

Series on Advances in Mathematics for Applied Sciences – Vol. 78

# ADVANCED MATHEMATICAL & COMPUTATIONAL TOOLS IN METROLOGY & TESTING VIII

*Editors*

**F Pavese**

**M Bär**

**A B Forbes**

**J M Linares**

**C Perruchet**

**N F Zhang**



World Scientific

**ADVANCED  
MATHEMATICAL &  
COMPUTATIONAL TOOLS IN  
METROLOGY & TESTING VIII**

## SERIES ON ADVANCES IN MATHEMATICS FOR APPLIED SCIENCES

---

*Published\*:*

- Vol. 64 Generalized Kinetic Models in Applied Sciences — Lecture Notes on Mathematical Problems  
*by L. Arlotti et al.*
- Vol. 65 Mathematical Methods for the Natural and Engineering Sciences  
*by R. E. Mickens*
- Vol. 66 Advanced Mathematical and Computational Tools in Metrology VI  
*eds. P. Ciarlini et al.*
- Vol. 67 Computational Methods for PDE in Mechanics  
*by B. D'Acunto*
- Vol. 68 Differential Equations, Bifurcations, and Chaos in Economics  
*by W. B. Zhang*
- Vol. 69 Applied and Industrial Mathematics in Italy  
*eds. M. Primicerio, R. Spigler and V. Valente*
- Vol. 70 Multigroup Equations for the Description of the Particle Transport in Semiconductors  
*by M. Galler*
- Vol. 71 Dissipative Phase Transitions  
*eds. P. Colli, N. Kenmochi and J. Sprekels*
- Vol. 72 Advanced Mathematical and Computational Tools in Metrology VII  
*eds. P. Ciarlini et al.*
- Vol. 73 Introduction to Computational Neurobiology and Clustering  
*by B. Tirozzi, D. Bianchi and E. Ferraro*
- Vol. 74 Wavelet and Wave Analysis as Applied to Materials with Micro or Nanostructure  
*by C. Cattani and J. Rushchitsky*
- Vol. 75 Applied and Industrial Mathematics in Italy II  
*eds. V. Cutello et al.*
- Vol. 76 Geometric Control and Nonsmooth Analysis  
*eds. F. Ancona et al.*
- Vol. 77 Continuum Thermodynamics  
*by K. Wilmanski*
- Vol. 78 Advanced Mathematical and Computational Tools in Metrology and Testing  
*eds. F. Pavese et al.*

\*To view the complete list of the published volumes in the series, please visit:  
[http://www.worldscibooks.com/series/samas\\_series.shtml](http://www.worldscibooks.com/series/samas_series.shtml)

# ADVANCED MATHEMATICAL & COMPUTATIONAL TOOLS IN METROLOGY & TESTING VIII

## Editors

**F Pavese**

*INRIM, Italy*

**M Bär**

*Physikalisch-Technische Bundesanstalt, Germany*

**A B Forbes**

*National Physical Laboratory, Middlesex, UK*

**J M Linares**

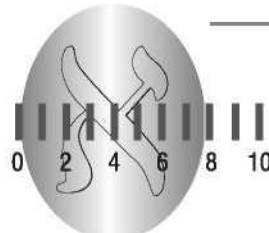
*Université de la Méditerranée, France*

**C Perruchet**

*UTAC, Montereau, France*

**N F Zhang**

*NIST, USA*



*Published by*

World Scientific Publishing Co. Pte. Ltd.

5 Toh Tuck Link, Singapore 596224

*USA office:* 27 Warren Street, Suite 401-402, Hackensack, NJ 07601

*UK office:* 57 Shelton Street, Covent Garden, London WC2H 9HE

**Library of Congress Cataloging-in-Publication Data**

AMCTM VIII (2008 : Paris, France)

Advanced mathematical and computational tools in metrology and testing : AMCTM VIII /  
edited by Franco Pavese ... [et al.].

p. cm. -- (Series on advances in mathematics for applied sciences ; v. 78)

Includes index.

ISBN-13: 978-981-283-951-0 (hardcover : alk. paper)

ISBN-10: 981-283-951-8 (hardcover : alk. paper)

1. Measurement--Congresses. 2. Physical measurements--Congresses. 3. Metrology--Congresses.  
I. Pavese, Franco. II. Title. III. Title: AMCTM 8.

QA465.A58 2008

530.8--dc22

2009001775

**British Library Cataloguing-in-Publication Data**

A catalogue record for this book is available from the British Library.

Copyright © 2009 by World Scientific Publishing Co. Pte. Ltd.

*All rights reserved. This book, or parts thereof, may not be reproduced in any form or by any means,  
electronic or mechanical, including photocopying, recording or any information storage and retrieval  
system now known or to be invented, without written permission from the Publisher.*

For photocopying of material in this volume, please pay a copying fee through the Copyright  
Clearance Center, Inc., 222 Rosewood Drive, Danvers, MA 01923, USA. In this case permission to  
photocopy is not required from the publisher.

Printed in Singapore.

## **Book Editors**

- F Pavese** (Istituto Nazionale di Ricerca Metrologica, Torino Italy)  
**M Bär** (Physikalisch-Technische Bundesanstalt, Braunschweig, Germany)  
**A B Forbes** (National Physical Laboratory, Teddington, UK)  
**J M Linares** (Université de la Méditerranée, Marseille, France)  
**C Perruchet** (UTAC, Paris, France)  
**N-F Zhang** (National Institute of Standards & Technology, Gaithersburg, USA)

*For the first seven Volumes see this Series vol. 16 (1994), vol.40 (1996), vol.45 (1997),  
vol.53 (2000), vol.57 (2001), vol.66 (2004) and vol.72 (2006)*



**IMEKO TECHNICAL COMMITTEE 21 " MATHEMATICAL TOOLS FOR MEASUREMENTS".**

**Chairperson:** F Pavese, Istituto Nazionale di Ricerca Metrologica (INRIM), Torino



**AMCTM 2008 CONFERENCE CHAIRPERSONS:** F.Pavese (INRIM), J-M Linares  
(Université de la Méditerranée)

## **INTERNATIONAL SCIENTIFIC COMMITTEE**

- Robert Douglas, National Research Council, Ottawa, Canada  
Alistair B Forbes, National Physical Laboratory, Teddington, UK  
Christophe Perruchet, UTAC, Paris, France  
Eduarda Côrte-Real Filipe, Instituto Português da Qualidade (IPQ), Caparica, Portugal  
Eric Benoit, Université de Savoie, Annecy, France  
Franco Pavese, Istituto Nazionale di Ricerca Metrologica (INRIM), Torino  
Isao Kishimoto, AIST, National Metrology Institute of Japan, Ibaraki, Japan  
Leslie Pendrill, SP Sveriges Tekniska Forskningsinstitut, Borås, Sweden  
Jean-Marc Linares, Université de la Méditerranée, Marseille, France  
Markus Bär, Physikalisch-Technische Bundesanstalt, Braunschweig, Germany  
Nicolas Fischer, Laboratoire National d'Essais et de Métrologie, Paris, France  
Patrizia Ciarlini, Istituto per le Applicazioni del Calcolo "M.Picone", Roma, Italy  
Wolfram Bremser, Bundesanstalt für Materialforschung und -prüfung, Berlin, Germany  
Nien-Fan Zhang, National Institute of Standards & Technology, Gaithersburg, USA

## **ORGANISED BY**

IMEKO TC21 [www.imeko-tc21.org](http://www.imeko-tc21.org)

Collège Français de Métrologie (CFM) [www.cfmetrologie.com](http://www.cfmetrologie.com)

## **Foreword**

This volume collects the refereed contributions based on the presentation made at the International Conference on Advanced Mathematical and Computational Tools in Metrology and Testing, held in Paris in June 2008. The conference was organised by IMEKO Technical Committee 21 “Mathematical Tools for Measurements” (<http://www.imeko-tc21.org>), the eighth in an evolving series, with “testing” appearing in the title for the first time in this volume. The aims of TC 21 activities, reflected in the book series, are:

- To present and promote reliable and effective mathematical and computational tools in metrology and testing.
- To understand better the modelling, statistical and computational requirements in metrology and testing.
- To provide a forum for metrologists, mathematicians, software and IT engineers that will encourage a more effective synthesis of skills, capabilities and resources.
- To promote collaboration in the context of EU and International Programmes, projects of EUROMET and EA and of other world regions, MRA requirements.
- To support young researchers in metrology, testing and related fields.
- To address industrial and societal requirements.

The themes in this volume reflect the importance of mathematical, statistical and numerical tools and techniques in metrology and testing and, addressing the challenge promoted by the Metre Convention, in enabling a mutual recognition for the measurement standards.

Torino, December 2008

The Editors

## **Contents**

<i>Foreword</i>	v
Sensitivity Analysis in Metrology: Study and Comparison on Different Indices for Measurement Uncertainty <i>A Allard and N Fischer</i>	1
Likelihood Maximization Against the Probability Density Function Shape <i>S Aranda, J-M Linares and J-M Sprauel</i>	7
Methods for Estimation of the Effect of Correlation at the Measurement of Alternating Voltage <i>T Barashkova</i>	14
Multi-Determination of Aerodynamic Loads Using Calibration Curve with a Polynomial and MLP Neural Network Combination <i>I M Barbosa, O A De Faria Mello, M L Colucci da Costa Reis and E del Moral Hernandez</i>	20
Uncertainty Analysis in Calibration of Standard Volume Measures <i>E Batista, N Almeida and E Filipe</i>	28
Virtual Atomic Force Microscope as a Tool for Nanometrology <i>V S Bormashov, A S Baturin, A V Zablotksiy, R V Goldshtain and K B Ustinov</i>	32
Development of a Mathematical Procedure for Modelling and Inspecting Complex Surfaces for Measurement Process <i>S Boukebbab, H Bouchenitfa and J-M Linares</i>	37
A Software Simulation Tool to Evaluate the Uncertainties for a Lock-in Amplifier <i>P Clarkson, T J Eward, P M Harris, K J Lines, F O Onakunle and I M Smith</i>	44

Measurement Uncertainty in a Non-Classical Context <i>G E D'Errico</i>	50
Comparison of Methods to Measure Uncertainty Based on the ISO Standards <i>L Del Dossi and D Zappa</i>	54
Methods for Aggregating Key Comparisons <i>R J Douglas and A G Steele</i>	61
Uncertainty Evaluation for Pose Estimation by Multiple Camera Measurement System <i>M Douilly, N Anwer, P Bourdet, N Chevassus and P Le Vacon</i>	73
Analysis of Dynamic Measurements: Compensation of Dynamic Error and Evaluation of Uncertainty <i>C Elster and A Link</i>	80
An Approach to Uncertainty Using Nested Analysis <i>M Do Céu Ferreira, A Furtado and E Filipe</i>	90
Proficiency Testing for Calibration Laboratories <i>E Filipe</i>	96
Nonlinear Least Squares and Bayesian Inference <i>A B Forbes</i>	104
Measurement Strategy Analysis for Out-of-Roundness Measurement with CMM <i>B Gapinski, M Rucki and M Pawlowski</i>	113
Dedicated Software Package for Pressure Regulation at 1 ppm Level Using a Gas-Controlled Heat Pipe <i>S Giunta, A Merlone, P Marcarino, S Botta and V Giovanetti</i>	118
Model Adequacy in Measurements: Estimation and Improvement <i>V A Granovsky and T N Siraya</i>	123

A New Guide for the Development and Assessment of Measurement Software <i>N Greif and G Parkin</i>	130
Current Issues in the Evaluation of Ionising Radiation Measurements <i>D Gridentschnig</i>	136
Modelling and Uncertainty Estimates for Numerically Reconstructed Profiles in Scatterometry <i>H Gross, A Rathsfeld and M Bär</i>	142
Kalman Filter Type Sequential Method with Stopping Rule for Calibration of Measurement Instruments <i>C Hajiyev</i>	148
Determination of Optimum Input Signals via D-optimality Criterion for Calibration of Measurement Instruments <i>C Hajiyev</i>	154
An Extension of the GUM Tree Method for Complex Numbers <i>B D Hall</i>	158
Digital Filtering for Dynamic Uncertainty <i>J P Hessling</i>	164
Considerations and Developments in Uncertainty Evaluations in Chemical Metrology <i>R Kaarls</i>	171
Quality by Design Applications to Analytical Methods in the Pharmaceutical Industry <i>R S Kenett and D A Kenett</i>	183
A Test of Linearity Using Covering Arrays for Evaluating Uncertainty in Measurement <i>R Kessel and R Kacker</i>	195
Challenges in Practical Dynamic Calibration <i>M Kobusch, T Bruns and E Franke</i>	204

Derivation of an Output PDF from Bayes' Theorem and the Principle of Maximum Entropy <i>I Lira, C Elster, W Wöger and M. Cox</i>	213
Evaluation of Uncertainties on Datum-System Reference <i>J Mailhe, J-M Linares and J-M Sprauel</i>	219
Possibility Distribution: A Useful Tool for Representing Coverage Intervals With and Without the Probability Density Knowledge <i>G P Mauris</i>	225
Implementation of Some Mathematical Approximation Methods of Functions for Study of the Factors which Influence the Ferment Activity of Beer Yeast <i>M R Milici, R Rotar and L D Milici</i>	231
Measurement Uncertainty Calculation Using MUSE: A Software Project to Support the Measurement Community with a Freely Available Implementation of GUM Supplement 1 <i>M Müller, M Wolf and M Rösslein</i>	237
Robust Line Detection for Line Scale Calibration <i>J A Muñoz-Gómez and C Galvan</i>	243
Analysis of Consistency of the Basic Concepts for the Expression of Uncertainty in Present International Written Standards and Guides <i>F Pavese</i>	249
An Optimised Uncertainty Approach to Guard-Banding in Global Conformity Assessment <i>L R Pendrill</i>	256
From GUM to Alternative Methods for Measurement Uncertainty Evaluation <i>M Priel</i>	262
The Propagation of Uncertainty Related to the Calibration Functions of Platinum Resistance Thermometers and Possible Correlation Effects <i>A S Ribeiro, J A Sousa, C O Costa, M G Cox and P M Harris</i>	273

Measurement of Characteristics Related to Human Perception <i>G B Rossi</i>	279
Lossless Compression of Computer Tomography Point Clouds <i>R Schmitt and P Fritz</i>	291
Declaration and Specification of a Geometrical Part in the Language of Geometric Algebra <i>P Serré, M Moinet and A Clément</i>	298
Modelling of Dynamic Measurement Systems and Uncertainty Analysis Employing Discretised State-Space Forms <i>K-D Sommer, U Hanebeck, M Krystek and F Sawo</i>	309
Optimal Decision Rules and Limits of Detection <i>J A Sousa and A B Forbes</i>	319
Validity of Expanded Uncertainties Evaluated Using the Monte Carlo Method <i>H Tanaka and K Ehara</i>	326
Model Based Uncertainty Analysis in Inter-Laboratory Studies <i>B Toman and A Possolo</i>	330
Gear Metrology of Statistical Tolerancing by Numerical Simulation <i>J-P Vincent, C Baudouin, J Bruyere, J-Y Dantan and R Bigot</i>	344
Transferring Monte Carlo Distributions in the Evaluation of Uncertainty <i>R Willink</i>	351
Mathematical Entropy and a Criticism of a Usage of the Principle of Maximum Entropy <i>R Willink</i>	357
Multivariate and Functional Clustering Applied to Measurements of Laboratory Analysis Systems <i>I Winzenborg, A Geistanger and U Stadtmüller</i>	361

Impact of Correlation in the Measured Frequency Response on the Results of a Dynamic Calibration <i>G Wiibeler, A Link, T Bruns and C Elster</i>	369
Uncertainty of Standard Concentrations, Calibration Line and Predictions <i>C Yardin and S Kaba</i>	375
The Concept of “Virtual Microscope” for Nanometrology <i>A V Zablotskiy, A S Baturin and V S Bormashov</i>	381
Orthogonal Distance Fitting of Precision Free-Form Surfaces Based on $l_1$ Norm <i>X C Zhang, X Q Jiang and P J Scott</i>	385
Allan Variance and the Uncertainty of Autocorrelated Measurements <i>N-F Zhang</i>	391
<i>Author Index</i>	405

## SENSITIVITY ANALYSIS IN METROLOGY: STUDY AND COMPARISON ON DIFFERENT INDICES FOR MEASUREMENT UNCERTAINTY

ALEXANDRE ALLARD, NICOLAS FISCHER

*Laboratoire national de métrologie et d'essais  
1 rue Gaston Boissier, 75724 Paris, France*

Sensitivity analysis is an important part of metrology, particularly for the evaluation of measurement uncertainties. It enables the metrologist to have a better knowledge of the measurement procedure and to improve it. A tool for sensitivity analysis is developed in the Guide for the evaluation of Uncertainty in Measurement (GUM) [1]. Supplement 1 to the GUM [2] that deals with Monte Carlo Methods (MCM) provides a similar sensitivity index known as “One At a Time” (OAT). Other sensitivity indices have been developed, but have not yet been used in metrology so far. In this paper, we put forward four indices and we compare them by means of metrological applications. We particularly focus on the Sobol indices [3], based on the evaluation of conditional variances. In order to compare the performance of these indices, we have chosen two examples, different from a mathematical point of view. The first example is the mass calibration example, mentioned in Supplement 1 to the GUM ([2], §9.3). It highlights the relevance of Sobol index to estimate interaction effects. The second example is based on Ishigami function, a non-monotonic function, ([3], §2.9.3). It leads to the conclusion that when the model is non-monotonic, indices based on partial derivatives and SRRC give wrong results, according to the importance of each input quantity.

### 1. Introduction to Sensitivity Analysis

Sensitivity analysis is a wide topic that has different interpretations regarding the scientific community (Statistics, numerical analysis...). In the uncertainty framework, sensitivity analysis is considered as Factor’s prioritization. The aim is then to identify the input quantities  $X_i$  that impact the most the variance of the output quantity  $Y$  from a quantitative point of view. It enables the metrologist to have a better knowledge of the measurement procedure and to improve it. Scientific literature and guides for uncertainty provide different indices  $S_i$  that are interesting to study in the metrologist context to identify the most relevant ones.

## 2. Sensitivity Analysis Indices

### 2.1. Partial Derivative Approach - GUM

According to the GUM approach, the sensitivity indices are based on the partial derivatives that have been calculated when applying the law of propagation of uncertainty (LPU).

$$S_i = \frac{\left( \frac{\partial f}{\partial x_i} \right)^2 u^2(x_i)}{u^2(y)} \quad (1)$$

These indices are the contributory uncertainties of the input quantities to the variance of the measurand in the linear case with independent input quantities.

### 2.2. “One At a Time” Index – GUM S1

The GUM-S1 (Appendix B) only suggests a “One At a Time” method to estimate sensitivity indices for a Monte Carlo method. The principle consists in holding all input quantities but one fixed at their best estimate while performing MCM. This provides the PDF for the output quantity having just that input quantity as a variable.

It can be seen as a generalization of the partial derivative approach adapted to Monte Carlo Method, where:

- $c_i = \frac{u_i(y)}{u(x_i)}$  is the sensitivity coefficient with  $u_i^2(y)$  is the variance of the measurand when all input quantities but  $X_i$  are fixed.
- $c_i^2 u^2(x_i)$  is the contribution to the variance
- $S_i = \frac{u_i^2(y)}{u^2(y)}$  is the ratio in the uncertainty budget

These indices are very intuitive. They are computed next to the propagation step and imply  $N$  more trials for Monte Carlo simulations for each sensitivity index to estimate.

### 2.3. Rank Correlation

In the case of a monotonic but nonlinear model, the Standardized Rank Regression Coefficient can be used as a sensitivity index:

$$SRRC(r_x; r_y) = \frac{\sum_{i=1}^n (r_{xi} - \bar{r}_x)(r_{yi} - \bar{r}_y)}{\sqrt{\sum_{i=1}^n (r_{xi} - \bar{r}_x)^2 \sum_{i=1}^n (r_{yi} - \bar{r}_y)^2}} \quad (2)$$

where  $r_x$  and  $r_y$  are respectively the rank vectors of the data  $X$  and  $Y$ .

We used the normalized indices in order to assess the relative contribution of  $Xi$ :

$$S_i = \frac{SRRC_i^2}{\sum_i SRRC_i^2} \quad (3)$$

These coefficients are easy to compute within Monte Carlo method and provide sensitivity indices simultaneously as the propagation step.

## 2.4. Variance Based Method - Sobol Indices

### 2.4.1. Definitions

Sobol [4] indices rely on a decomposition of the variance of the output quantity into terms of increasing dimensionality. These terms are the variances of the conditional expectation of  $Y$  (conditionally to  $Xi$ ), suitable measures of the importance of  $Xi$ .

$$V(Y) = V(E[Y|X_i]) + E[V(Y|X_i)] \quad (4)$$

$$V_i = V(E[Y|X_i]), \quad V_{ij} = V(E[Y|X_i, X_j]) - V_i - V_j,$$

$$\dots, \quad V_{1\dots p} = V(Y) - \sum_{i=1}^p V_i - V_j - V_k$$

First order Sobol indices measure the main effects of the variables  $Xi$ :

$$S_i = \frac{V(E[Y|X_i])}{V(Y)} \quad (5)$$

Second order Sobol indices measure the interaction effects of the quantities  $Xi$  and  $Xj$ :

$$S_{ij} = \frac{V_{ij}}{V(Y)} \quad (6)$$

One important property is that the sum of all the indices is equal to one.

#### 2.4.2. Estimation

The estimation of Sobol indices is based on two  $M$ -sample of the input quantities  $X_i^{(1)}$  and  $X_i^{(2)}$ , where  $M$  is the number of Monte Carlo trials. For instance, first order Sobol indices are estimated according to:

$$\hat{S}_i = \frac{1}{M} \sum_{k=1}^M f\left(X_{k,1}^{(1)}, \dots, X_{k,p}^{(1)}\right) f\left(X_{k,1}^{(2)}, \dots, X_{k,i-1}^{(2)}, X_{k,i}^{(1)}, X_{k,i+1}^{(2)}, \dots, X_{k,p}^{(2)}\right) \quad (7)$$

Such an estimation has been implemented on both R and Matlab and the dispersion of the estimations has been controlled with bootstrap methods and also with standard deviations on the indices.

### 3. Examples

#### 3.1. Mass Calibration

We consider the calibration of a weight  $W$  as described in GUM S1 [2]:

$$m_w = (mrc - dmrc) \left( 1 + (a - 1200000) \left( \frac{1}{rhow} - \frac{1}{rhor} \right) \right) \quad (8)$$

The input quantities are defined as follows:

- a Gaussian distribution with 100 000 mean and 0.05 standard deviation is assigned to  $mrc$  ( $X_1$ , mg)
- a Gaussian distribution with 1.234 mean and 0.02 standard deviation is assigned to  $dmrc$  ( $X_2$ , mg)
- a uniform distribution between  $1.1 \cdot 10^6$  and  $1.3 \cdot 10^6$  is assigned to  $a$  ( $X_3$ , mg/m<sup>3</sup>)
- a uniform distribution between  $7 \cdot 10^9$  and  $9 \cdot 10^9$  is assigned to  $rhow$  ( $X_4$ , mg/m<sup>3</sup>)
- a uniform distribution between  $7.95 \cdot 10^9$  and  $8.05 \cdot 10^9$  is assigned to  $rhor$  ( $X_5$ , mg/m<sup>3</sup>)

Table 1. Results of sensitivity indices for mass calibration

Variable	LPU 1st order	LPU 2nd order	OAT - GUM S1	Ranks	Sobol
$X_1$	0.862	0.445	0.437	0.862	0.439
$X_2$	0.138	0.071	0.070	0.135	0.068
$X_3$	0.000	0.000	0.000	0.003	0.000
$X_4$	0.000	0.000	0.000	0	0.000
$X_5$	0.000	0.000	0.000	0	0.000
Interaction $X_3 \cdot X_4$	-	0.483	-	-	0.489
Interaction $X_3 \cdot X_5$	-	0.001	-	-	0.004

Indices based on the ranks, first order partial derivatives and OAT do not allow estimate the interaction effects. Thereby they lead to an underestimation of the importance of the variables  $X_3$  and  $X_4$  in the uncertainty budget.

### 3.2. Ishigami Function

This function is a very well known example used in the literature; see [3] to illustrate the importance of the choice of the suitable sensitivity indices.

$$Y = \sin(X_1) + 7(\sin(X_2))^2 + 0.1X_3^4 \sin(X_1) \quad (9)$$

A uniform distribution between  $-\pi/10$  and  $\pi/10$  is assigned to  $X_1$ ,  $X_2$  and  $X_3$ . The calculation of Sobol indices has been implemented with R and Matlab and the quality of the estimation has been controlled with bootstrap methods.

Table 2. Results of sensitivity indices for Ishigami function

Variable	LPU 1st order	OAT	Ranks	Sobol - Matlab	Sobol - R
$X_1$	1.000	0.448	1	0.312	0.315
$X_2$	0.000	0.552	0	0.442	0.443
$X_3$	0.000	0.000	0	0.000	0.000

Interaction  $X_1 \cdot X_3$ :  $S_{13} = 0.245$  only available within the variance based decomposition of Sobol. In addition, due to the non-linear and non-monotonic

model, Ranks and LPU 1<sup>st</sup> order indices do not provide the correct contributions of the input quantities.

#### 4. Conclusion

When performing a MC Method, under the assumptions of linearity or monotony, one should prefer easy to handle indices, OAT and ranks correlation indices. When applying the Sobol's theory, no assumptions are made on the mathematical model of measurement regarding linearity or monotony. It offers then the ideal theoretical background to the problematic of sensitivity analysis in the sense of Factor's prioritization. It allows the computation of interaction effects simultaneously as the propagation of uncertainty. However the computational execution time of the model is a major concern when using complex codes and could be a strong limit to the estimation of the Sobol indices.

#### Acknowledgments

The authors would like to thank Bertrand Iooss for his comments and advices on the use of the R sensitivity package.

#### References

1. BIPM, IEC, IFCC, ISO, IUPAC, IUPAP, *Guide to the Expression of Uncertainty in Measurement* (1995).
2. BIPM, IEC, IFCC, ISO, IUPAC, IUPAP, *Evaluation of measurement data – Supplement 1 to the “Guide to the expression of uncertainty in measurement” – Propagation of distributions using a Monte Carlo method Final draft* (2006).
3. A.Saltelli, K.Chan, E.M.Scott, *Sensitivity Analysis*, Wiley (2000).
4. I.M. Sobol, *Sensitivity Estimates for Nonlinear Mathematical Models*, Mathematical Modelling and Computational Experiments (1993)
5. <http://cran.cict.fr/src/contrib/Descriptions/sensitivity.html>

## LIKELIHOOD MAXIMIZATION AGAINST THE PROBABILITY DENSITY FUNCTION SHAPE

SEBASTIEN ARANDA,

*Laboratory EA(MS)<sup>2</sup>, Université Aix-Marseille  
13625 Aix-en-Provence, France*

JEAN-MARC LINARES, JEAN-MICHEL SPRAUEL

*Laboratory ISM, UMR CNRS 6233, Université Aix-Marseille  
13625 Aix-en-Provence, France*

The goal of this article is to propose a criterion based on an adequate real distribution. In order to do this, the criterion must be able to integrate any type of distribution like unsymmetrical distributions, which are characteristic of the PDF shapes left by some manufacturing processes. To carry out this objective, two tasks should be realised. First, a criterion has to be constructed using the statistical approach. And next, the behaviour of the likelihood function against different kinds of PDF shape may be studied to define the most appropriate form of this function.

### 1. Introduction

The recent evolution of the manufacturing processes, during the last decades, has allowed designers to reduce clearances in mechanical products. It has greatly impacted the measuring and control scheme, based on coordinate measuring machines, by bringing tolerance intervals much closer to measurement uncertainties. In consequence, to reduce or control the gap between a measured set of points and its best-fitted geometrical element has become one of the most important modern metrology's challenges. This article focuses on this topic by presenting a study based on a statistical best-fit method. This one is able to minimise and estimate the gap between the knowledge of a real surface and its mathematical representation, i.e. best-fitted feature. Many researches have been conducted to find an optimal best-fit method and a great number of solutions have been proposed to solve this problem [1-2]. Two major points of view can be discerned. Some consider that the best representing geometrical feature is found when the minimum of a given mathematical function deriving from the distances between the feature and a set of points is reached. While others consider that the best-representing feature should be

evaluated by a statistical mean like a regression analysis method. But whatever the considered points of view, fitting a feature imposes to make or accept a hypothesis concerning the distribution of the points around this one. In the last raised point of view, which based on statistical approach, the hypothesis relative to the point's distribution is entirely part of the best-fit criterion. The goal of best-fit process is to identify the feature parameters which maximize the probability that the point's distribution matches an attempted one. At the opposite, in the first point of view which is based on a deterministic approach, the hypothesis relative to the point's distribution is not part of the criterion. It has to be accepted. The objective consists in optimizing a mathematical function that defines a metrological aspect of the point's distribution. For example, the least square method tries to define the parameters which minimize the square sum of the distances between the measured points and the feature. Authors proved [3] that it leads to promote a normal distribution of the points around the best-fitted feature (figure 1).

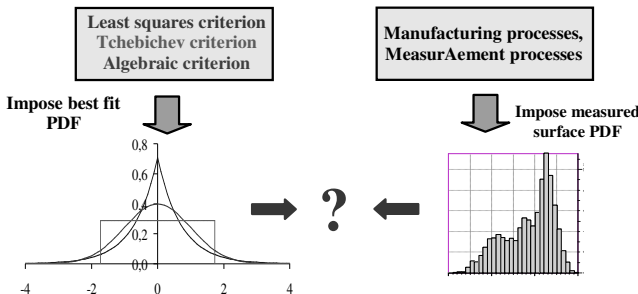


Figure 1: difference between manufactured PDF and criterion PDF.

## 2. Statistical Best-Fit Approach

In this article, surface best-fit will be considered as a statistical process, thus falling within the trend of thought led by Professors Estler and Cox [4]. The real surface is considered as an infinite number of points which represents an unknown population. The only information source available about it is a sample of measured points. The best-fit process goal is to estimate two geometrical characteristics of the real surface population which are: its position and its orientation. It is very important to notice that the objective is to estimate the geometrical characteristics of the real, and unknown, surface population and not the measured point ones. The interest of this approach comes from its ability to deliver information on the real point's population, i.e. measured surface, with a few number of measured points. It allows, for example, making conclusions

about the extreme fitted feature of the real and unknown surface while Least Squares approach only permits to build conclusions about the measured extreme feature of the points.

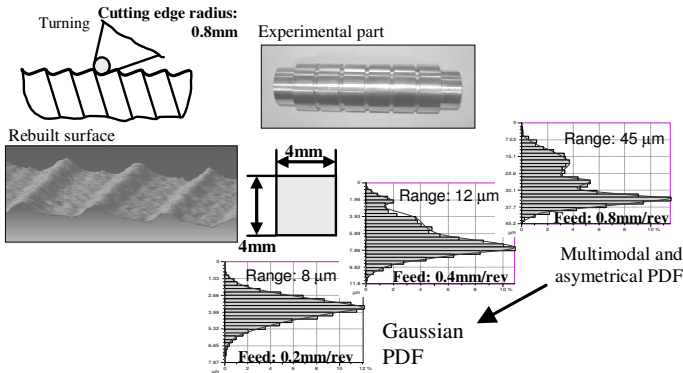


Figure 2: impact of the manufacturing process parameter onto point's distribution.

Such a goal can be reached by linking the sample of measured points to the real surface population with an attempted Probability Density Function (PDF). This one introduces additional information by describing how the points of the real surface, thus also the sample ones, are distributed around the mean feature (figure 2). It depends significantly on the manufacturing process used to generate the surface and can be estimated by using some knowledge about the manufacturing process, strategy and parameters [5]. Estimation of the PDF is a very important part of the best-fit process because it greatly influences its results.

Once estimated, the PDF can be used to build a likelihood function (LF) which will allow evaluating the quantity of information contained in the points sample regarding to a particular position and orientation of the fitted feature.

As more the likelihood is high, more the feature is representative of the real surface; the best-fit method will simply consist to identify the feature parameters which maximise the previously proposed LF.

Next paragraphs will discuss about the definition of the two main points of the proposed best-fit method, whose are the representation of the attempted Probability Density Function and the definition of the likelihood estimator.

### 3. Definition of Probability Density Function (PDF)

The PDF is a key parameter of the statistical best-fit approach. As a generic approach is researched, we choose to define the PDF by the way of numerical

estimation derived from a machining simulation. This solution allows taking profit of the great number of works done on the machining simulation theory and permits to model any kind of PDF shape. As a first approach, the basic and intuitive numerical of the PDF should be a histogram (figure 2). The sizes of the classes are derived from the result of a machining simulation. This simple solution issues one main limitation caused by the step effect, due the non-linearity of the PDF histogram, which should avoid the success of the likelihood maximization. Taking more points to build the histogram should be a solution to reduce the step effect. But it will never totally avoid while it will greatly increase the calculation time. A better solution remains in using a core function fitting of the basic histogram. It consists in fitting a reasonable histogram, i.e. build from a reasonable number of points, by a sum  $f(x)$  of normal laws (figure 3).

$$f(d_k) = \sum_{i=1}^{i=q} \frac{1}{\sigma_i \sqrt{2\pi}} \text{Exp}\left(-\frac{1}{2} \cdot \frac{(d_k - m_i)^2}{\sigma_i^2}\right) \quad (1)$$

The law parameters are defined by minimising the residual gap between the probability estimation give by the function  $S(x)$  and the probability reference represented by the histogram.

$$W = \sum_{k=1}^{k=n} e_k^2 \quad \text{with} \quad e_k = P_k - f(d_k) = P_k - \sum_{i=1}^{i=q} \frac{1}{\sigma_i \sqrt{2\pi}} \text{Exp}\left(-\frac{1}{2} \cdot \frac{(d_k - m_i)^2}{\sigma_i^2}\right) \quad (2)$$

This representation of the PDF is very useful because it provides a continuous and derivable function. The next figure illustrates the fitting of 14 classes histogram build from 200 points by three Gaussian cores.

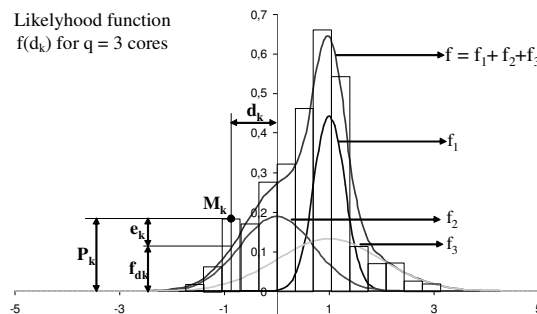


Figure 3: definition of a linear PDF estimation by a Gaussian core fitting of a histogram.

#### 4. Definition of the Likelihood Criterion Function

Depending on the manufacturing process, the PDF shape may be symmetrical, unsymmetrical, unimodal or multimodal. For example, grinding operation will lead to a Gaussian shape while milling and turning operations will lead to unsymmetrical and slightly multimodal shapes. More over, the attempted PDF is not only due to the manufacturing process. The measuring process will also influence and deform the distribution of the measured points (figure 4). But the criterion should give good likelihood estimation for every kind of PDF shapes.

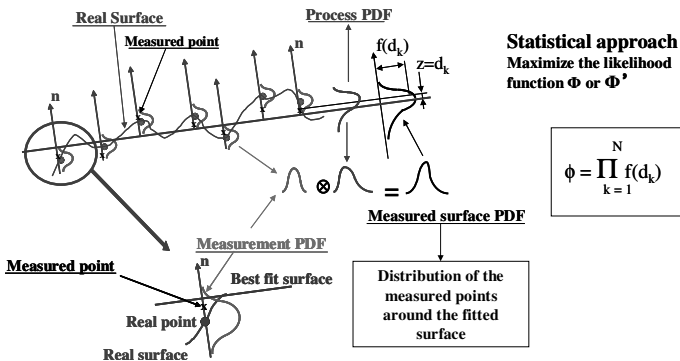


Figure 4: principle of the likelihood approach and the determination of the measured PDF.

By definition, the LF consists in the product of the probabilities given by the PDF for all the measured points and the likelihood criterion remains to perform a maximization of this function against the parameters' feature. The success of the maximization search is closely linked to two mains aspects of the LF shape:

- The LF has to be concave. Else it will admits more than one local's minimum and the success of the optimization is not guarantied.
- The gradient of the LF has to be always different from zero and should vary the more continuously as possible.

Let's discuss about this two points, starting by the second one i.e. the gradient. As presented on the next figure, the previously proposed LF lead to a high gradient around  $x = -1.5$  and a quasi null gradient over  $x = -2.5$  and  $x = 0$ . It makes the research of the maximum difficult or even impossible. A more stable approach should consist in maximising the logarithm of the LF (figure 5). With this particular expression the LF gradient evolves more continuously and is always different from zero.

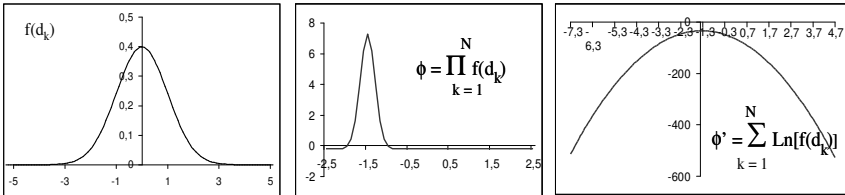


Figure 5: impact of the criterion definition onto the likelihood function.

More-over, the product of  $n$  terms closed to zero, which can lead to computational rounding errors, is converted into a steadier sum. Let's now focuses on the concavity of the LF, witch depends directly on the shape of the PDF one. The next figure, obtained by simulation, shows the effect of slightly bimodal PDF on the LF shape (figure 6). It shows that the LF can remain concave and thus maximizable though the slightly by-modality of PDF. Complementary works, not presented here, shown that a high multi-modality is needed to make the LF unoptimizable. But, as the measured PDF seems to remain generally slightly multi-modal does not represent a problematic issue.

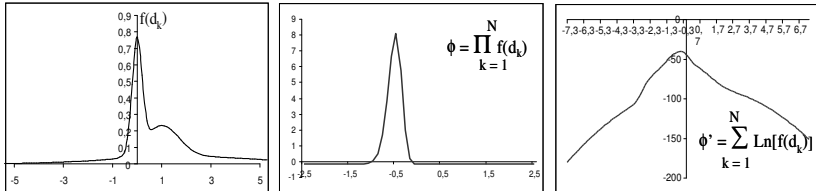


Figure 6: impact of PDF shape onto the likelihood function.

## 5. Conclusion

After exposing the concept of statistical best-fit approach, this article has proposed a criterion based on an adequate real PDF (i.e. unsymmetrical and slightly-multimodal). To reach this objective, two key points have been addressed. First, two formulations of the LF have been proposed. And next, the effect of the PDF shape on the LF concavity, which traduces the ability to correctly maximize it, has been discussed.

## References

1. P. Bourdet, A. Clement, "A study of optimal-criteria identification based on the small displacement screw model", Annals of CIRP, vol. **37** (1988).
2. G. Goch, U. Tschudi, "Universal Algorithm for the alignment of Sculptured Surfaces", Annals of CIRP, vol. **41**, n°1 (1992).

3. J.M. Sprauel, J.M. Linares, P. Bourdet, "Contribution of non linear optimization to the determination of measurement uncertainties", 7<sup>th</sup> CIRP Seminar on Computer Aided Tolerancing, pp.285-292 (2001).
4. W.T. Estler, "Measurement as Inference: fundamental Ideas", Annals of the CIRP, **vol. 48/2** (1999).
5. S. Aranda, J.M. Linares, J.M. Sprauel, P. Bourdet, "Surface best fit: Generated distribution of the real manufacturing process", Models for Computer Aided Tolerancing in Design and Manufacturing, **vol. 37** (2007).

## METHODS FOR ESTIMATION OF THE EFFECT OF CORRELATION AT THE MEASUREMENT OF ALTERNATING VOLTAGE\*

TATJANA BARASHKOVA

*Virumaa College of Tallinn University of Technology, Järveküla tee 75  
Kohila-Järve, 30328, Estonia*

In this article developed by the author the variant of system of covariance calculation is presented, which leads to the precise results of the measurements and based on: the least-squares method, criteria of uniformity of several correlation coefficients, "expert-statistical" method. Use of the above mentioned methods has allowed to increasing the reliability of the results of measurements of an alternating current voltage.

### 1. The Research on the Effect of Correlation in the Measurement of Alternating Voltage

The proposed calibration method for measuring thermoelectric voltage transducers was based on the studies carried out in the METROSERT electrical measurement laboratory in order to verify the developed model of alternating voltage measurement. A method was proposed to reduce the measured dimension. A sample correlation coefficient was taken as the dimension reduction criterion. The relative difference (deviation) of the alternating current voltage from the equivalent direct current voltage is usually taken as the measured. The value of this measured within the operating frequency range is the metrological characteristic of the calibrated thermoelectric transducer. The uncertainty of the alternating voltage standard is estimated to be at the level of the root-mean-square deviation of the results of measurement of the relative difference between the direct current voltage and alternating current voltage. There is a regularly renewed calibration certificate on the transfer standard FLUKE with a table of expanded uncertainty regarding frequency and voltage. Following the recommendations of the company FLUKE, the uncertainties brought in by other means of measurement are excluded due to the specific nature of the measurements. Thus, the uncertainty of the results of calibration of

---

\* This work was carried out with the support of the Estonian Ministry of Education Science Grant No. 142506s03 and the Estonian Science Foundation Grants No. 5621 and No. 6172

alternating current voltage standards with the use of thermoelectric transducers comprises the FLUKE uncertainty and the uncertainty of the relative correction. Such laboratories as LABORATOIR CENTRAL DES INDUSTRIES ELECTRIQUES, LABORATOIR NATIONAL METROLOGIE LNM, using a simple method for estimating the alternating current voltage, i.e. Zero method, have obtained inferior metrological characteristics than those obtained in estimation with the use of alternating current voltage measurement model. The method, described in the paper, allows taking into account the variability of the conditions in the measuring laboratory without using any indeterminate functional relation. Using the developed method, any laboratory can raise the quality of measurement as well as apply for certification of its quality management system as being compliant with the requirements of ISO/IEC 17025 standard. The method, described in the paper, is based on the expert evaluation of the measured. Precision instruments can perform the role of experts the same as a group of specialists. In the METROSERT laboratory, a small scale experiment has been carried out to verify the efficiency of the model of precise measurement of alternating voltage. The main emphasis was made on modeling the experiment with the use of a random number generator. The proposed method would allow to produce a good reference standard on the basis of the transfer standard of the alternating current voltage unit FLUKE 792A. Having the evidence of the continuous stability of the source of direct current voltage, having measured the temperature gradient and stability lapse rate and using the results of international comparisons as expert estimates, the measuring laboratories can obtain accreditation to have the right for the calibration of alternating current voltage standards. In the work, such methods of covariance estimation have been studied, which allow to make the measurement results more precise in case the observation data have different degrees of precision and are correlated. To compare the results of the measurements accomplished at different times, a test of the homogeneity of several correlation coefficients has been applied. It is a known fact that during the estimation of any output value it is impossible to be sure that the input values' correlation ratios can be neglected. Therefore, in practice any function under investigation has to be estimated with the use of sampled data and such methods of statistics estimation, which will specify the covariance of dependent variables. For example, if the function under investigation is hypothetically linear, the input values' correlation ratio is estimated with the use of a sampled correlation coefficient, applying statistical or empirical methods. Operating just a small number of sampled input values, it is not possible to be sure that the function is linear. Likewise, in the absence of sufficient amount of statistical data it is impossible to be sure that the correlated random values follow the Gaussian distribution model. The deficit of input data implies the possibility for the functional relationship to be of a monotonic non-

linear nature. The following issues have been solved within the project in order to raise the trustworthiness of the correlation analysis results. The methods have been developed to estimate the uncertainty of standard model of alternating current voltage in case of correlated and unequal precision measurement results. Methods of multivariate mathematical statistics have been included in the measurement methodology in order to reduce the instability estimates of alternating current voltage. The variability of measurement conditions of alternating voltage has been taken into account for the situation, when the precise functional relationships between the measured and the mentioned conditions are not known. The possibilities to reduce the degree of the measurements' equation and the number of informative parameters have been analyzed. Also, the influence of random deviations on the correlation ratio of random values in measurement of alternating voltage has been studied. The implementation of the above-mentioned methods has allowed improving the reliability of the measurement results of alternating current voltage. The statistical analysis has made it possible to obtain the best estimation of the alternating voltage measured. Estonia does not possess a reference standard for alternating current voltage. It is very important for a state to have a standard that produces the required alternating current voltage with a relative uncertainty under  $30 \cdot 10^{-6}$ . The received functional dependence allowed to determining the contribution of each input quantity to uncertainty of an alternating voltage estimation that, in turn, led to the improvement of model of measurement. The tasks solved in the project will make it possible to produce in Estonia, on the basis of the transfer standard of the voltage unit Fluke 792 A, a reference standard of alternating current voltage within the range from 100 mV to 1000 V with frequency within the range from 10 Hz to 1 MHz.

## 2. Expert Statistical Method

The general number of the parameters influencing the investigated value of an alternating voltage is large. If these parameters are registered on every  $i$  – limit of measurement the multivariate measurements will turn out. It is necessary to subject these available multivariate measurements to statistical processing for reception of more reliable objective function.

$$\begin{aligned} U'_{0\approx} &= f(U_{x\approx}, U_{x\equiv}, U_{0\approx}, U_{0\equiv}) = \\ &= \alpha + \beta_1 U_{x\approx} + \beta_2 U_{x\equiv} + \beta_3 U_{0\approx} + \beta_4 U_{0\equiv} \end{aligned} \quad (1)$$

"Expert-statistical" method [1, 2, 3] has allowed to receiving the best estimation of value of an alternating voltage of 50 Hz frequency, dependent on the correlated input quantities.

1. Statistical part of initial data. As it was already mentioned above, input variables  $U_{x \approx}, U_{x \equiv}, U_{0 \approx}, U_{0 \equiv}$  were measured on each  $i$ -limit of measurement every  $j$ -day of experiment. Therefore the statistical part of initial data is represented in the form of

$$\mathbf{X}^j = \begin{pmatrix} U_{x \approx}^1, U_{x \approx}^2, \dots, U_{x \approx}^i \\ U_{x \equiv}^1, U_{x \equiv}^2, \dots, U_{x \equiv}^i \\ U_{0 \approx}^1, U_{0 \approx}^2, \dots, U_{0 \approx}^i \\ U_{0 \equiv}^1, U_{0 \equiv}^2, \dots, U_{0 \equiv}^i \end{pmatrix} \quad (2)$$

2. Expert part of initial data concerns to data on the estimations  $U'_{0 \approx}$ , received after corresponding statistical processing of "expert" data (Tabl.1). Data about  $U'_{0 \approx}$  are represented in the form of

$$\mathbf{Y}_{ij} = \begin{pmatrix} (U'_{0 \approx})_{11}, (U'_{0 \approx})_{21}, \dots, (U'_{0 \approx})_{i1} \\ (U'_{0 \approx})_{12}, (U'_{0 \approx})_{22}, \dots, (U'_{0 \approx})_{i2} \\ \dots \dots \dots \dots \dots \dots \dots \dots \\ (U'_{0 \approx})_{1j}, (U'_{0 \approx})_{2j}, \dots, (U'_{0 \approx})_{ij} \end{pmatrix} \quad (3)$$

Where  $(U'_{0 \approx})_{ij}$  – the expert estimation of a alternating voltage, received in a frequency range 50 Hz on  $i$ -limit of measurement in  $j$ -day of experiment.

3. Estimating of unknown parameters of criterion function is reduced to the usual scheme of the regression analysis. The criterion of the least-squares method [2] assesses the parameters of objective function as the solving of optimization problems of a kind

$$\sum_{j=1}^5 \sum_{i=1}^{10} \frac{1}{\sigma_{ij}^2} [(U'_{0 \approx})_{ij} - f(U_{x \approx}, U_{x \equiv}, U_{0 \approx}, U_{0 \equiv})]^2 \rightarrow \min \quad (4)$$

where  $\sigma_{ij}$  characterizes uncertainty of an estimation of result on  $i$ -limit of measurement on  $j$ -day of experiment.

The optimization problems solution (4) looks as follows

$$\begin{aligned} U'_{0 \approx} = & 3,17 \cdot 10^{-5} + 0,092794403 \cdot U_{x \approx} - 0,092794692 \cdot U_{x \equiv} + \\ & + 6,67365 \cdot 10^{-7} \cdot U_{0 \approx} + 0,983076135 \cdot U_{0 \equiv} \end{aligned} \quad (5)$$

Table 1. Complete result of calculation of  $\Delta$  and  $\Delta'$ 

$U_{x=}$	$U_{0=}$	$U_{x\equiv}$	$U_{0\equiv}$	$\Delta = \frac{U_{0\equiv} - U_{0=}}{U_{0\equiv}} \times 10^{-6}$	$\Delta' = \frac{U'_{0\equiv} - U'_{0=}}{U'_{0\equiv}} \times 10^{-6}$
V	V	V	V	V	V
1	0,91272248	10	0,91272226	9,999710	29
2	0,82148018	9	0,82147801	8,999700	33
3	0,73022863	8	0,73022799	7,999750	31
4	0,63898620	7	0,63898690	7,000200	29
5	0,54769387	6	0,54769273	5,999791	35
6	0,45641487	5	0,45641467	4,999860	28
7	0,36509764	4	0,36509701	3,999830	43
8	0,27380322	3	0,27380349	2,999890	37
9	0,18248528	2	0,18248517	1,999900	50
10	0,09111343	1	0,09111147	0,999960	40

$(U_{0=})_{il} = 89 \cdot 10^{-5} + 10,95(U'_{x=})_{il}$        $(U_{0\equiv})_{il} = 87 \cdot 10^{-5} + 10,95(U'_{x\equiv})_{il}$   
 $(U_{x=})_{il} = -8,1 \cdot 10^{-5} + 0,091(U'_{0=})_{il}$        $(U_{x\equiv})_{il} = -7,9 \cdot 10^{-5} + 0,091(U'_{0\equiv})_{il}$   
 $r = 0,998$        $r = 0,998$

The received functional dependence allowed to determining the contribution of each input quantity to uncertainty of an alternating voltage estimation that, in turn, led to the improvement of model of measurement (Figure 1.)

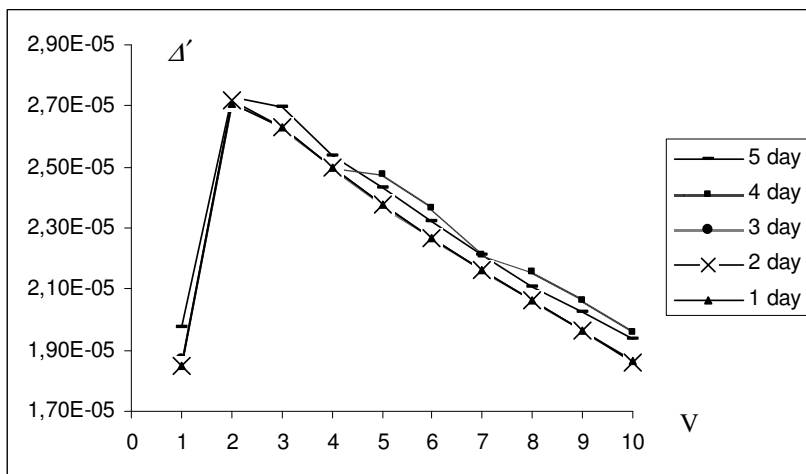


Figure 1. Complete result of calculation of  $\Delta'$  with the “expert–statistical” method from experimental data of five days of measurements

## Acknowledgments

The author expresses thanks to the professor Rein Laaneots, and also Andrei Pokatilov, Toomas Kübarsepp, the Grand Joint Ventures METROsert, for help on work.

## References

1. S. A. Aivazian, et al., *Applied Statistics: Classification and Dimensionality Reduction*. Moscow: Finance and Statistics, 1988 (in Russian)
2. T. Barachkova and R. Laaneots, *L'expérience de covariation entre des valeurs devant les mesures d'une tension alternative*. 12<sup>ème</sup> congrès international de métrologie, 20–23 Juin 2005, Lyon-France
3. R. Laaneots and O. Mathiesen, *An Introduction to Metrology*. Tallinn: TUT Press, 2006

## MULTI-DETERMINATION OF AERODYNAMIC LOADS USING CALIBRATION CURVE WITH A POLYNOMIAL AND MLP NEURAL NETWORK COMBINATION

ITAMAR MAGNO BARBOSA

*Department of Electronic Systems Engineering, Escola Politécnica de São Paulo  
Av. Prof. Luciano Gualberto, São Paulo, CEP 05508-900, Brazil*

OLYMPIO ACHILLES DE FARIA MELLO

*Director of the Institute of Aeronautics and Space  
Praça Mal. Eduardo Gomes, 50, São José dos Campos, CEP 12228-904, Brazil*

MARIA LUÍSA COLLUCCI DA COSTA REIS

*Aerodynamics Division, Instituto de Aeronáutica e Espaço  
Praça Mal. Eduardo Gomes, 50, São José dos Campos, CEP 12228-904, Brazil*

EMÍLIO DEL-MORAL-HERNANDEZ

*Department of Electronic Systems Engineering, Escola Politécnica de São Paulo  
Av. Prof. Luciano Gualberto, São Paulo, CEP 05508-900, Brazil*

The central aim of this study is to improve the accuracy of multivariate Calibration Curves employing Polynomial and Multi Layer Perceptrons Neural Networks. The proposed method considers a Reference (or Principal) Function represented by a polynomial and a Deviate Function represented by a Multilayer Perceptron Artificial Neural Network (MLP). It has been observed that the MLP results in decreasing data spread around the fitting Calibration Curve (CC).

### 1. Instrumentation

During the wind tunnel tests at the TA2 aerodynamic facility, showed in Figure (1), a six component external balance is used to measure three forces  $F_1$ ,  $F_2$  and  $F_3$  (N) and three moments  $F_4$ ,  $F_5$ ,  $F_6$  (Nm) acting on the model. The electrical output load cell readings  $S_i$  ( $i = 1$  to 6), units in (mV), are respectively measured and the loads  $F_i$  are obtained from multivariate Calibration Curve (CC). The 6-Degrees of freedom -DOF external balance calibration is performed prior to model testing by applying 73 combinations of known loads,

which yield 73x6 cell readings. From these known loads and cell readings, a multivariate CC is obtained through approximation techniques [1].



Figure 1. The TA-2 wind tunnel test section.

## 2. Methodology

### 2.1. Fitting by Polynomial Only

The current standard procedure at the Aerodynamic Lab is to use a Multivariate Polynomial of Second Order Degree with independent term equal to zero to fit a Calibration Curve, Eq. (1). To find the parameters  $a_n$  ( $n = 1$  to 27) the least squares method is used, through Eq. (2) [5]:

$$F_i = a_1 S_1 + \dots + a_6 S_6 + a_7 S_1 S_2 + \dots + a_{21} S_5 S_6 + a_{22} S_1^2 + \dots + a_{27} S_6^2 \quad (1)$$

$$\vec{a} = \begin{pmatrix} \vec{S}^T & \vec{S} \end{pmatrix}^{-1} \vec{S}^T \vec{F} \quad (2)$$

where:  $\vec{a}$  -parameters matrix;  $\vec{S}$  -design matrix;  $\vec{F}$  -loads matrix.

## 2.2. Fitting by Multilayer Perceptron (MLP) Only

The MLP may be represented by a graph, as shown in Figure 2, and by the mathematical modelling shown in equation (3a) or (3b). The nodes are Artificial Neurons (Perceptrons) and each one represents a mathematical transformation in equation (3a) or (3b) [4].

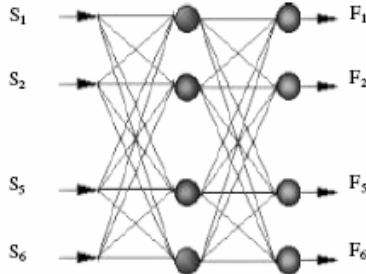


Figure 2. The architecture of MPL of several outputs.

$$F_i = \sum_{n=1}^N \text{hip.tg.} \left\{ W_{2in} \left[ \text{hip.tg.} \left( \sum_{n=1}^N \sum_{k=1}^6 W_{lnk} S_k \right) \right] \right\} + C \quad (3a)$$

$$F_i = \sum_{n=1}^N \left\{ W_{2in} \left[ \text{hip.tg.} \left( \sum_{n=1}^N \sum_{k=1}^6 W_{lnk} S_k \right) \right] \right\} + C \quad (3b)$$

Error minimization is performed by linearisation of errors and least squares procedure. The aim is to decrease the indicator Sum of Squared Errors (*SSE*). Equations (4) and (5) represent the error minimization algorithm and the *SSE*, respectively [2]:

$$\vec{w}(n+1) = \vec{w}(n) - \left[ \vec{J}^T(n) \vec{J}(n) + \lambda \vec{I} \right]^{-1} \vec{J}^T(n) \vec{e}(n) \quad (4)$$

$$SSE = \sum_1^N e^2 \quad (5)$$

where:  $\vec{w}(n+1)$  is the synaptic weight (next value);  $\vec{w}(n)$  is the synaptic weight (present value);  $\vec{J}$  is the Jacobean Matrix;  $\vec{e}$  is the error matrix;  $e^2$  is the squared error; and  $\lambda$  is the learning rate.

### 2.3. Fitting by Combination between Polynomial and MLP

The combination of Polynomial and MLP involves a first approximation of the Calibration Curve (CC) by a Polynomial only: the “Reference Function”. This approximation generates  $F'_i$ , which deviate  $D_i$  in relation to the actual measured values  $F_i$ . Provided that these errors  $D_i$  are systematic, then they can be approximated by a second function: the “Deviate Function” (DF). This DF may be approximated by a MLP. This latter approximation generates  $D'_i$ , which also deviate  $d_i$  in relation to  $D_i$ . Eventually we summarize the values  $F'_i$  and  $D'_i$  resulting in  $F''_i$ . Provided that Polynomial and MLP converge to  $F_i$  and  $D_i$  respectively, then  $d_i$  will be lower than  $D_i$ . These relations are represented in Eqs. (6) and (7):

$$F_i = F'_i + D_i = F'_i + D'_i + d_i = F''_i + d_i \quad (6)$$

$$D_i = D'_i + d_i \quad (7)$$

## 3. Results

### 3.1. The Polynomial Approach

In this phase, the two different polynomials  $P1$  and  $P2$  employed to represent the Calibration Curve are presented in Table 1, along with the values of the SSE of the polynomial least squares fitting for the calibration number 1 and for the prediction of the second and third calibration data set. The prediction consists in maintaining the parameters found in least squares fitting and, supplying different S values originating from subsequent calibrations, thereby obtaining new  $F'_i$  values.

Table 1. Polynomials employed to represent the Calibration Curve, SSE values of fitting CC and predictions.

Polynomial	Math model	SSE Fitting	SSE Pred. 1	SSE Pred. 2
$P_1$	$P_1 = a_1S_1 + a_2S_2 + a_3S_3 + \dots + a_6S_6$	11.5712	7.5379	5.2584
$P_2$	$P_2 = P_1 + a_7S_1S_2 + a_8S_1S_3 + \dots + a_{21}S_5S_6$	2.5268	2.7095	6.7200

### 3.2. The MLP Approach

Figure 3 presents the comparison between the SSE of both the MLP and the polynomial  $P2$ , as a function of the number of neurons in the hidden layer. We utilized a MLP following Eq. (3a). The learning of the MLP and polynomial fitting results are related to the first calibration data set. Figure 3 also shows the MLP and polynomial predictions for the second and third calibration data sets. Learning and prediction processes were performed using the hyperbolic tangent transfer function in the hidden layer and in the output layer.

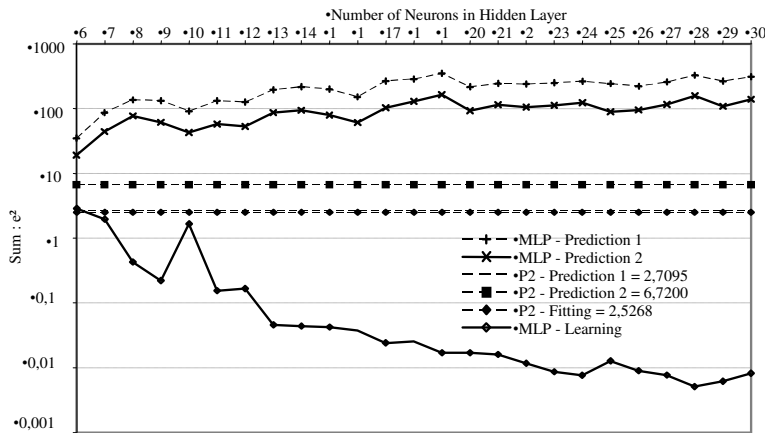


Figure 3. Comparison between the SSE of the learning process of the MLP and the polynomial fitting  $P2$ . The prediction of the second and the third Calibration Curves are also compared.

### 3.3. Combination of MLP and Polynomial Approaches

The MLP and Polynomial combination procedure consists of the following phases:

1. Summation of the fitted load  $F'_i$ , originated from the polynomial fitting, and the errors  $D'_i$  estimated by MLP. The net errors of the combination are equal to the MLP errors  $d_i$ ;
2. Maintaining the polynomial fitting estimated parameters and the synaptic weights resulting from the MLP learning process, to predict the load values  $F(pred)$  predicted for subsequent calibrations, by supplying new values of load cell readings; and

3. Evaluating the prediction errors, which are the differences between the predicted values  $F(pred)$  and the loads, applied in the new calibration processes.

We performed a combination with Polynomial P1 as Reference Function (RF) and an MLP as Eq. (3a). The SSE of learning or regression and SSE of Prediction 1 and 2 are presented in Figure 4. It is observed that using around 36 to 39 neurons in the hidden layer is enough to reach reasonably small variations in Performance Function value, for these calibration data sets.

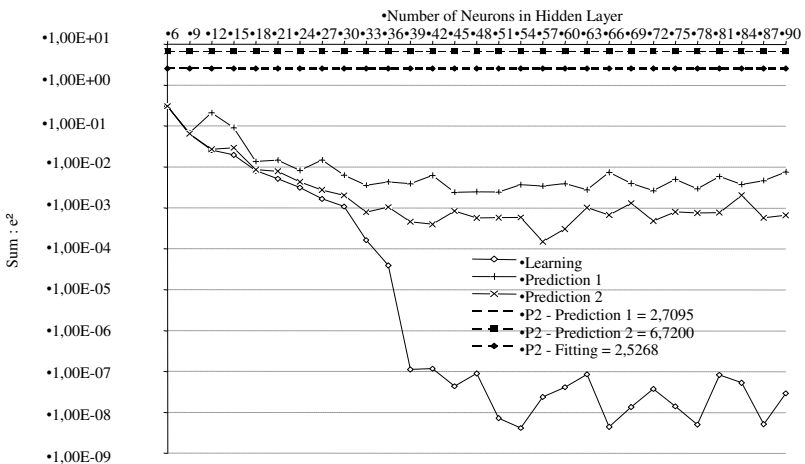


Figure 4. Comparison between the SSE of polynomial  $P_2$  and the SSE of the combination with P1 and MLP, in the learning and prediction mode.

### 3.4. Other Indicators for Performance Function

We have analyzed other indicators besides the SSE in new data sets. New calibrations have been combined in one, two or three sets of measurements and several indicators of fitting performance were observed. We utilized a new MLP following Eq. (3b). Table 2 summarizes these results for new data. For empty cells the indicator is not defined. Indicators such as Mean Squared Error,  $MSE$ , and Standard Deviation of Fitting, “ $s$ ”, decrease as the complexity of mathematical modeling increases. This brings the possibility that net uncertainty computation would decrease.

#### 4. Conclusions

The SSE value of fitting has predominantly decreased as the complexity of mathematical modeling increases or the number of neurons in the hidden layer increases.

The decrease of the SSE is not certain to occur in the prediction. It has been observed that the more one confines the MLP learning, the more one departs from the prediction of subsequent calibrations.

The approach proposed in this study which combines MPL and polynomial resulted in improved SSE for the prediction of the aerodynamic loads, when using P<sub>1</sub> as Reference Function. For the data sets under consideration, using around 36 to 39 neurons in the hidden layer is enough to reach reasonably small variations in Performance Function value.

Other indicators such as Mean Squared Error (*MSE*) and Standard Deviation of Fitting, “*s*”, also decrease as the complexity of mathematical modeling increases.

Further studies must be conducted in order to search for proper MLP configurations which result in improved prediction accuracies when detecting non-linear behaviour of the calibration process.

Table 2. Comparing other indicators of Performance Fitting. Considered Load: F<sub>6</sub>.

Polynomial P <sub>2</sub>	Number of Hidden Neurons in MLP (Deviate Function). Reference Function = P <sub>1</sub>				Number of considered sets of measurements
	6	12	18	24	
Sum Squared Errors <i>MSE</i>					
120.3316	0.9958	0.8019	0.2665	0.0273	1 set
241.1826	1.6711	1.6748	0.4426	0.0444	2 sets
614.1008	5.3627	0.5066	0.6573	0.1000	3 sets
Mean Squared Error ( <i>MSE</i> ) = sqrt ( <i>SSE</i> / Number of Errors )					
0.5241	0.0477	0.0428	0.0247	0.0079	1 set
0.5247	0.0437	0.0437	0.0225	0.0071	2 sets
0.6836	0.0639	0.0196	0.0224	0.0087	3 sets
Standard Deviation of Fitting ( <i>s</i> )					
2.1115					1 set
2.0597	0.1579				2 sets
1.9643	0.1957	0.0863			3 sets

## REFERENCES

1. Barbosa, I. M.; Del-Moral-Hernandez, E.; Reis, M. C. C.; Mello, O. A. F., “Measurement Uncertainty Contribution to the MLP Neural Network Learning”, *Metrology and Measurement System*, v. XIV, p. 101-116 (2007).
2. Devore, J.L., *Probability and Statistics*, 6th ed., Thomson Books Cole, 2004.
3. INMETRO, “Vocabulário Internacional de Termos Fundamentais e Gerais de Metrologia” (International Vocabulary of Basic and General Terms in Metrology), 4<sup>th</sup> ed., Rio de Janeiro (2005).
4. Haykin, S. S., *Neural Network: A Comprehensive Foundation*, 2<sup>nd</sup> ed., Prentice-Hall, 1999.
5. Bevington, P. R., *Data Reduction and Analysis for the Physical Sciences*, McGraw-Hill Book Company, USA, 1969.

## UNCERTAINTY ANALYSIS IN CALIBRATION OF STANDARD VOLUME MEASURES

ELSA BATISTA, NELSON ALMEIDA, EDUARDA FILIPE

*Instituto Português da Qualidade, Rua António Gião, 2 – Caparica, Portugal*

Standard test measures can be calibrated using the gravimetric or the volumetric methods according to the needed accuracy. In this paper is presented and compared the evaluation of the data and uncertainty of both gravimetric and volumetric method. The model for calculating the measurement uncertainty and the methodology for the evaluation of the uncertainty components are described for both gravimetric and volumetric methods. It is also described the cases where two reference volume measures are used to determine the volume of a single instrument in the volumetric method.

### 1. Introduction

Standard volume measures are used for testing measuring systems for liquids, like fuel dispensers, water meters, fuel meters and road tanks. Calibration of standard volume measures can be performed by using a volumetric or a gravimetric method depending on the needed accuracy.

The gravimetric method is the standard method used by both National Metrology Institutes (NMIs) and accredited laboratories to calibrate high accuracy volumetric equipment. The method consists on weighing the standard volume measure when empty and again when full up with water (the calibration liquid) to the reference line. The difference obtained in the weighing gives the mass of contained or delivered liquid, which is then converted to volume using the appropriated formula described in the ISO 4787 standard [1].

The volumetric calibration involves the transfer of a volume of liquid between the reference volume measure and the standard volume measure. All care has to be taken to ensure that a complete transfer takes place, observing drying and draining procedures and other well established and documented experimental techniques [2].

### 2. Uncertainty Evaluation

Measurement uncertainty is estimated for both methods following the Guide to the expression of uncertainty in measurement (GUM) [3]. The measurement model is presented along with the standard uncertainties components, the

sensitivities coefficients, the combined uncertainty and the expanded uncertainty.

## 2.1. The Measurement Model and Uncertainty Components

For gravimetry and for a reference temperature of 20 °C, the following model was used [2]:

$$V_{20} = f(m, \rho_A, \rho_W \rho_B, t, \gamma, V_{\text{men}}) = (m_2 - m_1) \times \frac{1}{\rho_W - \rho_A} \times \left(1 - \frac{\rho_A}{\rho_B}\right) \times [1 - \gamma(t - 20)] + \delta V_{\text{men}} \quad (1)$$

The standard uncertainties are due to the mass measurement ( $m_2 - m_1$ ), water density ( $\rho_W$ ), mass pieces density ( $\rho_B$ ), air density ( $\rho_A$ ), cubic thermal expansion coefficient of the material of the standard volume measure ( $\gamma$ ), water temperature ( $t$ ) and the meniscus reading. For volumetry with a reference temperature of 20 °C, the following model was used [3]:

$$\begin{aligned} V_{20} &= f(V_0, t_p, t_r, \gamma_p, \gamma_r, \beta_L, V_{\text{men}}) = \\ &V_0 \times [1 + \gamma_p(t_p - 20) - \beta_L(t_p - 20) - \gamma_r(t_r - 20)] + \delta V_{\text{men}} \end{aligned} \quad (2)$$

In this case the standard uncertainties considered are the reference volume measure ( $V_0$ ), cubic thermal expansion coefficient of the material of the reference ( $\gamma_p$ ) and of the standard volume measure ( $\gamma_r$ ), cubic thermal expansion coefficient of the liquid ( $\beta_L$ ), water temperature in the reference ( $t_p$ ) and in standard volume measure ( $t_r$ ) and the variability of the meniscus reading. In the case where two reference volume measures of the same nominal volume are used, equation 2 can be rewritten as the following as  $V_1 \cong V_2 \cong V_0$ :

$$V_{20} = V_0 [2 + \gamma_p(t_{p1} - 20) + \gamma_p(t_{p2} - 20) - \beta_L(t_{p1} - 20) - \beta_L(t_{p2} - 20) - 2\gamma_r(t_r - 20)] + \delta V_{\text{men}} \quad (3)$$

If we call:  $\theta = (t_{p1} - 20)$ ,  $\theta_1 = (t_{p2} - 20)$ ,  $\theta_2 = (t_r - 20)$

$$\text{Then: } V_{20} = V_0 [2 + \gamma_p(\theta + \theta_1) - \beta_L(\theta + \theta_1) - 2\gamma_r\theta_2] + \delta V_{\text{men}} \quad (4)$$

## 2.2. Combined and Expanded Uncertainty

Combined uncertainty for the gravimetric method:

$$\begin{aligned} u(V_{20}) &= \left[ \left( \frac{\partial V_{20}}{\partial m} \right)^2 u^2(m) + \left( \frac{\partial V_{20}}{\partial \rho_w} \right)^2 u^2(\rho_w) + \left( \frac{\partial V_{20}}{\partial \rho_A} \right)^2 u^2(\rho_A) + \left( \frac{\partial V_{20}}{\partial \rho_B} \right)^2 u^2(\rho_B) \right. \\ &\quad \left. + \left( \frac{\partial V_{20}}{\partial \gamma} \right)^2 u^2(\gamma) + \left( \frac{\partial V_{20}}{\partial t} \right)^2 u^2(t) + u^2(\text{men}) \right]^{\frac{1}{2}} \end{aligned} \quad (5)$$

Combined standard uncertainty for the volumetric method:

$$u(V_{20}) = \left[ \left( \frac{\partial V_{20}}{\partial V_0} \right)^2 u^2(V_0) + \left( \frac{\partial V_{20}}{\partial \gamma_p} \right)^2 u^2(\gamma_p) + \left( \frac{\partial V_{20}}{\partial t_p} \right)^2 u^2(t_p) + \left( \frac{\partial V_{20}}{\partial \beta_L} \right)^2 u^2(\beta_L) \right. \\ \left. + \left( \frac{\partial V_{20}}{\partial t_R} \right)^2 u^2(t_R) + \left( \frac{\partial V_{20}}{\partial \gamma_R} \right)^2 u^2(\gamma_R) + u^2(men) \right]^{\frac{1}{2}} \quad (6)$$

Combined standard uncertainty for the volumetric method but using two reference volume measures of the same capacity:

$$u(V_{20}) = \left[ \left( \frac{\partial V_{20}}{\partial V_0} \right)^2 u^2(V_0) + 2 \left( \frac{\partial V_{20}}{\partial V_1} \right) \left( \frac{\partial V_{20}}{\partial V_2} \right) (u(V_1)u(V_2)r(V_1, V_2)) + \left( \frac{\partial V_{20}}{\partial \gamma_p} \right)^2 u^2(\gamma_p) + \left( \frac{\partial V_{20}}{\partial \theta} \right)^2 u^2(\theta) \right. \\ \left. + \left( \frac{\partial V_{20}}{\partial \beta_L} \right)^2 u^2(\beta_L) + \left( \frac{\partial V_{20}}{\partial \theta_1} \right)^2 u^2(\theta_1) + \left( \frac{\partial V_{20}}{\partial \theta_2} \right)^2 u^2(\theta_2) + \left( \frac{\partial V_{20}}{\partial \gamma_R} \right)^2 u^2(\gamma_R) + u^2(men) \right]^{\frac{1}{2}} \quad (7)$$

The  $u(men)$  for the gravimetry depends on the operator skills and the neck diameter of the standard volume measure, in volumetry  $u(men)$  it also depends on the repeatability of the meniscus reading. From the determined values of  $k$ -factor and of the combined standard uncertainty of the measurand, the expanded uncertainty was deduced by  $U = k \times u(V_{20})$ .

In the gravimetric and volumetric calibration using one reference volume measure the variables are not correlated. In the other case (eq. 7) the two volumes are correlated by the use of the same mass comparator. From the experimental values this term is negative but negligible.

### 3. Experimental Results

Two standard volume measures of 5 L and 20 L, normally used for verification of petrol pumps, were calibrated using the methods described above, the results are the following:

Table 1. Calibration results of two standard volume measures

Nominal Volume (L)	Gravimetry		Volumetry	
	True Volume (L)	$U$ (L)	True Volume (L)	$U$ (L)
5	5.0046	0.0015	5.007	0.002
20	20.0213	0.0051	20.019	0.007
20 (two references)			20.017	0.010

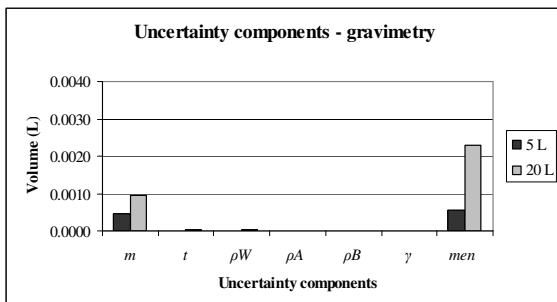


Figure 1. Uncertainty components for gravimetry

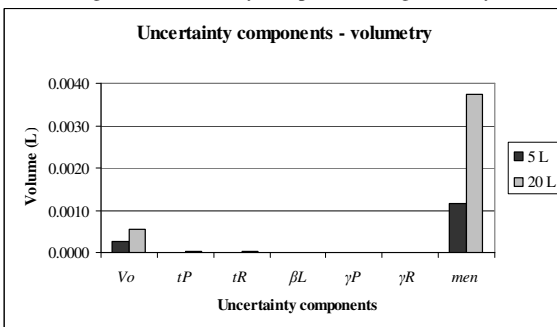


Figure 2. Uncertainty components for volumetry using one standard volume measure

#### 4. Concluding Remarks

As expected, the expanded uncertainty for the volumetric method is larger than for the gravimetric method due to the accuracy of the used standard (weighing scale). Also if two reference volume measures are used in the volumetric method the uncertainty is larger due also to the increase of the variability in the meniscus reading. Both in the gravimetric and volumetric methods the largest uncertainty component is the meniscus which is mainly dependent on the operator skill.

#### References

1. ISO 4787, Laboratory glassware - Volumetric glassware - Methods for use and testing of capacity; Genève, (1984).
2. OIML R 120, Standard capacity measures for testing measuring systems for liquids other than water, Paris (1996).
3. BIPM, IEC, IFCC, ISO, IUPAC, IUPAP, OIML, Guide to the expression of uncertainty in measurement (GUM), Genève, (1995).
4. Workshop on calibration of volume standards - DAM-Munich-1998

## VIRTUAL ATOMIC FORCE MICROSCOPE AS A TOOL FOR NANOMETROLOGY

V.S. BORMASHOV, A.S. BATURIN, A.V. ZABLOTSKIY

*Moscow Institute of Physics and Technology (State University),  
Institutskiy per. 9, Dolgoprudny, Moscow region, 141700, Russia  
bormashov@bk.ru*

R.V. GOLDSHTEIN, K.B. USTINOV

*Institute of Problems in Mechanics Russian Academy of Science,  
prosp. Vernadskogo 101 bl.1, Moscow, 119526, Russia*

Novel concept of linear dimension measurements by means of AFM is described. The main idea of this concept is based on simultaneous analysis of the simulation data obtained on “virtual atomic force microscope” and the experimental results. The physical model of AFM, which is the key element of the concept, is described in this paper.

### 1. Introduction

Atomic force microscope (AFM) is commonly used to study a surface morphology of specimens and its physical properties at the nanometer scale. Despite great progress in probe microscopy most of AFM methods are able to give only so called “contrast maps”, which represent a qualitative distribution of certain specimen characteristic over its surface. Ordinary approach to linear dimensions measurements using AFM consists in determining a model of specimen from physical measurements of that specimen. This is so called an “inverse” problem. Unfortunately there is no universal algorithm to find a solution of this problem if specimen dimensions decrease to nanometer scale [1]. This is the main reason limiting AFM usage as a tool for nanometrology. In our previous work [2] we proposed to use a simulation data obtained by “virtual microscope” and corresponding experimental results jointly to measure specimen linear dimensions and estimate their uncertainties. In this concept “virtual microscope” is a software tool that represents a numerical AFM model. In this work we propose a physical model that describes an AFM operation.

### 2. “Virtual AFM” Features

Four main modules are used to simulate AFM operation: scanning system, deflection registration system, feedback system and probe-specimen interaction.

In our work we deal with only a contact mode of AFM operation to avoid complicated artifacts that might be caused by bistability in tapping mode.

## 2.1. Scanning system

To simulate a real 3D-scanning system it is more feasible to consider at the beginning a single one-dimensional piezoelement that corresponds to a single scanner axis. Interpreting a numerous experimental data we conclude that there are two turning points, which are specific points characterizing each piezoelement (see point A and B on Figure 1). These points limit possible piezoelement deformations  $Z_{\min}$  and  $Z_{\max}$  at given voltages  $V_{\min}$  and  $V_{\max}$  applied by control system. There is another unique parameter  $k$  that characterizes hysteresis of piezoelement, which is a maximum difference between scanner's coordinates when it moves in the opposite directions taken at the same voltage  $(V_{\min}+V_{\max})/2$ . Value of  $k=0$  means absence of hysteresis.

Now we assume that piezoelement is situated in some initial state that corresponds to voltage  $V_0$  and coordinate  $Z_0$ . Changing a voltage to value  $V$  causes the piezoelement move toward a one of the turning points and its coordinate is given by

$$Z(V) = a(V - V_0)^2 + b(V - V_0) + Z_0, \quad (1)$$

where simulation parameters  $a$  and  $b$  could be found by using the condition  $Z(V_{\max}) = Z_{\max}$  for increasing voltage or  $Z(V_{\min}) = Z_{\min}$  for decreasing voltage. The second condition is determined by parameter  $k$ . The found values of  $a$  and  $b$  should be recalculated each time when the voltage derivative change a sign. The values of  $V$  and  $Z$  at that moment should be taken as new values of  $V_0$  and  $Z_0$ .

Let now consider a dynamics of piezoelement movement, which exhibits essential drift. The main reason of scanner drift is a creep of piezoelement [3]. The simplest model of creep is given by equation

$$Z(t) = Z_1 - (Z_1 - Z_0)\gamma + (Z_1 - Z_0)\gamma \lg(t/\tau), \quad (2)$$

where  $\gamma$  is a dimensionless parameter that characterizes a drift speed of scanner,  $Z_0$  and  $Z_1$  – scanner coordinates calculated by using eq. (1) at voltage change from  $V_0$  to  $V_1$ . Equation (3) is valid for a time  $t \geq \tau$ , where  $\tau$  is a model parameter that gives a time scale of scanner creep. This parameter could also be considered as a scanner delay for rapid voltage change. To simulate piezoelement movement during time  $0 < t < \tau$  spline approximation was used. Simulation results obtained by above-mentioned algorithm are shown in Fig. 1.

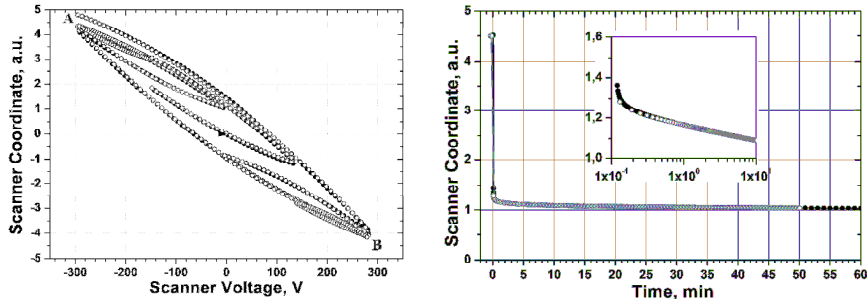


Figure 1. AFM scanner hysteresis (left) and creep (right). Black dots are experimental data and gray pricked dots are simulation results.

In scope of our model the 3D scanner is a combination of three independent one-dimensional scanners. Each of them satisfies to equations (1) and (2). The vector  $\mathbf{c}$  of resulting 3D scanner position in laboratory frame is given by

$$\mathbf{c} = (f_1(\mathbf{r}) \quad f_2(\mathbf{r}) \quad f_3(\mathbf{r}))^T, \quad (3)$$

where  $\mathbf{r}$  is a vector constructed of three individual 1D scanners' positions at given voltages,  $f_i$  is a function describing movement along  $i$ -th axis of laboratory frame. The set of  $f_i$  functions is estimated from non-orthogonality calibration procedure.

## 2.2. Feedback system

To simulate a feedback system operation we used a standard PID regulator algorithm that could be found elsewhere [4].

## 2.3. Optical registration system

In optical registration module we consider a nonlinear detector response on cantilever bend deformation. This phenomenon could be explained by different factors such as nonregular shape of laser spot, poor adjustment of optical system, nonlinear transfer function of electronics etc. To find dependence between cantilever bend and detector response it is possible to use a universal method for calibration of optical system.

## 2.4. Probe-specimen interaction module

Designations used to describe an interaction problem of AFM probe contact with surface are represented in Fig. 2. Coordinate frame in Fig. 2 coincides with AFM scanner's frame. Axis  $t$  is a projection on  $XY$  plane of direction of

maximum slope (derivative) of surface profile in the vicinity of contact point. Surface profile  $f(x, y)$  and probe shape  $g(x, y)$  are assumed to be known.

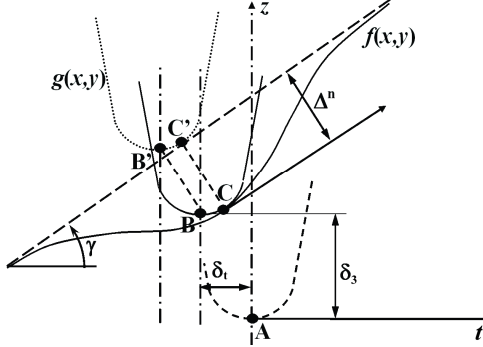


Figure 2. Schematic of contact problem to simulation of probe-specimen interaction.

Here we assume that the curvature radius of surface is larger than a radius of probe. We also introduce some auxiliary points in Fig. 2. Point A is a position of probe's tip with coordinates  $(x_0, y_0, z_0)$  that corresponds to initial state. Probe's tip is situated in this position if one removes the specimen. Point B' is a position of probe's tip with coordinates  $(x_B, y_B, z_B)$  if only cantilever deformation due to specimen surface shape is taken into account. Point C' is a real contact point of probe with coordinates  $(x_C, y_C, z_C)$  when its tip is in position B. Points B and C designate the same points of probe as B' and C' when elastic deformations are taken into account in addition to cantilever deformation.

Let introduce displacement of probe  $\delta_X = x_B - x_0$ ,  $\delta_Y = y_B - y_0$ ,  $\delta_Z = z_B - z_0$  relatively to initial state and position of contact point  $\xi_X = x_B - x_C$ ,  $\xi_Y = y_B - y_C$ ,  $\xi_Z = z_B - z_C$  relatively to probe's tip. To find a probe's tip position it is necessary to minimize a potential energy of interaction given by

$$\varepsilon = \min_{\delta_i, \Delta^n} \left[ \frac{1}{2} A_{ij} \delta_i \delta_j + \frac{8}{15} \left( \frac{E_p}{1 - v_p^2} + \frac{E_s}{1 - v_s^2} \right) \Delta^n^{5/2} \sqrt{R} \right], \quad (4)$$

$$\text{where } \delta_1 = \delta_X + \Delta^n \cos \gamma \frac{\partial f}{\partial x}, \quad \delta_2 = \delta_Y + \Delta^n \cos \gamma \frac{\partial f}{\partial y},$$

$$\delta_3 = h(x_0 + \delta_X, y_0 + \delta_Y) - z_0 - \Delta^n \cos \gamma.$$

Minimization is performed at boundary conditions

$$\delta_Z(x_0, y_0, z_0) = h(x_0 + \delta_X, y_0 + \delta_Y) - z_0, \quad \Delta^n \geq 0. \quad (5)$$

In above equations  $A_{ij}$  is a stiffness matrix of cantilever;  $\delta_i$  corresponds to displacements  $\delta_1, \delta_2, \delta_3$  that gives corrected probe's tip position,  $\Delta^n$  is an elastic

deformation,  $h(x, y)$  is a convolution surface that gives all possible positions (normal coordinate) of probe's tip,  $v_p$  and  $v_s$  are Poisson coefficients and  $E_p, E_s$  are Young modulus of probe and specimen correspondingly,  $R$  is an effective contact radius in contact point. Convolution surface is given by equation

$$h(x, y) = \min_{\xi, \eta} [f(x + \xi, y + \eta) - g(\xi, \eta)]. \quad (6)$$

To solve the system of equations (4)-(6) we propose to use a step-by-step method. First of all it is necessary to calculate a convolution surface that gives a first approximation for probe displacement. Then we can calculate a  $\delta_x, \delta_y, \delta_z$  taking into account only cantilever bend (elastic deformation is neglected). Using second approximation as initial conditions it is possible to minimize (4) and find a real tip position.

### 3. Conclusion

One of the important parts of AFM measurement concept is a realistic computer simulation of AFM operation taking into account all important drawbacks of AFM which are influence on the measurements uncertainties. For the scanning system we take into account hysteresis, piezocreep and nonorthogonality. The ordinary used assumption that sample and probe are absolute rigid bodies was expanded taking into account probe's finite size, elastic and adhesion interactions in the contact. The model describe in the paper provides a basis for realistic simulation of typical commercial atomic force microscope.

### Acknowledgments

Authors acknowledge the Russian Ministry of Education and Science (Federal Agency of Science and Innovation, contract 02.513.11.3224 and Grant of Federal Agency of Education RNP.2.1.2.9353) for financing of this research.

### References

1. P.C. Sabatier. *J. Math. Phys.* **41**, 4082 (2000).
2. A. V. Zablotskiy, A. S. Baturin, V. S. Bormashov, R. M. Kadushnikov, N. A. Shturkin, *Nanotechnology in Russia* **11-12**, 40 (2007).
3. G.A.G. Cidade, G. Weissmuller, P.M. Bisch. *Rev. Sci. Instrum.* **69**, 3593 (1998).
4. Liptak, Bela. *Instrument Engineer's Handbook: Process Control*. Radnor, Pennsylvania: Chilton book Company, 20-29 (1995).

## DEVELOPMENT OF A MATHEMATICAL PROCEDURE FOR MODELLING AND INSPECTING COMPLEX SURFACES FOR MEASUREMENT PROCESS

SALIM BOUKEBBAB, HICHEM BOUCHENITFA

*Laboratoire de Mécanique, Faculté des Sciences de l'Ingénieur  
Université Mentouri Constantine, Campus Châab Ersas,  
25017 Constantine, Algérie  
Tel/fax : +213 (0) 31 81 88 53 / 63  
E-mail : [boukebbab@umc.edu.dz](mailto:boukebbab@umc.edu.dz)*

JEAN MARC LINARES

*Institut des Sciences du Mouvement/GIBO  
CNRS UMR 6233, Université de la Méditerranée  
Institut Universitaire Technologique  
Avenue Gaston Berger  
13625 Aix en Provence cedex  
Tel: + 33 (0) 4 42 93 90 96  
E-mail : [Jean-marc.linares@univmed.fr](mailto:Jean-marc.linares@univmed.fr)*

The design and the manufacture of free form surfaces are being a current practice in the industry. Thus the problem of the parts conformity of complex geometry is felt more and more. By this work, a mathematical procedure for modelling and inspecting complex surfaces in measurement process is presented including the correction of geometrical deviations within manufacturing process. The method is based on the Iterative Closest Point (I.C.P.) algorithm for alignment stage between nominal surface and measured points. The finite elements method for geometric compensation STL model generally obtained by a triangulation of nominal model using Computer Aided Design (CAD) software; is used in our proposal. An industrial application concerning a rapid prototyping technology process is presented. This last is used for manufacturing of real parts obtained from a STL file format.

### 1. Introduction

By definition the inspection of the mechanical parts is the comparison between measurement results and the theoretical topology of surfaces in order to check the conformity after an industrialising step. So the development of a complete inspection system and a quality control of manufactured parts require the coordination of a set of complex processes allowing data acquisition, and their comparison with a reference model. The automation of this function is currently

based on alignment methods of measured points resulting from an acquisition process and these nominal surfaces.

In this paper, a mathematical procedure for modelling and inspecting complex surfaces in measurement process is presented. This procedure enables the correction of relative deviations within manufacturing process, and it is based on two techniques. The first one uses the Iterative-Closest-Point (ICP) algorithm, which is a well-known method to best fit a 3D set of points to a 3D model. This technique minimizes the sum of squared residual errors between the set of points and a model. The second uses the finite elements method in order to compensation STL model (figure 1).

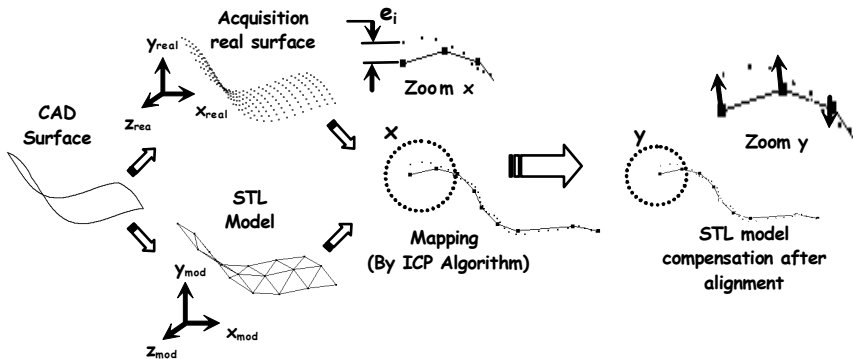


Figure 1. Principal step of model correction.

The distances  $e_i$  (i.e. form defects), between nominal surface and measured points, calculated after alignment stages are necessary for correcting the errors cumulated during the manufacturing phase [1].

An industrial application, concerning a rapid prototyping technology process, is presented for validation of this approach. As already pointed out, the prototyping technology is used for manufacturing a physical model starting from a STL format file obtained by Computer Aided Design (CAD) software.

## 2. Presentation of the Mathematical Procedure

In current state of the metrology software, the inspection of elementary surfaces is not a problem, and most CMMs realize numerically compensation of the geometric alignment deviations. On the other hand, the inspection of surfaces

which have geometries of a higher complexity like gears, sculptured surfaces...etc represents a major challenge, because the problems related to the parts conformity are being felt more and more. For this, in our proposal, the ICP (Iterative Closest Point) algorithm method will be used.

The ICP algorithm is a well-known method for registering a 3D set of points to a 3D model. Since the presentation of the ICP algorithm by Besl and McKay [2], many variants have been introduced. The new propositions affect one or more stages of the original algorithm to try to increase its performances, specially, accuracy and speed. This method minimizes the sum of squared residual errors between the set of points and the model. The ICP algorithm finds a registration that is locally the best fit using the least-squares method [3]. Its main goal is to find the optimal rigid transformation which will corresponds as well as possible a set of measured points  $\mathbf{P}$  to a geometrical model  $\mathbf{M}$ , using the singular value decomposition function (figure 2).

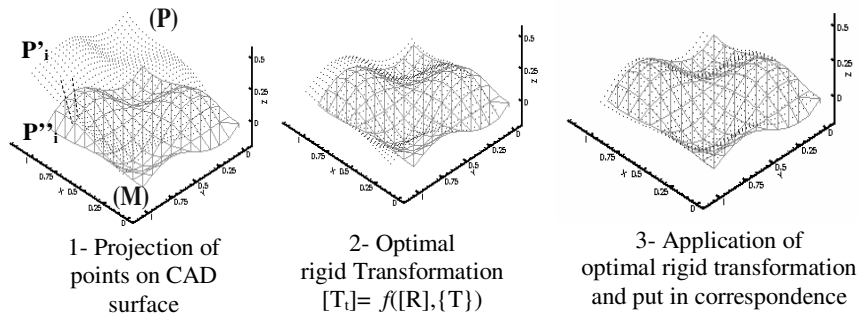


Figure 2. Principal steps of the I.C.P. algorithm.

The parameters of the rigid transformation between the sets of points  $P_i'$  and  $P_i''$  must minimize the cost function:

$$\frac{1}{N} \sum_{i=1}^N \| P_i'' - [T_t] \times (P_i') \|^2 \quad (1)$$

A rigid transformation  $[T_t]$  consists in the rotation matrix  $[R]$  and the translation vector  $\{T\}$  giving the iterative transformation  $P_i'' = [R] \times P_i' + \{T\}$  ( $P_i'$  will be transformed into a point  $P_i''$ ). This algorithm requires an initial estimate of the registration; because the computation speed and registration accuracy depend on how this initial estimate is chosen [3]. The compensation of

STL model is realized by the finite elements method. The elements of model are triangular surfaces; its equation has the form:

$$z = w + \alpha_2 \times x + \alpha_3 \times y \quad (2)$$

The formulation of the plane equation in terms of the coordinates of nodes  $Z_i$ , (figure 3) enables us to write the variations  $e_i$  at nodes level between a point  $M_i$  and the plane element:

$$e_i = z_{Mi} - z_i \quad (3)$$

By replacing the Eq. (2) in Eq. (3) one obtains:

$$e_i = z_{Mi} - [w + \alpha_2 \times x + \alpha_3 \times y] \quad (4)$$

By making the approximation according to the previous relation, the optimal parameters will be determined:  $(w, \alpha_2, \alpha_3)_{\text{Opt}}$ . However, the approximation by finite elements consists in calculating optimal displacements to nodes  $N_i$  (figure 3).

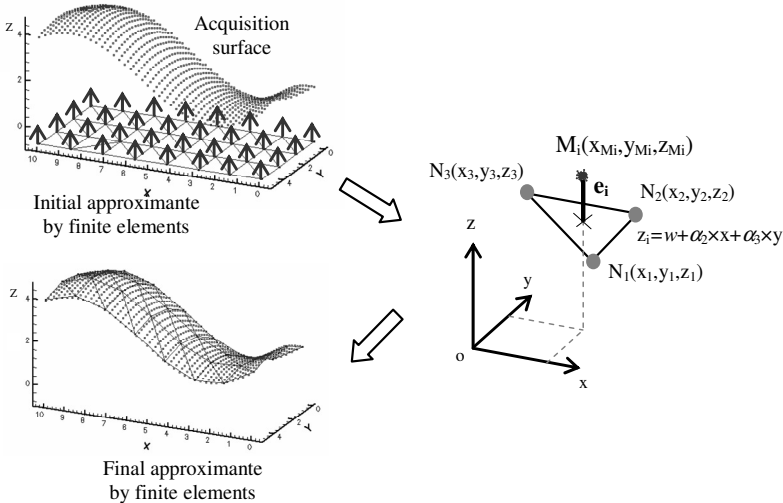


Figure 3. Approximation surface by finite elements.

The writing of the variables ( $w, \alpha_2, \alpha_3$ ) in terms of nodes coordinates leads to the following equation:

$$Z_i = \sum_{i=1}^{n=3} f_i(x, y) \times z_i \quad (5)$$

It should be noted that  $f_1(x,y)$ ,  $f_2(x,y)$  and  $f_3(x,y)$  are substitutions equations. After having reformulated the equation of the triangular elementary surface in terms of nodes coordinates  $\mathbf{Z}_i$ , the Eq (4) can be written in the following form:

$$e_i = z_{Mi} - \left[ \sum_{i=1}^{n=3} f_i(x, y) \times z_i \right] \quad (6)$$

The optimization of the least square criterion is used to determine the optimal variables  $(\mathbf{Z}_1, \mathbf{Z}_2, \mathbf{Z}_3)$ , obtained by these equations:

$$\frac{\partial \sum_{i=1}^n \|e_i\|^2}{\partial z_1} = \frac{\partial \sum_{i=1}^n \|e_i\|^2}{\partial z_2} = \frac{\partial \sum_{i=1}^n \|e_i\|^2}{\partial z_3} = 0 \quad (7)$$

The Eq. (7) gives a linear system with symmetrical matrix and its resolution permits to calculate the optimal coordinates  $Z_1$ ,  $Z_2$  and  $Z_3$  of nodes  $N_1$ ,  $N_2$  and  $N_3$ . The surface of total approximation is obtained by the assembly of the triangular surface elements. A data processing model was developed under a programming language for validation.

### 3. Application for Rapid Prototyping Technology

In this application, the part manufacturing by the rapid prototyping technology is treated (figure 4). This process is used for manufacture of the real part starting from a STL format file obtained by Computer Aided Design (CAD) software [4]. The standard data interface between CAD software and the prototyping machine is the STL file format, which approximates the shape of a part using triangular facets.

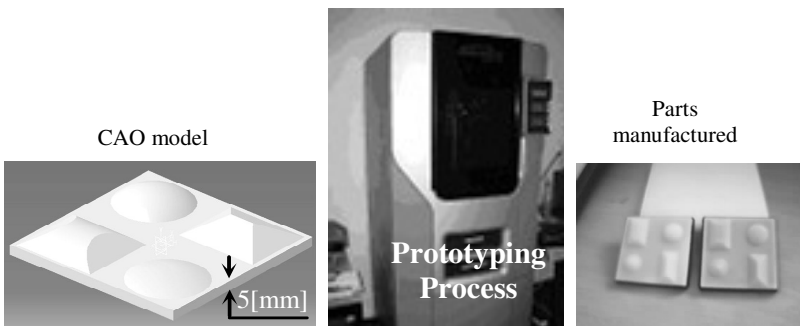


Figure 4. Prototyping technology process.

The manufacturing of parts, by the prototyping technology, consists to the reproduction of STL model by deposit of plastic with a hot temperature [5]. In this technology, the temperature of the print head is near of 250 °C. So, under the effect of heat a deformation is observed on the parts with a low thickness (figure 5).

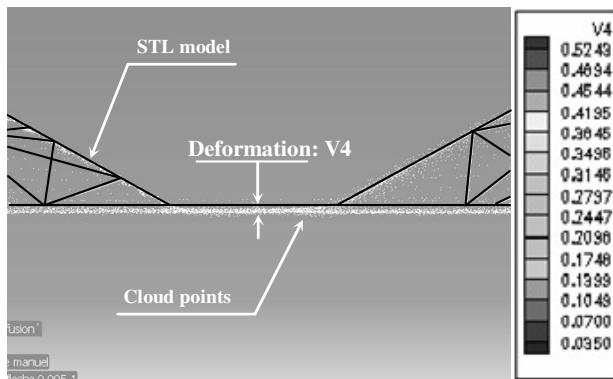


Figure 5. Alignment step with an aim of compensation STL model.

This deformation represents an inevitable deviation in this manufacturing process, and is detected after alignment step (using the ICP algorithm) between the STL model and the set of points of real surface obtained after measurement phase. This deformation varies from 0,035 to 0,5243 [mm] in absolute value. Using the knowledge of this real deviation, a new STL model obtained by the finite elements method including the inverse deviation is constructed. The new parts are made using this new STL model on the rapid prototyping machine.

#### 4. Conclusion

The mechanical productions of freeform surfaces are being a current practice in the industry. The conformity problem of the mechanical parts is felt more and more. The objective of the present work consists to propose one mathematical procedure for modelling and inspecting freeform surfaces. This proposal allows correcting deviations within manufactured parts. This procedure is built on two algorithms. The first algorithm is used for alignment between the measured points and the CAD model. It permits to determine the thermal deformation of the manufactured part. The second one is based on the finite elements method for including in the STL model the deformation compensation. An industrial application has been treated for validating the proposed method.

## References

1. S. Boukebbab, H. Bouchenitfa, H. Boughouas and J.M. Linares, *Applied Iterative Closest Point algorithm to automated inspection of gear box tooth*, International Journal of Computers & Industrial Engineering 52 pp162-173 (2007).
2. P.J. Besl and N.D. McKay, *A Method for Registration of 3-D shapes*, IEEE Transactions on Pattern Analysis and Machine Intelligence, 14(2), pp239–256, (1992).
3. B. Ma and R.E. Ellis, *Robust registration for computer-integrated orthopedic surgery: Laboratory validation and clinical experience*, International Journal of Medical Image Analysis 7, pp 237–250 (2003).
4. T. Fischer, M. Burry and J. Frazer, *Triangulation of generative form for parametric design and rapid prototyping*, International Journal of Automation in Construction 14, pp233– 240 (2005).
5. R.A. Buswell, R.C. Soar, A.G.F. Gibb and A. Thorpe, *Freeform Construction: Mega-scale Rapid Manufacturing for construction*, International Journal of Automation in Construction 16, pp 224–231 (2007).

## A SOFTWARE SIMULATION TOOL TO EVALUATE THE UNCERTAINTIES FOR A LOCK-IN AMPLIFIER

P. CLARKSON, T. J. ESWARD, P. M. HARRIS, K. J. LINES, F. O. ONAKUNLE,  
I. M. SMITH\*

*National Physical Laboratory, Teddington, Middlesex, TW11 0LW, UK*  
*\*E-mail: ian.smith@npl.co.uk*

A simulation of a lock-in amplifier, based on the Monte Carlo method, has been developed to allow metrologists to understand how uncertainties propagate through a mathematical model of the instrument. Examples of its use are presented. The software is available from the NPL web site.

### 1. Introduction

Lock-in amplifiers are widely used in metrology to extract sinusoidal (AC) signals of specific frequencies from signals buried in noise. The mathematical basis of their operation is the orthogonality of sinusoidal functions. The user's signal is multiplied by two nominally orthogonal reference signals, the resulting signals are filtered and the DC components of the filtered signals are combined to obtain estimates of the amplitude and phase of the signal component of interest.

A software simulation tool to investigate the behaviour of a lock-in amplifier has been developed. The simulation tool allows the user to enter values for the parameters that define a test signal and those that characterise the operation of the instrument. The user may also associate uncertainties with many of the parameter values and a Monte Carlo method<sup>6</sup> is applied to show how the uncertainties propagate through a mathematical model of the instrument.

### 2. Principles Of The Lock-in Amplifier

The operation of a lock-in amplifier is well described by Stanford Research Systems<sup>2</sup> and by Schofield.<sup>1</sup>

The test signal is made of components of the form

$$V^{\text{sig}}(t) = A_{\text{sig}} \sin(\omega_{\text{sig}} t + \theta_{\text{sig}}), \quad \omega_{\text{sig}} = 2\pi f_{\text{sig}},$$

describing the signal of interest and other signals, including noise, in which the signal of interest is embedded. The internal oscillator of the lock-in amplifier generates a digitally synthesized sine wave defined by its frequency  $f_{\text{ref}}$ , amplitude  $A_{\text{ref}}$ , and sampling rate  $f_s$ .

When an external reference signal, such as that acting as the excitation signal for the experiment, is provided to the amplifier, a phase-locked-loop (PLL) is used to phase-lock the internal oscillator sine wave to the reference signal. The PLL introduces phase noise to the internal oscillator sine wave, so that the instantaneous phase shift between the sine wave and the external reference signal is not zero, but the average of the instantaneous phase shifts can be assumed to be zero. In the absence of an external reference signal, the internal oscillator signal may itself be used as the excitation signal.

A second sine wave, of the form

$$V^{\text{X,ref}}(t) = A_{\text{ref}} \sin(\omega_{\text{ref}} t + \theta_{\text{ref}}), \quad \omega_{\text{ref}} = 2\pi f_{\text{ref}},$$

phased-shifted by  $\theta_{\text{ref}}$  from the internal oscillator sine wave, provides the reference input to the first (X) phase-sensitive-detector (PSD). A third sine wave, of the form

$$V^{\text{Y,ref}}(t) = A_{\text{ref}} \sin(\omega_{\text{ref}} t + \theta_{\text{ref}} + \theta_{\text{orth}}),$$

phase-shifted from the second sine wave by  $\theta_{\text{orth}} = 90^\circ$ , provides the reference input to the second (Y) PSD.

The PSDs multiply the amplified, filtered and digitized test signal by the two reference signals to give output signals with components of the form

$$\begin{aligned} V^{\text{X}}(t_i) &= A_{\text{sig}} A_{\text{ref}} \sin(\omega_{\text{sig}} t_i + \theta_{\text{sig}}) \sin(\omega_{\text{ref}} t_i + \theta_{\text{ref}}) \\ &= \frac{1}{2} A_{\text{sig}} A_{\text{ref}} [\cos((\omega_{\text{sig}} - \omega_{\text{ref}}) t_i + (\theta_{\text{sig}} - \theta_{\text{ref}})) \\ &\quad - \cos((\omega_{\text{sig}} + \omega_{\text{ref}}) t_i + (\theta_{\text{sig}} + \theta_{\text{ref}}))], \end{aligned}$$

and

$$\begin{aligned} V^{\text{Y}}(t_i) &= A_{\text{sig}} A_{\text{ref}} \sin(\omega_{\text{sig}} t_i + \theta_{\text{sig}}) \sin(\omega_{\text{ref}} t_i + \theta_{\text{ref}} + \theta_{\text{orth}}) \\ &= \frac{1}{2} A_{\text{sig}} A_{\text{ref}} [\sin((\omega_{\text{sig}} - \omega_{\text{ref}}) t_i + (\theta_{\text{sig}} - \theta_{\text{ref}})) \\ &\quad + \sin((\omega_{\text{sig}} + \omega_{\text{ref}}) t_i + (\theta_{\text{sig}} + \theta_{\text{ref}}))]. \end{aligned}$$

The output signals from the PSDs are low-pass filtered to obtain the respective DC components corresponding to  $\omega_{\text{sig}} = \omega_{\text{ref}}$ :

$$X = \frac{1}{2} A_{\text{sig}} A_{\text{ref}} \cos(\theta_{\text{sig}} - \theta_{\text{ref}}), \quad Y = \frac{1}{2} A_{\text{sig}} A_{\text{ref}} \sin(\theta_{\text{sig}} - \theta_{\text{ref}}),$$

from which are obtained

$$R = \frac{2}{A_{\text{ref}}} \sqrt{X^2 + Y^2}, \quad \theta = \tan^{-1} \left( \frac{Y}{X} \right),$$

estimates of, respectively, the amplitude  $A_{\text{sig}}$  and phase difference  $\theta_{\text{sig}} - \theta_{\text{ref}}$  of the component of the test signal at the frequency of the reference signals.

### 3. Monte Carlo Calculation

The basis for the evaluation of measurement uncertainty is the propagation of probability distributions. In order to apply the propagation of probability distributions, a measurement evaluation model of the generic form  $Y = f(\mathbf{X})$  relating input quantities  $\mathbf{X} = (X_1, \dots, X_N)^T$ , about which information is available, and an output quantity  $Y$ , about which information is required, is formulated. Information concerning  $\mathbf{X}$  is encoded as probability distributions. An implementation of the propagation of probability distributions provides a probability distribution for  $Y$ , from which can be obtained an estimate  $y$  of  $Y$  and the standard uncertainty  $u(y)$  associated with the estimate. Particular implementations are the GUM uncertainty framework<sup>3</sup> and a Monte Carlo method.<sup>4-6</sup> The Monte Carlo method has a number of advantages. It is applicable regardless of the nature of the measurement evaluation model, i.e., whether it is linear or non-linear, and the types of probability distribution characterizing the input quantities. It makes no assumption about the distribution of  $Y$ , and the calculation of model sensitivity coefficients is not required since the only interaction with the measurement evaluation model is to evaluate the model for values of the input quantities.

For the lock-in amplifier, the input quantities include the properties of the instrument, such as the quality of the reference signals and the low-pass filter. For a simulated test signal, the input quantities can also include properties of that signal. There are two output quantities, the amplitude and phase difference of the component of the test signal at the frequency of the reference signals.

### 4. Simulation Software Tool

A software tool has been developed to allow (a) simulated (sine or square wave) signals, defined in terms of probability distributions for amplitude, phase, frequency, amplitude noise and jitter noise, and (b) signals read in from data files, to be processed. The operation of the lock-in amplifier is determined by assigning probability distributions to the parameters defining

the internal oscillator (reference signals), analogue-to-digital conversion and low-pass filter. A Monte Carlo calculation is used to investigate the influence of the different parameters on the evaluation of the output quantities and the performance and limitations of ideal and imperfect instruments. Results, comprising estimates of the output quantities and the associated standard uncertainties, are provided.

The overall aim of the software is to help answer questions about how well an instrument can recover a signal from noise and about the dispersion of values obtained.

The software has been compiled into a standalone Windows executable and is available to download from the NPL website.<sup>7</sup>

## 5. Results

The simulation software has been applied to a real signal consisting of a 50 Hz square wave with amplitude noise, measured over a period of 20 seconds. Fig. 1 shows a screenshot of the front-panel of the simulation software with the graph showing the initial portion of this measured signal.

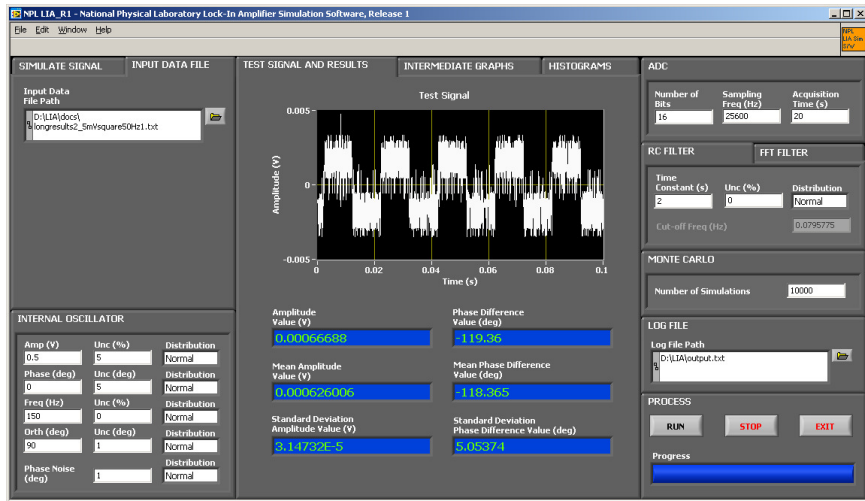


Fig. 1. Screenshot of front-panel of the lock-in amplifier simulation software.

The measured signal was first processed using a software simulation of an ideal instrument, i.e., setting the uncertainties associated with the values of the parameters defining the properties of the instrument to zero,

and evaluating the amplitudes of the first (50 Hz), third (150 Hz) and fifth (250 Hz) harmonics,<sup>a</sup> where the metrologist's estimate of the frequency of the fundamental (50 Hz) has been accepted as being correct.

A Monte Carlo calculation of 10 000 trials was then undertaken, setting standard uncertainties for the values of the amplitude (as 5 %), phase (as 5°) and orthogonality angle (as 1°) of the reference signals, and phase noise (as 1°).<sup>b</sup> The frequency of the internal oscillator was kept constant at 50 Hz.

Table 1 compares the values of the amplitudes of the three harmonics obtained for an ideal instrument, and the results (estimates and associated relative standard uncertainties) from the Monte Carlo calculation.

Table 1. Amplitude values for the first three odd integer harmonics: ideal instrument and imperfect instrument.

Frequency (Hz)	Ideal instrument		Relative standard uncertainty (%)
	Estimate (mV)	Estimate (mV)	
50	1.879	1.880	5.0
150	0.626	0.626	5.0
250	0.375	0.375	5.0

The agreement between the estimates returned by the ideal and imperfect instruments indicates that, on average, the estimates are not sensitive to imperfections in the instrument. The values of the standard uncertainties obtained for an imperfect instrument (and those from other Monte Carlo calculations for this signal) suggest that the uncertainty associated with an estimate of the amplitude of a harmonic of the test signal is predominantly influenced by that associated with the value of the amplitude of the internal oscillator signal.

---

<sup>a</sup>A square wave  $S(t)$  of amplitude  $A$  and angular frequency  $\omega$  can be expressed as an infinite sum of odd integer harmonics:

$$S(t) = \frac{4A}{\pi} \left[ \sin(\omega t) + \frac{1}{3} \sin(3\omega t) + \frac{1}{5} \sin(5\omega t) + \dots \right].$$

<sup>b</sup>In each Monte Carlo trial, values of amplitude, phase and orthogonality angle of the reference signals, and phase noise are sampled from the corresponding probability distributions. Estimates of the amplitude and phase difference are then calculated.

## 6. Conclusions

A software simulation of a lock-in amplifier has been developed that allows the user to analyse both simulated and real (measured) signals. The software implements a model of a lock-in amplifier and provides a means of investigating the propagation of uncertainties through the model using a Monte Carlo method.

Future investigation using simulated signals, i.e., signals having well-defined properties, and real signals, will be undertaken to obtain a better understanding of the effectiveness of lock-in amplifiers in recovering signals (in terms of their amplitude and phase) from noise. Setting a non-zero value for the uncertainty associated with one parameter at a time will help build an understanding of which parameters are most significant.

It is hoped that the simulation tool will prove to be useful to metrologists in understanding results obtained using a lock-in amplifier in the laboratory.

## Acknowledgements

The work described here was supported by the National Measurement System Directorate of the UK Department for Innovation, Universities and Skills as part of the NMS Software Support for Metrology programme.

## References

1. Schofield J H 1994 Frequency-domain description of a lock-in amplifier *Am. J. Phys.* **62** pp 129–133
2. Stanford Research Systems 1993 *Model SR830 DSP Lock-In Amplifier* ©1993 by Stanford Research Systems, Inc. Sunnyvale, California
3. BIPM, IEC, IFCC, ISO, IUPAC, IUPAP and OIML 1995 *Guide to the expression of uncertainty in measurement* 2nd edn (Geneva, Switzerland: International Organisation for Standardisation) ISBN 92-67-10188-9
4. BIPM, IEC, IFCC, ILAC, ISO, IUPAC, IUPAP and OIML 2008 *Evaluation of measurement data — Supplement 1 to the “Guide to the expression of uncertainty in measurement” — Propagation of distributions using a Monte Carlo method* (Sèvres, France: Joint Committee for Guides in Metrology)
5. Cox M G and Harris P M 2006 SSfM Best Practice Guide No 6, Uncertainty evaluation *Technical report DEM-ES-011* (Teddington, UK: National Physical Laboratory)
6. Cox M G and Siebert B R L 2006 The use of a Monte Carlo method for evaluating uncertainty and expanded uncertainty *Metrologia* **43** pp S178–188
7. Software Support for Metrology: Software Downloads, [www.npl.co.uk/server.php?show=ConWebDoc.2644](http://www.npl.co.uk/server.php?show=ConWebDoc.2644).

## MEASUREMENT UNCERTAINTY IN A NON-CLASSICAL CONTEXT

GIAMPAOLO E. D'ERRICO

*Istituto Nazionale di Ricerca Metrologica (INRIM)  
Strada delle Cacce 73, Torino (I), e-mail: g.derrico@inrim.it*

Diverse approaches to measurement uncertainty have been proposed as alternatives to well-established statistical methods. Some are founded on deductive inference systems that dismiss one law or another of classical logic, and purport processing of uncertainty in non-classical terms, e.g., fuzzy sets or belief measures. Intuitionistic logic, a deductive inference system where the law of excluded middle need not hold, is a case-study: since the logic of uncertainty is essentially inductive, a major point at issue is the viability of an intuitionistic probability calculus. An objective of this paper is to set the relevance of such a non-classical context to quantitative treatments of measurement uncertainty.

### 1. Introduction

An essential requirement of an uncertainty logic is non-truth-functionality [1]. Probability calculus (PC) proves to uniquely provide a non-truth-functional paradigm satisfying all the laws of classical logic (CL). Non-classical paradigms (fuzzy sets, many-valued logics) instead dismiss some classical law, and treat uncertainty by use of a mutable stock of *ad hoc* truth-functional rules. A related question is robustness of PC against dismissal of any classical laws. An answer is given by evidence theory that includes axiomatic PC as a particular case [2]. An alternative is to change the logic underlying PC from CL to a non-CL, such as intuitionistic logic (IL). If so, since the law of excluded middle need not hold in IL, PC would be challenged to integrate the lack of this law within the non-truth-functionality of the logic of uncertainty. Section 2 telescopes an outlook on such a paradigm change (2.1), focusing then on measurement uncertainty (2.2), and Section 3 points out some provisional conclusions.

### 2. Uncertainty in the Context of Intuitionistic Logic

#### 2.1. *Probability Calculus from an Intuitionistic Standpoint*

Let  $\alpha, \beta$  represent well formed formulae (wff) in the formal language of a propositional logic with classical connectives for disjunction  $\vee$  ('or'),

conjunction  $\wedge$  ('and'), negation  $\neg$  ('not'). If  $\mapsto$  represents the classical logic consequence,  $\alpha$  is true (respectively, false) if the theorem  $\mapsto \alpha$  holds, i.e., if  $\alpha$  is a  $\mapsto$  thesis (respectively, an  $\mapsto$  antithesis). For instance, the fact that the principle of excluded middle holds in this logic is represented by the statement that  $(\alpha \vee \neg \alpha)$  is a  $\mapsto$  thesis. The expression  $\alpha \mapsto \beta$  means that  $\beta$  is a consequence of  $\alpha$ ; while  $\alpha$  and  $\beta$  are incompatible (mutually exclusive) if their conjunction  $(\alpha \wedge \beta)$  is false (is an  $\mapsto$  antithesis). Such a logic system is truth-functional if the truth value of a wff depends exclusively on, and is completely determined by, the truth values of its components, e.g.,  $(\alpha \wedge \beta)$  is true if and only if  $\alpha$  is true and  $\beta$  is true. If  $P(\cdot)$  is the probability measure of a PC, with application to wff,  $P(\cdot)$  is a function mapping propositions in the real interval  $[0,1]$ . Based on this underlying logic, the classical Kolmogorovian axioms can then be re-expressed as follows [3]:

$$P(\alpha) = 1 \text{ if } \alpha \text{ is a } \mapsto \text{ thesis ,} \quad (1)$$

$$P(\alpha) = 0 \text{ if } \alpha \text{ is an } \mapsto \text{ antithesis ,} \quad (2)$$

$$P(\alpha) \leq P(\beta) \text{ if } \alpha \mapsto \beta , \quad (3)$$

$$P(\alpha) + P(\beta) = P(\alpha \vee \beta) + P(\alpha \wedge \beta) . \quad (4)$$

Classical rules for PC can be easily derived. E.g.,  $P(\neg \alpha) = 1 - P(\alpha)$  follows from Eq. (1), Eq. (2) and Eq. (4); putting  $\beta = \neg \alpha$ , Eq. (1) gives  $P(\alpha \vee \neg \alpha) = 1$  and Eq. (2)  $P(\alpha \wedge \neg \alpha) = 0$ , so that Eq. (4) becomes  $1 = P(\alpha) + P(\neg \alpha)$ .

On Eq. (4) is based the principle of addition of probabilities of mutually exclusive, incompatible, wff:

$$P(\alpha \vee \beta) = P(\alpha) + P(\beta) \text{ if } P(\alpha \wedge \beta) = 0 . \quad (5)$$

If a measure  $\pi(\cdot)$  is used instead of  $P(\cdot)$  to express a state of complete uncertainty on  $\alpha$  by allowing both  $\pi(\alpha) < 1/2$  and  $\pi(\neg \alpha) < 1/2$ , the following sub-additive inequality includes Eq. (5) as a special case:

$$\pi(\alpha \vee \beta) \geq \pi(\alpha) + \pi(\beta) \text{ if } \pi(\alpha \wedge \beta) = 0 . \quad (6)$$

Thus, sub-additivity allows the probability of the disjunction of two incompatible wff to be less than unit. The mathematical theory of evidence [2], for instance, is a paradigm where sub-additivity holds in the form of Eq. (6).

If the law of excluded middle is maintained, i.e., if  $\mapsto(\alpha \vee \neg\alpha)$  holds in the underlying logic, Eq. (5) yields:

$$\pi(\alpha) + \pi(\neg\alpha) \leq 1 = \pi(\alpha \vee \neg\alpha). \quad (7)$$

However, if the logic underlying PC is IL, the law of excluded middle need not hold. In this case, an intuitionistic probability (IP) would still allow a non-truth-functional treatment of uncertainty. Provided the consequence relation is interpreted in intuitionistic term (i.e.,  $(\alpha \vee \neg\alpha)$  is not a  $\mapsto$  thesis), an IP calculus may still be formalized by Eqs. (1-5): in particular, it is not necessary to rule out additivity expressed by Eq. (5).

## 2.2. Applicability to Measurement Uncertainty

IP may find application in situations where the law of excluded middle is questioned: to asses its relevance to measurement, let uncertainty be represented in terms of a real interval of values the measurand can plausibly range within.

For example, let  $q, r, s$  be real quantities obeying a physical formula  $\lambda = \lambda(q, r, s)$  such that  $q = rs$ , and let  $U_q, U_r, U_s$  represent uncertainty intervals associated to their respective measurement results. Since triplets  $\hat{q} \in U_q, \hat{r} \in U_r, \hat{s} \in U_s$  exist such that  $\hat{q} = \hat{r}\hat{s}$ , the instance  $\hat{\lambda} = \lambda(\hat{q}, \hat{r}, \hat{s})$  of the formula is true. But there also exist triplets  $q_0 \in U_q, r_0 \in U_r, s_0 \in U_s$  such that  $q_0 \neq r_0 s_0$ , i.e. the instance  $\lambda_0 = \lambda(q_0, r_0, s_0)$  is false. If so, however, a formula  $\neg\lambda_0$  can be either true or false. In fact, on one hand, there exist triplets  $\{q^+ \neq q_0 \in U_q, r^+ \neq r_0 \in U_r, s^+ \neq s_0 \in U_s\}$  such that  $q^+ = r^+ s^+$ , and therefore the formula  $\neg\lambda_0 = \lambda(q^+, r^+, s^+)$  is true; on the other hand, there exist also triplets  $\{q^- \neq q_0 \in U_q, r^- \neq r_0 \in U_r, s^- \neq s_0 \in U_s\}$  such that  $q^- \neq r^- s^-$ , and therefore  $\neg\lambda_0 = \lambda(q^-, r^-, s^-)$  is false. Thus, in the formal language introduced above, the disjunctive wff  $(\lambda_0 \vee \neg\lambda_0)$  instantiates a failure of the law of exclude middle.

Nevertheless, this failure cannot be managed by application of a deductive IL. Rather, an inductive inference system is required, that can be as well based on a classical or intuitionistic probability calculus (the underlying logic is immaterial in this respect). In fact,  $(\lambda_0 \vee \neg\lambda_0)$  is not a  $\mapsto$  thesis; but, while  $\hat{\lambda} = \lambda(\hat{q}, \hat{r}, \hat{s})$  is definitely true (the triplet is constrained to  $\hat{q} = \hat{r}\hat{s}$ ), triplets  $(q_0, r_0, s_0), (q \neq q_0, r \neq r_0, s \neq s_0)$  can vary over their domain of definition. Being affected by presence of unconstrained variables, the truth value of a formula  $(\lambda_0 \vee \neg\lambda_0)$  remains undetermined—unless a suitable measure is defined on the domain, so that a formula is assigned a truth degree ranging in between falsehood and truth. Perspicuously, this entails an area outside the province of bivalent logic.

The main point is the logic of uncertainty is intrinsically not truth-functional: a facet of this situation is that a set-theoretic representation of uncertainty, as expressed in terms of real intervals (or fuzzy sets [1]), implies a translation of truth-functional connectives into set operations, again resorting to truth-functionality. This means an undertaking bound to inventing somehow cumbersome procedures, if compared to the construct of stochastic dependence/independence, implemented by probability calculus to trespass deductive inference, the realm of (classical or non-classical) tautologies, to enter inductive inference, the realm of learning from experience.

As to usual practice of quantitative estimation of measurement uncertainty, compliance with IP is redundant—uncertainty being conveniently computed by use of conditional probabilities, 2-place functions  $p(\cdot|\cdot)$ . In the case in point, if  $z$  is a real measurand and  $\mathbf{x} = (x_1, \dots, x_i, \dots, x_n)$  is the result of  $n$  observations of  $z$ , the probability density function  $p(z|\mathbf{x})$  denotes the posterior probability for  $z$  to range in  $dz$ , given  $\mathbf{x}$ . In fact, a measurement uncertainty estimate expressed in terms of standard deviation of  $p(z|\mathbf{x})$ , is immune to side-effects related to set-theoretic representations of uncertainty.

### 3. Conclusion

Attractiveness of intuitionistic logic (IL) is mainly due to formalization initiated by Heyting [4] and Kolmogorov [5]: it has given rise to interest in many fields, e.g., in probability theory. Intuitionistic probability allows to violate the law of excluded middle while preserving additivity of probability functions. In the light of the investigation performed so far, the following conclusions may be drawn:

- IL provides useful tools for refining treatments of epistemic uncertainty;
- calculus of (conditional) probability is the rational to model and estimate measurement uncertainty by means of statistical methods.

### References

1. G.E. D'Errico, “Paradigms for uncertainty treatment: A comparative analysis ...”, *Measurement* (2008), doi: 10.1016/j.measurement.2008.09.001.
2. G.J. Klir, T.A. Folger, *Fuzzy Sets, Uncertainty, and Information*, Prentice Hall, Englewood Cliff, New Jersey (1988).
3. D. Weatherston, *Notre Dame Journal of Formal Logic* **44** (2), 111 (2003).
4. A. Heyting, “Die formalen Regeln der intuitionistischen Logik” (1930), Italian translation in: *Dalla logica alla metalogica (From logic to metalogic)* (E. Casari, ed.), pp. 195-212, Sansoni, Firenze (1979).
5. A.N. Kolmogorov, “O printsipe tertium non datur” (1925), It. tr. in: *From logic to metalogic* (E. Casari, ed.), pp. 167-194, Sansoni, Firenze (1979).

## COMPARISON OF METHODS TO MEASURE UNCERTAINTY BASED ON THE ISO STANDARDS

LAURA DELDOSSI, DIEGO ZAPPA

*Department of Statistical Sciences, Catholic University, L.go Gemelli 1  
Milan, 20123, Italy*

In this paper we compare ISO 5725 and GUM from a statistician point of view. In particular we report some considerations on the relevant role of the interactions among the variables in the equation model, we emphasize the importance to apply standard ANOVA technique if the measurand is measurable and we give some warnings concerning the application of the expanded uncertainty when the variables that are involved are few.

### 1. Introduction

Quantitative evaluation of the uncertainty of a measurement is necessary to take the right decision in judging whether the differences among the results of an experiment or the variability of a process are due to either an out of control process or to a not capable measurement system. This is true especially because process variation is generally becoming small due to technological improvements and therefore the measurement procedures must be tested to assess their adequateness (see, for a review [1]). In the last fifteen years the International Organization of Standardization (ISO) has produced several documents on uncertainty measurement. The most important ones are the international standards ISO 5725:1994 (Part 1-6) [2] and the ISO “Guide to the expression of uncertainty in measurement” (GUM) [3] published in 1995, both proposing a method to calculate the uncertainty of a measurement.

In section 2 analogies and differences between the two methods are illustrated and some warnings to the ISO users are given in order to avoid wrong applications of the standards and, consequently, wrong evaluation to measure uncertainty. Some notes are given in section 3 on two other ISO technical specifications recently published on measurement uncertainty (ISO/TS 21748:2004 [4], ISO/TS 21749:2005 [5]) where an attempt has been made to combine ISO 5725 and GUM’s approach.

## 2. ISO 5725 and GUM: a Comparison

ISO 5725 deals with accuracy (trueness and precision) of measurement methods and results. Key points of this procedure are the following:

1. the measurement method yields “measurement  $y$  on a continuous scale and it gives a single value”
2. it is based on a collaborative study, that is an interlaboratory experiment in which identical material is measured using the same standard method in different laboratory with different operators using different equipment
3. the model explaining the measurand  $Y$  depends on the experimental design used to obtain the measurement. It is generally a random effect model such as

$$Y = \mu + B + E \quad (1)$$

where  $\mu$  is the general mean,  $B$  is the bias due to the laboratory component, assumed to be  $N(0, \sigma_L^2)$ ,  $E$  is the random error under repeatability conditions assumed to be  $N(0, \sigma_E^2)$ ,  $B$  and  $E$  are supposed to be uncorrelated

4. the uncertainty is measured as the reproducibility standard deviation,  $\sigma_R = (\sigma_L^2 + \sigma_E^2)^{0.5}$  and it is estimated using the analysis of variance (ANOVA) method
5. there are no rules to obtain the so called confidence interval at a stated probability level (usually 0.95) around  $y$  (expanded uncertainties)

On the contrary the characteristics of the GUM method are:

1. it assumes that  $Y$  may be not directly measured
2. as a consequence of 1. no experimental design to obtain  $y$  is requested
3.  $Y$  depends on  $m$  measured input quantities  $X_1, \dots, X_m$  through a known equation called measurement equation

$$Y = f(X_1, X_2, \dots, X_m). \quad (2)$$

To avoid non linearities in (2), the Taylor series expansion of (2) is often calculated in the neighbourhood of  $(x_1, x_2, \dots, x_m)$ . The latter are either the mean of  $n$  independent repeated measurements of each of the  $X_1, X_2, \dots, X_m$  (called type A method) or the expected mean obtained from the assumed probability density function (PDF) of each of the  $X_i$  (called type B method). Truncating the expansion at the first order, (2) may be approximated as

$$Y \approx c_0 + \sum_{i=1}^m c_i X_i \quad (3)$$

where  $c_i = [\partial f / \partial X_i]_{X_i=x_i}$  ( $i=1,..m$ ) are called the “sensitivity coefficients”

4. the estimate,  $y$ , of the measurand is obtained either from (2), if  $f$  is known or from (3) substituting  $(X_1, X_2, \dots, X_m)$  by  $(x_1, x_2, \dots, x_m)$ .

The uncertainty of  $Y$  is evaluated through the “law of propagation of uncertainty” as

$$u_c^2(y) = \sum_{i=1}^m c_i^2 u^2(x_i). \quad (4)$$

(4) is called the combined standard uncertainty

5. the expanded uncertainty  $U_p$  is given by

$$U_p = k_p u_c(y) \quad (5)$$

where  $k_p$  is known as coverage factor, generally calculated using an appropriate percentile of the  $t$ -Student or of the standardized normal distribution, such that the interval  $[y \pm U_p]$  should encompass a fraction  $p$  of the values that could reasonably be attributed to the measurand.

From the beginning GUM was a widely adopted standard approach, probably because it was considered a method so easy that its application seemed to be achievable without the need of “at least one member of the panel with experience in the statistical design and analysis of experiments” as ISO 5725 did. Furthermore GUM gave the possibility to take into consideration the uncertainty of type B, that is uncertainties generally specified by judgment based on non-statistical available information. The experimenter has to prepare the “uncertainty budget”, that is the list of all input variables  $X_i$  in equation (2) with the corresponding  $u(x_i)$  and  $c_i$ . Then  $u_c(y)$  is computed using the law of propagation of the uncertainties (4). In (4) also the covariances should be inserted if the input variables are not independent as it is often mentioned in the GUM, but nothing is said on how to compute the covariances or, on the other side, how to prove that the input variables are independent. It is evident that sampling from  $X_i$  marginally with respect to all the other variables does not allow to evaluate the dependence among the variables. The consequences are that applying (4), the uncertainty  $u_c(y)$  can be overestimated or underestimated depending on the sign of the covariances.

Finally the expanded uncertainty  $U_p$  is obtained by choosing the coverage factor  $k_p$  on the basis of the normal or  $t$ -Student distribution. About the opportunity to this choice, we remind the many criticism appeared in the metrological literature (see e.g. the special issue of *Metrologia* in 2006) and the new proposal for obtaining the complete probability density function (pdf) of the measurand  $Y$  by Monte Carlo simulation (see [6]). To check the

approximations that comes from (5), we computed the cumulative density function of the convolution of  $X_1$  and  $X_2$ , supposing  $X_1 \sim N(0, \sigma^2)$  (intended here as a type A variable) and  $X_2 \sim U(-a, a)$  (intended here as a type B uniform random variable), and also of  $X_1$ ,  $X_2$  and  $X_3$ , supposing  $X_3 \sim U(-b, b)$ . We noticed that as much as the variance of  $X_2$  (or  $X_2$  and  $X_3$ ) increases with respect to  $\sigma^2$ , then the solution (5) will return a width of the confidence interval related to the measurement wider than the one obtained by the exact convolution procedure. It may be supposed that (5) is a good solution only if the variances due to type B variables do not dominate with respect to the variance of the type A variables (generally supposed to be gaussian).

On the other hand the standard approach proposed in ISO 5725 is based on the assumption to run an experimental design to obtain  $y$ . The main by-products of such a choice are: 1) the randomization of the trials in the design reinforces confidence on the assumed normal distribution of the random effects; 2) the experimental design gives the possibility to estimate, if they exist, interactions among factors and to take them into account (the latter is in particular not possible in the GUM procedure); 3) numerous statistical results are available to obtain approximated confidence intervals of variance components as Modified Large Sample (MLS) (see [7], [8]), Generalized Confidence Intervals (GCI) (see, e.g., [9]) and Simulated Confidence Intervals (SCI) [10], and they could easily be used in this metrological context.

So we think that ISO 5725 approach is preferable to measure uncertainty if  $Y$  can be measured directly. Only if it is not possible, GUM approach can be adopted but with some cautions. For some particular circumstances (linearity of the function  $f$ , normality assumption, independence of the input variables) the two approaches give the same results.

### **3. A Possible Conciliation between the ISO 5725 and the GUM Approach**

Few years ago two ISO technical specifications were published ([4] and [5]) attempting to combine ISO 5725 and GUM's approaches to remove some doubts came out from the GUM prescriptions.

ISO 21749 follows the approach taken in GUM but proposes to use the analysis of variance to estimate uncertainties of components classified as Type A. Then familiarity with data analysis, and specific particular statistical techniques are requested by this technical specification. As in ISO 5725, the variability of the manufacturing process is generally not taken into consideration in the model but measurements of reference standards are used to provide data on the measurement process itself. The novelty of this approach consists on the introduction of nested designs with the corresponding ANOVA table to estimate the uncertainties, because of time-dependent sources of variability or of measurement configuration (differences due to different instruments, operators, geometries) and material inhomogeneity, and the use of GUM approach to

compute the expanded uncertainty. Some considerations are necessary. While the use of nested designs are justified to take into account time-dependent sources of variability, it is not clear why nested design is introduced to estimate uncertainties due to measurement configuration and material inhomogeneity. For the latter a crossed design with random or mixed effects should be the right design. In this sense the ANOVA table in the example 8 of [5] “Type A evaluation of uncertainty from a gauge study” is not appropriate. This gauge capability study involves a mixture of the crossed and nested effects model and then it needs a suitable design of experiment that enables to estimate both the uncertainties due to random or to fixed effects with a single ANOVA table. Furthermore, once the various variance components are estimated, the expanded uncertainty is obtained following the GUM procedure and the coverage factor is based on the *t*-Student distribution with degrees of freedom approximated by the Welch-Satterwhaite formula. Other statistical methods proposed in these last years in the ANOVA context as MLS, GCI and SCI, produce intervals whose width is generally shorter.

ISO 21748 deals with the evaluation of measurement uncertainties using data obtained from studies conducted in accordance with ISO 5725-2, that is relative to the interlaboratory experiments in presence of reproducibility data. These studies yield performance indicators ( $s_E$  and  $s_R$ ) estimated on the basis of model (1) which form a specification for the method of performance. But in the practice  $s_R$  does not necessarily include variation of all the effects that influence a measurement result. This is the reason for which this guidance introduces the following statistical model

$$Y = \mu + \delta + B + \sum_{i=1}^m c_i X_i + E \quad (6)$$

where, in particular,  $\delta$  is a term representing the intrinsic bias due to the measurement method,  $X_i \sim N(0, u^2(x_i))$  and the summation is over those effects subject to deviations other than those incorporated in  $B$  or  $E$ . Then model (6) is a combination of (1), used by the ISO 5725, and (3), used by the GUM approach, with the addition of the measurement method bias  $\delta$ . It is based on the idea that effects not observed within the context of the collaborative study shall be negligible or explicitly allowed for according to a simple rule: they are considered negligible if their uncertainties are less than 0.2 times the correspondent expected one. The main factors that are likely to change between collaborative study and routine testing are, for example, sampling process, inhomogeneity, changes in test-item type. Their uncertainties have to be added to increment the reproducibility variance of the collaborative studies. There would be other effects that may operate in particular instances, such as factors which are held constant or which vary insufficiently during collaborative studies. The guidance proposes to estimate these effects separately, either from

experimental variation or by prediction from established theory and, only if not negligible, adding components in (6).

In our opinion there is a risk in this procedure. Including uncertainties components in subsequent steps does not allow to take into account once again the interactions among factors. Then it should be better, if possible, to modify suitably the native experimental design of the collaborative trial. For example, if factors are quantitative, one can refer to the so called combined array approach (see [11]) in which the controllable factors as well as the noise factors, which typically arise in the real production/utilization of goods, are unified in a single experimental design. This requires that the noise factors can be reproduced as controllable factors in a laboratory or in a pilot plant level; as a consequence in the computation of the variance of the response variable, the uncertainties that come from the true realization of the noise factors are considered. This approach is different from the one proposed in [4] as it allows to take into account also all the interactions between controllable and noise factors.

#### **4. Conclusion**

If the response variable  $Y$  is directly measurable, the design of a suitable experiment and the use of the correspondent ANOVA table provide the best approach to estimate the different sources of variation derived from a measurement system.

Even if in ISO standards the uncertainty due to the manufacturing process is never taken into account as “measurement of check standards are used”, often the factor “part” should be considered along with its interaction with the other factors. The use of mixed effect model is also suggested to consider fixed and random factors in a single factorial (crossed or nested) experiment to estimate all uncertainties components (systematic and random) with a single ANOVA table.

When  $Y$  is not directly measurable or there are significant input components classified as type B, the GUM approach can be applied, with some caution in the interpretation of the expanded uncertainty as it is relevant the right choice of the coverage factor and the interaction among factors.

#### **References**

1. R.K. Burdick, C.M. Borror, D.C. Montgomery, *Journal of Quality Technology* **35**, 342-354 (2003).
2. ISO 5725:1994 (1-6), (1994).
3. ISO, *Guide to the Expression of Uncertainty in Measurement*, (1995).
4. ISO/TS 21748:2004 (2004).
5. ISO/TS 21749:2005, (2005).

6. JCGM 101 *Evaluation of measurement data – Supplement 1 to the GUM – Propagation of distributions using a Monte Carlo method* (2008).
7. F.A. Graybill, C. Wang C., *JASA* **75**, 372, 869-873 (1980).
8. R.K. Burdick, G.A. Larsen, *Journal of Quality Technology*, **29**, 3, 261-273 (1997).
9. R.K. Burdick, C.M. Borror, D.C. Montgomery, ASA-SIAM Series on Statistics and Applied Probability (2005).
10. L. Deldossi, D. Zappa, in Proceedings of ENBIS-DEINDE 2007, 105-116 (2007).
11. D.C. Montgomery Wiley, New-York (2001).

## METHODS FOR AGGREGATING KEY COMPARISONS

R.J. DOUGLAS, A.G. STEELE

*Institute for National Measurement Standards*

*National Research Council Canada*

*Ottawa, Ontario K1A 0R6, Canada*

Key comparisons aim to demonstrate agreement, within claimed uncertainties, of measurements made by National Metrology Institutes (NMIs). Chi-squared-like tests of this agreement can be strengthened by increasing the number of independent measurements by aggregation: grouping measurement comparisons into larger sets where an averaged test of expected agreement is still of practical interest.

Measurements can have their agreement evaluated relative to reference values; or relative to each other to test unmediated agreement. One might average over artefacts, or over measurement ranges, or over techniques of measurement, or over all the comparisons run by a particular consultative committee (CC), or over all CCs. One might want to average over agreement for measurements from a particular NMI, or average over all participants from a particular region, or average over all participants in the key comparison data base. We show how the relative weights of subgroups of measurements should be chosen to balance the influence of the different subgroups in the aggregation irrespective of the number of measurements in the subgroup.

### 1. Introduction

#### 1.1. Testing Comparisons

For key comparisons [1], the agreement of experimental results  $\{x_i\}$  with some ideal result  $x_0$  is usually evaluated relative to the claimed randomness, i.e. the uncertainties. Often, individual results are evaluated with equivocal conclusions: the main problem is to strengthen these conclusions with larger sets of results.

Formal testing often uses a normalized error parameter,  $E_n$ , that we normalize to the standard uncertainty (coverage factor  $k = 1$ ).

$$E_n = \frac{(x_i - x_0)}{u(x_i - x_0)}. \quad (1)$$

With  $E_n$ , a comparison result can be tested against a fixed acceptance criterion such as  $|E_n| < 2$ ; or against a criterion that tries to take into account the shape of this specific uncertainty distribution, such as  $|E_n| < k_i$  (its coverage factor for a stated coverage probability such as 95%).

In either case, the criterion for acceptance characterizes what is meant by “the absence of compelling evidence to reject the null hypothesis” – the hypothesis of agreement within the range expected from the claimed uncertainties. This is a *scientific* test that can, on its own, only identify when new science is convincingly present; but cannot, on its own, offer really strong support for the hypothesis of ideal agreement.

### **1.2. *The Main Problem for Testing Comparisons***

The weakness of the testing can be compounded by an expectation of non-repeatability of the test’s decision. For example, with a comparison that either just passes or just fails any  $E_n$  criterion for acceptance: for a randomized but minuscule re-scaling of the uncertainties claimed for the comparison, we can see that *half* of the repeated tests would be expected to give the *opposite* decision. This unpalatable expectation about the non-repeatability of decisions can always be present unless participants claim a perfect repeatability in their measurements.

Within a single laboratory, these difficulties are addressed by repeating a measurement many times and pooling the results, often with an aggregating test statistic (such as a chi-squared, or mean-square  $E_n$ ). By increasing the number of measurements upon which the decision is being based, we can usually improve the repeatability expected for the decision. In this paper we aim at applying aggregation to diverse key comparisons, identifying and addressing issues of equitable post-facto treatment for the diverse comparisons in a quest for the advantage of having been “measured many times”.

Although both the repeatability and the testing may each be expressed as a probability based on the uncertainties claimed by the participants, they are expressed in different probabilistic domains that should not be conflated when both concepts are being considered. For *repeatability* there can be as many probability domains as there are repeatability conditions. For *testing* the distributions’ locations are constrained for each participant by one of several forms of “agreement with...” as the test’s null hypothesis.

### **1.3. *Aggregation for Testing Comparisons***

In describing a group of diverse comparisons using an aggregating statistic, we seek a consensus that the comparisons’ measurements share some essential characteristic that is of interest. This may be simple: a stable artefact as the shared measurand, with  $E_n$  testing mediated by a reference value [1], or perhaps using unmediated pair differences [1,2]. However, since  $E_n$  is dimensionless,

there is no prohibition on aggregating over very diverse measurands – provided that a convincing case can be made that the aggregate is meaningful.

Sometimes, a group of comparisons may be easy to appreciate as a candidate for aggregation. For example, if a group of nominally identical artefacts is circulated in a comparison, it may be quite easy to form a consensus that it is appropriate to report on agreement that has been aggregated over all artefacts. However, with such similar measurands extra care may be needed to read the uncertainty budgets for indications of covariant uncertainty components that we would want to take into account in characterizing the aggregated results.

The reasons for aggregating comparisons are not necessarily this obvious. For example, aggregating the results from a key comparison in “mass” with one from “time interval” might initially seem subject to the adage that one should not “compare apples with oranges”. The aggregator has the responsibility of making the case for the underlying similarity: for testing the interlaboratory consistency of mass measurements – on apples as well as on oranges, the case for aggregation would be simple. For mass and time interval, the underlying unifying question may be more subtle – for example, unified by a focus on the quality system of two or more NMIs – within their claimed uncertainties, do their quality systems deliver interoperable results? A CC might aggregate results over all its key comparisons, to report on the average “state of agreement” for its entire scope of measurements. Although the case for aggregation over any set of very-different comparisons may need to be more carefully explained, it may also be easier to justify their non-covariance or independence.

The most familiar aggregating statistic in measurement science is a (reduced) chi-squared-like statistic: the mean-square  $E_n$ . Departures from the analytic reduced-chi-squared form can be gracefully handled by Monte Carlo simulation, to extend the chi-squared testing formalism to reference values that are not the weighted mean, to the all-pairs-difference chi-squared, and to non-Gaussian uncertainty claims. Monte Carlo simulation can handle as easily many other aggregating statistics (such as any Holder, or  $L_p$  norm) that may be useful in special circumstances, so the choice of statistic should not be chosen merely for its ease of computability. Chi-squared testing uses the square of the  $L_2$  norm: the root-mean-square (RMS)  $E_n$ . It is very familiar to all those who deal with least-squares fitting, and as such we think that it is the most appropriate method to convey confidence about aggregates to a wide audience.

For some aggregates of interest, it may be appropriate to be able to balance the influence of subgroups containing quite different numbers of measurements. To appreciate how to do this, let us consider chi-squared-like aggregation.

## 2. Chi-squared-like Testing

### 2.1. Agreement-hypothesis Testing

To illustrate the use of different weighting for different key comparisons or subgroups of measurements, we consider a generalized chi-squared-like aggregate (which includes the equally-weighted aggregate as a special case):

$$\chi^2 = \sum_{j=1}^J a_j \sum_{i=1}^{I_j} \left[ \frac{x_{ij} - x_{0j}}{u(x_{ij} - x_{0j})} \right]^2 = \sum_{j=1}^J a_j z_j. \quad (2)$$

It is aggregating over  $J$  comparisons, with the  $j$ -th comparison consisting of  $I_j$  measurements  $\{x_{ij}\}$  being compared to  $j$ -th comparison's reference value  $x_{0j}$  with its departure normalized to the standard uncertainty of its departure.

Within the  $j$ -th comparison, Equation 2 follows the widespread convention that all labs' normalized departures from the reference value are given equal weight in the test, even when a pilot lab has made more measurements than all other participants combined. To extend equal weighting of lab results across all comparisons, the  $a_j$ 's would be chosen to be equal. Alternatively, the relative size of the  $a_j$ 's could be chosen to accord equal weight to each comparison's chi-squared aggregate,  $z_j$ , irrespective of the number of lab results. In either case, the overall scaling could be chosen to create a reduced chi-squared-like test: the ways for doing this are developed below.

The essence of chi-squared-like testing of agreement is to evaluate [2, 3] the probability density function (PDF) of  $\chi^2$  (equation 2) from the PDFs of the  $x_{0j}$  subject to the constraint that for the  $x_{ij}$ , their PDFs' means agree with the means of the PDFs of the  $x_{0j}$ . Statements of probability resulting from this  $\chi^2$  PDF are to be viewed as predictions, based on the claimed uncertainties, that are conditional on the assumption of ideal agreement. This is the distribution that is used to evaluate the aggregated results' metrological compatibility with the hypothesis of "ideal agreement with the reference values  $\{x_{0j}\}$ ", quoting the probability that this constrained  $\chi^2$  would be greater than the experimental  $\chi^2$ . If this probability exceeds a pre-chosen tolerance for the chance of falsely rejecting the agreement hypothesis (chosen, for example at 5% [4]), then the agreement hypothesis is accepted since the comparison exhibits insufficiently compelling evidence for rejecting it. For any particular set of uncertainty distributions, this tolerance can be expressed as a cutoff value  $\chi_c^2$  for  $\chi^2$ , calculated from the  $\chi^2$  PDF, and the acceptance criterion becomes  $\chi^2 < \chi_c^2$ .

## 2.2. Chi-squared-like Testing – Equal Weights for Measurements

Chi-squared-like aggregates can be properly evaluated for any comparison by Monte Carlo simulation, and their PDFs approximated to any precision that may be needed. To demonstrate the ways that aggregates may be used, scaled, balanced and combined, it is helpful to develop the classical chi-squared as a straightforward exercise in propagating uncertainty distributions to the analytic chi-squared distribution. This simple exercise is commonly eclipsed by the subtleties of the brilliant theorems that define and extend the applicability of the analytic chi-squared distribution. With the Monte Carlo method available, we need not concern ourselves overly with the theorems and the existence of analytic closed forms for the integrals.

We can follow the simple story of the PDF developing as we aggregate. For developing the classical chi-squared, we can follow the aggregation analytically, with  $N$  independent Gaussian distributions, constrained to be zero-mean. In Equation 2, for group  $j$ ,  $N$  would be  $I_j$ , and we can simplify by using external reference values  $x_{0j}$ . The zero-mean Gaussian would be in the variable  $x_{ij} - x_{0j}$ , with standard deviation  $u(x_{ij} - x_{0j})$ . The variable  $(E_n)_{ij} = (x_{ij} - x_{0j}) / u(x_{ij} - x_{0j})$  will have a standard-normal distribution (zero mean, standard deviation = 1, variance = 1).

The next step is to change variables: in  $y = (x_{ij} - x_{0j}) / u(x_{ij} - x_{0j})$  we have a standard normal distribution,  $f(y) = (2\pi)^{-1/2} \exp(-y^2/2)$ , (Figure 1-a). We want to express this as a function  $g$  of a new variable  $v = y^2$ :  $g(v) = f(y = v^{1/2}) | dy/dv|$ , which for  $v \geq 0$  is proportional to  $v^{1/2} \exp(-v/2)$ . The Gaussian's symmetry simplifies adding probabilities of the two distinct branches:  $f(y = -v^{1/2}) | dy/dv| dv$  and  $f(y = +v^{1/2}) | dy/dv| dv$ . Normalized on its range  $[0, \infty)$ , we have the analytic chi-squared with degrees-of-freedom = 1:  $g(v) = (2\pi)^{-1/2} v^{1/2} \exp(-v/2)$ , (Figure 1-b), with mean = 1, and variance about the mean = 2.

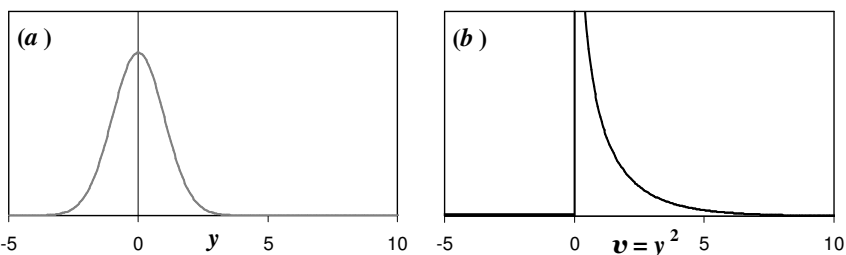


Figure 1. A Gaussian PDF (a) for a random variable  $y$  gives rise to a PDF for  $y^2$  (b) that is a chi-squared with degrees-of-freedom = 1.

We can now consider the PDF of the simplest aggregate, following the way that the constrained chi-squared develops as we aggregate over each result. In Equation 2, for equal weights (e.g.  $a_j = 1$ ), each time an additional term is added in the sum over  $i$ , the PDF of the already-aggregated terms is convoluted with the PDF of the additional term, a chi-squared with degrees-of-freedom = 1. As shown in Figure 2, the result for aggregating  $N$  equally-weighted results is a chi-squared with degrees-of-freedom =  $N$  (because the reference value is an external reference value):  $[2^{N/2} \Gamma(N/2)]^{-1} z^{(N-2)/2} \exp(-z/2)$ , with mean  $N$  and variance  $2N$ .

Those used to combining uncertainties for a measurement equation that is a simple sum (such as a series of corrections applied to a measurement) should feel at home with Figure 2's picture of the aggregation. Other than the fact that each distribution is non-Gaussian, all is familiar. We can see the central limit theorem's shape prediction – the PDF for the aggregate (in column 3) is tending towards a Gaussian as we increase the number  $N$  of aggregating results. It is centred at the sum of the means ( $N$  in this case), with variance the sum of the individual variances ( $2N$  in this case). By dividing the aggregate by the sum of the means, (column 4), we obtain the *reduced  $\chi^2$*  form with a mean of 1; the standard deviation of the reduced  $\chi^2$  is  $\sqrt{2}/\sqrt{N}$ , narrowing as  $N$  increases. The essence of equity can be appreciated in Figure 2: to contribute equally to the aggregate's breadth the variance of column 2 in each row should be the same.

To increase  $N$ , measurements may be repeated and aggregated. The measurements may be made on the same artefact at different times, or at more or less the same time on different artefacts with nominally identical measurands. Of the wide range of non-prohibited aggregations that might be considered, this type would perhaps be the easiest to explain.

In practice, the reference value may not be external, the claimed distributions may not be Gaussian, the results may not be independent, and the aggregate may even be taken to test unmediated agreement [2]. In any of these cases, the required PDF departs from the analytic chi-squared, but it can easily be evaluated by Monte Carlo simulation, constrained to force “agreement”. A analogue of Figure 2 could be constructed from the Monte Carlo histograms.

In discussing the use of chi-square-like statistics for testing, as described in section 2.1, it is useful to emphasize that the overall scaling is irrelevant as long as the scaling is identical for (1) the experimental  $\chi^2$  and (2) the  $\chi^2$  used in the specific evaluation of the PDF. The overall scaling of the  $\{a_j\}$  in Equation 2 can be chosen to suit the user's convenience, and we generally prefer the reduced-chi-squared scaling (right column in Figure 2) that is so widely familiar in the context of least-squares fitting.

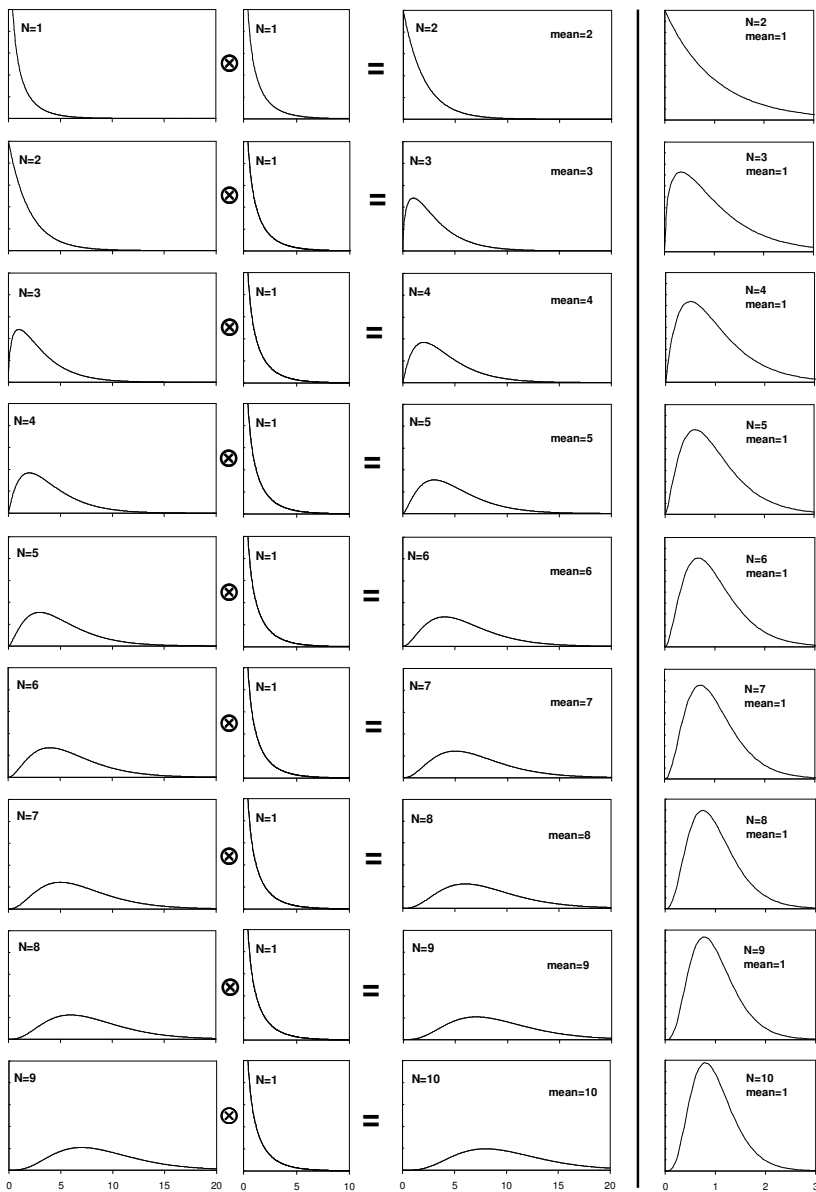


Figure 2. Mean-square aggregation of  $N = 2 \dots 10$  standard-normal variates by repeated convolution ( $\otimes$ ) with a  $\chi^2$  having degrees-of-freedom (DoF) = 1, generating a  $\chi^2$  with DoF =  $N$  in column 3, and thence a reduced  $\chi^2$  in column 4, also with DoF =  $N$ . The basis for equity in the aggregation is the equal variance of the  $\chi^2$  from each distribution in column 2.

### 2.3. Chi-squared-like Testing – Balancing Comparisons of different $N$

If the aggregation is intended to accord each measurement the same weight, we would be unconcerned that some comparisons have vastly more measurements than other comparisons. Within a single comparison, the pilot lab often has performed 10 or more times as many measurements as any other lab, yet is usually accorded the same weight as any other lab in consistency testing. Similarly, if our intent for the aggregate is to report equitably on a set of comparisons, we have to address the reality that some comparisons are repeated at 5-day intervals [5] while others are repeated at 4-decade intervals [6] – the dynamic range in the number of measurements in a comparison can be at least 1000:1. In any aggregate over all mass comparisons and all time comparisons, we need both a method for equitable aggregation, *and* a simple explanation for why this method is appropriate.

The development of the chi-squared aggregate in Section 2.2 above can provide the simple insight we require for an appropriate way of balancing comparisons within the aggregate. There, we saw how each measurement was accorded equal weight by its equal contribution of variance to the variance of the  $\chi^2$  aggregate. If we wish to shift away from according equal weight to each measurement, and instead accord equal weight to each comparison (or group of comparisons), then all we need do is to define a weighted aggregate that scales the variance of each comparison's  $\chi^2$  (constrained aggregate) so that their scaled variances are equal.

Let us follow how this would apply to the simple case of aggregating  $J$  key comparisons in Equation 2. This would be a test of the claimed metrological compatibility of the results with the experiment's key comparison reference value (KCRV) for the  $j$ -th comparison,  $x_{0j}$ . Since  $x_{0j}$  is usually algorithmically derived from the  $\{x_{ij}\}$ , the variability of  $x_{0j}$  due to the variability expected from the claimed uncertainties of the  $\{x_{ij}\}$ , will need to be taken into account. Also, any departures of the uncertainty distributions from Gaussians, and any significant covariances will need to be considered. It is straightforward to do this by Monte Carlo simulation, and evaluate the means and variances that we will need for balancing the aggregated  $\chi^2$  across the  $J$  different comparisons.

For an audience of practical measurement scientists, we prefer to do the Monte Carlo simulation by resampling *measurements* from the uncertainty distributions, rather than resampling values for the measurand as we might do for an audience of theoreticians and statisticians. The processing for each KCRV is defined in terms of the concrete measurements, although for distributions that are symmetric about the reporting value the fiducial argument leads us to

conclude that there should be no difference [7]; and even for distributions that are asymmetric about their reporting mean value, the  $\chi^2$  is not expected to show any difference between these two resampling methods. To evaluate the characteristics of the  $\chi^2$  distributions, they are resampled from distributions with means constrained to agree with the mean of the reference value distribution – a simple implementation of this is to constrain the resampled measurements to be from zero-mean distributions. (In practice, we have found this to work well, even for median KCRVs.)

From this constrained model of the uncertainties (with agreement forced upon average values), in the Monte Carlo simulation we resample  $K$  times ( $K \sim 10^5$  or more) and index each set of resampled values with the index  $k$ :  $\{(x_{ij})_k\}$ . For the  $k$ -th set, the simulated KCRV for the  $j$ -th subset is  $(x_{0j})_k$ , obtained by the same algorithm as was used for the experimental KCRV.

Sometimes, the algorithm may involve steps, such as the presence or absence of specific methods for outlier rejection, that may not be definitively described for the experimental comparison – leading to difficulties in simulating the KCRV. If KCRVs create substantive difficulties, we advocate using pair-difference chi-squared-like statistics as a truly unmediated [8] test of the within-uncertainty interoperability of the experimental results of the comparisons [2], which can also be equitable aggregated across diverse comparisons [9].

Where the documentation allows the KCRVs to be simulated adequately, the  $k$ -th simulation run has its agreement-constrained chi-squared calculated as

$$\chi_k^2 = \sum_{j=1}^J a_j \sum_{i=1}^{I_j} \left[ \frac{(x_{ij})_k - (x_{0j})_k}{u(x_{ij} - x_{0j})} \right]^2 = \sum_{j=1}^J a_j (z_j)_k. \quad (3)$$

To obtain equitable treatment of the  $J$  comparisons, the weights  $\{a_j\}$  are chosen to each contribute equal broadening in the sum over the  $J$  terms of Equation 3. When the  $J$  comparisons are independent (actually, “uncorrelated” usually suffices, since we are using Monte Carlo simulation and rarely need to multiply marginal probability density functions), we can recognize that the variance of  $\chi_k^2$  will be the sum of the variances of the  $J$  comparisons, and the balancing of the comparisons is then very nearly a simple exercise in balancing variances.

The mean  $c_j$  of  $z_j$  is determined by resampling  $K$  times ( $10^5$  times or more)

$$c_j = K^{-1} \sum_{k=1}^K (z_j)_k = K^{-1} \sum_{k=1}^K \sum_{i=1}^{I_j} \left[ \frac{(x_{ij})_k - (x_{0j})_k}{u(x_{ij} - x_{0j})} \right]^2, \quad (4)$$

and the variance  $\text{var}_j$  of  $z_j$  about its mean is determined by

$$\text{var}_j = K^{-1} \sum_{k=1}^K [z_j - c_j]^2, \quad (5)$$

and since we want all the  $j$  broadenings of the chi-squared aggregate to balance, where each broadening is given by  $(a_j^2 \text{var}_j)$ , we assign the weights  $a_j$  as

$$a_j = \frac{b}{\sqrt{\text{var}_j}}, \quad (6)$$

where  $b$  is a constant that may be chosen to suit our convenience. Thus we can create a reduced chi-squared-like statistic, with a mean equal to 1. For independent comparisons, the overall mean is  $b \sum_{j=1}^J a_j c_j$ , so we would choose

$$b = \left[ \sum_{j=1}^J a_j c_j \right]^{-1} \quad (7-a)$$

to obtain a reduced chi-squared-like aggregate, whose agreement-constrained distribution has a mean value of 1.

If there are significant covariances between comparisons that are accounted for in the Monte Carlo model, a different Monte Carlo run should evaluate  $b$

$$b = \left[ K^{-1} \sum_{k=1}^K \sum_{j=1}^J a_j \sum_{i=1}^{I_j} \left[ \frac{(x_{ij})_k - (x_{0j})_k}{u(x_{ij} - x_{0j})} \right]^2 \right]^{-1}, \quad (7-b)$$

and the quality of the relative balancing from Equation 6 could then be judged by the departure from equality of the variance (evaluated by Monte Carlo simulation) of the  $J$  partial chi-square aggregates, each of  $J - 1$  comparisons, excluding in turn each comparison. This evaluates the equality of the broadening from the distribution of  $a_j z_j$  in its proper context of the broadening that it induces when it is the last comparison considered. If  $A$  is the overall Monte-Carlo variance of the weighted chi-squared of  $J$  comparisons, and  $B_j$  is the Monte Carlo variance of the  $J - 1$  comparisons (excluding comparison  $j$ ) then the variability of  $(A - B_j)^{1/2}$  quantifies how successful our balancing strategy has been. This could provide an “improved” balancing method, but the tolerance for residual imbalance would usually be quite large, and if the simple method doesn’t work well, it may be wiser to consider whether only one of the covariant comparisons should be included in the aggregation.

The same principles can be applied recursively to balance over diverse attributes [9]: measurements, artefacts, ranges, similar measurands, measurands in the same field, or all key comparisons under the auspices of a particular CC.

The aggregation can be restricted to focus on results involving a specific NMI, or a specific RMO; or could address the entire SI.

## 2.4. Scaled Convolution

In the context of CIPM key comparisons, new comparisons are always being added to the BIPM database. The definitive evaluation, accounting for any reported covariances between comparisons, would be done by repeating the Monte Carlo simulation. However, commonly the additional comparisons to be incorporated will be regarded as independent of other comparisons, and in this case a short-cut exists which may be helpful.

If we were not doing weighted aggregation, to combine a Monte Carlo histogram of the PDF of the current aggregate  $f(\zeta_1)$  with the Monte Carlo histogram of the chi-squared aggregate of the new comparisons  $g(\zeta_2)$ , we could numerically convolute them to get the PDF of the sum,  $\zeta = \zeta_1 + \zeta_2$ :  $f \otimes g(\zeta)$ .

For two independent random variables  $\xi$  and  $\psi$ , with PDFs  $f(\xi)$  and  $g(\psi)$ ; their general linear combination  $w = \alpha\xi + \beta\psi$ , can be shown to have a PDF given by a “scaled convolution”  $f \langle \alpha \otimes \beta \rangle g(w)$  (a non-standard operator):

$$f \langle \alpha \otimes \beta \rangle g(w) = \beta^{-1} \int_{-\infty}^{\infty} f(\xi) g\left(\frac{w - \alpha\xi}{\beta}\right) d\xi. \quad (8)$$

With  $\alpha = \beta = 1$ , we recover the familiar convolution integral, while for  $\alpha = 1$ ,  $\beta = -1$ , we recover the correlation integral. Numerical integration of Equation 8 could be used as an alternative to re-simulating the entire BIPM database for each new comparison:  $\alpha$  and  $\beta$  would be determined by the methods described above in Equations 4-7.

## 2.5. The Chi-squared-like Decision

In the aggregation over comparisons, after the weights  $\{a_j\}$  and the scale factor  $b$  have been determined, a final Monte Carlo run can create a histogram of the constrained  $\chi_k^2$  (Equation 3), approximating the constrained PDF of the  $\chi^2$  aggregate,  $PDF(z)$ . From the chosen tolerance  $T$  (e.g.  $T = 5\%$ ) for falsely rejecting the null hypothesis, we can obtain the corresponding cutoff value of  $\chi^2$ ,  $\chi_c^2$  from:

$$\int_{\chi_c^2}^{\infty} PDF(z) dz = T. \quad (9)$$

If  $\chi_e^2$ , the comparison’s experimental  $\chi^2$ , is greater than  $\chi_c^2$  then the agreement hypothesis is rejected by this criterion.

Equivalently, if  $\mathbf{P}$  (the integral of  $PDF(z)$  from  $z = \chi_e^2$  to  $\infty$ ) is less than  $\mathbf{T}$ , then the agreement hypothesis is rejected by this criterion. Even in the absence of a pre-agreed tolerance  $\mathbf{T}$ , the value of  $\mathbf{P}$  for this comparison allows anyone to use their own tolerance as the basis for their own decision about whether or not the agreement hypothesis is to be rejected.

### 3. Conclusion

A framework for aggregating and balancing diverse key comparisons has been presented, aiming at allowing chi-squared-like aggregates of dissimilar key comparisons to be used and appreciated with appropriate graphically-based explanations of the balancing. The underlying similarity that is the essence of the aggregation will still need to be crafted and presented for each new case.

### References

1. CIPM, Mutual recognition of national measurement standards and of calibration and measurement certificates issued by national metrology institutes,(1999). See [http://www.bipm.org/utils/en/pdf/mra\\_2003.pdf](http://www.bipm.org/utils/en/pdf/mra_2003.pdf) for the text of the arrangement, and for its Appendix B of comparison results see [http://kcdb.bipm.org/AppendixB/KCDB\\_ApB\\_search.asp](http://kcdb.bipm.org/AppendixB/KCDB_ApB_search.asp)
2. R. J. Douglas and A. G. Steele “Pair-difference Chi-squared Statistics for Key Comparisons” *Metrologia* **43** 89-97 (2006).
3. A. G. Steele and R. J. Douglas “Chi-squared Statistics for KCRV Candidates” *Metrologia* **42** 253-261 (2005).
4. M. G. Cox “The Evaluation of Key Comparison Data” *Metrologia* **39** 589-595 (2002).
5. CCTF K001.UTC See  
[http://kcdb.bipm.org/appendixB/KCDB\\_ApB\\_info.asp?cmp\\_idy=617&cmp\\_cod=CCTF-K001.UTC&prov=exalead](http://kcdb.bipm.org/appendixB/KCDB_ApB_info.asp?cmp_idy=617&cmp_cod=CCTF-K001.UTC&prov=exalead)
6. G. Girard “The Third Periodic Verification of National Prototypes of the Kilogram” (1988-1992) *Metrologia* **31** 317-336 doi: [10.1088/0026-1394/31/4/007](https://doi.org/10.1088/0026-1394/31/4/007) (1994)
7. R. J. Douglas, A.G. Steele, B.M. Wood and K.D. Hill, “A useful reflection”, *Metrologia* **42** (5), L35-L39, doi: [10.1088/0026-1394/42/5/L03](https://doi.org/10.1088/0026-1394/42/5/L03) (2005).
8. R.J. Douglas and A.G. Steele, “Avoiding a Complex Reference Value”, *Metrologia* **45**, L13 (2008).
9. A. G. Steele and R. J. Douglas “Establishing confidence from measurement comparisons” *Meas. Sci. Technol.* **19** doi: [10.1088/0957-0233/19/6/064003](https://doi.org/10.1088/0957-0233/19/6/064003) (2008).

## UNCERTAINTY EVALUATION FOR POSE ESTIMATION BY MULTIPLE CAMERA MEASUREMENT SYSTEM

MARC DOUILLY<sup>1,2</sup>, NABIL ANWER<sup>1</sup>, PIERRE BOURDET<sup>1</sup>,

NICOLAS CHEVASSUS<sup>2</sup>, PHILIPPE LE VACON<sup>2</sup>

<sup>1</sup>*LURPA, Ecole Normale Suprieure de Cachan, 61 Av du Prsident Wilson  
Cachan, 94230, France*

<sup>2</sup>*EADS IW, 12 Rue Pasteur  
Suresnes, 92150, France*

In this paper, a multiple camera measurement system is presented for the pose (position and orientation) estimation of a robot end-effector for assembly. First, a multiple camera geometric model is introduced for the 3D pose estimation of the end-effector and the identification of the intrinsic and extrinsic parameters of cameras. Second, an uncertainty propagation model is derived from the geometric model that enables the number of cameras to be chosen, the relative position between cameras and finally uncertainty evaluation for pose estimation. Experimental results are presented in the last section of this paper.

### 1. Introduction

Modern industrial trends in aeronautics and space have placed an increasing demand on the subject of robotics and robot manipulators and hence the attention of many researchers from different engineering and science areas. The emphasis on sensor-guided robots, off-line programming, robot calibration, to name a few, contributed to reach some sort of maturity and important research results toward efficiency and ease of use of robots for many applications (assembly and welding, product inspection and testing,...) through the enhancement of the accuracy, the speed and the flexibility of robots.

Robot calibration is the process of enhancing the accuracy of a robot manipulator through modification of the robot control software [1]. Calibration process encompasses four steps: Kinematic modeling, Pose measurement, Kinematic identification and Kinematic compensation. A wide account of robot calibration literature is provided in [2], [3] and [4].

Robot calibration can be done using multiple cameras setup. Position measurement using cameras first requires careful calibration of the cameras. These calibrated cameras define afterward the robot world coordinate frame. Optimal camera alignment [5] (number of cameras, relative pose) and evaluation of the accuracy of the resulting system is an important issue toward pose measurement.

In this paper, a multiple camera measurement system is presented for the pose estimation of a robot end-effector for assembly applications requiring extremely tight tolerances. First, a multiple camera geometric model is introduced for the 3D pose estimation of the end-effector and the identification of the intrinsic and extrinsic parameters of cameras. Second, an uncertainty propagation model is derived from the geometric model that enables the number of cameras to be chosen, the relative position between cameras and finally uncertainty evaluation for pose estimation. Experimental results and software development are presented in the last section of this paper.

## 2. Multiple camera geometric model

### 2.1. The Pin-hole model

The Pin-hole model [6] assumes a correspondence between real object point and image point through a straight line that passes through the focal point of the camera. Its also described as the linear projective transformation from the projective space  $\Re^3$  into the projective plane  $\Re^2$  represented as follows:

$$M_{\text{Cam}} = \begin{pmatrix} f_x & 0 & u_0 & 0 \\ 0 & f_y & v_0 & 0 \\ 0 & 0 & 1 & 0 \end{pmatrix} \begin{pmatrix} r_{11} & r_{12} & r_{13} & t_x \\ r_{21} & r_{22} & r_{23} & t_y \\ r_{31} & r_{32} & r_{33} & t_z \\ 0 & 0 & 0 & 1 \end{pmatrix} = \begin{pmatrix} m_{11} & m_{12} & m_{13} & m_{14} \\ m_{21} & m_{22} & m_{23} & m_{24} \\ m_{31} & m_{32} & m_{33} & m_{34} \end{pmatrix} \quad (1)$$

The camera matrix  $M_{\text{Cam}}$  contains intrinsic parameters (the scale factors and the image center) and extrinsic parameters (the transformation from world coordinates to the camera coordinates).

The world coordinates and the image coordinate systems are related by the following equations under undistorted camera model assumptions:

$$\begin{cases} u_C = \frac{m_{11}X_C + m_{12}Y_C + m_{13}Z_C + m_{14}}{m_{31}X_C + m_{32}Y_C + m_{33}Z_C + m_{34}} \\ u_C = \frac{m_{21}X_C + m_{22}Y_C + m_{23}Z_C + m_{24}}{m_{31}X_C + m_{32}Y_C + m_{33}Z_C + m_{34}} \end{cases} \quad (2)$$

It is now possible to express 3D world coordinates from the camera coordinates  $(u_{iC} \ v_{iC})^T$  when considering multiple camera system ( $1 \leq i \leq n$ ) by solving a standard least square fitting which minimize the location error of points in the image plane  $e = A \times b - c$  described as follows:

$$A = \begin{pmatrix} \vdots \\ m_{11,i} - m_{31,i}u_{iC} & m_{12,i} - m_{32,i}u_{iC} & m_{13,i} - m_{33,i}u_{iC} \\ m_{21,i} - m_{31,i}v_{iC} & m_{22,i} - m_{32,i}v_{iC} & m_{23,i} - m_{33,i}v_{iC} \\ \vdots \\ m_{34,i}u_{iC} - m_{14,i} & m_{34,i}v_{iC} - m_{24,i} & \vdots \end{pmatrix} \quad (3)$$

$$c = \begin{pmatrix} \vdots \\ X_C \\ Y_C \\ Z_C \end{pmatrix} \quad b = \begin{pmatrix} X_C \\ Y_C \\ Z_C \end{pmatrix}$$

The result can be written:

$$\begin{cases} X_C = f_1(\dots, u_{iC}, v_{iC}, \dots) \\ Y_C = f_2(\dots, u_{iC}, v_{iC}, \dots) \\ Z_C = f_3(\dots, u_{iC}, v_{iC}, \dots) \end{cases} \quad (4)$$

## 2.2. Pose calculation

Least square fitting is also used to calculate the pose of a marked object. The position of markers on the object  $C_{Obj,j}$  ( $X_{Obj,j} \ Y_{Obj,j} \ Z_{Obj,j}$ )<sup>T</sup>,  $1 \leq j \leq p$  ( $p$  markers) is known and  $C_{Meas,j}$  ( $X_{Meas,j} \ Y_{Meas,j} \ Z_{Meas,j}$ )<sup>T</sup>,  $1 \leq j \leq p$  is measured by the multiple camera system yielding to the following equation where  $P_{Obj,Meas}$  is the Pose Matrix:

$$\begin{aligned} C_{Meas,j} &= P_{Obj,Meas} \cdot C_{Obj,j} \\ \text{or} \\ P_{Obj,Meas} &= g(C_{Meas,j}, C_{Obj,j}), 1 \leq j \leq p \end{aligned} \quad (5)$$

## 2.3. Visibility model

To track the robot end-effector, all its positions in the working volume need to be visible through the placed reference markers on the end-effector. A Marker Visibility Volume (a set of geometrical properties that allow an optimal camera position) is defined for each marker position on the robot end-effector.

Visibility volumes intersection and camera field of view enables then to extract a set of optimal positions and orientations of cameras (Fig. 1).

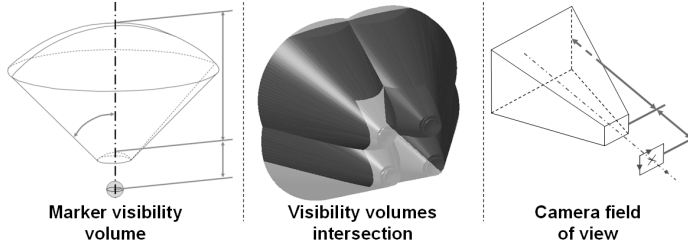


Fig. 1. Visibility model for the optimal relative pose of cameras

### 3. Uncertainty evaluation

From a metrological view camera-based measurement have a stated measurement uncertainty. In real applications the final measurement uncertainty is affected by many factors such as illumination, edge effects, the operator, and non-regularities of the object to be measured.

The study carried out here explores uncertainty on the position of the centers of markers when their position on the camera coordinate system is measured (Eq. 3 and Eq. 4).

According to [7] and [8] several approaches to propagating uncertainty could be used. One approach is to use Monte Carlo methods, which is highly general but computationally expensive. Our approach uses an analytical method based on covariance propagation method expressed as follows:

$$\text{Cov}(f(\dots, u_{iC}, v_{iC}, \dots)) = J_{f/\vec{u}} \times \text{Cov}(\vec{u}) \times J_{f/\vec{u}}^T, 1 \leq i \leq n$$

$$\text{Cov}(\vec{u}) = \begin{pmatrix} \ddots & & & 0 \\ & \text{Var}(u_{iC}) & \text{cov}(u_{iC}, v_{iC}) & \\ & \text{cov}(v_{iC}, v_{iC}) & \text{Var}(u_{iC}) & \\ 0 & & & \ddots \end{pmatrix} \quad (6)$$

$$J_{f/\vec{u}} = \begin{pmatrix} \frac{\partial f_1}{\partial u_{1C}} & \frac{\partial f_1}{\partial v_{1C}} & \dots & \frac{\partial f_1}{\partial u_{nC}} & \frac{\partial f_1}{\partial v_{nC}} \\ \frac{\partial f_2}{\partial u_{1C}} & \frac{\partial f_2}{\partial v_{1C}} & \dots & \frac{\partial f_2}{\partial u_{nC}} & \frac{\partial f_2}{\partial v_{nC}} \\ \frac{\partial f_3}{\partial u_{1C}} & \frac{\partial f_3}{\partial v_{1C}} & \dots & \frac{\partial f_3}{\partial u_{nC}} & \frac{\partial f_3}{\partial v_{nC}} \end{pmatrix}$$

$\text{Cov}(\vec{u})$  : Covariance matrix of centers of a marker on  $n$  image planes  
 $J_{f/\vec{u}}$  : Jacobian matrix of  $f$  around  $C$  ( $1 \leq i \leq n$ ) on each camera

$$\text{Cov}(f(\vec{u})) = \begin{pmatrix} \text{Var}(X_C) & \text{cov}(X_C, Y_C) & \text{cov}(X_C, Z_C) \\ \text{cov}(Y_C, X_C) & \text{Var}(Y_C) & \text{cov}(Y_C, Z_C) \\ \text{cov}(Z_C, X_C) & \text{cov}(Z_C, Y_C) & \text{Var}(Z_C) \end{pmatrix} \quad (7)$$

Once we obtain the covariance matrix for a given marker in the measurement space, we can apply the same method to estimate uncertainties for  $p$  points of an object seen by  $n$  cameras to extract uncertainties on the orientation and the position of the object in the measurement space:

$$\text{Cov}(g(\mathbf{C}_{\text{Meas},j}, \mathbf{C}_{\text{Obj},j})) = J_{g/\bar{c}} \cdot \text{Cov}(\mathbf{C}_{\text{Meas},j}, \mathbf{C}_{\text{Obj},j}) \cdot J_{g/\bar{c}}^T \quad (8)$$

#### 4. Experimental results

Experiments based on a two cameras measurement system are shown to validate the uncertainty propagation application. (Fig. 2) depicts the measurement of the center of a marker on each camera (10 000 measurement). (Fig. 3) shows the resulting calculation of the corresponding 3D point (world coordinates system).

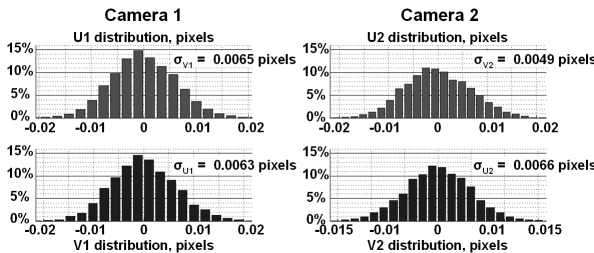


Fig. 2. Experimental results on image planes (2 cameras)

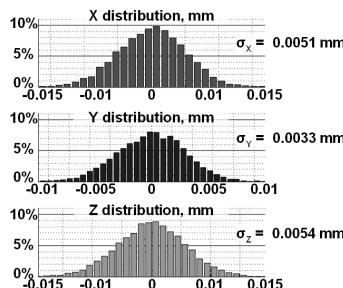


Fig. 3. Experimental results of the corresponding 3D point

Monte Carlo simulation is used here as a sampling method for analyzing uncertainty propagation. Inputs (coordinates on image plane) are randomly generated from probability distributions (normal or uniform) using MINITAB®. Results of the simulation are showed here (Fig. 4 and Fig. 5).

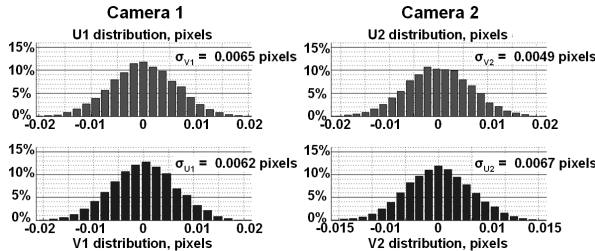


Fig. 4. Sampling on image planes (2 cameras)

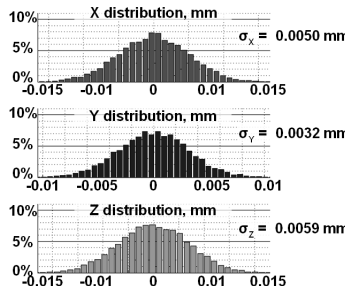


Fig. 5. Stochastic uncertainty propagation results

MAPLE® software has been used to calculate an explicit solution of the analytical model based on covariance propagation (Eq. 6). The covariance matrix of the corresponding 3D point (Eq. 7) is computed and the results as highlighted hereafter show similar results (experimental, stochastic uncertainty propagation and explicit solution for covariance propagation).

$$\text{Cov}(f(\vec{\bar{u}})) = \begin{pmatrix} 2.533e^{-5} & -1.828e^{-6} & -1.828e^{-6} \\ -1.828e^{-6} & 2.533e^{-5} & -1.828e^{-6} \\ -1.558e^{-5} & -1.828e^{-6} & 2.533e^{-5} \end{pmatrix} \quad \begin{aligned} \sigma_X &= 0.0050\text{mm} \\ \sigma_Y &= 0.0032\text{mm} \\ \sigma_Z &= 0.0068\text{mm} \end{aligned} \quad (9)$$

## 5. Conclusion

This paper presents models used for the setup and the validation of a multiple camera based measurement system for the pose estimation of a robot end-effector.

The multiple camera model based on linear projective transformation on image plane coupled with the visibility model lead to a geometric model for multiple camera measurement (number of cameras and relative position and orientation between cameras) and enable world coordinates calculation and 3D object pose estimation.

The study carried out here explores uncertainty on the position of the centers of markers when their position on the camera coordinate system is measured. The uncertainty propagation approach described here is based on stochastic uncertainty propagation as well as an explicit solution for covariance propagation.

Experimental results showed similar results compared to stochastic uncertainty propagation and explicit solution for covariance propagation when using two cameras.

## References

1. Hanqi Zhuang, Zvi S. Roth, *Camera-Aided Robot Calibration*, CRC Press (1996)
2. Kevin L. Conrad, Panayiotis S. Shiakolas, *Robotic Calibration Issues : Accuracy, Repeatability and Calibration*, 8<sup>th</sup> Mediterranean Conference on Control & Automation, Patras, Greece (2000)
3. Hans-Gerd Mass, *Dynamic Photogrammetric Calibration of Industrial Robots*, Videometrics V, SPIE Proceedings Series Vol. 3174, SPIEs 42nd Annual Meeting, San Diego (1997)
4. Albin Sunnanbo, *Laser Feedback Control for Robotics in Aircraft Assembly*, PhD thesis, Linkping, (2003)
5. Philippe A. Cefontaine, Marc Schirski, Daniel Bndgens and Torsten Kuhlen, *Camera Setup Optimization for Optical Tracking in Virtual Environments*, Eurographics Symposium on Virtual Environments, (2006)
6. Radu Horaud, Olivier Monga, *Vision par ordinateur*, p.151-153, (1995)
7. NF ENV 13005 : *Guide to the expression of uncertainty in measurement*, (1999)
8. Joint committee for guides in metrology, *Evaluation of measurement data - Supplement 1 to the Guide to the expression of uncertainty in measurement, Propagation of distributions using a Monte Carlo method*, (2006)

## ANALYSIS OF DYNAMIC MEASUREMENTS: COMPENSATION OF DYNAMIC ERROR AND EVALUATION OF UNCERTAINTY

CLEMENS ELSTER, ALFRED LINK

*Physikalisch-Technische Bundesanstalt Berlin  
Abbestrasse 2-12, 10587 Berlin, Germany*

Sensors employed for dynamic measurements often show a non-perfect dynamic behaviour. By taking the instantaneous output of the sensor as an estimate of the time-dependent value of the measurand, the so-called dynamic error emerges. We assume that a linear time-invariant system is appropriate to model the dynamic input-output behaviour of the sensor, and we propose digital filtering for the compensation of the dynamic error. A procedure for the design of the digital compensation filter is described, and the evaluation of the uncertainty associated with the application of this filter is considered. Finally, the benefit of the dynamic compensation and proposed uncertainty treatment is illustrated in terms of simulations for a particular relevant dynamic model.

### 1. Introduction

The task of analyzing dynamic measurements is encountered in many applications such as the determination of a time-dependent force or acceleration [1], or the analysis of atmospheric measurements [2]. Typically, the sensors employed for these measurements show a non-ideal dynamic behaviour, i.e. the instantaneous output of these sensors depends not only on the instantaneous value of the measurand but also on its past values. While the goal in the design of the sensors is to attenuate these dynamic effects by adding appropriate analogue filters [3], they often cannot be fully eliminated. When using the instantaneous sensor output as an estimate of the measurand, the dynamic error is introduced which often is ignored [4]. For instance, for accelerometers the current standard [5] for dynamic calibration upon shock excitations determines the ratio of the peak amplitudes of the accelerometer output signal and the applied excitation. Such proceeding, however, is appropriate only for low frequency shocks [6].

Often, the assumption of a linear and time-invariant (LTI) system is appropriate for the description of the input-output behaviour of a sensor. Then, the dynamic error can be eliminated or reduced by subsequent digital filtering,

cf., e.g., [7-10]. We propose to construct such a compensation filter as a cascade of a correction filter and a lowpass filter. The lowpass filter ensures that high frequency noise is attenuated. The correction filter is designed such that its frequency response approximates the reciprocal of the frequency response of the sensor within the frequency range of interest. For the calculation of the filter coefficients, a least-squares procedure is proposed. Application of the compensation filter to the discretized and quantized sensor output signal then yields a discrete-time estimate of the measurand. The evaluation of uncertainty associated with this estimate is considered in the framework of the GUM [11], taking into account the uncertainties associated with the sensor model as well as a noise process which is assumed to model analogue-to-digital conversion errors. Closed formulae are given for an FIR-type compensation filter. We finally illustrate the proposed analysis in terms of simulations for a second-order model cascaded by an additional analogue fourth-order Bessel lowpass filter.

## 2. Sensor Model and Estimation Task

Figure 1 shows schematically the considered measurement process. The time-dependent value  $x_c(t)$  of the measurand acts as the input to the sensor whose output is denoted by  $y_c(t)$ . A subsequent analogue-to-digital conversion (ADC) yields the discrete-time signal  $y(n)$ ,  $n = 0, 1, \dots$ . This signal is processed by the compensation filter to obtain the discrete-time estimate  $\hat{x}(n)$  of  $x_c(t)$  at the times  $t_n = n \cdot T_s$ , where  $f_s = 1/T_s$  denotes the sampling frequency. We model ADC errors by a zero-mean stationary noise process  $W(n)$  and we assume knowledge about its autocovariance function  $c_\tau = E[W(n)W(n+\tau)]$ . We therefore assign the uncertainties  $u(y(n)) = \sqrt{c_0}$  and  $u(y(n), y(n+\tau)) = c_\tau$  to the discrete-time output signal  $y(n)$  which serves as the input to the compensation filter.



Figure 1. Block scheme of measurement and subsequent compensation.

We assume that the sensor can be modelled by the continuous-time LTI system with system function

$$G(s) = \sum_{k=0}^L B_k s^k / \left( 1 - \sum_{k=1}^M A_k s^k \right). \quad (1)$$

$G(s)$  may include an analogue anti-aliasing filter preceding the ADC. If we denote by  $X(s)$  and  $Y(s)$  the Laplace transforms of  $x_c(t)$  and  $y_c(t)$ , then  $Y(s) = G(s)X(s)$  holds. The frequency response of the LTI system (1) is given by  $G(j\Omega)$ , and  $|G(j\Omega)|$  is assumed to not approach zero within the radian frequency range  $|\Omega| \leq \bar{\Omega}$  of interest. Also, the spectrum of  $x_c(t)$  and hence that of  $y_c(t)$  is assumed to be (essentially) zero for  $|\Omega| > \bar{\Omega}$ . Finally, the sampling frequency  $f_s$  has been chosen large enough so that the Nyquist frequency  $f_s/2$  exceeds  $\bar{\Omega}/2\pi$ .

The parameters  $\theta = (A_1, \dots, A_M, B_0, \dots, B_L)^T$  of the system function (1) need to be determined by dynamic calibration measurements. We assume that the LTI system (1) has been identified by analyzing dynamic calibration measurements [12, 13]; cf. [14] for the particular example of accelerometer identification. In the following we assume that an estimate  $\hat{\theta}$  of the parameters  $\theta$  including the associated uncertainty matrix  $U(\hat{\theta})$  is available where  $[U(\hat{\theta})]_{kl} = u(\hat{\theta}_k, \hat{\theta}_l)$ . The estimate  $\hat{\theta}$  is assumed to be independent of the  $y(n)$ . The task to be considered is to determine estimates  $\hat{x}(n)$  of  $x_c(t)$  at the discrete times  $t_n = n \cdot T_s$  together with associated uncertainties  $u(\hat{x}(n))$  and  $u(\hat{x}(n), \hat{x}(n+m))$ .

### 3. Design of Compensation Filter and Dynamic Estimation

The compensation filter is constructed as a cascade of a digital correction filter and a digital lowpass filter. The correction filter is designed such that its frequency response approximately equals the reciprocal of the frequency response of the sensor within the frequency region  $|\Omega| \leq \bar{\Omega}$  of interest. The role of the lowpass filter is to damp high (ADC) frequency noise. Within  $|\Omega| \leq \bar{\Omega}$ , the lowpass filter should have no essential influence. Since correction and lowpass filter are both LTI systems, the order of their application has no influence. The design of the digital filters follows well-known techniques of digital signal processing, cf. [15].

#### 3.1. Correction Filter

Let

$$g_{\text{cor}}(z) = \sum_{k=0}^{L_{\text{cor}}} b_{\text{cor},k} z^{-k} \left/ \right( 1 - \sum_{k=1}^{M_{\text{cor}}} a_{\text{cor},k} z^{-k} \right. \quad (2)$$

denote the system function of the sought digital correction filter. The frequency response  $F(\Omega)$  of (the mixed continuous-time discrete-time system given by) the sensor system (1) followed by an ideal ADC and the digital filter (2) is

$$F(\Omega) = G(j\Omega)g_{\text{cor}}(e^{j\Omega/f_s}). \quad (3)$$

That is, for the continuous-time input  $x_c(t) = e^{j\Omega t}$ , the discrete-time output  $y(n)$  is given by  $y(n) = F(\Omega) \cdot e^{j\Omega n/f_s}$ . Ideally, the correction filter compensates the influence of the sensor, and the frequency response  $F(\Omega)$  equals one within the frequency region  $|\Omega| \leq \bar{\Omega}$  of interest. The coefficients of the correction filter can be determined by minimizing a sum of weighted least-squares

$$\sum_k w_k |e^{-j\Omega_k \tau_{\text{cor}}} / G(j\Omega_k) - g_{\text{cor}}(e^{j\Omega_k/f_s})|^2 \quad (4)$$

at suitably chosen frequencies  $\Omega_1, \Omega_2, \dots$ . The additional inclusion of the linear phase  $e^{-j\Omega_k \tau_{\text{cor}}}$  in (4) shifts the output of the correction filter by the time  $\tau_{\text{cor}}$ . Provided that the time delay  $\tau_{\text{cor}}$  has been chosen appropriately and that the order of the correction filter is sufficiently high, a good approximation can be reached [16]. The weighting scheme in (4) may be extended to a non-diagonal weighting matrix.

When an IIR filter is designed, i.e.  $M_{\text{cor}} > 0$  in (2), care must be taken in order to obtain a stable filter; in this case, the optimization must constrain the poles of (2) to be within the unit circle. In contrast to an IIR filter, no constraints need to be considered for the design of an FIR correction filter in order to guarantee its stability. Furthermore, the determination of its coefficients according to the minimization of (4) can be done by *linear* least-squares.

For the remainder of this paper we consider the case of an FIR correction filter  $g_{\text{cor}}(z)$ . The determination of its coefficients by minimizing (4) is an ordinary least-squares task which is solved in terms of linear algebra, cf. [17]. Since the estimates  $\hat{\theta}$  of the parameters of the LTI system (1) are uncertain, so is the estimate of the frequency response  $G(j\Omega_1), G(j\Omega_2), \dots$  derived from them and entering into (4). The uncertainties  $U(\hat{\theta})$  associated with  $\hat{\theta}$  are easily propagated through the least-squares analysis to yield the uncertainties associated with the obtained estimates of the coefficients of the correction filter. Care must be taken in case the design matrix of the linear least-squares task is ill-conditioned; in this case a minimum norm solution should be chosen which is obtained in terms of an SVD of the design matrix of the least-squares problem, cf. [17].

### 3.2. Lowpass Filter

Typically, the frequency response of a sensor decays at higher frequencies. Therefore, the gain of the correction filter is expected to grow (rapidly) for high frequencies. The lowpass filter is applied to damp this behaviour and to attenuate high frequency noise. The lowpass filter is designed such that the frequency region  $|\Omega| \leq \bar{\Omega}$  of interest is within its passband, and that a sufficient damping is reached for high frequencies. The frequency response  $F(\Omega)$  of the sensor system (1) followed by a digital lowpass filter  $g_{\text{low}}(z)$  and the correction filter  $g_{\text{cor}}(z)$  is given by

$$F(\Omega) = G(j\Omega) g_{\text{cor}}(e^{j\Omega/f_s}) g_{\text{low}}(e^{j\Omega/f_s}). \quad (5)$$

A precise filter design task would require to quantify the filter behaviour within the passband and within the stop band. We propose to use a linear phase FIR filter using windowing techniques [15] and to control its cutoff frequency. The order of the filter has to be chosen high enough so that a large (prescribed) attenuation of the frequency response (5) as well as of  $g_{\text{cor}}(e^{j\Omega/f_s}) g_{\text{low}}(e^{j\Omega/f_s})$  in the stopband is reached. The lowpass filter introduces the additional linear phase  $e^{-j\Omega\tau_{\text{low}}}$ , so that ideally (5) reads  $F(\Omega) = e^{-j\Omega\tau}$  within  $|\Omega| \leq \bar{\Omega}$  where  $\tau = \tau_{\text{low}} + \tau_{\text{cor}}$ .

### 3.3. Dynamic Estimation

The time-dependent value of the measurand is estimated by applying in sequence the lowpass and the correction filter to the discretized and quantized sensor output, cf. figure 1. Let

$$y_{\text{low}}(n) = \sum_{k=0}^{L_{\text{low}}} b_{\text{low},k} \cdot y(n-k) \quad (6)$$

denote the lowpass filtered sensor output signal, and

$$x(n - n_{\tau}) = \sum_{k=0}^{L_{\text{cor}}} b_{\text{cor},k} \cdot y_{\text{low}}(n-k) \quad (7)$$

the output of the correction filter when applied to the lowpass filtered sensor signal.  $n_{\tau} = (\tau_{\text{cor}} + \tau_{\text{low}})/T_S$  denotes the known time shift induced by the correction and the lowpass filter. Relation (7) together with (6) can be viewed as a model in terms of the GUM [11]. By inserting the estimates  $\hat{y}(n)$  (i.e. the recorded sensor output signal) and the estimates  $\hat{b}_{\text{cor},k}$  of the filter coefficients

$b_{\text{cor},k}$  of the correction filter into (6) and (7), the estimates  $\hat{x}(n - n_\tau)$  are obtained.

#### 4. Uncertainty Evaluation

The subsequent uncertainty evaluation assumes that reconstruction errors of the evaluation model (7) can be neglected, i.e. the size of these errors is assumed to be small as compared to resulting uncertainties (10). To ease notation, we introduce the vectors  $\hat{\mathbf{y}}_{\text{low}}(n) = (\hat{y}_{\text{low}}(n), \dots, \hat{y}_{\text{low}}(n - L_{\text{cor}}))^T$  where  $L_{\text{cor}}$  denotes the order of the FIR correction filter in (7) and its coefficients  $\hat{\mathbf{b}} = (\hat{b}_{\text{cor},0}, \dots, \hat{b}_{\text{cor},l})^T$  with  $l = L_{\text{cor}}$ . Since the lowpass filter coefficients in (6) are known, the uncertainty matrix  $\mathbf{U}(\hat{\mathbf{y}}_{\text{low}}(n))$  with elements  $[\mathbf{U}(\hat{\mathbf{y}}_{\text{low}}(n))]_{(l+1)(m+1)} = u(\hat{y}_{\text{low}}(n-l), \hat{y}_{\text{low}}(n-m))$  associated with  $\hat{\mathbf{y}}_{\text{low}}(n)$  is determined from the relations

$$u(\hat{y}_{\text{low}}(n), \hat{y}_{\text{low}}(n+m)) = \sum_{k_1=0}^{L_{\text{low}}} \sum_{k_2=0}^{L_{\text{low}}} b_{\text{low},k_1} \cdot b_{\text{low},k_2} \cdot c_{m+k_1-k_2}, \quad (8)$$

where  $c_\tau$  denotes the given autocovariance function of the noise process  $W(n)$  modelling ADC errors. Note that the right hand side of (8) does not depend on  $n$ . Using the compact notation and inserting estimates, we obtain from (7)

$$\hat{x}(n - n_\tau) = \hat{\mathbf{b}}^T \hat{\mathbf{y}}_{\text{low}}(n), \quad (9)$$

from which

$$\begin{aligned} & u^2(\hat{x}(n - n_\tau)) \\ &= \hat{\mathbf{b}}^T \mathbf{U}(\hat{\mathbf{y}}_{\text{low}}(n)) \hat{\mathbf{b}} + \hat{\mathbf{y}}_{\text{low}}^T(n) \mathbf{U}(\hat{\mathbf{b}}) \hat{\mathbf{y}}_{\text{low}}(n) + \text{Tr}(\mathbf{U}(\hat{\mathbf{y}}_{\text{low}}(n)) \mathbf{U}(\hat{\mathbf{b}})) \end{aligned} \quad (10)$$

follows, cf. also [10]. In (10),  $\text{Tr}$  denotes trace of a square matrix, and  $\mathbf{U}(\hat{\mathbf{b}})$  denotes the uncertainty matrix associated with the estimated parameters of the correction filter. Note that the result (10) would be obtained by a propagation of distributions [18,19], irrespective of the particular form of the distribution assigned to the input quantities, provided that its first and second order moments are consistent with the given estimates and uncertainty matrices. Application of the GUM (first-order Taylor series expansion) would yield only the first two terms on the right hand side of (10). For the covariances,

$$\begin{aligned} & u(\hat{x}(n - n_\tau), \hat{x}(m - n_\tau)) = \hat{\mathbf{b}}^T \mathbf{U}(\hat{\mathbf{y}}_{\text{low}}(n)) \hat{\mathbf{y}}_{\text{low}}^T(m) \hat{\mathbf{b}} \\ &+ \hat{\mathbf{y}}_{\text{low}}^T(n) \mathbf{U}(\hat{\mathbf{b}}) \hat{\mathbf{y}}_{\text{low}}(m) + \text{Tr}(\mathbf{U}(\hat{\mathbf{y}}_{\text{low}}(n)) \hat{\mathbf{y}}_{\text{low}}^T(m) \mathbf{U}(\hat{\mathbf{b}})) \end{aligned} \quad (11)$$

is obtained, where

$$[\mathbf{U}(\hat{\mathbf{y}}_{\text{low}}(n)\hat{\mathbf{y}}^T_{\text{low}}(m))]_{(k+1)(l+1)} = u(\hat{\mathbf{y}}_{\text{low}}(n-k), \hat{\mathbf{y}}_{\text{low}}(m-l)). \quad (12)$$

When the uncertainty matrix  $\mathbf{U}(\hat{\mathbf{b}})$  is small and can be neglected, the uncertainties (10) and covariances (11) are independent of the measurand and can be calculated in advance. Note that estimation and calculation of uncertainties may be carried out in real time, cf. [10].

## 5. Example

The sensor model  $G(s) = G_{\text{2nd}}(s)G_B(s)$  is considered for an illustration where

$$G_{\text{2nd}}(s) = S_0 \frac{\omega_0^2}{s^2 + 2\delta\omega_0 s + \omega_0^2} \quad (13)$$

is a second-order model with static gain  $S_0$ , damping  $\delta$  and resonance frequency  $\omega_0$ , and  $G_B(s)$  is the system function of an analogue fourth order Bessel filter with cutoff frequency  $\omega_A$ . The second-order model is appropriate to describe, for instance, the input-output behaviour of accelerometers [14]. The Bessel filter represents an additional analogue filter designed to attenuate ‘ringing’, cf. results below. We used the model  $G(s) = G_{\text{2nd}}(s)G_B(s)$  to illustrate the procedures and to conduct simulations, where the parameters  $S_0 = 1$ ,  $\delta = 0.02$ ,  $f_0 = f_A = 50$  kHz and  $f_s = 500$  kHz were chosen.

Figure 2 shows the frequency response of the sensor system, the compensation filter and the compensated sensor system. The frequency response of the compensated sensor system has a linear phase response and shows below 80 kHz only a small deviation of its magnitude from one. The correction filter has been determined using an FIR filter with 20 coefficients and an additional delay of  $\tau_{\text{cor}} = 10 \cdot T_s$ . For the least-squares fit, 200 equidistantly spaced frequencies up to 100 kHz were used using uniform weights. As lowpass filter, an order 60 windowed (Kaiser window with Kaiser window parameter 8) linear phase lowpass FIR filter was chosen with cutoff frequency 75 kHz, implying an additional delay of  $\tau_{\text{low}} = 30 \cdot T_s$ . For the simulations, we used the Gaussian test signal shown in Figure 3 whose spectrum has support in the resonance region of the second-order system. Figure 3 also shows the difference between this test signal and the (numerically determined, time-shifted) sensor output signal with and without subsequent digital filtering.

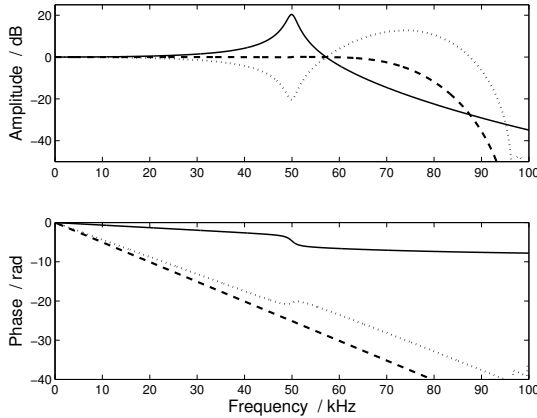


Figure 2. Frequency response of the sensor system with (dashed) and without (solid) compensation. The dotted curve shows the frequency response of the compensation filter.

The sensor output signal shows oscillations ('ringing') caused by the resonance of the second-order system which are also observed in real acceleration measurements. For this example, the size of the dynamic error reaches 10%. The compensation filter eliminates the distortion of the sensor output signal.

In a next step, we ran many simulations to assess the performance of the compensation filter and to also consider the proposed uncertainty evaluation. Here, also additive noise was included in the sensor output signal which models quantization (and possibly other) errors. For this we used white Gaussian noise with standard deviation  $\sigma = 0.001$ . For the analysis of the data, however, different parameters were used than those used for numerically calculating the sensor output. More precisely, for each single simulation run, parameters  $\hat{\theta}$  used for the *analysis* were drawn from an  $N(\theta, U(\hat{\theta}))$  distribution, where  $U(\hat{\theta})$  was assumed diagonal with relative uncertainties for  $S_0$ ,  $f_0$  and  $\delta$  of 0.2%, 2% and 20%, respectively. In this way, the uncertainty of the parameters used for the analysis was reflected. Using 200 repeated simulations, we then conducted the root mean square errors of the estimated input signal as well as the (ensemble) mean of the uncertainties calculated for each estimate. Figure 4 shows the corresponding results. The root mean square errors appear to be in good accordance with mean uncertainties. The calculated uncertainties showed only a small variation between the different simulation runs.

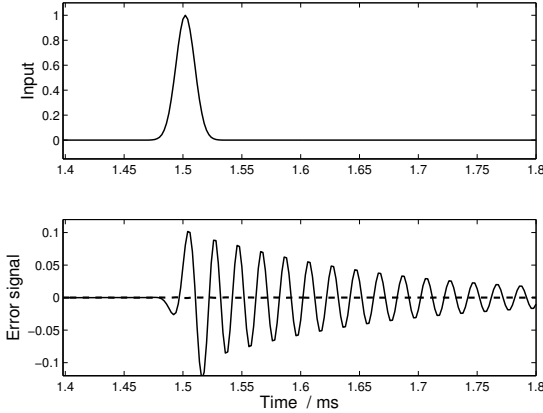


Figure 3. Top: Gaussian test signal. Bottom: Difference signal between sensor input and output with (dashed) and without (solid) subsequent application of the digital compensation filter.

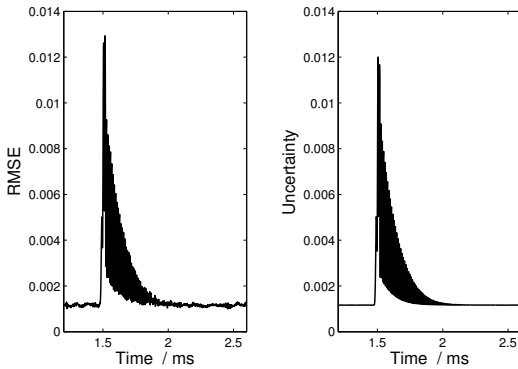


Figure 4. Results for dynamic analysis. Left: Root mean square errors (RMSE). Right: Mean of uncertainties  $u(\hat{x}(n))$  for Gaussian test signal and  $\sigma = 10^{-3}$  for size of sensor output noise.

## 6. Conclusion

Digital filtering has been proposed for the compensation of dynamic errors when the input-output behaviour of the employed sensor is governed by linear time-invariant system. Uncertainty evaluation has been considered, taking into account a noise process modelling ADC errors as well as the uncertainty associated with the sensor model. The proposed analysis has been assessed in terms of simulations. The results show that the dynamic analysis allows improved estimates and uncertainties to be determined. It is concluded that

metrology can benefit from the application the proposed techniques in the field of dynamic measurements.

## References

1. T. Bruns, A. Link and C. Elster, *Proc. of XVIII IMEKO World Congress*, Rio de Janeiro, Brazil (2006).
2. B. Saggin, S. Debei and M. Zaccariotto, *Measurement* **30**, 223 (2001).
3. M. Jafaripanah, B. M. Al-Hashimi and N. M. White, *IEEE Trans. Instrum. Meas.* **54**, 245 (2005).
4. J. P. Hessling, *Meas. Sci. Technol.* **17**, 2740 (2006).
5. ISO, International Standard 16063-13, International Organization for Standardization, Geneva (2001).
6. A. Link, A. Täubner, W. Wabinski, T. Bruns and C. Elster, *Measurement* **40**, 928 (2007).
7. R. Pintelon, Y. Rolain, M. Vanden Bossche and J. Schoukens, *IEEE Trans. Instrum. Meas.* **39**, 116 (1990).
8. I. Kollar, R. Pintelon, Y. Rolain, J. Schoukens, *IEEE Trans. Instrum. Meas.* **40**, 659 (1991).
9. A. L. Shestakov, *IEEE Trans. Instrum. Meas.* **45**, 250 (1996).
10. C. Elster, A. Link and T. Bruns, *T. Meas. Sci. Technol.* **18**, 3682 (2007).
11. BIPM, IEC, IFCC, ISO, IUPAC, IUPAP and OIML. *Guide to the Expression of Uncertainty in Measurement* Geneva, Switzerland: International Organization for Standardization ISBN 92-67-10188-9 (1995).
12. R. Pintelon and J. Schoukens. *System identification: a frequency domain approach*, IEEE Press, Piscataway (USA) (2001).
13. L. Ljung. *System identification: Theory for the user*, Prentice Hall, 2<sup>nd</sup> edition (1999).
14. A. Link, A. Täubner, W. Wabinski, T. Bruns and C. Elster, *Meas. Sci. Technol.* **17**, 1888 (2006).
15. A. V. Oppenheim and R. W. Schafer. *Discrete-Time Signal Processing*, Prentice Hall, Englewood Cliffs, NJ (1989).
16. R. Vuerinckx, Y. Rolain, J. Schoukens and R. Pintelon, *IEEE Trans. Signal Process.* **44**, 2339 (1996).
17. G. H. Golub and C. F. van Loan. *Matrix Computations*, The John Hopkins University Press, Baltimore and London (1996).
18. BIPM, IEC, IFCC, ILAC, ISO, IUPAC, IUPAP, and OIML. Supplement 1 to the “Guide to the expression of uncertainty in measurement”. Joint Committee for Guides in Metrology, Bureau International des Poids et Mesures, JCGM 101, to appear
19. M. G. Cox and B. R. L. Siebert, *Metrologia* **43**, 178 (2006).

## AN APPROACH TO UNCERTAINTY USING NESTED ANALYSIS

MARIA DO CÉU FERREIRA, ANDREIA FURTADO, EDUARDA FILIPE

*Portuguese Institute for Quality  
Rua António Gião, 2  
2829-513 Caparica Portugal*

This communication focuses the Portuguese experience in the field of the refractometers metrological requirements, namely the analyses of variance with a nested experimental design applied to the liquid standards used in metrological control.

### 1. Introduction

The refractometers are instruments, which measure the refractive index using the phenomenon of light refraction. According the most common definitions, the refractive index  $n$  of a homogeneous substance is the ratio of the speed of light in vacuum to the speed of light in the substance concerned.

One important application of refractometry in the field of metrology is the measurement of sugar in the must of the grape, which foresees the alcoholic concentration of the produced wine. The refractive index for grape must and sugar solutions are expressed relative to that of air and the white light. It is a dimensionless quantity (dimension 1).

Within the framework of Portuguese Metrological System, a regulation was put in force in 1992 that establishes the operational procedures as well as the requirements of the National Legal System. Consequently, all refractometers models approved by the Portuguese Institute for Quality (IPQ) are subject to legal verification, which is undertaken according to the OIML<sup>1</sup> recommendation. By this recommendation the standards are used to carry out tests for metrological control and to calibrate instruments before and after the tests performed using vintaging musts. The chemical-physical principle applied is related with the must fermentation, which produce a representative quantity of alcohol, where the sugar concentration is proportional to the expected alcoholic content, in terms of percent volume of alcohol (% vol).

## 2. Standard's Preparation

The standards used in the verification of refractometers should be standard solutions of saccharose or glucose. Due to unstable saccharose solution, glucose solutions are generally used. To prepare such solution, it used mustard essence (allyl isothiocyanate), tartaric acid and purified water in three different mass concentrations, by gravimetric method at  $(20\pm 5)$  °C and normal atmospheric pressure. For each standard, the mass fraction is determined from the refractive index displayed by the standard refractometer. The relationship is in agreement with OIML R 124 table giving the correspondence between the refractive index and conventional sugar mass fraction of the must (expressed as %). Three different standards were prepared with different sugar concentration (and proportional % vol. of alcohol): 6% vol, 11% vol and 16% vol. Such solutions were kept in a cool and dark environment.

## 3. Measurement Configuration

This study was performed according a two-level nested analysis of variance [2] with two cycles of experiences: 90 days for the first cycle and 45 days for the second one. At level 1, the measurements were taken over a short time and at level 2 the measurements were taken over  $k$  days where the replicates  $j$  are nested within days. For each cycle, it was prepared three different concentration solutions (bottle n. 1, 2 and 3), which were split in several sub-samples.

### 3.1 Statistical Model

The establishment of a proper model for a property value is a complex task, which should be carried out with great care to account for all relevant details of the procedures. In terms of ANOVA [2], for this two-level nested design, the samples are at the level of groups and the repeatability of the measurements method is found within the groups. The basic model reads as

$$Y_{kj} = \mu + \tau_k + \varepsilon_{kj} \quad (1)$$

where  $Y_{kj}$  is the result of a single measurement in the experiment,  $\mu$  is the expectation of  $Y_{kj}$  which is the value that  $Y_{kj}$  takes up when the number of repeated measurements tends to infinity,  $\tau_k$  is a bias term, due to the differences in the extracts. The variable is assumed to be normally distributed, with mean zero and variance  $\sigma^2$ . Furthermore, it is assumed that  $\tau_k$  is independent of all  $\varepsilon_{ki}$  which are also normally distributed, with mean zero and variance  $\sigma^2$ . According ISO/TS 21749 [2, §5.2.3] the scattering of data for ANOVA, can be

expressed in terms of sums of squared differences for the day effect  $SS_D$  and for the error effect  $SS_E$ , which express the levels of analysis variance. The mean square for random effects and for the day effect was also calculated.

#### 4. Homogeneity Study

A homogeneity study is necessary in order to demonstrate that the batch of bottles (units) is sufficiently homogeneous. It was performed the within-bottle (5 mL) and the between-bottle homogeneity testing, according ANOVA approaches [3]. Computing the row data from measurements results, the variance components were quantified, with ANOVA expressed in terms of sums of squares and mean squares differences from variability sources (between-day and within-day) with 136 degrees of freedom  $v$  in the 1<sup>st</sup> cycle and 86 in the 2<sup>nd</sup> cycle. Table 1 display the results, where it is observed a fully agreement among measurements with insignificant variability of the homogeneity.

Table 1. 1<sup>st</sup> and 2<sup>nd</sup> Cycle ANOVA

Source	$v$		SS		MS		Expected mean square	
	1 <sup>st</sup>	2 <sup>nd</sup>	1 <sup>st</sup>	2 <sup>nd</sup>	1 <sup>st</sup>	2 <sup>nd</sup>	1 <sup>st</sup>	2 <sup>nd</sup>
6 % vol								
Day	33	15	$1.657 \times 10^{-07}$	$7.956 \times 10^{-08}$	$5.177 \times 10^{-09}$	$5.304 \times 10^{-09}$	$5.177 \times 10^{-09}$	$5.304 \times 10^{-09}$
Error	136	64	$2.305 \times 10^{-07}$	$1.005 \times 10^{-07}$	$1.746 \times 10^{-09}$	$1.570 \times 10^{-09}$	$1.746 \times 10^{-09}$	$1.570 \times 10^{-09}$
SUM	169	79	$3.961 \times 10^{-07}$	$1.800 \times 10^{-07}$	$3.157 \times 10^{-11}$	$6.714 \times 10^{-11}$		
11 % vol.								
Day	33	15	$2.780 \times 10^{-07}$	$6.682 \times 10^{-08}$	$8.425 \times 10^{-09}$	$4.455 \times 10^{-09}$	$8.425 \times 10^{-09}$	$4.455 \times 10^{-09}$
Error	136	64	$3.773 \times 10^{-07}$	$1.419 \times 10^{-07}$	$2.774 \times 10^{-09}$	$2.217 \times 10^{-09}$	$2.774 \times 10^{-09}$	$2.217 \times 10^{-09}$
SUM	169	79	$6.553 \times 10^{-07}$	$2.087 \times 10^{-07}$	$4.985 \times 10^{-11}$	$5.639 \times 10^{-11}$		
16 % vol.								
Day	33	15	$4.445 \times 10^{-07}$	$8.734 \times 10^{-08}$	$1.347 \times 10^{-08}$	$5.823 \times 10^{-09}$	$1.347 \times 10^{-08}$	$2.122 \times 10^{-09}$
Error	136	64	$7.342 \times 10^{-07}$	$5.085 \times 10^{-07}$	$5.399 \times 10^{-09}$	$7.945 \times 10^{-09}$	$5.399 \times 10^{-09}$	$7.945 \times 10^{-09}$
SUM	169	79	$1.179 \times 10^{-07}$	$5.958 \times 10^{-07}$	$7.970 \times 10^{-11}$	$7.370 \times 10^{-11}$		

#### 5. Stability Test

The evaluation of data from a stability study is a check if any trend in the data can be observed. In this work, it was adopted a linear approximation as a suitable model for the stability studies [3] that can be expressed as:

$$\bar{Y} = b_0 + b_1 \bar{X} \quad (2)$$

where  $b_0$  (intercept) and  $b_1$  (slope) are the regression coefficients which can be computed from the following expressions:

$$b_1 = \frac{\sum_{i=1}^J (X_i - \bar{X})(Y_i - \bar{Y})}{\sum_{i=1}^J (X_i - \bar{X})^2} \quad (3), \quad b_0 = \bar{Y} - b_1 \bar{X} \quad (4)$$

where  $\bar{X}$  is the average of days between measures and  $\bar{Y}$  is the average value of measure. The estimate for the intercept can be computed from by equation 4. From error analysis, the expressions for the standard deviations in  $b_1$  and  $b_0$  can expressed as

$$s(b_1) = \frac{s}{\sqrt{\sum_{i=1}^J (X_i - \bar{X})^2}} \quad (5) \quad \text{where} \quad s^2 = \frac{\sum_{i=1}^J (Y_i b_0 - b_1 X_i)^2}{J - 2} \quad (6)$$

Table 2. Data from stability study

Standard (Refractive Index)	$b_0$	$b_1 (10^{-6})$	$s(b_1)$	$t_{0.95;J-2}.s(b_1)$
1 <sup>st</sup> Cycle				
1.35106	1.351	2.386	0.0486	0.0990
1.36371	1.364	4.495	0.0460	0.0937
1.37578	1.376	-6.613	0.0634	0.1290
2 <sup>nd</sup> Cycle				
1.35108	0.633	1.118	0.0228	0.0218
1.36365	0.639	2.107	0.0216	0.0206
1.37576	0.645	-3.099	0.0298	0.0284

Based on  $s(b_1)$  and an appropriate  $t$ -factor (for a number of degrees of freedom equals  $J-2$ ),  $b_1$  can be tested for significance (table 2). The Student's factor for  $J-2$  degrees of freedom and  $p = 0.95$  (95 % level of confidence) equals 2,037. Since  $|b_1| < t_{0.95;J-2}.s(b_1)$  the slope is insignificant [3]. As a consequence, no instability was observed (Table 2).

## 6. Evaluation of Measurement Uncertainty

The uncertainty calculation of the refractive index must be in agreement with the principles of GUM<sup>4</sup>, with a proper model for a property value where all factors included have significantly contributed. For this, the analysis of variance

was used as a statistical technique to derive standard uncertainties from homogeneity, stability and characterization data. According literature<sup>3</sup>, the model can be expressed as follows:

$$u_{CRM} = \sqrt{u_{char}^2 + u_{bb}^2 + u_{lts}^2 + u_{sts}^2} \quad (7) \quad u_{bb} = \sqrt{\frac{MS_D - MS_E}{J} + \frac{MS_E}{J} \cdot e^{-\frac{MS_D}{MS_E}}} \quad (8)$$

where  $u_{char}^2$  is the standard uncertainty from characterization,  $u_{bb}^2$  the standard uncertainty from between-bottle,  $u_{lts}^2$  the standard uncertainty from long-term stability and  $u_{sts}^2$  the standard uncertainty from short-term stability.

The value of uncertainty from characterization is based on the uncertainty evaluation of the method of measurement. According literature, one possible way to evaluate the homogeneity contribution to standard uncertainty,  $u_{bb}$ , is to use the Federer<sup>5</sup> equation (8).

The value of  $u_{lts}$  is obtained from the results drawn in table 1 with a shelf life  $t$  of 145 days; which can be considered a long-term stability standard uncertainty. Following the same line of reasoning as for the homogeneity study, the influence of the measurement variability on the estimate of the degradation rate is calculated. According regression function, the value's slope are consider as conservative estimate of degradation, as shown in table 2.

The short-term stability uncertainty,  $u_{sts}^2$ , is associated with any extra effects due to transport of the samples. The knowledge of standards composition is important and allows giving better advice in order to maintain the initial condition. Furthermore, IPQ certificates promote this procedure and the validity of the uncertainty on the certificate should be constant during the lifetime of the standard. The table below represents the values of each standard uncertainty. As can be seen the major standard uncertainty is from long-term stability and material characterization.

Table 3. Raw data from standard uncertainty components

Standard (% vol)	Refractive Index	$\mu_{car}$ ( $10^{-5}$ )	$\mu_{bb}$ ( $10^{-5}$ )	$\mu_{lts}$ ( $10^{-5}$ )	$\mu_{sts}$ ( $10^{-5}$ )	$\mu_{CRM}$ ( $10^{-4}$ )
1 <sup>st</sup> Cycle						
6	1.35106	8.75	2.65	7.87	2.62	1.23
11	1.36371	9.48	3.41	1.48	3.36	1.07
16	1.37578	7.12	4.13	2.18	4.02	0.94
2 <sup>nd</sup> Cycle						
6	1.35108	6.75	2.75	3.67	2.73	0.86
11	1.36365	4.25	2.25	6.95	2.12	0.87
16	1.37556	7.84	1.84	9.98	2.06	1.29

The coverage factor  $k$  used by expanded uncertainty is determined on the basis of the normal distribution of refractive index with a 95 % level of confidence. Figure 1 plotted the values of expanded uncertainty,  $U$ , for each reference material.

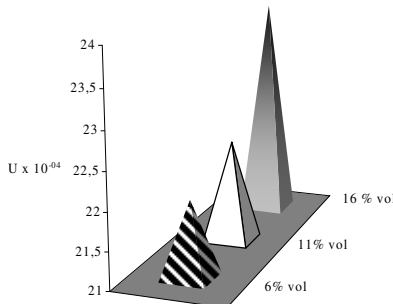


Figure 1. Expanded Uncertainty,  $U$ , of the Reference Material

## 7. Conclusion

Based on the approach of a single method, in a single laboratory, we showed how data from nested two-level design describe and evaluate the uncertainty.

Globally the results are quite satisfactory with uncertainty budgets in the same level, according with the reference value of standard material.

In order to improve the results with lower uncertainty, it is recommended to minimize the influence of analytical variations which can be reduced increasing the number of replicates and the period of the stability study.

## References

1. OIML R 124 (1997), Refractometers for the measurement of the sugar content of grape must.
2. ISO/TS 21749 (2005), Measurement uncertainty for metrological applications – repeated measurements and nested experiments.
3. Guide 35 (2006), Reference materials – General and statistical principles for certification.
4. BIPM, IEC, IFCC, ISO, IUPAC, IUPAP, OIML, *Guide to the Expression of Uncertainty in Measurement (GUM)*, 2nd ed., International Organization for Standardization, Genève, 1995, pp 11, 83-87.
5. Federer WT (1968) J Royal Stat Soc C 17: 171-176 Uncertainty calculations in the certification of reference materials.

## PROFICIENCY TESTING FOR CALIBRATION LABORATORIES

EDUARDA FILIPE

*Instituto Português da Qualidade, Rua António Gião, 2  
2829-513 Caparica, Portugal  
efilipe@mail.ipq.pt*

The proficiency testing (PT), as described by the ISO Guide 43 “is the use of interlaboratory comparisons (ILCs) for purpose of the determination of laboratory testing or measurement performance...”. The NMIs traditionally organize the ILCs for the NABs providing the travelling standards, the reference(s) value(s) and at the end perform the statistical analysis of the laboratory results. The goal of this article is to discuss the existing approaches for the calibration laboratories ILCs evaluation and propose a basis for the validation of the laboratories measurement capabilities.

### 1. Introduction

The proficiency testing (PT), as described by the ISO Guide 43 [1] “is the use of interlaboratory comparisons (ILCs) for purpose of the determination of laboratory testing or measurement performance and one of the main uses of PT schemes is to assess laboratories’ ability to perform tests competently. ... Participation in PT schemes provides laboratories with an objective means of assessing and demonstrating the reliability of the data they are producing”. All the PT schemes have in common the comparison of test and measurement results obtained by two or more laboratories.

The proficiency testing policy and plan are designed by the National Accreditation Boards (NABs) in collaboration with the National Metrology Institutes (NMIs). The type of ILCs are identified in order to comply with the requirements of the regional and international organizations, namely the European Accreditation (EA) and the International Laboratory Accreditation Cooperation (ILAC), needed for the maintenance of these Boards at the multilateral agreements (MLA) of recognition of the calibration certificates or reports issued by a signatory country.

The NMIs traditionally organize the ILCs providing the travelling standards, the reference(s) value(s) and at the end perform the statistical analysis of the laboratory results. These results are evaluated by performance statistics

usually the  $E_n$  numbers and the different types of scores as defined by the ISO Guide 43 and more recently by the ISO 13528 standard [2]. These performance statistics are obtained by the ratio of the differences between the participating laboratory results and the reference or assigned values<sup>1</sup> and the combined expanded uncertainty (95%) –  $E_n$  numbers, or the combined uncertainty (68%) –  $Z, Z', \xi$ ...scores of these two values.

In order that an ILC is a reliable tool for a laboratory to validate their measurement capability it is needed that the NMI provides a travelling standard better – in terms of accuracy class or uncertainty, than the accredited best measurement capability (BMCs) of the laboratories. Although this situation encloses the majority of the cases, there are cases where the limited resolution of the measuring instruments does not permit the requirement of a reference value uncertainty inferior to one third of the uncertainty of the participating laboratories.

The goal of this article is to discuss the calibration laboratories ILCs evaluation and propose a basis for the validation of the laboratories BMCs.

## 2. General Principles and Concepts

The new VIM:2007 [3] defines measurement result (result of measurement) as the set of quantity values being attributed to a measurand together with any other *available relevant information ...*" and in Note 2 "A measurement result is generally expressed as a single measured quantity value and a measurement uncertainty ... . This is one of the changes from the previous edition where measurement result was defined as a value attributed to a measurand and will require the revision of the standards related with the ILCs as it will be needed that the laboratories should indicate a reliable estimate of their uncertainties. This is already a practice in the generality of the calibration laboratories especially in the "physics area" and will be generalized to the other sectors.

The ISO 13528:2005 standard defines proficiency testing as the determination of laboratory testing performance by means of ILCs and this performance can be described essentially by three properties: laboratory bias, stability and repeatability. For the case of calibration laboratories the ILCs are usually carried on to evaluate the laboratory bias. The travelling standard and assigned value are, as referred, provided by a Reference Laboratory, usually a NMI. The performance statistic preferred is the  $E_n$  numbers defined as:

---

<sup>1</sup> Assigned value: value attributed to a particular quantity and accepted, sometimes by convention, as having an uncertainty appropriate for a given purpose [2].

$$E_n = \frac{x - X}{\sqrt{U_{Lab}^2 + U_{ref}^2}} \quad (1)$$

Where  $X$  is the assigned value determined by the Reference Laboratory;  $U_{ref}$  is the expanded uncertainty of  $X$  and  $U_{lab}$  is the expanded uncertainty of a participant's result  $x$ . The critical value is 1.0 so a result is considered satisfactory to  $|E_n| \leq 1$  and unsatisfactory for  $|E_n| > 1$ . The laboratories uncertainty evaluation should be consistent with the published documents, namely the GUM and the Reference Laboratory should guarantee that their uncertainties are reported it in a uniform way.

When the uncertainty of the travelling standard obtained by the Reference laboratory is better than one third of the laboratories uncertainties this value will not influence significantly the comparison uncertainty for a specific laboratory and its BMC can be validated by the ILC by the difference of its value from the assigned value and the “comparison uncertainty” calculated by equation (2), as it is considered that there is independence between the laboratory value and the assigned value.

$$U_{comp} = \sqrt{U_{lab}^2 + U_{ref}^2} \quad (2)$$

The NABs ask frequently the NMIs to evaluate the performance of the accredited laboratories when calibrating industrial measuring instruments (MIs). These services usually are not provided by the NMIs and in these cases the NMIs have to buy the MIs, perform its characterization, specially its stability and finally calibrate the instrument. These MIs usually have a fixed resolution that is the major component of uncertainty (case of digital balances, callipers, etc...). Even with the best instrumentation the NMI is not able to “decrease” this intrinsic component of uncertainty and for this reason the reference value will have an uncertainty that will “penalise” the laboratory comparison uncertainty. The BMC's laboratories for this reason cannot be validated.

It is proposed in this cases to use the “Procedure A” as described in [4] for the evaluation of NMIs key comparison data. In this procedure it is calculated as reference value the weighted mean of the laboratories values. This estimator uses for the weights the inverse of the squares of the associated standard uncertainties.

$$X = \hat{\mu} = \frac{\sum_i \psi_i \cdot x_i}{\sum_i \psi_i} \quad \therefore \quad \psi_i = \frac{1}{u^2(x_i)} \quad (3)$$

$$\frac{1}{u(X)} = \sqrt{\sum_i \psi_i} \quad \text{or} \quad u(X) = \frac{1}{\sqrt{\sum_i \psi_i}} \quad (4)$$

This consensus value will be considered as the “assigned value” of the ILC if all the results are consistent statistically. So it is needed to perform a consistency test, assuming the “normality of the data”, using the statistic:

$$\chi^2_{\text{obs}} = \sum_i \frac{(x_i - X)^2}{\psi_i} \quad (5)$$

Under the null hypothesis that all  $n$  measurement results are consistent and independent of each other, this statistic follows a  $\chi^2$  distribution with  $n-1$  degrees of freedom.

Calculating the critical value of this sampling distribution for a given significant level (usually  $\alpha=5\%$ ) we accept the null hypothesis if

$$\chi^2_{\alpha, n-1} > \chi^2_{\text{obs}} \quad \therefore \quad \alpha = 5\% \quad (6)$$

and the reference value with the corresponding uncertainty will be the assigned value for the ILC.

If the null hypothesis is false, for the cases where the statistic  $\chi^2_{\text{obs}}$  is superior to the critical value, means that not all measurement results belong to the same population. This situation is typical of most ILCs data sets. The discrepant values should be identified by:

$$|x_i - X| > U_{\text{comp}} \quad (7)$$

After discarding the discrepant values the remaining ones will be used to calculate the weighted mean and the assigned value will be found.

In all cases where the assigned value is a calculated one the comparison uncertainty  $U_{\text{comp}}$  will be smaller due to the dependence between the laboratory value and the assigned value, described in [4] App. C:

$$U_{\text{comp}} = \sqrt{U_{\text{lab}}^2 - U_{\text{ref}}^2} \quad (8)$$

In this case the  $E_n$  formula should change to:

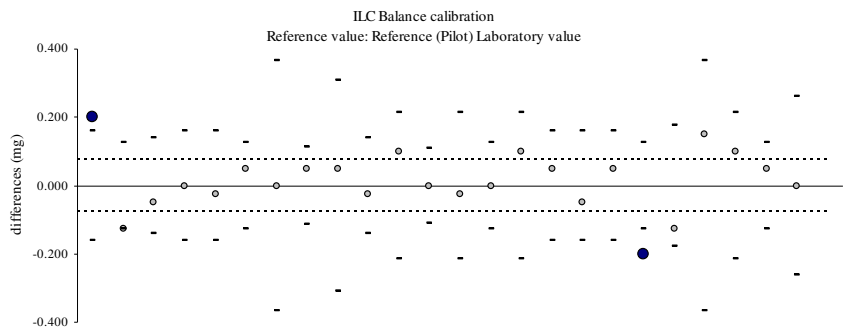
$$E_n = \frac{x - X}{\sqrt{U_{\text{lab}}^2 - U_{\text{ref}}^2}} \quad (9)$$

As it can be seen in the following examples this reference value will have an uncertainty compatible to the laboratories value validation.

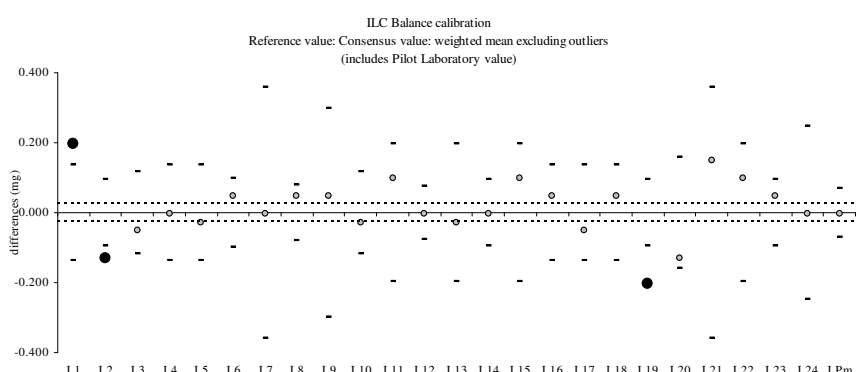
### 3. ILC examples

#### 3.1. ILC- Balance calibration

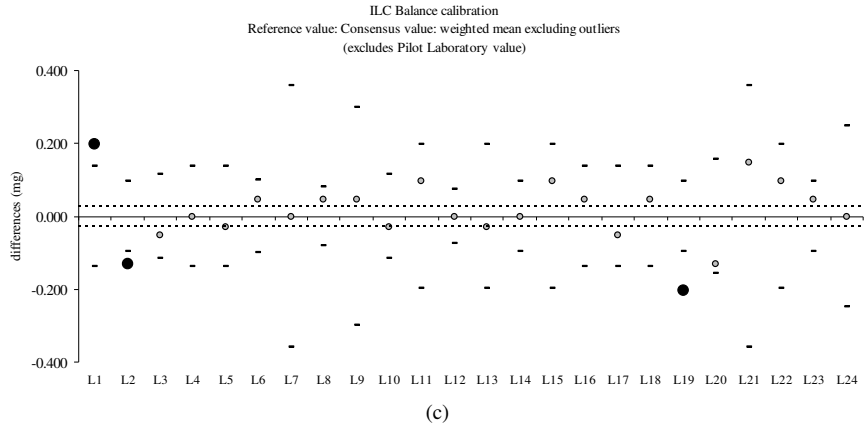
This ILC was performed with a digital balance with a 0.1 mg resolution. To the 24 participants laboratories was asked to calibrate a balance that was in the NMI laboratory under stable conditions. The MI drift was controlled at regular intervals by the reference laboratory. The ILC results for  $m = 50$  g are shown in Fig. 1.



(a)



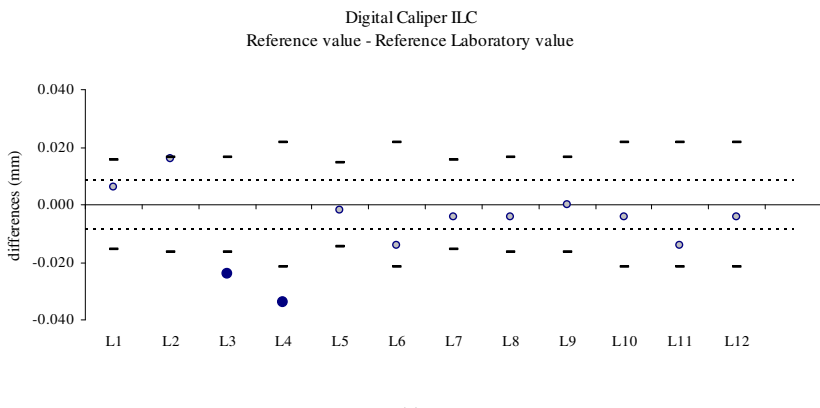
(b)



**Figure 1.** (a) Zero line: Reference (Pilot) Laboratory value ( $X$ ): 50.00017 g. Dotted line:  $U(X)$ : 0.075 mg. (b) Zero line: Calculated assigned value excluding outliers (black dots) ( $X$ ): 50.00017 g. Dotted line:  $U(X)$ : 0.026 mg. The Reference laboratory was included at the calculation (L<sub>Pm</sub>) of the assigned value.(c) Zero line: Calculated assigned value excluding outliers (black dots) ( $X$ ): 50.00017 g. Dotted line:  $U(X)$ : 0.028 mg. The Reference laboratory was not included at the assigned value.

### 3.2. ILC: Digital Caliper calibration

This ILC was performed with a digital caliper with a 0.001 mm resolution that circulated among the 12 participant's laboratories. It was asked to calibrate this MI for several points. The ILC results for nominal  $l = 300$  mm are shown in Fig. 2.



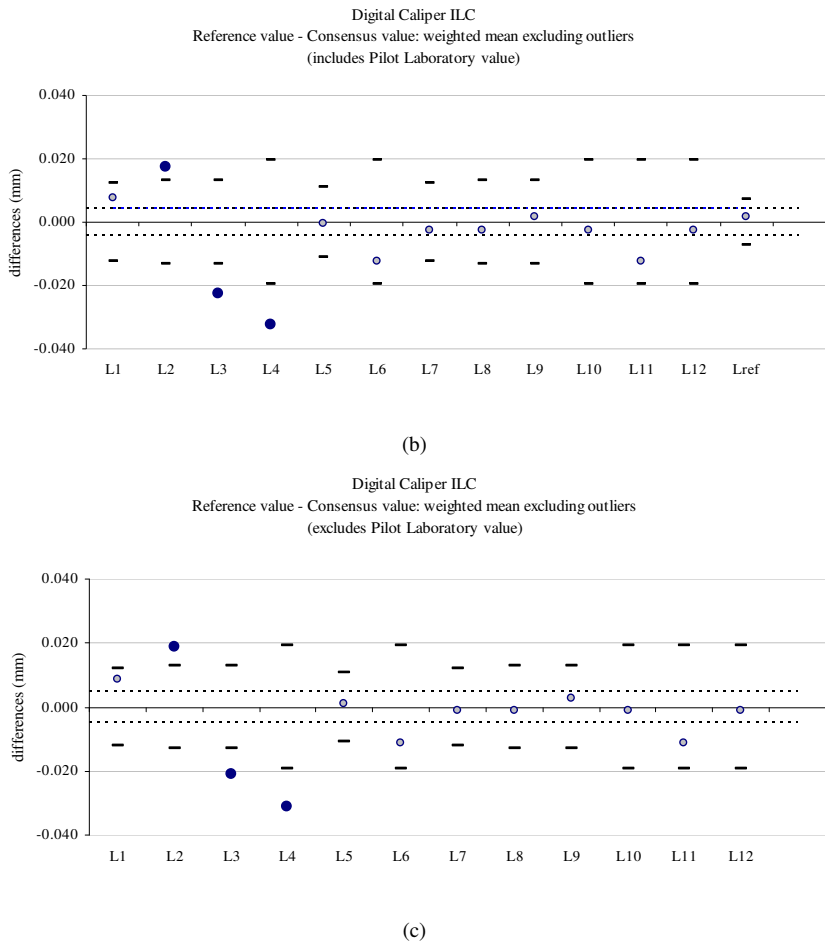


**Figure 2.** (a) Zero line: Reference Laboratory value ( $X$ ): 300.024 mm. Dotted line:  $U(X)$ : 0.0086 mm.  
 (b) Zero line: Calculated assigned value excluding outliers (black dots): 300.022 mm. Dotted line:  $U(X)$ : 0.0044 mm. The Reference laboratory was included at the calculation (LPm) of the assigned value.  
 (c) Zero line: Calculated assigned value excluding outliers (black dots): 300.021 mm. Dotted line:  $U(X)$ : 0.0050 mm. The LPm was not included at the assigned value.

From the figures in the b) and c) cases it can be noticed the small influence of the reference laboratory value and uncertainty in the assigned value uncertainty.

#### **4. Conclusions**

It was proposed a procedure for the evaluation of Proficiency testing by ILCs performed with calibration laboratories for the cases where the resolution of the measuring instruments limits the reference value uncertainty.

#### **Acknowledgements**

The author thanks the colleagues from IPQ Mass and Length laboratories for the comparison data availability.

#### **References**

1. ISO/IEC Guide 43-1:1997, Proficiency testing by interlaboratory comparisons. Part 1: Development and operation of proficiency testing schemes.
2. ISO 13528:2005, Statistical methods for use in proficiency testing by interlaboratory comparisons.
3. ISO/IEC GUIDE 99:2007, International vocabulary of metrology - Basic and general concepts and associated terms (VIM).
4. M. G. Cox, The evaluation of key comparison data. *Metrologia*, 2002, 39, 589-595.

## NONLINEAR LEAST SQUARES AND BAYESIAN INFERENCE

ALISTAIR B. FORBES

*National Physical Laboratory  
Teddington, Middlesex, UK, TW11 0LW  
alistair.forbes@npl.co.uk*

Many data analysis problems in metrology involve fitting a model to measurement data. Least squares methods arise in both the parameter estimation and Bayesian contexts in the case where the data vector is associated with a Gaussian distribution. For nonlinear models, both classical and Bayesian formulations involve statistical distributions that, in general, cannot be completely specified in analytical form. In this paper, we discuss how approximation methods and simulation techniques, including Markov chain Monte Carlo, can be applied in both a classical and Bayesian setting to provide parameter estimates and associated uncertainty matrices. While in the case of linear models, classical and Bayesian methods lead to the same type of calculations, in the nonlinear case the differences in the approaches are more apparent and sometimes quite significant.

*Keywords:* Parameter estimation; Bayesian inference; Markov chain Monte Carlo; uncertainty

### 1. Introduction

We consider a model [1] in which a response variable is measured subject to random effects:

$$y_i = \phi(\mathbf{x}_i, \boldsymbol{\alpha}) + \epsilon_i, \quad i = 1, \dots, m. \quad (1)$$

Here,  $y_i$  is the measured response,  $\phi(\mathbf{x}_i, \boldsymbol{\alpha})$  the modelled response depending on variable values  $\mathbf{x}_i$  and parameters  $\boldsymbol{\alpha} = (\alpha_1, \dots, \alpha_n)^T$ ,  $n \leq m$ , and  $\epsilon_i$  represents a random effect. Corresponding to variable values  $\{\mathbf{x}_i\}_{i=1}^m$ , which we assume are known accurately, the data vector  $\mathbf{y} = (y_1, \dots, y_m)^T$  is a point in  $\mathbb{R}^m$ . Given  $\{\mathbf{x}_i\}_{i=1}^m$ ,  $\boldsymbol{\alpha} \mapsto \phi(\boldsymbol{\alpha}) = (\phi(\mathbf{x}_1, \boldsymbol{\alpha}), \dots, \phi(\mathbf{x}_m, \boldsymbol{\alpha}))^T$  describes an  $n$ -dimensional *model surface* in  $\mathbb{R}^m$ . We can think of the observed vector  $\mathbf{y}$  as a perturbation of an (unknown) point  $\phi(\boldsymbol{\alpha})$  on this surface, where  $\boldsymbol{\alpha}$  describes the true state of the system. We assume that

the perturbation has the probabilistic characterisation  $\mathbf{y} \in N(\phi(\boldsymbol{\alpha}), \sigma^2 I)$ , with  $\sigma$  known, i.e.,  $\mathbf{y}$  is a sample from a multivariate normal distribution centred on the (unknown)  $\phi(\boldsymbol{\alpha})$ . This paper considers the question: given that  $\mathbf{y}$  has been observed, what can be said about  $\boldsymbol{\alpha}$ ; in particular, what is the best estimate  $\mathbf{a}$  of  $\boldsymbol{\alpha}$  and what is its associated uncertainty? In section 2, we describe the parameter estimation approach to answering this question while section 3 describes the Bayesian inference approach that determines a state of knowledge distribution for  $\boldsymbol{\alpha}$ . Sections 4 and 5 discuss how summary information about the state of knowledge distribution can be derived using approximation and sampling methods. Section 6 describes a numerical example and our concluding remarks are given in section 7.

## 2. Parameter Estimation Approach

The least squares (LS) method [4] is an example of a parameter estimation method. The LS estimate  $\mathbf{a}$  minimises  $d(\mathbf{y}, \boldsymbol{\alpha}) = \|\mathbf{y} - \phi(\boldsymbol{\alpha})\|$ , i.e., determines  $\mathbf{a}$  such that  $\phi(\mathbf{a})$  is the point on the surface  $\phi(\boldsymbol{\alpha})$  closest to  $\mathbf{y}$  as measured in the Euclidean norm. The optimal  $\mathbf{a}$  is such that

$$\mathbf{J}^T \mathbf{f} = \mathbf{0}, \quad \mathbf{f} = \mathbf{f}(\boldsymbol{\alpha}) = \mathbf{y} - \phi(\boldsymbol{\alpha}), \quad J_{ij} = J_{ij}(\boldsymbol{\alpha}) = \frac{\partial f_i}{\partial \alpha_j}, \quad (2)$$

an  $n \times n$  system of equations involving the Jacobian matrix  $J$ . The left-hand side depends on  $\boldsymbol{\alpha}$  and  $\mathbf{y}$  and the equations implicitly define the solution  $\mathbf{a} = \mathcal{A}(\mathbf{y})$  as a function of  $\mathbf{y}$ . Regarding  $\mathbf{y}$  as an input and  $\mathbf{a}$  as an output, if we associate a distribution with  $\mathbf{y}$  then, in theory, we can propagate this distribution through to that associated with  $\mathbf{a}$ . If we knew that  $\mathbf{y} \in N(\phi(\mathbf{a}^*), \sigma^2 I)$  for some  $\mathbf{a}^*$  then, using linearisation about  $\mathbf{a}^*$ , it is possible to show using the law of propagation of uncertainty [2] (LPU) that, approximately,

$$\mathbf{a} \in N(\mathbf{a}^*, V_{\mathbf{a}}), \quad V_{\mathbf{a}} = \sigma^2 (\mathbf{J}^T \mathbf{J})^{-1}, \quad (3)$$

where the Jacobian matrix  $J$  is evaluated at  $\mathbf{a}^*$ . This tells us that if  $\boldsymbol{\alpha} = \mathbf{a}^*$ , the LS estimate is approximately distributed as  $N(\mathbf{a}^*, V_{\mathbf{a}})$ . We can use Monte Carlo (MC) sampling methods [2] to determine a more accurate estimate of the distribution for  $\mathbf{a}$ , given  $\boldsymbol{\alpha} = \mathbf{a}^*$ : we sample  $\mathbf{y}_q \in N(\phi(\mathbf{a}^*), \sigma^2 I)$ , and evaluate  $\mathbf{a}_q = \mathcal{A}(\mathbf{y}_q)$ ,  $q = 1, \dots, M$ . The mean of the distribution for  $\mathbf{a}$  is estimated by  $\sum_q \mathbf{a}_q / M$ , etc. Both the LPU and MC approaches start with a plausible candidate  $\mathbf{a}^*$  for  $\boldsymbol{\alpha}$ . Given an observed data vector  $\mathbf{y}$  we can take for  $\mathbf{a}^*$  the LS estimate itself.

In the parameter estimation approach, we determine an estimate of the distribution  $p(\mathbf{a} | \boldsymbol{\alpha} = \mathbf{a}^*)$  for the parameter estimates  $\mathbf{a}$  given a known value

$\alpha^*$  of the parameters  $\alpha$ . The distribution can be realised as a frequency distribution corresponding to the experimental procedure of measuring the same artefact characterised by parameter values  $\alpha^*$ , recording data vectors  $y_q$  and then calculating parameters estimates  $a_q$ . The resulting distribution provides a characterisation of the measurement and parameter estimation method [3].

### 3. Bayesian Inference Approach

The probability density  $p(\eta|\alpha)$  describes the distribution associated with observing data vector  $\eta$  given that the model is described by parameters  $\alpha$ . From this point of view,  $p(\eta|\alpha)$  is a family of distributions parametrized by  $\alpha$ . An observed data vector  $\eta = y$  provides information about which members from this family are more likely than others in the form of a distribution  $p(\alpha|y)$ , the density for  $\alpha$ , given  $y$ . Intuitively, the further  $y$  is from  $\phi(\alpha)$ , the less likely  $\alpha$  is, i.e., if  $p(y|\alpha)$  is small then  $p(\alpha|y)$  should also be small, etc. Bayes' theorem [6,8] states that  $p(\alpha|y) \propto p(y|\alpha)p(\alpha)$ , showing that  $p(\alpha|y)$  varies with  $p(y|\alpha)$  and  $p(\alpha)$ . Bayes' theorem provides the calculation for the following hypothetical situation. A large number of artefacts with accurately calibrated values  $a_q$  distributed according to  $p(\alpha)$  are measured, obtaining measurement results  $y_q \in N(\phi(a_q), \sigma^2 I)$ . If  $y_q = y$  (within some tolerance), we make a note of the calibrated value  $a_q$ . Then such noted  $a_q$  are drawn from the distribution  $p(\alpha|y)$ . In other words, if the calibrated values for the artefacts to be measured are distributed according to  $p(\alpha)$ , then the artefacts giving the same measurement result as  $y$  have calibrated values distributed according to  $p(\alpha|y)$ .

The distribution  $p(\alpha)$  is often called the prior distribution, while  $p(\alpha|y)$  is termed the posterior distribution. The distribution  $p(\alpha)$  should be assigned to capture what is known about  $\alpha$  independent from (or prior to) the data  $y$ . If not much is known  $p(\alpha)$  is set to be a non-informative prior, often  $p(\alpha) \propto 1$ . For many situations in which the data  $y$  carries all or nearly all the information about  $\alpha$ , the posterior distribution is dominated by  $p(y|\alpha)$  and the precise form of the prior distribution has no practical influence on the posterior distribution.

Bayes' theorem determines  $p(\alpha|y)$  in terms of  $p(y|\alpha)$  and  $p(\alpha)$  up to a multiplicative constant. In order to make inferences about  $\alpha$ , e.g., determine its mean and variance, it is necessary to estimate that constant. Two approaches can be implemented, the first to find an analytic approximation to the distribution, the second to sample from the distribution.

#### 4. Approximating The Posterior Distribution

For the model  $\mathbf{y} \in N(\phi(\boldsymbol{\alpha}), \sigma^2 I)$  and prior distribution  $p(\boldsymbol{\alpha}) \propto 1$ , the posterior distribution is given by

$$p(\boldsymbol{\alpha}|\mathbf{y}) \propto p(\mathbf{y}|\boldsymbol{\alpha}) \propto \exp\left\{-\frac{1}{2\sigma^2}d^2(\mathbf{y}, \boldsymbol{\alpha})\right\}, \quad d(\mathbf{y}, \boldsymbol{\alpha}) = \|\mathbf{y} - \phi(\boldsymbol{\alpha})\|, \quad (4)$$

showing that the shape of the distribution is determined by the distance function  $d(\mathbf{y}, \boldsymbol{\alpha})$ . If  $\phi(\boldsymbol{\alpha})$  is linear in  $\boldsymbol{\alpha}$  then  $d^2(\mathbf{y}, \boldsymbol{\alpha})$  is quadratic in  $\boldsymbol{\alpha}$  and  $p(\boldsymbol{\alpha}|\mathbf{y})$  is therefore a multinormal distribution centred on the least squares estimate  $\mathbf{a}$  of  $\boldsymbol{\alpha}$ . For the nonlinear case, we can use a linear approximation  $\phi(\boldsymbol{\alpha}) \approx \phi(\mathbf{a}) + J(\boldsymbol{\alpha} - \mathbf{a})$  determined about the nonlinear least squares estimate. Using this approximation,  $d^2(\mathbf{y}, \boldsymbol{\alpha})$  is approximated by a quadratic function and, to first order,  $p(\boldsymbol{\alpha}|\mathbf{y}) \approx N(\mathbf{a}, V_{\mathbf{a}})$ , where  $V_{\mathbf{a}}$  is as in (3). We can determine a more accurate approximation to  $p(\boldsymbol{\alpha}|\mathbf{y})$  by determining a quadratic approximation to  $\phi(\boldsymbol{\alpha})$  and using this to calculate a more accurate quadratic approximation to  $d^2(\mathbf{y}, \boldsymbol{\alpha})$  which leads to a second, more accurate, Gaussian approximation

$$p(\boldsymbol{\alpha}|\mathbf{y}) \approx N(\mathbf{a}, V_{\mathbf{a}}^Q), \quad V_{\mathbf{a}}^Q = \sigma^2 \left( J^T J + \sum_i f_i G_i \right)^{-1}, \quad G_{i,jk} = \frac{\partial^2 f_i}{\partial \alpha_j \partial \alpha_k}. \quad (5)$$

The matrix  $V_{\mathbf{a}}^Q = \sigma^2 H^{-1}$ , where  $H$  is the matrix of second partial derivatives of  $d^2(\mathbf{y}, \boldsymbol{\alpha})/2$  with respect to  $\alpha_j$ . Note that  $V_{\mathbf{a}}^Q$  depends on  $\mathbf{y}$  through  $f_i = y_i - \phi(\mathbf{x}_i, \boldsymbol{\alpha})$ .

#### 5. Sampling From The Posterior Distribution

For accurate data and model surfaces that are approximately linear, the distance function  $d(\mathbf{y}|\boldsymbol{\alpha})$  is approximately quadratic, in which case the posterior distribution  $p(\boldsymbol{\alpha}|\mathbf{y})$  will be approximated reasonably well by the Gaussian distribution  $N(\mathbf{a}, V_{\mathbf{a}})$  derived from the least squares estimate. Markov chain Monte Carlo (MCMC) techniques [5,6] can be used to generate a sample from  $p(\boldsymbol{\alpha}|\mathbf{y})$  from which more accurate information about  $p(\boldsymbol{\alpha}|\mathbf{y})$  can be derived, as in standard MC approaches. For our purposes, a Markov chain is a sequence of parameter values  $\mathbf{a}_q$ ,  $q = 1, 2, \dots$ , exploring the parameter space. Given a distribution  $p(\boldsymbol{\alpha})$  (usually a posterior distribution), we wish to construct a chain such that the samples  $\mathbf{a}_q$  eventually represents a sample from  $p(\boldsymbol{\alpha})$ .

A random walk is an example of a Markov chain. Consider

$$\mathbf{a}_q = c \mathbf{e}_q + d \mathbf{a}_{q-1}, \quad \mathbf{e}_q \in N(0, 1), \quad c^2 + d^2 = 1. \quad (6)$$

If  $a_{q-1}$  is distributed with density  $p_{q-1}(\alpha)$  then the density for  $a_q$  is given by a convolution

$$p_q(\alpha) = \int_{-\infty}^{\infty} p_{q-1}(\beta)p(\alpha, \beta)d\beta, \quad (7)$$

defined by  $p(\alpha, \beta)$ , known as the transition kernel. Starting from any distribution  $p_0$ , the repeated application of the convolution operator defines a sequence of densities  $p_q$  that converges to  $p_N$ , the density associated with  $N(0, 1)$ . The constants  $c$  and  $d$  govern the speed of convergence: the larger  $d$ , the slower the convergence. Figure 1 shows the convergence of a uniform distribution to a Gaussian distribution for  $d = 0.5$  and  $d = 0.9$  and  $q = 1, 2, 4, 8, 16$ .

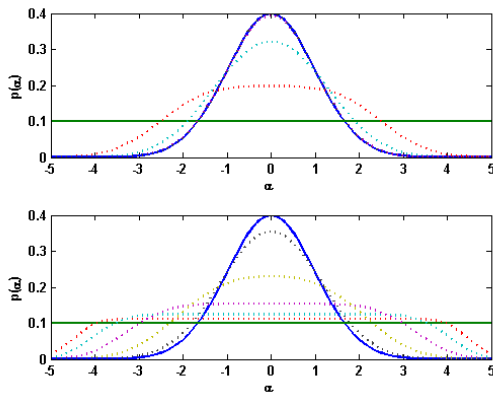


Fig. 1. Convergence of a uniform distribution to the limiting Gaussian distribution for the random walk (6) for  $q = 1, 2, 4, 8, 16$  and  $d = 0.5$  (top) and  $d = 0.9$  (bottom).

MCMC algorithms are based on determining transition kernels  $p(\boldsymbol{\alpha}, \boldsymbol{\beta})$  such that i) the chain converges to the target distribution  $p(\boldsymbol{\alpha})$  with

$$p(\boldsymbol{\alpha}) = \int p(\boldsymbol{\beta})p(\boldsymbol{\alpha}, \boldsymbol{\beta})d\boldsymbol{\beta}, \quad (8)$$

and ii) the chain is ergodic. The latter condition ensures that if the chain has converged to its stationary distribution, then the samples  $\boldsymbol{a}_q$  generated by the chain are representative samples from  $p(\boldsymbol{\alpha})$ , in the sense, for example, that the mean of the samples converges to the mean of the distribution. For an ergodic chain, the samples  $\boldsymbol{a}_q$  visit all regions of parameter space

infinitely often and the frequency with which they visit a region is proportional to the probability mass for that region. The speed at which the chain moves through the parameter space will determine how large a sample we need in order to obtain accurate estimates of the distribution mean and variance, for example. The rate at which sample averages converge to the corresponding distribution expectations depends on the autocorrelation structure described in terms of the covariances  $\gamma_k = \text{cov}(\mathbf{a}_q, \mathbf{a}_{q+k})$ . If the chain takes very small steps so that the autocorrelation is high, then we will need to wait a long time to obtain accurate averages. For the random walk example, if  $d$  is large, the autocorrelation is high.

### 5.1. Metropolis-Hastings Independence Sampling

The Metropolis-Hastings algorithms [5,6] provide a flexible method of defining Markov chains with a target stationary distribution. One implementation is as follows. Suppose we want to sample from  $p(\boldsymbol{\alpha})$  and that  $\hat{p}(\boldsymbol{\alpha})$  is an approximating distribution for  $p(\boldsymbol{\alpha})$  from which it is easy to sample. Given  $\mathbf{a}_0, p_0 = p(\mathbf{a}_0)$  and  $\hat{p}_0 = \hat{p}(\mathbf{a}_0)$ , the chain is generated in the following steps. For  $q = 1, 2, \dots, M$ ,

- I Sample  $\mathbf{a}^*$  from  $\hat{p}(\boldsymbol{\alpha})$  and evaluate  $p^* = p(\mathbf{a}^*)$ ,  $\hat{p}^* = \hat{p}(\mathbf{a}^*)$  and ratio  $r_q = p^* \hat{p}_{q-1} / p_{q-1} \hat{p}^*$ .
- II Sample  $u_q \in R[0, 1]$ . If  $u_q \leq \min\{1, r_q\}$  set  $\mathbf{a}_q = \mathbf{a}^*$ ,  $p_q = p^*$ , and  $\hat{p}_q = \hat{p}^*$ . Otherwise set  $\mathbf{a}_q = \mathbf{a}_{q-1}$ ,  $p_q = p_{q-1}$ , and  $\hat{p}_q = \hat{p}_{q-1}$ .

In order to calculate the ratio  $r_q$  it is only necessary to know  $p$  and  $\hat{p}$  up to a multiplicative constant, allowing the procedure to be implemented for Bayesian inference. The scheme ensures that the proposed  $\mathbf{a}^*$  is accepted with probability  $\min\{1, r_q\}$ . If  $\hat{p}(\boldsymbol{\alpha}) = p(\boldsymbol{\alpha})$ , then  $r_q = 1$  and the proposal is always accepted and the  $\mathbf{a}_q$  are independent samples from  $p(\boldsymbol{\alpha})$ . If the ratio  $r_q$  is likely to be very small, then we may have to wait many iterations for successful steps. This can happen, for example, if  $\hat{p}$  has relatively small density where  $p$  has significant density. In the case of low acceptance rates, the sample generated will have a high autocorrelation. Ideally, the acceptance rate for the chain should be in the region 0.2 to 0.4 [6].

In our application,  $p(\boldsymbol{\alpha}) = p(\boldsymbol{\alpha}|\mathbf{y})$ , the posterior distribution associated with the model  $\mathbf{y} \in N(\boldsymbol{\phi}(\boldsymbol{\alpha}), \sigma^2 I)$ , and  $\hat{p}(\boldsymbol{\alpha})$  is related to the normal distribution  $N(\mathbf{a}, V\mathbf{a})$  centred on the least squares estimate  $\mathbf{a}$  of  $\boldsymbol{\alpha}$ . In order to reduce the risk that  $\hat{p}$  significantly under-represents  $p$  far from the LS estimate we choose for  $\hat{p}$ , a  $t$ -distribution  $t_\nu(\mathbf{a}, V\mathbf{a})$ , where  $\nu$  is a small integer number of degrees of freedom, say between 4 and 10.

Let  $J$  be the Jacobian matrix (2) at the least squares solution  $\mathbf{a}$  and  $R$  its  $n \times n$  upper-triangular factor formed from the QR factorisation [1,7] of  $J$ . Then  $V_{\mathbf{a}} = \sigma^2 (R^T R)^{-1} = \sigma^2 R^{-1} R^{-T}$ . The Metropolis-Hastings scheme can be implemented as follows. For  $q = 0, 1, \dots, M$ ,

- I Draw  $\mathbf{v}_q \in N(0, I)$  and  $s_q^2 = \mathbf{v}_q^T \mathbf{v}_q / \nu$ .
- II Draw  $\mathbf{d}_q \in N(0, I)$ , solve  $R\mathbf{e}_q = \mathbf{d}_q$ , and set  $\mathbf{a}^* = \mathbf{a} + \sigma \mathbf{e}_q / s_q$ ,

$$F^* = \frac{1}{2\sigma^2} d^2(\mathbf{y}, \mathbf{a}^*), \quad \hat{F}^* = \frac{\nu + n}{2} \log \left( 1 + \frac{\mathbf{d}_q^T \mathbf{d}_q}{\nu s_q^2} \right). \quad (9)$$

- III If  $q = 0$ , set  $q = 1$  and go to I. Otherwise, evaluate

$$r_q = \exp\{F_{q-1} - F^* + \hat{F}^* - \hat{F}_{q-1}\}. \quad (10)$$

- IV Draw  $u_q \in R[0, 1]$ . If  $u_q < r_q$ , set  $\mathbf{a}_q = \mathbf{a}^*$ ,  $F_q = F^*$ , and  $\hat{F}_q = \hat{F}^*$ . Otherwise, set  $\mathbf{a}_q = \mathbf{a}_{q-1}$ ,  $F_q = F_{q-1}$ ,  $\hat{F}_q = \hat{F}_{q-1}$ ,  $q = q + 1$  and go to I.

In the above scheme,  $\mathbf{a}^*$  is a draw from  $\hat{p}(\mathbf{a}) = t_\nu(\mathbf{a}, V_{\mathbf{a}})$ , and  $F^* = -\log p(\mathbf{a}^*)$  and  $\hat{F}^* = -\log \hat{p}(\mathbf{a}^*)$ , up to additive constants. The scheme requires only a standard normal and uniform random number generators.

## 6. Numerical Example: Exponential Decay

We illustrate the least squares and Bayesian inference approaches on simulated data involving an exponential decay model of the form

$$y_i = \alpha_1 e^{-\alpha_2 x_i} + \alpha_3 + \epsilon_i, \quad \epsilon_i \in N(0, \sigma^2). \quad (11)$$

The parameter  $\alpha_1$  gives the response at time  $x = 0$  and  $\alpha_3$  the limiting response. Simulated data were generated for 6 abscissae values  $\mathbf{x} = (0.4, 0.6, 0.8, 1.0, 1.2, 1.4)^T$  for the case  $\boldsymbol{\alpha} = (4.1, 2.5, 0.1)^T$  and  $\sigma = 0.05$ .

Figure 2 graphs the estimates of  $p(\alpha_1|\mathbf{y})$  and  $p(\alpha_3|\mathbf{y})$  estimated using the MCMC scheme described above with  $\nu = 6$ , with 20 chains generated each of length 1000 after an initial ‘burn-in’ period of 1000 samples to ensure sufficient convergence of the chains. The figure also shows i) the corresponding Gaussian approximations (solid curves) to these distributions centred on the least squares solution with variance matrix  $V_{\mathbf{a}}$  as in (3), and ii) the  $t$ -distributions used in the MCMC simulations.

Figure 3 gives the representations of the posterior distributions for the case where the prior distribution for  $\alpha_3$  applies the constraint  $\alpha_3 \geq 0$ . This constraint is easily incorporated into the simulation scheme. Due to correlation, the constraint on  $\alpha_3$  also has an impact on  $p(\alpha_1|\mathbf{y})$ . While parameter

estimation schemes can take into account constraints in determining values for the parameters, they provide no mechanism to assess the impact of the constraints on the associated uncertainties.

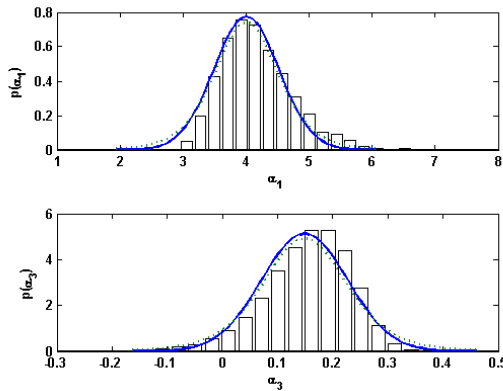


Fig. 2. Posterior distributions  $p(\alpha_1|y)$  (top) and  $p(\alpha_3|y)$  (bottom) along with their Gaussian approximations (solid curves). The dotted curves are the  $t$ -distributions used in the Metropolis-Hastings simulation.

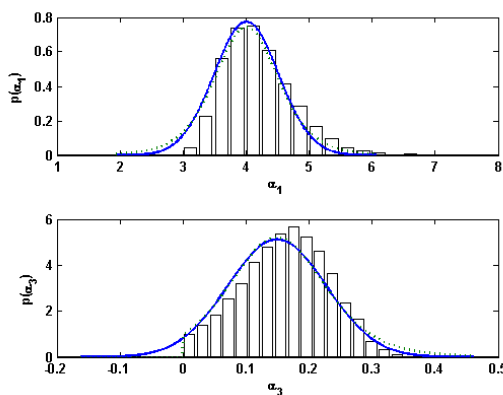


Fig. 3. As Fig. 2 but incorporating the constraint  $\alpha_3 \geq 0$ .

## 7. Summary and Concluding Remarks

For mildly nonlinear models and normally distributed random effects, the distribution  $p(\boldsymbol{a}|\boldsymbol{\alpha})$  associated with the least squares parameter estimates and the distribution  $p(\boldsymbol{\alpha}|\mathbf{y})$  for the parameters  $\boldsymbol{\alpha}$  given the observed data  $\mathbf{y}$  are likely to be approximated well by the same multivariate Gaussian distribution based on a linearisation of the model surface about the least squares estimate. The two distributions nevertheless different. The former describes the likely variation in the parameter estimates and can be estimated using standard Monte Carlo techniques. The latter summarises the information about  $\boldsymbol{\alpha}$  derived from the data and model assumptions, including the prior distribution  $p(\boldsymbol{\alpha})$ , and can be approximated using Markov chain Monte Carlo methods. A simple implementation of a Metropolis-Hastings algorithm suitable for model fitting in metrology has been described.

## Acknowledgements

The author is grateful to the AMCTM Organising Committee for its support and to Dr Ian Smith, NPL, for comments on a draft of this paper. This work was funded by the UK's Department of Innovation, Universities and Skills as part of the Software Support for Metrology Programme.

## References

1. R. M. Barker, M. G. Cox, A. B. Forbes, and P. M. Harris. SSfM Best Practice Guide No. 4: Modelling Discrete Data and Experimental Data Analysis. Report DEM-ES-018, National Physical Laboratory, Teddington, UK, 2007.
2. M. G. Cox and P. M. Harris. SSfM Best Practice Guide No. 6, Uncertainty evaluation. Report DEM-ES-011, National Physical Laboratory, Teddington, UK, 2006.
3. M. G. Cox, G. B. Rossi, P. M. Harris, and A. Forbes. A probabilistic approach to the analysis of measurement processes. *Metrologia*, 45(5):493–502, 2008.
4. A. B. Forbes. Parameter estimation based on least-squares methods. In F. Pavese and A. B. Forbes, editors, *Data modeling for metrology and testing in measurement science*, New York. Birkhauser-Boston. In press.
5. D. Gamerman. *Markov chain Monte Carlo: Stochastic Simulation for Bayesian inference*. Taylor & Francis, New York, 1997.
6. A. Gelman, J. B. Carlin, H. S. Stern, and D. B. Rubin. *Bayesian Data Analysis*. Chapman & Hall/CRC, Boca Raton, Fl., second edition, 2004.
7. G. H. Golub and C. F. Van Loan. *Matrix Computations*. John Hopkins University Press, Baltimore, third edition, 1996.
8. D. S. Sivia. *Data Analysis: a Bayesian Tutorial*. Clarendon Press, Oxford, 1996.

## MEASUREMENT STRATEGY ANALYSIS FOR OUT-OF-ROUNDNESS MEASUREMENT WITH CMM<sup>1</sup>

BARTOSZ GAPINSKI, MIROSLAW RUCKI, MICHAL PAWLOWSKI

*Division of Metrology and Measurement Systems, Poznan University of Technology  
Piotrowo str 3. PL-60965 Poznan, POLAND*

In the paper, the recommendations on the parameters of a circle measurement with CMM (Coordinate Measuring Machine) have been presented. The method of uncertainty estimation for the measured circle has been presented, too. The influence of the parameters of measured detail underwent discussion, like the type of form deviation and dimensional tolerances, as well as influence of the measurement method, particularly, number of probing points, CMM permissible error and fitting element type. The simulations and experimental measurement proved that the minimal number of probing points is not recommended. On the other hand, in the touch-trigger measurement, too large number of points does not increase the accuracy of measurement. As a result, the recommendations on the probe points number and CMM accuracy have been presented.

### 1. Introduction

Coordinate Measurement Machines (CMM) are universal, accurate and quick measuring devices [1]. To exploit them effectively, the appropriate measurement strategy should be worked out. One of the most often measured details are shaft/bore joints. CMM is able to measure not only the form deviations, but provide also the information on dimensions and position of the measured object [2]. The investigations enabled to formulate some recommendations on the correct measurement of the circle taking into consideration its expected form deviation (the type and value), CMM accuracy and the fitting element.

### 2. Strategy of the Roundness Measurement with CMM

A contact measurement with Coordinate Measuring Machine could be performed in two ways: touch trigger or scanning [3]. Scanning measurement allows to collect a large number of probing points in a relatively short time and to gain full information on the measured profile. However, many of existing CMMs are equipped with touch trigger probing heads. They are much cheaper

---

<sup>1</sup> The researches are financed by the Polish Government Science Support in the years 2006-2008

and measure with higher accuracy. So, it is important to analyze the touch trigger measurement and to ensure its highest effectiveness and correctness.

The type and value of the form deviation are also of great importance. The accuracy of the CMM is described by ISO 10360:2000 with following parameters [3]:  $MPE_E$  – maximum permissible error of indication of CMM for size measurement;  $MPE_P$  – maximum permissible probing error;  $MPE_{Tij}$  – maximum permissible scanning probing. Standard ISO/TS 12181-1:2003 [4] determines four possible reference elements: LSCI – Least Squares Reference Circle; MZCI – Minimum Zone Reference Circles, MCCCI – Minimum Circumscribed Reference Circle and MICI – Maximum Inscribed Reference Circle. Eventually, the uncertainty of measurement should be evaluated [5]. In case of the circle measurement, different values of uncertainty would be obtained for the centre position, diameter and the form deviation value.

### 3. Simulations and Experimental Researches

To achieve optimal exploitation of CMM, the appropriate measurement strategy must be prepared. In the touch trigger probing method, the number of probing points is one of important factors. Mathematically, 3 points are enough to define a circle, but the measurement could not be based on 3 points only. In order to match the out-of-roundness type and the CMM's accuracy with the required number of probing points, the CYRKIEL program was worked out. It generates the number of probing points which ensure the metrologically correct results of measurement (fig. 1) [6, 7]. In simulations, as well as in the experiments, the out-of roundness with equal lobes was examined.

<b>Nominal parameters</b>		<b>Permissible error of CMM</b>	
Diameter [mm]	100.000	Constant error A [um]	0.0
Upper tolerance	35	Factor K	0.0
Lower tolerance	0	Distribution	steady
<b>Out-of-roundness type</b>		<b>Simulation parameters</b>	
<input checked="" type="checkbox"/> Number of harmonic function	2	Initial number of points	4
100 [%]	-045° 00' 00"	Number of repetitions	25
<input type="checkbox"/> Number of harmonic function	3	Initial angle offset	+00° 00' 00"
40 [%]	-030° 00' 00"	Change of angle offset	003° 36' 00"
<input type="checkbox"/> Number of harmonic function	7	Increment of points number	1
20 [%]	-018° 00' 00"	Number of measuring series	125
<input type="checkbox"/> Number of harmonic function	13	Final number of points	128
20 [%]	-007° 00' 00"		

Figure 1. Decisional window of the CYRKIEL program

The simulations performed with CYRKIEL program proved that there is certain limit of points number. When it is exceeded, any larger number of probing points could provide the increase of accuracy smaller than the measurement uncertainty. At the same time, it is clearly seen that when the probing points number is small, the dispersion of the results is large (Fig. 2, 3). Hence, there is a need to gain information on appropriate points number. The results of simulations underwent the experimental check. For that purpose, CMMs with various accuracies were used: DEA Global 7.7.5, Wenzel LH 54 and Sheffield Discovery D8. Additionally, the measured details were checked with the specialized roundness measurement device Talyrond 73 by Taylor Hobson. The measurement results remained in agreement with the simulations.

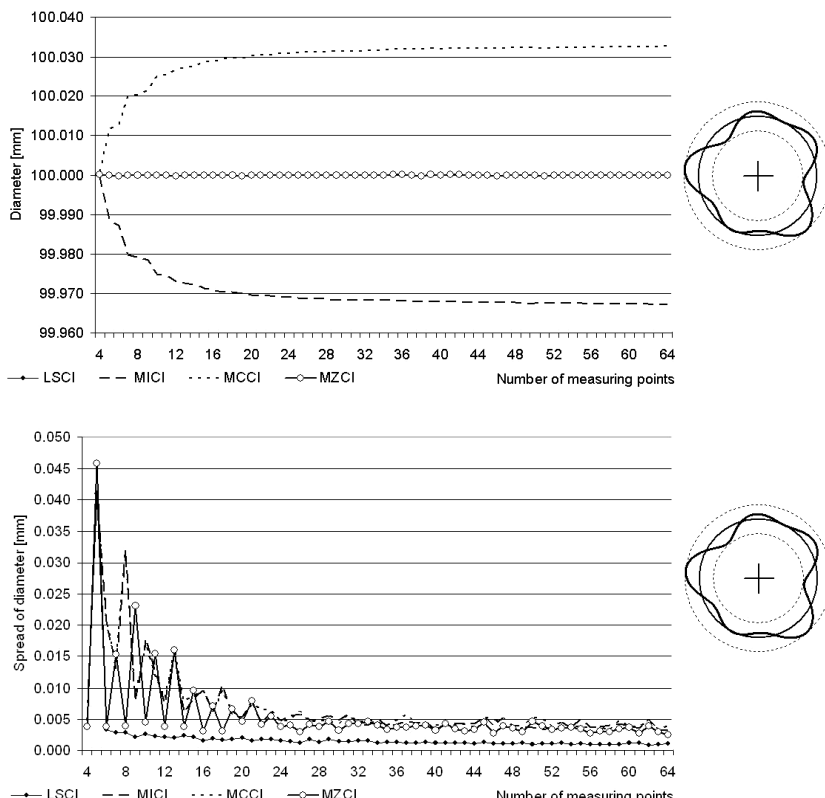


Figure 2. Example of the simulation results of the ring with diameter  $\varnothing 100$  mm and form deviation 0.034 mm: influence of the probing points number on the achieved diameter (upper); range of the values for various angle position of the ring related to the coordinate system (lower)

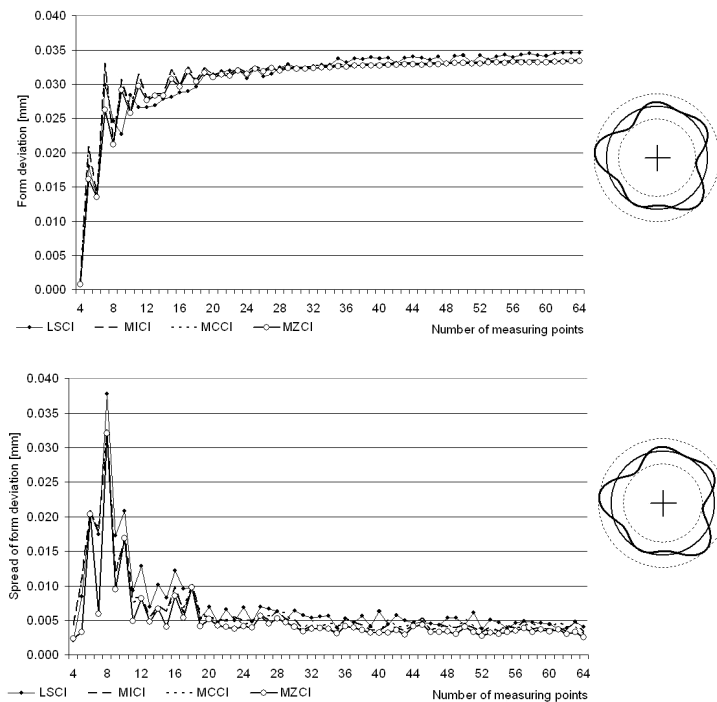


Figure 3. Example of the simulation results of the ring with diameter Ø100 mm and form deviation 0.034 mm: influence of the probing points number on the achieved value of form deviation (upper); range of the achieved values for various angle position of the ring related to the coordinate system (lower)

#### 4. Recommendations for the Roundness Measurement with CMM

To choose the appropriate number of the probing points, the uncertainty of the measurement could be taken as a reference value. In that case, the number of the probing points ensures the measurement with the uncertainty equal to the uncertainty of the CMM. In that case, according to the Standard [3], accuracy of CMM could be considered its data  $MPE_E = \pm(1.5+L/333) \mu\text{m}$ . As it was mentioned above, the uncertainty of the measurement (type A) should be calculated independently for the particular tasks: circle centre position ( $X, Y$ ), diameter ( $D$ ) and form deviation ( $RN$ ). The evaluated uncertainty for those tasks was  $U_{95(X,Y)} = 0.0015$ ,  $U_{95(D)} = 0.0009$ ,  $U_{95(RN)} = 0.0008 \text{ [mm]}$  respectively. Hence, the recommended number of probing points could be different for those three measured parameters. The example of generated recommendations is presented in the Table 1. It should be stated, however, that the recommended numbers are not always even.

Table 1. Recommended number of probing points for certain types of form deviations and measurement uncertainties (measured detail was of diameter 100 mm; its form deviation 0.040 mm); X, Y – coordinates of the circle centre, D – diameter, RN – roundness deviation; CMM accuracy  $MPE_E = \pm(1.5+L/333) \mu\text{m}$

Fitting element	X ; Y	Oval D	RN	Type of out-of-roundness			X ; Y	D	RN
				3-lobing		4-lobing			
LSCI	12	12	48	8	12	42	10	12	38
MZCI	24	48	48	16	36	42	16	22	38
MICI	24	48	48	16	24	42	20	34	38
MCCI	20	24	36	16	32	32	20	20	28

## 5. Conclusions

CMMs are uniform and flexible devices able to replace in some applications a specialized measuring devices. However, they require a metrologically correct measurement strategy. The CMM's uncertainty, number of probing points and fitting element must be taken into consideration.

## References

- 1 Nuemann H. J.: *Präzisionsmesstechnik in der Fertigung mit Koordinatenmessgeräten*, Renningen, ISBN 3-8169-2211-2, 2004.
- 2 Gapinski B.: Application of the Coordinate Measuring Technique for Roundness Measurement, *Development of Mechanical Engineering as a Tool for the Enterprise Logistics Progress – SCIENCE REPORT – Project CII-PL-0033-01-0506*, Poznan, Poland 2006, pp. 257-266.
- 3 ISO 10360:2000: Geometrical Product Specification (GPS) – Acceptance and reverification tests for coordinate measuring machines (CMM), *International Organization for Standardization*, 2000.
- 4 ISO/TS 12181-1:2003: Geometrical Product Specifications (GPS) – Roundness – Part 1: Vocabulary and parameters of roundness, *International Organization for Standardization*, 2003.
- 5 Hemdt A.: *Matematische Grundlagen der Koordinatenmesstechnik*. VDI-Bildungswerk, Achen.
- 6 Grzelka M., Pawłowski M., Gapinski B.: Expert Programs Supporting the Form Deviations Measurement, *IV. International Congress on Precision Machining ICPM 2007*, Sandomierz 25-28.09.2007; ISBN 978-83-88906-916; Vol.1, pp. 303-310.
- 7 ISO/TS 14253-2:1999 Geometrical Product Specifications (GPS) – Inspection by measurement of workpieces and measuring equipment – Part 2: Guide to the estimation of uncertainty in GPS measurement, in calibration of measuring equipment and in product verification; International Organization for Standardization, 2003.

## DEDICATED SOFTWARE PACKAGE FOR PRESSURE REGULATION AT 1 PPM LEVEL USING A GAS-CONTROLLED HEAT-PIPE

SALVATORE GIUNTA<sup>1</sup>, ANDREA MERLONE<sup>2</sup>, PIERO MARCARINO<sup>2</sup>,  
SIMONE BOTTA<sup>3</sup>, VALTER GIOVANETTI<sup>4</sup>

<sup>1</sup> *Avio SpA, V. I° Maggio, Rivalta, Italy*

<sup>2</sup> *Istituto Nazionale di Ricerca Metrologica, Str. delle Cacce, Torino, Italy*

<sup>3</sup> *Politecnico di Torino, c.so Duca degli Abruzzi, Torino, Italy*

<sup>4</sup> *Istituto di Ricerca sull'Impresa e lo Sviluppo – CNR, Str. delle Cacce, Torino, Italy*

A new pressure controller has been designed and developed at the Italian Istituto Nazionale di Ricerca Metrologica (INRIM). It allows pressure regulations at 1 ppm by means of a Gas-Controlled Heat-Pipe, that realizes the liquid-vapor phase transition of its working fluid. Thanks to the thermodynamic relation  $p(T)$ , linking the pressure  $p$  and the temperature  $T$  of the working fluid, the pressure control algorithm can use a thermometer as a pressure sensor, reaching in this way better pressure control than those obtainable using commercial pressure gauges. Dedicated electronics circuits and software have been developed at INRIM for the complete control of the electronics, I/O interfacing routines, PID and auto-calibrating control functions, data acquisition modules and “real-time” control. The paper reports the structure of the software, its main features and the capabilities of the whole system.

### 1. Introduction

Studies to define the International Temperature Scale ITS-90 are carried on at INRIM in the framework of determining liquid/vapor phase transition curves for the primary platinum resistance thermometry between the aluminum and silver fixed points [1]. In this field, the system named "Temperature Amplifier" [2] requires the use of two Gas-Controlled Heat-Pipes (GCHPs) coupled to the same pressure line and controlled by means of a specific system, designed and made at the INRIM. Interest in the temperature amplifier proposed by the INRIM has been shown by the laboratories of several National Metrology Institutes. New pressure-controlled GCHPs have been made and at least three different types are now available, depending on their use (research or calibration) and the temperature field required.

The GCHP realizes the liquid-vapor phase transition of the working fluid contained. Being the temperature  $T$  thermodynamically related to the pressure  $p$ , the temperature control can be obtained by means of the pressure regulation. In a previous Temperature Amplifier the fine pressure regulation in the GCHPs was obtained using a movable bellows. This was an experimental system provided with a specially developed software [3], and has been used for several research purposes [4, 5], achieving promising results for its further improvement and commercialization. Today a new series of devices is commercially available both for calibration and for research purposes. The new system consists of new GCHPs, a new pressure controller and a new software to obtain the automatic pressure regulation. The new pressure controller is portable and easier to be used. This controller is initially dedicated to several application: it will be used for the “Temperature Amplifier”, for thermometer calibration facilities and for the realization of a pressure transfer standard for interferometric manobarometers.

## 2. Software

The developed software is a package divided in forms, modules and user friendly windows and virtual consoles. Each window executes several instructions and subroutines, from the system start-up, configuration and initialize, to the lowest automation, up to the finest pressure set point achievable. A “manual” window allows to give to the operator a complete control on all the instrument involved. A view of the electro-valves scheme and a virtual panel of the resistance bridge allow to change any of reading parameters and to manually control the electro-valves opening/closing also for a desired interval expressed in milliseconds. The high level automation achieved is obtained by means of a series of data extrapolation and PID subroutines. Time dependable evaluations sub-routines are continuously running, since the electro-valves action can reach a “real time” control within 10 ms. The temperature stability is estimated as a standard deviation of a series of resistance values measured. Non significant values are filtered in real time and a data-log file is generated in order to record any event during the acquisition and control. Pressure and temperature values are continuously stored, together with all the significant information. Thermometers calibrations for comparisons are also possible and automatic “self-heating” evaluation subroutines are available too. Programmable measurements campaign can also be performed by the developed package.

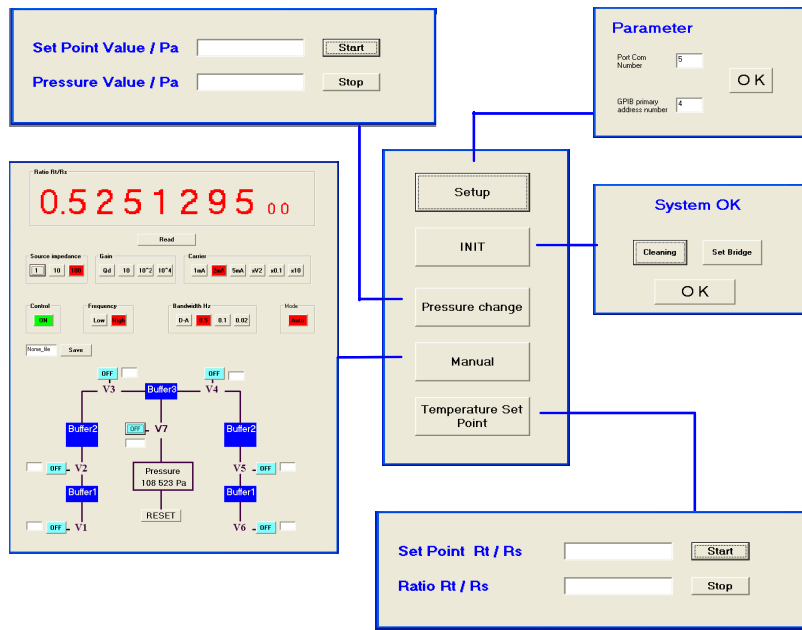


Figure 1. Main forms

## 2.1. Lowest Automation Level

It just brings the pressure to a decided set point value, using a MKS pressure sensor, without keeping it at that level. It acts on the electro-valves, opening the high (or low) pressure one, if the desired value is lower (or higher) than the starting one. When the ratio between the pressure value and the set point is 2%, it stops its action. This procedure is useful when a big pressure change is required.

## 2.2. Fine Regulation

A specific subroutine is used to maintain pressure and temperature set points in a complete automatic way, keeping all the valuable information under the operator's control. A gross regulation of pressure is obtained using a MKS pressure sensor with a sensibility of  $10^{-3}$ , the temperature is controlled within  $\pm 0,1$  °C. The fine pressure regulation is obtained using a resistance bridge as

pressure sensor with a sensibility of  $10^{-7}$  reaching a temperature controlled within 1 mK by directly setting a desired value in resistance.

### 3. Pressure Controller

The pressure controller is made of a series of volumes which are put in communication acting on several electro-valves.

Considering two different volumes  $V_i$  and  $V_j$  containing the same gas at the same temperature and at the pressures  $p_i$  and  $p_j$  respectively, the opening of an electrovalve, interposed among the two volumes, brings the final pressure to a value proportional to the ration between  $V_i$  and  $V_j$ . By accurately designing the volumes and operating the correct electro-valves opening-closing sequence, the whole system reaches the finest pressure control capabilities.

#### 3.1. Dedicated Electronics

The circuits are developed to allow the automatic pressure regulation. A microcontroller is programmed to communicate via RS232 with the PC which sends the commands to drive the electro-valves and to read the acquisition from the pressure sensor.

### 4. Preliminary results

The first results obtained with the new pressure controller and the developed software in a mercury heat-pipe demonstrate good controlling capabilities. A pressure control within few tenth of pascal has been achieved in the whole range between 50 kPa and 300 kPa.

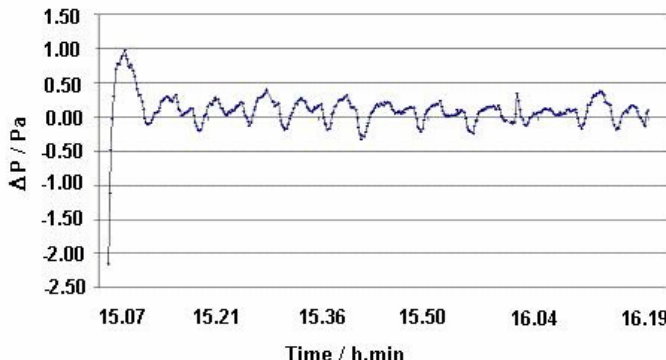


Figure 2. Pressure stability at  $p = 108\,000$  Pa.

These are preliminary results: a further improvement can be achieved introducing a “continue auto-tuning algorithm” that will allow the system to reduce the still appreciable regulation fluctuation: this will ensure the ppm level. An example of pressure control at 108 kPa is reported in next figure.

## 5. Conclusions

The described software has been developed to reach a pressure control at the ppm level, using a GCHP. The control system uses a resistance bridge and a SPRT as pressure sensor and an innovative pressure controller as actuator. The system can be used for several research and calibrations purposes. In a preliminary version, the software has been tested using a mercury GCHP and an ASL F18 resistance bridge, giving remarkable results in the range between 50 kPa and 300 kPa. Some improved control subroutines will allow the extension of the range, down to 5, by means of an “auto-tuning” principle, still under investigation. Moreover, the software will be extended to other application considering the use of other devices for the resistance readings (different bridges or multimeters), and also other GCHP, filled with different working fluids (water, cesium). Finally, the whole system, will be used for the circulating prototype of a “Temperature Amplifier”, under the Euromet project n. 772.

## References

1. Marcarino P., Merlone A., “Towards new temperature standards for contact thermometry above 660 °C”, *Metrologia*, 39, pp. 395-398 (2002).
2. P. Marcarino, A. Merlone, ”Thermodynamic Temperature Amplification By Means Of Two Coupled Gas-Controlled Heat-Pipes”, “Temperature: its measurement and control in Science and Industry”, v. 7, part 2, p. 951 – 956
3. A.Merlone, B.Cavigioli, P.Marcarino, *A new Software for the Automation of accurate Pressure Regulation in Gas controlled Heat-Pipes*, Advanced Mathematical and Computational Tools in Metrology, vol.5, Series on Advances in Mathematics for Applied Sciences vol. 57, World Scientific, Singapore, 2001, 265-269.
4. Merlone A., Dematteis R., Marcarino P., “Gas-Controlled Heat Pipes for Accurate Liquid-Vapour Transitions Measurements”, *International Journal of Thermophysics*, 24 No. 3, pp. 695-712 (2003).
5. Marcarino P., Merlone A., “Gas-Controlled Heat-Pipes for Accurate Temperature Measurements”, *Applied Thermal Engineering*, n. 23/9, pp. 1145-1152 (2003).

## MODEL ADEQUACY IN MEASUREMENTS: ESTIMATION AND IMPROVEMENT

V. A. GRANOVSKY, T. N. SIRAYA<sup>†</sup>

*Central Scientific-Research Institute “ELEKTROPRIBOR”,  
30, Malaya Posadskaya St., 197046, St. Petersburg, RUSSIA*

Adequacy improvement problem is discussed for measurement models. The main practical situations, which require improving models, are revealed and described. The peculiarities of model improvement algorithms are outlined and compared for these cases. Measurement result is proposed to be extended by including model inadequacy characteristics.

### 1. Introduction

By this paper a series of works is prolonged, which deal with the key role of models in measurements, and especially with the problem of model adequacy. Measurement procedure is investigated as a complex system of various elements; for instance, it may be schematically presented as in fig. 1, with two associated and interactive rows of elements [1]. The first (upper) row consists of the real objects, such as physical bodies and measuring instruments, and also of their properties, operations and processes. Mathematical models for the respective elements of the first row form the second row; these include measurand, models for measuring instruments and experimental data, data processing algorithms, measurement results and errors (uncertainties).

While measurement being realized, the operator usually does not pay due attention to all the elements of measurement model. For instance, metrological characteristics of measuring instruments (as models of the latter) are generally regarded as significant elements. However, the experimental procedure model and the method of measurement are habitually just meant or disregarded; so the experimental procedure is actually taken alike to similar cases. The model of physical body under investigation and that of its property (or measurand) are rarely stated explicitly. Although the experimental data model is usually

---

<sup>†</sup> Work partially supported by grant 08-08-00678-a of the Russian Foundation for Fundamental Investigations.

presented, it is next to never founded. The data model is generally suggested (on default) to be stochastic one, with Gaussian distribution of data.

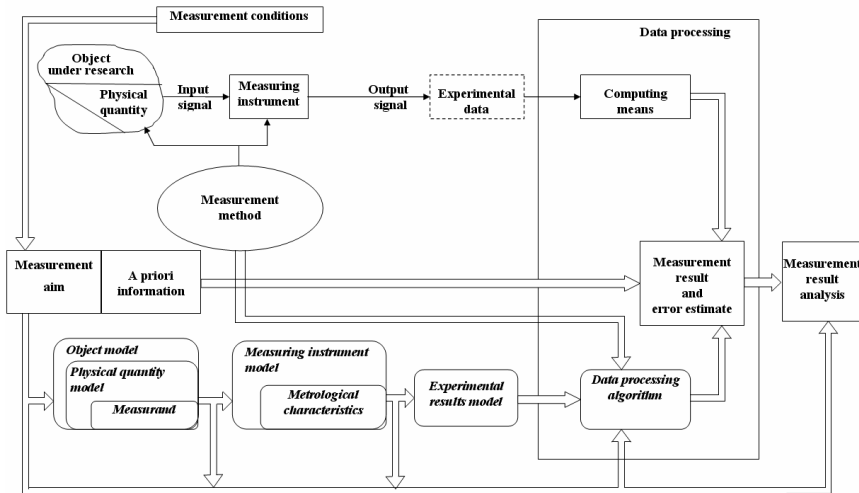


Figure 1. General measurement structure

So the general model of measurement circumstances or MMC, including all the model elements above, is never stated strictly and completely. At the same time, the measurement result (that is, measurand estimate and its error/uncertainty) may be correctly interpreted (and properly understood) only within the limits of MMC.

Similar fundamental contradictions of result interpretation are valid for model-founded reasoning in all applied fields [2]; they are naturally connected with the model adequacy analysis and validation. These problems are particularly significant just for metrology, since the problem of measurement errors estimation is of prime importance for this case.

In this report an attempt is made to outline the ways for measurement model improvement in order to overcome the difficulties in measurement result interpretation and presentation.

## 2. General Methodology

Various aspects of measurement model investigations are essential for metrology and measurement science [3-5], including main ways of model construction and adequacy (validation) problems [6-8].

The series of earlier authors' papers [8-10] are primarily directed to clear recognizing of the fundamental imperfection of the customary form of the measurement result presentation, and to outline the practical ways for its improvement based on model adequacy analysis. So, the major principles of the model adequacy analysis for measurements are formulated, and the main aspects of adequacy problem are considered in [8], such as formal (internal) and physical (external) adequacy, qualitative and quantitative ones. Various scales for inadequacy characteristics estimation are also discussed. The procedure of model improvement via step-by-step extension was investigated in [9], so it was intended for formulating and estimating of the model inadequacy characteristics.

Thus on the basis of the analysis it was suggested [8, 10] to extend the presentation of measurement result, including inadequacy characteristics of the model used to obtain this result. On the other hand, it suggests the practical reasons and natural limits for improvements of measurement model adequacy. Really, the measurement model may be considered as sufficiently adequate in case, when inadequacy error is negligible for the declared purpose or small relatively to the total measurement error. Just in this case it would be reasonable to reduce the information to two estimates - measurand value and error (uncertainty). Otherwise, it would be sensible to indicate model inadequacy characteristics or / and improve the model adequacy.

General scheme for construction, use and improvement models for measurement problems is presented in Fig. 2. The scheme demonstrates the step-by-step process of constructing a set of models for a measurement problem,

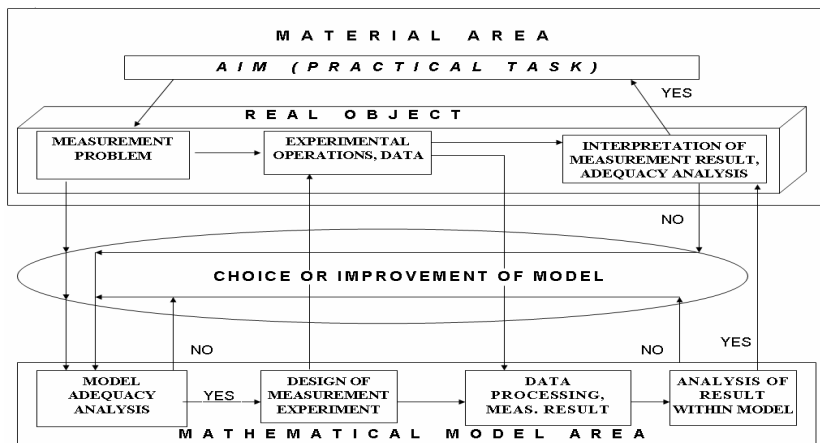


Figure 2. General scheme for construction, use and improvement models for measurement problem

which arises from practical tasks; the necessity is also shown for model adequacy analysis on different levels, both model and object ones.

Although the outlined way of model adequacy analysis may seem somewhat abstract, it really proves to be relevant for measurement practice. In particular, it turns out to be quite efficient in combination with the basic measurement model, shown at fig. 1. Thus, it may help to reveal the potential sources, producing various kinds of model inadequacy, and therefore, it could also outline the ways for model improvement.

### **3. Main Situations of Models Improvement**

Studying measurement problems, one ought to single out several typical situations, which call for the model improvement. It may be based on condition, if there is any general measurement model, which contains the current one. There are three main practical cases stated below. It is natural, that algorithms for model improvement and the necessary data are different for these cases.

a) Measurement procedure is a priori planned as a multistage process, or it is necessary to find an initial approximation for the precision method. A typical case is that zero error of a measuring instrument is corrected (at the first stage of a precise measurement). The numerous examples are offered when the calibration curves are estimated or tested. Here the total error of calibration curve  $f(X)$  consists of two components:

$$\delta f(X) = \delta_c f(X) + \delta_a f(X). \quad (1)$$

Thus the first component  $\delta_c f(X)$  is due to the approximation of the function  $f(X)$  within the assumed family of curves (for instance, linear functions); the second component  $\delta_a f(X)$  is the inadequacy error, caused by the deviations of the real curve from the assumed family (for instance, non-linearity error).

It is essential, that in this case the formal “general” model is usually known, and there are natural characteristics of the model effectiveness. Thus, the main tendencies for model improvement are usually known a priori. However, the specific ways for these may be quite different, so the choice of the way and comparison of the improved models are just relevant topics. For example, while starting from initial linear function, the most popular way of improvement is just to pass to polynomials (of limited degree). But in general it is not the best way; in many cases homographic or exponential functions turn out to be more appropriate.

b) Measurement of the highest precision (under given resources) is just a situation, which contains model improvement as an integral part. This is just an opposite case for the previous one, as here the “general” model is usually unknown or indefinite.

There are several subgroups of this case. So, numerous examples are presented by the measurements on primary standards, and so called super-precise ones [5]. Then measurement procedures contain both optimal design of measurement, and complex data processing. They may be realized as iterative procedures, including redefinition of the measurand. These are the most precise measurements under given technical and economic resources.

Somewhat different group of measurements arises when the fundamental physical limits of precision are investigated. For instance, it comprises a redefinition of a unit of quantity, based on modern physical effects, in order to obtain higher precision of unit realization and/or more effective data fusion.

c) Decision on the model improvement is taken *a posteriori*, on the basis of data analysis. There are two main variants, according to stage of analysis and decision. At the first case, the internal adequacy analysis is carried out within the model accepted, based on data obtained and assumptions taken. For instance, the properties of data are obviously different from what are expected according to the model assumed, and it is confirmed by the statistical analysis of data.

As an example the navigational determinations may be mentioned, when the increasing errors (trends) are to be corrected with use of GPS/GLONASS.

At the second case, several measurement results of the same quantity are compared, which are obtained by different methods (e. g., based on differing physical principles), and consequently – based on different measurement models. If one reveals an essential disagreement between these results, it is necessary to improve some of models, or co-ordinate all the models. Here the directions of model improvement are not known *a priori*, but they are discovered via data analysis. Often it is necessary to improve the physical model of the object, even if the initial model was not presented explicitly, or to extend MMC. One of the ways is to carry out the arbitration or independent measurements, being more precise than the compared ones. It is essential that MMC for the latter to be the most complete model and the measurand to be fixed as common one.

As above, the use of GPS/GLONASS serves as example for solution of a difficulty, when there are discrepancies of the object position determinations by various methods and instruments. In this case GPS/GLONASS may serve as an arbitration instrument.

It is to be noted that investigation for model adequacy improvement is only one aspect of model quality. In practice it is necessary to take into account resource restrictions, expenses for model construction, and the tools for solving problem within model. It implies that sometimes it is reasonable to use simple models. Being economical, clear and simple in use, stable under perturbations, these may be preferable than more adequate, but complex ones.

#### **4. Conclusions**

The above analysis leads to a conclusion that MMC is to be considered as an inalienable element of the measurement description and result presentation. Taken beyond the well defined model, the result of measurement does not allow interpretation; so it could not be used in practice. Thus it implies that it is necessary to make definition for result of a measurement [11] more precise through a set of estimates for measurand, error (uncertainty), and model inadequacy. So, definition 2.10 [11] may be extended as follows:

Notes 1 The information about the quantity may be presented as a set of three estimates, which are obtained for measurand value, error (uncertainty) and inadequacy characteristic.

2 If the measurement model is considered to be sufficiently adequate (i.e., inadequacy is negligible for the declared purpose), it is common to reduce the information to two estimates – measurand value and error (uncertainty).

Practical realization of this proposal requires solving the following problems:

- classification of MMC, based on main properties of the measurement elements and stages;
- definition of general set of model inadequacy measures or characteristics, and coordinated subsets for the main groups of MMC;
- development of methods for estimating of inadequacy characteristics for the main groups of MMC;
- formulation of criteria for testing inadequacy characteristics to be negligible for certain purpose.

#### **References**

1. Granovsky V. A., Siraya T. N. Methods of data processing in measurements. Leningrad, Energoatomizdat, 1990 (in Russian).
2. Peshel M. Modelling of signals and systems. Berlin, Veb Verlag Technique, 1978.

3. Abdullah F., Finkelstein L., Khan S. H., Hill W. J. Modeling in measurement and instrumentation. An overview, Measurement, 1994, v. 14, N 1, p. 41-53.
4. Finkelstein L. Measurement and instrumentation science. An analytical review Measurement, 1994, v. 14, N 1, p. 3-14.
5. Finkelstein L., Grattan K. T. V. (Eds.) Concise Encyclopedia of Measurement and Instrumentation, Pergamon, Oxford, 1994.
6. Butler B.P., Cox M.G., Forbes A.B, Harris P.M., Lord G.J. Model validation in the context of metrology: A survey. NPL Report CISE 19/99, 1999.
7. Eward T., Lord G., Wright L. Model validation in continuous modeling. NPL Report CMSC 29/03. – 2003.
8. Granovsky V.A., Siraya T.N. Mathematical tools in metrology: adequacy problem In “AMCTM 1999. EuroConference on Advanced Mathematical and Computational Tools in Metrology”. Oxford, 1999.
9. Granovsky V.A., Siraya T.N. Adequacy of Mathematical tools in metrology: step-by-step approach In Advanced Mathematical Tools in Metrology, V, Singapore, 2001. World Scientific, pp. 185-192.
10. Granovsky V.A., Siraya T.N. Measurement quality characteristics in metrology: systemic approach “Proc. XVII IMEKO World Congress”, 2003, Dubrovnik.
11. International Vocabulary of Basic and General Terms in Metrology, 3rd ed., BIPM 2008.

## A NEW GUIDE FOR THE DEVELOPMENT AND ASSESSMENT OF MEASUREMENT SOFTWARE

NORBERT GREIF

*Physikalisch-Technische Bundesanstalt  
Abbestr. 2-12, 10587 Berlin, Germany  
E-mail: norbert.greif@ptb.de*

GRAEME PARKIN

*National Physical Laboratory  
Hampton Road, Teddington, TW11 0LW, United Kingdom  
E-mail: graeme.parkin@npl.co.uk*

The aim of this article is to outline the purpose and rationale for a new software guide for measurement systems software. The progress on constructing the guide is described. The work is being done in collaboration with the Physikalisch-Technische Bundesanstalt (PTB) and the National Physical Laboratory (NPL).

### 1. Introduction

Software is an intrinsic part of metrology. It is used in instruments to control experiments, store and process measurement data, analyse and display results and to implement many mathematical techniques. A great number of innovations in metrology have been enabled through the use of software for simulations or complex analysis. For example, the international temperature scale ITS-90 requires the processing of high order polynomials and can only be practically implemented using software. Given this reliance, improvements in the quality of software and reduced cost of its development are vital to the effective delivery of metrology.

However, due to the increasing complexity of and dependency on software, there are considerable concerns over its quality. A study by NIST in 2000 stated that ‘Software bugs, or errors, are so prevalent and so detrimental that they cost the U.S. economy an estimated \$59.5 billion annually’. There is every reason to believe that Europe suffers in a similar way. NPL’s recent audits of instrument manufacturers, based on Software Sup-

port for Metrology (SSfM) Best Practice Guide 1, Validation of Software in Measurement Systems,<sup>1</sup> and several examinations of measurement software carried out by the PTB's Software Testing Laboratory,<sup>2</sup> have indicated that software engineering techniques, especially development and testing techniques, are not widely used.

A software guide that has been developed and accepted by leading NMI's would be more widely used and effective in the measurement community to overcome the deficiencies in software quality. For this reason PTB and NPL are currently collaborating on a proposed new guide.

## 2. Purpose of the Guide

The purpose of the proposed new guide is to enable

- developers of measurement software to know what they have to do to produce fit-for-purpose software; and
- assessors of measurement software to confirm that the developed software is fit-for-purpose.

By fit-for-purpose software we mean software that meets domain-specific measurement standards, relevant software quality standards and best software engineering practice.

The guide will also

- include a glossary of software terms to provide a common understanding of terminology in software development, software verification and validation and further essential phases of the software life cycle;
- give descriptions of appropriate techniques to be used in the development and assessment of software;
- provide risk categories with the appropriate techniques to be used for each risk level (see section 4);
- provide check lists for developers and assessors where possible; and
- where possible provide examples.

Today, there does not exist such an international software guide for measurement scientists. Consequently, based on the stated need and some initial discussions outlined in the remainder of this article, PTB and NPL have started to develop the proposed new software guide.

### **3. Main Aims of the Guide**

The following sections discuss the main aims of the guide and the approaches to deliver these aims. The proposed common view of PTB and NPL is presented.

#### ***3.1. Who Is the Guide for?***

This guide is aimed at those who implement and assess measurement software. These include at least scientists, e.g. metrologists, and instrument manufacturers. It is also applicable for testing and calibration laboratories to prove that the software used is fit-for-purpose.

#### ***3.2. Structure and Type of the Guide***

Due to the complexity of software development it is expected that there will be one main guide and some supplementary guides. The supplementary guides will include more detailed information on specific software aspects, e.g. programming language style and coding standards or static analysis. The work on the guides is based on the NPL's current SSfM Best Practice Guide 1 and the PTB's system of guidance documents for developing and assessing software.

The main guide will be developed first. Using a risk based approach (see section 4), the guide will be practical, short, and self-contained.

#### ***3.3. Types of Measurement Software***

The guide will cover all types of measurement software including COTS software, embedded software, control of instruments, mathematical processing and GUI software, developed for a laboratory application or for an instrument.

#### ***3.4. Process View versus Product View?***

By process view we mean gathering evidence during the software development via preventive process audits to show that the software is fit-for-purpose as compared to analytical testing the final or some intermediate software product or system (product view).

Generally, the quality of software can be determined from the quality of the final software product, its intermediate products and also by the underlying processes of the software lifecycle.

Product quality can be evaluated on the basis of internal product characteristics (e.g. results of static analyses), or on the basis of external product characteristics (e.g. results of dynamic functional tests). Consequently, software quality assurance consists of measures such as the assessment and improvement of software lifecycle processes via audits. These measures need to be taken as early as possible in the software lifecycle as it is more costly to correct at the later stages of development. The two main aspects of software quality, product and process view, are inseparable, and they supplement each other. The logical consequence from this is that analytical and preventive aspects of quality assurance have to be linked and directed towards the common objective of software quality.

The guide will consider both aspects of software quality and will concentrate on the process of providing evidence that the software product is fit-for-purpose.

### ***3.5. Software Lifecycle***

Based on the process view, the whole software lifecycle will be considered as it affects whether, the software is fit-for-purpose. To serve as the base for the software guide, a software process reference model is being derived from the international standard ISO/IEC 12207. Due to the aim of practicability, only the essential key process areas are being selected. Currently it is proposed, that the process reference model includes: requirements specification, design, implementation, testing, and operation/maintenance. Structuring the software processes helps to categorise the diversity of the recommended development and assessment techniques, and the different activities of life-cycle processes.

### ***3.6. Relationship with other International Standards***

There are many software standards covering different aspects of software. However, they do not cover what the proposed guide will include. Where necessary, relevant software standards will be taken into consideration. Currently, these include: IEC 61508, ISO/IEC 12207, ISO/IEC 15504 and ISO/IEC 25000 series. Wherever applicable, descriptions, requirements and recommendations of the guide will be traced back to relevant software standards.

#### 4. Risk-based Approach

No software can be shown to be completely error free due to the infeasibility of complete testing and impracticality of mathematical proof. The application of various techniques can reduce the number of errors in the software, but the more techniques that are applied the more expensive the software is to develop. Software to be used in a safety-critical environment will require more effort than that in a non safety-critical one. A risk-based approach provides a means to determine how much effort should be used in the development of software that is suitable for the application and for the consequences of when it goes wrong. The guide will provide a risk assessment procedure based on the international standards ISO/IEC 16085 and ISO/IEC 27005. Firstly, the guide will define risk categories based on measurement software specific risk factors with appropriate risk levels. To keep simple the risk assessment and the following procedure of determining techniques for each risk category, in a second step, the set of risk factors with different risk levels is mapped to an unified risk index, the so-called Measurement Software Index (MSI). Based on the general MSI (a function of all risk factors) selected development and assessment techniques have to be assigned to the defined MSI levels for each of the selected software life-cycle processes. To provide a simple risk assessment procedure, PTB and NPL are proposing the following fundamental process:

- Initially, the risk factors are restricted to the following: level of control complexity, level of processing complexity, and level of system integrity, which is considered to be composed of at least the criticality elements safety issues, security issues, or environmental issues. However, the proposed risk factors and corresponding levels can be expanded by further domain-specific aspects if needed.
- The number of risk levels for each basic risk factor is restricted to four (very low, low, high, very high).
- The number of risk levels for the general Measurement Software Index (MSI) is restricted to five (0, 1, 2, 3, 4).

For each of the three risk factors and for each of the four corresponding risk levels, a set of measurement software oriented characteristics has been drafted to derive the relevant risk level. Characteristics for the risk factor control complexity are, for example,

- the impact of software control functions on measurement processes,
- the influence of the software on measurement results or

- the number and complexity of software interactions with other software/hardware subsystems.

Based on these risk-oriented characteristics, a proposal for the MSI as a function of the risk categories has been elaborated. Each combination of risk factors and risk levels has been mapped to a MSI of 0 to 4.

The remaining problem is the assignment of appropriate software development and assessment techniques to be used to the MSI levels. For each MSI level, the guide has to recommend which techniques and, specifically, what level of activity for each lifecycle process should be used. For that purpose, the following are being developed:

- a list of practical development and assessment techniques;
- appropriate levels of activity for each selected process of the software lifecycle (process requirements);
- assignments of selected techniques and process requirements to the MSI levels for each of the selected lifecycle processes.

Based on the agreed assumptions and the final decisions to be derived, a simple risk assessment procedure relating to ISO/IEC 27005 and ISO/IEC 16085 will be implemented by the guide. Thus, the user of the guide can ensure that the user's software is fit-for-purpose concerning the main risks of the user's specific domain.

## 5. Conclusions

There is the need for an international software guide for metrologists which contains all that is required to develop fit-for-purpose software as currently none exists.

The concept of the international software guide is being jointly developed by PTB and NPL. It takes a risk-based approach. Further details of the concept are still being developed.

It is proposed that BIPM is approached to develop and publish the guide as an international software guide for the measurement community.

## References

1. RM Barker, Brian Wichmann, Graeme Parkin , *SSfM Best Practice Guide No 1: Validation of Software in Measurement Systems DEM-ES 014*, ISSN: 1744-0475, (National Physical Laboratory, January 2007).
2. Norbert Greif , *Software Testing and Preventive Quality Assurance for Metrology*, in: *Computer, Standards & Interfaces*, 28(2006)3, 286-296, ISSN: 0920-5489, Elsevier.

## CURRENT ISSUES IN THE EVALUATION OF IONISING RADIATION MEASUREMENTS

DIETER GRIENTSCHNIG

*Chemical Laboratories, Böhler Edelstahl GmbH & Co KG, Mariazeller Str. 25,  
8605 Kapfenberg, Austria*

The ISO 11929 standards series for characteristic limits of ionising radiation measurements shall be replaced by a single standard the current draft of which is ISO/DIS 11929:2008. Its scrutiny reveals that it is conditional on an arbitrary extension of the parameter space and of the likelihood function into the unphysical region not in line with ordinary Bayesian statistics and that some of the equations it includes are unfavourable.

### 1. Introduction

Ionising radiation is usually measured by detectors which produce individual electric pulses. In general, the background effect due to ambient radiation and other causes has to be taken into account. Therefore, determining the level of radiation of a sample necessitates subtraction of the background count rate measured without sample from the gross count rate obtained with the sample. For calculating the activity of the sample this count rate difference has to be divided by the detection efficiency and e.g. in the case of a wipe test also by the wiping efficiency and the area wiped.

Traditionally conventional statistics has been applied to derive a decision threshold and a detection limit for radiation measurements. Most of these calculations take only the uncertainty due to counting statistics into account and use a Gaussian approximation for the frequency distribution of the net count rate. Widely used equations for the decision threshold and the detection limit derived in that way can be found for instance in the pioneering paper by Currie.<sup>1</sup>

In 1998 Weise<sup>2</sup> used Bayesian statistics for deriving formulae of the decision threshold and the detection limit for a gross minus background count rate measurement, based upon Poisson distributions of the numbers of pulses counted. In the same paper<sup>2</sup> he also employed a general approach established earlier,<sup>3</sup> utilizing Bayesian statistics and the principle of maximum entropy, which may be applied to any mathematical model of measurement and is not limited to particular probability distribution functions of the input quantities. It became the blueprint for all parts of the ISO 11929 standards series published

from 2005 onwards, whereas its parts 1 to 4 are still founded on the conventional statistics concept. Now the whole ISO 11929 standards series shall be replaced by a single standard. Its current draft<sup>4</sup> is entirely based on the new approach striving to achieve the following three objectives:

1. All uncertainty components of the measurand shall be taken into account, not only uncertainty due to counting statistics.
2. Bayesian statistics shall be employed to combine all uncertainty contributions. This objective is motivated by the preceding one which requires the combination of Type A and Type B uncertainties according to the GUM<sup>5</sup>. Although the GUM does not prescribe the use of Bayesian statistics as a prerequisite for combining different types of uncertainty, only in a Bayesian framework such an operation is accepted to be well-founded.<sup>3</sup>
3. The decision threshold and the detection limit shall be defined in such a way that the ensuing equations do not differ significantly from those of conventional statistics and that existing practices therefore can be maintained if the uncertainty originates only from counting statistics.<sup>2</sup> Thus, in the latter case the revision of the standard aims at replacing its theoretical framework without changing the numerical results it produces.

## **2. Scrutiny of the ISO/DIS 11929:2008 Concept**

### **2.1. Terms and Definitions**

The theoretical foundations of ISO/DIS 11929:2008<sup>4</sup> are explained in its Annex F. It will be reviewed in the sequel, adopting and explaining its symbols.

In ISO/DIS 11929:2008 the measurand quantifies the ionising radiation emanating from a sample. Therefore, its smallest true value  $\tilde{y}$  corresponds to the absence of such radiation and is 0, whereas its observed values  $y$  resulting from measurement are not restricted to the positive half-axis. This means that the parameter space<sup>6</sup> is  $\Pi = [0, \infty)$  and the sample space<sup>6</sup>  $\Sigma = (-\infty, \infty)$ . The conditional probability of the estimated value  $y$  given the true value  $\tilde{y}$  is denoted by  $f(y|\tilde{y})$ . Considered as a function of  $y$  for fixed  $\tilde{y}$  it is called the sampling distribution<sup>6</sup> if  $y$  is used as a test statistic in hypothesis testing. For a constant value  $y$  the mathematical expression of  $f(y|\tilde{y})$  represents a function of  $\tilde{y}$  which is called the likelihood function or simply the likelihood. Sometimes a separate symbol like  $l(\tilde{y}, y)$ ,<sup>7</sup>  $L(\tilde{y}; y)$  or inexpeditiously also  $L(\tilde{y}|y)$  is introduced for it whereas  $f_0(\tilde{y}|y)$  is chosen in ISO/DIS 11929:2008. There the prior distribution of  $\tilde{y}$  is denoted by  $f(\tilde{y})$ . The conditional probability of the true value  $\tilde{y}$  given the estimated value

$y$  represents the posterior distribution if it is interpreted as a function of  $\tilde{y}$  for fixed  $y$ . Due to Bayes' theorem it can be expressed as

$$f(\tilde{y} \mid y) = \frac{f_0(\tilde{y} \mid y)f(\tilde{y})}{\int_{\Pi} f_0(\tilde{y}' \mid y)f(\tilde{y}')d\tilde{y}'}, \quad \tilde{y} \in \Pi, y \in \Sigma. \quad (1)$$

For such a nonnegative parameter  $\tilde{y}$  a prior of the form  $1/\tilde{y}$  is quite common although it cannot be normalized. Only for the widely used and also improper uniform prior the posterior distribution is proportional to the likelihood.

## 2.2. Extension of the Parameter Space

ISO/DIS 11929:2008 actually uses the extended parameter space  $\Xi = (-\infty, \infty)$ , but with a Heaviside step function prior which is unity for  $\tilde{y} \geq 0$  and zero elsewhere. In these circumstances the equivalent of Eq. (1) reads

$$f(\tilde{y} \mid y) = \frac{f_0(\tilde{y} \mid y)f(\tilde{y})}{\int_{\Xi} f_0(\tilde{y}' \mid y)f(\tilde{y}')d\tilde{y}'}, \quad \tilde{y} \in \Xi, y \in \Sigma, \quad (2)$$

corresponding to Eq. (F.2) in ISO/DIS 11929:2008. Equation (2) does not conform to customary Bayesian statistics which assumes the parameter space to be restricted in such a way that prior distributions are strictly positive.<sup>7</sup> The posterior density function given by Eq. (2) reaches to  $\tilde{y} < 0$  where it is zero. The likelihood function is also formally extended to negative  $\tilde{y}$  values. Since  $f_0(\tilde{y} \mid y)$  equals  $f(y \mid \tilde{y})$  and represents the conditional probability of the estimated value  $y$  given the true value  $\tilde{y}$  it remains unclear what this probability for an impossible and thus hypothetical true value  $\tilde{y} < 0$  should mean. Moreover, it is completely irrelevant which values are attributed to  $f_0(\tilde{y} \mid y)$  for  $\tilde{y} < 0$  because the prior vanishes there and thus multiplication with the prior gives zero anyway.

## 2.3. Application of the Principle of Maximum Entropy

The observed value  $y$  called primary measurement result<sup>4</sup> is calculated by inserting the estimates of the input quantities into the mathematical model of the measurement. Its standard uncertainty  $u(y)$  results from combining the standard uncertainties of the estimates of all input quantities in the way established by the GUM<sup>5</sup>. Next, the maximum-entropy distribution of expectation  $y$  and variance  $u^2(y)$  defined in the extended parameter space  $\Xi$  is calculated and employed as the likelihood function. The motivation for this approach is the belief that using the combined standard uncertainty calculated from both Type A and Type B uncertainties as the standard deviation of a distribution would be theoretically

sound for the likelihood function but not for the sampling distribution. Insertion of the ensuing Gaussian distribution into Eq. (2) gives the posterior

$$f(\tilde{y} | y) \propto \exp\left(-\frac{(\tilde{y} - y)^2}{2u^2(y)}\right) \cdot f(\tilde{y}), \quad \tilde{y} \in \Xi, y \in \Sigma. \quad (3)$$

The fact that its location parameter and its scale parameter are  $y$  and  $u(y)$  respectively is only due to the extension of the parameter space. Applying the principle of maximum entropy with respect to the original parameter space would result in a location parameter less than  $y$  and a scale parameter greater than  $u(y)$ .<sup>8</sup> Therefore, the arbitrary extension of the parameter space does not only lead to a different notation but to a posterior distribution  $f(\tilde{y}|y)$  of sometimes substantially different shape.

#### **2.4. Sampling Distribution Allowing for all Uncertainty Contributions**

Given the relation between the likelihood function and the sampling distribution,  $f_0(\tilde{y}|y) = f(y|\tilde{y})$ , Eq. (2) for Bayes' theorem with respect to the extended sample space may also be written as

$$f(\tilde{y} | y) \propto f(y | \tilde{y}) f(\tilde{y}), \quad \tilde{y} \in \Xi, y \in \Sigma. \quad (4)$$

Since  $f(\tilde{y})$  vanishes for  $\tilde{y} < 0$  a comparison of Eqs. (3) and (4) permits  $f(y|\tilde{y})$  to be evaluated only for  $\tilde{y} \geq 0$  and yields the sampling distribution

$$f(y | \tilde{y}) \propto \exp\left(-\frac{(\tilde{y} - y)^2}{2u^2(y)}\right), \quad \tilde{y} \in \Pi, y \in \Sigma. \quad (5)$$

Thus, ISO/DIS 11929:2008 is based upon the very unusual approach of deriving the sampling distribution from the posterior distribution. But by examining the calculation of the foregoing expression it becomes apparent that in fact the posterior distribution plays no part in it. Actually, Eq. (5) is obtained without mentioning Bayes' theorem and the posterior distribution by simply applying the identity  $f(y|\tilde{y}) = f_0(\tilde{y}|y)$ , extending the parameter space and inserting the maximum-entropy distribution for  $f_0(\tilde{y}|y)$ . It seems that the detour taken in ISO/DIS 11929:2008 is meant to impart a Bayesian character to the likelihood function in order to justify using a standard uncertainty combined of Type A and Type B uncertainties as a basis of its maximum-entropy distribution.

Equation (5) considered as a function of  $y$  for a certain  $\tilde{y}$  does not represent a Gaussian distribution because the denominator of the argument of the exponential function depends on  $y$ . However, in Eq. (5) the variance  $u^2(y)$  of the likelihood function  $f_0(\tilde{y}|y)$ , which is a function of  $\tilde{y}$  for given  $y$ , is approximated

by the variance  $\tilde{u}^2(\tilde{y})$  of the sampling distribution  $f(y|\tilde{y})$ , i.e. the distribution of  $y$  for fixed true value  $\tilde{y}$ . Although  $y$  may be negative whereas  $\tilde{y}$  may not it is assumed that in practice  $y$  is close enough to  $\tilde{y}$  and the dependence of  $u^2$  on  $y$  sufficiently weak for this approximation to be acceptable. This results in the approximate equation of the sampling distribution,

$$f(y|\tilde{y}) \propto \exp\left(-\frac{(\tilde{y}-y)^2}{2\tilde{u}^2(\tilde{y})}\right), \quad \tilde{y} \in \Pi, y \in \Sigma, \quad (6)$$

which leads in the usual manner to the equations for the decision threshold,  $y^* = k_{1-\alpha} \tilde{u}(0)$ , and the detection limit,  $y^\# = y^* + k_{1-\beta} \tilde{u}(y^\#)$ , where  $k_{1-\alpha}$  and  $k_{1-\beta}$  signify the respective quantiles of the normal distribution.

## 2.5. Application to Poisson Distributed Counts

For a net count rate measurement the numbers of gross counts  $n_g$  and of background counts  $n_0$  are Poisson distributed and with the respective counting times  $t_g$  and  $t_0$  the approach of ISO/DIS 11929:2008 leads to the decision threshold<sup>4</sup>

$$y^* = k_{1-\alpha} \sqrt{\frac{n_0}{t_0} \left( \frac{1}{t_g} + \frac{1}{t_0} \right)}. \quad (7)$$

It is identical to the equation of conventional statistics for the Gaussian approximation. However, the posterior distribution of the true number of background counts for a number  $n_0$  of pulses counted and uniform prior is not a Poisson distribution of variance  $n_0$ , but a gamma distribution of variance  $n_0 + 1$ . Thus the decision threshold formula resulting from Bayesian statistics reads<sup>2</sup>

$$y^* = k_{1-\alpha} \sqrt{\frac{n_0+1}{t_0} \left( \frac{1}{t_g} + \frac{1}{t_0} \right)}. \quad (8)$$

The difference between Eqs. (7) and (8) is not only conceptually significant but also of practical importance because for a small true number of background counts the probability of the error of the first kind deviates more strongly from  $\alpha$  for Eq. (7) than for Eq. (8).<sup>9</sup>

## 2.6. Coverage Interval for the Measurand

Due to the characteristics of the posterior distribution given by Eq. (2) or (3) the probabilistically symmetric coverage interval for the measurand stipulated by ISO/DIS 11929:2008 leads to the awkward result that it never includes zero and

in certain circumstances not even the posterior mode. Thus, it seems to indicate that regardless of the coverage probability chosen complete absence of radiation could be excluded. Since ionising radiation measurement is a sensitive field such an interpretation might lead to unwarranted irritation. This would be avoided by establishing a coverage interval of shortest length instead, which is easy to calculate for the truncated Gaussian distribution present.<sup>10,11</sup>

### 3. Conclusion

With the intention of achieving the three objectives reported in the introduction ISO/DIS 11929:2008 adopts a concept that includes a questionable extension of the parameter space and of the likelihood function. The choice to set up just this extended likelihood function by the primary measurement result and the combined standard uncertainty seems at least as arbitrary as the usual combination of Type A and Type B uncertainties this approach is meant to replace.

### References

1. L. A. Currie. Limits for Qualitative Detection and Quantitative Determination — Application to Radiochemistry. *Anal. Chem.*, 40:586–593, 1968.
2. K. Weise. Bayesian-statistical decision threshold, detection limit, and confidence interval in nuclear radiation measurement. *Kerntechnik*, 63:214–224, 1998.
3. K. Weise and W. Wöger. A Bayesian theory of measurement uncertainty. *Meas. Sci. Technol.*, 4:1–11, 1993.
4. ISO/DIS 11929. Determination of the characteristic limits (decision threshold, detection limit and limits of the confidence interval) for measurements of ionizing radiation — Fundamentals and application. International Organization for Standardization, Geneva, 2008.
5. *Guide to the Expression of Uncertainty in Measurement*, Second edition. International Organization for Standardization, Geneva, 1995.
6. J. Bernardo and R. Rueda. Bayesian Hypothesis Testing: A Reference Approach. *Internat. Statist. Rev.*, 70:351–372, 2002.
7. J. M. Bernardo. Bayesian Statistics. In: R. Viertl (ed.) *Probability and Statistics, Encyclopedia of Life Support Systems (EOLSS)*. Eolss Publishers, Oxford, 2003.
8. E. T. Jaynes. Prior Probabilities. *IEEE Trans. Sys. Sci. Cybernet.*, sec-4:227–241, 1968
9. D. J. Strom and J. A. MacLellan. Evaluation of eight decision rules for low-level radioactivity counting. *Health Phys.*, 81:27–34, 2001.
10. R. J. A. Little. The statistical analysis of low-level radioactivity in the presence of background counts. *Health Phys.*, 43:693–703, 1982.
11. B. P. Roe and M. B. Woodroffe. Setting Confidence Belts. *Phys. Rev.*, D63:13009, 2001.

## MODELLING AND UNCERTAINTY ESTIMATES FOR NUMERICALLY RECONSTRUCTED PROFILES IN SCATTEROMETRY

HERMANN GROSS, ANDREAS RATHSFELD\*, MARKUS BÄR

*Physikalisch-Technische Bundesanstalt, Abbestr. 2-12, 10587 Berlin;*

*\*Weierstrass Institute for Applied Analysis and Stochastics, Mohrenstr. 39, 10117 Berlin,  
Germany*

With decreasing feature sizes of lithography masks, increasing demands on metrology techniques arise. Scatterometry as a non-imaging indirect optical method is applied to periodic line-space structures in order to determine geometric parameters like side-wall angles, heights, top and bottom widths and to evaluate the quality of the manufacturing process. The numerical simulation of the diffraction process is based on the finite element solution of the Helmholtz equation. The inverse problem seeks to reconstruct the grating geometry from measured diffraction patterns. The uncertainties of the reconstructed geometric parameters essentially depend on the uncertainties of the input data. We compare the results obtained from a Monte Carlo procedure to the estimations gained from the approximative covariance matrix of the profile parameters close to the optimal solution and apply them to EUV masks illuminated by plane waves with wavelengths in the range of 13 nm.

### 1. Introduction

In scatterometry the sample to be examined is irradiated with monochromatic or broadband light at different angles of incidence, and the reflected or transmitted light is measured in an angle-resolved way. Scatterometric measurements are shown schematically in Fig. 1. As no imaging optics is used, profile parameters of the etched structure and optical material properties can be determined only indirectly from the measured scattered light. The fractions of the light energy in the individual diffraction directions, i.e. their efficiencies, and the phase shifts are strongly marked by the profile, structure and distribution of the optical indices. Thus, the inverse problem is here a profile reconstruction: geometric parameters must be derived from the measured reflected and transmitted modes. Fig. 2 shows the parameterization of the cross-section over one period (840 nm) of a typical line-space structure for lithography in the extreme ultraviolet wavelength range. The line is a symmetric bridge made of three layers of different materials with typical dimensions of 55nm height and 140nm width. A

multilayer stack with a period of 7nm beneath the line-space structure enables the reflection of EUV waves.

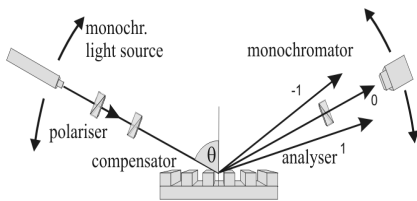


Figure 1. Scatterometric measurement scheme.

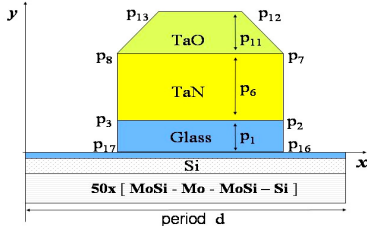


Figure 2. Typical EUV mask of line-space structures over a MoSi multilayer stack.

## 2. Mathematical Modeling – Direct Problem

The mathematical basis for modelling the propagation of electromagnetic waves in matter are Maxwell's equations. Their numerical solution represents a direct problem. From the data of the incident light and from characteristic parameters of the irradiated grating, the efficiencies and phase shifts for the different diffraction directions are calculated. We use the finite element method (FEM) for the forward calculations on mask profiles.

Since the polarized incident wave can be represented as a superposition of a TE- and a TM-polarized mode, i.e. of waves with the electric field vector oscillating normally and parallel, respectively, to the plane of incidence, Maxwell's equations for the electromagnetic field in the time-harmonic case reduce to the scalar Helmholtz equation over one period of the cross-section domain of the mask specimen (cf. the details in [1,2]):

$$\Delta u(x, y) + k^2 u(x, y) = 0 \text{ with } k = k(x, y) = \omega \sqrt{\mu_0 \epsilon(x, y)} \quad (1)$$

Here, the unknown  $u$  is the z-component of the electric resp. magnetic field, the wave number  $k$  is constant in each area of the mask specimen filled by the same material, and  $\omega$  is the circular frequency of the incident plane wave. FEM solution of this boundary value problem and the so-called Rayleigh representation of  $u(x, y)$  provides a general solution above and below the mask. For the areas above or below the grating structure, the following splitting into propagating plane waves and evanescent modes hold in the TE case:

$$E_z(x, y) = \sum_{n=-\infty}^{\infty} A_n^+ \exp(i\beta_n^+ y + i\alpha_n x) + A_0^{inc} \exp(-i\beta_0^+ y + i\alpha x),$$

for  $y \geq b^+$  (above) (2)

$$E_z(x, y) = \sum_{n=-\infty}^{\infty} A_n^- \exp(-i\beta_n^- y + i\alpha_n x), \text{ for } y \leq b^- \text{ (below)} \quad (3)$$

$$\text{with } k^\pm = k(x, b^\pm), \alpha_n = k^+ \sin \theta + \frac{2\pi}{d} n \text{ and } \beta_n^\pm = \sqrt{(k^\pm)^2 - \alpha_n^2}.$$

For the approximation accuracy of FEM the quotient optical wavelength over period of the grating structure is important. If it is markedly smaller than 1, e.g. 1/100, lots of oscillations occur, and the approximation is bad or the calculation times become unacceptably long. However, by means of a suitable extension of the method (GFEM: generalized FEM) - as offered by the DIPOG software package [4] - also such cases can be calculated accurately and with reasonable effort.

### 3. Inverse Problem

The inverse problem consist in determining the parameters  $p_j, j = 1, \dots, J$  describing the geometry of the grating from the measured efficiency/phase shift values. An equivalent optimization problem is set up with the following objective functional which is to be minimized:

$$f(\{p_j\}) = \sum_{l=1}^L \sum_{m=1}^M \sum_{n=(n,\pm):n \in U^\pm} b_n^\pm(\lambda_l, \theta_m) \left[ e_n^\pm(\lambda_l, \theta_m) - c_n^\pm(\lambda_l, \theta_m) \right]^2 \quad (4)$$

Hereby,  $\lambda_l, l = 1, \dots, L$  and  $\theta_m, m = 1, \dots, M$  are the wavelengths or angles of incidence of the measurement. The  $c_n^\pm(\lambda_l, \theta_m)$  designate the measured efficiencies or phase shifts, and  $b_n^\pm(\lambda_l, \theta_m)$  are freely chosen weight factors. The  $e_n^\pm(\lambda_l, \theta_m)$  are the efficiencies or phase shifts calculated by FEM for the grating with the parameters  $p_j, j = 1, \dots, J$ . The values of the grating parameters are varied until the minimum of the functional has been found. Theoretically, the uniqueness of the minimum solution for the parameter identification of the grating cannot be proved. Practically, accurate results will be achieved if there is a sufficient number of measured values and if the bounds for the sought parameters have been chosen appropriately.

An example of the objective functional  $f$  as a function of two grating parameters (layer thickness  $p_6$  and a lateral coordinate  $p_7$ ) is shown in Fig. 3. The functional was defined choosing  $b_n^\pm = 1$  and including the deviation terms

from the diffraction orders -11 to 11 over three different wavelengths and one angle of incidence (cf. Fig. 3, left). A distinct minimum can be seen at exactly the right point. However, the figure also shows that an unfavourable choice of the initial value for the layer thickness, i.e. a value greater than 60 nm or smaller than 50 nm, leads to a false reconstruction result. The gradient-based optimization procedures applied would then find the local minima of the neighbouring valleys. A more suitable choice of the weight factors  $b_n^\pm$  and the choice of an optimal subset of the measured data included into the functional  $f$  improve the shape of the graph such that disturbing secondary minima disappear (cf. Fig. 3, right). Thus the optimization converges faster, and the final approximate solution is less dependent of the initial choice of parameters. This sensitivity enhancement is based on optimizing the conditioning of some Jacobian matrices [cf. the details in 2,3].

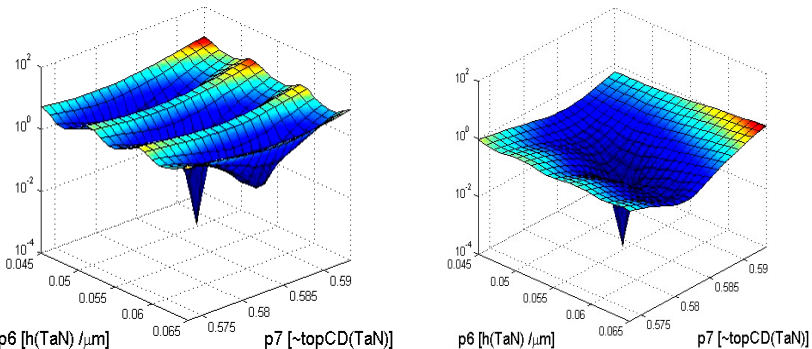


Figure 3. Left: objective functional of the reconstruction test for an EUV mask with complete simulated data set. Right: weighted objective functional based on an optimal subset of 12 data values.

#### 4. Uncertainty Estimation

Clearly, the measured efficiency values  $c_n^\pm$  entering the numerical algorithm have an uncertainty. It is important to see how these uncertainties affect the accuracy of the reconstructed parameter values. To analyze this, a simple model is considered: Suppose that systematic effects can be neglected and that the values of uncertainty contribution to  $c_n^\pm$  are normally distributed (Gaussian)

with zero mean and standard deviation  $u_{c_n^\pm} = \sqrt{(a \cdot c_n^\pm)^2 + (b_g)^2}$ . Then, one

identifies the uncertainties of the input data with  $u_{c_n^\pm}$ . The first term  $a \cdot c_n^\pm$  represents a linearly dependent noise with a constant factor  $a$  (e.g.  $a = 0.01$ ). The second term accounts for a background noise independent of the measured efficiencies or phase shifts (typical value of  $b_g$  is  $10^{-5}$ , i.e.,  $b_g = 0.001\%$ ).

First we apply a Monte Carlo method similar to the recommendations in Supplement 1 of the GUM [5], i.e., complete profile reconstructions are repeated many times, e.g.  $M$  times, with randomly perturbed simulated data. So a distribution of the reconstructed parameters is generated and their deviations from the true values can be calculated. In a first test, the data set consists of only 12 efficiencies values for an optimally chosen index set of data included into the summation of the objective functional  $f$ . We use N2s-12 as an initial for this data set. For these efficiencies, their distribution around the undisturbed values is shown in Fig. 4, left. To these  $M$  sets of efficiencies, the numerical reconstruction algorithm is applied, and  $M$  approximate solution vectors for the sought profile parameters, e.g.,  $p_6$ ,  $p_7$ , and  $p_{16}$  of the line-space structure already shown, are obtained (cf. Fig. 4, right). The ranges between lower and upper quartiles are indicated by boxes, and the medians by lines. In a further test, the full simulated data set (N2s-415), consisting of 415 efficiency values for four different wavelengths and three different angles of incidence, is used. As expected, the range of the resulting profile parameters is clearly reduced in the case of substantially larger data sets. However, a 1 nm range is reached already for the smaller data set consisting of only 12 optimally chosen efficiency values.

Alternatively, a faster way to estimate the uncertainties is to follow a proposal by Al-Assaad and Byrne [6]. If the mapping  $(p_j) \mapsto (e_n^\pm)$  is assumed to be locally almost linear, at least for  $(p_j)$  close to the point of the optimal solution, then the uncertainties of the reconstructed parameters are, again, normally distributed random numbers with zero mean. The standard deviation  $\sigma_j$  of  $p_j$  is the square root of the  $j^{\text{th}}$  main diagonal entry of the covariance matrix  $\text{Cov}$  given by the following approximation:

$$\text{Cov} = \left[ J_u^T \cdot J_u \right]^{-1}, \quad J_u := \left( \frac{\partial e_n^\pm}{\partial p_j} \quad \frac{1}{u_{c_n^\pm}} \right)_{n,j}. \quad (5)$$

If the two examples (N2s-12, N2s-415) of an EUV mask reconstruction are calculated by means of this covariance method, the results are comparable with those of the Monte Carlo experiments. In fact we observe deviations up to 30% for N2s-12 and up to 10% for N2s-415.

For all parameters investigated and reconstructed with simulated measurement data and even for optimal input data sets of a moderate size, the relative uncertainties have been found to be smaller than 2 %. Of course, these results are valid under the assumption, that the uncertainties resulting from the inaccuracies in the geometric modelling of the line-space structure are neglected respectively are much smaller than the uncertainties of the measured efficiencies or phase shifts, ranging from 1 to 3 % in the numerical examples. In further investigations the impact of effects like non-periodic details of real mask structures, e.g., roughness in the interfaces of the multilayer stack beneath the line-space structure, on the uncertainties of the reconstructed parameters will be examined.

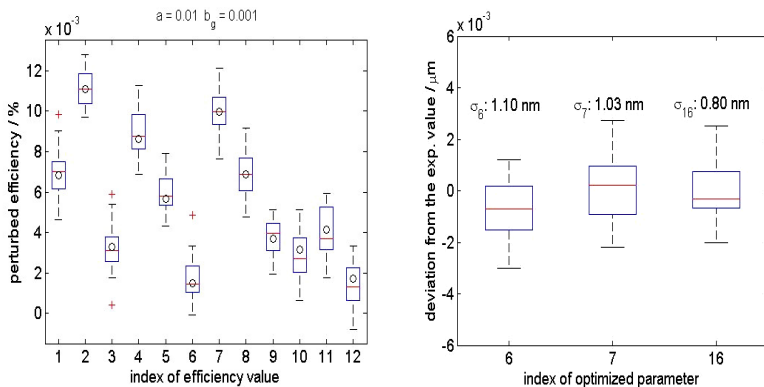


Figure 4. Effect of perturbed efficiencies (left) of a set of 12 values on the reconstructed parameters of an EUV mask, shown as deviation from the true values (right).

## References

1. H. Gross, R. Model, M. Bär, M. Wurm, B. Bodermann and A. Rathsfeld, *Measurement* **39**, 782 (2006).
2. H. Gross and A. Rathsfeld, *Waves in Random and Complex Media*, **18:1**, 129 (2008).
3. H. Gross, A. Rathsfeld, F. Scholze, M. Bär and U. Dersch, *Proc. of SPIE* **6617**, 66171B-1 (2007).
4. J. Elschner, R. Hinder, A. Rathsfeld and G. Schmidt, *DIPOG Homepage*, <http://www.wias-berlin.de/software/DIPOG>.
5. BIPM, IEC, IFCC, ILAC, ISO, IUPAC, IUPAP and OIML 2006 Evaluation of measurement data - Supplement 1 (to appear)
6. R. M. Al-Assaad and D. M. Byrne, *J. Opt. Soc. Am. **24** (2)*, 330 (2007).

## KALMAN FILTER TYPE SEQUENTIAL METHOD WITH STOPPING RULE FOR CALIBRATION OF MEASUREMENT INSTRUMENTS

CHINGIZ HAJIYEV

*Istanbul Technical University, Faculty of Aeronautics and Astronautics,  
Maslak, 34469, Istanbul, Turkey*

In this paper a Kalman filter type algorithm for estimating a calibration characteristic of measurement instruments is presented. That approach gives a rigorous derivation of a recurrent algorithm for estimating the parameters of the calibration curve with the incorporation of the errors in reproducing the inputs. A new approach has been proposed for the generation of stopping rule in calibration characteristics identification problem. The proposed stopping rule defines the coefficients estimation halt and makes possible to determine sufficient number of measurements to attain required accuracy of calculated estimates. As an example, the problem of calibration of a differential pressure gauge using standard pressure setting devices (piston gauges) is examined.

### 1. Introduction

A measuring instrument is calibrated in measurement engineering by means of a high-precision standard instrument that reproduces standard signals for particular measurement intervals, which pass to the instrument and produce output signals that define the calibration characteristic.

The least squares method (LSM) is a technique widely used in practice for processing experimental data [1-3]. In the measurement instruments calibration problem LSM is used for the statistical estimation with high accuracy of coefficients in calibration curves. As is known [1], the use of LSM has limitations. For one thing, values of the arguments  $x(k), k = 1, \dots, n$  used to plot a relation  $y = f(x)$  may be measured with a certain error. The main relation for results of measurements in this case takes the form

$$y(k) = f[x(k) + \delta_x(k)] + \delta_y(k), \quad (1)$$

where  $\delta_x(k)$  and  $\delta_y(k)$  are the errors in argument and output coordinate, respectively. In such a situation, the use of LSM gives usually biased results and what is important incorrect estimates of their errors. Standard instruments for calibration (which reproduce the inputs) also have errors, and LSM in that case may lead to erroneous results.

In this paper a Kalman filter type algorithm for estimating a calibration characteristic of measurement instruments with account of the input signals errors is presented. A new approach for the generation of stopping rule in calibration characteristic identification problem is proposed. Combining the sequential calibration algorithm with the proposed stopping rule provides the required accuracy with the minimum number of measurements, which substantially reduces the economical and time expenses.

## 2. Problem Formulation

Consider calibrating a measurement instrument by means of standard setting devices. The calibration characteristic of the measurement instrument is described adequately by an  $m$ -order polynomial

$$y = a_0 + a_1 p + a_2 p^2 + \dots + a_m p^m \quad (2)$$

The measurement equation is written as

$$z_y(k) = a_0 + a_1 p(k) + a_2 p^2(k) + \dots + a_m p^m(k) + v(k), \quad k = 1, \dots, n, \quad (3)$$

where  $v(k)$  is the Gaussian random measurement errors with zero mean and variance  $\sigma^2$ . It was assumed that values of arguments  $p(k), k = 1, \dots, n$  (values generated by standard setting devices) were known with errors. It is required to design algorithm for the calibration curve (2) coefficients estimation with allowance for the reproduced input signals errors which provides the required calibration accuracy with the minimum number of measurements.

## 3. Algorithm for Estimation of the Calibration Curve Coefficients Regarding Errors in the Inputs

We represent Eqs. (2) and (3) in vector form

$$y(k) = \boldsymbol{\phi}^T(k) \boldsymbol{\theta}^T \quad (4)$$

$$z_y(k) = \boldsymbol{\phi}^T(k) \boldsymbol{\theta} + v(k), \quad k = 1, \dots, n \quad (5)$$

where  $\boldsymbol{\phi}^T(k) = [1, p(k), p^2(k), \dots, p^m]$  is the input vector (regression vector),  $\boldsymbol{\theta}^T = [a_0, a_1, a_2, \dots, a_m]$  is the vector of unknown (to be estimated) parameters. This class of model is of interest for the reason that familiar, efficient and simple methods can be used to estimate the parameter vector  $\boldsymbol{\theta}$ . However, these methods were developed for the special case where the regression vector  $\boldsymbol{\phi}(k)$  is accurately known. However, if this vector was measured with an error, the existing methods give inaccurate (biased) results and incorrect error estimates.

Our goal in this study was to design an estimation algorithm for a linear regression model with allowance made for the regression vector error.

Expression (5) includes the input coordinate error  $v(k)$  and the regression vector error  $\delta_\varphi(k)$ . Allowing for this, we obtain

$$\begin{aligned} z_y(k) &= [\boldsymbol{\varphi}(k) + \delta_\varphi(k)]^T \boldsymbol{\theta}(k) + v(k) = \boldsymbol{\varphi}^T(k) \boldsymbol{\theta}(k) + \delta_\varphi^T(k) \boldsymbol{\theta}(k) + v(k) \\ &= \boldsymbol{\varphi}^T(k) \boldsymbol{\theta}(k) + \delta_{rd}(k) \end{aligned} \quad (6)$$

where  $\delta_{rd}(k) = \delta_\varphi^T(k) \boldsymbol{\theta}(k) + v(k)$  is the reduced error.

In what follows, the measurement error  $z_y(k)$  is expressed in terms of the reduced error. The reduced error variance is

$$D_{\delta_{rd}}(k) = \sigma^2 + \boldsymbol{\theta}^T(k) D_\varphi(k) \boldsymbol{\theta}(k), \quad (7)$$

where  $D_\varphi(k)$  is the covariance matrix of input variable errors, whose diagonal elements are variances of the corresponding components of the regression vector  $\boldsymbol{\varphi}(k)$ . Applying the optimum linear Kalman filter [4] to model (3)-(4) and keeping in mind that the variance of measurement error  $z_y(k)$  is determined by expression (7), we obtain

$$\hat{\boldsymbol{\theta}}(k) = \hat{\boldsymbol{\theta}}(k-1) + K(k)[z_y(k) - \boldsymbol{\varphi}^T(k) \hat{\boldsymbol{\theta}}(k-1)], \quad (8)$$

$$K(k) = \frac{P(k-1)\boldsymbol{\varphi}(k)}{\boldsymbol{\varphi}^T(k)P(k-1)\boldsymbol{\varphi}(k) + \hat{\boldsymbol{\theta}}^T(k-1)D_\varphi(k)\hat{\boldsymbol{\theta}}(k-1) + \sigma^2} \quad (9)$$

$$P(k) = P(k-1) - \frac{P(k-1)\boldsymbol{\varphi}(k)\boldsymbol{\varphi}^T(k)P(k-1)}{\sigma^2 + \boldsymbol{\varphi}^T(k)P(k-1)\boldsymbol{\varphi}(k) + \hat{\boldsymbol{\theta}}^T(k-1)D_\varphi(k)\hat{\boldsymbol{\theta}}(k-1)} \quad (10)$$

where  $K(k)$  is the gain of the filter and  $P(k)$  is the covariance matrix of the estimation errors, the iteration step  $k$  indicates the ordinal number of the conducted experiment.

The Eqs. (8)-(10) represent a recurrent procedure and makes it possible to estimate the calibration characteristic (2) regarding errors in the reproduction of input signals.

#### 4. Generation of Calibration Procedure Stopping Rule

The results of the general mathematical theory of optimal stopping rules [5], a latter-day branch of probability theory, have not enjoyed any appreciable application in the generation of stopping rules in parametric identification

problems. This situation is attributable to the complexity of adapting various statistical tests of a general nature to real applied problems and algorithms.

In application to multidimensional parametric identification problems [6] the stopping rule based on comparing the statistics of the differences between two successive estimates is introduced. That rule can be used for stopping the calibration procedure of measurement instruments through following statistic:

$$r_i^2 = (\hat{\boldsymbol{\theta}}_i - \hat{\boldsymbol{\theta}}_{i-1})^T D_{\Delta\theta_i}^{-1} (\hat{\boldsymbol{\theta}}_i - \hat{\boldsymbol{\theta}}_{i-1}) \leq \varepsilon, \quad (11)$$

where  $D_{\Delta\theta_i}$  is the covariance matrix of the discrepancy between two successive estimates  $\hat{\boldsymbol{\theta}}_i$  and  $\hat{\boldsymbol{\theta}}_{i-1}$ , and  $\varepsilon$  is a predetermined small number. The discrepancy  $\hat{\boldsymbol{\theta}}_i - \hat{\boldsymbol{\theta}}_{i-1}$  has a normal distribution, since it is a linear combination of two Gaussian random variables. With these considerations in mind it is known that the statistic  $r^2$  has a  $\chi^2$  distribution with  $n$  degrees of freedom ( $n$  is the number of dimensions of the vector  $\boldsymbol{\theta}$ ), and the threshold values of  $r^2$  can be found by determining the tabulated values of the  $\chi^2$  distribution for a given level of significance. It is evident from relation (11) that the smaller the value of  $r^2$ , the greater will be the consistency of the estimates. Usually in the testing of consistency in such cases the lower limit of the confidence interval must be equal to zero, and the upper limit is determined by the level of significance  $\alpha_i$ .

To test the consistency of the estimates, the level of significance  $\alpha_i$  is adopted, which corresponds to the confidence coefficient  $\beta_i = 1 - \alpha_i$ . The threshold  $\chi_{\beta_i}^2$  is specified in terms of this probability, using the distribution of the investigated statistic  $r^2$ :

$$P\{\chi^2 < \chi_{\beta_i}^2\} = \beta_i, \quad 0 < \beta_i < 1. \quad (12)$$

The estimation process is stopped when

$$r_i^2 < \chi_{\beta_i}^2, \quad (13)$$

since further measurements yield insignificant improvement in the calibration characteristic. If the quadratic form  $r^2$  is larger than or equal to the specified threshold  $\chi_{\beta_i}^2$ , estimation should be continued. This stopping rule can be used to make a timely decision to stop the calibration process, and it does not require large computational expenditures.

The covariance matrix ( $D_{\Delta\theta_i}$ ) of the discrepancy between two successive estimates  $\hat{\boldsymbol{\theta}}_{i-1}$  and  $\hat{\boldsymbol{\theta}}_i$  may be written in the form [6]

$$D_{\Delta\theta_i} = P_{i-1} - P_i. \quad (14)$$

## 5. Calibration Coefficients Estimation by Dividing the Calibration Intervals into Halves

If the calibration curve is nonlinear, the entire calibration interval should be covered, because taking a decision to stop the process with an incomplete calibration interval may lead to errors. The calibration of an instrument in such a case is proposed to be performed on dividing the calibration intervals into halves. One first performs calibration measurements at the initial, middle, and final points of the calibration interval, and from the measurements  $z_y(1)$ ,  $z_y(n^*) = z_y(n/2)$  and  $z_y(n)$  via filter (8)-(10) calculates the corresponding estimates for the unknown calibration coefficients (if  $n/2$  is not an odd number, then as  $n^*$  one should take the nearest even number). Then the subintervals  $[1, n^*]$  and  $[n^*, n]$  are again divided into two equal parts, and in the middle points in each part the calibration measurements are fulfilled and through (8)-(10) the estimated coefficients are refined. That procedure is continued until (13) is not true. If the inequality (13) holds, then the coefficient estimation is stopped. The estimates obtained at the stopping moment will determine the calibration characteristic. As a consequence, the calibration of the measurement instrument is performed with the required accuracy on the minimum number of calibration measurements.

The calculation results for the confidence bound  $\chi_{\beta_1}^2 = 0.115$  (which corresponds to the confidence probability  $\beta_1 = 0.01$ ) are given in Fig. 1.

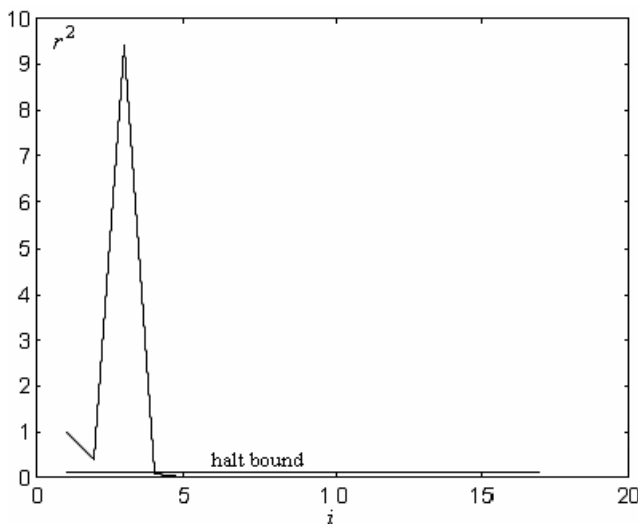


Figure 1. Behavior of statistic  $r^2$  when proposed calibration algorithm was used

As it is seen from these results, after the fifth step of estimation, according to the decision rule (13) the calibration should be stopped because further measurements lead only to a slight improvement in the calibration curve and are considered undesirable. Comparison of the obtained calibration results show that the proposed algorithm provides the required calibration accuracy with a smaller number of measurements.

The calibration algorithm with the stopping rule is tested on actual pressure measurements. Calibration values and the absolute and relative calibration errors show that the calibration errors are insignificant.

## 6. Conclusion

A sequential method with stopping rule for calibration of measurement instruments is presented. The presented method differs from existing calibration methods in that it incorporates the errors in the inputs. It is based on an algorithm of Kalman filter type, where one uses the characteristics of the reduced errors as the measurement ones. The algorithm improves the accuracy of the estimates and gives reliable evaluations of their errors.

A new approach has been proposed for the generation of stopping rule in calibration characteristics identification problem. The proposed stopping rule defines the coefficients estimation halt and makes possible to determine sufficient number of measurements to attain required accuracy of calculated estimates in practice. The reduction of the number of the calibration measurements reduces the economical and time expenses. That is particularly important in flight calibration of flying vehicles devices, where the cost of each measurement is high.

## References

1. V. A. Granovsky and T. N. Siraya, *Methods for Processing Experimental Measurement Data* (in Russian), Energoatomizdat, Leningrad, 1990.
2. L. Ljung, *System Identification. Theory for the User*, Prentice-Hall, Inc., Sweden, 1987.
3. A. A. Abdullayev and Ch. M. Gadzhiev, Metrological Support to Data-Acquisition Systems for Oil-Product Accounting, *Measurement Techniques*, **36**, 9 (1993) 977-981.
4. A. P. Sage and J. L. Melse, *Estimation Theory with Application to Communication and Control*, McGraw-Hill, New York, 1972.
5. Y. S. Chow, H. Robbins and D. Siegmund, *Great Expectations: The Theory of Optimal Stopping*, Houghton Mifflin, Boston, Mass, 1971.
6. Ch. Hajiyev, Stopping of Algorithms and Faults Detection in Kalman Filter Application. *Proc. of the 7<sup>th</sup> Mediterranean Conference on Control and Automation (MED 99)*, June 28-30, 1999, Haifa, Israel, pp. 2133-2142.

## DETERMINATION OF OPTIMUM INPUT SIGNALS VIA D-OPTIMALITY CRITERION FOR CALIBRATION OF MEASUREMENT INSTRUMENTS

CHINGIZ HAJIYEV

*Istanbul Technical University, Faculty of Aeronautics and Astronautics,  
Maslak, 34469, Istanbul, Turkey*

A procedure for optimal selection of sample input signals via D-optimality criterion to get the best calibration characteristics of measuring apparatus is proposed. As an example the problem of optimal selection of standard pressure setters when calibrating differential pressure gage is solved.

### 1. Introduction

The cost of a measuring instruments increases with its accuracy. Therefore low cost accurate measurement devices are one of the main goal of engineers. One way of reducing the cost of accuracy is the calibration process. This paper deals with the calibration of a low cost sensor with a high accurate one.

The main question is the evaluation of accurate calibration characteristics with a few number of experimental data. In the existing works for calibration of measurement apparatus the equidistant sample signals are used. On the other hand, though it is paradoxical, the application of equidistant sample signal to get the best calibration characteristic is erroneous. Therefore it is required to determine the optimal sample signals composition with a view to get the best calibration characteristics (planning experiment problem).

Different measures, all based on the dispersion matrix of the calibration coefficients estimation errors, can be chosen as criteria to design optimal inputs. In this study the *D-optimality* criterion is chosen as optimality criterion to determine the optimal input signals for calibration of measurement instruments. This criterion is the overall measure in terms of the volume of the estimation error ellipsoid, which is proportional to the determinant of dispersion matrix of the estimation errors. Therefore the input signals determined via *D-optimality* criterion minimize the determinant of dispersion matrix.

### 2. Problem Statement

From practical considerations the calibration curve should be in a polynomial form as follows

$$y_i = a_0 + a_1 p_i + a_2 p_i^2 + \dots + a_m p_i^m \quad (1)$$

where  $y_i$  is the output of the low cost transducer and  $p_i$  are the outputs of the high precision transducer,  $a_0, a_1, \dots, a_m$  are the calibration curve coefficients. Measurements contain random Gaussian noise with zero mean and  $\sigma^2$  variance. Let the calibration curve coefficients be denoted as  $\tilde{\theta} = [a_0, a_1, \dots, a_m]^T$ . The coefficients in these polynomials were evaluated in [1] by the least squares method. The expressions used to make the evaluation had the form:

$$\tilde{\theta} = (\tilde{X}^T \tilde{X})^{-1} (\tilde{X}^T \tilde{z}); \quad \tilde{D}(\hat{\theta}) = (\tilde{X}^T \tilde{X})^{-1} \sigma^2 \quad (2)$$

where  $\tilde{z}^T = [z_1, z_2, \dots, z_n]$  is the vector of the measurements,  $\tilde{X}$  is the matrix of the known coordinates (here,  $p_1, p_2, \dots, p_n$  are values that are producible by the standard instruments),  $\tilde{D}(\hat{\theta})$  dispersion matrix of the calibration coefficients' estimation errors.

The values of  $p_1, p_2, \dots, p_n$  the outputs of the high accuracy transducer, should be such that the polynomial characteristics given by (1) best approximates the real calibration characteristics. Thus the problem can be stated as follows: Find the values of  $p_1, p_2, \dots, p_n$  such that the values of  $a_0, a_1, \dots, a_m$  are optimum in a sense that a given performance criterion is minimum.

As mentioned above the matrix  $\tilde{D}$  can be used as a measure of the error between the low cost transducer and the high precision transducer. The *D-optimality* criterion is used in this study as an optimality criteria, i.e

$$\min_{p_i} \left[ \det \left( \tilde{X}^T \tilde{X} \right)^{-1} \sigma^2 \right] \quad (3)$$

is sought. The values of  $p_1, p_2, \dots, p_n$  found by solving the above equations should be in the range  $0 - p_{\max}$ . Otherwise the solution is invalid.

### 3. The Solution Algorithm

Let the objective function is denoted as:

$$f(p_1, p_2, \dots, p_n) = \det \{ \tilde{D}(p_1, p_2, \dots, p_n) \}. \quad (4)$$

As explained above the problem is a constrained optimization problem. The objective function is a multivariable, nonlinear, continuous and has derivative in the considered interval. Assume that the minimum of  $f(p_1, p_2, \dots, p_n)$  exists for the following values of  $p_1, p_2, \dots, p_n$ :  $\boldsymbol{p}^* = [p_1^*, p_2^*, \dots, p_n^*]^T$ . In order that  $\boldsymbol{p}^*$  is a minimum of (6), the following conditions should be satisfied [2]

$$\nabla f(\boldsymbol{p}^*) = 0 \quad (5)$$

$$\nabla^2 f(\boldsymbol{p}^*) \text{ is semi positive} \quad (6)$$

where  $\nabla$  denotes the gradient.

The extremum condition given by (5) can explicitly be written as:

$$\frac{\partial[\det\{\tilde{D}(p_1, p_2, \dots, p_n)\}]}{\partial p_i} = 0, \quad i = \overline{1, n}. \quad (7)$$

When the derivatives in (7) is calculated  $n$  algebraic equations with  $n$  unknowns are obtained.

$$Q_i(p_1, p_2, \dots, p_n) = 0, \quad i = \overline{1, n} \quad (8)$$

where  $n$  denotes the number of measurements. After proper mathematical transformations, the determinant of  $\tilde{D}$  dispersion matrix can be found. Having taken the corresponding derivatives one has a system of  $n$  algebraic equations with  $n$  variables. With a view to find all the possible solutions of the system one can apply numeric methods of searching that are simply realized by a computer.

#### 4. Computational Results

The results of determination of optimum input signals for calibration of measurement apparatus for the case of  $m = 2$  and  $n = 5$  are given below. In the calculations the following data and initial conditions are taken.

- Calculation of optimum input signals is performed for the differential pressure gage "Sapphir-22DD". The range of the transducer is  $0 \leq p_i \leq 1600$  bar. The differential pressure gage errors are subjected to normal distribution with zero mean and the standard error deviation  $\sigma_i = 2,6$  bar [1].

- Calibration characteristics of the differential pressure gage is described by 2 order polynomial.

The optimum input signals for calibration of above mentioned differential pressure gage are evaluated via Eqs. (8). The method is used to obtain the optimum coefficients of the characteristic polynomial for the *D-optimality* criteria. Closed form algebraic Eqs. (8) is calculated to solve the equation given in (3). The software program MATHEMATICA is used to find the optimum values of  $p_i^*(i \neq 1, i \neq n)$ . The optimum input values for the case of  $n = 5$  are tabulated in Table 1.

Table 1. Optimum and equal calibration intervals for  $n = 5$

Calibration intervals	$p_1$	$p_2$	$p_3$	$p_4$	$p_5$
Optimum intervals	0	256	800	1344	1600
Equal intervals	0	400	800	1200	1600

The obtained values of optimum input signals for calibration of differential pressure gage are checked via actual experiments. Calibration of differential pressure gage is made by the help of the standard measuring instrument. The

standard instrument reproduced pressure signals corresponding optimum and equal calibration intervals. The results of experimental checking are presented in the Fig.1.

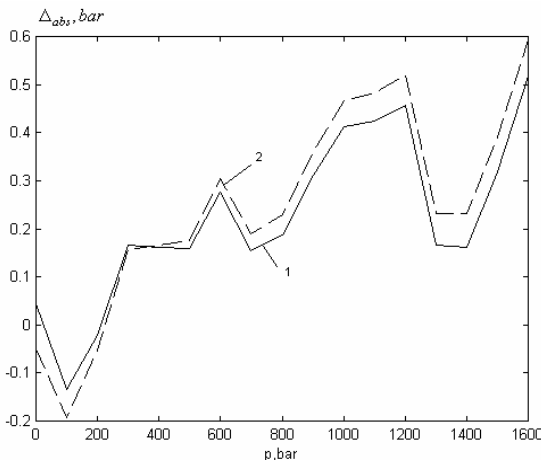


Figure 1. Absolute calibration errors: calibration was performed by using, optimum calibration intervals (1) and equal calibration intervals (2).

As it is seen from presented results, the calibration errors corresponding to optimum calibration intervals are considerably smaller than in the case of equal calibration intervals. The experiment results confirm the correctness of the obtained theoretical results.

## 5. Conclusion

The paper shows that the accuracy of the calibration characteristics of measuring apparatus substantially depends on the values of reproduced sample input signals. A procedure for optimal selection of sample input signals to get the best calibration characteristics of measuring apparatus was proposed. The  $D$ -optimality criterion was used as an optimality criterion in this study. This criterion is the overall measure in terms of the volume of the estimation error ellipsoid, which is proportional to the determinant of dispersion matrix of the estimation errors.

## References

1. A. A. Abdullayev and Ch. M. Gadzhiyev, Metrological Support to Data-Acquisition Systems for Oil-Product Accounting, *Measurement Techniques*, **36**, 9 (1993) 977-981.
2. G. V. Reklaitis, A. Ravindran, K. M. Ragsdell, *Engineering Optimization, Methods and Applications*, Vol.1, John Wiley and Sons, New York, 1983.

## AN EXTENSION OF THE GUM TREE METHOD FOR COMPLEX NUMBERS

BLAIR D. HALL

*Measurement Standards Laboratory of New Zealand, Industrial Research Ltd.,  
PO Box 31-310 Lower Hutt 5040, New Zealand  
E-mail: b.hall@irl.cri.nz*

An uncertain complex number is an entity that encapsulates information about an estimate of a complex quantity. Simple algorithms can propagate uncertain complex numbers through an arbitrary sequence of data-processing steps, providing a flexible tool for uncertainty calculations supported by software. The technique has important applications in modern instrumentation systems. Some radio-frequency measurements are discussed.

### 1. Introduction

Some difficulty has been reported<sup>1</sup> in evaluating the measurement uncertainty of instrumentation systems using the recommendations of the *Guide to the Expression of Uncertainty in Measurement* (GUM).<sup>2</sup> The operation of modern systems is often thought of in terms of more than one step of data-processing, instead of the single measurement function required by the GUM's *Law of Propagation of Uncertainty* (LPU). Moreover, a complete sequence of steps may not be carried out at each measurement (e.g., instrument calibration contributes to uncertainty but is not usually repeated each time). Also, if a function of measurement results is of interest, the handling of uncertainties associated with systematic errors requires special care.

For measurements of real-valued quantities, a *GUM Tree* design technique for modular systems has been developed to address these issues.<sup>3</sup> It introduces the notion of an *uncertain number*, an entity encapsulating information about an estimate of a quantity that can be propagated using simple algorithms.<sup>4,5</sup> GUM Tree systems provide full LPU uncertainty propagation for multi-step data processing, which can be represented succinctly using an uncertain number notation (much like matrix and complex

number notations represent lower-level computations).

This paper introduces the idea of an *uncertain complex number* (UC) for complex quantities based on a bivariate form of the LPU that supports multi-step data-processing.<sup>6</sup> The essential features of the GUM Tree technique are unchanged: the algorithms and structure of an UC are analogous to the real-valued counterparts, although matrices and complex numbers replace real-number parameters.

## 2. Mathematical Details

A one-step approach to propagation of uncertainty in complex-valued problems has been described.<sup>7</sup> This section presents a mathematically equivalent procedure that can be extended to multi-step problems.

In the notation used, complex quantities are in bold italics, like  $\mathbf{t}$  or  $\boldsymbol{\alpha}$ ; bold capitalized Roman letters represent matrices, like  $\mathbf{R}$ . Real quantities are in plane italics and the real and imaginary components of a complex number are labeled 1 and 2, respectively, like  $\mathbf{t} = t_1 + it_2$ . The standard uncertainty of a scalar  $t_1$  is written  $u(t_1)$  and the correlation associated with scalars  $t_1$  and  $t_2$  is written  $r(t_1, t_2)$ .

### 2.1. Single-Step Uncertainty Evaluation

A measurement procedure for a complex quantity of interest, the *measurand*, can be represented as a function of all the quantities that influence the measurement,

$$\mathbf{Y} = \mathbf{f}(\mathbf{X}_1, \dots, \mathbf{X}_l). \quad (1)$$

An estimate  $\mathbf{y}$  can be obtained by evaluating this function with influence quantity estimates,  $\mathbf{x}_1, \dots, \mathbf{x}_l$ . A standard uncertainty,  $u(x_{ij})$ ,  $i = 1, 2$ ;  $j = 1, \dots, l$ , is associated with each of the real and imaginary components.

A measure of the contribution to uncertainty in  $\mathbf{y}$  from the estimate  $\mathbf{x}_j$  is the *component of uncertainty* matrix

$$\mathbf{U}_{\mathbf{x}_j}(\mathbf{y}) = \frac{\partial \mathbf{y}}{\partial \mathbf{x}_j} \mathbf{U}_{x_j}(\mathbf{x}_j) \quad (2)$$

$$= \begin{bmatrix} \frac{\partial y_1}{\partial x_{1j}} & \frac{\partial y_1}{\partial x_{2j}} \\ \frac{\partial y_2}{\partial x_{1j}} & \frac{\partial y_2}{\partial x_{2j}} \end{bmatrix} \begin{bmatrix} u(x_{1j}) & 0 \\ 0 & u(x_{2j}) \end{bmatrix}. \quad (3)$$

The component of uncertainty matrices associated with the influence quantities can be used to evaluate the variance-covariance matrix associated

with  $\mathbf{y}$ , which characterises the measurement uncertainty,

$$\mathbf{V}(\mathbf{y}) = \sum_{i=1}^l \sum_{j=1}^l \mathbf{U}_{\mathbf{x}_i}(\mathbf{y}) \mathbf{R}(\mathbf{x}_i, \mathbf{x}_j) \mathbf{U}'_{\mathbf{x}_j}(\mathbf{y}) \quad (4)$$

$$= \begin{bmatrix} u^2(y_1) & u(y_1, y_2) \\ u(y_1, y_2) & u^2(y_2) \end{bmatrix}, \quad (5)$$

where the correlation coefficients associated with a pair of complex quantities, or of a single quantity, are the elements of<sup>a</sup>

$$\mathbf{R}(\mathbf{x}_i, \mathbf{x}_j) = \begin{bmatrix} r(x_{1i}, x_{1j}) & r(x_{1i}, x_{2j}) \\ r(x_{2i}, x_{1j}) & r(x_{2i}, x_{2j}) \end{bmatrix}. \quad (6)$$

## 2.2. Multi-Step Uncertainty Problems

Some procedures are better represented by a sequence of equations<sup>b</sup>

$$\mathbf{Y}_1 = \mathbf{f}_1(\Lambda_1), \dots, \mathbf{Y}_p = \mathbf{f}_p(\Lambda_p), \quad (7)$$

where  $\Lambda_i$  is the set of arguments of the  $i^{\text{th}}$  function,<sup>c</sup> and  $\mathbf{Y} = \mathbf{Y}_p$ .

The uncertainty calculation (4) still applies. However, each component of uncertainty in  $\mathbf{y}$  is now evaluated recursively; the  $i^{\text{th}}$  step being<sup>d</sup>

$$\mathbf{U}_{\mathbf{x}_j}(\mathbf{f}_i) = \sum_{\mathbf{y}_k \in \Lambda_i} \frac{\partial \mathbf{f}_i}{\partial \mathbf{y}_k} \mathbf{U}_{\mathbf{x}_j}(\mathbf{y}_k). \quad (8)$$

This is a key result. It shows that all that is required to obtain the components of uncertainty of an intermediate result  $\mathbf{y}_i$  are the partial derivatives of  $\mathbf{f}_i$  with respect to its direct inputs (elements of  $\Lambda_i$ ) and the components of uncertainty associated with those inputs.<sup>e</sup> The result shows that data processing can be arranged to evaluate the result and the components of uncertainty at an intermediate step before proceeding to the next step. This is exploited by the GUM Tree technique to automate the step-by-step evaluation of intermediate results and components of uncertainty in software.

<sup>a</sup>Note, this matrix is not symmetric, because, in general,  $r(x_{1i}, x_{2j}) \neq r(x_{2i}, x_{1j})$ .

<sup>b</sup>For the description of multi-step calculations, we now adopt the convention that *only* influence quantities are represented by  $\mathbf{X}$ , or  $\mathbf{x}$ , whereas  $\mathbf{Y}$ , or  $\mathbf{y}$ , may be used for *either* influences *or* (intermediate) results. The measurand may be written without a subscript, but all other intermediate quantities are subscripted.

<sup>c</sup>These arguments may be the results of earlier steps, or influence quantities.

<sup>d</sup>Recursion stops when  $\mathbf{y}_k$  refers to an influence estimate, not an intermediate result.

<sup>e</sup>In this equation,  $\frac{\partial \mathbf{f}_i}{\partial \mathbf{y}_k}$  is actually the Jacobian matrix of the bivariate function (c.f. equation (3)), so the method applies even when the complex function  $\mathbf{f}_i$  is not analytic.

### 3. Uncertain Complex Numbers

The notion of an UC entity arises from the concurrent processing of intermediate results and components of uncertainty in multi-step problems. By associating UCs with quantity estimates, data processing can be expressed succinctly in terms that are directly related to the physical quantities involved, while the low-level propagation of uncertainty is hidden. Moreover, UC expressions can be programmed into a computer without additional analysis, such as derivation of sensitivity coefficients, etc.<sup>3f</sup>

Some terminology is associated with UC notation. For example, a UC equation corresponding to (1) could be written as  $y = f(x_1, \dots, x_l)$ , with typewriter font used to represent UCs. The function arguments are all associated with influence quantity estimates: a complex value and a pair of standard uncertainties define these UCs, which are referred to as *elementary*. On the other hand,  $y$  is an *intermediate* UC, defined by a function.<sup>g</sup> UCs have a number of numerical properties that can be evaluated, including *value* and *component of uncertainty*. Implicitly, the UC function  $f()$  defines  $\mathbf{y}$  as well as the set of component of uncertainty matrices required to obtain the covariance in (4). The value of  $y$  is the estimate  $\mathbf{y}$ , obtained by processing data according to the defining equations in the usual way. The component of uncertainty of  $y$  with respect to  $x_j$  is the matrix  $\mathbf{U}_{x_j}(\mathbf{y})$  defined in (3). In software,  $f()$  is automatically decomposed into a sequence of basic UC operations that evaluate  $y$  in a procedure analogous to the evaluation of  $\mathbf{y}$  by basic complex operations.<sup>5</sup>

### 4. Application and Discussion

The application of UCs to some important types of radio-frequency (RF) measurement has been investigated recently: measurement of RF power, and measurement of complex reflection coefficients with a vector network analyser (VNA) were studied.<sup>8</sup> A common feature of these studies was the importance of the uncertainty arising from instrument ‘calibration’.<sup>h</sup> A calibration procedure estimates measurement errors that can be adjusted during normal instrument operation. This is generally done by recording the instrument’s response to a number of well-characterised reference stimuli.

---

<sup>f</sup>Software support provides an UC data type and a library of basic mathematical operations that can be used to form arbitrary UC expressions.

<sup>g</sup>The distinction between elementary and intermediate UCs is analogous to the independent and dependent variables of ordinary mathematics.

<sup>h</sup>Calibration is colloquial; ‘correction’ is a more appropriate metrological term.

A calibration procedure will give rise to a number of equations of the form<sup>i</sup>

$$f_{\text{cal}}(a_i, b_i, \dots, v, w, \dots; E_1, E_2, \dots; \alpha_i, \gamma_i) = 0, \quad (9)$$

which are solved to obtain the correction parameters  $E_1, E_2, \dots$ . The UCs  $a_i, b_i, \dots, v, w, \dots$  are associated with errors: indexed terms ( $a_i, b_i$ , etc), refer to independent errors (e.g., electronic instrumentation noise), while  $v, w, \dots$  are associated with fixed errors (e.g., the unknown error in a particular reference value). The nominal value of the reference,  $\alpha_i$ , and the instrument's response,  $\gamma_i$ , are pure numbers with no uncertainty.

During normal operation, an adjustment function is used to map an instrument response to an UC for the measured quantity. This can be represented by an equation of the form<sup>i</sup>

$$y_i = f_{\text{adj}}(a_i, b_i, \dots, v, w, \dots; E_1, E_2, \dots; \gamma_i), \quad (10)$$

where  $a_i, b_i, \dots, v, w, \dots$  are the independent and systematic uncertainties and  $\gamma_i$ , is the uncorrected instrument response, with no uncertainty. The correction parameters  $E_1, E_2, \dots$  here ensure that uncertainties due to calibration errors are propagated correctly to the measurement result  $y_i$ .

The RF calibration and measurement procedures were described in these studies as sequences of equations. Using UC data processing software, the correction parameter uncertainties from calibration were propagated in the adjustment functions and measurement results were processed further, to obtain UCs for the ratio and difference of measurements. At all stages, intermediate UC properties could be evaluated, allowing an assessment to be made of the relative importance of various errors. The results showed that errors during calibration introduced correlation between measurement results, which, when propagated further, affected the uncertainty of the ratios and differences significantly. For instance, in the VNA measurement of reflection coefficients, the uncertainty associated with the calculated ratios and differences was a factor of 10 lower than a similar calculation that treated the measurement results as independent.<sup>j</sup> Similarly, in the case of RF power measurements, the relative uncertainty of the power measurement ratios was actually less than the relative uncertainty of the individual measurements, because of uncertainty about calibration error in the meter's scale factor. Had the measurement uncertainties been treated as inde-

---

<sup>i</sup>Although we write this as a single equation, it is often a sequence of equations.

<sup>j</sup>The trace of the covariance matrices was used as the magnitude of the uncertainty.

pendent, the relative uncertainty in the ratio would have been more than double.

It is no surprise that calibration errors lead to correlation between measurement results. However, a comprehensive uncertainty analysis of these measurement scenarios is rarely undertaken because of the complexity of the error models. Our study shows that an UC analysis is straightforward when problems are formulated as a sequence of equations.

The GUM Tree technique, and the associated idea of an uncertain complex number, are new tools to apply established methods of uncertainty analysis. They provide a powerful algorithmic approach that is particularly suited to large, complicated problems, such as those presented by many modern measuring instruments. They also provide a way of seamlessly propagating uncertainty during any post-processing of measurement results. Indeed, now that embedded computers are an ubiquitous part of most measuring instruments, there is ample opportunity for designers to incorporate these tools as internal routines. To do so would herald a new generation of measurement systems: capable of reporting both an estimate of the *value* of a quantity of interest and most, if not all, of the information needed to evaluate the *uncertainty* in that estimate.

## References

1. B. Anderson, Keynote Address, NCSL International Workshop and Symposium, (Washington, DC, July, 2001)  
see <http://metrologyforum.tm.agilent.com/ncsli2001.shtml>.
2. BIPM, IEC, IFCC, ISO, IUPAC, IUPAP and OIML *Guide to the Expression of Uncertainty in Measurement*, 2<sup>nd</sup> edn. (Geneva, ISO, 1995).
3. B. D. Hall, Computer Standards and Interfaces (2006) **28**(3), 306–310.
4. B. D. Hall, Advanced Mathematical and Computational Tools in Metrology VI, (World Scientific, 2004) pp 199–208.
5. B. D. Hall, Metrologia (2006) **43** L56-L61.
6. B. D. Hall, Metrologia (2004) **41** 173-177.
7. N. M. Ridler and M. J. Salter, Metrologia (2002) **39** 295-302.
8. B. D. Hall, Working with CGUM: RF Measurement Examples, (Industrial Research Ltd. Manual 81, 2007), [Online: <http://mst.irl.cri.nz/>]

## Acknowledgement

This work was funded by the New Zealand Government as part of a contract for the provision of national measurement standards.

## DIGITAL FILTERING FOR DYNAMIC UNCERTAINTY

JAN P. HESSLING

*SP Technical Research Institute of Sweden, Measurement Technology  
Box 857, SE-501 15 Borås, Sweden*

Evaluation of measurement uncertainty is essential for all kinds of calibration procedures. The widely accepted approach may directly be applied in static or stationary measurements but gives little support for transient conditions. To remedy this situation, the sensitivities to the uncertainty of input variables which are normally constant, are here generalized to be time-dependent and derived by means of digital filtering. Arbitrarily varying measurands are allowed but the system must be linear and time-invariant. The approach is illustrated for a common accelerometer system.

### 1. Introduction

There is an emerging need for improved treatment of transient dynamic effects [1,2] in the evaluation of uncertainty [3] – when dynamic aspects are relevant they are often strongly dominating and involve several parts of the measurement system of different character. For instance, a weakly damped mechanical sensor requires an electrical filter to operate satisfactory. All relevant parts should be, but are often not in practice, included in any dynamic compensation, evaluation of uncertainty, or estimation of error etc.

Temporal correlations of non-stationary signals are non-trivial to account for when estimating the measurement uncertainty. Even though the measurement *system* generally is time-invariant, the *measurement* is time-dependent and typically non-ergodic. In contrast to the stationary case, ensemble and time averages – corresponding to conditions of reproducibility and repeatability, respectively – then have completely different meanings. The measurement uncertainty (MU) should be associated to an ensemble of measurements, all with the same time-dependent measurand, but with different realizations of the measurement system and conditions. The ensemble thus reflects the variation of parameters and conditions consistent with the dynamic calibration. The dynamic uncertainty (DU) may in turn be defined as the contribution to the MU due to the uncertainty of the time-dependence of the estimated measurand. As such the DU varies in time, in stark contrast to static or

stationary measurements. At present, there have been few attempts to define and evaluate the DU [2].

Digital filters [4] can be used for many of the tasks of dynamic evaluation. Besides dynamic correction [2, 5] of the dynamic error [1] due to a non-perfect response, they may be used for evaluating the DU. A stochastic dynamic model of the measurement system must then be known. The contribution due to the uncertainty of the model (DUM) can be evaluated with a bank of digital filters, one filter for each model parameter. Applied to any measured signal it gives the time-dependent sensitivities between the time-invariant parameter uncertainties and the DUM varying in time. These sensitivity signals are comparable to the constant sensitivity ( $c_i$ ) coefficients [3] for stationary signals. A general method for synthesizing DUM filter banks is presented here as a part of the framework of dynamic metrology [6]. By way of illustration, the DUM will be evaluated for a common system for measuring acceleration.

## 2. Time-Dependent Sensitivity

The model equation for a dynamic measurement is given in terms of a system of differential equations in time rather than any instantaneous algebraic equation [3]. This gives rise to the fundamental dynamic concepts of time delay and wave form distortion [1], beyond the amplification which is an essentially linear static aspect. Many differential model equations may nevertheless conveniently be formulated as algebraic equations by using the Laplace transform. By means of parametric system identification [7] this description can be found directly from calibration results. The analysis can then proceed as in the GUM [3] to produce expressions for the uncertainty in the s-domain. Just as the Laplace transform converted a time domain description to the s-domain, an inverse transform is required for real time analysis. The inverse Laplace transform is however not a practical tool. Digital filtering is more convenient and frequently used for realizing the inverse transform. In this context, a method to synthesize digital filters for evaluating the DUM in fact suggests itself:

1. Determine the model equation for the measurement. That is, an algebraic s-domain equation with uncertain parameters.
2. Find a propagator of deterministic parameter *errors* (section 2.1).
3. Derive the corresponding propagator of *uncertainty* (section 2.2).
4. Realize the propagator of uncertainty as a digital filter (section 2.3).

The estimation of the DUM will then resemble the present standard, but with time-dependent sensitivities found by filtering of the measured signal, rather than constant sensitivities found by differentiation of an algebraic model equation.

## 2.1. Error Propagator

The model equation of the measurement is conveniently formulated in terms of the transfer function  $H(s)$  of the measurement system. If the Laplace transform of the input and output signals are  $X(s)$  and  $Y(s)$ , respectively,

$$Y(s) = H(s)X(s), \quad H(s) = K \frac{\prod_{m=1}^m (1-s/z_m)}{\prod_{l=1}^L (1-s/p_l)}. \quad (1)$$

The transfer function is here expressed, as is common, in terms of zeros ( $z_m$ ) and poles ( $p_l$ ) usually obtained by parametric system identification [7]. Now assume there are associated errors ( $\Delta z_m$ ) of ( $\Delta p_l$ ) in these parameters describing the deviation between the true and identified model. A linearization as in the GUM [3] chapter 5, of the s-plane model equation yields,

$$\begin{aligned} \frac{\Delta H(s)}{H(s)} &= -\sum_q \rho_q \cdot E_q(s), \quad \Delta Y(s) = \frac{\Delta H(s)}{H(s)} Y(s) \\ \rho_q &= \frac{\Delta q}{|q|}, \quad \begin{cases} q = \{z_m, p_l\} \equiv |q|e^{i\alpha} \\ \Delta q = \{\Delta z_m, -\Delta p_l\} \end{cases}, \quad E_q(s) = \frac{s/|q|}{s/|q| - e^{i\alpha}}. \end{aligned} \quad (2)$$

This describes how the relative parametric errors  $\rho_q$  propagate according to  $E_q(s)$  into the measured signal. For dynamic estimation of the measurand / dynamic correction it is the inverse transfer function  $H^{-1}(s)$ , that is applied to the measured signal  $Y(s)$ . For modeling or estimation of dynamic error [1,6], it is the transfer function  $H(s)$  that is applied to the measurand  $X(s)$ . The difference in these two cases is just an interchange of poles and zeros to switch between  $H(s)$  and  $H^{-1}(s)$ , which results in different signs of the signal errors. The root-mean-square errors and consequently the DUM will thus be the same in both cases. To simplify the presentation, the DUM will be formulated for dynamic correction, or expressed differently, for the dynamic estimator  $\hat{X}(s) = \hat{H}^{-1}(s) \cdot Y(s)$  of the measurand. The estimated error signal  $\Delta \hat{y}(t)$  can then be written in terms of implicitly time-dependent sensitivities  $c_q(\hat{y})$  found

by convolving/filtering (\*) the estimated measurand  $\hat{x}(t)$  with the impulse responses  $e_q(t)$  corresponding to the dynamic propagators  $E_q(s)$ ,

$$\Delta\hat{x}(t) = \sum_q \rho_q c_q(\hat{x}), \quad c_q(\hat{x}) = e_q(t) * \hat{x}(t). \quad (3)$$

## 2.2. Statistical Analysis

The measurement system and the error propagators in Eq. (2) are time-invariant but the time-dependence of the measurand results in a non-ergodic measurement. Ensemble and time averages will thus have completely different meanings. The DU relates to an ensemble of measurements, all with the same time-dependent measurand  $x(t)$  but with different realizations of the measurement system. Since physical signals are real-valued, all poles and zeros must either be real, or complex-conjugated in pairs. The two contributions from the conjugated parameters of each pair are therefore first summed to account for their correlation, before the statistical analysis is made. For simplicity, assume the parameter errors  $\rho_q$  for  $\text{Im}(q) \geq 0$  are unbiased and uncorrelated, and  $\arg(\rho_q)$  uniformly distributed. The variance  $u_c^2$  of the error signal  $\Delta\hat{x}(t)$  will then read ( $\bar{\rho}$  denotes complex conjugation of  $\rho$ ),

$$\begin{aligned} u_c^2(\hat{x}) &= \sum_{\text{Im}q \geq 0} u_q^2 c_q^2(\hat{x}) \quad \langle \rho_p \bar{\rho}_q \rangle = \delta_{pq} \cdot u_q^2, \quad \langle \rho_q \rangle = 0 \\ c_q(\hat{x}) &= \begin{cases} \varsigma_q^{(11)}(\hat{x}) & , \quad \text{Im}(q) = 0 \\ \sqrt{2} \cdot |\varsigma_q^{(12)}(\hat{x}) - \exp(i\alpha) \varsigma_q^{(22)}(\hat{x})| & , \quad \text{Im}(q) > 0 \end{cases} \\ \varsigma_q^{(mn)}(\hat{x}) &= e_q^{(mn)}(t) * \hat{x}(t), \quad E_q^{(mn)}(s) = \frac{\hat{s}^m}{(\hat{s} - e^{i\alpha})(\hat{s} - e^{-i\alpha})^{n-1}}, \quad \hat{s} \equiv \frac{s}{|q|} \end{aligned} \quad (4)$$

As in the GUM [3], the sensitivity signals  $c_q$  multiply the parametric uncertainties  $u_q$  and the summation is quadratic. However, the sensitivities depend implicitly on time via the time-dependence of the estimated measurand  $\hat{x}(t)$ .

## 2.3. Synthesis of Digital Sensitivity Filter

The continuous time dynamic sensitivity systems  $E_q^{(mn)}(s)$  in Eq. (4) will here be realized as digital filters utilizing a mapping method [5]. The mapping is mainly chosen for its simplicity. A drawback is its fairly low utilization ratio

which reduces the usable bandwidth. Time-reversed filtering is used for stabilization. If post-processing is not allowed, more complicated methods of stabilization may be required. Neither of these limitations should be of any significance for evaluating the uncertainty. The CT poles and zeros are then, for sampling rate  $T_S$ , mapped to DT according to,

$$q \rightarrow \exp(qT_S). \quad (5)$$

The coefficients of the digital uncertainty filters  $E_q^{(mn)}(z)$  are given in Table 1.

Table 1. Input  $\{b_k\}$  and output  $\{a_k\}$  filter coefficients,  
 $y_k + a_1 y_{k-1} + a_2 y_{k-2} = b_0 x_k + b_1 x_{k-1} + b_2 x_{k-2}$ , of the three sensitivity  
filters, expressed in CT poles  $qT_S \equiv u + iv$ .

	$E_q^{(11)}(z)$	$E_q^{(12)}(z)$	$E_q^{(22)}(z)$
$b_0, b_1, b_2$	1, -1, 0	$ qT_S (0, 1, -1)$	(1, -2, 1)
$a_1$	$-e^u$	$-2e^u \cos(v)$	$-2e^u \cos(v)$
$a_2$	0	$e^{2u}$	$e^{2u}$

### 3. Example – Accelerometer System

The DUM sensitivity signals  $c_q(\hat{x})$  will here be illustrated for a common system for measuring acceleration. It consists of an accelerometer with resonance frequency  $f_C$  and a relative damping  $\zeta = 0.02$ , and a fourth order Bessel filter with cross-over frequency  $0.75f_C$ . The combined sensitivity signal  $c \equiv \sqrt{\sum c_q^2}$  relevant for equal relative parameter uncertainties, is shown in Fig. 1.

The dynamic model of this measurement system consists of six complex-valued poles in three pairs but no zeros,

$$p = 2\pi f_C \left( -\zeta \pm i\sqrt{1-\zeta^2}, -0.493 \pm 0.623i, -0.679 \pm 0.203i \right). \quad (6)$$

The measurand is chosen to be a Gaussian pulse of high bandwidth ( $0.50f_C$ ).

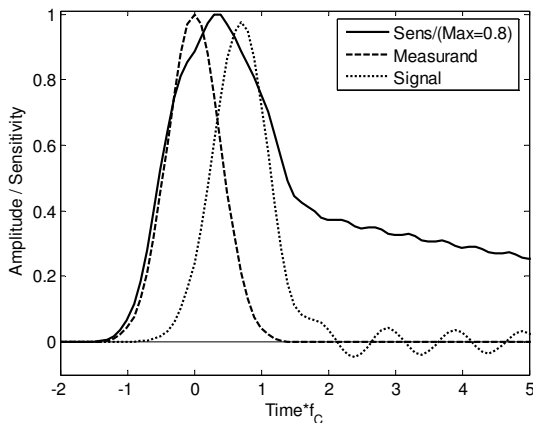


Figure 1. The combined DUM sensitivity (Sens) for a Gaussian pulse of acceleration (Measurand). The measured acceleration (Signal) is shown for comparison. As an example, 1% uncertainty in magnitude of the parameters leads to a maximum measurement uncertainty of 0.8% .

#### 4. Conclusions

A general digital filtering method to evaluate the time-dependent measurement uncertainty due to the dynamic model has been proposed. The uncertainty refers to the variability of the response of the measurement system and excludes the systematic dynamic error due to the non-ideal model, which has been treated elsewhere. The combined uncertainty was illustrated for a common transducer system for measuring acceleration. The required dynamic model is supposed to be obtained using the well established methods of parametric system identification. The synthesis of the digital uncertainty filters as well as their application to measured signals is simple and only involves elementary mathematical operations and standard filter operations.

#### Acknowledgments

Financial support from National Metrology, of the Swedish Ministry of Industry, Employment and Communication, grant 38:10, is gratefully acknowledged.

#### References

1. Hessling J P *Meas. Sci. Technol.* **17** 2740 (2006)
2. Elster C, Link A and Bruns T *Meas. Sci. Technol.* **18** 3682 (2007)

3. ISO GUM 1995 *Guide to the Expression of Uncertainty in Measurement* edition 1993, corrected and reprinted 1995 (Geneva, Switzerland: International Organisation for Standardisation)
4. Chi-Tsong Chen 2001 *Digital Signal Processing* (New York: Oxford University Press)
5. Hessling J P *Meas. Sci. Technol.* **19** 075101 (2008)
6. Hessling J P *Meas. Sci. Technol.* **19** 084008 (7p) (2008)  
Special feature: *ISMTII 2007, 8th Int. Symp. on Measurement Technology and Intelligent Instruments (Sendai, Japan, 24–27 Sept. 2007)*
7. Pintelon R. and J. Schoukens 2001 *System Identification: A Frequency Domain Approach*, IEEE Press, Piscataway (USA)

## CONSIDERATIONS AND DEVELOPMENTS IN UNCERTAINTY EVALUATIONS IN CHEMICAL METROLOGY

ROBERT KAARLS

*President, CIPM Consultative Committee for Amount of Substance, Metrology in Chemistry (CCQM), Bureau International des Poids et Mesures BIPM, Pavillon de Breteuil, Sèvres*

In many cases the overall measurement uncertainty in a chemical measurement result is highly determined by the uncertainty components generated during the sample preparation process. Extra components are caused by inhomogeneity and instability of the samples to be measured or under test. The measurement uncertainty is further determined by the eventual application of recovery procedures and the consequences of commutability problems. In several cases the measurement result is method dependent. In order to have comparable measurement results it is essential that the measurand is defined very precisely. Metrological traceability to the SI is not (yet) possible in all cases. Procedures for the calculation of measurement uncertainty in chemical measurements as carried out by the National Metrology Institutes are still under consideration. Likewise the uncertainty in the reference value of an inter-laboratory comparison, for example a Key Comparison, is still debated, as well as the determination of the uncertainty claimed with a Calibration and Measurement Capability (Best Measurement Capability in the scope of an accreditation) of a measurement or testing laboratory. So far, measurement uncertainty related to sampling is left aside. An overview will be given of achievements and challenges with regard to measurement uncertainty evaluation in chemical measurement institutes.

### 1. The CIPM Mutual Recognition Arrangement

The CIPM Mutual Recognition Arrangement (CIPM MRA) was first signed during the General Conference on Weights and Measures, held in Paris on 14 October 1999. The CIPM MRA is a mutual recognition of national measurement standards and of calibration and measurement certificates issued by National Metrology Institutes (NMIs). It is operated by the BIPM as one of the activities in the scope of the Inter-Governmental Treaty of the Metre Convention fostering the establishment of a credible and reliable global measurement system, traceable to long term stable international measurement standards as defined by the International System of Units SI. The CIPM MRA calls upon:

- the operation by each NMI of a suitable way of assuring quality, by applying a quality system in conformity with the ISO/IEC 17025 (or

equivalent) and when relevant also in conformity with the ISO Guide 34;

- results of Key Comparisons leading to a quantitative measure of the degree of equivalence of national measurement standards;
- successful participation in other appropriate supplementary and bilateral comparisons.

It has to be noted that national measurement standards include not only realizations of the SI units in the form of artifacts, but also calibration and measurement capabilities, used to realize measurement results in terms of the SI units, as well as Certified Reference Materials (CRMs). The role of the NMIs is to deliver traceability to their customers. In general this can be done through different processes, depending on the area of metrology, like:

- calibration of (secondary) measurement standards, transfer standards, measuring instruments, etc.;
- value assignment of CRMs, that are delivered to the customers, like calibration solutions and matrix CRMs for validation of measurement procedures and eventually for, but not preferably, recovery corrections;
- value assignment of customer's "in-house" reference materials;
- value assignment of reference materials used in Proficiency Testing schemes (PTs).

It has to be remarked here that in many countries not only the original NMI by law is charged with the realization and maintenance of national measurement standards and the dissemination of traceability to all customers. Inasmuch as in many countries the NMI does not cover all areas of metrology, other expert institutes may also become charged to be responsible for the "national measurement standards" of a group of well defined quantities. In these cases these expert institutes have been officially designated by the responsible authorities in the country, being the government or the co-ordinating NMI, and are known as Designated Institutes (DIs). In several countries this is the case for physical measurement standards, but in particular in the field of metrology in chemistry this is often the case as metrology in chemistry is a rather new discipline and many NMIs do not cover the whole field.

Currently the CIPM MRA has been signed by some 79 Member States and Associate States and Economies and 2 international organizations (IAEA and JRC IRMM), representing about 200 NMIs and other Designated Institutes.

The BIPM publishes all the data with respect to the CIPM MRA on its website in the so-called CIPM MRA database, indicated as the KCDB ([www.bipm.org/kcdb](http://www.bipm.org/kcdb)).

The database does not only show the names of the participating countries and their NMIs and DIs but also in another part the results of the Key Comparisons. In a third part of the database the claimed Calibration and Measurement Capabilities of the participating NMIs and DIs are published after, on the basis of the results of Key Comparisons, the capabilities and competences have been demonstrated and a quality system review has taken place and has demonstrated compliance with ISO/IEC 17025 and eventually also with ISO Guide 34.

Recently, in agreement with the International Laboratory Accreditation Cooperation –ILAC, a CMC has been defined as “*a calibration and measurement capability available to customers under normal conditions*”:

(a) *as published in the BIPM key comparison database (KCDB) of the CIPM MRA; or*

(b) *as described in the laboratory’s scope of accreditation granted by a signatory to the ILAC Arrangement*”.

A number of notes annexed to this definition clarifies the definition. With respect to chemical analysis the notes remark that the measurement uncertainty claimed in a CMC is based on the inherent performance of the available measurement method for typical stable and homogeneous samples; and measurement uncertainty claimed for a listed CRM, as the means of delivering traceability to the customer, includes the influence of instability, inhomogeneity and sample size. It is also noted that national measurement standards supporting CMCs from a NMI or DI are either themselves primary realizations of the SI or are traceable to primary realizations of the SI at other NMIs or DIs through the framework of the CIPM MRA.

## **2. Consultative Committee for Amount of Substance, Metrology in Chemistry – CCQM**

The CCQM has been established by the CIPM as one of its advisory scientific committees in 1993. The aim and tasks are:

- to establish worldwide comparability through
  - traceability to the SI, or if not (yet) possible to other internationally agreed references,
  - developing primary and other methods of higher order,
  - databases and
  - primary (pure) reference materials and
  - validation of traceable methods and procedures and measurement uncertainty calculations

- to organize Pilot Study comparisons and Key Comparisons;
- to liaise with all stakeholders;
- to contribute to the establishment of a globally recognized system of national measurement standards and facilities and the implementation of the CIPM MRA;
- to advise the CIPM and the BIPM on metrology in chemistry.

With metrological traceability is meant traceability to the International System of Units – SI, or if not yet possible to other internationally agreed references, like for pH or in the case of biological activity for example to the International Standards and International Units of the WHO.

For chemical measurement results this means in particular traceability to the mole in the case of amount of substance. However, in many cases the chemical measurement results are also expressed in terms of:

- amount fraction : mol/mol
- amount concentration : mol/m<sup>3</sup>
- mass concentration : kg/m<sup>3</sup>
- amount content : mol/kg
- mass fraction : kg/kg

(or expressed in multiples or sub-multiples).

Examples of potential primary methods are: gravimetry, titrimetry, coulometry, calorimetry (differential scanning calorimetry), isotope dilution mass spectrometry, cavity ring down spectrometry and instrumental neutron activation analysis. However, these methods are only to be considered as primary methods when the method is fully understood and correctly applied.

A typical traceability chain in metrology in chemistry is given in Figure 1. Basic building blocks for establishing traceability in chemical metrology are pure compounds, calibrators, calibration solutions and Certified Reference Materials. Therefore purity analysis is of high importance. In most cases this is done by determining the impurities; so, by determining (100% minus impurities).

In many cases the measurement result may be dependent on the method/procedure applied. One could consider this as fixing all types of influence quantities. Nevertheless as long as the measurement result is expressed in terms of the SI, traceability is claimed to the SI. As long as everyone uses the same method, global comparability of measurement results can be obtained.

A major reason for discrepancies between measurement results in comparisons is often caused by a not strictly application of the measurement procedure and/or by an unclear understanding and definition of the measurand.

It means that de facto one is measuring different measurands and thus no comparability of measurement results can be obtained.

Major uncertainty components contributing to the overall uncertainty in the measurement are caused by the way the sample is prepared, like dilution, extraction, clean up, contamination, separation, etc. Further uncertainty components that contribute are the homogeneity (bulk, within-bottle, between-bottle, etc.), stability and sample size and recovery correction in case a CRM is used for calibration. Finally, in a number of cases like in bio activity measurements, also commutability issues may have to be considered.

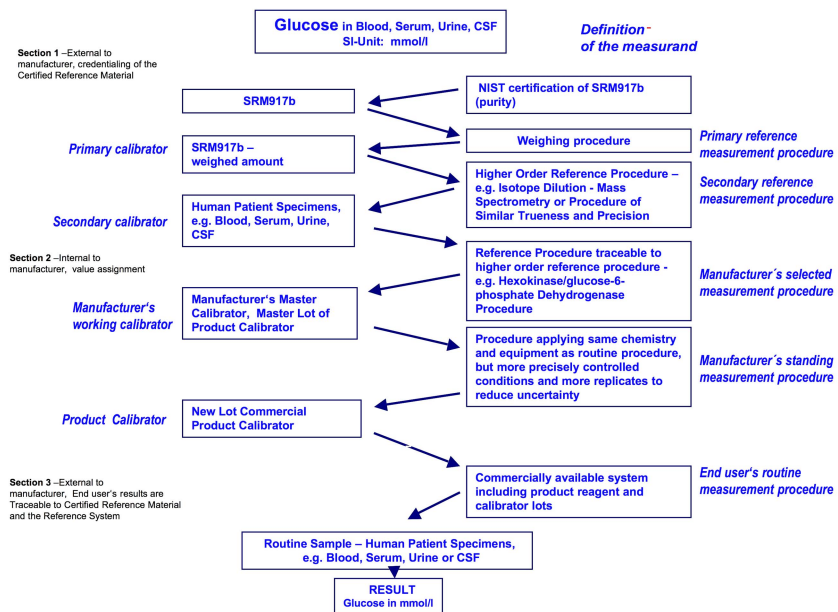


Figure 1. Typical example of a traceability chain in metrology in chemistry (in this case for glucose in blood).

### 3. Key Comparisons and the Key Comparison Reference Value –KCRV

The CIPM MRA defines a Key Comparison (KC) as “*one of the set of comparisons selected by a Consultative Committee to test the principle techniques and methods in the field*”. And as a note it is added that KCs may include comparisons of representations of multiples and sub-multiples of SI base and derived units and comparisons of artefacts. This definition has to be interpreted as that the best available techniques, methods and procedures used to realize the claimed CMC at a NMI or DI have to be tested. Of course, depending

on the claimed measurement uncertainty, NMIs and DIs may apply different techniques and methods and procedures.

The aim of the KC is to provide evidence that a claimed CMC in the scope of the CIPM MRA is credible.

Further, the CIPM MRA defines the KCRV as "*the reference value accompanied by its uncertainty resulting from a CIPM KC*". In other words, the KCRV intends to be the best estimate of the "true" value of the measurand under consideration; that is the measurand one intends to measure. So, the KCRV is a close, if not the best, approximation to the SI value.

As it is the role of the NMIs to deliver credible traceability to the SI to their customers, it is clear that the NMI has to demonstrate how well it can deliver the best estimate of the "true" value of a measurand within its claimed measurement range and claimed measurement uncertainty. Thus, in order to assess this we must have an accurate value of this best estimate.

In organizing comparisons in the field of metrology in chemistry in general we have sufficient samples available to involve all interested NMIs and DIs in the world at once in the comparison. And all NMIs and DIs that have CMC claims or are planning to have CMC claims in the same field have to join in this comparison. Due to a lack of samples at a later time and also for reasons of economy it is often not possible to repeat the same exercise at a later moment in time. As a consequence however, in the KC the different participating laboratories are applying "higher" order and "lower" order methods, depending on their capabilities and CMC claims. Another issue to consider is that in many cases the number of participating institutes is rather small. This all has consequences for the way we have to treat the results and how the KCRV could be calculated.

Driven by the aims and the rules of the CIPM MRA it is clear that the KCRV has to be calculated on the basis of the best available results in the KC or by an independent primary method, like gravimetry. In the case that the KCRV is calculated on the basis of results of participants in the KC only those results obtained by the application of techniques and measurement procedures that are most suitable and accurate can be used. This does of course not exclude any institute from participation, while all results will still be published in the KCDB.

However, participation of all institutes in the KC leads to the participation of a very inhomogeneous group of NMIs and DIs, some of them having longstanding experience, others just joining in the field and having less experienced staff, while they also may apply "higher" as well as "lower" order methods.

These considerations lead to a situation where we have to decide that the best estimate of the “true” value for the KCRV has to be determined on the basis of a (limited) selected group of participants having experience and applying the most suitable, reliable and accurate techniques, methods and procedures. This dilemma does of course not exist when the KCRV is determined *á priori* by an independent primary method.

For calculating the KCRV the CCQM will select usable measurement results on the basis of:

- sound scientific considerations, informed when appropriate by statistical considerations;
- results of properly applied primary methods;
- results of properly applied most accurate methods of higher order;
- results of NMIs and DIs that have proven to be knowledgeable and have the right capabilities and competences, e.g. proven by good results in earlier KCs and pilot study comparisons and being able to determine realistic measurement uncertainties.

Once a selection has been made with respect to which results will be used for calculating the KCRV a choice has to be made for the method of calculating. The KCRV may be calculated as an arithmetic mean, weighted mean, median or another method. As mentioned before in many KCs only a small number of institutes participate. This means that statistical tests have low power to detect discrepant values.

#### K44 - trace metals in sewage sludge

by measurand, 4-5 data      By courtesy of D. Duewer, NIST

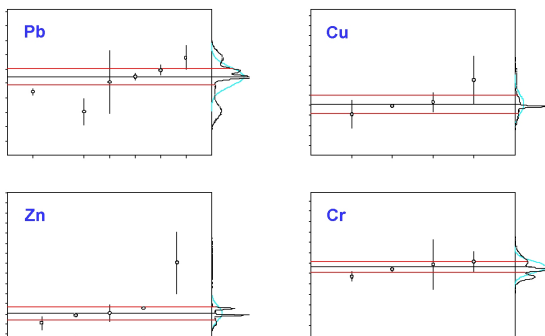


Figure 2. Grouped by measurand with 4 or 5 participants.

Therefore, in most of the cases either a simple mean or a simple median is used for the determination of the KCRV.

Figures 2 and 3 give some examples of results in a KC. By applying a technique developed by Dave Duewer one can get an impression on the robustness of the results.

**K44 – trace metals in sewage sludge  
by measurand, 2-3 data**

By courtesy of D. Duewer, NIST

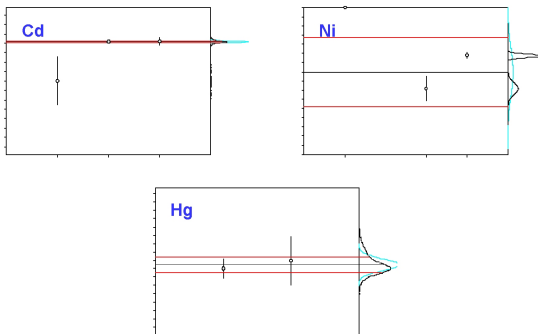


Figure 3. Grouped by measurand with 2 or 3 participants.

Homogeneity effects should be taken into account by the coordinating NMI for purposes of determining a KCRV that relates to a common measurand, by using increased standard uncertainties in place of the  $u(x_i)$ . Similarly other effects, such as stability, should be treated. Supposing that homogeneity effects have been well characterized by the coordinating NMI in terms of a standard uncertainty  $u_{wb}$  for within-bottle effects and a standard uncertainty  $u_{bb}$  for between-bottle effects and further supposing that homogeneity is modelled as a random variable, and that NMI  $i$  receives one bottle containing the material of concern from a batch, making a number  $n_i$  of indications of the property, each of which is regarded as a realization of that variable, then, for purposes of determining a KCRV that relates to a common measurand, in place of  $u(x_i)$ , a value given by the quadrature sum of  $u(x_i)$ ,  $u_{wb}/n_i^{1/2}$  and  $u_{bb}$  should be used.

#### 4. Degree of Equivalence –DoE

The CIPM MRA defines the Degree of Equivalence (DoE) as the degree to which the value of a measurement standard is consistent with the KCRV. This is expressed quantitatively by the deviation from the KCRV and the uncertainty of

this deviation. This means that the DoE refers to the deviation from the KCRV and the combined uncertainty of the KCRV and the NMIs measurement result:

$$D_i = x_i - x_{KCRV} \quad (1)$$

The expanded uncertainty of the DoE is then:

$$U(D_i) = 2 \sqrt{(u(x_i)^2 + u(x_{KCRV})^2)} \quad (2)$$

In case of an independent KCRV:

$$U(D_i) = 2 \sqrt{(u(x_i)^2 + u(x_{KCRV})^2)} \quad (3)$$

The question is now how the claimed CMC of a NMI and in particular the claimed measurement uncertainty relates to the result obtained in a KC. The CIPM MRA is not clear in how to calculate an acceptable uncertainty on the basis of the DoE. Assuming that corrections have been made for known errors or biases, then as a consequence a bias showing up in the result of a KC, being the deviation from the KCRV, has to be considered as an overlooked or underestimated component of uncertainty  $u(x_{dev})$ .

The expanded uncertainty to be claimed in the CMC should then be calculated as:

$$U(x_{CMC}) = 2 \sqrt{(u(x_{dev})^2 + u(x_i)^2 + u(x_{KCRV})^2)} \quad (4)$$

However, other opinions on the relationship between the DoE and the uncertainty claimed in a CMC exist.

Of course, the NMI concerned may also withdraw its original CMC and study first why its result in the KC is deviating more than expected.

The above approach is naturally in particular valid in cases where we are considering a claimed CMC that is directly one-to-one underpinned by a KC. Another question, not yet answered, is what does the result in a KC say about many other claimed CMCs that belong to the same area of metrology in chemistry but that are not directly underpinned by a one-to-one KC. Remembering that, for example, in the food area there are some 50 to 60 elemental species of importance and that there are more than 105 organic species in some 107 chemical matrices covering 12 orders of magnitude in concentration (1 g/g proximates, dietary fiber through 1 pg/g mycotoxins, PAHs, dioxins, PCBs, then it is clear that only a very limited number of KCs can be carried out compared to the enormous amount of different CMCs. The

CCQM is now studying how the claimed CMCs in the field of metrology in chemistry can be best tested by carrying out real Key Comparisons testing the basic competences a NMI or DI must have in order to produce credible and reliable measurement results with realistic uncertainty statements in the field of metrology in chemistry where it has capabilities. This may lead to a situation that somewhat different approaches may be used in for example the organic, inorganic or gas analysis field.

Basic competences to be tested are for example:

- contamination control and correction
- sample dissolution and preparation
- purity assessment (small and large molecules)
- analysis of isotope ratios
- gravimetric preparations
- controlling matrix effects
- ICP-MS, graphite furnace, X-ray fluorescence, etc.
- Chromatographic analysis, IDMS, etc.

A paper by Dave Duewer also suggests that based on the results in many comparisons one could come to certain decisions with respect to the capabilities and competences of an NMI. On the basis of a number of measurement results grouped by participant, as given in Figure 4, one could also draw some conclusions with respect to the credibility of participating NMIs.

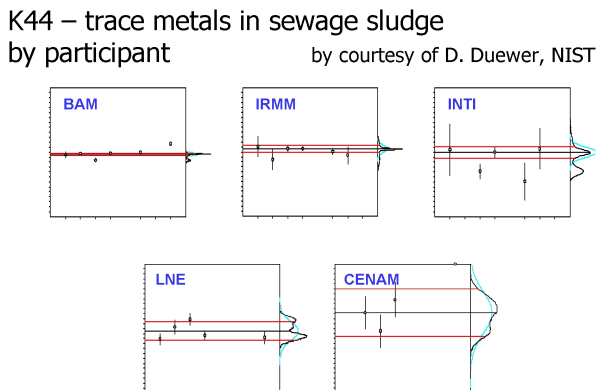


Figure 4. Results grouped by participant.

In the field of gas analysis such an approach may also be feasible because over the last 10 years a good database of results can be composed.

## **5. Uncertainties Claimed in CMCs and in Listed CRMs**

One of the basic principles of the CIPM MRA is that the MRA should be very transparent. Therefore all results of KC and other supplementary comparisons are published with disclosing the names of the participating NMIs and DIs. This transparency also requires that there is a clear link between the DoE demonstrated in a KC and the claimed measurement uncertainty in a CMC. Thus, the claimed CMC cannot have an uncertainty smaller than the DoE obtained in a relevant comparison. Equally, as listed CRMs as the means of delivering traceability to the customer, must have certified values based on the institutes own measurement capabilities, the uncertainty stated in the certified CRM value cannot be smaller than the uncertainty claimed in the CMC(s) used to assign the certified value. Of course, by assigning values to CRMs the certification processes described in the ISO Guides 34 and 35 should be taken into account.

## **6. Conclusions and the Way Forward**

For logistic and economic reasons all NMIs and DIs having claimed measurement capabilities in the area that will be underpinned by a defined KC, have to participate in that KC. This means that in the KC higher order and lower order methods are applied and that experienced and less experienced institutes participate. Moreover, in a considerable number of KCs the number of participants is very limited. Therefore, in most of the cases one cannot simply apply statistical methods to calculate the KCRV and its uncertainty.

Decisions on how to deal with the results in a KC have to be made on a case by case basis and should only be made on sound scientific considerations informed by applicable statistics.

Still further study is needed for developing guidance on how to deal with uncertainties in the KCRV due to inhomogeneity and stability issues.

The relationship between the DoE and the claimed uncertainty in a CMC has to be defined. Equally the relationship between the uncertainty claimed in a CMC and the uncertainty claimed in a listed CRM has to be defined. Much more studies will be carried out to develop guidance for judging CMCs that are not directly underpinned by a KC result. So, still the question has to be answered on “how far does the light shine?”.

Further studies are now carried out with respect to what is the best way of testing claimed capabilities and competences of the NMIs and DIs. This may lead to approaches different from what has been done so far.

### Acknowledgments

The author likes to thank the following participants in the two CCQM ad hoc Working Groups on the KCRV and Efficient and Effective Testing for their very useful input in the discussions: Prof. Maurice Cox (NPL), Dr. Martin Milton (NPL), Dr. Steve Ellison (LGC), Dr. Mike Sargent (LGC), Dr. Dave Duewer (NIST), Dr. Reenie Parris (NIST), Dr. Greg Turk (NIST), Dr. Willie May (NIST), Dr. Lindsey Mackay (NMIA), Dr. Jochen Vogl (BAM), Dr. Wolfram Bremser (BAM), Dr. Robert Wielgosz (BIPM).

### References

1. M. Barranco and J. R. Buchler, *Phys. Rev. Cf***22**, 1729 (1980).
2. H. Müller and B. D. Serot, *Phys. Rev. C***52**, 2072 (1995).
3. V. Baran, M. Colonna, M. Di Toro and A. B. Larionov, *Nucl. Phys. A***632**, 287 (1998).
4. Mutual recognition of national measurement standards and of calibration and measurement certificates issued by national metrology institutes, CIPM, Paris, 14 October 1999
5. Calibration and Measurement Capabilities in the context of the CIPM MRA, BIPM, 2008
6. Guide to the implementation of the CIPM MRA,BIPM, 2008
7. D. L. Duewer, Reenie M. Parris, Steven L.R. Ellison, draft paper on Sound Metrological Approach to Assigning CCQM KCRVs and U95(KCRV)
8. V. Baran, M. Colonna, M. Di Toro and V. Greco, *Phys. Rev. Lett.* **86**, 4492 (2001).

## QUALITY BY DESIGN APPLICATIONS TO ANALYTICAL METHODS IN THE PHARMACEUTICAL INDUSTRY

RON S. KENETT

*KPA Ltd., Raanana, Israel*  
*ron@kpa.co.il*

DAN A. KENETT

*Teva Pharmaceutical Ind. Ltd., Rehovot, Israel*  
*Dan.Kenett@teva.co.il*

A process is well understood when all critical sources of variability are identified and explained, variability is managed by the process, and product quality attributes can be accurately and reliably predicted over the design space. Quality by Design (QbD) is a systematic approach to development that begins with predefined objectives, emphasizes product and process understanding and sets up process control based on sound science and quality risk management. The FDA and ICH have recently started promoting QbD in an attempt to curb rising development costs and regulatory barriers to innovation and creativity. QbD is partially based on the application of multivariate statistical methods and a statistical Design of Experiments strategy to the development of both analytical methods and pharmaceutical formulations. In this paper, we review the basics of QbD and emphasize their impact on the development of analytical measurement methods in the innovative, generic and biosimilar pharmaceutical industry.

### 1. Background

A process is well understood when all critical sources of variability are identified and explained, variability is managed by the process, and product quality attributes can be accurately and reliably predicted over the design space. Processes must meet current good manufacturing practices to ensure that drug products meet safety and efficacy requirements. Traditionally, this requirement has been met by performing process validation studies on initial manufacturing batches. It has been recognized that this approach is unlikely to fully represent routine manufacturing and therefore unlikely to cover all potential sources of variability (e.g., raw materials, operators, shifts, reactor vessels). Moheb Nasr, director of the Office of New Drug Quality Assessment at FDA, has identified this issue as a challenge to the regulatory process and stated that there is currently a "focus on process validation and not process understanding" [14]. Quality by Design is about changing this approach.

Quality by Design (QbD) is a systematic approach to development that begins with predefined objectives, emphasizes product and process understanding and sets up process control based on sound science and quality risk management. The FDA and ICH have recently started promoting QbD in an attempt to curb rising development costs and regulatory barriers to innovation and creativity [3, 8, 9, 15]. An operational definition of QbD in analytical methods has been proposed by Borman et al from GSK (see [2]). We build on their approach, emphasizing the specific needs of biosimilar products. QbD can be described as a four stage process addressing both design and control. The stages are:

*I. Design Intent:* The Active Pharmaceutical Ingredient (API) chemical and physical characteristics and Drug Product (DP) performance targets are identified for the commercial product.

*II. Design Selection:* The API manufacturing process and the DP formulation and manufacturing process are selected to achieve the Design Intent for the commercial product.

*III. Control Definition:* The largest contributors to Critical Quality Attributes (CQA) variability are established and controls defined to ensure process performance expectations are met.

*IV. Control Verification:* The performance of the API and DP processes in manufacturing are measured to verify that the controls are effective and the product performance acceptable.

QbD is partially based on the application of multivariate statistical methods [4, 5, 6, 10, 22] and a Statistical Design of Experiments strategy [9, 10, 11, 22] to the development of both analytical methods and pharmaceutical formulations. In defining the controls (Stage 3), a QbD process is applied again to the design of the analytical methods in order to provide the necessary controls. The next section is a general review of the application of QbD to the development of analytical methods in the chemical and biotechnological pharmaceutical industry.

## **2. Analytical Challenges of Biopharmaceutical Products**

The biopharmaceutical industry has emerged from the development of recombinant DNA techniques in the 1980s. Today more than 120 therapeutic proteins are widely used for treating cancer, anemia, rheumatoid arthritis etc and are saving millions of lives. The most common cellular expression systems used to manufacture therapeutic proteins include bacteria, yeast, mammalian cells and insect cells. The choice of expression system depends on factors such as type of target protein, intellectual property rights and economy of manufacture.

Bacterial systems offer rapid and cheap expression, but cannot express complex proteins which are glycosylated and require an in vitro folding and tag removal step during downstream processing. Yeast generally expresses the target protein in its native form to the medium but expression levels are very low. Insect cells provide many advantages of the mammalian cell characteristics but currently there are no such products approved. A large stake of the 40 billion dollar biopharmaceutical market is composed of recombinant proteins produced in large bioreactors of 10-25,000 liters with engineered mammalian cells. The production cost of such processes is very high and can reach 1 million dollars per batch.

In recent years, some of the early patents set by the biotechnology innovator companies are beginning to expire opening the grounds for generic versions of biopharmaceuticals called biosimilar or follow-on biologics. Although no regulatory infrastructure presently exists in the U.S. for biosimilars, the regulatory systems are fast responding to this need, in response to intense political pressure to provide cheaper life saving drugs. For more background see [16]. In fact, by definition, the development and the production of biosimilar products fits very well the QbD paradigm as the target quality attributes sought of a biosimilar product are those of the innovator product on the market. Therefore from early development stages, comparability assessments need to be performed with innovator product by an array of analytical methods which probe the structure, the modifications, the activity, the specificity, the purity, the size and the stability of the product. As stated by health authorities (EMEA guideline on similar biological medicinal products CHMP/437/04), the success of the biosimilar development approach will depend on the ability to characterize the product and therefore to demonstrate the similar nature of the concerned products. Biological medicinal products are usually more complex and therefore more difficult to characterize than chemically derived medicinal products. In addition, there is a spectrum of molecular complexity among the various products (recombinant DNA, blood or plasma-derived, immunological, gene and cell-therapy, etc.). Moreover, parameters such as the three-dimensional structure, the amount of acidic-basic variants or post-translational modifications such as the glycosylation profile can be significantly altered by changes, which may initially be considered to be 'minor' in the manufacturing process. Thus, the safety/efficacy profile of these products is highly dependent on the robustness and the monitoring of quality aspects.

As a consequence of these conditions, the standard generic approach (demonstration of bioequivalence with a reference medicinal product by appropriate bioavailability studies) is not appropriate, while the approach based

on a comparability exercise needs to be followed. Innovators of well characterized biotech products also perform comparability exercises after manufacturing changes. The challenges and approaches used to demonstrate comparability of a well characterized biopharmaceutical can be as varied and complex as the products themselves. The quality attributes of a biotech product are traditionally associated only with specifications, not a "design space" approach indicating method of action. The International Conference on Harmonization (ICH) Q6 defines specifications as "a list of tests, references to analytical procedures, and appropriate acceptance criteria which are numerical limits, ranges, or other criteria for the tests described." Ideally, the acceptance criteria should be set to meet well-established requirements such as those representing product performance. However, such information is often missing and specifications are set by establishing the likely range of acceptable values to be seen in production data. When reviewing acceptance criteria set using preproduction data, regulators tend to favor the 3-sigma limits that are used for control charts. In practice, limits set using data from a small number of batches are almost always too tight [17] with the risk of rejection of "good batches". Some outstanding issues relate to comparability (e.g. process scale up and scale down versus current process scale of biosimiliar versus innovator product) and to the setting of product specifications, when only a limited number of batches are available. This situation is particularly relevant for products produced in large bioreactors.

In sum, pharmaceutical Drug Products are typically small molecules, often very stable, mostly without a device and produced by chemical synthesis. In contrast, biopharmaceutical Drug Products are large, complex molecules where stability requires special handling and the delivery device is often a key differentiator. Biopharmaceutical DP are produced in living organisms at comparatively high costs and are highly sensitive to manufacturing changes. In the next section we focus on the QbD development of analytical methods emphasizing statistical methods that help address these challenges.

### **3. Development of Analytical Methods**

The application of QbD to the development of analytical methods, at stage III, follows the same four steps process outlined above. Specifically, we have the following steps first presented in [2]:

*i. Method Design Intent:* The analytical method performance criteria are identified for the methods intended to be used for commercial product release.

*ii. Method Design Selection:* The method conditions are selected to achieve the Design Intent for the commercial release methods.

*iii. Method Control Definition:* The largest contributors to variability in the method performance characteristics are established and controls defined to ensure method performance expectations are met.

*iv. Method Control Validation:* The performance of the analytical method in use in a manufacturing environment is measured to verify that the method controls are effective and the method performance acceptable.

Analytical methods performance criteria are driven by an understanding of the process monitoring and control requirements, including the process critical quality attributes (CQAs) and specification limits. CQAs are identified by uncovering the characteristics of a drug substance or a drug product that needs to be controlled, to ensure the safety or efficacy of a product. The criteria for evaluating methods measuring these CQAs include, among others:

*Precision:* the requirement for the method variability to be a small proportion of the specification.

*Selectivity:* the determination of which impurities actually need to be monitored at each step and ensuring adequate discrimination between them

*Sensitivity:* ensuring the method is sufficiently sensitive relative to the specification limit in order to achieve effective process control.

These criteria address the aspects of the method that are required to facilitate ease of use in routine operation (e.g., analysis time, acceptable solvents, available equipment). Opportunities for the implementation of improved or new technology also need to be identified. These criteria can be generated by performing an analysis of the voice of the customer (VoC) (i.e., the aspects of a method that are considered important for the quality control laboratories within manufacturing where the commercial methods will be operated). Fundamental to design selection is the method-development phase. To develop a QbD method, the method performance criteria must be understood as well as the desired operational intent that the eventual end user would wish to see in the method. To deliver the latter, methods must take into account the VoC. Traditional approaches to analytical method validation and analytical method transfer, rely on a one time evaluation of the method and do not provide a high level of assurance of method reliability. The limited understanding of a method obtained through these traditional approaches has often led to poor technology transfer exercise from development into use in commercial manufacturing facilities. The fact that significant analytical method variables are not fully explored, leads to post transfer method failures. When transfers fail, significant resources are often required to attempt to remedy the causes of the transfer failure, usually at a time when there is considerable pressure to support the introduction and launch of a new product.

The desired state is to be able to prove that the method will be reliable (robust and rugged) throughout the life cycle of its use. This can be achieved by a risk assessment for identifying potential variables and determine which robustness and ruggedness experiments are to be performed. The latter can be tested as part of a measurement systems analysis study in which the most likely sources of variability are identified and studied (see [10]). All the knowledge (not just the technology) should then be transferred; any future changes to the method or the environment in which it is operated should be risk assessed; and, if appropriate, equivalency should be demonstrated as part of an overriding change-control procedure.

Analytical method robustness testing typically involves evaluating the influence of small changes in the operating conditions. Ruggedness testing identifies the degree of reproducibility of test results obtained by the analysis of the same sample under various normal test conditions such as different laboratories, analysts, and instruments. The term "robustness" has been used differently when describing chemical processes where processes, are defined as robust if they have the ability to tolerate the expected variability of raw materials, operating conditions, process equipment, environmental conditions, and human factors.. In the analytical world, it includes factors affecting robustness and ruggedness.

#### **4. Statistical Methods in the Application of QbD**

The application of QbD to the development of analytical methods is supported by an extensive statistical methodology. In particular we briefly review some of the following topics. In parenthesis are names of some of the software products supporting the approach and is provided only as informative data.

- Statistical Design of Experiments (MINITAB, JMP)
- Simulation experiments (DryLab, VisiMix, DynoChem)
- Stochastic emulators (TITOSIM)
- Variable fidelity experimentation
- Combining expert opinions with physical end simulation experiments
- Response surface methodologies (MINITAB, JMP)
- Multi-objective optimization (MINITAB, JMP, TITOSIM)
- Multivariate methods (MINITAB, JMP)

#### 4.1. Statistical Design of Experiments

Statistically designed experiments are now recognized as essential for rapid learning and thus for reducing time-to-market while preserving high quality and peak performance (see [10, 22]). The application of statistically designed experiments, in the development of analytical methods, is reported in [2, 15]. One example is the design of an HPLC method used to determine eight biogenetic amines as dabsyl derivatives [18]. The system consists of an Agilent 1050 High Performance Liquid Chromatography, with a variable-wavelength UV-vis detector and a model 3396-A integrator. The list of factors and their levels, used in the statistically designed experiment is presented in Table 1.

Table 1. Factors and levels in HPLC experiment described in [18].

Upper level (1)	Lower level (-1)	Nominal Value	Factor
2	0	1	Gradient Profile
42	38	40	Column Temp (C)
44	36	40	Buffer Conc. (mM)
5.2	4.8	5	Mobile-phase Buffer pH
451	441	446	Detection Wavelength (nm)
0.25	0.21	0.23	Triethylamine (%)
10.5	9.5	10	Dimethylformamide (%)

The specific experimental array used in the experiment is a  $2^{7-4}$  Fractional Factorial experiment with 3 center points, is described in Table 2.

Table 2. Experimental array of experiment described in [18].

Gradient	Temp	Conc	Buf	pH	Wave	perc	Perc
1	1	1	1	1	1	1	1
2	1	1	-1	-1	1	-1	-1
3	1	-1	1	1	-1	-1	-1
4	1	-1	-1	-1	-1	1	1
5	-1	1	1	-1	-1	1	-1
6	-1	1	-1	1	-1	-1	1
7	-1	-1	1	-1	1	-1	1
8	-1	-1	-1	1	1	1	-1
9	0	0	0	0	0	0	0
10	0	0	0	0	0	0	0
11	0	0	0	0	0	0	0

The array consists of 11 experimental runs that involve combining the design factors levels in a balanced set of combinations. The statistically designed experiment approach is maximizing the learned information for a

given experimental budget. From the experimental plan in Table 2, one can deduce the main effects of the 7 factors on various responses such the method resolution (see Figure 1).

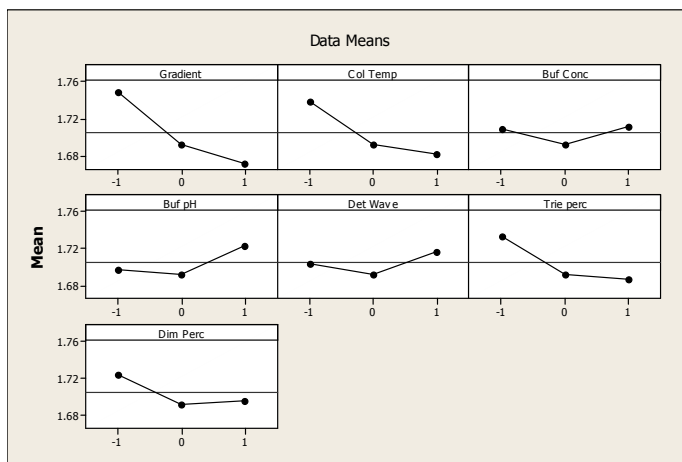


Figure 1. Main effects of factors on method resolution from data in [18].

From this analysis, one can determine that Gradient Profile and Column Temperature are active factors affecting resolution. A contour plot display of the method's design space accounting for non linear effects, in terms of Gradient Profile and Column Temperature, is presented in Figure 2.

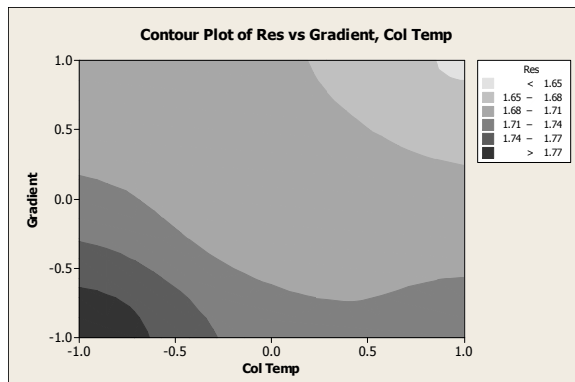


Figure 2. Contour plot of effect of Gradient Profile and Column temperature on method resolution from data in [18].

The Fractional Factorial design used in the development of the HPLC method provided a full exploration of the design space in terms of main effects and robustness properties. These experiments are physical experiments and require optimization in experimental set up complexities and budget limitations. In contrast, simulation experiments provide new opportunities for quick and extensive learning (see [11]). Such experiments are described next.

#### **4.2. Simulation Experiments and Stochastic Emulators**

Modern simulation platforms provide efficient and effective opportunities for conducting experiments and learn about the impact of design factors on CQAs. For example *VisiMix* enables mathematical modeling of mixing phenomena. It conducts calculation of average and local characteristics of mixing flow and distribution of concentration, including simulations of “non perfect” mixing. Another software product focused on the development of analytical methods from the Molnar-Institute is *DryLab*. This simulator simplifies and speeds the process of developing good chromatographic separations or methods by allowing to model changes in separation conditions using a personal computer. One more example is *DynoChem* which is used for fitting chemical reaction models, prediction of scale-up conditions, optimization of laboratory and production results, equipment characterization and shows the effect of scale dependent physical phenomena (mixing, heat transfer, mass transfer). Dynochem can be used for simulation of reactions performed in homogenous environment. When mixing is not ideal and the solution is not homogenous, VisiMix can be used for finding the required mixing conditions. In recent years, a comprehensive statistical methodology has been developed to exploit such simulation platforms, see [1, 11, 20, 21, 22].

#### **4.3. Bayesian Models**

In [18], information from expert opinion, computer experiments and physical experiments are combined in a simple regression model of the form:

$$\mathbf{Y} = f(\mathbf{X}, \boldsymbol{\beta}) + \boldsymbol{\varepsilon} \quad (1)$$

In this model  $\mathbf{X}$  represents the design space corresponding, for example, to the values of the factors in Table 1. In this example  $\mathbf{X}$  is a  $8 \times k$  matrix,  $k$  representing the number of observations in the experiments, the first column consisting of the value '1" used to accommodate the average response. The vector  $\boldsymbol{\beta}$  represents the values of the model coefficients, in this case of dimension 7, and  $\mathbf{Y}$  represents the  $k$  observations, for example of method resolution. Combining these results with the expert opinion posteriors we derive

a second posterior distribution and then adding estimates from physical experiments through Markov Chain Monte Carlo we calculate the final distribution for  $\beta$ .

$$\text{Stage 1}(\mathbf{Y}_o) \rightarrow \text{Stage 2}(\mathbf{Y}_o + \mathbf{Y}_c) \rightarrow \text{Stage 3}(\mathbf{Y}_o + \mathbf{Y}_c + \mathbf{Y}_p) \quad (2)$$

A related approach called "variable fidelity experiments" has been proposed in [7] to combine results from experiments conducted at various levels of sophistication. These methods can be used to derive specification limits reflecting the expected variability of the response  $\mathbf{Y}$  in the design space described by  $\mathbf{X}$ .

#### **4.4. Response Surface Methodology**

Response surface methodology (RSM) is a strategy for exploring the relationship between controllable factors and important response variables. RSM makes extensive use of statistically designed experiments and regression models. A key element to RSM is the notion of sequential learning where initial experiments help focus attention on the most important factors, subsequent steps help to bring these factors to settings that achieve good results, and finally efficient statistical modeling techniques are used to estimate how these factors affect the response variables of greatest importance (see [9, 10, 13, 22]). Using this approach, one can optimize the design of the HPLC method described in Table 1 to achieve maximum resolution on the bottom left corner of Figure 2.

#### **4.5. Multivariate Methods**

Data collected by analytical methods is typically multivariate. DP specifications are almost always presented in a univariate format, one variable at a time. Multivariate statistics offer an effective approaches to set specifications and describe DP performance. For example, in [4], Multivariate tolerance regions are used to specify the performance of a product by considering the combined distribution of its CQA characteristics. Such an approach accounts for the correlation structure between CQAs thus enhancing sensitivity and specificity of the analytical methods. For more on multivariate approaches to process control and specification setting see [5, 6, 10, 22].

### **5. Summary and Conclusions**

The application of QbD to the development of analytical methods is providing an opportunity to revise traditional concepts and procedures for designing and validating analytical methods and setting specifications in drug

products. In this paper, we outline the challenges faced by modern medicinal products, and their generic and biosimilar counterparts. These challenges can be addressed by statistical methodologies such as statistically designed experiments, multivariate methods, Bayesian models, simulation experiments and stochastic emulators. The paper is meant to be only a high level introduction to these topics referring the reader to references for more details.

### **Acronyms**

QbD - Quality by Design	API - Active Pharmaceutical Ingredient
DP - Drug Product	CQA - Critical Quality Attribute
VoC - Voice of the Customer	FDA - Food and Drug Administration

### **Software Products for simulations and QbD statistical analysis**

DryLab – <http://www.molnar-institut.com/cd/indexe.htm>  
 DynoChem – <http://www.scale-up.com/index.html>  
 JMP – <http://www.jmp.com/>  
 MINITAB – <http://www.minitab.com/>  
 OntoSpace – <http://www.ontonix.com/>  
 TITOSIM – <http://www.titosim.com/>  
 VisiMix – <http://www.visimix.com/>

### **References**

1. Bates, R., Kenett R., Steinberg D. and Wynn, H. (2006), Achieving Robust Design from Computer Simulations, *Quality Technology and Quantitative Management*, **3**, 2, pp. 161-177.
2. Borman, P., Nethercote, P., Chatfield, M., Thompson, D., Truman, K. (2007), "The Application of Quality by Design to Analytical Methods", *Pharmaceutical Technology*.
3. Food and Drug Administration (2006), Guidance for Industry Quality Systems Approach to Pharmaceutical CGMP Regulations.
4. Fuchs, C. and Kenett, R. (1988), "Appraisal of Ceramic Substrates by Multivariate Tolerance Regions", *The Statistician*, **37**, pp. 401-411.
5. Fuchs, C. and Kenett, R. (1998), "Multivariate Tolerance Regions and F-tests", *Journal of Quality Technology*, **19**, pp. 122-131.
6. Fuchs, C. and Kenett, R. (1998), *Multivariate Quality Control: Theory and Applications*, Marcel Dekker Inc., New York.
7. Huang D., Allen T. (2005), Design and analysis of variable fidelity experimentation applied to engine valve heat treatment process design, *Journal of the Royal Statistical Society (C)*, **54**, 2, pp. 443-463.

8. ICH (2006), The International Conference on Harmonization of Technical Requirements for Registration of Pharmaceuticals for Human Use, Quality Guideline Q8 Pharmaceutical Development.
9. Kenett, R. and Stark, Y. (2008), "Drug Development Strategy: The interface between QbD and statistical methods" Global Pharmaceutical Conference on Practical Application of QbD in Accelerated Development, Frankfurt, Germany.
10. Kenett, R. and Zacks, S. (1998), *Modern Industrial Statistics: Design and Control of Quality and Reliability*, Duxbury Press, San Francisco, 1998, Spanish edition 2000, 2<sup>nd</sup> paperback edition 2002, Chinese edition 2004.
11. Kenett, R.S. and Steinberg, D. (2006), New Frontiers in Design of Experiments, *Quality Progress*, pp. 61-65, August.
12. Kennedy M. and O'Hagan, A. (2000), Predicting the output of a complex computer code when fast approximations are available, *Biometrika*, **87**, pp.1-13.
13. Myers R., Montgomery D., Vining G., Borror C., Kowalski S. (2004), Response Surface Methodology: A Retrospective and Literature Survey, *Journal of quality technology*, **36**, 1, pp. 53-77.
14. Nasr, M. (2007), "Quality by Design (QbD) – A Modern System Approach to Pharmaceutical Development and Manufacturing – FDA Perspective", FDA Quality Initiatives Workshop, Maryland, USA.
15. Nethercote, P. (2008), "Implications of QbD Approach on Analytical Method Development, Validation, Transfer and Change Control", Global Pharmaceutical Conference Practical Application of QbD in Accelerated Development, Frankfurt, Germany.
16. Niazi, K. (2006), *Handbook of Biogeneric Therapeutic Proteins Regulatory, Manufacturing, Testing, & Patent Issues*, CRC Press.
17. Orchard, T. (2006), "Setting acceptance Criteria from Statistics of the Data", *BioPharm*, **19**, pp.34-46.
18. Reese C., Wilson A., Hamada M., Martz H., Ryan K. (2004), Integrated Analysis of Computer and Physical Experiments, *Technometrics*, **46**, 2, pp. 153-164.
19. Romero R., Gasquez, D., Sanshez, M., Rodriguez, L. and Bagur, M. (2002), "A Geometric Approach to Robustness testing in Analytical HPLC", *LC GC North America*, **20**, pp. 72-80.
20. Sacks, J., Welch, W., Mitchell, T. and Wynn, H. (1989), Design and Analysis of Computer Experiments, *Statistical Science*, **4**, pp. 409-435.
21. Santner, T. J., Williams, B. J., Notz, W. I. (2003), *The Design and Analysis of Computer Experiments*. Springer Verlag, New York..
22. *Wiley Encyclopedia of Statistics in Quality and Reliability* (2007), Ruggeri, F., Kenett R. and Faltin, F. (editors in chief), J. Wiley.  
<http://mrw.interscience.wiley.com/emrw/9780470061572/home>

## A TEST OF LINEARITY USING COVERING ARRAYS FOR EVALUATING UNCERTAINTY IN MEASUREMENT

RÜDIGER KESSEL, RAGHU KACKER

*NIST, Mathematical and Computational Sciences Division,  
100 Bureau Drive, Gaithersburg, MD 20899-8910, USA*

Since the Guide to the Expression of Uncertainty in Measurement (GUM) was published in 1993 it has changed the evaluation of physical and chemical measurements. Nowadays almost all high level measurements include a detailed evaluation of uncertainty. This allows the scientific community to do the next step and evaluate uncertainty for derived evaluations like parameter fittings. The evaluation of the uncertainty for complicated parameters like the results from non-linear fitting procedures can be carried out in two steps. The first step is a sensitivity analysis of the evaluation algorithm and a test of mutual independence of the parameters. If the fitting algorithm is sufficiently robust a linear model is derived from the fitting algorithm which is then used in a second step to evaluate the uncertainty of the fitting parameters. This paper discusses the sensitivity analysis in detail with the emphasis on possibilities to check for robustness and linearity. An efficient method based on covering arrays is presented to test for hidden couplings between the input parameters inside the evaluation model.

### 1. Introduction

In science and metrology results are often calculated based on different data and given values. A wide variety of techniques and procedures are employed including linear and non-linear fitting, optimization and simulation. Traditionally these techniques provide little support for calculating and propagating uncertainty. Also the calculations may require complicated computer calculations which may be expensive to execute. The approach which we propose here is to treat the existing algorithms and calculation schemes as black boxes, where the relation between input and output is defined by some unknown or partly unknowable function. For the calculation of the uncertainty associated with the results we follow the Guide to the Expression of Uncertainty in Measurement (GUM) [1]. The GUM propagates estimates and standard uncertainties for the input quantities using a linear approximation of the measurement function. Figure 1 illustrates a general measurement function from the GUM [1]. The GUM approach does not require complete knowledge of probability density functions (pdfs) for the input quantities. Generally, the estimates and uncertainties for the input quantities can be more reliably determined than complete pdfs. Therefore the GUM approach is more widely applicable than other approaches such as the Monte Carlo Simulation [2] which

require knowledge of pdfs. In the discussion of the efficiency of the different computational approaches it is generally assumed that the evaluation of the black box model consumes by far the most resources.

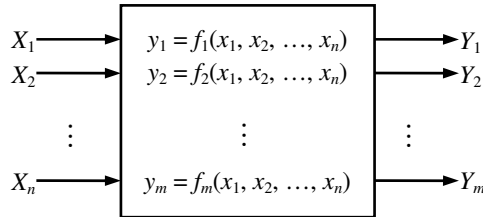


Figure 1. General measurement function

The GUM method can be applied to any kind of calculation scheme where we assume that we calculate some number  $m$  of results  $Y_k$  based on  $n$  input quantities  $X_i$  and therefore  $m$  functions  $f_k$  exist which link the input to the output (see Figure 1). Fortunately we do not need to know the functions in detail. To employ the GUM method it is enough if we know a linear equivalent of the functions around the value of the input quantities.

If the partial derivatives of the functions  $f_k$  are known, the linear equivalent of the functions can be calculated by a first order Taylor series expansion as described in the GUM. A numerical alternative to use the GUM approach which does not require evaluation of partial derivatives is described in [3]. This numerical approach, often referred to as spread-sheet method is popular among chemists.

The mainstream GUM method works well only if the unknown functions do not deviate too much from their linear approximations. Therefore we describe methods to evaluate the difference between the black box model and the linear approximation to test whether the linearized model is adequate. We have implemented the methods described here in a Python [4] script. In the last section we discuss some aspects of the implementation.

## 2. Calculation of the Linear Model

The propagation of uncertainty according to the GUM is based on an equivalent linear model for the measurement function. The GUM proposes a first order Taylor series expansion to calculate the linear model. Alternatively numerical methods can be used. We use here the spread-sheet method [3].

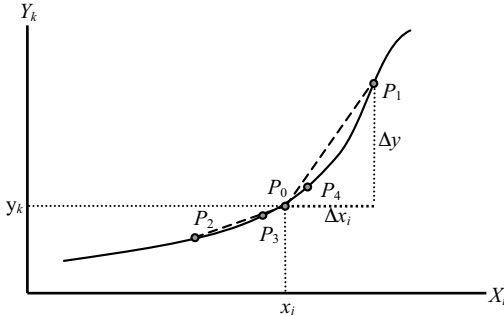


Figure 2. Linearization of function  $f_k(\dots, x_i, \dots)$  with 5-point linearity test

The idea is simply to substitute the partial derivative in the Taylor expansion by the quotient of differences

$$\frac{\partial y_k}{\partial x_i} \cong \frac{\Delta y_k}{\Delta x_i} = \frac{y_{k,1} - y_{k,0}}{x_{i,1} - x_{i,0}} = c_{k,i} \text{ with } k = 1 \dots m, i = 1 \dots n \quad (1)$$

assuming a function  $y_k = f_k(x_1, x_2, \dots, x_n)$  is given and the relation between the result  $y_k$  and an input  $x_i$  is similar to the illustration in Figure 2.  $P_0$  is given by the value of  $x_i$  and result of  $f_k(\dots, x_i, \dots)$ . Now we choose another point with coordinates  $P_1 : [x_i + \Delta x_i, f_k(\dots, x_i + \Delta x_i, \dots)]$ . We can estimate the sensitivity by the slope of a straight line through  $P_0$  and  $P_1$ . If we would be interested in the best estimate of the slope in  $P_0$  we would decrease  $\Delta x_i$  to some minimal value based on the numerical resolution of the computer calculation. Since we are not interested in the slope at the exact point  $P_0$  but rather in an uncertainty interval around  $P_0$  we can choose  $\Delta x_i$  to be equal to the given (or assumed) uncertainty  $u(x_i)$ . The number of model evaluations to calculate the linear model is  $n + 1$ , so the method scales with  $n$ .

In practice it is useful to calculate not only the sensitivities (Eq. 1) but also the relative sensitivities

$$S_{k,i} = c_{k,i} \cdot \frac{x_i}{y_k}. \quad (2)$$

With the relative sensitivities it is possible to judge if the sensitivity analysis is reasonable. The relative uncertainty multiplied by the relative sensitivity leads to the relative uncertainty contribution. A value for the relative sensitivity greater than one indicates that the black box model magnifies the uncertainty of the particular input quantity and further if the value is much larger than one it indicates that the black box model may not be numerically robust.

### 3. Linearity Checks

In the preceding section we presented the well-known spread-sheet approach to extract a linear model from a given model which may be non-linear. Now we discuss several possible linearity checks. All linearity checks calculate quotients of differences similar to Eq. 1 and compare the result with some combination of the sensitivities found in the previous section. The model will be considered sufficiently linear if the sensitivities agree within 5%.

#### 3.1. Three and Five Point Calculation

The calculation of the linear model can be extended by choosing additional points and calculating the slope of the straight lines through them. Figure 2 illustrates this for 5 points. With  $P_0$ ,  $P_1$  and  $P_2$  we can calculate two slopes for plus and minus  $u(x_i)$ . By comparing the two slopes we can detect whether  $P_0$  is close to a local extreme, or whether  $f_k(\dots, x_i, \dots)$  has a significant curvature around  $x_i$ . By adding two more points with a significantly smaller  $\Delta x_i$  we can test whether the curvature is significantly changing in an interval around  $x_i$ . In general the sensitivity can be calculated for the different points with the following equation:

$$c_{k,i}(w) = w \cdot \frac{f_k(\dots, x_i + \frac{u(x_i)}{w}, \dots) - f_k(\dots, x_i, \dots)}{u(x_i)}. \quad (3)$$

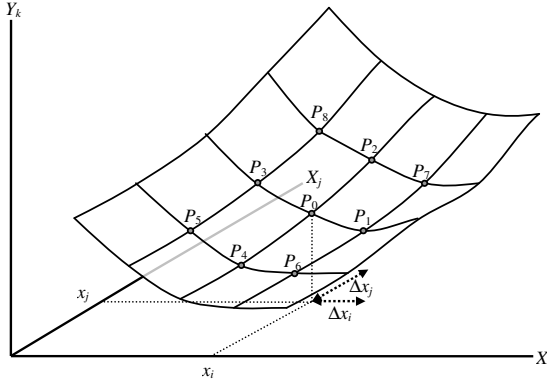
The parameter  $w$  determines  $\Delta x_i$  expressed as a fraction of  $u(x_i)$ . Useful values for  $w$  are 1,  $-1$ , 10 and  $-10$ . This leads to the criteria for sufficient linearity

$$\left| \frac{c_{k,i}(1)}{c_{k,i}(-1)} - 1 \right| < \varepsilon_{\text{lin}}, \quad \left| \frac{c_{k,i}(1)}{c_{k,i}(10)} - 1 \right| < \varepsilon_{\text{lin}} \quad \text{and} \quad \left| \frac{c_{k,i}(-1)}{c_{k,i}(-10)} - 1 \right| < \varepsilon_{\text{lin}}, \quad (4)$$

with  $\varepsilon_{\text{lin}}$  being the selected linearity limit of 0.05. The number of model evaluations to calculate the linearity check is  $(p-1) \cdot n + 1$  with  $p$  being the number of points used for the check, so the method scales with  $n$ .

#### 3.2. All Pairs Coupling Test

The linearity check discussed in the last section is a robust method to check for sufficient linearity within one input parameter but it does not check for any coupling between parameters (input quantities). An example of such coupling is the product of two input quantities  $Y = X_1 \cdot X_2$ . This example is of some relevance in metrology. A significant deviation from the linear model can be observed if the value of one or both of the quantities is small compared to the uncertainty of the value. The three and five point linearity check will not detect this situation.

Figure 3. Evaluation of the function  $f_k(\dots, x_i, x_j, \dots)$  around  $P_0$ 

If we want to check for this kind of non-linearity in the black box model, we need to calculate additional points. We choose a pair of input quantities  $x_i$  and  $x_j$  for which we want to analyze the model. Figure 3 illustrates the method. During the three point linearity check we have already calculated  $P_0$ ,  $P_1$ ,  $P_2$ ,  $P_3$  and  $P_4$ . So we know the linear sensitivity in  $x_i$  and  $x_j$  to be  $c_{k,i}(1)$  and  $c_{k,j}(1)$ .

Now we can evaluate the model at  $P_5$ ,  $P_6$ ,  $P_7$  and  $P_8$  and calculate the difference from the center point  $P_0$ :

$$d_k(w_i, w_j) = f_k(\dots, x_i + \frac{u(x_i)}{w_i}, x_j + \frac{u(x_j)}{w_j}, \dots) - f_k(\dots, x_i, x_j, \dots) \quad (5)$$

with  $w_i$  and  $w_j$  being either plus or minus one. Table 1 shows the relation between the points and the  $w_i$  and  $w_j$  values.

Table 1. Combinations of  $w_i$  and  $w_j$ 

Point	$w_i$	$w_j$
$P_5$	-1	-1
$P_6$	+1	-1
$P_7$	+1	+1
$P_8$	-1	+1

A similar difference can be calculated for the linear model

$$l_k(w_i, w_j) = c_{k,i}(1) \cdot \frac{u(x_i)}{w_i} + c_{k,j}(1) \cdot \frac{u(x_j)}{w_j}. \quad (6)$$

The coupling can be checked by evaluating the following condition:

$$\left| \frac{d_k(w_i, w_j) - l_k(w_i, w_j)}{l_k(w_i, w_j)} \right| < \epsilon_{\text{lin}}. \quad (7)$$

Since it is not known in advance which of the input quantities might be coupled we need to repeat the check for all pairs. The number of model evaluations to calculate the all-pairs coupling check is  $(n^2-n)/2$ , so this method scales as  $n^2$  if  $n$  is large.

### 3.3. Covering Array Based Coupling Test

The all pairs coupling test discussed in the previous section is a useful method to judge whether a black box model has some significant pair-wise coupling between the input parameters. Unfortunately the evaluation may be costly because it scales with  $n^2$ . Especially for complicated data fitting and expensive simulation runs when the number of input parameters is large (greater 20) this analysis is expensive. Much more resources are needed for the coupling test than for the extraction of the linear model.

To overcome this problem we look for couplings between several pairs in one run. Instead of varying just one pair of input parameters we vary several pairs in one run and check for significant differences. With all runs we have to ensure that all combinations of input pair variations appear in the runs. This is an application of so called covering arrays [5]. Covering arrays are used in software testing as optimized test patterns for finding parameter interaction faults which are hidden couplings in software programs. So a covering array is an optimized test pattern for a coupling check. The covering are constructed in such a way that all necessary patterns are covered by the arrays. The covering arrays have as many columns as the black box model has input parameters. Every row is a separate test case. The number of rows depends on the number of parameters, the number of discrete values for each parameter and the strength of the array. The strength is a measure of the complexity of the interactions that can be detected. For the application of the coupling test we need a binary array with strength of two. A number of different algorithms exist to generate covering arrays in an efficient way [6].

The covering array (for an example see Table 2) contains a row with  $n$  values which are either  $-1$  or  $+1$ . For every row of the covering array the difference

$$d_k^*(w_1, \dots, w_n) = f_k(x_1 + \frac{u(x_1)}{w_1}, \dots, x_n + \frac{u(x_n)}{w_n}) - f_k(x_1, \dots, x_n) \quad (8)$$

is calculated from one extra black box model evaluation. The  $w_1 \dots w_n$  are the pattern values from the rows of the covering array. We also need a similar value

$$l_k^*(w_1, \dots, w_n) = \sum_{i=1}^n c_{k,i}(1) \cdot \frac{u(x_i)}{w_i} \quad (9)$$

based on the assumption that the model is perfectly linear. In Eq. 9 the  $w_1 \dots w_n$  are the same pattern values as in Eq. 8. Under the condition that

$$\left| \frac{d_k^*(w_1, \dots, w_n) - l_k^*(w_1, \dots, w_n)}{l_k^*(w_1, \dots, w_n)} \right| < \epsilon_{lin}, \quad (10)$$

we can judge whether or not any coupling is observable with this test pattern. If no significant coupling shows up during any of the model evaluations we can conclude that the linear model is representing the behavior of the black box model for small changes in the input values. It is possible that a coupling in one pair of parameters may be compensated by another coupling in another parameter and we are not observing the coupling with the combinatorial pattern. This can only be detected with the all pairs approach with a much higher cost.

Table 2. Example of a binary covering array of strength 2 for 10 parameters

run	$w_1$	$w_2$	$w_3$	$w_4$	$w_5$	$w_6$	$w_7$	$w_8$	$w_9$	$w_{10}$
1.	-1	-1	-1	-1	-1	-1	-1	-1	-1	-1
2.	-1	+1	+1	+1	+1	+1	+1	+1	+1	+1
3.	+1	-1	+1	-1	+1	-1	+1	-1	+1	-1
4.	+1	+1	-1	+1	-1	+1	-1	+1	-1	+1
5.	-1	+1	+1	-1	-1	-1	-1	+1	+1	-1
6.	-1	-1	-1	+1	+1	+1	+1	-1	-1	+1
7.	-1	+1	+1	+1	+1	-1	-1	-1	-1	-1
8.	-1	-1	-1	-1	-1	+1	+1	+1	+1	+1
9.	+1	-1	+1	-1	-1	+1	+1	+1	-1	-1
10.	+1	-1	-1	+1	+1	-1	-1	-1	-1	+1

The number of model evaluations to calculate the combinatorial coupling check is dependent on the number of rows in the covering array. For a large number of parameters the upper bound scales with  $\log_2(n)$ .

#### 4. Implementation

The linear model approximation and the different linearity checks were implemented in a Python script [4], which can call an arbitrary command line program to execute the black box model calculations.

The basic flow chart is shown in Figure 4. Based on the original data file a number of modified test data files are generated to calculate the linear model and to perform the linearity checks. All data is stored in text files (csv). The necessary covering arrays are generated with the command line version of the software tool FireEye [6].

The test data files are used by the black box model which generates the result files. Since the model calculations are independent from each other it is possible to execute several runs of the model in parallel. After all runs of the model are completed the linear model is generated and the linearity checks are

run. For test purposes the black box model can be replaced by a white box model with a known algebraic equation system. This allows verifying the script by testing that the correct linear system is determined for well defined equations.

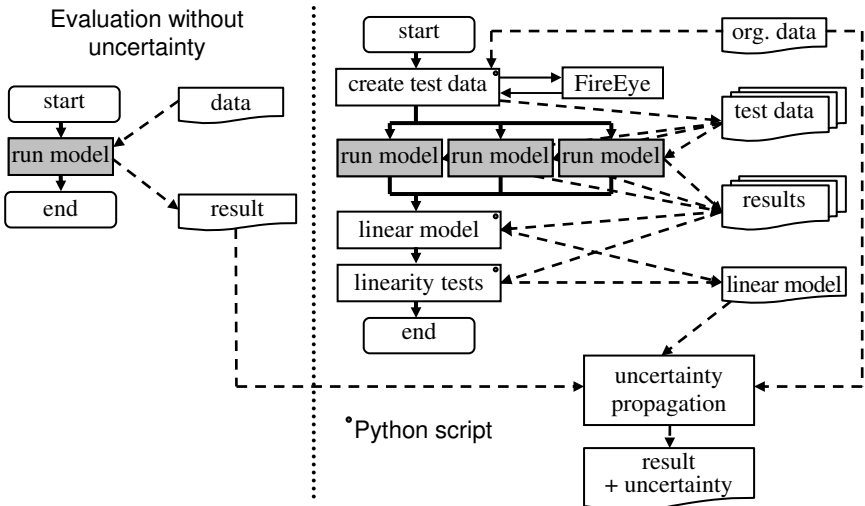


Figure 4: Flow chart of the linear model generation

## 5. Conclusions

It is well-known that the standard GUM method can be applied to any kind of result evaluation if the evaluation model is sufficiently linear. The so-called spread-sheet method can be efficiently used to calculate the sensitivities of an equivalent linear model for the measurement. If the result evaluation is available in the form of a command line program which can be called by a script language it is possible to generate automatically an equivalent linear model which can then be used to propagate the uncertainty. In this way the propagation of uncertainty can be added to virtually any kind of computerized result evaluation without any change to the existing code.

Additionally we propose some useful linearity and coupling tests to verify that the basic assumption about the sufficient linearity of the model can be justified. We introduce covering arrays as a way to find efficient test cases. The combination of linear model generation, three-point linearity test and coupling test based on covering arrays is an efficient way to establish a linear model which allows us to use mainstream GUM uncertainty propagation. The proposed approach is not a mathematical proof of linearity; however, it is of

practical use especially useful in cases when the calculation of the result evaluation requires a lot of computing resources.

## References

- [1] BIPM *et. al.* Guide to the Expression of Uncertainty in Measurement (GUM). ISBN 92-67-1011889, 1<sup>st</sup> Edition (1993) 2<sup>ed</sup> Edition (1995).
- [2] BIPM *et. al.* Supplement 1 to the GUM: Propagation of distributions using a Monte Carlo method. 2008)
- [3] Kragten J. *Analyst*. 119:2161–2166 (1994)
- [4] Python Programming Language, <http://www.python.org>
- [5] Lawrence, J. F. *et. al.* Binary Covering Arrays. submitted (2008)
- [6] FireEye: Executable copies can be obtained from kuhn@nist.gov

## CHALLENGES IN PRACTICAL DYNAMIC CALIBRATION

MICHAEL KOBUSCH, THOMAS BRUNS, ERNST FRANKE

*Physikalisch-Technische Bundesanstalt (PTB),  
Bundesallee 100, 38116 Braunschweig, Germany*

High precision calibration of electromechanical transducers using dynamic loads is a field of rapidly growing demand in industries. But in contrast, the number of validated methods or even written standards is still close to negligible considering the number of measurands concerned. For this reason, the Physikalisch-Technische Bundesanstalt (PTB) has put increasing effort into the field of dynamic measurement of mechanical quantities in the past several years. The dynamic measurands covered so far by this R&D initiative include acceleration, force, pressure and torque. New dynamic calibration facilities have been developed, applying either periodic or shock excitations and using either primary or secondary calibration methods. The working principles of these calibration devices are described subsequently as well as the different approaches for the dynamic characterization of transducers, like step response, impulse response or harmonic response, respectively. From the scientific point of view, the harmonization of different dynamic calibration results is an essential prerequisite towards future standardization work. Despite the different technical realizations, the mathematical procedures and the problems for a dynamic characterization of transducers as well as the dissemination of the dynamic units are generally similar. These challenges are now approached by methods of a model-based calibration, which seem to give very promising results.

### 1. Introduction

With an increased number of dynamic applications in all fields of industry along with the growing demand for precise measurements, the dynamic calibration of electromechanical transducers is becoming more and more important. This relates to a great variety of time-varying mechanical quantities, beginning with acceleration and angular acceleration, up to dynamic force, pressure and torque. These quantities are commonly measured in industrial praxis, e.g. in production engineering, material testing, automation, robotics, mining and oil industry, food industry, automotive and aviation industry just to mention some. Depending on the specific application and its dynamic load, signals of different behavior in the time and frequency domain will occur, from gradual and step-like changes to periodical variations, shock pulses or random noise.

In contrast to the importance of dynamic measurements, only few dynamic calibration methods have been validated today and the number of written standards is very small considering the number of measurands concerned. This dissatisfying metrological situation motivated the Physikalisch-Technische Bundesanstalt (PTB), the national metrology institute of Germany, to start a research and development initiative, putting increased efforts in the field of dynamic measurement of mechanical quantities over the past several years. The measurands covered so far include acceleration, angular acceleration, force, pressure and torque. Within the scope of this initiative, several new dynamic calibration facilities based on primary or secondary calibration methods have been developed, applying either periodic or shock excitation. The primary calibration methods investigated here use a laser interferometer as reference, whereas the secondary methods perform a comparison with a reference transducer. In praxis, the calibration method to be chosen is usually related to the considered dynamic load and it is therefore still useful to have different methods at hand. With respect to future standardizations and disseminations of the dynamic units, the calibration facilities provide the technical means for the research on scientifically accepted calibration methods including their specific uncertainty budgets. These investigations are required for the characterization of the transducer's dynamic behavior to be expressed in its technical specifications or its calibration certificate.

## 2. Dynamic Calibration of Electromechanical Transducers

A brief overview about the dynamic calibration facilities at PTB is given in the following for the dynamic measurands *acceleration* (shock, sinusoidal), *force* (shock, sinusoidal) and *pressure* (shock). Moreover, a development in the field of dynamic torque was launched recently and the results will be taken as a vantage point for further research and development [9].

### 2.1. Acceleration Calibration

Calibrations of acceleration transducers and angular acceleration transducers with primary methods using sinusoidal excitation as well as shock excitation are well established [1] and described by a series of international standards [2]. In accordance to these standards, four primary sine calibration devices with overlapping frequency ranges (0.1 Hz – 20 Hz, 0.4 Hz – 63 Hz, 10 Hz – 2.5 kHz, 10 Hz – 20 kHz) are operated at PTB for regular calibration services. The example presented in figure 1 shows the high frequency (HF) acceleration standard for excitations up to 20 kHz. The acceleration transducer to be

calibrated (DUT, device under test) is mounted onto an air-borne armature which is excited by an electrodynamic vibration exciter (shaker). Traceability of the input acceleration is achieved by a laser-Doppler interferometer (LDI). Parasitic vibrations from the environment are suppressed by a vibration isolation system. According to ISO 16063-11, the calibration result is the frequency response (in amplitude and phase) of the transducer's sensitivity (ratio of output voltage and input acceleration) at selected frequency points. For magnitude of sensitivity, this calibration device provides a measurement uncertainty of 0.1 % to 0.5 %.

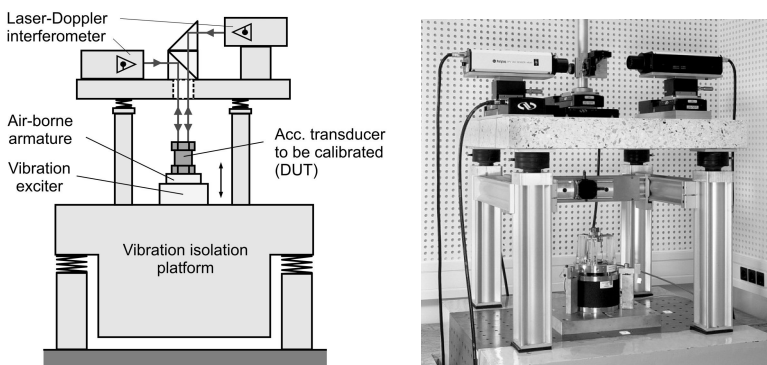


Figure 1. HF acceleration standard

The unit of angular acceleration at sinusoidal excitation is realized by a primary calibration device using a rotational exciter with air-borne armature. Its specifications are: frequency range 0.3 Hz – 1 kHz, angular acceleration 1 rad/s<sup>2</sup> – 1400 rad/s<sup>2</sup>. Traceability is achieved by an LDI directed onto a reflective holographic diffraction grating (retro-reflection in first order of diffraction) which is fixed at the lateral surface of the cylindrical rotor. For this optical geometry, the interferometer senses a component of the tangential velocity proportional to the angular velocity to be measured [4].

Two primary calibration devices are in service for shock calibrations, one for low intensity (LI) shock pulses (50 m/s<sup>2</sup> – 9000 m/s<sup>2</sup>), the other for high intensity (HI) shocks (5 km/s<sup>2</sup> – 100 km/s<sup>2</sup>). Photographs of both facilities are shown in figure 2. The typical calibration result according to ISO 16063-13 is the shock sensitivity  $S_{sh}$ , which is defined as the ratio between the pulse peak values of the transducer output voltage  $u_{peak}$  and the acceleration  $a_{peak}$ . Traceability of acceleration is again achieved by an LDI. The LI shock acceleration standard measuring device uses a hammer-anvil principle with air-borne mass bodies. A spring-driven acceleration mechanism hits on a hammer,

which itself impacts on an anvil that carries the DUT at its backside. The duration of the Gauss-shaped acceleration pulses range from 1 ms to 10 ms, depending on the selected mass bodies and hammer tips (example of 2 ms is shown in figure 3). The working principle of the HI shock acceleration standard measuring device is based on the propagation of an elastic shock wave in a long bar. The device features three bars of 4 m length each, of different material (steel or titanium) and different cross sections. The DUT is mounted at the end surface of these Hopkinson bars. The shock pulses are generated via a pneumatically-driven ball accelerator and a pulse mitigator, resulting in short dipole pulses of about 70  $\mu$ s to 300  $\mu$ s pulse width. Elastic reflections at the bars' ends lead to pulse repetitions after few milliseconds (1.7 ms for Ti, see figure 3), depending on the elastic wave velocity within the solid material.

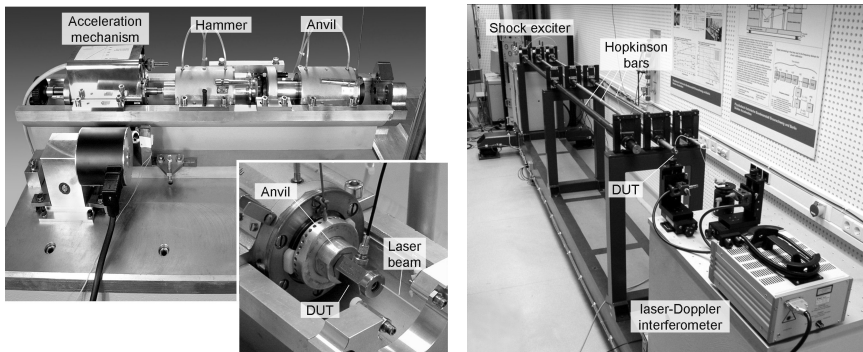


Figure 2. Shock acceleration standard measuring devices, LI shock (left), HI shock (right)

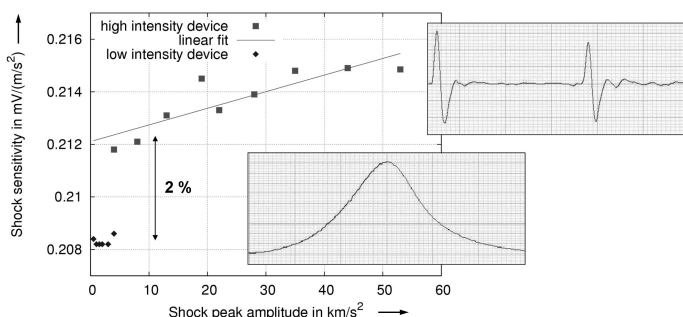


Figure 3. Comparison of shock calibration results and shock signals: HI device (upper plot, dipole pulse and its first reflection), LI device (lower plot, Gaussian pulse of 2 ms), time scale is 0.5 ms/division for both plots.

Experiences prove that both facilities obviously give different calibration results [3]. Whereas the transducer's sensitivity for LI shock agrees well with that from sine calibrations at the reference frequency of 160 Hz, the HI shock value deviates for about 2 % for the example given in figure 3. Model calculations provide evidence that the deviation is caused by the different spectral content of the LI and HI shock pulses. These deviations increase with shorter pulse duration, i.e. higher frequency content, as the transducer's axial resonance becomes more and more excited.

## 2.2. Dynamic Force Calibration

After establishing linear and angular acceleration devices for primary calibrations with sinusoidal and shock excitation, the development moved on to dynamic force [5, 6]. For some years now, PTB maintains sinusoidal and shock force calibration facilities on a research and development level. Here, primary and secondary methods are currently investigated. However, the state of a regular service to customers is still some steps away. For primary calibrations, traceability of dynamic force is achieved according to Newton's law which defines force as the product of mass and acceleration. The measurement of dynamic forces is consequently based on acceleration measurements achieved by laser-Doppler interferometry.

As an example, a primary calibration device for sine force calibrations of up to 10 kN amplitude and 2 kHz excitation frequency is shown in figure 4. An electrodynamic vibration exciter generates a sinusoidal motion of its air-borne armature carrying the force transducer under test with a selectable seismic mass on top. The dynamic input of the force transducer is the inertia force of the accelerated seismic mass.

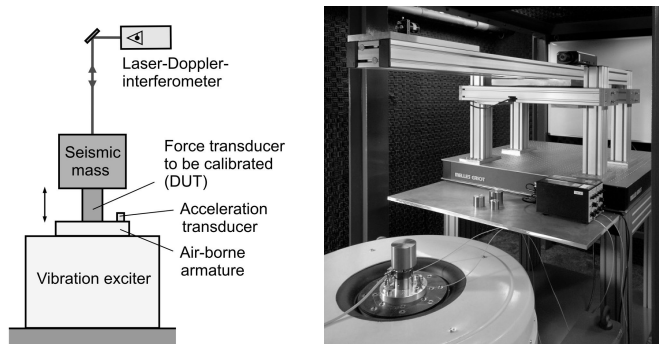


Figure 4: 10 kN periodic force calibration device

Two facilities for the primary calibration of shock forces have been developed in recent time. The first technical realization is a device for shock forces up to 20 kN peak amplitude, a second one for forces up to 250 kN is under construction. In each device, shock forces are generated by the collision of two air-borne mass bodies with the DUT placed in between and LDIs measure the course of motion of both masses. Figure 5 depicts the working principle of the bigger machine. A hydraulic drive accelerates the impacting mass of about 100 kg which then collides with the force transducer fixed at the reacting mass which is initially at rest.

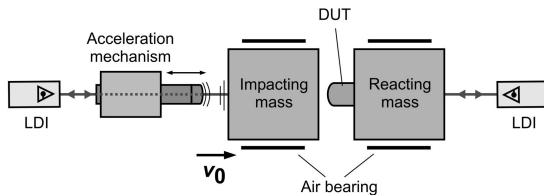


Figure 5. Principle of the 250 kN impact force calibration device

### 2.3. Dynamic Pressure Calibration

For the calibration of dynamic pressure [7], as required for example in various fields of ballistics, explosion protection and car engineering, two new facilities using step and impulse response procedures are already providing regular service on a secondary level at PTB [8]. This means, traceability is derived from statically calibrated reference transducers. Therefore, the pitfalls of dynamic effects, although certainly present, may not have been clearly visible in the daily work.

A calibration device for quasi-static pressure up to 450 MPa uses a high speed double valve to generate pressure steps of durations of some seconds. Dynamic effects show up here in deviations from the dynamic synchronization between reference transducer and DUT.

For calibrations of short pressure pulses, the laborious procedure of a gun barrel firing of prepared ammunition could be replaced by a ball drop device (see figure 6) which generates half-sine pulses of up to 800 MPa amplitude, similar duration (3 ms), but much better reproducibility. Here, a steel ball of 7 kg is dropped from an adjustable height and impacts onto a punch protruding into a pressure chamber filled with hydraulic liquid.

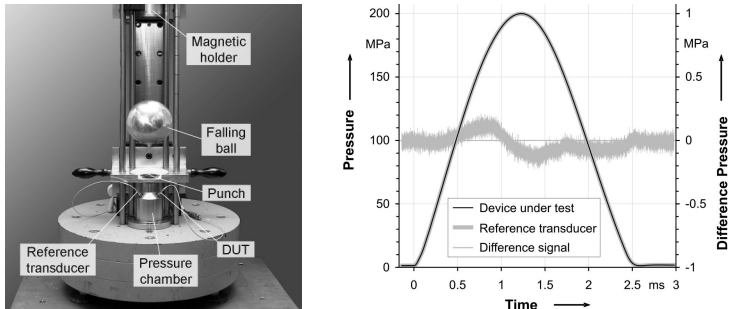


Figure 6. Ball drop device for the secondary calibration with pressure pulses and typical signals

### 3. Model-based Characterization of Transducers

A focal point of recent research is the characterization of the transducer's dynamic behavior in order to provide the user with the basis to estimate the measurement properties in an intended dynamic application. The set of dynamic parameters to be determined and to be specified in the transducer's datasheet or calibration certificate should be suitable for all measurement principles, mechanical designs as well as calibration methods applied. As a general objective, results from different calibration devices using differing excitation signals should become transferable. In addition to the static sensitivity or its low frequency value, respectively, some data with dynamic relevance like the fundamental resonance frequency, mass and stiffness values is occasionally given today. But to be more general, an approach of a model-based dynamic characterization is proposed [10 – 13] that shall describe the dynamic measurement performance of the transducer in a given application. In order to identify the sought model parameters from performed calibration measurements, an identification process has to vary the model parameters until the data sets measured by the transducer and predicted by the model are in the best possible agreement.

Investigations of the dynamic calibration of acceleration transducers and force transducers have shown that the dynamic behavior of these transducers is well described by a model of spring-coupled mass bodies, where the coupling to the mechanical environments is taken into account by adequately chosen boundary conditions. Mathematically, such a model can be expressed by a system of second order ordinary differential equations. Taking the example of the model of a force transducer (see figure 7), its 2-mass standard model with one degree of freedom consists of two model masses coupled via a visco-elastic spring element (stiffness  $k$ , damping  $d$ ). The force-proportional elongation  $x(t)$  of

the spring represents the model's output signal; input signals are known accelerations or external forces, depending on the considered application. The structural parts of the transducer (head mass  $m_H$ , base mass  $m_B$ ) at both sides of the spring and the coupled mechanical parts have to be adequately allocated into the resulting model masses  $m_{H^*}$  and  $m_{B^*}$ . For the primary sine force calibration (see figure 4), the accelerations  $a_{H^*}(t)$  and  $a_{B^*}(t)$  of both model masses are known input quantities. And in case of the primary shock force calibration according to the principle given in figure 5, known inputs are the inertia forces  $F_1(t)$  and  $F_2(t)$  measured at the impacting mass bodies.

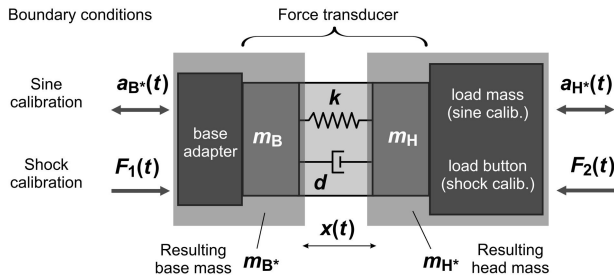


Figure 7. Spring-mass-damper model for the sine and shock force calibration of a force transducer

#### 4. Summary and Outlook

Concentrated efforts in the dynamic calibration of transducers for mechanical quantities have been made in recent years. It became evident that it is necessary to harmonize results from different dynamic calibration methods in order to go for scientifically accepted standards. Results achieved by shock or periodic excitations have to be made comparable. In case of shock, the mere evaluation of pulse peak values gives inconsistent results as the different spectral signal content is not taken into account.

Furthermore, there are still a lot of open questions to be answered. For example, which units should be chosen for the traceability of the dynamic measurands? What could be the procedures for the dissemination of the dynamic units, by transfer standards? And what should be specified in the certificate of the transducer? Another challenge is the specification of the uncertainty of a dynamic calibration. Anyway, adding some aspects regarding modeling and data analysis it will become evident that despite big differences in technical realizations, the mathematical procedures and problems for the dynamic characterization of transducers and for the dissemination of a unit for dynamic measurement are very similar if not even identical. These points will now be

approached by methods of a model-based parameter identification which is currently under development in a joined effort of different working groups at PTB.

## References

1. H.-J. v. Martens, A. Täubner, W. Wabinski, A. Link, H.-J. Schlaak: Laser interferometry - tool and object in vibration and shock calibrations, Proc. of SPIE Vol. 3411 (1998), 195-206.
2. ISO 16063 series: Methods for the calibration of vibration and shock transducer, International Organization for Standardization, Geneva.
3. A. Link, A. Täubner, W. Wabinski, T. Bruns, C. Elster: Calibration of accelerometers: determination of amplitude and phase response upon shock excitation, Meas. Sci. Technol., 17 (2006), 1888-1894.
4. A. Täubner, A. v. Martens, H.-J.: Measurement of angular acceleration, angular velocities and rotation angles by grating interferometry, Measurement, 24 (1998), 21-32.
5. R. Kumme: Investigation of the comparison method for the dynamic calibration of force transducers, Measurement, 23 (1998), 239-245.
6. M. Kobusch, Th. Bruns, L. Stenner, S.-P. Schotte: Impulse force investigations of strain gauge sensors, Proceedings of IMEKO TC3 19th International Conference, 2005, Cairo, Egypt.
7. J. Hjelmgren: Dynamic measurement of pressure – a literature survey, SP Report 2002:34, [www.sp.se/](http://www.sp.se/).
8. E. Franke, F. Jäger: Neue dynamische Mess- und Kalibrierverfahren für Druckimpulse bis 800 MPa (8000 bar), in: Sensoren und Messsysteme 2004, VDI Berichte Nr. 1829, 2004, S. 163-170.
9. Th. Bruns, M. Kobusch: Traceability of dynamic force and torque calibrations by means of laser-Doppler-interferometry, Proc. of SPIE Vol. 5503 (2004), 602-607.
10. Th. Bruns, A. Link, C. Elster: Current developments in the field of shock calibration, Proc. of XVIII IMEKO World Congress, 2006, Rio de Janeiro, Brazil.
11. M. Kobusch, A. Link, A. Buss, Th. Bruns: Comparison of shock and sine force calibration methods, Proc. of IMEKO TC3 & TC16 & TC22 International Conference, 2007, Merida, Mexico.
12. A. Link, A. Täubner, W. Wabinski, T. Bruns, C. Elster: Modelling accelerometers for transient signals using calibration measurements upon sinusoidal excitation, Measurement, 40 (2007), 928-935.
13. C. Elster, A. Link, T. Bruns: Analysis of dynamic measurements and determination of time-dependent measurement uncertainty using a second order model, Meas. Sci. Technol. 18 (2007), 3682-3687.

## DERIVATION OF AN OUTPUT PDF FROM BAYES' THEOREM AND THE PRINCIPLE OF MAXIMUM ENTROPY

I. LIRA

*Department of Mechanical and Metallurgical Engineering  
Pontificia Universidad Católica de Chile  
Vicuña Mackenna 4860, Santiago, Chile  
E-mail: ilira@ing.puc.cl*

C. ELSTER AND W. WÖGER

*Physikalisch-Technische Bundesanstalt (PTB)  
Abbestrasse 2-12, 10587 Berlin, Germany  
E-mail: clemens.elster@ptb.de*

M. COX

*Mathematics and Scientific Computing, National Physical Laboratory (NPL)  
Teddington, Middlesex, TW11 0LW, UK  
E-mail: maurice.cox@npl.co.uk*

In the recently issued Supplement 1 to the GUM a Monte Carlo method is proposed for the evaluation of measurement uncertainty. The method is based on Bayes' theorem and the principle of maximum entropy (PME). These two tools are used to assign probability density functions (PDFs) to the input quantities entering a measurement model, which are then combined using the rules of probability calculus to find the PDF associated with the output quantity. The expectation of the latter PDF will usually be taken as the best estimate of the output quantity, and the square root of its variance will be taken as the associated standard uncertainty. Furthermore, coverage intervals having specified probabilities of containing the value of the output quantity can be calculated. The method is general, in the sense that it is not restricted to linear models. In this paper, some details on the application of Bayes' theorem and of the PME in assigning PDFs to the input and output quantities are reviewed.

### 1. Introduction

The uncertainty framework proposed in the Guide to the Expression of Uncertainty in Measurement<sup>1</sup> (GUM), while useful in many practical situ-

ations, is limited to linear or linearized measurement models to which the Central Limit Theorem can be applied. Furthermore, to a certain extent the GUM framework is inconsistent, because it mixes frequency-based statistical techniques with Bayesian-type analysis. (In the former measurement data are used to evaluate the unknown parameters of sampling distributions. In the latter, information about all quantities involved in a measurement task, together with the measurement model, are used to encode the state of knowledge or degree of belief about any or all of these quantities in the form of probability density functions —PDFs— with known parameters.)

Supplement 1 to the GUM<sup>2</sup> (S1-GUM), recently issued by the Joint Committee for Guides in Metrology (JCGM), is free from these drawbacks. It proposes a Monte Carlo method that consists of generating a random sample of the input quantities by drawing values from the corresponding PDFs. The measurement model is then used to obtain a value for the output quantity that can be considered as drawn from the output PDF. Therefore, by repeating this process a large number of times, the output PDF is generated numerically.

In a previous paper,<sup>3</sup> the relation between S1-GUM and Bayesian analysis was succinctly outlined. In the present paper we provide further clarifications on this relation. We focus on the derivation of the input and output PDFs from Bayes' theorem and the principle of maximum entropy. The possibility of previous information about the measurand being available is included in the analysis.

## 2. The Output PDF

In both the GUM and the S1-GUM the measurement model is written as

$$Y = f(\mathbf{X}), \quad (1)$$

where  $Y$  is the output quantity, or measurand, and  $\mathbf{X}$  is the set of  $N$  input quantities  $X_1, \dots, X_N$ . A subset  $\mathbf{Z}$  of the input quantities may be measured in the course of the evaluation process, generating measurement data  $D_{\mathbf{Z}}$ . Additional information  $I_{Y, \mathbf{X}, \mathbf{P}}$  about some or all quantities (including the measurand) and about a set  $\mathbf{P}$  of  $M$  (nuisance) parameters  $P_1, \dots, P_M$  may be previously available through other means. (An example of one of these parameters is given in section 3.)

The goal of the analysis is to encode the state of knowledge about the output quantity in the form of a PDF  $g_Y(\eta | D_{\mathbf{Z}}, I_{Y, \mathbf{X}, \mathbf{P}})$ , where  $\eta$  is a variable that represents the possible values of the measurand, by taking into

account the measurement model, the data  $D_Z$  and the information  $I_{Y,X,P}$ . To this end the analysis starts from the PDF  $g_{Y,X}(\eta, \xi | D_Z, I_{Y,X,P})$  encoding the state of knowledge about all quantities in equation (1), where  $\xi$  is the set of variables representing the possible values of the input quantities. From the product rule of probabilities, this PDF may be decomposed as

$$g_{Y,X}(\eta, \xi | D_Z, I_{Y,X,P}) = g_X(\xi | D_Z, I_{X,P}) g_{Y|X}(\eta | I_Y, \xi), \quad (2)$$

where  $g_X(\xi | D_Z, I_{X,P})$  is the PDF for the input quantities given the data  $D_Z$  and given also the pre-existing information  $I_{X,P}$  about these quantities and about the parameters  $P$ , and  $g_{Y|X}(\eta | I_Y, \xi)$  is the PDF for the output quantity conditional on the values  $\xi$  and given the pre-existing information  $I_Y$  about the measurand.

The output PDF can now be obtained by marginalization, that is, by integrating the right-hand side of (2) over all input quantities:

$$g_Y(\eta | D_Z, I_{Y,X,P}) = \int_{-\infty}^{\infty} \cdots \int_{-\infty}^{\infty} g_X(\xi | D_Z, I_{X,P}) g_{Y|X}(\eta | I_Y, \xi) \prod_{i=1}^N d\xi_i. \quad (3)$$

The expectation  $E(Y)$  of this PDF will usually be taken as the best estimate  $y$  of the measurand, and the square root of its variance  $V(Y)$  will be taken as the associated standard uncertainty  $u(y)$ . An expanded uncertainty can be defined as the half-length of an interval that encompasses a given large fraction of the unit area under the PDF  $g_Y(\eta | D_Z, I_{Y,X,P})$ . However, this definition is useful only if the latter PDF is symmetric and unimodal, and if the interval is centred on the expectation. A more general concept is that of coverage interval, defined as above but with arbitrary left or right bounds.

If desired, the state of knowledge about any one of the input quantities, say  $X_j$ , may similarly be updated:

$$g_{X_j}(\xi_j | D_Z, I_{Y,X,P}) = \int_{-\infty}^{\infty} \cdots \int_{-\infty}^{\infty} g_X(\xi | D_Z, I_{X,P}) g_{Y|X}(\eta | I_Y, \xi) d\eta \prod_{i \neq j}^N d\xi_i \quad (4)$$

### 3. Bayes' Theorem

The integrands in equations (3) and (4) may be obtained through the application of Bayes' theorem.<sup>4</sup> For the PDF  $g_X(\xi | D_Z, I_{X,P})$ , the theorem

gives

$$g_{\mathbf{X}}(\boldsymbol{\xi}|D_{\mathbf{Z}}, I_{\mathbf{X}, \mathbf{P}}) \propto \int_{-\infty}^{\infty} \dots \int_{-\infty}^{\infty} l(\boldsymbol{\zeta}, \boldsymbol{\pi}|D_{\mathbf{Z}}) g_{\mathbf{X}, \mathbf{P}}(\boldsymbol{\xi}, \boldsymbol{\pi}|I_{\mathbf{X}, \mathbf{P}}) \prod_{i=1}^M d\pi_i, \quad (5)$$

where  $\boldsymbol{\zeta}$  and  $\boldsymbol{\pi}$  are the possible values of  $\mathbf{Z}$  and  $\mathbf{P}$ , respectively, and the normalizing constant is such that  $g_{\mathbf{X}}(\boldsymbol{\xi}|D_{\mathbf{Z}}, I_{\mathbf{X}, \mathbf{P}})$  integrates to one. In this equation,  $l(\boldsymbol{\zeta}, \boldsymbol{\pi}|D_{\mathbf{Z}})$  is the likelihood function conditional on the data  $D_{\mathbf{Z}}$  about the quantities  $\mathbf{Z}$ , and  $g_{\mathbf{X}, \mathbf{P}}(\boldsymbol{\xi}, \boldsymbol{\pi}|I_{\mathbf{X}, \mathbf{P}})$  is the PDF that expresses the state of knowledge about all input quantities and about all parameters  $\mathbf{P}$ , excluding the data. Note that since  $\mathbf{Z}$  is a subset of  $\mathbf{X}$ , then  $\boldsymbol{\zeta}$  is a subset of  $\boldsymbol{\xi}$ .

Typically, the quantities  $\mathbf{Z}$  will be independent from each other. Data  $D_Z$  about any one of them, say  $Z$ , may consist of a series of  $n_Z \geq 2$  measurement values  $z_1, \dots, z_{n_Z}$ . Usually, these values are assumed to be drawn independently from a Gaussian sampling (frequency) distribution with unknown expectation  $Z$  and unknown variance  $V$  with possible values  $\nu$ , so the likelihood function is

$$l(\zeta, \nu|z_1, \dots, z_{n_Z}) \propto \prod_{i=1}^{n_Z} \frac{1}{\nu^{1/2}} \exp\left(-\frac{(\zeta - z_i)^2}{2\nu}\right), \quad (6)$$

where the variance has been taken as one of the nuisance parameters  $\mathbf{P}$ . If there is no pre-existing information  $I_{Z,V}$ , a non-informative PDF  $g_{Z,V}(\zeta, \nu) \propto 1/\nu$  ( $-\infty < \zeta < \infty, 0 < \nu < \infty$ ) leads to the marginal PDF  $g_Z(\zeta|D_Z)$  that includes the data being a scaled and shifted  $t$ -distribution with  $n_Z - 1$  degrees of freedom. (For the variance to exist in this case, it is required that  $n_Z$  be at least 4). PDFs that include the data  $z_1, \dots, z_{n_Z}$  obtained under other assumptions have also been derived.<sup>4</sup>

The PDF  $g_{Y|\mathbf{X}}(\eta|I_Y, \boldsymbol{\xi})$  in equation (2) can also be obtained using Bayes' theorem. In effect, since in this context the values  $\boldsymbol{\xi}$  of the input quantities are given, they are to be considered as "data". We then have

$$g_{Y|\mathbf{X}}(\eta|I_Y, \boldsymbol{\xi}) \propto l(\eta|\boldsymbol{\xi}) g_Y(\eta|I_Y). \quad (7)$$

The likelihood  $l(\eta|\boldsymbol{\xi})$  cannot in this case be derived from a sampling distribution. The reason is that given the model (1), if the input quantities take on the values  $\boldsymbol{\xi}$  the output quantity can only be equal to  $\eta = f(\boldsymbol{\xi})$ . Thus,  $l(\eta|\boldsymbol{\xi}) = \delta(\eta - f(\boldsymbol{\xi}))$ , where  $\delta(\cdot)$  denotes the Dirac delta function. Thus<sup>5</sup>

$$g_{Y|\mathbf{X}}(\eta|I_Y, \boldsymbol{\xi}) = \delta(\eta - f(\boldsymbol{\xi})) g_Y(\eta|I_Y). \quad (8)$$

If no information about the measurand is previously available, other than it must comply with the measurement model, then  $g_Y(\eta) \propto 1$  and  $g_{Y|X}(\eta|\xi) = \delta(\eta - f(\xi))$ , which is the case considered in S1-GUM.

(More generally, if the measurement model is implicit, of the form,  $h(Y, X) = 0$ , the delta function in the above expressions should be changed to  $\delta(h(\eta, \xi))$ .)

#### 4. The Principle of Maximum Entropy

The principle of maximum entropy (PME)<sup>6</sup> is used in Bayesian analysis to construct PDFs based on information that cannot be interpreted as measurement data about the quantities involved. This is the case of the PDFs  $g_Y(\eta|I_Y)$  and  $g_X(\xi|I_{X,P})$ . For example, if the possible values  $\eta$  of the measurand are known to lie on the given interval  $(a, b)$ , the PME leads to the PDF  $g_Y(\eta|a, b) = 1/(b - a)$  for  $a < \eta < b$  and zero otherwise, that is, a uniform distribution over the given interval.

The S1-GUM provides guidance about using other maximum entropy PDFs. The case for which the information about an input quantity  $X$  consists of an estimate  $x$  and associated standard uncertainty  $u(x)$  is worth clarifying. It is well known that in this case the maximum entropy PDF  $g_X(\xi|x, u(x))$  is a Gaussian distribution with expectation  $x$  and variance  $u^2(x)$ . However, some authors<sup>7</sup> interpret this distribution as the likelihood function conditional on the datum  $x$  assumed to be drawn from a Gaussian distribution with unknown expectation  $X$  and given variance  $u^2(x)$ . Bayes' theorem with a non-informative PDF  $g_X(\xi) \propto 1$  then leads to the same result for the PDF  $g_X(\xi|x, u(x))$ , albeit through a different reasoning.

It should finally be noted that Bayes' theorem is not essential for the analysis above to be considered "Bayesian". For example, consider a situation in which there are no data and no previous knowledge about the measurand. The output PDF  $g_Y(\eta|I_X)$  will then be evaluated starting with a PDF  $g_X(\xi|I_X)$  obtained from previous evaluations or otherwise derived from the PME.

#### 5. Conclusion

Equations (3) and (4) are the basic equations of this paper. Equation (3) (with  $g_{Y|X}(\eta|\xi) = \delta(\eta - f(\xi))$ ) is also the starting point of S1-GUM. The Monte Carlo method proposed in that document is merely a numerical way of computing the output PDF  $g_Y(\eta|D_Z, I_{Y,X,P})$  (and also the PDFs  $g_{X_j}(\xi_j|D_Z, I_{Y,X,P})$ ) once the PDFs  $g_X(\xi|D_Z, I_{X,P})$  and  $g_{Y|X}(\eta|I_Y, \xi)$

have been obtained. We hope that in this paper the role played by Bayes' theorem and the principle of maximum entropy in finding the latter two PDFs has been clarified.

### Acknowledgments

The support of Fondecyt (Chile) research grant 1060752 is gratefully acknowledged.

### References

1. BIPM, IEC, IFCC, ISO, IUPAC, IUPAP and OIML, *Guide to the expression of uncertainty in measurement* (International Organization for Standardization, Geneva, Switzerland, corrected and reprinted 1995).
2. BIPM, IEC, IFCC, ILAC, ISO, IUPAC, IUPAP and OIML, *Evaluation of measurement data — Supplement 1 to the “Guide to the expression of uncertainty in measurement” — Propagation of distributions using a Monte Carlo method*. Joint Committee for Guides in Metrology, JCGM 101, to appear.
3. C. Elster, W. Wöger and M. G. Cox, *Metrologia* **44**, L31 (2007).
4. I. Lira and W. Wöger, *Metrologia* **43**, S249 (2006).
5. C. Elster, *Metrologia* **44**, 111 (2007).
6. W. Wöger, *IEEE Trans. Instr. Measurement* **IM-36**, 655 (1987).
7. D. S. Sivia, *Data Analysis. A Bayesian Tutorial* (Oxford Science Publications, Great Clarendon Street, Oxford OX2 6DP, 2006).

## EVALUATION OF UNCERTAINTIES ON DATUM-SYSTEM REFERENCE

JEAN MAILHE

*Laboratory EA(MS)<sup>2</sup>, Université Aix-Marseille, Avenue Gaston Berger 13625 Aix en Provence, France*

JEAN-MARC LINARES, JEAN-MICHEL SPRAUEL

*Laboratory ISM, UMR6233, Université Aix-Marseille, Avenue Gaston Berger 13625 Aix en Provence, France*

International standards provide, with the Geometrical Product Specification (GPS), tools for geometric specification and verification of mechanical parts based on tolerance zones (TZ). A TZ represents a domain space in which the real surface must be included. This space domain defines the set of geometries which are functionally equivalent. In a part design, numerous TZ are constraints related to a reference system. This last one is an ideal geometry, called datum, associated to real surfaces, called datum feature. A datum can be simple, if it is related to one datum feature, or forming a datum-system reference if it is related to two or three real surfaces. In this case, there is a hierarchy in the fitting process between the datum-system and the set of datum features. Hence, a primary, secondary and a tertiary datum should be considered. It is now commonly admitted that measurements are tainted with uncertainties. These uncertainties on datum feature estimations are propagated to the datum-system reference and then propagated to all TZ positions. Thus, considering the level arm effect between the datum and the TZ, uncertainties on TZ positions can become quickly of the same order of magnitude as the maximal admissible defect specified on product geometry. This paper presents a method permitting to estimate uncertainties on a datum-system reference.

### 1. Introduction

To guarantee the well working of a mechanical part, the measurement of its surfaces is a compulsory task. International standards provide, with the Geometrical Product Specification (GPS), tools for geometric specification and verification of mechanical parts based on tolerance zones (TZ). A TZ represents a domain space in which the real surface must be included. This space domain defines the set of geometries which are functionally equivalent. In a part design, numerous TZ are constraints related to one or more reference systems. These last are ideal geometries, called datum, (plane, straight-line, point ...) associated to real surfaces, called datum feature. A datum can be simple, if it is related to

one datum feature, or forming a datum-system reference if it is related to two or three real surfaces. In the case of a datum-system reference, there is a hierarchy in the fitting process between the datum-system and the set of datum features. Hence, a primary, secondary and a tertiary datum should be considered in this paper. In this case, the secondary datum is depending on primary datum and the tertiary datum is depending on both primary and secondary datum. It is now commonly admitted that measurements are subject to uncertainties. These uncertainties associated with measurement of datum features are propagated to the datum-system reference. Finally, these calculated uncertainties are propagated to all TZ positions. Thus, due to leverage effect between the datum and the TZ, uncertainties associated with TZ position can become quickly of the same order as the maximal admissible defect of product geometry.

## 2. General Principle

With a mathematical point of view, the estimation of a datum reference is done by a fitting between a coordinate system  $(C, \mathbf{e}_1, \mathbf{e}_2, \mathbf{e}_3)$ , modeling the datum-system reference, and one to three independent estimations of real surfaces (figure 1), called datum features.

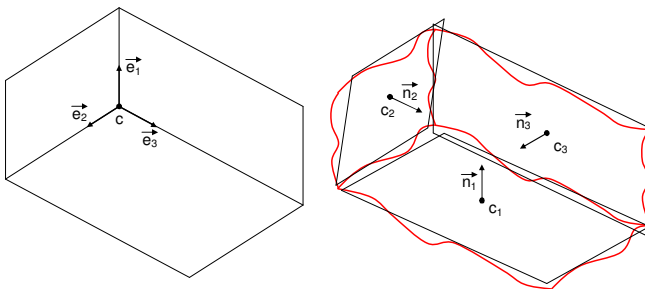


Figure 1. Datum feature estimation problem

The proposed method is made of three steps:

- The first one is the modeling of the datum features, which is done by random vectors  $(C_i, \mathbf{n}_i)$ . Their mean position and orientation, and their covariance matrix will be estimated from sets of measured points.
- In the second step, the association between datum features and the datum-system reference is expressed under a form of a linear equation system. A function  $f$  (1) providing the reference geometrical parameters, depending on datum features parameters, must be written.

$$\begin{aligned} f : \Re^{6 \times 3} &\mapsto \Re^{12} \\ C, e_1, e_2, e_3 &= f(C_1, n_1, C_2, n_2, C_3, n_3) \end{aligned} \quad (1)$$

- In the third step, the datum feature uncertainties will be propagated, through function  $f$ , to the datum-system reference.

## 2.1. Datum Feature Modeling

Currently, a Coordinate Measuring Machine (CMM) performs a discrete sampling of a real surface. Measurement data is a set of points describing a real surface. Then, this set of points is best fitted to the surface model, a plane in our case. This operation permits the estimation of the feature, but presents three sources of uncertainties: the surface model [1], the sampling strategy [2] and classical measurement uncertainties. The model chosen, to represent mean values and variances of the datum feature estimation, is the random vector. Each coordinate of the random vector is a stochastic variable representing a geometric parameter of the fitted surface model. In our case, the plane is represented by a point and a vector  $(C_i, n_i)$  (2), described by six coordinates [3]:

$$\mathbf{P} = \begin{bmatrix} C_x & C_y & C_z & n_x & n_y & n_z \end{bmatrix}^T \quad (2)$$

The best fitting is done by the maximization of the likelihood function applied to a Gaussian distribution [4][5]. As the point/vector model is not minimal, the best fitting is performed on three free parameters and then propagated to the random vector  $\mathbf{P}$ .

$$\varphi = \left( \frac{1}{\sigma \sqrt{2\pi}} \right)^n e^{-\frac{1}{2} \sum_{i=1}^n \left( \frac{d_i}{\sigma} \right)^2} \Rightarrow \sum_{i=1}^n d_i \frac{\partial d_i}{\partial P_i} = 0 \quad (3)$$

The variance of association residues are next propagated to the geometric parameters. This propagation permits calculating the covariance matrix of the random vector.

$$\text{cov}(P_k, P_l) = \sum_{i=1}^N \left( \frac{\partial P_k}{\partial d_i} \right) \left( \frac{\partial P_l}{\partial d_i} \right) \text{var}(d_i) \Rightarrow \mathbf{cov}(\mathbf{P}) = \mathbf{J} \cdot \text{var}(\mathbf{d}_i) \cdot \mathbf{J}^T \quad (4)$$

## 2.2. Datum-System Reference Modeling

The datum-system reference is made of three orthogonal planes depending on three datum features (real surfaces). The primary face of the datum-system

reference must be tangent to the material and minimizing the maximal gap to the first datum feature (real surface). The secondary face of the datum-system reference must be tangent to the mater and minimizing the maximal gap to the second datum feature (real surface) while being perpendicular to the primary face of the datum-system reference. The tertiary face of the datum-system reference must be tangent to the third datum feature and perpendicular to both primary and secondary datum. This association results in eight possible contact configurations depending on the orientation between each datum feature. It is possible to detect the actual configuration by testing the sign of the scalar product of each normal vector of the planes fitted to the datum features. Three Heaviside functions are included to obtain a unique linear equation system including the whole configurations. Then, to obtain the Jacobian operator permitting uncertainty propagation, the total derivative of the linear system is written under a matrix form.

### 2.2.1. Calculation of Datum-System Reference Basis

The calculation of the mean orientation of the datum-system reference does not depend on the contact configuration. Hence, the expression of the vectors characterizing this coordinate system is simplified. In the case of three datum features, the following vectors are obtained. The first datum feature totally constrains the first vector of the basis by an equality relation:

$$\mathbf{e}_I = \mathbf{n}_I \Leftrightarrow \begin{cases} e_{Ix} & n_{Ix} \\ e_{Iy} & n_{Iy} \\ e_{Iz} & n_{Iz} \end{cases} \quad (5)$$

The second vector of the basis is obtained by projection of the orientation vector of the second datum feature on the plane orthogonal to previous vector:

$$\mathbf{e}_2 = \frac{P_{\mathbf{n}_I}(\mathbf{n}_2)}{\|P_{\mathbf{n}_I}(\mathbf{n}_2)\|} = \frac{\mathbf{n}_2 - \mathbf{n}_I \cdot (\mathbf{n}_I \cdot \mathbf{n}_2)}{\|\mathbf{n}_2 - \mathbf{n}_I \cdot (\mathbf{n}_I \cdot \mathbf{n}_2)\|} \quad (6)$$

Finally, the third vector is calculated to form an orthonormal basis:

$$\mathbf{e}_3 = \mathbf{e}_1 \wedge \mathbf{e}_2 \quad (7)$$

To facilitate the calculation of the Jacobian operator, this vector can be obtained, directly, from the random vectors of the first and second datum features:

$$\mathbf{e}_3 = \frac{\mathbf{n}_1 \wedge \mathbf{n}_2}{\|\mathbf{n}_1 \wedge \mathbf{n}_2\|} \quad (8)$$

### 2.2.2. Datum-System Reference Origin Calculation

The expression of the mean localization issue comes from the management of the different contact configurations. As shown in figure 2, they are eight possible contact configurations.

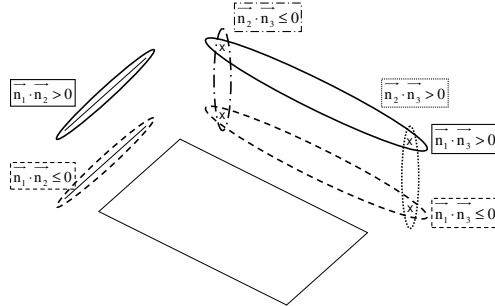


Figure 2. Contact configurations

The contact configuration can be found by the sign of the scalar product of all combinations of the normal vectors. Whatever the configuration, finding the origin of the coordinate system is done by calculating the intersection of three planes. This calculation leads to a linear problem. Of course, the definition of these planes depends on the contact configuration. Hence, is it possible to write a unique linear system by using the Heaviside function, which permits the modeling of limit between two contact configurations. In the case of three datum features, the following semi-linear system is obtained:

$$\begin{cases} OC \cdot \vec{n}_1 = OC \cdot \vec{n}_1 \\ OC \cdot \vec{n}_2 = OC_2 \cdot \vec{n}_2 - H_t(-\vec{n}_1 \cdot \vec{n}_2) \cdot h_t \cdot \vec{n}_1 \cdot \vec{n}_2 \\ OC \cdot \vec{n}_3 = OC_3 \cdot \vec{n}_3 - H_t(-\vec{n}_1 \cdot \vec{n}_3) \cdot h_t \cdot \vec{n}_1 \cdot \vec{n}_3 - H_t(-\vec{n}_2 \cdot \vec{n}_3) \cdot h_2 \cdot \vec{n}_2 \cdot \vec{n}_3 \end{cases} \quad (9)$$

where  $H_t(x)$  represents the Heaviside function.

### 2.3. Uncertainties Propagation from Datum Features to Datum-System Reference

The final point is to express the covariance matrix of the geometrical parameters of the datum-system reference. The estimation is done by linear propagation of the datum features covariance matrix to actual coordinate system. The propagation is done by the classical formula:

$$Cov(C, e_1, e_2, e_3) = J \cdot Cov(C_1, \vec{n}_1, C_2, \vec{n}_2, C_3, \vec{n}_3) \cdot J^T \quad (10)$$

The Jacobian operator can be separated into two blocks, one for the origin and one for the basis.

It has however to be accounted for the fact that the basis is built to be orthonormal. This introduces covariance terms between the different components.

The Jacobian matrix of origin construction is finally obtained by following expression:

$$X \cdot J_{oc}^T = Ga \Leftrightarrow J_{oc} = X^{-1} \cdot Ga \quad (11)$$

where:  $Ga$  is the matrix representing the total derivative of linear system (9).

### 3. Conclusion

In the field of Geometrical Product Verification, the impact of datum feature uncertainties is almost always underestimated. Their impact on verification results is often amplified by the distances between the datum-system reference and the specified surfaces.

### References

1. J Mailhe, JM Linares, JM Sprauel, P Bourdet, Geometrical checking by virtual gauge, including measurement uncertainties, *CIRP Annals-Manufacturing Technology* 2008, **57**, 513-516.
2. A. Weckenmann, J. Lorz, S. Beetz, Monitoring coordinates measuring machine by user-defined calibrated parts. In: proceeding of the 9<sup>th</sup> CIRP seminar on computer aided Tolerancing. 2005. CD-Rom.
3. J. Bachmann, J.M. Linares, S. Aranda, J.M. Sprauel, Process measurement impact on the verification uncertainty. *Series on advanced in mathematics for applied sciences* 2004, **66**, 149-158.
4. S. Aranda, J. Mailhé, J.M. Linares, J.M. Sprauel, Contribution to surface best fit enhancement by the integration of the real point distributions. *Series on advanced in mathematics for applied sciences* 2006, **72**, 258-261.
5. J.M. Sprauel, J.M. Linares, J. Bachmann, P. Bourdet, Uncertainties in CMM Measurements, Control of ISO Specifications. *Annals of the CIRP* 2003, **52**, 423-26.

## POSSIBILITY DISTRIBUTION: A USEFUL TOOL FOR REPRESENTING COVERAGE INTERVALS WITH AND WITHOUT THE PROBABILITY DENSITY KNOWLEDGE

GILLES P. MAURIS

*LISTIC, Université de Savoie, Domaine Universitaire  
74 944 Annecy Le Vieux, France*

This paper deals with a fuzzy/possibility representation of measurement uncertainty that often arises in physical domains. The construction of the possibility distribution is based on the stacking up of probability coverage intervals issued from the probability density. When the probability density is unknown but different amounts of information such as symmetry, unimodality, support or standard deviation are available, corresponding possibility distributions dominating probability coverage intervals can be built. They are compared to the coverage intervals obtained by using the maximum entropy principle.

### 1. Introduction

Uncertainty is a key concept for the measurement expression. Indeed, In many application domains, it is important to take the measurement uncertainties into account, especially in order to define around the measurement result, an interval which will contain an important part of the distribution of the measured values, that is, a coverage interval. To build such coverage intervals, the ISO guide recommends to use a coverage factor  $k$ , determined on the basis of measurer's pragmatics if the probability distribution is not known [1]. In a lot of situations, the assumption of Gaussian distribution is quite satisfied (due to the Central Limit Theorem), but it is not always the case. It is why many authors have proposed to use a maximum entropy approach for assigning a probability distribution to a measurable quantity handled as a random variables [2]. The maximum entropy approach is an extension of the Laplace indifference principle which says that: "when there is no reason to do otherwise, assign all outcomes equal probability". The possibility theory [3] offers an alternative approach to this treatment of incomplete knowledge. It proposes a more comprehensive way to express ignorance by considering a family of probability distributions instead of a single one. The main purpose of this paper is to present how we can replace the *ceteris paribus* probability approach by a *ceteris incognitis* possibility approach fully representing the lack of knowledge on the measurement

probability density. As the two approaches both allow to derive coverage intervals, these intervals provide a good way to make comparisons between the probability maximum entropy principle and the possibility maximum specificity principle we propose in this paper.

The paper is organized as follows. In section 2, we recall basics of the possibility theory with a special focus on the links between a possibility distribution and probability coverage intervals. The third section presents possibility models of some common situations of information shortage, and their comparison with a conventional maximum principle entropy approach. Some concluding remarks point out the interest of the approach and some future developments.

## 2. Possibility Representation of Measurement Distribution

### 2.1. Basics of Possibility Theory

A fundamental notion of the possibility theory [3] is the possibility distribution, denoted  $\pi$ , which is in the measurement context an upper semi-continuous mapping from the real line to the unit interval:  $\pi : R \rightarrow [0, 1]$ . Thus  $\pi$  is a fuzzy subset but with specific semantics for the membership function. Indeed, a possibility distribution describes the more or less plausible values of an uncertain variable  $X$ . The possibility distribution is such that  $\sup_{x \in R} \pi(x) = 1$ , and the associated possibility measure, denoted  $\Pi$ , is defined as follows:

$$\forall A \subset R, \Pi(A) = \sup_{x \in A} \pi(x)$$

and  $\Pi$  satisfies a maxitivity property [3]:

$$\forall A, B \subset R, \Pi(A \cup B) = \max(\Pi(A), \Pi(B)) .$$

An important point is that a possibility distribution  $\pi$  defines a probability family  $\mathcal{P}(\pi) = \{P, \forall A, P(A) \leq \Pi(A)\}$  [4]. In the measurement context, this fact can be useful when it is not possible to identify one specific probability density. Finally, a key concept for our purpose is the specificity notion. A possibility distribution  $\pi_1$  is called more specific (i.e. more thinner) than  $\pi_2$  as soon as the possibility inclusion is satisfied, i.e.  $\forall x, \pi_1(x) \leq \pi_2(x)$ . In this latter case,  $\pi_1$  is said more informative than  $\pi_2$ .

### 2.2. Possibility versus Probability

Let us assume that the considered random variable  $X$  corresponding to the measurement  $x$  is continuous on the set of reals and is described by a

probability density  $p, F$  being its corresponding cumulative probability function. A coverage interval of probability level  $\beta$  (denoted  $I_\beta$ ) is defined as an interval for which the probability  $P_{out}$  to be outside this interval  $I_\beta$  does not exceed  $\alpha =_{\text{def}} 1 - \beta$ . We can impose the coverage intervals to be defined around a same point  $x^*$ , generally the mean or the median of measurements. It has been proven in [5] that stacking coverage intervals on top of one another leads to a possibility distribution (denoted  $\pi^*$  having  $x^*$  as modal value). In fact, in this way, the  $\alpha$ -cuts of  $\pi^*$ , i.e.  $A_\alpha = \{x | \pi^*(x) \geq \alpha\}$  are identified with the coverage interval  $I_\beta^*$  of probability level  $\beta = 1 - \alpha$  around the nominal value  $x^*$ . Thus, the possibility distribution  $\pi^*$  encodes the whole set of coverage intervals in its membership function. Moreover, this probability/possibility transformation satisfies:  $\forall A \subset R, \Pi^*(A) \geq P(A)$ , with  $\Pi^*$  and  $P$  the possibility and probability measures associated respectively to  $\pi^*$  and  $p$ . The most specific possibility distribution (i.e. the one corresponding to coverage intervals with minimal length) among those that dominate  $p$  is obtained from the level cuts of the probability density [5] (which are in the multi-modal case constituted of unions of intervals). This most specific possibility associated to  $p$  is called optimum and is denoted  $\pi^{\text{opt}}$ . The expression of  $\pi^{\text{opt}}$  is:

$$\pi^{\text{opt}}(x) = 1 - \int_{p(y) > p(x)} p(y) dy \quad (1)$$

For symmetric unimodal (with mode  $m$ ) probability densities, Eq. (1) becomes:

$$\pi^m(m-t) = \pi^m(m+t) = P(|X-m| \geq t) = 2(1-F(t)) \quad (2)$$

The possibility distribution is thus simply related to the cumulative probability function  $F$ .

### 3. Possibility Distribution of Some Situations of Information Shortage

The key concept of specificity will be used for considering situations when the probability density function of measurement is not known, but some parameters are available, e.g. the support, the mode, the mean, the standard deviation. Knowing one or many of such parameters does not fix the probability density function uniquely. In fact, it defines a family of probability distributions  $\mathcal{P}$  that may be in some common cases be represented by a possibility distribution  $\pi$  those  $\alpha$  cuts contain the  $1-\alpha$  coverage intervals of all the probability distributions of  $\mathcal{P}$ . This is equivalent to find a bound for the probability  $P(|X-m| \geq t)$  when the knowledge of  $p$  is not available. Therefore

the determination of such a maximum specific possibility distribution according to the available information is clearly related to probability inequalities.

### **3.1. Case of Finite Support Probability Distribution**

Let us consider first the case where the only available information is that any possible measurement values is in the interval  $[a, b]$ . Therefore, the corresponding possibility distribution is a rectangular distribution having a possibility value of 1 in  $[a, b]$ . If in addition, it is known that the probability distribution is unimodal with mode  $m$ , then the triangular possibility distribution  $\pi_r^m$  with mode  $m$  (see fig 1) dominates all the probability distributions lying in the considered family. This result has been established in [6] for the case of symmetric probability distributions and in [7] for the case of asymmetric distributions. Clearly this result corresponds to a Bienaymé-Chebyshev-like probabilistic inequality built from the  $\alpha$  cuts of  $\pi_r^m$ . Note that the assumption of bounded support is crucial in getting this piecewise linear representation.

### **3.2. Case of Infinite Support Probability Distribution**

If only the mean  $\mu$  and the standard deviation  $\sigma$  are known, the possibility distribution can be obtained from the Bienaymé-Chebychev inequality [8]:

$$\pi_{BC}(\mu + t) = \pi_{BC}(\mu - t) = \min(1, \frac{\sigma^2}{t^2}) \quad (3)$$

If the probability distribution is unimodal and symmetric, the inequality can be improved by using the Gauss-Winkler inequality [8]. This leads to the following possibility distribution expression:

$$\begin{aligned} \pi_{GW}(\mu + t) &= \pi_{VP}(\mu - t) = 1 - \frac{t}{\sqrt{3}\sigma} && \text{if } t \leq \frac{2}{\sqrt{3}}\sigma \\ \pi_{GW}(\mu + t) &= \pi_{VP}(\mu - t) = \frac{4\sigma^2}{9t^2} && \text{if } t \geq \frac{2}{\sqrt{3}}\sigma \end{aligned} \quad (4)$$

### **3.3. Comparison of the Possibility and Maximum Entropy Approaches**

Let us recall that maximum entropy consists for incomplete knowledge (leading in fact to a family of probability distributions) in selecting a single one in the family having the maximum entropy proposed by Shannon [2]. When only the support is known, the probability density is the uniform density and the

associated possibility distribution is a triangular possibility distribution. Therefore we obtain the same results as the maximum specificity possibility approach as shown in figure 1. If the mode is known, but not equal to the middle of the support, then a asymmetric triangular possibility distribution is obtained. Note that introducing unimodality constraint in the maximum entropy principle can be considered but it is not straightforward [9].

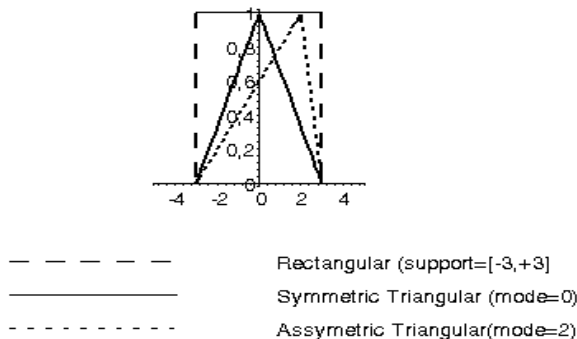


Figure 1. Examples of possibility distribution associated to a finite support probability family

When the mean  $\mu$  and the standard deviation  $\sigma$  are known the maximum entropy density is a Gaussian density [2].

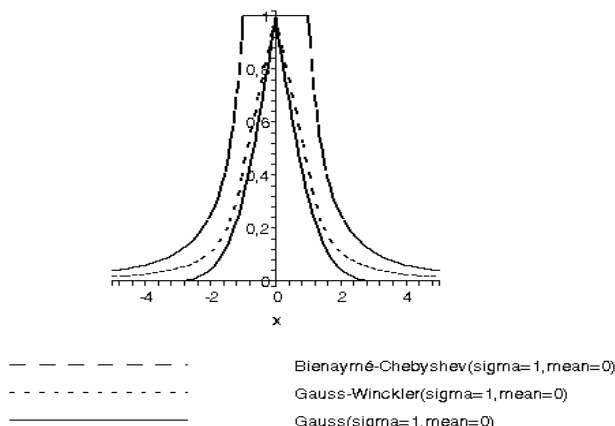


Figure 2. Examples of possibility distribution associated to an infinite support probability family

The figure 2 shows that the coverage intervals obtained from the maximum entropy principle does not include the ones from the possibility approach. In

fact, imposing the maximal entropy consists to add an arbitrary information, i.e. that is not observed. In addition, it can be seen in figure 2 that the more available the information, the more specific is the associated possibility distribution.

#### 4. Conclusion

A possibility distribution can encode all the coverage intervals of a probability density and can also represent a family of probability distributions. Thus the possibility distribution provides an interesting way to represent different amounts of knowledge about measurement distribution, especially for probability densities with a support, a mode, and/or a standard deviation constraint. The coverage intervals results have been compared with those obtained by a maximum entropy principle approach. This allows to highlight the effect of adding knowledge which is either not available or unverified. Further developments will deal with how considering more knowledge (e.g. higher moments) in the possibility representation

The presented results suggest that in measurement problems with incomplete probability density knowledge, the maximum entropy principle can be replaced by a weaker maximum specificity principle for possibility distributions. Of course, the maximum specific possibility distribution in agreement with available information may fail to be unique, and the issue of choosing between in such a case is an intriguing one that constitutes interesting topics of future research.

#### References

1. ISO, *Guide to the Expression of Uncertainty in Measurement* (1993)..
2. W. Woeger, *Meas. Tech.*, **V46**, No 9, 815 (2003).
3. L.A. Zadeh, *Fuzzy Sets and Systems*, **V1**, No 1, 3 (1978).
4. D. Dubois, *Computational Statistics and Data Analysis*, **V54**, No1, 47 (2006).
5. D. Dubois, L. Foulloy, G. Mauris, H. Prade, *Reliable Computing*, **V10**, No 4, 273 (2004).
6. G. Mauris, V. Lasserre, L. Foulloy, *Measurement*, **V29**, No3, 165 (2001).
7. C. Baudrit, D. Dubois, *Computational Statistics and Data Analysis*, **V51**, No 1, 86 (2006).
8. R. Savage, *J. of The Research of the NBS*, **V65**, No3, 211 (1961).
9. P.L. Brockett, A. Charnes, K. Paick, *IEEE Trans. On Information Theory*, **V41**, No3, 824 (1995).

## **IMPLEMENTATION OF SOME MATHEMATICAL APPROXIMATION METHODS OF FUNCTIONS FOR STUDY OF THE FACTORS WHICH INFLUENT THE FERMENT ACTIVITY OF BEER YEAST\***

MARIANA-RODICA MILICI, RODICA ROTAR, LAURENȚIU-DAN MILICI

*Electrical Engineering Department, University of Suceava, University Street no.13  
Suceava, Romania*

The study proposes to find the most efficient way to grow the intracellular trehalose content through beer yeast suspending into trehalose solutions by different concentrations, at different thermo-stating temperatures and in different contact times, taking into account that this technique allows the passive transfer of exogenous trehalose inside the cells both at a new propagated cell population, and at cells resulted from an industrial inoculum.

### **1. The Factors Which Influent the Beer Yeast Fermentation Activity**

The rejoinder life cycle, determined by number of complete divisions of each individual cell is genetic controlled, but influenced by medium conditions. After the cell divided by a certain number, enters into the cell senescence, loosing definitively the multiplication capability and finally dies. The chronological life cycle, defined as maximum outliving time of the cells maintained in the stationary growing stage and characterized by a temporary loosing of multiplication capability due to the nutrients absence, constitutes an important controlling instrument of degeneration at the macromolecular level and of cell death rate.

The study object is to evaluate in which measure the supplementation of yeast inoculum with linoleic acid succeed to minimize the negative effect of the thermal shock stress factor on the one side, and the subduing to repetitive running of fermentation cycles, on the other side.

The study proposes to find the most efficient way to grow the intracellular trehalose content through beer yeast suspending into trehalose solutions by different concentrations, at different thermo-stating temperatures and in different contact times, taking into account that this technique allows the passive transfer

---

\* This work is supported by the SPEEDVIRT project, through contract 137-CEEX II03/02.10.2006

of exogenetic trehalose inside the cells both at a new propagated cell population, and at cells resulted from an industrial inoculum.

Due to the reduced volume, the yeast cell, as all microbial cells, is extremely sensible at the variation of bio-synthesis parameters, especially at the concentration variations of nutritive substratum. The nutrient concentration increasing determines, usually, a stimulation of microbial metabolism, but only till a limit value over that the concentration increasing even remain without effect, or has a negative influence on cellular physiology through substratum inhibition or through the osmotic pressure increasing.

The fermentation conditions are very important for rapid starting and fermentation in good conditions of the unfermented beer:

- chosen propagation method;
- yeast dose chosen at impregnation, correlated with the impregnation temperature and multiplication degree during the fermentation process, correlated with the impregnation dose and fermentation duration;
- aeration and agitation;
- fermentation temperature and pressure;
- chosen fermentation duration and dimension and form of fermentation recipients;
- getting in, purification and cheeping of the yeast.

Temperature is one of the most important physical parameters, deeply involved, through its effects, in the increasing of fermentation capability. The temperature variations have effect over the efficiency of substratum transformation, over the nutritive requests of the yeast and over the fermentation speed.

Repetitive re-impregnations affect the fermentation capability of beer stem because occur changes in cellular wall physiology, is affected the integrity of the membrane mitochondrial functions. Those effects extending is a phenomenon that depends on species and can be strengthened in case of using of yeast at the "high-gravity" unfermented beer fermentation, more and more used technique.

The influence factors with physical-chemical character (osmotic pressure, hydrostatical pressure, hydrodynamic detension force during manipulation, pH, temperature, content of oxygen, ethanol, carbon dioxide), and the nutritional influences (HG unfermented beers, required sources of carbohydrates and nitrogen, the content of inorganic zinc and magnesium ions, of vitamins and phosphorus) have a outstanding influence over the cellular growing and fermentation capability of yeast.

## 2. Comparing of Viability of Cells From Fermented Mediums in Different Conditions, After 24, 72, 120 Hours

Because in the large majority of cases the tests direct to a real function of real variable, the approximation of this characteristic, in the specified cases, consists in the approximation of a real function, approximation named interpolation too. The approximation of the certain real function is made by simple and easy utilized functions, especially through implementation of the computing of the values of this function. Because the real function set is a linear dimensional infinite space, while the function sets in which we look for the approximation are dimensional finite spaces, in actual fact, the abstract problem that stand on the base of approximation techniques consists in replacing of one element from an dimensional infinite space by representatives of one dimensional finite space. To can specify the “approximation” notion and to can appreciate the error made through the above specified replacing, the using of “norm” mathematical concept is needed.

Considering a real linear space  $X$ , we define on it the norm symbolical noted by:  $\| \cdot \| : X \rightarrow \mathbb{R}$ , having the properties (that satisfy the axioms):

- a)  $\|f\| \geq 0, \forall f \in X$
  - b)  $\|f\| = 0 \Rightarrow f = 0$
  - c)  $\|\alpha f\| = |\alpha| \cdot \|f\|, \forall \alpha \in \mathbb{R}, \forall f \in X$
  - d)  $\|f + g\| \leq \|f\| + \|g\|, \forall f, g \in X$
- (1)

If on the linear space  $X$  it was defined the norm  $\| \cdot \|$ ,  $X$  is a normalized linear space. On these terms we could specify the “approximation” of one function from normalized linear space  $X$ , defining what means a best approximation.

Considering the dimensional infinite functions space  $X$ , normalized by  $\| \cdot \|$  and  $X_m$  a linear subspace of  $X$ , dimensional finite with  $\dim(X_m) = m$ , we define the notion of approximation of one function  $f \in X$  by function  $g_m \in X_m$  considering  $\|f - g_m\|$  as a measure of the error that is made if instead of the function  $f$  is used the function  $g_m$ . It is naturally on these terms to say that  $g_m$  is the best approximation of  $f$  if:

$$\left\| f - \overline{g_m} \right\| = \inf_{g_m \in X_m} \left\| f - \overline{g_m} \right\| = \alpha_m \quad (2)$$

The main question which is mooted consists in the fact that from the given definition doesn't result that always is a best approximation, not that this, in case it exists, is unique. A much delicate problem, that requires approximations in its turn, is the effective computing of the best approximation in case it exists.

In many cases, in the function approximation theory is sufficient a hypothesis flimsier than the existence of one norm on the space  $X$  namely is

sufficient the existence of one semi-norm on  $X$  that is a function noted also  $\| \cdot \|$ :  $X \rightarrow \mathbb{R}$ , but satisfying only the axioms a, b and d from (1). The existence and oneness of a best approximation is assured by the next theorems which will be enounced without demonstration.

Generally, when we know data on certain moments of time, we can find a continuous function that approximates the evolution of these data. Now there are known several kinds of approximation functions able to approximate data that have a certain evolution.

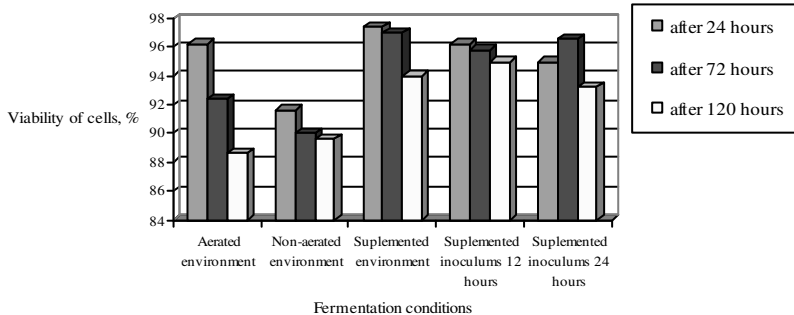


Figure 1. Comparing of viability of cells from fermented environment in different conditions, after 24, 72, 120 hours

As is shown in figure 1, the viability of cells is the lowest in conditions offered by non-aerated medium. In the aerated medium, viability is initial low, but decreases against the end of the fermentation. The greatest number of viable cells was registered in the medium in which was linoleic acid, even under the form of a supplement for medium, or under the form of a supplement for inoculums yeast.

### 3. Conclusions

After the progress recorded by the pasteur's and hansen's researches which obtained, through isolating techniques, the first culture of pure yeast, other ways to optimize the yeast fermentation activity was limited. This fact is due to that the classical techniques to improve biological the yeast stem are heavy, non-specific and not always applicable to the non-spore beer yeast.

The obtained data after comparative study of yeast cells supplemented or not with linoleic acid that fermented in aerated, non-aerated or non-aerated but supplemented with linoleic acid mediums, indicate:

- The yeast contained in the supplemented inoculums demonstrated a growing and led to a fermentation degree comparable with that yeast which fermented the aerated non-fermented yeast.

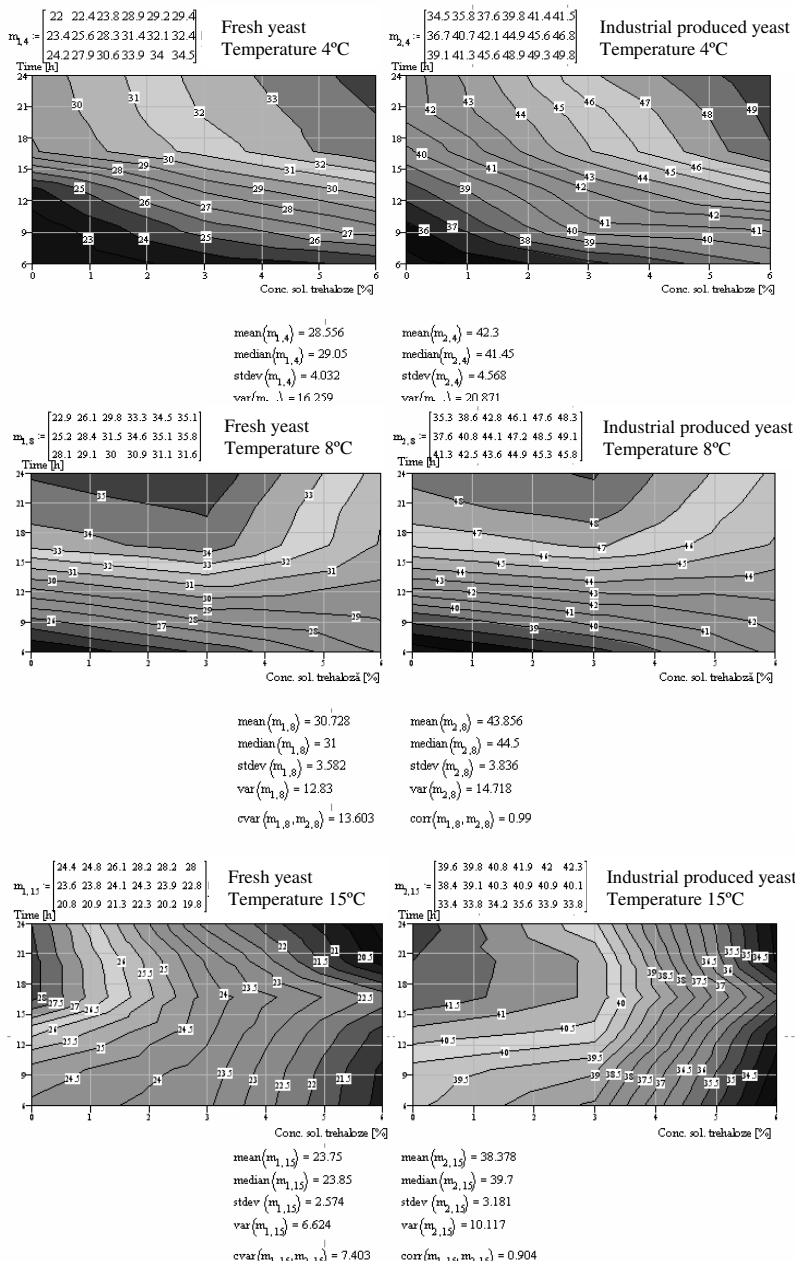


Figure 2. The evolution of intracellular concentration at constant temperature

The cells from supplemented medium and those that belong to inoculums supplemented with linoleic acid with a contact time of 12, respectively 24 hours are characterized by a certain progressive dynamic regarding the fermentation intensity.

- The quantity of generated biomass is greater in the supplemented and in that fermented by cells from inoculums supplemented with linoleic acid.
- The greatest number of viable cells is recorded even in the medium in that was presented the linoleic acid, or in that fermented by cells supplemented with linoleic acid.
- The trehalose intracellular content of the cells supplemented at a contact time of 12 hours, at the initial moment clear-cut superior, decrease drastically in the first 24 hours of fermentation, what indicates the increasing of the cells' capability to synthesize the trehalose, during the time of contact with the linoleic acid, to use as reserve-carbohydrate in lag stage, but the reserve after 120 hours of fermentation in a greater measure than the cells from aerated, non-aerated and supplemented with linoleic acid medium.
- The fermentation degree of the aerated non-fermented beers or of those impregnated with inoculums supplemented with linoleic acid is lower, but the differences are very small.
- The capability to reduce the diacetil, correlated with the beer's vitality, is clear-cut superior at the cells from the inoculums supplemented with acid.

The results indicate that the variant of supplementing the beer inoculums with linoleic acid is an alternative for medium aerating.

## References

1. G. A. Hulse, *Yeast Propagation*, Brewing Yeast Fermentation Performance, Smart, K., (ed.), Blackwell Science, Oxford, pag. 251-256 (2003).
2. A. Lentini, P. Rogers, V. Higgins, I. Dawes and M. Chandler, *The Impact of Ethanol Stress on Yeast Physiology*, Brewing Yeast Fermentation Performance, Smart, K., (ed.), Blackwell Science, Oxford, pag. 25-38 (2003).
3. N. Moonjai, K. J. Verstrepen., F. R. Delvaux, G. Derdelinckx and H. Verachtert, *The effects of linoleic acid supplementation of cropped yeast on its subsequent fermentation performance and acetate ester synthesis*, J. Inst. Brew., 108(2), pag. 227-235 (2002).
4. S. M. van Zandycke, R. Siddique and K. A. Smart, *The role of membrane in predicting yeast quality*, MBAA TQ, vol. 40, no. 3, pag. 169-173 (2003).
5. L. D. Milici and M. R. Milici, *Computing systems using in engineering*, Publishing House of the University of Suceava, 262 pag., ISBN 973-666-100-8 (2004).

# MEASUREMENT UNCERTAINTY CALCULATION USING *MUSE*

## A SOFTWARE PROJECT TO SUPPORT THE MEASUREMENT COMMUNITY WITH A FREELY AVAILABLE IMPLEMENTATION OF GUM SUPPLEMENT 1

MARTIN MÜLLER, MARCO WOLF

*Institute of Computational Science, ETH Zürich 8092 Zürich, Switzerland*

MATTHIAS RÖSSLEIN

*Materials-Biology Interactions, Empa St. Gallen 9014 St. Gallen, Switzerland*

*MUSE* (Measurement Uncertainty Simulation and Evaluation) is a software tool for the calculation of measurement uncertainty based on the Monte Carlo method (MCM) as recommended by the first supplement to the GUM (GS1). It is shown here how a simple example can be implemented in the application language of *MUSE*. An overview of the possible parameters that can be set is given.

### 1. Introduction

Nowadays it's getting more and more important to prove the quality of measurement results, and in particular to demonstrate the fitness for purpose by giving a measure of the confidence that can be placed on the result. This requires to include the degree to which a result would be expected to agree with other results. A worldwide accepted and used measure of this is the measurement uncertainty.

The way to evaluate the measurement uncertainty for any type of a measurement was only developed in the last two decades. In 1993, the International Standardization Organization (ISO) published the *Guide to the Expression of Uncertainty in Measurement* [3] (GUM). As the uncertainty propagation introduced by GUM has different limitations [5], a supplemental guide [2] to GUM (GS1) was published. It recommends the Monte Carlo method (MCM) to propagate the distributions of the input quantities through the equation of the measurement if the model is nonlinear,

or the input quantities cannot be adequately represented by their first two moments. In such cases the uncertainty propagation of GUM can lead to useless results, whereas MCM uses all the available information to calculate the probability density function (PDF) of the output quantity.

The goal of the software project *MUSE* is to support the metrologists with a tool to calculate the measurement uncertainty according to GS1. The software is freely available from the project homepage [1] and implements all aspects of the guideline. In the following we show, how to use the tool and how the different parameters of an uncertainty calculation can be controlled.

*MUSE* uses an XML-based language for the description of measurements. There are two different types of XML files in *MUSE* to specify a measurement. *Basic models* describe on the one hand input quantities whereas the *simulation description* defines how the basic models interact. The specification of the measurement in *MUSE* starts at the same point as GUM with the equation

$$Y = f(X_1, \dots, X_n) \quad (1)$$

of the measurand  $Y$  where the  $X_i$  are the input quantities. In the following we show the possible elements of the hierarchical structure of a model description and a simulation description. To this end, we use a rather simple example to show the different aspects of *MUSE* where the equation of the measurand is given by  $Y = f(X_1, X_2) = \sqrt{X_1^2 + X_2^2}$ . Its input quantities are both described by Gaussian distributions with a mean value of 1 and a standard deviation of 1, i.e.  $X_1 \sim N(1, 1)$  and  $X_2 \sim N(1, 1)$ .

## 2. Basic Models

*MUSE* allows a structured modeling of the measurement formula by using so called *basic models*. The *root element* of a model description file needs to be the XML element `<model name="gauss" targetid="g">` where the attributes `name` and `targetid` must be set. The attribute `name` identifies the model whereas the attribute `targetid` specifies the resulting *influence*, i.e. the return value of the model. The main idea behind basic models is to define all of the input quantities,  $X_i$  in formula (1), in separate files and use these files in the simulation description. An input quantity of formula (1) can either be described by a single probability density function (PDF) or by a combination of PDFs. A model description with one influence described by a single PDF can be defined as shown in the first example below.

---

```

1 <model name="gauss" targetid="g">
2   <influence id="g" name="gauss">
3     <distribution>
4       <gauss>
5         <mu>1</mu>
6         <sigma>1</sigma>
7       </gauss>
8     </distribution>
9   </influence>
10 </model>

```

---

The element `<influence>` contains just one element `<distribution>` defining a single PDF for the influence in this model. It is possible to access all PDFs implemented in *MUSE* using such a model description. This is done by changing the element `<gauss>` to the element that corresponds to the designated distribution and adapting the parameters. A list of all available distributions is given on the project homepage [1]. So called *subinfluences* can then be used to combine PDFs in a model description. Subinfluences are defined in a section delimited by the element `<influences>` as shown in the second model description.

---

```

1 <model name="x12" targetid="g">
2   <influence id="g" name="x12">
3     <formula>pow(X1,2) + pow(X2,2)</formula>
4     <influences>
5       <influence id="X1" name="X1" model="gauss"/>
6       <influence id="X2" name="X2" model="gauss"/>
7     </influences>
8   </influence>
9 </model>

```

---

This basic model reuses the basic model `gauss` defined in the first model. The element `<formula>` in a model description states then the relation between defined influences using all available functions and operators of *MUSE*. To reuse basic models with different parameters without touching the model definition file directly *MUSE* allows to set parameters of a model from outside.

### 3. Simulation Description

The input quantities of equation (1) are modeled in *MUSE* using basic models which are defined in model description files as shown in the previous section. The equation of the measurand needs to be specified after defining

the input quantities of a measurement. This is done in *MUSE* in a separate XML file, the simulation description. There, so called *instances* of basic models are defined. An instance of a model represents an influence quantity with individual setups and the name of the instance can then be used to access this instance. The simulation description below instantiates the model `x12` defined above by `<instance name="X12" model="x12"/>`. The equation of the measurand is then built based on this instances.

---

```

1 <simulation>
2   <initialization>
3     <instance name="X12" model="x12"/>
4   </initialization>
5   <calculation>
6     <uncertainty>sqrt(X12)</uncertainty>
7   </calculation>
8 </simulation>

```

---

The root element of the simulation description is the element `<simulation>` followed by an initialization section starting with the element `<initialization>`. Here all instances of the used basic models are defined and the parameters of these models can be set. The calculation section follows specifying the relation between the instances of the basic models after the initialization section.

The calculation section starts with the element `<calculation>`. A lot of attributes can be set to control the calculation for this element which are described in the next section. The equation of the measurand is then specified with the element `<uncertainty>`. Here the formula  $f$  is defined as a string using all functions and operators of *MUSE*. Using the basic model `x12` from above we can hence define the simulation of the example with the equation of the measurand given by  $Y = f(X_1, X_2) = \sqrt{X_1^2 + X_2^2}$  by building an instance of this model and taking the square root of this instance. As the model `x12` returns `pow(X1,2) + pow(X2,2)`, where `X1` and `X2` are Gaussian distributions, we end up with the overall equation of the measurand `sqrt(pow(X1,2) + pow(X2,2))`.

*MUSE* contains a lot of additional features to GS1 like the modeling of calibrations, measurement series and so on. They are also controlled via the simulation description, but an elaboration on these features would go beyond the scope of this paper and is given elsewhere [1].

## 4. Calculation Parameters

*MUSE* allows to control all important calculation parameters of a simulation. They are defined as attributes of the element `<calculation>` in the simulation description. A complete list of the attributes is given on the project homepage [1]. One parameter that can be controlled here is the number of Monte Carlo runs. Therefore, the attribute `mcsimulations` needs to be set. It is also possible to activate the adaptive Monte Carlo procedure described in GS1 via this attribute. Another attribute with the name `rngenerator` defines which *pseudo random number generator* *MUSE* takes to produce randomly values from the PDFs of the input quantities. It is possible to choose between the generator of Wichmann and Hill or the Mersenne Twister. Details and comparisons of these generators are given in *MUSE: Computational aspects of a GUM supplement 1 implementation* [4].

As a Monte Carlo simulation delivers one possible value for the PDF of the output quantity for each run, the resulting numbers need to be summarized to get the best estimate, the standard uncertainty or the coverage interval. To this end, the so called *analyze package* of *MUSE* can be turned on using the element `<analyse mode="on"/>` in the calculation section. By activating this module, a statistical output file is generated containing all relevant information of the PDF of the output quantity and also data to plot a histogram. This file can then be used to visualize the results using for example the tool *MuseView* which comes with *MUSE*. To see how the statistical parameters are calculated, which algorithms are used to propagate the distributions through the equation of the measurand in an efficient way and all other computational aspects of *MUSE* see reference [4].

## 5. Conclusion

*MUSE* is a powerful and freely available implementation of GS1 and supports therefore the measurement community with a tool to utilize the content of GS1. All the given distributions and all other aspects like the adaptive procedure, the calculation of the different types of coverage intervals and the recommended random number generator are implemented. In addition, *MUSE* supports calculations including complex valued quantities, the consideration of calibrations and the modeling of measurement series and processes. All steps done by *MUSE* are highly optimized. Therefore *MUSE* allows the metrologist to run evaluations of the measurement uncertainty with an excellent computational performance and with well balanced memory usage.

*MUSE* provides a structured and clear design for the modeling process. To this end, so called basic models are used to separate different influences in individual files and to compose the overall equation of the measurement using these models. Hence, the software facilitates the handling of large measurements scenarios. Due to the structured modeling and the usage of a state of the art Monte Carlo calculation core *MUSE* can be used in numerous different scientific areas to obtain an approximation of the PDF for the measurand. Based on this PDF it is possible to demonstrate the fitness for purpose by giving a measure of the confidence that can be placed on the result.

## References

1. *MUSE* - Measurement Uncertainty Simulation and Evaluation. Website, 2008. Software package, <http://www.mu.ethz.ch/muse>, ETH Zürich and Empa St. Gallen.
2. BIPM Joint Committee for Guides in Metrology (JCGM). Evaluation of Measurement Data-Supplement 1 to the 'Guide to the Expression of Uncertainty in Measurement'-Propagation of Distributions using a Monte Carlo Method. 2008.
3. International Organization for Standardization. *Guide to the Expression of Uncertainty in Measurement*. International Organization for Standardization (ISO), Central Secretariat, Geneva, 1 edition, 1995.
4. M. Müller, M. Wolf, and M. Rösslein. *MUSE*: Computational aspects of a GUM supplement 1 implementation. *Metrologia*, 45:586–594, 2008.
5. M. Müller, M. Wolf, M. Rösslein, and W. Gander. Limits of the uncertainty propagation: examples and solutions using the Monte Carlo method. In *Proceeding, 13th International Metrology Congress*, 2007.

## ROBUST LINE DETECTION FOR LINE SCALE CALIBRATION

JOSÉ ANTONIO MUÑOZ-GÓMEZ

*Departamento de Ingenierías, CUCSUR, Universidad de Guadalajara, Av.  
Independencia Nacional 151, Autlán, Jalisco, C.P. 48900, México*

CARLOS GALVAN

*Centro Nacional de Metrología (CENAM), km 4,5 Carretera a los Cues  
Mpio. El Marques, Querétaro C.P. 76241, México*

A novel method for detection of lines in a digital image used in line scale calibration process is described. The line images are recorded by a moving microscope and a CCD camera. This method is based on the center of the line instead of the edges of the line. Line detection is one of the most important problems in the line scale calibration. This method uses a Gabor filter for each row in the digital image. Likewise, based on robust statistics, some outlier points due to imperfections in the mark on the scale are ignored.

### 1. Introduction

The measurement of graduated lines scales is one of the most important tasks in the traceability chain for the measurement of the unit of length. Before 1961, the length of a meter was defined as the distance between two graduation lines on a platinum-iridium meter prototype based in Paris. The development of stabilized lasers and the methods for determining their frequencies leaded the Conference General des Poids et Mesures to redefine the unit of length in terms of the velocity of light in 1983. In practical measurements, the unit of length is often measured by using optical interferometry.

There are several instruments designed to make line scale calibration using laser interferometers, some of them use a photoelectric microscope in order to observe graduation lines. The position of the microscope (or scale) is measured by the laser interferometer [4, 5]. Those measurements can be taken while the microscope is located on the graduation line or dynamically when the microscope position moves through the graduation lines. Other instruments utilize a CCD in order to observe the line position even statically or dynamically [3, 6].

In both cases the main goal in the calibration process is to detect accurately the center of the scale mark. This work shows a novel method to determine, in a

robust way, the best fitted line to the center of the scale mark contained in a digital image. This task is required when we use a CCD camera in a line scale calibration process, and certain discontinuities due to manufacturing such as scratches on the scale surface.

This kind of problems appear when the scale is type I or II according with DIN 866 or JIS B 7541 grade 0 or 1. With this type of scales, we cannot obtain homogeneous digital signal in CCD, thus image processing procedures to locate adequately the center of line are needed.

## 2. Model Description

The proposed scheme is organized on three stages, for the convenience of exposition we consider that each image only contains one mark. Firstly, for each row in the image, we detect the centers of the mark. Secondly, based on the detected centers, we adjust (by robust statistics) a line. Finally, we establish a relation between the lines and the global coordinates. These steps are described in the following sections.

## 3. Center Detection

The detection of the center line for each column with a sub-pixel precision is based on the complex Gabor filter; this is a well known quadrature filter. This process is done for every row in the image. The Gabor filter is designed in space domain defined by:

$$h(x) = g(x)[\cos(\omega x) + j \sin(\omega x)], \quad (1)$$

where  $g(x)$  is a Gaussian function with  $\sigma=\omega/4$ , and  $\omega=\pi/d$ , where  $d$  correspond to measurement of the width of the mark in pixels. When a convolution between the Eq. (1) and a signal that contains a scale mark is performed, we obtain a signal from which the maximum magnitude estimates the center of the mark. Besides, based on the phase, we determine the center of the mark with sub-pixel precision. This process is showed in Figure 1.

Once the maximum of the magnitude is located, we look for the phase of the filtered signal for a phase zero value. We must to take into account that we are working with digital data, so it makes difficult to find the exact value. For this purpose, we calculate a line (by least squares fitting) using the values of the phase corresponding to the pixels located around the neighborhood of the maximum magnitude. With this procedure, we can determine the center of the line with sub-pixel resolution.

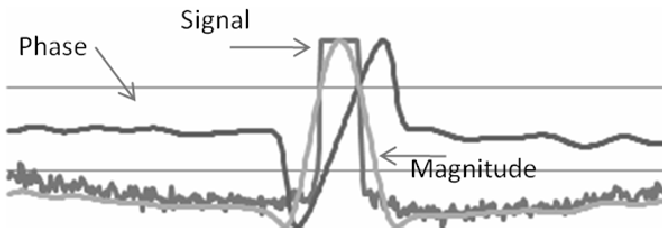


Figure 1. Gabor filter applied to a signal (noise one), and the results are the phase and magnitude.

The filter is applied for each row in the digital image obtaining the points required to estimate the line equation which describes the observed mark. This process is also hold when the digital image has more than one mark. This can be done by making a summation of the intensity values for each column. A percentage indicating the probability to find a mark is established. With these local maxima is possible to search this position in the filtered signals.

#### 4. Robust Scale Mark Estimation

As a second step in the proposed scheme, is to adjust a straight line to the points located in the previous section. It is well known that the least square data fitting is sensitive to the outlier data. In the images that have been used to test this algorithm some outliers can be found. For example, in the image shown in Figure 2 we can see several points which does not correctly indicate the center of the line. These points show the presence of little scratch on the scale mark.

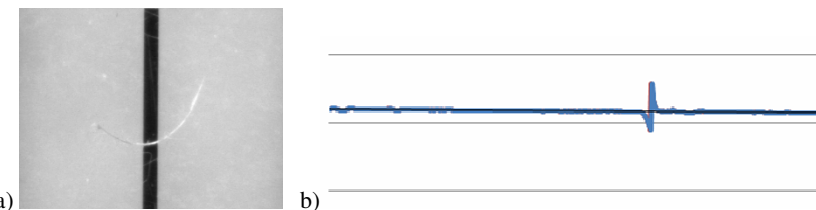


Figure 2. a) Line Scale mark with a scratch. b) Values of the center of line for each row from image 2a.

The difference in the line mark equation parameters including all points and those outliers points eliminated manually is about 0.7 pixels.

To solve this problem we have use a robust estimator for the line scale equation. We propose to use an M-estimator [7]; where the goal is to determine the unknown parameters by minimizing the residual errors of the cost function:

$$U(m, b, \alpha) = \sum \rho(y_i - mx_i - b). \quad (2)$$

The truncated quadratic function  $\rho$  is described in Eq. (3), where  $\psi$  is called the influence function.

$$\rho(x) = \begin{cases} x^2 & |x| < \alpha \\ k & \text{otherwise} \end{cases} \quad \psi(x) = \begin{cases} x & |x| < \alpha \\ 0 & \text{otherwise} \end{cases} \quad (3)$$

With this selection, the algorithm is similar to the original least square algorithm, but only the points which satisfy the influence function are taken into account. However, the  $\alpha$  parameter is data dependent, so we propose an iterative method. First the estimation is made with all points (traditional least squares). In consecutive steps, this parameter can be reduced up to reach a percentage of total points. In our experiments this value is set at 60%.

Based on the above described procedure, for each mark in the image we determine the two parameters of the straight line. As can be seen, the slope can be used as additional information to verify the quality of the scale mark. This information is not counted into account in the present work; further work in this direction is beginning undertaken.

## 5. Robust Pixel Length Determination

Finally, it is necessary to map the local position of the detected lines (image reference) to a global reference. For this process we use the next relation:

$$z^w = z_i + \beta x_i, \quad (4)$$

where  $z^w$  corresponds to the real position for  $i$ th-line, and  $\beta$  is the scale factor for each pixel in the CCD. This process takes interferometer readings and positions for the same line along calibration process. In practice, the first line is taken for different images along CCD interval, in order to determine this factor. The scale factor  $\beta$  is calculated by solving the following system of equations:

$$z_0 + \beta x_0 = z_1 + \beta x_1 = \dots = z_n + \beta x_n = z^w. \quad (5)$$

To solve Eq. (5), we decide to continue with robust statistics by using an M-estimator with the Hampel function, see [7], given by:

$$\rho(x) = x^2 / 2(1+x^2). \quad (6)$$

Using this function, the optimal value for the factor  $\beta$  is found by minimizing the cost function given by Eq. (7). In this case, we used an iterative

algorithm based on the gradient of the cost function (nonlinear least square). This algorithm requires a good initial guess, this is obtained from the relation  $\Delta z / \Delta b$ ; which represents the difference between the real position for a specific line and the values obtained for this mark in the images.

$$\min_{\beta} \left\{ U(\beta) = \sum_{\{i,k\} \in C} \rho(z_k + \beta x_k - (z_i + \beta x_i)) \right\}. \quad (7)$$

With the factor  $\beta$  and the sensor coordinates, the center of each mark is mapped to a global coordinates obtaining the distances for all graduated lines. A detailed explanation of the proposed scheme can be found in [1]. Also, the mechanical system is described in [2].

It should be observed that the M-estimator can be characterized by his influence function which determines how the residuals are weighted. We choose different functions (see Eq. (3), Eq. (6)) based on the knowledge of the data distribution of the analyzed data.

## 6. Results

The purpose of this section is to test the proposed method. We exemplify the algorithm by analyzing two cases. This method has been used in the CENAM's line scale calibration bench [2]. This device uses a laser interferometer to measure the position of a Vision System. These instruments are used by CENAM to calibrate different kind of line scales, eventually is also used to calibrate measurement tapes. The results depicted in this section do not consider the errors of the mechanical system, because they are not considered in the proposed model.

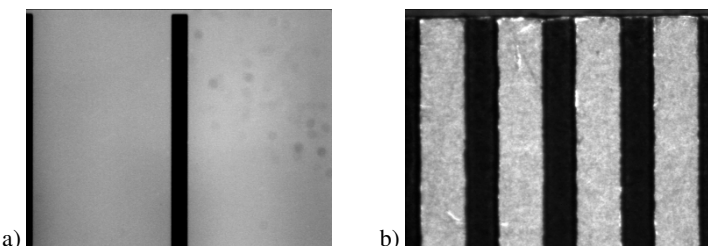


Figure 3. a) Glass scale according to JIS B 7541 Grade 0, b) Steel scale according to DIN 866 Type A.

In Figure 3 we show different types of images that can be seen in the calibration process. In Figure 3a the edges of the line are well defined. In contrast, Figure 3b shows several little scratches around of the edges in each mark.

For images like those shown in Figure 3a (1mm scale resolution), a standard deviation about 40 nm is obtained. Pixel length is about  $3.2 \mu\text{m}$ , this value is obtained with a standard deviation of 32 nm. In Figure 3b, a standard deviation of 65nm is registered, this value is due to the scratches.

### Acknowledgments

The first author extends his thanks to PROMEP-México for his partial supporting under project 103.5/08/2919. We express our gratitude to the referees for their many valuable suggestions that improved this article. The help of final revision from Dr Omar Aguilar is also greatly appreciated.

### References

1. J. A. Muñoz-Gómez, Medición Robusta de Líneas Graduadas Utilizando un Sistema de Visión, Master Thesis, CIMAT, Guanajuato, México, 2001.
2. H. Gonzalez, C. Galvan and J. A. Muñoz, Image Processing Automatic Interferometric Calibration System for Line Scales, Proceeding of SPIE Annual Meeting 2003 San Diego, Cal USA August 2003.
3. A. Lassila, E. Ikonen and K. Riski; Interferometer for calibration of graduated line scales with moving CCD camera as a line detector; Applied Optics, Vol. 33, No. 16, 1 June 1994, 3600-3603.
4. J. S. Beers, K. B. Lee, Interferometric measurements of length scales at the National Bureau of Standards, Precis. Engen. 4, 205-214 (1982).
5. Chao-Jung Chen, Sheng-Hua Lu, Huang-Chi Huang, and Ren-Huei Hsu; Automatic calibration of measuring tapes with friction driver and a image processor.
6. H. Heister; Zur automatischen Kalibrierung geodätischer instrumente, Phd. Thesis in Studiengang Vermessungswesen Universität der Bundeswehr München, 1988.
7. R. J. Huber, Robust Statistics, Wiley Series in Probability on Mathematical Statistics, 1981.

## **ANALYSIS OF CONSISTENCY OF THE BASIC CONCEPTS FOR THE EXPRESSION OF UNCERTAINTY IN PRESENT INTERNATIONAL WRITTEN STANDARDS AND GUIDES**

FRANCO PAVESE

*INRIM, strada delle Cacce 73  
Torino, 10135, Italy, [f.pavese@inrim.it](mailto:f.pavese@inrim.it)*

At present, several international written standards and guides are available, dealing with the expression of uncertainty in measurement, calibration and testing, and concerning the definition of the basic concepts and related nomenclature and basic methods for data analysis. An inspection and comparison of these texts, which were prepared in a time span of more than twenty years, shows that, to different degrees, not all of them are consistent with each other, probably due mainly to an advancement of the discussion and of agreed solutions that took place in the indicated time span and that can be observed for most of them. The paper addresses an attempt to identify what appear the more serious inconsistencies that in author's view should be removed in the process of revision started for several of them.

### **1. Introduction**

The standardisation of procedures for the statistical processing of measurement data, namely for the assessment of measurement uncertainty, is essential to science, as well to the work in the enterprises and in private and public laboratories, in particular in field-testing but also, increasingly, in field-laboratories of calibration. A prerequisite for these procedures to provide a sound help to their users, also from a legal point of view, is that the terms used in the written standard are consistent with each other and with the specialised internationally-recognised sources of terminology.

The lack of a common language and common understanding of basic concepts, such as repeatability, reproducibility, accuracy, systematic effects or error, true value, bias, Type A and B uncertainty components, etc., and of the underlying assumptions, would generate ambiguity in the interpretation of the guidelines or prescriptions and confusion in the application of the procedures.

At present, several international written standards and guides are available from various bodies, dealing with the expression of uncertainty in measurement, calibration and testing, and concerning the definition of the basic concepts and related nomenclature. Consistency with each other is usually given for granted.

This paper is focusing on the analysis of some of the most critical problems occurring when inconsistencies are instead observed to occur and on the different approaches sometimes being used for the fields of calibration and of testing.

## 2. A critical review of problems in the GUM

The GUM [1] is based, first of all, on the following principle: “*The concept of uncertainty adopted in this Guide is based on the measurement result and its evaluated uncertainty rather than on the unknowable quantities ‘true’ value and error*”, i.e. on “*observable quantities*”, where “*the term ‘true value of a measurand’ ... is not used in this Guide because the word ‘true’ is viewed as redundant*”, since “*the ‘true’ value of the measurand (or quantity) is simply the value of the measurand (or quantity)*”. In addition, the Guide is actually dealing with the “*the realized quantity*” that is “*an approximation of the measurand*”, the latter being defined according to VIM 2<sup>nd</sup> edition (1993) [2] “*the quantity subject to measurement*”. However, the GUM states, “*neither the value of the realized quantity nor the value of the measurand can ever be known exactly*”, thus also the value of the measurand and the value of the realized quantity are as *unknowable* as the ‘true’ value is. The GUM also states, “*for all practical purposes associated with the measurement*” the measurand “*value is unique*” and “*a unique ‘true value’ is only an idealized concept*”, though they are said in GUM to carry the same meaning. Anyhow, the measurement is only dealing with the realized quantity, an approximation to the measurand, for the unknowable value of which there is no reason to be unique. Yet, the GUM indicates that “*remaining error*”, difference to the “*value of the measurand*”, “*values of measurand due to incomplete definition*” are unknowable contributions. Therefore, they are not included in the “*result of measurement*”, and are only indicated to contribute to a so-called “*final result of measurement*”.

A second basic principle of the GUM is that “*the result of the measurement of the realized quantity is corrected for the difference between that quantity and the measurand*”. However, both terms of the difference, “*realized quantity*” and “*measurand*”, are not observable. The first because its value is as unknowable as that of the “*quantity*” (“*Neither the value of the realized quantity nor the value of the measurand can ever be known exactly*”), the second because the knowledge of the measurand can only be approximated. In fact, “*it is assumed that the results of a measurement have been corrected for all recognized significant systematic effects*” and that, “*after the correction, the expectation or expected value of the error arising from a systematic effect is zero*”. However,

this statement would imply that no unrecognised<sup>1</sup> systematic effects should exist (while they are assumed instead to exist –though unknowable– in the GUM Appendix D, and in DIN 1319 [3]) and that the correction should be exact. Both instances are unverifiable.

A third basic principle of GUM is that, “*implicit in this Guide is the assumption that a measurement can be modelled mathematically to the degree imposed by the required accuracy of the measurement*” and that “*the mathematical model of the measurement procedure that transforms the set of repeated observations into the measurement result is of critical importance since, in addition to the observations, it generally includes various influence quantities that are inexactly known*”. Thus, a mathematical model is used and the uncertainty propagation law, in place of the variational method, to take into account the effect on the measurement result of the variability of the influence quantities: the variational method is only recommended for checking model incompleteness. It is unclear if the application of this principle is alternative to the determination of reproducibility. Still, model incompleteness is assumed *not* to contribute to the variance of the “*result of measurement*”, but to be only a random unknowable contribution to that of the “*final result of measurement*”: it should rather be considered as a *non-uniqueness*, since it is responsible for the multiplicity of the measurand values. Yet, no mention can be found in the GUM of the fact that in *empirical* or *theoretical* models the values of the model parameters are determined from basically different processes.

Concerning uncertainty components, instead of classifying them according to repeatability and reproducibility, the GUM defines two types. The first is “*Type A ... method of evaluation of a standard uncertainty by the statistical analysis of a series of observations*” this uncertainty component being “*obtained from a Type A evaluation calculated from a series of repeated observations*”. However, by also stating that “*variations in repeated observations are assumed to arise because influence quantities that can affect the measurement result are not held completely constant*”, the GUM is inconsistent with the universally adopted definition of ‘repeated measurements’ excluding the variability of any influence quantity “*over a short period of time*” [2, 4]. Actually, the concept of “*influence quantity*” variability is not a characteristic of ‘repeatability’ (“*repeated observations*”) but of ‘reproducibility’ –and the concept of “*systematic effects*” is a characteristic of

---

<sup>1</sup> the word “*recognized*” carries an ambiguity about the fact that, after identification, investigation bringing to the correction would consist of experimental determinations or of inference from modelling.

‘accuracy’, or ‘trueness’ in testing. In fact, according to the definition of ‘influence quantity’ in GUM and VIM 2<sup>nd</sup> Edition [2] (“*quantity that is not the measurand but that affects the result of the measurement*”) and in VIM 3<sup>rd</sup> Edition [2] (“*quantity that, in a direct measurement, does not affect the quantity that is actually measured, but affects the relation between the indication and the measurement result*”), the variability of the influence quantities is the entire and only potential sources of the systematic effects (or error)<sup>2</sup>, thus of the reproducibility generally broader variability with respect to repeatability: “*measurement precision under reproducibility conditions of measurements*” are those “*condition of measurement in a set of conditions that includes different locations, operators, measuring systems, and replicate measurements on the same or similar objects*” (noting, “*the different measuring systems may use different measurement procedures*”, a condition not generally allowed in testing).

The second component is “*Type B ... method of evaluation of a standard uncertainty by means other than the statistical analysis of a series of observations*”, i.e. “*... founded on a priori distributions*”, which is said to be based on *prior* knowledge not always based on experimental verification, but this does not seem to reconcile with the GUM basic principle of only using “*knowable quantities*”.

### **3. The ‘true value’ in IEC 60359**

Contrarily to GUM, which is not using the term ‘true value’ but is making use of the *concept*, for the IEC 60359 [5] the concept of true value is not only unknowable, but is said to be also unnecessary for the stated objective of the measurement, to be able to obtain measurement results that are compatible with each other: “*The uncertainty of a valid result of a measurement shall be such as to ensure compatibility with all other valid measurements of the same measurand*”. A recent definition of “*metrological compatibility*” can be found in VIM 3<sup>rd</sup> Edition: “*property of all pairs of measurement results for a specified measurand, such that the absolute value of the difference of the measured quantity values is smaller than some chosen multiple of the standard measurement uncertainty of that difference*”. It is not clear how this can reconcile with GUM principles, since the latter assumes *a priori* the measurements to be ‘repeated’, so excluding *a priori* the possibility of ‘non compatibility’ after the corrections are applied.

---

<sup>2</sup> Time is almost never an influence quantity in itself, but in time the influence quantities can show a variability.

#### 4. A critical review of problems in the VIM 2008

The 3<sup>rd</sup> Edition of the VIM is said to have been written in order to become consistent with all its contemporary Guides and standards [6].

In practice, one can observe some difficulties in having fulfilled this goal. For example, in VIM Type A evaluation of measurement uncertainty arises from “*evaluation of a component of measurement uncertainty by a statistical analysis of quantity values obtained under defined measurement conditions*”, where the conditions can be “*repeatability condition of measurement, intermediate precision condition of measurement and reproducibility condition of measurement*”. The addition of the latter two conditions looks as a very useful specification, but they are not deducible from the GUM document.

Still, in the VIM definition of reproducibility, already reported in Section 2, the specification “*or similar objects*” can be understood only in some specific contexts. In general, “*similar*” is too a generic concept and “*object*” could not be the appropriate word. While it can probably correctly be used in testing, in metrology its use should, e.g., be excluded for artefact standards.

A more basic problem in VIM appears to be the definition of “*systematic measurement error*”: “*Component of measurement error that in replicate measurements remains constant or varies in a predictable manner*”. In fact, a systematic error constant in value (stable influence quantities) is only assumed to be the condition for repeated measurements (and “*over a short period of time*”); and, what about its *unpredictable* variability. Also the three Notes to the definition place some problems.

“*NOTE 1 —A reference quantity value for a systematic measurement error is a true quantity value, or a measured quantity value of a measurement standard of negligible measurement uncertainty, or a conventional quantity value*”. In order to talk of “*measurement error*” the two terms of the difference producing the error should be comparable. However, the first value is unknowable, the second value has an uncertainty associated to it, the third value is not directly comparable with the measured value and may be affected by an uncertainty.

“*NOTE 2 —Systematic measurement error, and its causes, can be known or unknown. A correction can be applied to compensate for a known systematic measurement error*”. This is in accordance with DIN 1319 but not with GUM.

“*NOTE 3 —Systematic measurement error equals measurement error minus random measurement error*”. The wording is consistent with the VIM definition (“*constant*”), but, instead, the random measurement error, for the GUM (and,

more generally, for non-repeated observations), includes a contribution due to the variability of systematic effects.

In addition, a few definitions look little informative (like tautologies), e.g., the ‘true value’ being “*quantity value consistent with the definition of a quantity*”.

## 5. A critical review of problems in some other relevant ISO standards

The ISO standards 5725 [7] and 3534 [4] considered here do not have the specific aim to deal with the concepts treated by GUM. However, there are basically two concepts that unavoidably overlap the same domain: trueness (true value) and bias.

As to the first, the definition of ‘trueness’ becomes somewhat confusing from a lexical viewpoint after VIM 3<sup>rd</sup> Edition specifying that “*measurement accuracy*” is “*closeness of agreement between a measured quantity value and a true quantity value of a measurand*” while “*measurement trueness*” is “*closeness of agreement between the average of an infinite number of replicate measured quantity values and a reference quantity value*”: at least unfortunate. ISO 5725 (1994) definition of the latter is “*closeness of agreement between the average value obtained from a large series of test results and an accepted reference value*”, a case of use of a ‘consensus value’ not explicitly treated in its different implications by GUM with respect to the ‘true value’.

As to ‘bias’, this concept is linked to the previous by ISO 5725 in saying, “*the measure of trueness is usually expressed in terms of bias*”. This specification is picturing the intrinsic difference of this concept in metrology and testing.

In testing, in fact, for ISO 5725-1 (1994) and 3534-1 (2003) bias is, accordingly, the “*difference between the expectation of the test results and an accepted reference value*”. However, ISO 3534-2 (2006) looks inconsistent in saying “*difference between the expectation of a test result or measurement result and a true value*”, because ‘true value’ and ‘reference value’ have different meanings. For problems in correcting bias, see [8].

In metrology, the term bias should not be used when it would refer to the ‘true value’; in all instances, GUM prescribes be corrected, so the “*result of the measurement*” according to GUM is bias-free. In VIM 3<sup>rd</sup> Edition ‘bias’ is the “*estimate of a systematic measurement error*”, thus a single value without variability, while, e.g., EA-4/16 (2003) [9] tells instead, “*the bias of a test method is usually determined by studying relevant reference materials or test samples ... The uncertainty associated with the determination of the bias is an*

*important component of the overall uncertainty*”. At least, two different words should be used.

For more comments on some of the issues illustrated in this paper see also [10].

## References

1. BIPM, IEC, IFCC, ISO, IUPAC, IUPAP, and OIML, *Guide to the Expression of Uncertainty in Measurement* (GUM), International Organization for Standardization, Geneva, 2<sup>nd</sup> edn (1995).
2. BIPM/ISO, *International Vocabulary of Basic and General Terms in Metrology* (VIM) 2<sup>nd</sup> (1993) and 3<sup>rd</sup> (2008) edns, <http://www.bipm.org>.
3. DIN 1319-1 *Fundamentals of metrology, Part I: basic terminology*, Berlin, Beuth (1995).
4. ISO 3534-1, *Statistics, Vocabulary and symbols, Part 1: General statistical terms and terms used in probability*, International Organization for Standardization, Geneva, 2<sup>nd</sup> edn (2006).
5. IEC 60359, *Electrical and electronic measurement equipment –Expression of performance*, International Organization for Standardization, Geneva, 3<sup>rd</sup> edn (2001).
6. C. Ehrlich, R. Dybkaer and W. Wöger, *Accred Qual Assur* (2007) 12: 201-218.
7. ISO 5725, *Accuracy (trueness and precision) of measurement methods and results*, International Organization for Standardization, Geneva, 2<sup>nd</sup> edn, 1994.
8. B. Magnusson and S.L.R. Ellison, *Anal Bioanal Chem* (2008) 390:201–213.
9. European Accreditation, *EA guidelines on the expression of uncertainty in quantitative testing*, EA-4/16, rev00, 2003.
10. F. Pavese, *Accred Qual Assur* (2007) 12: 525-534.

## AN OPTIMISED UNCERTAINTY APPROACH TO GUARD-BANDING IN GLOBAL CONFORMITY ASSESSMENT

LESLIE R PENDRILL

*SP Technical Research Institute of Sweden, Measurement Technology  
Box 857, SE-501 15 Borås, Sweden, [leslie.pendrill@sp.se](mailto:leslie.pendrill@sp.se)*

A traditional approach in conformity assessment to minimizing the risks of incorrect decision-making associated with measurement uncertainty is to apply ‘guard-bands’ which narrow the zone of acceptance by some fraction of the measurement uncertainty. Criticism of the guard-band approach has included increased costs for the supplier in meeting the narrower acceptance zone as well as the fact that the new acceptance limits will in time become new *de facto* specification limits. The present work applies an optimized uncertainty methodology to analyse the consequences of guard-banding in terms of an economic decision theory approach. The methodology is of general applicability but is illustrated in the present work in the simple case of pre-packaged goods priced linearly with the amount of content. Optimum strategies for the supplier are illustrated in terms of minimizing production and testing costs, while at the same time maintaining satisfactory levels of customer satisfaction.

### 1. Introduction

In recent years there has been an increasing interest and enhanced insight into decision-making gained when extending classical, purely statistical treatment of customer and supplier risks [1 - 3], towards a more ‘stakeholder’ motivated (and ultimately optimised) approach in terms of effective costs associated with manufacture, testing and incorrect decision-making [4 - 9].

The present work examines a traditional approach in conformity assessment to minimizing the risks of incorrect decision-making associated with measurement uncertainty in which ‘guard-bands’ narrow the zone of acceptance by some fraction of the measurement uncertainty [1]. Discussion is in terms of new decision-theory tool – the “operating cost characteristic” [9] – which, together with the optimized uncertainty methodology [4, 8], provides a complete, 3D surface to illustrate the optimum level of measurement effort as a balance against costs associated with the consequences of incorrect decision-making, as recently published by the author [9].

The methodology is of general applicability but is illustrated in the present work in the simple case of homogeneously pre-packaged goods priced linearly with the amount of content.

## 2. Introducing Cost into Conformity Assessment Risks

In general, the impact of a wrong decision in conformity assessment is expressed as a risk  $R$ , defined as the probability  $p$  of the wrong decision occurring multiplied by the cost  $C$  of the consequences of the incorrect decision:

$$R = p \times C \quad (1)$$

as an example of the more general, historical expression of statistical expectation. [The traditional treatment of the two kinds of decision-making risks – consumer (or customer) risk and producer (or supplier) risk – in purely statistical terms is well-known.] In this section, new expressions for decision-making risks including costs are presented, together with a novel tool – the operating cost characteristic curve – as an extension of traditional statistical tools, with the addition of an economic decision-theory approach. Complementarity with the optimised uncertainty methodology [4, 8] is emphasised in the concluding remarks.

### 2.1 Inspection by Variable

Acceptability by variable is based on inspection of the distance of observed product value from the specification limit(s) for product value.

*Example:* A manufacturer of 500 g packets of pre-packaged coffee powder finds in production a net result of  $497 \pm 8$  g for one particular daily run of  $N_{\text{lot}} \approx 10^5$  packets. Observed variations are dominated by actual changes in the amount of powder,  $x$ , from packet to packet, described by the probability density function (PDF)  $g_{\text{entity}}(x)$ . The metrological control of the content of pre-packages according to actual legislation in international legal metrology [9] has as targets to ensure that the mean value of the actual content of a batch is at least equal to the value declared on the product label and, at the same time, that the dispersion of the actual content of single packages around the mean value is kept as small as possible. To protect the customer, a lower limit,  $L_{SL,x} = 485$  g, is typically set as a one-sided tolerance interval for the contents of pre-packaged goods in conformity assessment requirements [9].

Measurement uncertainty [10, 11] is relatively small, typically 1 g ( $k = 2$ ) as described by the measurement PDF  $g_{\text{test}}(\eta, y_m)$ .

## 2.2 Operating Cost Characteristics and Optimised Uncertainty

Incorrect acceptance of a non-conforming object on inspection will lead to customer costs associated with out-of-tolerance product. Overall costs,  $E$ , consisting of a sum of testing costs,  $D$ , and the costs,  $C$ , associated with customer risk, can be calculated with the expression:

$$E(\eta, \sigma) = D(\eta, \sigma) + C(\eta) = \frac{D}{\sigma^2} + \int_{\eta \in R_{PV}} C(\eta) \cdot g(\eta | \hat{\eta}) \cdot d\eta \quad (2)$$

with  $\hat{\eta} \in R_{PV}$ , where  $R_{PV}$  denotes the region of permissible values and  $\sigma$  is a measure of dispersion.

Overall costs  $E(\eta, \sigma)$ , according to (2) can be either plotted over:

- a range of quantity values of  $L_{SL} - H \cdot s_p \leq \hat{x} \leq L_{SL} + H \cdot s_p$  for a given dispersion,  $\sigma = s_p$ , and ‘guard-band’ factor  $H$  – yielding an “operating cost characteristic” [9] [figure 1] analogous to the traditional, probability-based operating characteristic
- a range of test uncertainties,  $\sigma$ , for a given mean quantity value  $\hat{x} \geq L_{SL}$ , the so-called “optimised uncertainty curve” [4, 8] [figure 2]

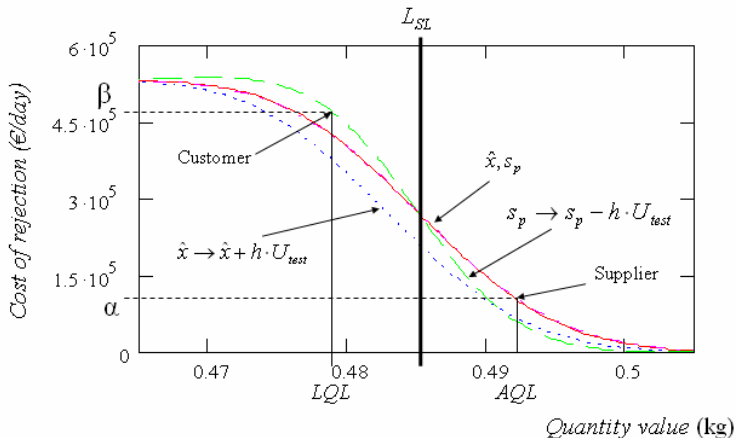


Figure 1. “Operating cost characteristics”: Daily costs of out-of-tolerance product as a function of quantity value (net mass) at a given production variation,  $\sigma = s_p = 8$  g for pre-packaged coffee with different strategies to satisfy guard-banding

Assuming a Gaussian distribution of product values and a linear cost model, expression (2) in the present case is given by:

$$E_{\text{product}} = \frac{D_{\text{product}}}{s_p^2} + \int_{-\infty}^{L_{SL}} C_{\text{global}} \cdot [- (y - y_{\text{nominal}})] \cdot \frac{1}{\sqrt{2\pi} \cdot s_p} e^{-\frac{(y - \hat{y})^2}{2s_p^2}} \cdot dy \quad (3)$$

Relevant costs are  $D_{\text{product}} = 50 \text{ € / day}$  at  $\sigma = s_p = 8 \text{ g}$  and  $C_{\text{global}} = N_{\text{tot}} \cdot C_{\text{specific}}$ , where  $N_{\text{tot}} = 10^5$  and  $C_{\text{specific}} = 10 \text{ € / kg}$ .

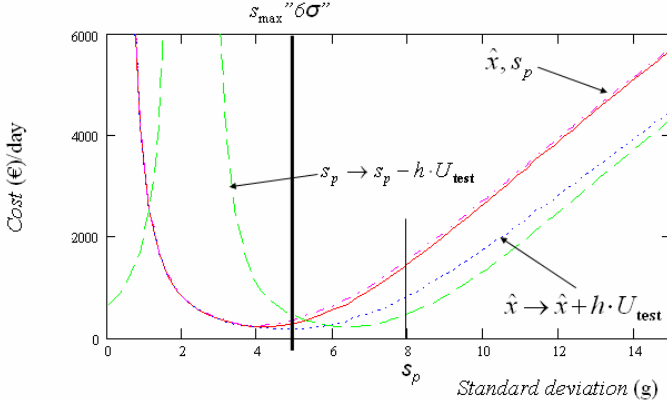


Figure 2. Optimised uncertainty: Daily costs of out-of-tolerance product as a function of production standard deviation,  $\sigma$ , for a given quantity value (net mass 497 g) for pre-packaged coffee with different strategies to satisfy guard-banding. (Note that test costs,  $D_{\text{test}}/s_p^2$ , diverge at zero standard deviation,  $s_p$ , as is evident in the dashed curve.)

Figure 2 shows overall costs as a function of production standard deviation, calculated with equation (3), indicating optimised (i.e. minimized) costs for different strategies of guard-banding. For comparison, a classical limit on production variation according to the famous ‘six-sigma’ approach to statistical process control (SPC) is shown ( $s_{\max} “6\sigma”$ ) in figure 2.

It is possible to view the two tools - the operating ‘cost’ characteristics and optimized sampling uncertainty methodologies – as together providing a complete basis for risk-assessment in conformity assessment: Overall costs could be plotted in three dimensions where at each fraction non-conforming product on the operating characteristic curve [shown in figure 1 for a given production variation,  $s_p$ , ( $= 5 \text{ g}$ )], the corresponding optimized uncertainty curve [shown in figure 2 shown for a given quantity value (net mass 497 g)] would cross in the orthogonal direction. In that way, the optimum uncertainty required at specific conformity assessment points, such as those for customer and supplier risks, could be identified. This provides the decision-maker with a more complete and arguably more relevant assessment of expectations and risks including additionally measures of impact, importance and consequence [9].

Examples of evaluations of expression (2) for optimized uncertainty by variable, including a nesting of product and measurement integrals and a cost function can be found in [8] and references therein.

### 2.3 Guard Bands and Production Strategies

Guard-banding [1, 2] reduces the *customer cost risk* associated with measurement uncertainty with the introduction of a lower acceptance limit  $L_{AL}$  inside a lower specification limit  $L_{SL}$  calculated with:

$$C_{\text{global}}(\hat{x}, L_{AL}, h) = \int_{\eta < L_{SL}} N_{\text{lot}} \cdot C(\eta) \cdot g_{\text{entity}}(\eta | \hat{x} + L_{AL}) \cdot d\eta \quad (4)$$

with guard-band  $L_{AL} = L_{SL} + h \cdot U_{\text{test}}$ , with some multiple of the (expanded) test uncertainty  $U_{\text{test}}$ ; and  $\hat{x} \geq L_{AL}$ . The equivalent expressions for customer risk in the case of an upper acceptance limit,  $U_{AL}$ , are obtained by inverting the signs throughout.

The gains for the customer from guard-banding at the same time oblige the supplier to take action to satisfy the narrower acceptance region in one of two ways:

- Minimising production variations
- Increasing the mean quantity of product

These two alternatives can be modeled using the above-mentioned optimised production variation methodology can be applied where decreasing customer risks through guard-banding are balanced against the increased costs of minimising production variation.

A guard band limit  $L_{AL}$  can be satisfied by *reducing product variation* with an amount equal to the width of the guard-band, i.e.,  $s_p \rightarrow s_p - h \cdot U_{\text{test}}$ .

The other approach open to the supplier of meeting tighter acceptance intervals narrowed by guard-bands is to *shift average product value* away from the specification limit with an amount equal to the width of the guard-band, i.e.,  $\hat{x} \rightarrow \hat{x} + h \cdot U_{\text{test}}$  in the case of a single, lower specification limit.

The associated increases in production cost can be judged from the optimised production (dashed) curves in figures 1 and 2.

## Acknowledgements

Thanks for discussions about the performance of the testing of different measurement instruments with Håkan Källgren, Jan-Erik Elander and Jonatan Westerberg and other colleagues at SP. The author has also benefited from participation in the Joint Committee for Guides in Metrology (JCGM), Working Group 1. This work has been partially financed by grant (2007) 38:10 National Metrology of the Swedish Ministry of Industry, Employment and Communication.

## References

1. David Deaver, "Guardbanding with Confidence," 1994 NCSL Workshop & Symposium, pp. 383-394, 1994
2. R.H. Williams and C.F. Hawkins, "The Economics of Guardband Placement," *Proceedings, 24<sup>th</sup> IEEE International Test Conference*, Baltimore, MD, Oct. 17-21, 1993 (MD).
3. AFNOR "Metrology and statistical applications - Use of uncertainty in measurement: presentation of some examples and common practice," FD x07-022, 2004
4. T. Fearn, S. Fisher, M. Thompson and S. Ellison, "A decision-theory approach to fitness for purpose in analytical measurement," *Analyst*, vol. 127, pp. 818 – 824, 2002
5. L.R. Pendrill, "Optimised measurement uncertainty and decision-making when sampling by variables or by attribute," *Measurement*, vol. 39, pp. 829-840, 2006;  
<http://dx.doi.org/10.1016/j.measurement.2006.04.014>.
6. L.R. Pendrill and H. Källgren, "Decision-making with uncertainty in attribute sampling," *Advanced Mathematical and Computational Tools in Metrology VII*, vol. 72, pp. 212 – 220, 2006, World Scientific, Singapore, ISBN 981-256-674-0.
7. L.R. Pendrill and H. Källgren, "Exhaust gas analysers and optimised sampling, uncertainties and costs," *Accred. Qual. Assur.*, vol. 11, no. 10, pp. 496 – 505, Oct. 2006
8. L R Pendrill "Optimised Measurement Uncertainty and Decision-Making in Conformity Assessment", 2007 NCSLi Measure, Vol. 2, no. 2, pp 76 – 86
9. L.R. Pendrill, "Operating 'cost' characteristics in sampling by variable and attribute" *Accred. Qual. Assur.*, July 2008, DOI: 10.1007/s00769-008-0438-y
10. G.B. Rossi and F. Crenna, "A probabilistic approach to measurement-based decisions," *Measurement*, vol. 39, pp. 101 – 119, 2006
11. JCGM WG1 "Evaluation of measurement data — The role of measurement uncertainty in deciding conformance to specified requirements", *draft GUM Supplement JCGM 106* March 2008

## FROM GUM TO ALTERNATIVE METHODS FOR MEASUREMENT UNCERTAINTY EVALUATION

MARC PRIEL

*Laboratoire national de métrologie et d'essais  
Centre for Scientific and Industrial Metrology  
1, rue Gaston Boissier 75724 Paris cedex 15, France*

Since the advent of the Guide to the expression of Uncertainty in Measurement (GUM) in 1995 laying the principles of uncertainty evaluation numerous projects have been carried out to develop alternative practical methods that are easier to implement namely when it is impossible to model the measurement process for technical or economical aspects.

In this paper the author presents the recent evolution of measurement uncertainty evaluation methods with GUM's supplements and several alternative methods for laboratories. The evaluation of measurement uncertainty can be presented according to two axes based on intra-laboratory and interlaboratory approaches.

The intra-laboratory approach includes : “the modelling approach” (application of the procedure described in chapter 8 of the GUM, GUM uncertainty framework) and “the single laboratory validation approach”.

The interlaboratory approaches are based on collaborative studies and they are respectively named “interlaboratory validation approach” and “proficiency testing approach”. The first one uses the statistical methods described in the standard ISO 5725 Accuracy (trueness and precision) of measurement methods and results and the recent ISO Technical Specification 21748 Guidance for the use of repeatability reproducibility and trueness estimates in uncertainty estimation. The second approach will certainly play an important role in the near future. A majority of testing laboratories are involved in Proficiency Testing Scheme and interested in the possibility to use the results of these exercises and the data accumulated along the time to evaluate their uncertainty. The most important application area of these approaches certainly concerns medicine laboratories. Recently, the medicine laboratories have been encouraged to evaluate their uncertainty of analysis, either by regulation or on voluntary basis in accreditation process.

### 1.1. *New Definitions from VIM 3<sup>rd</sup> Edition*

The new edition of the International Vocabulary of Metrology – Basic and General Concepts and Associated Terms (VIM) 3<sup>rd</sup> [1] edition introduce new definitions for the two terms: measurement result and uncertainty, these new definitions are in accordance with the evolution of the concept of uncertainty. The new definitions are:

Measurement result (VIM 2.9)

*Set of quantity values being attributed to a measurand together with any other available relevant information.*

It is important to consider that a measurement result is not a single value but a set of values often expressed as a probability density function (PDF) Measurement uncertainty (VIM 2.26)

*Non negative parameter characterizing the dispersion of the quantity values being attributed to a measurand, based on the information used*

It seems very clear that the probability density function (PDF) representing the result is often summarized by the expectation and the variance (or the standard deviation) of the density function (PDF) that are the two statistics that the user of a measurement result is provided with.

## **1.2. Why is it Important to Report an Uncertainty with a Measurement Result ?**

The introduction of the GUM expresses clearly the reasons why is it important to report an uncertainty: “*When reporting the result of a measurement of a physical quantity, it is obligatory that some quantitative indication of the quality of the result be given so that those who use it can assess its reliability. Without such an indication, measurement results cannot be compared either among themselves or with a reference value given in a specification or standard*” [2].

Whatever the method used to evaluate the measurement uncertainty, this information is always necessary to support decision, conformity assessment etc...

## **1.3. Use of Uncertainty in Conformity Assessment**

It is now recognized in the testing community that it is as important to communicate the uncertainty on a specific measurement, as it is to report the measurement result itself. It is also clear that a measurement or a test result without an assessment of its quality is completely useless. It is impossible to compare different measurements of the same measurand or parameter without knowing the uncertainty. The assessment of results conformity with a specification limit calls for knowledge of the uncertainty of the result, in order to “evaluate” the conformance or non-conformance decision. Measurement and test results are the basic information underlying the statement of conformity of many products and activities. Figure 1 illustrates the risk related to a decision when uncertainty is considered. The figure presents a case where the measurement result is higher than the specification limit.

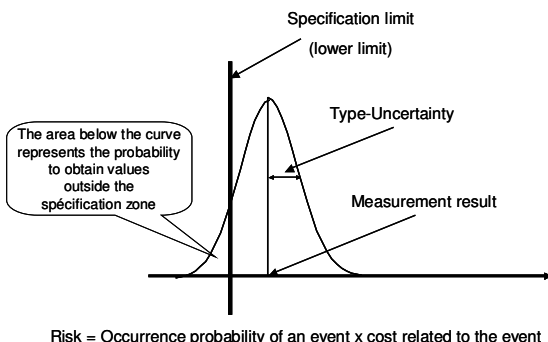


Figure 1. Illustration of the risk related to a decision when the uncertainty of measurement is considered.

In principle, the conformance can be asserted but due to the uncertainty of measurement, some values (which could be attribute to the measurand) could be below the limit. In this case, if the conformance is declared there is a risk of making a wrong decision and the probability of occurrence of this decision is evaluated by the area defined by the curve of the PDF and the limit. Up to now, only the ILAC Guide G8 [3] has given some practical rules to tackle this problem, but the TC 69 Technical Committee “Statistical Methods” of ISO has a working group on this subject.

## 2. Approaches to Uncertainty Evaluation

### 2.1. *GUM is the Master Document*

The Guide to the Expression of Uncertainty in Measurement (GUM) is recognized by the scientific community as the master document on measurement uncertainty. The GUM is based on sound theory and provides a consistent and transferable evaluation of measurement uncertainty.

### 2.2. *Why is it Important to Develop Alternative Methods in Addition to the GUM*

The application of the GUM uncertainty framework requires knowledge of the concept by the user, a mathematical model of the measurement process, the evaluation of standard uncertainties. But in many fields this is not used for technical, cultural or economical aspects. For instance, modeling the measuring process may not be feasible at least with reasonable effort.

Two main arguments presented in international documents are incentives to find alternative solutions: The ISO/CEI 17025 standard « General requirements for the competence of testing and calibration laboratories » opens alternative prospects: [...] *In certain cases the nature of the test method may preclude rigorous, metrologically and statistically valid, calculation of uncertainty of measurement. In these cases the laboratory shall at least attempt to identify all components of uncertainty and make a reasonable estimation, and shall ensure that the form or reporting of the result does not give a wrong impression of uncertainty. Reasonable estimation shall be based on knowledge of the performance of the method and on the measurement scope and shall make use, for example, previous experience and validation data [...]* In the same way ILAC (International Laboratory of Accreditation and Cooperation) has published a guide ILAC G17/2002 [4] Introducing the concept of uncertainty in testing in association with the application of standard ISO / CEI 17025 which present some clues for using existing data for uncertainty evaluation : [...] *The basis for the estimation of uncertainty of measurement is to use existing knowledge. Existing experimental data should be used (quality control chart, validation, round robin test, PT, handbooks etc.[...]*

### 2.3. Classification of the Different Approaches

Figure 2 shows a classification of the different methods.

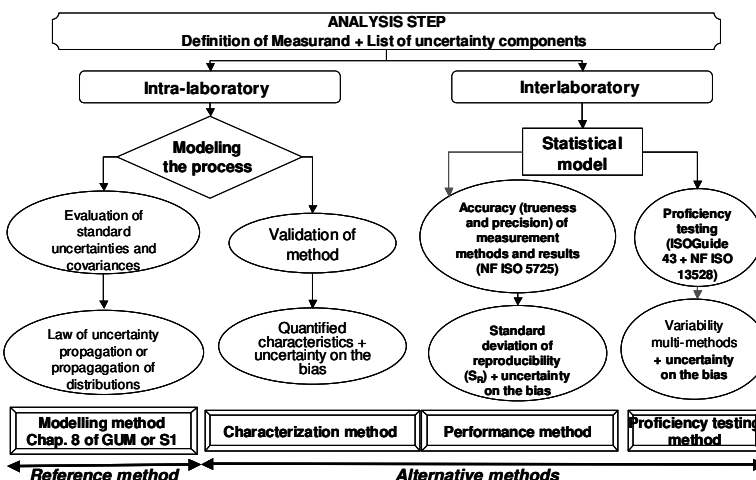


Figure 2. Classification of the different methods.

This classification is based on a distinction between uncertainty evaluation carried out by the laboratory itself (the intra-laboratory approach) and uncertainty evaluation based on collaborative studies (the interlaboratory approach). These approaches have been presented in several documents [5], [6]. The two approaches are then subdivided as follows:

- The intra-laboratory approaches: modelling of the measurement process with use of the law of propagation of uncertainty; and the single-laboratory validation approach.
- The interlaboratory approaches: use of “performance method” (ISO 5725) [7]; and “proficiency method” (ISO-Guide 43) [8].

#### ***2.4. Requirements Common to the Different Approaches***

Whichever method is used, it is always important:

- To define clearly, without ambiguity, the measurand or characteristic to be measured, analyzed or tested.
- To analyze carefully the measuring or testing process in order to identify the major components of uncertainty and to consider whether they are taken on board in the application of the propagation law of uncertainty or if they are active during the repetition of observations organized to evaluate repeatability and reproducibility or if they are included in collaborative studies.

It is also important to admit that, in some situations, we are not in a position to identify the components of the uncertainty.

#### ***2.5. Presentation of Intra-Laboratory Approaches***

##### ***2.5.1. The “Modelling Method”***

The GUM procedure for the evaluation of uncertainty is described in chapter 8 of the GUM. This procedure is based on a model (measurement model) formulated to take into account the interrelation of the input quantities that influence the measurand. The model includes corrections to take systematic effects into account; such corrections are essential to achieve traceability to stated references (e.g. CRMs, reference measurement procedures, SI units).

Contributions to uncertainty may be evaluated either by the statistical analysis of series of observations (type A evaluation) or by any other means (type B evaluation). Separate contributions, however evaluated, are expressed in

the form of standard deviations and are combined by using the law of propagation of uncertainty to evaluate the combined uncertainty on the result.

Two procedures can be used to evaluate the measuring uncertainty: the propagation law of uncertainty or the propagation of distributions by Monte Carlo simulation.

### 2.5.2. The “Characterization Method”

The single-laboratory validation approach uses the results of an experimental design organized for internal validation of the method. A chemist, say, wants to confirm that the performance capabilities of a method under consideration are consistent with the requirements of the application. It is accordingly necessary to evaluate the method performance capabilities, which is done with the help of characteristics such as repeatability, linearity, trueness.... This is fully described in the Eurachem guide, "The Fitness for Purpose of Analytical Methods: A Laboratory Guide to Method Validation and Related Topics" [9]. The most important of these characteristics are selectivity/specificity, repeatability, reproducibility (or intermediate precision VIM 3<sup>rd</sup> Edition 2.24), linearity, sensitivity, limit of detection, limit of quantification, ruggedness/robustness, and trueness. The “Characterization method” consists in establishing a simplified model to express the measurement process:

$$y = m + C_{True} + C_{Lin} + \sum_i c_i x_i + e \quad (1)$$

where

$y$ : an observed result

$m$ : (unknown) expectation of ideal results

$c_{True}$ : correction for trueness of the method

$c_{lin}$ : correction for nonlinearity

$c_i x_i$ : effects of factors of influence, with their sensibility coefficient

$e$ : random error term

The various terms of the equation (1) are assumed to be uncorrelated.

The estimation of the variance is:

$$u^2(y) = u^2(C_{True}) + u^2(C_{Lin}) + \sum_i c_i^2 u^2(x_i) + s_r^2 \quad (2)$$

where

$u(c_{True})$ : uncertainty of trueness

$u(c_{lin})$ : uncertainty of non-linearity

$u(x_i)$ : uncertainty of factors of influence

$s_r^2$ : the estimated variance of  $e$  (repeatability)

This approach can be used when the laboratory has access to references (CRMs, reference methods, etc.); without these possibilities, a Proficiency Testing Scheme may be an interesting solution.

## **2.6. Presentation of the Interlaboratory Approach**

The interlaboratory approach is based on the treatment of laboratories comparisons. It may be useful to remind the different objectives of interlaboratory comparison. Figure 3 illustrates the three types of laboratory comparisons.

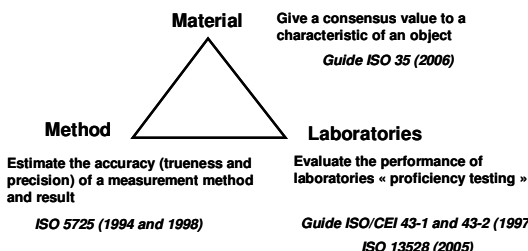


Figure 3. The 3 objectives of an interlaboratory comparison.

The comparisons relating to the method or to the laboratories will be used and described in the next paragraphs.

### **2.6.1. The “Performance Method”**

When for any reason a model describing the measuring process is not available, the major sources of variability can often be assessed by interlaboratory studies as stated in ISO 5725, “accuracy (trueness and precision) of measurement methods and results”, which provides estimates of repeatability (repeatability standard deviation  $s_r$ ), reproducibility (reproducibility standard deviation  $s_R$ ), and sometimes trueness of the method (measured as a bias with respect to a known reference value). This approach is fully described in ISO/TS 21748 [10], “Guidance for the use of repeatability, reproducibility and trueness estimates in measurement uncertainty estimation”.

Before the results of the interlaboratory comparison are used, it is very important compare the measurand under consideration and the measurand of the interlaboratory comparison attentively. In some cases, if any factors likely to influence the measurement results are not adequately covered by the collaborative study (sampling step, preparation of the sample, lyophilized

sample in place of human serum), because it is common practice to distribute prepared materials in collaborative study, etc.), they must be introduced in the model with the term  $\sum_i c_i x_i$  and their contribution to the total variance evaluated.

The statistical model presented in equation (3) is appropriate for analysis of measurement results. The hypothesis of this method is that the different factors (uncertainty components) will be estimate through the variance between laboratories

$$y = m + \delta + B + \sum_i c_i x_i + e \quad (3)$$

where

$y$ : an observed result

$m$ : (unknown) expectation of ideal results

$\delta$  : bias of measurement method

$B$ : laboratory component of bias

$x_i$  : deviation of factors that are assumed to possibly change between the collaborative study and the routine measurement

$c_i$ : sensitivity coefficient

$e$ : random error term

The various terms of equation (4) are assumed to be uncorrelated. The estimation of the variance is:

$$u^2(y) = u^2(\hat{\delta}) + s_L^2 + \sum c_i^2 u^2(x_i) + s_r^2 \quad (4)$$

where

$u(\hat{\delta})$  : uncertainty associated with  $\delta$

$s_L^2$ : estimated variance of  $B$

$u(x_i)$ : uncertainty associated with  $x_i$

$s_r^2$ : estimated variance of  $e$

with reproducibility given by:  $s_R^2 = s_L^2 + s_r^2$ . The model becomes:

$$u^2(y) = u^2(\hat{\delta}) + s_R^2 + \sum c_i^2 u^2(x_i) \quad (5)$$

Since this approach focuses on the performance of the method, it is sometimes referred as a “top-down” approach.

### 2.6.2. *The “Proficiency Testing Method” (PT Method)*

For several measurement fields the organization of PT constitutes one of the favorite means for the evaluation of laboratory competences. Currently, the main use of PT schemes consists in calculating the difference between the result of a laboratory and a consensus value established by the PT provider and then comparing this difference with the dispersion of the results.

Nevertheless, the relative disadvantage of PT samples is the lack of traceable reference values similar to those for certified reference materials. Consensus values in particular are prone to occasional error. This certainly demands due care in their use for uncertainty estimation, as indeed due care is recommended in recent PT protocols [11].

It seems evident that from the analysis of the deviation within the values obtained by one laboratory and the value assigned for the comparison, it is possible to obtain some interesting information on the bias of the laboratory. PT schemes can thus give information on systematic errors for laboratories and for a kind of measurement, when no reference materials are available.

The interlaboratory standard deviation (between laboratories) from on going studies can be used in several ways. For any customer using the analytical service, PT data is a key indication of the overall performance of laboratories. For a laboratory the standard deviation can be used as a first estimation of the standard uncertainty. But in a majority of situations, the uncertainty evaluated through this approach seems excessive. A promising method to improve the uncertainty still exploiting the results from a PT scheme is then the combination with the single laboratory validation approach.

## 2.7. *The Combination of Methods*

In practice, very often a combination of the various approaches needs to be used to assess the uncertainty. In the biomedical field, a project developed by the CHU (Centre Hospitalier Universitaire) of Rangueil, (Toulouse) and the LNE, has permit to propose a method of uncertainty evaluation for medicine laboratories. This method is fully described in [12]. The principle is based on the exploitation of the existing data, combining the results of the validation of the method (indicated as “characterization of the method” in figure 1) and those of the PT scheme (“PT method” in figure 1). In order to validate the approach CHU and LNE applied it on a practical case of a dosage of glucose in a sample of human plasma and a good coherence were found between this approach and the modelling approach.

### 3. Conclusions

In a recent past, testing laboratories were arguing against the evaluation of uncertainties because of its difficulties. Many of them were reluctant to apply the law of propagation of uncertainty with its apparent mathematical complexity. This paper presents several alternative approaches for laboratories, in particular ones based on interlaboratory comparisons.

But the difficulties remain the same, whatever the method used to evaluate the uncertainty of a result. It is essential to define the measurand clearly and to analyze the measuring process carefully in order to identify the factors that influence the result. These two tasks make greater demands on technical competencies in measurement techniques than on mathematical skills.

We have shown that the exploitation of the data deriving from PT schemes only suffers from the main drawback that the standard uncertainty can result quite higher than the one calculated by the modelling approach. This is due to the fact that this approach takes into account all the variability due to the different analytical methods that do not always have the same sources of uncertainty.

A promising method to improve the uncertainty still exploiting the results from a PT scheme is then the combination of the “PT approach” with the “characterization of method approach”. In any case, these new approaches to uncertainty evaluation will undoubtedly facilitate the presentation of results, their comparability, and their traceability to SI units.

### References

1. Guide ISO 99:2007 International Vocabulary of Metrology – Basic and General concepts and Associated Terms (VIM) 3<sup>rd</sup> edition
2. Guide to the expression of uncertainty in measurement (GUM), BIPM 1995
3. ILAC G8 1996 Guidelines on Assessment and Reporting of Compliance with Specification (based on measurements and tests in a laboratory)
4. ILAC G17/2002 Introducing the concept of uncertainty in testing in association with the application of the standard ISO / CEI 17025
5. EA–4/16 – Guidelines on the expression of uncertainty in quantitative testing, European co-operation of accreditation, 2004
6. Eurolab Technical Report N° 1/2007 Measurement uncertainty revisited: Alternative approaches to uncertainty evaluation
7. ISO 5725 Standard Accuracy (trueness and precision) of measurement methods and results

8. ISO/CEI Guide 43 (1997) Development and operation of laboratory proficiency testing
9. The fitness for purpose of analytical methods: A laboratory guide to method and related topics, Eurachem (1998) [www.eurachem.org](http://www.eurachem.org)
10. ISO/TS 21748 “Guidance for the use of repeatability, reproducibility and trueness estimates in measurement uncertainty estimation”
11. M Thompson, S L R Ellison, R Wood ; (2006) « The International Harmonized Protocol for the proficiency testing of analytical chemistry (IUPAC Technical Report) ; Pure Appl. Chem. 78: 145-196
12. P. Fisicaro, S. Amarouche, B. Lalere, G. Labarraque, M. Priel, Approaches to the uncertainty evaluation based on proficiency testing schemes in chemical measurements Accreditation and Quality Assurance

## THE PROPAGATION OF UNCERTAINTY RELATED TO THE CALIBRATION FUNCTIONS OF PLATINUM RESISTANCE THERMOMETERS AND POSSIBLE CORRELATION EFFECTS

A. S. RIBEIRO<sup>1</sup>, J. A. SOUSA<sup>2</sup>, C. O. COSTA<sup>1</sup>, M. G. COX<sup>3</sup>, P. M. HARRIS<sup>3</sup>

<sup>1</sup>*National Laboratory of Civil Engineering, 1700-066 Lisbon, Portugal*

<sup>2</sup>*Madeira Regional Laboratory of Civil Engineering, 9000-264 Funchal, Portugal*

<sup>3</sup>*National Physical Laboratory, Teddington, Middlesex TW11 0LW, UK*

In metrology laboratories, the transfer of traceability from primary standards (fixed points) to standard platinum resistance thermometers (SPRTs) is often based on the use of in-house methodologies with the fixed points defined by the International Temperature Scale, ITS-90. This process, however, is not simple, since different calibration functions apply to different temperature sub-intervals. The process has two stages: (1) estimation of the calibration parameters of the SPRT, and (2) the use of those calibration parameter estimates to obtain temperatures from measured values of electrical resistance. A relevant discussion is whether to use the above two stages or an approach given by combining them, taking into account the correlation associated with the calibration parameter estimates. In such cases, a further uncertainty component (a covariance) should be evaluated and included in the uncertainty budget. An example of application is given regarding the calibration and use of 25 Ω SPRTs in a metrology laboratory, considering two overlapping temperature sub-intervals. The comparison of the two approaches as regards the evaluation of uncertainty is the main concern of this paper.

### 1. Introduction

The International Temperature Scale ITS-90 [1] states that “between the triple point of equilibrium hydrogen (13,8033 K) and the freezing point of silver (961,78 °C)  $T_{90}$  is defined by means of platinum resistance thermometers calibrated at specific sets of defining fixed points and using specified interpolation procedures”. ITS-90 states that the evaluation of measurement uncertainty in the first comparison step in a traceability chain should be obtained with the highest degree of accuracy, as it is the initial component in the propagation of uncertainty within the chain.

The use of this traceability relation is widespread in primary and secondary metrology laboratories, where the use of SPRTs as transfer standards is important in the metrological infrastructure, being applied directly in the temperature domain and influencing many temperature-dependent quantities.

A previous paper [2] considered the evaluation of measurement uncertainty related to ITS-90 calibration functions and the comparison of a Monte method (MCM) and the GUM uncertainty framework [3]. This paper extends this work to examine correlation effects related to these functions, and the use of uncertainty information in further temperature measurement. The symbology, reference functions and constants of ITS-90 are used.

## 2. Measurement Model: Two-Stage and Single-Stage Approach

Temperature evaluation according to ITS-90 comprises two stages, a *calibration stage* and an *interpolation stage*, each comprising a sequence of operations. The sequence for the sub-interval (0 °C, 419,527 °C) is as follows:

### *Calibration stage*

1. Measure electrical resistance  $R_j$  at reference temperature  $T_j$ , for  $j = 1, 2, 3$ ;
2. Form the resistance ratios  $W_j = R_j/R_0$ , for  $j = 1, 2$ ; transform the  $T_j$  to  $t_j$  (°C);
3. Evaluate  $W_r(T_j)$  using 
$$W_r(t_j) = C_0 + \sum_{i=1}^9 C_i [(t_j / ^\circ\text{C} - 481) / 481]^i$$
 for  $j = 1, 2$ ;
4. Solve the equations  $W_j - W_r(T_j) = a(W_j - 1) + b(W_j - 1)^2$ ,  $j = 1, 2$ , for  $a$  and  $b$ .

### *Measurement interpolation stage*

5. Measure electrical resistance  $R$  at the unknown temperature  $T$  ( $\equiv t$  in °C);
6. Form the resistance ratio  $W = R/R_0$  (possibly using a new measured value for  $R_0$ , introducing for modelling purposes a new corresponding quantity  $\tilde{R}_0$ , say);
7. Form the reference resistance ratio  $W_r = W - a(W - 1) - b(W - 1)^2$ ;
8. Obtain  $t$  from the inverse function 
$$t = D_0 + \sum_{i=1}^9 D_i [(W_r(t) - 2,64) / 1,64]^i$$
.

$T$  is obtained from  $t$  in Step 8. Other sub-intervals have different formulae in steps 3 and 8. The traditional approach views this sequence as a two-stage process (Figure 1). In the calibration stage, the input quantities  $T_1$ ,  $T_2$ ,  $R_0$ ,  $R_1$  and  $R_2$  are provided to obtain the output quantities  $a$  and  $b$ . Then  $a$  and  $b$ , together with  $R_0$  (or  $\tilde{R}_0$ ) and  $R$ , become input quantities to the interpolation stage giving the output quantity  $T$ . Alternatively, the sequence could be treated as a single-stage process.

The comparison of the two approaches as regards the evaluation of uncertainty is the main concern of this paper.

### 3. Uncertainty Evaluation Using a Monte Carlo Method

To implement a Monte Carlo method (MCM), a mathematical model is used to relate an output quantity  $Y$  to input quantities  $X$  [4]. Here  $X$  corresponds to the fixed points and electrical resistances, and  $Y$  to the required temperature  $T$ . MCM propagates a large number of random draws from distributions characterizing  $X$  through the model to provide random draws from the distribution for  $Y(T)$ . From this output distribution the required information for  $T$  can readily be obtained, namely, a best estimate of  $T$ , the associated standard uncertainty, and a coverage interval for a prescribed coverage probability [5].

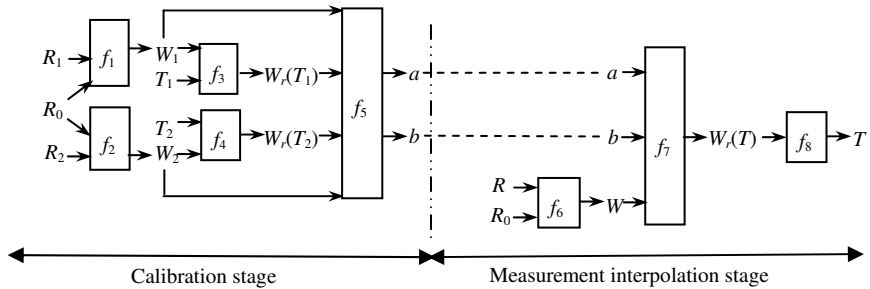


Figure 1. Chain of functions. The  $f_i$  denote mathematical models relating to the steps in the sequence of operations. For instance  $f_6$  is the determination of  $W$  from  $R$  and  $R_0$

Uncertainty evaluation is implemented differently according to the approach taken. For the two-stage approach, the calibration stage requires the generation of random sequences for the input quantities  $T_1$ ,  $T_2$ ,  $R_0$ ,  $R_1$  and  $R_2$  characterized by appropriate Gaussian distributions. These values are used to provide random draws from the joint distribution for the parameters  $a$  and  $b$ , and thence summary information for  $a$  and  $b$  consisting of their estimates and the associated covariance matrix. This summary information is used to establish an approximating bivariate Gaussian distribution for  $a$  and  $b$ . The interpolation stage requires the generation of random sequences for the quantities  $a$  and  $b$  (from this joint distribution) and  $R_0$  (or  $\tilde{R}_0$ ) and  $R$  to give random draws from the distribution for  $T$  and thence the required estimate, associated standard uncertainty and an expanded uncertainty. If it is equivalent for practical purposes to the single-stage approach, this two-stage approach can be useful when the two stages are to be applied by different users at different times.

The single-stage approach is easier to apply because it requires only the generation of random sequences for the input quantities  $T_1$ ,  $T_2$ ,  $R_0$  (and possibly  $\tilde{R}_0$ ),  $R_1$ ,  $R_2$  and  $R$ , the parameters  $a$  and  $b$  considered only as intermediate quantities in the computation.

#### 4. Practical Study for Two Interpolation Sub-Intervals of an SPRT

The propagation of uncertainty for both approaches is illustrated here using the calibration data for interpolation sub-intervals  $I_1$  and  $I_2$  of an SPRT given in Tables 1 and 2.

Table 1. Calibration data for an SPRT in the sub-interval  $I_1$  (0 °C to 419,527 °C)

Quantity	Fixed point temperature	Standard uncertainty	Quantity	Measured resistance	Standard uncertainty
$T_0$ / °C	0,010 00	0,000 21	$R_0/\Omega$	25,483 983	0,000 010
$T_1$ / °C	231,928 00	0,000 38	$R_1/\Omega$	48,230 983	0,000 010
$T_2$ / °C	419,527 00	0,000 52	$R_2/\Omega$	65,456 727	0,000 010

Table 2. Calibration data for an SPRT in the sub-interval  $I_2$  (-38,834 4 °C to 29,764 6 °C)

Quantity	Fixed point temperature	Standard uncertainty	Quantity	Measured resistance	Standard uncertainty
$T_1$ / °C	-38,834 40	0,000 22	$R_1/\Omega$	21,511 817	0,000 010
$T_0$ / °C	0,010 00	0,000 25	$R_0/\Omega$	25,482 744	0,000 010
$T_2$ / °C	29,764 60	0,000 18	$R_2/\Omega$	28,492 611	0,000 010

In  $I_2$  different relationships are used,  $I_2-$  for negative temperatures and  $I_2+$  otherwise, as described in section 2.

Table 3 gives the results obtained for  $I_1$  using MCM and  $10^6$  trials with a single-stage approach and a measured electrical resistance of 51,545 723 Ω with associated standard uncertainty 0,000 010 Ω. The results are estimates, 95 % coverage intervals and the computational accuracy [6, page 68] achieved.

Table 3. MCM results obtained for  $I_1$  with a single-stage approach

Quantity	Estimate	Expanded uncertainty	Computational accuracy	
$x$	$\hat{x}$	$U_{95}(\hat{x})$	$L^-$	$L^+$
$a \times 10^4$	-1,99(8)	0,084	0,000 4	0,000 5
$b \times 10^5$	-2,44(1)	0,58	0,003	0,004
$T(R)/\text{°C}$	267,165 8	0,000 8	$4 \times 10^{-6}$	$4 \times 10^{-6}$

The single-stage approach for  $I_2-$  and  $I_2+$ , was applied for measured electrical resistances of 23,266 937 Ω ( $R^-$ ) and 27,267 903 Ω ( $R^+$ ) and different reference functions. The results are presented in Table 4. The results for the

parameters  $a$  and  $b$  are not shown because they are of similar magnitude as the parameters presented in Table 3. However, the correlation associated with the estimates of  $a$  and  $b$  is very different for  $I_1$  and  $I_2$  (Figures 2 and 3). A possible explanation for the singular lack of correlation for  $I_2$  is that different reference functions are applied in the calibration stage, depending on the ITS reference temperature being lower or higher than 0 °C.

Table 4. MCM results obtained for  $I_2$  with a single-stage approach

Quantity	Estimate	Expanded uncertainty $U_{95}(\hat{x})$	Computational accuracy	
$x$	$\hat{x}$		$L^-$	$L^+$
$T(R^-) / ^\circ\text{C}$	-21,723 0	0,000 3	$1,7 \times 10^{-6}$	$1,8 \times 10^{-6}$
$T(R^+) / ^\circ\text{C}$	17,624 7	0,000 3	$1,7 \times 10^{-6}$	$1,6 \times 10^{-6}$

For the evaluation of temperature and measurement uncertainty in the second stage, it is required to generate new random sequences for the parameters  $a$  and  $b$  using the joint distribution for these quantities obtained from the first stage. The correlation diagrams so obtained were indistinguishable from Figures 2 and 3.

Finally, Table 5 presents results using MCM for the two-stage approach, which are comparable with regard to the respective uncertainties to those for the one-stage approach.

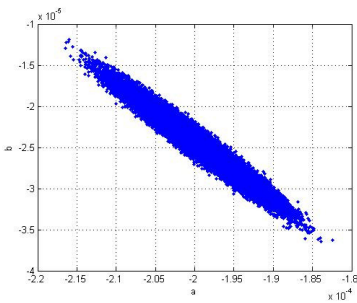


Figure 2 – Correlation diagram for the sequences for  $a$  and  $b$  for  $I_1$

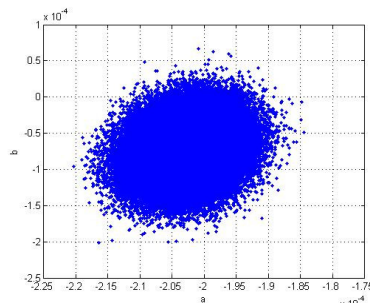


Figure 3 – As Figure 2 but for  $I_2-$

## 5. Conclusions

This paper has discussed the use of a single- and two-stage approach applied to the ITS-90 methodology, demonstrating that comparable measurement uncertainties can be obtained. The following conclusions are drawn:

Table 5. MCM results obtained for  $I_1$  and  $I_2$  with the two-stage approach

Quantity	Estimate	Expanded uncertainty	Computational accuracy	
$x$	$\hat{x}$	$U_{95}(\hat{x})$	$L^-$	$L^+$
$T(R)/^\circ\text{C}$	267,164 4	0,000 8	$1,3 \times 10^{-5}$	$1,2 \times 10^{-5}$
$T(R')/^\circ\text{C}$	-21,722 8	0,000 3	$1,8 \times 10^{-6}$	$1,9 \times 10^{-6}$
$T(R^+)/^\circ\text{C}$	17,624 8	0,000 3	$2,0 \times 10^{-6}$	$1,9 \times 10^{-6}$

1. The results appear to be insensitive to the assumption that, in the two-stage process, the calibration parameters have a joint Gaussian distribution;
2. Knowledge of the correlation depends on the temperature sub-interval. It is relevant to point out that in the overlapping region of sub-intervals  $I_1$  and  $I_2+$ , the measurement uncertainties are larger for the latter, possibly due to the negative correlation found in  $I_1$ , and this can be a criterion for adopting the calibration function associated with  $I_1$ ;
3. If the quantities corresponding to the two measured values of  $R_0$  are regarded as identical, the results obtained by MCM are negligibly different from those in which the quantities are regarded as different and independent. This conclusion was established in a related study.

## References

1. H. Preston-Thomas. The International Temperature Scale of 1990 (ITS-90). *Metrologia* **27**, 3–10 (1990).
2. A. Silva Ribeiro, J. Alves e Sousa, C. Oliveira Costa, M. Pimenta de Castro and Maurice G. Cox. Uncertainty evaluation and validation of a comparison methodology to perform in-house calibration of platinum resistance thermometers. *Int J Thermophysics DOI 10.1007/s10765-008-0409-x, Springer Science +Business Media, LLC 2008* (2008).
3. BIPM, IEC, IFCC, ISO, IUPAC, IUPAP, OIML. Guide to the Expression of Uncertainty in Measurement (Geneva, Switzerland: International Organization for Standardization, 1995), ISBN 92-67-10188-9.
4. W. Bich, M. G. Cox and P. M. Harris. Evolution of the Guide to the expression of uncertainty in measurement, *Metrologia* **43**, S161–S166 (2006).
5. C. W. Meyer and D. C. Ripple. Determination of the uncertainties for ITS-90 realization by SPRTs between fixed points. *Metrologia* **43**, 327-340 (2006).
6. P. Mac Berthouex and L. C. Brown. Statistics for Environmental Engineers, CRC Press, USA (1994).

## MEASUREMENT OF CHARACTERISTICS RELATED TO HUMAN PERCEPTION

GIOVANNI B. ROSSI

*Università degli Studi di Genova - DIMEC,  
Via All'Opera Pia 15A Genova, I-16145, Italia*

Measurement of characteristics related to human perception is discussed. A historical background is provided to explain how this subject has been critical for the entire science of measurement. Some current research activities are then surveyed and future research needs are addressed, including instrumentation, methods and models. Theoretical aspects are discussed and a new criterion for assessing measurability, which may be particularly useful for perceptual characteristics, is proposed.

### 1. Introduction

The measurement of characteristics related to human perception deserves great attention for both scientific and practical reasons. From the scientific standpoint, they are essential for the understanding of human perception, which in turn is basic for the study of cognitive functions. From the practical side, such measurements are inherently appealing, since they are customer oriented, highly informative and provide direct information on the perceived quality of devices and environment. The challenge is to enable such measurements to be as reliable as those occurring in physics and engineering, despite of the high inter and intra individual variability of sensory responses. This requires an interdisciplinary approach, embracing the physical, biological, psychological and social sciences. It is necessary to reach some agreement on the basic concepts and terms, to find a common language and, possibly, to develop a unified general theory of measurement.

In this paper the historical development of the subject will be briefly reviewed, starting from the origin of the theory of measurement in the 19<sup>th</sup> century, mentioning the schism between physicists and psychologists that arose in the middle of the 20<sup>th</sup> century and then outlining some of the relevant parallel development in the two areas, up to the present day.

Then current and future research needs will be reviewed, including instrumentation, methods and theoretical aspects. A new criterion for measurability will be proposed, that tries to combine scientific rigour and

openness to innovation and may be useful for addressing future studies in this area.

## 2. Historical background

### 2.1. *From the Origins to the Schism of the 1930s*

The reflection on the nature and the foundation of measurement is relatively recent and traceable to the midst of the 19<sup>th</sup> century. The start of these reflections is usually ascribed to Helmholtz, who considered what is the meaning of expressing through numbers situations of real objects and under what circumstances are we allowed doing so [2]<sup>\*</sup>. His answer was simple and convincing: if the characteristic is the amount of something, it may be thought as the sum of a number of elementary parts, or units, of that something. In this case measurement is equivalent to the counting of such units. This had been also recognised by Maxwell, but Helmholtz proceeded further and pointed out that, in order for measurement to take place, *the characteristic must have empirical properties similar to those that enable counting* that are order and addition.

This line of thought was continued by Campbell, in the beginning of the 20<sup>th</sup> century [4], who extended, in some regards, but radicalised also, Helmholtz's position. He emphasised, from a foundational standpoint, the role of "physical addition" in the construction of a reference measurement scale. Basically addition allows, once a unitary element has been chosen, to generate multiples and submultiples. So, once that the unit has been fixed, all the other elements of the scale may be assigned a unique value, since that value is constrained by the additivity property. Furthermore, since this procedure can not be applied to all the quantities, he stressed the importance of distinguishing between fundamental and derived quantities. The latter are derived from others thanks to an accepted physical law and this – he put in evidence – ensures their measurability.

Still by the end of the 19<sup>th</sup> century the Convention of the Metre was signed, which constitutes an international infrastructure for metrology. So at the turn from the 19<sup>th</sup> to the 20<sup>th</sup> century the paradigm of physical measurement, to quote Finkelstein, was firmly established [18].

But even prior to Helmholtz, Fechner, the recognised father of psychophysics had expressed the need of measuring phenomena, to put psychology on a sound scientific basis [1]. Yet, the measurement of sensation

---

\* The references have been listed in chronological order, in order to provide an overview of the historical development of the subject.

can not be as direct as that of physical quantities; rather it needs to be mediated by an accepted psychophysical law.

The problem of the measurability of sensory events was explicitly raised in the 1930s by the British Association for the Advancement of Science (BAAS) that appointed in 1933 a Committee to discuss and report about that. The Committee, composed by physicists and psychologists did not reach any agreement. Basically, the psychologists claimed that the result of a psychophysical experiment can not be expressed in purely physical terms, since it is based on perceived equalities and inequalities of sensations. On the other hand, physicists argued that Fechner's law, which was at that time the basis for indirectly measuring the intensity of a sensation, can not be proved unless it is possible to directly measure sensations, and sensations are not directly measurable, in their view, since they are not additive. So the final report, published in 1939, concluded with the impossibility of reconciling the two parts [5]. This caused a division in the scientific community with consequences up to the present day.

## **2.2. Twentieth Century Development**

After the BAAS Report, measurement in the two communities had an essentially parallel development in the two areas of physics/engineering and psychology, with noteworthy achievement in both of them, but with little communication.

On the psychological side, an extension of the scope of measurement must be mentioned, with the birth of what is more properly called psychometrics [3]. Whilst in psychophysics a characteristic of an object is investigated, as perceived by an average observer, in psychometrics the focus is rather on characters or traits of individuals, measured as responses to standard test items [8].

Concerning psychophysics, the contributions of Stevens must be mentioned. He provided replies to the arguments that were raised in the BAAS Committee against the measurability of sensory events. It was argued that sensations were not directly measurable and he introduced magnitude estimation, an experiment in which subjects describe the intensity of their sensations, as evoked by physical stimuli, by free number assignments [7]. The method was contested by some, but is still widely used today and in several cases it produces fairly reproducible results.

It was also argued, in the Committee, that physical addition was a necessary condition for measurement, and Stevens replied by proposing his famous fourfold classification of measurement scales [6]. In doing so he adopted a different perspective as the one by Helmholtz and Campbell: what characterises

a scale is not only the empirical relation that it is able to represent, but rather the kind of information it conveys. So a scale, in his view, is best connoted by the class of mathematical transformations that leave it unaffected. In this way it is possible to consider a broader range of empirical relations and additivity is no longer as important.

In a summary, with Stevens the psychophysics of the 20<sup>th</sup> century proved to be able to overcome the reservations raised in the BAAS Committee and measurement continued to be extensively used in that area [10-11]. More recently a noteworthy refinement of magnitude estimation was proposed by Berglund, the “master scaling” approach, which allows a kind of calibration of individual responses by the use of standard stimuli, with significant reduction of the influence of individual differences [19].

In the meantime physical measurements also evolved, although, as we have already noted, on a parallel track. Very remarkable was the systematisation of the International System of units (SI) in 1960, and the inclusion of luminous intensity as one of the base quantities. This is particularly relevant for our purposes, since it measures the physiological response to a physical stimulus. So the idea of explicitly accounting for persons’ responses was officially accepted in the SI [14, 20]. Yet this case has remained so far isolated although some interest in measurement related to perception seems now to be growing. The 21<sup>st</sup> CGPM (1999) [20] on the one hand recognised the need of new quantities in the emerging areas of Earth resources, the environment, human well-being, on the other was quite strict in requiring that such quantities should conform to the paradigm of derived measurement, traceable, as we have seen, to Campbell. Such measurements should be “in terms of well-characterised SI units so that they are reliable in the long term, are comparable worldwide and are linked to other areas of science and technology through the world’s measurement system established and maintained under the Metre Convention” – according to that resolution.

In the second half of the 20<sup>th</sup> century, a noteworthy systematisation of the theory of measurement was achieved under the so called representational approach [9, 12]. In such a framework, the notion of measurement scale is central and it encompasses what makes a measurement possible and meaningful. Indeed scales are characterised both by the empirical relations or operations that they are able to represent and by the class of admissible transformations that they may safely undergo. As an example, a ratio scale, the one that applies to most of the quantities in the SI, for example mass and length, represents both the empirical relation of order and the empirical operation of addition, and it may undergo similarity transformations, that is multiplication for a positive

constant. Such a transformation occurs when we change the conventional unit. A summary of the main scales considered in the representational systematisation is presented in Table 1.

Table 1. Summary of the main scales considered in the representational theory.

Empirical structure	Empirical relations	Scale type	Representation	Admissible transformations
NOMINAL	Equivalence among elements in each class	NOMINAL	$a \sim b \Leftrightarrow m(a) = m(b)$	Bi-univocal
ORDER	Weak order among the objects	ORDINAL	$a \succ b \Leftrightarrow m(a) \geq m(b)$	Monotone increasing
DIFFERENCE	As above plus weak order among intervals	INTERVAL	$\Delta_{ab} \succ \Delta_{cd} \Leftrightarrow m(a) - m(b) \geq m(c) - m(d)$	Linear positive $m' = \alpha m + \beta$ $\alpha > 0$
EXTENSIVE	As above plus a concatenation operation	RATIO	$a \sim b \circ c \Leftrightarrow m(a) = m(b) + m(c)$	Similarity $m' = \alpha m$ $\alpha > 0$

Noteworthy, in this approach the two standpoints that we have encountered in this brief historical survey, one based on empirical relations (Campbell) and one centred on admissible transformations (Stevens), are merged.

Although developed mainly in the area of behavioural sciences, this theory is now quite popular also among physicists and engineers, mainly thanks to the contribution of Finkelstein [13]. He proposed a well known definition of measurement, as the “a process of empirical, objective assignment of symbols to attribute of objects and events of the real world, in such a way as to represent them or to describe them”. In this definition the term “to represent” clearly points at the representational approach.

Lastly, at the end of the century the interest for quantities related to perception significantly increased in the physical metrology community, and the notion of *soft metrology* appeared. According to a report of the National Physical Laboratory (NPL) [17], soft metrology refers to “measurement techniques and models which enable the objective quantification of properties which are determined by human perception”, where “the human response may be in any of the five senses: sight, smell, sound, taste and touch”. The term soft here should not be intended in a negative sense, just as software is by no mean less important than hardware in computer science.

### 3. “Measuring the Impossible”

An important recent opportunity for progressing in our understanding of measurement related to perception has recently appeared with a European Call on “*Measuring the Impossible*”. This was a part (technically a “pathfinder”) of a more general session on *New and Emerging Science and Technology* (NEST) [24], which underlines the new and visionary atmosphere that backgrounds such matters. In this Call an explicit mention is made of the many reasons that push towards more research effort in this area. They include *scientific arguments*, “many phenomena of significant interest to contemporary science are intrinsically multidimensional and multi-disciplinary, with strong cross-over between physical, biological and social sciences”, *economic aspects*, “products and services appeal to consumers according to parameters of quality, beauty, comfort, which are mediated by human perception” and *social reasons*, “public authorities, and quasi public bodies such as hospitals, provide citizens with support and services whose performance is measured according to parameters of life quality, security or wellbeing”. Several projects have been launched on this topic, some of which are briefly mentioned here, just to give a feeling of what is going on.

The project MONAT, “Measurement of naturalness”, leaded by NPL, aims at measuring the naturalness of materials, such as fabrics, as the result of visual appearance and touch. The former is influenced by parameters as colour, texture, gloss and white light reflectance, the latter by thermal conductivity, hardness, surface topography and friction coefficient. This requires the measurement of physical and psychophysical characteristics, and their combination in order to account for multi sensory perceptual response and interpretation.

As another example, the project SYSPAQ, “Innovative sensor system for measuring perceived air quality”, coordinated by the Technical University of Berlin, aims at linking chemical measurements to sensory perception, for improving indoor air quality.

CLOSED, “Closing the loop of sound evaluation and design”, chaired by the Institut de Recherche et de Coordination Acoustique/Musique (France), aims at improving products by using perception information at the design stage.

Several other projects are currently at work that can not be mentioned here. For best benefiting of these activities, the need of a coordination action has been envisaged and implemented as MINET, *Measuring the Impossible Network* [25]. Technically, this is a Coordination Action, chaired by the University of Stockholm, for promoting discussion, cooperation and synergy among researchers operating in this field. This includes the implementation of a website

[25], including a database on the available expertise, the organisation of workshops and “think tank” events. In particular, recently an International Course has been held in Genova, Italy, on “Theory and methods of measurement with persons” [28]. The Course offered twenty lectures from scholars and scientists from all over Europe and USA that may be grouped in four main categories

- measurement in different disciplines (physics, psychology, behavioural and social sciences),
- theory and logics of measurement,
- multidimensional measurements and
- implementation areas.

The major challenge has been to have experts from different discipline work together, seeking a common language, and to develop a coherent lay out for such a multifaceted subject. Some of the main research challenges are now to be discussed.

## **4. Current and Future Research Activities**

### **4.1. A Concise Overview**

Intense research activity is required, in my opinion, on several distinct but complementary and synergic subjects.

Instrumentation-oriented research concerns both the measurement of the physical stimuli and of physiological responses. From the time of the “schism” the progress in these areas has been enormous and this would be, in itself, a good reason for reconsidering things. Concerning for example sound measurement, we now not only have high accurate measurement microphones, but also binaural recording devices, that allow measuring the acoustic stimuli as they appear at the input of the auditory system, sophisticated reproduction devices and processors and algorithms for the required signal processing. In the case of sight, we can measure not only luminous intensity and colour, but also parameters concerning the interaction between light and matter, as well as properties of surfaces, such has texture, which also involves sophisticated signal processing. Similar considerations apply for the other senses also.

Concerning the measurement of physiological responses, several techniques are available, a special place being held by brain imaging [15]. Roughly, there are two main approaches based either on the electromagnetic characteristic of the neural activity of the brain, including electroencephalography (EEG) and magneto-encephalography (MEG), or on the emodynamic paradigm, that is effects related to the blood flux associated to brain activity, comprising

functional magnetic resonance imaging (fMRI) and positron emission tomography (PET). These techniques are in rapid evolution, due to their great value in neurophysiology. For our standpoint, several metrological issues are of interest, including spatial and time resolution, measurement level (that is on which kind of measurement scale may their output be interpreted), calibration issues and, most important, how they correlate to subjective responses.

In fact, all these instrumentation-related possibilities should not make us forget that the testing of subjects remains the main track to psychological measurement [10, 11, and 22]. Several methods are available, ranging from the traditional methods of psychophysics, the method of limits, of average error and of constant stimuli, traceable to Fechner, and aiming at evaluating thresholds, just perceptible variations and, in general, equalities or inequalities of sensations, to the methods introduced by Stevens, magnitude and ratio estimation and production, to more advanced approaches, such as the master scaling technique [19]. Such methods have also benefited from the experiment-design techniques developed in the area of statistics. Other investigation techniques have been developed in the area of psychometrics, as we have briefly mentioned, and are based on the use of questionnaires [8].

So, in a summary, we have now several methods for gathering information from the real world and we must focus on how to best use such information. This is where measurement theory comes to play.

#### **4.2. Some Theoretical Issues**

Several conceptual and theoretical issues are, in my opinion, of prime interest in this area, including

- the language,
- the concept of measurement scale,
- the concept of measuring system (or instrument),
- the logic (deterministic, probabilistic, fuzzy...),
- the issue of measurability,
- multidimensional measurements,
- the development of unique system of measurable characteristics,
- issues related to models and complexity.

*Language* has been a main issue in the scientific and philosophical debate of the 20<sup>th</sup> century. In the metrology community a noteworthy revision of linguistic terms has been undertaken since the 1980s, with the publication of the International vocabulary of basic and general terms in metrology (1984), now at its third edition [27]. It is interesting to note the evolution of such editions, since

there has been a trend in including more disciplinary areas. It may be envisaged that in a near future man-related measurements may have a role there. Moreover, in the workshops and think tank events organized in the MINET, the issue of language soon emerged. It is natural that in a multidisciplinary environment this be a challenge. Yet with the revision of terms a revision of concepts and theories must also be considered, which may be beneficial for the entire world of measurement. In my opinion, it may be useful to concentrate on few terms that are necessary for expressing any theory of measurement [30].

One such term and concept is the *measurement scale*. This is central in the representational theory, as we have seen, and should be given more consideration in physical measurement also. For example, in primary metrology it is common to speak of units, yet what needs establishing is rather a reference scale. The confusion arises since it is somewhat taken from granted that the scale is of a ratio type and so it is fixed up to an arbitrary constant, the unit indeed. Yet when a primary reference experiment is devised, for example optical interferometry in the case of length, a system is realised that generates not only a situation corresponding to the unitary value, but also its multiples and submultiples: that is, what is actually generated is a reference scale.

Although we know much about scales nowadays, much research work is still needed, for ensuring that this concept is really common to measurement in both physical and behavioural sciences. This include, for example, a probabilistic formulation, a better understanding of the notion of scale in the case of derived quantities, a better systematization of the many psychological testing methods. In my opinion, such a research effort may be beneficial for physical metrology also. As an example, a precise definition of the uncertainty of a primary standard may outcome, as well as general criteria for the evaluation of inter-comparisons.

The concept of *measuring system*, or instrument, has a strange history. Although scientific instruments have been key in the development of modern science since the time of Galileo, it is curious to see how they have been ignored in the investigation on the foundation of measurement. Campbell himself, although being a physicist and plausibly well aware of the practical importance of instruments, denied their theoretical import and emphasized the role of the scale. Only very recently has the theoretical role of the measuring system been outlined. In particular, it is important to consider whether this is important only for physical measurements or for psychological ones also. I think that a general definition of measuring system is possible, which is also applicable to measurements that involve persons [26].

The question of the *logic* is transversal to all the above. If uncertainty is recognised as an essential aspect in measurement, a probabilistic or a fuzzy logic may be best suited. Systematic studies in these latter perspectives are still in their infancy.

*Measurability* will be addressed in the next section.

As outlined in the “Measuring the Impossible” Call, *multidimensionality* occurs when human perception and interpretation are involved. When shifting from one-dimensional to multidimensional measurements significant changes occur. In one dimension the key property is – as already recognized by Helmholtz and Campbell – order, whilst in the multidimensional case distance plays a key role. Moreover the problem of dimension reduction is also very important. My feeling is that in this area much effort has been spent in the development of data processing methods and tools, not paralleled by a proportional commitment to foundational aspects. For future work it would be wise to have foundational studies proceed together with the mathematical and numerical development of models and methods.

Considering the development of the SI we have noted the benefit of having the involved quantities treated as elements of a system [29]: a good point to be investigated in the future is whether and *to what extent physical and perceptual characteristics may be a part of the same system*.

Lastly, human perception and interpretation of, say, the living or working environment, may be understood through the mediation of *modelling*. Modelling of such functions raises the issue of *complexity*: this is another research frontier which is close to measurement.

### 4.3. Measurability

For dealing with this last issue we have to go back to the origins and to the problems raised by Helmholtz and Fechner. The problem of measurability is still open and, in this regard, I have recently made a proposal that is briefly recalled here.

I suggest that the general procedure for ensuring the measurability of a characteristic consists of the following steps:

1. to define the class of objects/events that manifest the characteristic,
2. to identify the empirical properties that define the characteristic,
3. to construct a reference measurement scale, that is to select a set of standard objects representative of the possible manifestations of the characteristic and to assign to each of them a measure that complies with empirical relations,

4. to find at least one empirical procedure for assigning measures to elements not included in the reference scale complying with empirical relations.

Than we may say that a characteristic is *measurable* if it is possible to satisfactorily apply the above procedure to it. As a final remark, it may seem that this procedure applies to fundamental measurement only, according to Campbell classification. In contrast, I suggest that the general framework is applicable to derived and conjoint measurements also: what makes a difference is essentially the way the reference scale is constructed. Anyway much more research is surely needed in this direction.

One final question for the reader: may the procedure above be a road map for the inclusion of some new perceptual quantity in the SI?

## 5. Final Remarks

The measurement of characteristic related to human perception and interpretation has been discussed, by briefly surveying the historical development of this subject from the 19th century up to the present day.

A reconsideration of such topic seems now to be possible and motivated by both scientific and socio-economical needs.

A new inter- and multidisciplinary perspective is envisaged that may be fruitful for the disciplines involved as well as for measurement science as a whole.

## References

1. G. T. Fechner, *Elemente der Psychophysik*, Leipzig: Breitkopf und Hartel, 1860, English translation: G. T. Fechner, *Elements of psychophysics*, Volume I, New York: Holt, Rinehart and Winston, 1966
2. H. von Helmholtz, *Zählen und Messen Erkenntnis – theoretisch betrachtet*, Philosophische Aufsätze Eduard Zeller gewidmet, Fuess, Leipzig, 1887
3. C. Spearman, *American Journal of Psychology* **15**, 201 (1904)
4. N. R. Campbell, *Physics – the elements*, (1920), reprinted as *Foundations of science*, Dover, New York, 1957
5. A. Ferguson, C. S. Myers, R. J. Bartlett, Qualitative estimates of sensory events, Final Report- British Association for the Advancement of Science, 1940, No. 2, 331-349
6. S. S. Stevens, *Science*, **103**, 667 (1946)
7. S. S. Stevens, Measurement, psychophysics and utility, in: C. W. Churchman & P. Ratoosh (Eds.), *Basic Concepts of Measurements*, Cambridge University Press, Cambridge, 1959, pp 1-49.

8. F. M. Lord, M. R. Novick, Statistical theories of mental test scores, Addison Wesley, Reading MA, 1968
9. D.H. Krantz, R.D. Luce and P. Suppes, and A. Tversky, Foundations of Measurement, Vol 1-3, Accademy Press, New York, 1971-1990.
10. F. Nowell Jones, History of psychophysics and judgement, in E. C. Carterette, M. P. Friedman (Eds.) Handbook of perception, vol. 2, Academic Press, New York, 1974
11. J. C. Baird, E. Noma, Fundamentals of scaling and psychophysics, Wiley, new York, 1978
12. F.S. Roberts, Measurement theory, Addison-Wesley, Reading, MA, 1979.
13. L. Finkelstein and M.S. Leaning, *Measurement* **2** 25 (1984).
14. R. A. Nelson, L. Ruby, *Metrologia*, **30** 55 (1993).
15. J. D. Bronzino (Ed.) The biomedical engineering handbook, CRC & IEEE Press, 1995
16. S. Muravyov, V. Savolainen, *Measurement*, **29**, 209 (2001)
17. M. R. Pointer, New directions – Soft metrology requirements for support from mathematics statistics and software, NPL Report CMSC 20/03, 2003.
18. L. Finkelstein, *Measurement* **34** 39 (2003).
19. B. Berglund, E. Harju, *European Journal of Pain*, **7** 323 (2003)
20. Rastello M L 2004 Photometry and photobiology: quantities and units, Proc. of 2nd Int. Symp. on Meas., An. and Modeling of Hum. Funct. and The 1st Mediterranean Conf. on Meas., Genova, 2004, 75-76
21. L. Finkelstein, *Measurement* **38** 267 (2005)
22. G. B. Rossi, F. Crenna, M. Panero, *Metrologia* **42** 97 (2005) .
23. G. B. Rossi, *Measurement*, **39** 34 (2006).
24. <http://www.cordis.lu/nest/>
25. <http://minet.wordpress.com/>
26. G. B. Rossi, *Measurement*, **40** 545 (2007)
27. ISO/IEC 2007 International Vocabulary of metrology - Basic and general concepts and associated terms (VIM)
28. <http://minet.wordpress.com/events/trainingcourse2008/>
29. A. Wallard, *Metrologia* **45** 119 (2008).
30. G. B. Rossi, Some key concepts and terms in measurement having a cross-disciplinary impact, 12<sup>th</sup> IMEKO TC1 andTC7 Symp. On Man, Science and Measurement, 3-5 September 2008, Annecy, France

## LOSSLESS COMPRESSION OF COMPUTER TOMOGRAPHY POINT CLOUDS

R. SCHMITT, P. FRITZ

*Laboratory for Machine Tools and Production Engineering  
RWTH Aachen University, Steinbachstraße 19, Aachen, 52074, Germany  
E-Mail: p.fritz@wzl.rwth-aachen.de*

This paper proposes a new method for an efficient lossless compression of computer tomography (CT) images. For this, we adapted a delta encoding scheme from PNG images to CT data by applying linear filter operations to the CT scans. After applying improved delta filters, we performed both run-length and entropy encoding using the deflate method. For the evaluation of the proposed methods, we performed CT scans of objects and compressed the resulting point clouds. As a result, we achieved an additional reduction of the data size compared to standard compression methods by up to 13.1 percent.

### 1. Introduction

The application of computer tomography (CT) in modern metrology is of continuing interest. Volumetric CT scans enable the non-destructive inspection of components whereas destructive inspection is time-consuming and expensive.

One major problem of computer-tomography measuring tasks is the size of the resulting scans. For example, the size of a medium-sized data set with a resolution of  $1000 \times 1000 \times 1000$  voxels and a bit depth per voxel of 16 bit is 1.9 GB. Hence, much effort has to be spent to carry out the measurement, to archive the data, or to transmit them to other manufacturing units. Instead of a lossy compression scheme as proposed in [1], we introduce a lossless method. Although the compression rates are lower, lossless compression methods do not affect the measurement uncertainty in further evaluation steps. This method is appealing for CT scanners for which customers demand performance acceptance tests: In contrast to lossy algorithms like JPEG or JPEG-2000, which discard seemingly less relevant information, with lossless methods, we can obtain a bit-by-bit reconstruction of the original data set. Hence, any additional conformance tests are needed when performing lossless compression methods on the scanned data.

Section 2 contains a review of related work on lossless compression techniques for 2D data and adapts them to volumetric CT data. Section 3 provides an empirical proof that our proposed method is superior to standard methods.

## 2. Proposed Compression Method

The most well known lossless compression format for 2D image data is *Portable Network Graphics (PNG)* [2, 3]. To compress the images, it uses a mix of several encoding paradigms. The first is *run-length encoding (RLE)* and detects repeating patterns in the data and encodes them with a single symbol. The method proposed in this paper uses a refined version of RLE that uses a sliding window to detect repeating patterns [4] (Figure 1a). Therefore, the number of different tokens within the data decreases after the RLE step.

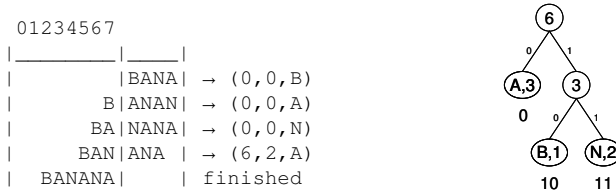


Figure 1: Standard encoding schemes. a) Example of run length encoding using a sliding window.  
b) Example of entropy encoding of 3 different tokens.

The second encoding scheme used for PNG and the proposed lossless CT-compression algorithm is *entropy encoding*. Tokens with a higher frequency are stored using fewer bits than tokens that appear only rarely, which provides a more bit-efficient representation of the data. Figure 1b provides an example of entropy encoding: The example data set (again, the word “banana”) consists of token *a* with frequency 3, *b* with frequency 1 and *n* with frequency 2. If each of the 6 tokens would be equally-sized coded with 2 bits, we would end up with 12 bits for the whole word. With Huffman encoding [5], the tokens are stored in a binary tree and are encoded with the path labels from the root to the leaf. In our example the data set is encoded with 9 bits, which is a compression rate of 25%. The combination of these 2 encoding paradigms is referred to as the *deflate* method [6] and is widely used for both image (PNG) and general data compression (ZIP).

This work focuses on the third method that is *delta encoding*. We split the CT scans into single image slides and perform several linear filter operations on each slide. The objective is to compute a *predictor* from the neighbor voxels

and save only the difference from the real voxel and the predicted value. If we assume that neighboring pixels would only differ slightly, a straightforward operation is using the upper or the left neighbor voxel within the same slide as predictor (see Figure 2). We adapted the more sophisticated Paeth filter [7] to 3 dimensions to incorporate interrelations of subsequent slices. This reduces the data redundancy, as changes of voxels from slide to slide are quite small. An optimal delta should be near to zero, as then the following encoding steps that are RLE and Huffman encoding achieve better encoding results on the repeating elements.

119	117	123	118
113	114	114	108
39	39	33	27
22	23	23	20
23	22	20	22
18	20	19	20

119	-2	6	-5
113	1	0	-6
39	0	-6	-6
22	1	0	-3
23	-1	-2	2
18	2	1	1

Figure 2: Example of delta encoding using the sub filter.

Let  $x$  be a CT scan with  $i$  rows,  $j$  columns and  $k$  layers and let  $x[i, j, k]$  denote a single voxel. For operations that do not consider the interrelationships of at least two layers, we denote a voxel for convenience  $x[i, j]$ . Now, we define several linear filters for preprocessing the data using a delta scheme:

The easiest filters operate on a single layer. The first is the *sub* filter that subtract each column by its predecessor column given by

$$x[i, j] = x[i, j] - x[i, j - 1] \quad (1)$$

and the equivalent *up* filter that operates on the rows of each layer given by

$$x[i, j] = x[i, j] - x[i - 1, j]. \quad (2)$$

The *average* filter is a combination of (1) and (2):

$$\begin{aligned} p[i, j] &= \lfloor (x[i - 1, j] + x[i, j - 1]) / 2 \rfloor \\ x[i, j] &= x[i, j] - p[i, j] \end{aligned} \quad (3)$$

A refined filter is the *Paeth* filter that also incorporates voxel changes in diagonal direction. We subtract the predicted voxel value from each other  $x[i, j, k]$  that will result in a minimal delta. The filter is defined by the pseudo code below:

```

for each voxel  $x[i, j, k]$  do
    a =  $x[i-1, j, k]$ 
    b =  $x[i, j-1, k]$ 
    c =  $x[i-1, j-1, k]$ 
    p = a + b - c
    pa = |p - a|
    pb = |p - b|
    pc = |p - c|
    if pa <= pb and pa <= pc then Pr = a
    elseif pb <= pc then Pr = b
    else Pr = c
     $x[i, j, k] = x[i, j, k] - Pr$ 

```

(4)

Now, we also take into account the interrelationships of neighboring layers by adapting the average filter to the *average-3D* filter:

$$\begin{aligned}
 p[i, j, k] &= \lfloor (x[i-1, j, k] + x[i, j-1, k] + x[i, j, k-1]) / 3 \rfloor \\
 x[i, j, k] &= x[i, j, k] - p[i, j, k]
 \end{aligned}
 \tag{5}$$

The adaptation of the Paeth filter is more sophisticated, because each voxel  $x$  has 7 neighbors in 3D (see Figure 3). Also, the calculation of  $p$  has to be modified to 3D. As in (4), we use a linear combination of neighboring voxels to estimate  $p$ . To select an optimal combination, we performed a grid search to estimate the optimal weights. To keep the energy of the predictor constant, the sum of the linear weights has to be equal to 1. Experiments have shown that for each voxel  $x$  selecting

$$p = a + b - c - d - e + f + g \tag{6}$$

provides the best results (Chapter 3). The remaining operations in Paeth 3D are analog to the standard Paeth filter.

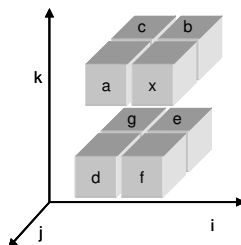


Figure 3: Naming of the neighbor voxels for the Paeth 3D operation.

### 3. Experimental Results

To evaluate our method, we performed and compressed 3 different CT scans that are a brush disk, a mobile phone and a noisy scanned chocolate egg that contains a hidden toy and should be an example for noisy data (see Table 1 and Figure 4). We performed all scans with an industrial CT with a starting resolution of  $1024 \times 1024 \text{ à } 800 \mu\text{m}$ . After the scan, we discard the space that contains no object and end up in the final object resolution.



Figure 4: CT scans of the experimental data. a) Brush disk, b) cell phone c) chocolate egg.

Table 1: Experimental setup

	Resolution	Layers	Size [MB]	SNR [dB]
Brush disk	$429 \times 408$	400	133	5.0
Cell phone	$912 \times 912$	503	797	27.4
Chocolate egg	$760 \times 760$	841	926	-0.1

Table 2 shows the performance of different delta filters on the testing data. The Paeth 3D filter was the most successful among all CT scans with an increase of the compression rate of 7.5 percent on the brush disk, 13.1 percent on the cell phone and only 2.5 percent on the chocolate egg.

Table 2: Compression rates of different delta filters.

	No delta [%]	Sub [%]	Up [%]	Average [%]	Average 3D [%]	Paeth [%]	Paeth 3D [%]
Brush disk	19.5	24.0	24.5	25.8	26.6	26.7	27.3
Cell phone	42.0	44.6	46.2	46.0	54.1	46.9	<b>55.1</b>
Chocolate egg	35.0	36.5	36.4	36.8	37.5	37.5	37.5

One reason for the good performance on the scanned mobile phone is that the portion of scanned air is lower than in the other scans. Air around or within a component result in noisy volume parts in the CT scans that have very low compression rates using lossless compression algorithms. As the chocolate egg has the lowest signal to noise ratio, the compression rates are much lower. Also, the lower the SNR of a CT scan, the smaller is the gain of using 3D delta filters.

For an optimal choice for the Paeth 3D predictor, we performed a grid search on the brush disk data to optimize the weights of the voxels a–g. Table 3 shows that the predictor in (6) is optimal. Interestingly, the third best combination of the optimization is the 2D Paeth and the fourth best the Average 3D filter.

Table 3: Combination weights of the 4 best Paeth predictors on the brush disk data.

Compression rate [%]	a	b	c	d	e	f	g
<b>27.3</b>	1	1	-1	-1	-1	1	1
26.7	1/3	1/3	0	1/3	0	-1/3	1/3
26.7	1	1	-1	0	0	0	0
26.6	1/3	1/3	0	0	0	1/3	0

Figure 5 illustrates the effect of delta filtering on an example CT scan: The range of possible gray values decreases considerably from  $\sigma = 1500$  to  $\sigma = 250$ , which yield the improved compression rates.

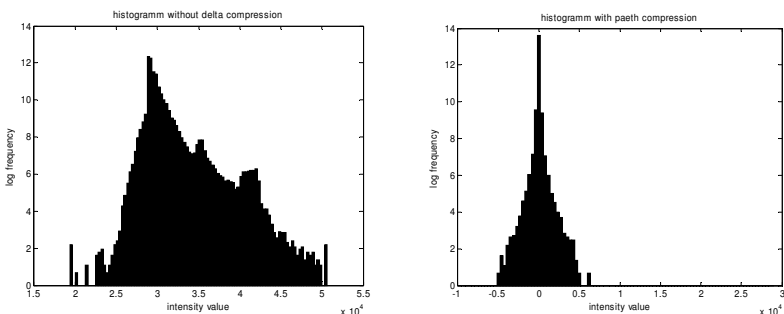


Figure 5: Histograms of different CT scans. a) without any delta filtering. b) with Paeth filter.

#### 4. Conclusions

We presented several methods for the lossless compression of CT data and proposed 3D-adapted delta compression filters. Experiments with 3 scanned objects proved that delta filtering improves the performance of run-length and Huffman

encoding especially on non-noisy data sets. Among all applied filters, the Paeth-3D filter was the most successful.

### Acknowledgments

We would like to thank Sebastian Pollmanns for providing the processed CT data. This work was funded by the Deutsche Forschungsgemeinschaft (DFG) under contract no. SCHM 1856/4-1.

### References

1. L. Ying and W.A. Pearlman, “Four-Dimensional Wavelet Compression of 4-D Medical Images Using Scalable 4-D SBHP”, in *Data Compression Conference*, pp. 233–242, 2007.
2. W3C, “PNG (Portable Network Graphics) Specification”, [www.w3.org/TR/PNG/](http://www.w3.org/TR/PNG/), Oct. 1996.
3. Greg Roelofs, *PNG: The Definitive Guide*, O'Reilly, Sebastopol, 1999.
4. J. Ziv and A. Lempel, “A Universal Algorithm for Sequential Data Compression”, in *IEEE Transactions on Information Theory*, vol. 23, no. 3, pp. 337–343, 1977.
5. D.A. Huffman: “A Method for the Construction of Minimum-Redundancy Codes”, in *Proceedings of the IRE*, vol. 40, no. 8, pp. 1098–1102, 1952.
6. P. Deutsch, *DEFLATE Compressed Data Format Specification*, RFC 1951, version 1.3, 1996.
7. A.W. Paeth, “Image File Compression Made Easy“, in J. Arvo (editor), *Graphic GEMS II*, Academic Press, San Diego, pp. 93–100, 1991.

## DECLARATION AND SPECIFICATION OF A GEOMETRICAL PART IN THE LANGUAGE OF GEOMETRIC ALGEBRA

PHILIPPE SERRE, MIREILLE MOINET

*Laboratoire d'Ingénierie des Systèmes Mécaniques et des Matériaux, LISMMMA  
Institut Supérieur de Mécanique de Paris, SUPMECA  
3, rue Fernand Hainaut, 93407 Saint-Ouen Cedex, France*

ANDRE CLEMENT

*Dassault Systèmes  
9, quai Marcel Dassault, 92156 Suresnes Cedex, France*

Declaration and specification of a geometrical part is formulated in the language of Geometric Algebra, a unified mathematical language based on Clifford algebra, developed by D. Hestenes since 1966. Some of the modern applications of Clifford geometric algebra are: computer vision, CAD systems, robotics and screw theory, automated theorem proving, symbolic algebra and numerical algorithms. First, we will recall as briefly as possible the TTRS theory and the thirteen geometrical constraints necessary and sufficient to specify any technical dimensions of a mechanical part and their “softgage” compatible with the ISO standard. Then we will give a description of the Geometric Algebra. Finally we will show how Geometric Algebra allows us to write down the thirteen constraints by an algebraic expression not only coordinate free but much more simple and taking into account the chirality of objects.

### 1. Introduction

To modelize a geometrical part in Computer Aided Design systems, two methods are widely used. The first one is the *procedural modelling*. Following this method, expected shapes are described by an ordered list of elementary constructions. For instance, a geometric object is: first an extrusion, second a revolution, third a hole, and so on. At each step, the position of the new element is defined with respect to any geometric element already constructed. The second method is the *declarative modelling* (or acausal modelling). Following this method, objects are described by a non-ordered set of geometric elements **and** a non-ordered set of geometric constraints between them. The geometric solution is provided by a specific solver (called GCS for Geometric Constraints Solver, see [1] and [2]).

Acausal modelling has many advantages compared to the procedural methods. In fact, “acausal” models are easy to build and modify (procedural

model are difficult to build and extremely hard to modify), “acausal” models require highly elaborated tools to handle them efficiently and “acausal” modelling is a convenient way to express specifications (procedural modelling is a convenient way to express explicit computations). For all these reasons, we consider “acausal” modelling is a well adapted solution to declare and specify a geometrical part, and we will present a new solution based on concepts of *Technologically and Topological Related Surfaces* (TTRS) and *Geometric Algebra* (GA).

TTRS theory was build by A. Clément in 1990 [3]. The study of the displacement group of the solids in the three-dimensional Euclidean space was the start point of his research. This group is divided into twelve subgroups. When a displacement is applied to a surface rather than a solid, this displacement may always be decomposed in two parts: the first part which really displaces the surface (and which can be called significant displacement), and the second part (possibly the identity displacement) which leaves the surface invariant in simply making it sliding on itself.

Finally, it is proved that all displacements, which leave surface invariant, belong to the same subgroup. That subgroup is called the invariance subgroup of the surface. Among the twelve subgroups of displacement, there exist only seven invariance subgroups of surfaces.

- $\{E\}$  Identity transformation,
- $\{T_u\}$  Unidirectional translation,
- $\{R_l\}$  Rotation about a line,
- $\{H_{L,p}\}$  Screw displacement,
- $\{C_r\}$  Translation combined with a rotation about an axis,
- $\{G_p\}$  Plane on plane movement,
- $\{S_o\}$  Spherical displacement.

The next stage of Clément’s work was the study of composition of these seven subgroups. By definition, an association between two subgroups must belong to another (or same) subgroup. This association, called TTRS, represents the relative position of one surface with respect to another one. So, TTRS is either a pair of surfaces, or a pair of TTRS, or a pair composed with a surface and a TTRS, belonging to the same solid. An important result was provided after the study of the twenty-eight association cases. In fact, it is proved that the number of reclassifying cases is equal to forty-four.

The number of reclassifying cases between points, lines and planes, is found when we remark that a point belongs to  $\{S_o\}$  subgroup, a line belongs to  $\{C_r\}$  subgroup and a plane belongs to  $\{G_p\}$  subgroup. In fact, it is demonstrated that

the number of reclassifying cases between point, lines and plane is equal to thirteen [4]. Thanks to these results, we know that the number of case studies is finite.

The other problem is to determine which solution is well adapted to represent geometric objects (only points, lines and planes here). Usual solutions are using coordinates of these objects in a specific Cartesian reference frame. In [5] D. Michelucci explains why this solution is often irrelevant in declarative modelling. He proposes another solution based on the Cayley-Menger determinants [6]. Also P. Serré, in [7] and [8], proposes a solution based on vector representation and metric tensor.

In this paper, geometric objects and TTRS are represented by Geometric Algebra language, a coordinate free formulation. The next section presents shortly the GA, and following section prove that TTRS can be represented by members of the GA.

## 2. Geometric Algebra, an Introduction

Geometric algebra and its extension to geometric calculus unify, simplify, and generalize vast areas of mathematics that involve geometric ideas [9]. They also provide a unified mathematical language for physics, engineering, and the geometrical aspects of computer science (e.g., graphics, robotics, computer vision) (see [10] and [11]).

There exist two main methods to present geometric algebra: top down or bottom up. The top-down method, useful only for mathematicians, starts from tensor algebra. In [12], B. Fauser and R. Ablamowicz explain: “The main advantage of the tensor algebra method is its formal strength. Existence and uniqueness theorems are most easily obtained in this language. Mathematicians derive almost algebras from the tensor algebra by a process called factorization. If one singles out a two-sided ideal  $I$  of the tensor algebra, one can calculate “modulo” this ideal. That is all elements in the ideal are collected to form a class called “zero”  $[0] = I$ . Every element is contained in an equivalence class due to this construction. Denote the tensor algebra as  $T(V) = R \oplus V \oplus \dots \otimes_n V \oplus \dots$  and let  $x, y, \dots \in V$  and  $L, M, \dots \in T(V)$ .

In the case of Clifford algebras, one selects an ideal of the form:  $I_{Cl} = \{X \mid X = L \otimes (x \otimes x - Q(x)I) \otimes M\}$ .

One could say that GA is a kind of “vectorization” on tensor algebra. On the other hand, the bottom-up method is good for engineers, starting from vector space and building step by step the GA. This is explained in the next section.

## 2.1. The Geometric Algebra

The most popular algebraic structure today for Euclidean  $n$ -space is the inner product space  $\mathbf{R}^n$ . This section describes a powerful extension of this structure, the geometric algebra  $\mathbf{G}^n$ .

- $\mathbf{G}^n$  has an associative noncommutative product with identity. The product is called the *geometric product*.
  - $\mathbf{G}^n$  is a vector space extending the vector space  $\mathbf{R}^n$ . It has dimension  $2^n$ . Its vectors are called *multivectors*. Scalars are multivectors.
  - The geometric product (left and right) distributes over multivector addition.
- We now elaborate individually these three aspects of  $\mathbf{G}^n$ . This will give us the rules for computing in  $\mathbf{G}^n$ . It will not prove that a mathematical structure satisfying the rules exists.

### 2.1.1. The geometric product

The geometric product of multivectors is based on a single rule. For every vector  $\mathbf{u}$  in  $\mathbf{R}^n$ ,

$$\mathbf{u}\mathbf{u} = \mathbf{u} \cdot \mathbf{u} \quad (1)$$

This equation shows that nonzero vectors have an inverse:  $\mathbf{u}^{-1} = \mathbf{u}/(\mathbf{u} \cdot \mathbf{u})$ .

Inner product between two vectors  $\mathbf{u}$  and  $\mathbf{v}$  is expanded as following:

$$\mathbf{u} \cdot \mathbf{v} = \frac{1}{2}((\mathbf{u} + \mathbf{v}) \cdot (\mathbf{u} + \mathbf{v}) - \mathbf{u} \cdot \mathbf{u} - \mathbf{v} \cdot \mathbf{v}) \quad (2)$$

Using equation (1) and distributivity property, we prove that

$$\mathbf{u} \cdot \mathbf{v} = \frac{1}{2}((\mathbf{u} + \mathbf{v})(\mathbf{u} + \mathbf{v}) - \mathbf{u}\mathbf{u} - \mathbf{v}\mathbf{v}) = \frac{1}{2}(\mathbf{u}\mathbf{v} + \mathbf{v}\mathbf{u}) \quad (3)$$

If  $\mathbf{u}$  and  $\mathbf{v}$  are orthogonal, then the equation (3) gives

$$\mathbf{v}\mathbf{u} = -\mathbf{u}\mathbf{v} \quad (4)$$

Example:  $(\mathbf{u}\mathbf{v})^2 = \mathbf{u}\mathbf{v}\mathbf{u}\mathbf{v} = -\mathbf{u}\mathbf{u}\mathbf{v}\mathbf{v} = -(\mathbf{u} \cdot \mathbf{u})(\mathbf{v} \cdot \mathbf{v})$ . Thus if  $\mathbf{u}$  and  $\mathbf{v}$  are nonzero, then  $(\mathbf{u}\mathbf{v})^2 < 0$ . Therefore  $\mathbf{u}\mathbf{v}$  is not a scalar or a vector. It is something new, a 2-vector (also called *bivector*).

### 2.1.2. Multivectors

We illustrate the vector space  $\mathbf{G}^n$  with  $\mathbf{G}^3$ . It is  $2^3 = 8$  dimensional. Let  $\{\mathbf{e}_1, \mathbf{e}_2, \mathbf{e}_3\}$  be an orthonormal basis of  $\mathbf{R}^3$ . Then a basis for  $\mathbf{G}^3$  is

- 1 : basis for 0-vectors (or scalars),
- $\{\mathbf{e}_1, \mathbf{e}_2, \mathbf{e}_3\}$  : basis for 1-vectors (or vectors),
- $\{\mathbf{e}_1\mathbf{e}_2, \mathbf{e}_2\mathbf{e}_3, \mathbf{e}_3\mathbf{e}_1\}$  : basis for 2-vectors (or bivectors),

- $\{\mathbf{e}_1\mathbf{e}_2\mathbf{e}_3\}$  : basis for 3-vectors (or trivectors).

We have used a specific orthonormal basis of  $\mathbf{R}^3$  to describe the vector space  $\mathbf{G}^3$ , but all orthonormal bases of  $\mathbf{R}^3$  give the same vector space  $\mathbf{G}^3$  with the same bivectors and trivectors.

### 2.1.3. Distributivity

To multiply any two multivectors expanded with respect to the basis above, use distributivity and the product rules. For example,

$$\begin{aligned}(2 - \mathbf{e}_1\mathbf{e}_2)(\mathbf{e}_1 + 3\mathbf{e}_2) &= 2\mathbf{e}_1 + 6\mathbf{e}_2 - \mathbf{e}_1\mathbf{e}_2\mathbf{e}_1 - 3\mathbf{e}_1\mathbf{e}_2\mathbf{e}_2 \\ &= 2\mathbf{e}_1 + 6\mathbf{e}_2 + \mathbf{e}_2 - 3\mathbf{e}_1 \\ &= -\mathbf{e}_1 + 7\mathbf{e}_2\end{aligned}$$

## 2.2. The Inner and Outer Products

We investigate the geometric product of two given vectors  $\mathbf{u}$  and  $\mathbf{v}$  in  $\mathbf{R}^n$ . Let  $\{\mathbf{e}_1, \mathbf{e}_2\}$  be an orthonormal basis for a plane containing the vectors. Let  $\mathbf{u} = a\mathbf{e}_1 + b\mathbf{e}_2$  and  $\mathbf{v} = c\mathbf{e}_1 + d\mathbf{e}_2$ . Then from the product rules,

$$\mathbf{u}\mathbf{v} = (ac + bd) + (ad - bc)\mathbf{e}_1\mathbf{e}_2 \quad (5)$$

### 2.2.1. The inner product

The first term on the right side of equation (5),  $(ac + bd)$ , is the usual inner product of  $\mathbf{u}$  and  $\mathbf{v}$  :  $\mathbf{u} \cdot \mathbf{v} = |\mathbf{u}||\mathbf{v}|\cos\theta$ .

### 2.2.2. The outer product

The second term on the right side of equation (5) is the *outer product* of  $\mathbf{u}$  and  $\mathbf{v}$  : This bivector is denoted  $\mathbf{u} \wedge \mathbf{v}$ . Just as  $\mathbf{u}$  represents an oriented length,  $\mathbf{u} \wedge \mathbf{v}$  represents an oriented area. For the factor  $(ad - bc)$  is the signed area of the parallelogram with sides  $\mathbf{u}$  and  $\mathbf{v}$  :  $|\mathbf{u}||\mathbf{v}|\sin\theta$

$I_2 \equiv \mathbf{e}_1\mathbf{e}_2$  specifies the plane in which the area resides. Thus

$$\mathbf{u} \wedge \mathbf{v} = (ad - bc)\mathbf{e}_1\mathbf{e}_2 = |\mathbf{u}||\mathbf{v}|\sin\theta I_2 \quad (6)$$

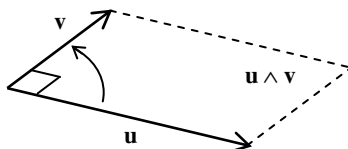


Figure 1: The bivector  $\mathbf{u} \wedge \mathbf{v}$ .

The inner product  $\mathbf{u} \cdot \mathbf{v} = |\mathbf{u}||\mathbf{v}|\cos\theta$  is intrinsic to the vectors, not depending on the basis  $\{\mathbf{e}_1, \mathbf{e}_2\}$ . So too with the outer product. For  $|\mathbf{u}||\mathbf{v}|\sin\theta$  is intrinsic. And if we rotate to another basis  $\begin{pmatrix} \mathbf{e}'_1 \\ \mathbf{e}'_2 \end{pmatrix} = \begin{pmatrix} \cos\alpha & \sin\alpha \\ -\sin\alpha & \cos\alpha \end{pmatrix} \begin{pmatrix} \mathbf{e}_1 \\ \mathbf{e}_2 \end{pmatrix}$  then  $\mathbf{I}'_2 = \mathbf{e}'_1 \mathbf{e}'_2 = \mathbf{I}_2$ .

### 2.2.3. The fundamental identity

Rewrite equation (5) in terms of the inner and outer products to obtain the *fundamental identity*

$$\mathbf{u}\mathbf{v} = \mathbf{u} \cdot \mathbf{v} + \mathbf{u} \wedge \mathbf{v} \quad (7)$$

Forget the coordinates of  $\mathbf{u}$  and  $\mathbf{v}$  which led to this equation. Remember that the geometric product of two vectors is the sum of a scalar and a bivector, both of which have a simple geometric interpretation.

## 2.3. Representing Subspaces

A *blade*  $\mathbf{B}$  for a subspace of  $\mathbf{R}^n$  is a product of members of an orthogonal basis for the subspace:  $\mathbf{B} = \mathbf{b}_1 \mathbf{b}_2 \cdots \mathbf{b}_k$ . We call  $\mathbf{B}$  a *k-blade*, or a blade of *grade k*. Nonzero scalars are 0-blades. Geometric algebra represents subspaces with their blades.

All blades of a subspace are scalar multiples of each other. For an  $i$ -dimensional subspace of  $\mathbf{R}^n$  has its own geometric algebra,  $\mathbf{G}^i$ . As with  $n$ -vectors in  $\mathbf{G}^n$ ,  $i$ -vectors in  $\mathbf{G}^i$  form a one dimensional subspace. They are the pseudoscalars of  $\mathbf{G}^i$ . A positive multiple of a blade represents the same subspace as the blade. A negative multiple represents the same subspace but with the opposite orientation (or with opposite *chirality*, see further).

The inverse of  $\mathbf{B}$  is  $\mathbf{B}^{-1} = \mathbf{b}_k \cdots \mathbf{b}_2 \mathbf{b}_1 / |\mathbf{b}_k|^2 \cdots |\mathbf{b}_2|^2 |\mathbf{b}_1|^2$

## 3. Geometric Constraints Represented as GA Objects

The aim of this section is to demonstrate that it is possible to represent the association of geometric objects as a member of Geometric Algebra. In this section, the proposed solution is illustrated with the association of two objects; these objects are points, lines and planes. To demonstrate the representation is relevant, we study the case of the association between two lines.

### 3.1. The Direction-Position Model

As we have seen before, subspaces of  $\mathbf{R}^n$  (points, lines, planes... through the origin) can be represented with blades of  $\mathbf{G}^n$ . This is the vector space model. In the affine space, we define the position of the geometric object with respect to the origin by a point. This representation is called “direction-position” model because a geometric object is defined by one “direction blade” and one “position vector” (see [13]).

#### 3.1.1. Geometric objects represented as members of GA

To express the relations linking the various parameters of the geometry, we must give a representation for each geometric element (here point, line and plane).

**Point.** A point  $P$  is represented as the bipoint  $OP$ . The bipoint  $OP$  is a vector called  $p$ . We can note that  $p \in \mathbf{R}^n$ .

**Line.** The representation of line is given by two vectors. The first one, called  $p$ , define the position of the line with respect to the origin of the affine space. The second one, called  $t$ , is the direction of the line.  $t$  is a unit vector. Then a point  $X$ , represented by the vector  $x$ , belongs to the line  $l$ , is expressed by the following relation

$$X \in l \Leftrightarrow (x - p) \wedge t = 0 \quad (8)$$

**Plane.** The representation of plane is given by a vector and a 2-blade. The first one, called  $p$ , define the position of the plane with respect to the origin of the affine space. The second one, called  $B$ , is the direction of the plane.  $B$  is a unit bivector. By analogy with the previous relationship, a point  $X$ , represented by the vector  $x$ , belongs to a plane  $\pi$ , is expressed by the following relation

$$X \in \pi \Leftrightarrow (x - p) \wedge B = 0 \quad (9)$$

#### 3.1.2. Geometric constraints represented as members of GA

To represent the association between two geometric elements by a GA multivector, we follow the following principle. The first term of that multivector is formed by the geometric product between the direction blades of each element. This term represents the association of directions.

A new vector models the relative position between the two elements. That vector represents the bipoint which begins at the point of the first element and finish at the point of the second element. So, the second term of the GA multivector is formed by the geometric product between the previous relative position vector, the direction blade of the first element and the direction blade of the second element.

Therefore, the association between two elements is represented by sum of the two terms of the GA multivectors. Table 1 gives expressions for different associations.

Note. In this section and for simplicity reasons, the relation-position vector is called  $\mathbf{p}_{ji}$ , with  $\mathbf{p}_{ji} = \mathbf{p}_j - \mathbf{p}_i$ .

Table 1: Expression of geometric constraints – case of position-direction model

	Point j	Line j	Plane j
Point i	$D_1 = \mathbf{p}_{ji}$	$D_2 = \mathbf{p}_{ji}\mathbf{t}_j$	$D_3 = \mathbf{p}_{ji}\mathbf{B}_j$
Line i	$D_4 = \mathbf{p}_{ji}\mathbf{t}_i$	$D_5 = \mathbf{t}_i\mathbf{t}_j + \mathbf{p}_{ji}\mathbf{t}_i\mathbf{t}_j$	$D_6 = \mathbf{t}_i\mathbf{B}_j + \mathbf{p}_{ji}\mathbf{t}_i\mathbf{B}_j$
Plane i	$D_7 = \mathbf{p}_{ji}\mathbf{B}_i$	$D_8 = \mathbf{B}_i\mathbf{t}_j + \mathbf{p}_{ji}\mathbf{B}_i\mathbf{t}_j$	$D_9 = \mathbf{B}_i\mathbf{B}_j + \mathbf{p}_{ji}\mathbf{B}_i\mathbf{B}_j$

**Case study.** Line-Line association (see Figure 2)

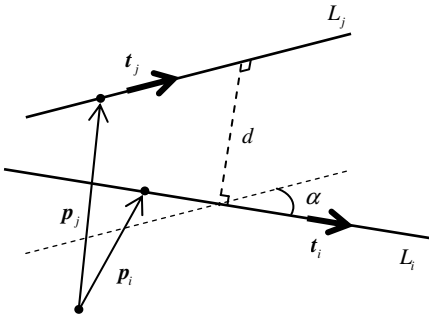


Figure 2: Parametrisation of a Line-Line association

The expansion of multivector  $D_5$  gives four grades. From grade zero until grade three:

$$\begin{aligned}
 D_5 &= \mathbf{t}_i\mathbf{t}_j + \mathbf{p}_{ji}\mathbf{t}_i\mathbf{t}_j \\
 &= \mathbf{t}_i \cdot \mathbf{t}_j + (\mathbf{t}_i \cdot \mathbf{t}_j) \mathbf{p}_{ji} - (\mathbf{p}_{ji} \cdot \mathbf{t}_j) \mathbf{t}_i + (\mathbf{p}_{ji} \cdot \mathbf{t}_i) \mathbf{t}_j + \mathbf{t}_i \wedge \mathbf{t}_j + \mathbf{p}_{ji} \wedge \mathbf{t}_i \wedge \mathbf{t}_j \quad (10) \\
 &= \langle D_5 \rangle_0 + \langle D_5 \rangle_1 + \langle D_5 \rangle_2 + \langle D_5 \rangle_3
 \end{aligned}$$

Geometric parameters defining the Line-Line association are angle  $\alpha$  and distance  $d$  (measured along the common perpendicular) between the two lines. To express  $\alpha$ , we expand the term  $\mathbf{t}_i\mathbf{t}_j$ , as follows:

$$\begin{aligned} \langle D_s \rangle_2 (\langle D_s \rangle_0)^{-1} &= (\mathbf{t}_i \wedge \mathbf{t}_j)(\mathbf{t}_i \cdot \mathbf{t}_j)^{-1} \\ &= \tan \alpha \mathbf{I}_2 \end{aligned} \quad (11)$$

With  $\mathbf{I}_2$  the unit 2-blade. The norm of the vector  $\langle D_s \rangle_2 (\langle D_s \rangle_0)^{-1}$  is equal to the tangent of the expected angle  $\alpha$ . Note that the unit bivector  $\mathbf{I}_2$  represents the vector plane containing vectors  $\mathbf{t}_i$  and  $\mathbf{t}_j$ .

To express  $d$ , we expand the two terms  $\mathbf{t}_i \wedge \mathbf{t}_j$  and  $\mathbf{p}_{ji} \wedge \mathbf{t}_i \wedge \mathbf{t}_j$ , as following:

$$\begin{aligned} (\langle D_s \rangle_3) (\langle D_s \rangle_2)^{-1} &= (\mathbf{p}_{ji} \wedge \mathbf{t}_i \wedge \mathbf{t}_j)(\mathbf{t}_i \wedge \mathbf{t}_j)^{-1} \\ &= \frac{1}{(\mathbf{t}_i \wedge \mathbf{t}_j)(\mathbf{t}_j \wedge \mathbf{t}_i)} (\mathbf{p}_{ji} \wedge \mathbf{t}_i \wedge \mathbf{t}_j)(\mathbf{t}_j \wedge \mathbf{t}_i) \\ &= du \end{aligned} \quad (12)$$

With  $u$ , the unit vector. The norm of the vector  $\langle D_s \rangle_3 (\langle D_s \rangle_2)^{-1}$  is equal to the expected length  $d$ . Note that the direction of the unit vector  $u$  is along the common perpendicular of the two lines.

Equations (11) and (12) provide the sought quantities that characterize the Line-Line association. For the other cases, we proceed the same way to prove that the appropriate multivector provide all expected geometric parameters.

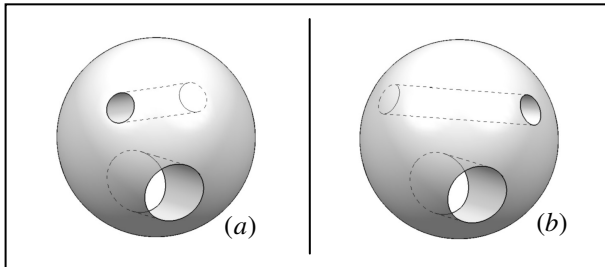


Figure 3: Objects with same geometric parameters and different shapes

As we can see on Figure 3, objects (a) and (b) are defined by the same geometric parameters  $d$  and  $\alpha$  but they don't have the same shape. When this problem occurs, we say that the two objects have an opposite chirality. This situation is well known in declarative modelling and it appears very often. In this case, the geometric constraints solver proposes one solution, sometimes the good one, but sometimes the bad one.

With the proposed solution, the user specifies the chirality between objects because GA language enables it. In the example, the 3-blade of multivector  $D_5$  provides the right information to distinguish between the two shapes (a) and (b). In fact, the 3-blade of multivector associated with object (a) is compared with the 3-blade of multivector associated with object (b). The quantity

$$\varepsilon_{ab} = \langle Da_5 \rangle_3 \langle Db_5 \rangle_3$$

is the chirality between TTRS (a) and TTRS (b). In the 3D space  $\varepsilon_{ab}$  is a scalar. If  $\varepsilon_{ab} < 0$  the chirality are the same, if  $\varepsilon_{ab} > 0$  are opposite.

#### 4. Conclusion

This paper has shown that Geometric Algebra language may model any system of elementary positioning geometric object (called TTRS) by a system of algebraic relations. This result is essential to practice acausal modelling (also called “equation-based object-oriented language”).

The main interest of the GA is to be a vector representation of portions of lines, plans and volumes totally independent of a Cartesian reference frame. In this sense, GA belongs to the family of coordinate free formulation. A secondary interest is the introduction of the inherent concept of chirality (distinction left / right) thanks to the non commutativity of geometric product. This notion of chirality is essential to distinguish a geometric object with his reflected image in a mirror when it is described by a textual description of a set of algebraic constraints.

Finally, the scope of this basic algebra is its universality to model all the physical sciences as was clearly demonstrated D. Hestenes. This paper has shown that, with this mathematical tool, we could model CAD geometric artifacts. Thus, we pave the way for the creation of a general acausal model which we will call "mechatronic". These models will represent physical phenomena that interact with geometry (mechanical, electrical, electromagnetism, ...).

#### References

1. D. Michelucci, S. Foufou, L. Lamarque, P. Schreck, *Geometric constraints solving: some tracks*, SPM '06: Proceedings of the 2006 ACM symposium on Solid and physical modeling, Cardiff, Wales, United Kingdom. ACM Press , pp. 185-196 (2006).
2. W. Bouma, I. Fudos, C.M. Hoffmann, J. Cai, R. Paige, *Geometric constraint solver*, Computer-Aided Design, Vol. 27.6, pp. 487-501 (1995).

3. A. Clément, A. Rivière, M. Temmerman, *Cotation tridimensionnelle des systèmes mécaniques*, PYC Editions (1994).
4. A. Clément, A. Rivière, P. Serré, C. Valade, *The TTRSS: 13 Constraints for Dimensioning and Tolerancing*, in Geometric Design Tolerancing: Theories, Standards and Applications, Hoda A. Elmaraghy (Editor), Chapman & Hall, pp 122-131 (1998)
5. D. Michelucci, *The next 100 papers about geometric constraint solving*, ISICAD conference on Geometric Constraints, Akademgorodok, Russia, (2004).
6. D. Michelucci, S. Foufou, *Using Cayley-Menger Determinants for Geometric Constraint Solving*, ACM Symposium on Solid Modeling, Genova, Italy (2004).
7. P. Serré, *Cohérence de la spécification d'un objet de l'espace euclidien à n dimensions*, PhD thesis, Ecole Centrale Paris (2000).
8. P. Serré, A. Clément, A. Rivière, *Vers une approche déclarative en CFAO. Application au mécanisme de Bennett*, 4th International Conference on the Integrated Design and Manufacturing in Mechanical Engineering, CDROM paper n°E6-2, 11 pages, Clermont-Ferrand, France, May 14-16 (2002).
9. A. MacDonald, *A Survey of Geometric Algebra and Geometric Calculus*, <http://faculty.luther.edu/~macdonal/>. (April 6, 2008).
10. D. Hestenes, *New Foundations for Classical Mechanics*, Kluwer Academic Publishers, Second Edition (1999).
11. C. Doran and A. Lasenby, *Geometric Algebra for Physicists*, Cambridge University Press, Fourth printing (2005).
12. B. Fauser, R. Ablamowics, *On the decomposition of Clifford Algebras of Arbitrary Bilinear form*, 5th International Conference on Clifford Algebras and their Applications in Mathematical Physics, Ixtapa, Mexico, June 27 - July 4, (1999).
13. D. Hestenes, G. Sobczyk, *Clifford Algebra to Geometric Calculus – A Unified Language for Mathematics and Physics*, D. Reidel Publishers (1984).

## MODELLING OF DYNAMIC MEASUREMENT SYSTEMS AND UNCERTAINTY ANALYSIS EMPLOYING DISCRETISED STATE-SPACE FORMS

KLAUS-DIETER SOMMER

*Physikalisch-Technische Bundesanstalt, Braunschweig, Germany*

UWE HANEBECK

*Universität Karlsruhe (TH), Karlsruhe, Germany*

MICHAEL KRYSTEK

*Physikalisch-Technische Bundesanstalt, Braunschweig, Germany*

FELIX SAWO

*Universität Karlsruhe (TH), Karlsruhe, Germany*

Modelling of a measurement is an indispensable prerequisite of modern uncertainty evaluation. Both, the ISO-GUM [1] and the supplement of the GUM [2] require to express the knowledge about the measurement process by a so-called model equation which represents the mathematical relationship between the relevant parameters, the influence quantities, the indication and the measurand(s). Nevertheless both documents are confined to lumped-parameter systems in the steady state. Since dynamic measuring systems gain more and more importance, modern uncertainty determination must develop appropriate modelling approaches for dealing with dynamic measurements. This paper exemplary describes a possible modelling approach for dynamic measurements that utilizes discretised state-space forms.

### 1. Introduction

For evaluating the measurement uncertainty, both, the ISO-GUM [1] and the supplement to the GUM [2] require to express the knowledge about a measurement process by the so-called model equation which represents the mathematical relationship between the relevant parameters, the influence quantities, the indication(s) and the measurand(s). But neither the GUM framework [1, 2] nor other relevant uncertainty documents provide any assistance on how to establish an appropriate mathematical model for

determining the measurement uncertainty. Moreover, both documents are confirmed to lumped-parameter systems in the steady state.

This paper describes a basic modelling approach that starts from a cause-and-effect analysis of the measurement process. For modelling dynamic effects in the time domain, discretised state-space forms are proposed. These mathematical forms originate from the signal-and-system theory. Due to their obvious advantage (see Section 4), they may also be applied on the modelling of measuring system.

## 2. The Cause-Effect Approach and the Inverse Model Equation

Generally, a model serves to evaluate an original system or to draw conclusions from its behaviour. In measurement, usually the measurand and other influence quantities may be seen as causative signals which are physically transformed by the measuring system into effects, such as, for example, indications. Therewith, the measuring system assigns values to the measurand(s), and the system is influenced by system-disturbing influence quantities. The cause-effect approach is the most commonly used and comprehensible methodology for representing basic relationships in modelling of measurements [3, 4].

A model that describes the cause-effect behaviour of a measuring system or sensor is often termed 'measurement equation' or 'sensor equation'. An example is given in Figure 1 [3, 4]: The indication of this temperature measurement  $X_1 = \vartheta_{\text{IND}}$  depends on both, the bath temperature  $Y = \vartheta_B$ , i. e. the measurand, and the instrumental error  $X_3 = \Delta\vartheta_{\text{Th}}$  of the thermometer used. Furthermore, the indication is affected by the temperature inhomogeneity of the bath, this effect is represented by the deviation  $\delta\vartheta_B$ . Then, the cause-effect relationship for this example can mathematically be expressed by  $X_1 = h(Y, X_2, X_3)$ .

In contrast to this, for determining the measurement uncertainty, usually an 'inverse model' is needed that establishes the relationship between the 'target quantity', i. e. the measurand  $Y$  and all relevant influence quantities and the indication,  $X_1, \dots, X_N$ . This model category is usually termed 'model equation', 'measurement reconstruction model' or 'model for evaluating the measurement uncertainty' [3]; it is generally expressed as

$$Y = f_M(X_1, \dots, X_N) \quad (1)$$

Figure 2 illustrates the difference between the two model categories.

In practice, due to its comprehensibility and assignability from the real system to the model, the cause-effect approach almost always forms the base for

modelling of measurements. The cause-effect approach itself is founded on the transfer behaviour of the functional elements of the measuring chain.

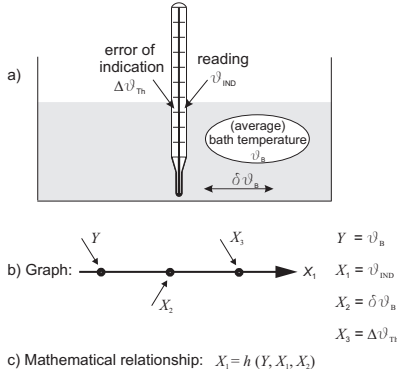


Figure 1. (a) Simplified example of a bath-temperature measurement. (b) Graph of the respective cause-and-effect relationship.

(c) Cause-and-effect relationship expressed in mathematical terms. Symbols:  $\vartheta_B$  – (average) bath temperature (measurand);  $\delta \vartheta_B$  – deviation due to the temperature inhomogeneity of the bath;  $\Delta \vartheta_{\text{th}}$  – indication(scale) error of the thermometer used;  $\vartheta_{\text{IND}}$  – indicated value [3, 4].

### 3. Describing and Modelling the Transfer Behaviour

Measuring systems are usually modelled the same way as any other technical information system. First, the system is decomposed and modularised into functional elements. Then, the transmission behaviour of each functional element is mathematically described. The so-called transfer function [5] relates the output signal to the input signal(s):

$$X_{\text{OUT}} = h(X_{\text{IN}}) \quad (2)$$

where  $X_{\text{IN}} = (X_{\text{IN}1}, \dots, X_{\text{IN}n})^T$  – input signal(s),  $X_{\text{OUT}}$  – output signal, and  $h$  – transfer function.

In measurement, the great majority of systems is treated as being linear and time invariant [6].

The transfer function of a time-invariant system or transmission element is represented by an algebraic equation (see Table 1). For a linear system, the transfer function consists of constant transmission factors,

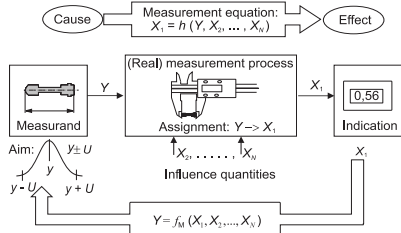


Figure 2. Comparison of model categories: 'Measurement equation' and 'Model equation' or 'reconstruction model' for the uncertainty evaluation [3, 4].

$$\underline{X}_{\text{OUT}} = h(\underline{X}_{\text{IN}}) = \underline{A} = (A_1, \dots, A_m)^T \quad (3)$$

where  $\underline{A} = (A_1, \dots, A_m)^T$  – constant factors.

Linear and time-invariant transfer functions can easily be inverted into the so-called model equation (see Equation (1) and Section 2).

Table 1: Survey on static and dynamic systems along with tools for their appropriate mathematical description [4].

	System class	Equation for general systems	Equation for linear systems
Static system	Algebraic equation	Equation without time dependencies: $\underline{Y} = f(\underline{X})$	Linear system of equations: $\underline{Y} = \underline{A}\underline{X}$
Dynamic systems	Description in time domain	Differential equation $\underline{Y}(t) = f(\underline{Y}^{(1)}, \underline{Y}^{(2)}, \dots, X, X^{(1)}, X^{(2)}, \dots, t)$	Linear differential eq. $\sum_{v=1}^n a_v \underline{Y}^{(v)} = \sum_{\mu=1}^m b_{\mu} \underline{X}^{(\mu)}$
		State space model $Z(t) = f(Z(t), X(t), t)$ $Y(t) = g(Z(t), X(t), t)$	$\dot{Z}(t) = AZ(t) + BX(t)$ $Y(t) = CZ(t) + DX(t)$
Dynamic systems	Description in frequency domain	Transfer function	$\underline{Y}(s) = G(s) \underline{X}(s)$ $G(s) = \frac{\sum_{\mu=0}^m b_{\mu} s^{\mu}}{\sum_{v=0}^n a_v s^v}$

To an increasing extend, dynamic measuring systems gain importance in metrology and industrial measurement. The time-dependent behaviour of these systems or transmission elements results from transient and storage effects affecting the quantity of interest. This might be explained with the example of an immersing liquid-in-glass thermometer (see Figure 3) [3, 4, 7]: A liquid-in-glass thermometer that indicates the ambient temperature  $\vartheta_a$  plus its (statical) instrumental error,  $\vartheta_{\text{IND}} = \vartheta_a + \Delta \vartheta_{\text{INST}}$ , is at time  $t_0$  being immersed into a water bath which has the temperature  $\vartheta_b$  (see Figure 3). Then, the cause-effect relationship of the measurement and temperature equalisation process may be expressed by the following differential equations

$$\vartheta_{\text{IND}} = \vartheta_b + \Delta \vartheta_{\text{INST}} - T \frac{d\vartheta_{\text{Th}}}{dt} \quad (4)$$

where  $T = \frac{m \cdot c}{\alpha \cdot A}$ ,  $\frac{d\vartheta_{\text{Th}}}{dt} \approx \frac{d\vartheta_{\text{IND}}}{dt}$ ,  $m$  – mass of the thermometer,  $c$  – specific heat capacity,  $\alpha$  – thermal transition factor,  $A$  – immersed surface area of the thermometer. Consequently, the model equation for evaluating the measurement uncertainty becomes

$$\vartheta_B = \vartheta_{\text{IND}} + \Delta\vartheta_{\text{INSTR}} - T \frac{d\vartheta_{\text{Th}}}{dt} \quad (5)$$

where  $T \cdot \frac{d\vartheta_{\text{Th}}}{dt} = \delta\vartheta_{\text{DYN}}(t)$  is the dynamic error component, whose expectation

is approximately  $\delta\vartheta_{\text{DYN}}(t) = (\vartheta_B - \vartheta_a) \cdot \exp\left(\frac{t - t_0}{T}\right)$  [3, 4, 7].

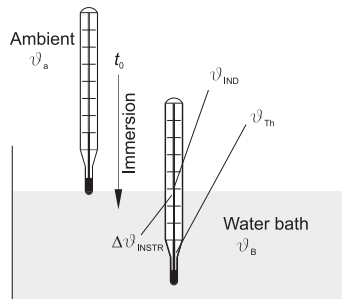


Figure 3. Example: Bath temperature measurement with necessary temperature equalisation of the thermometer used [4]. Symbols see text.

In general, dynamic measuring systems can be classified as lumped-parameter systems or distributed parameter systems. The key characteristic of a lumped-parameter system is that the state of the system, which uniquely describes the system behaviour, depends only on time. It is generally described by a set of ordinary differential equations [5]. Table 1 gives an overview on the mathematical tools used for the description of static and dynamic systems in both, the time domain and the frequency domain [4, 5, 6].

It should be noted that in today's practice, the system description is usually discretised. Discretization allows for treating almost all systems as being linear (for the discrete time) and offers advantages for digital signal processing.

#### 4. State-Space Forms

Whereas for linear and linearizable system the model equation is usually established by reversing the mathematical cause-effect relationship expressed by the transfer function, in case of non-linearizable and dynamic measuring systems this might be awkward.

A useful alternative way seems to be to describe dynamic measurements by means of the so-called space-state forms that in general consists of a system equation (6) and a so-called output equation (7) [5, 6]:

$$\mathbf{Z}^{(1)} = f_s [\mathbf{Z}(t), \mathbf{X}_{\text{IN}}(t), t] \quad (6)$$

$$\mathbf{X}_{\text{OUT}}(t) = f_{\text{OUT}} [\mathbf{Z}(t), \mathbf{X}_{\text{IN}}(t)], \quad (7)$$

where the state vector  $\mathbf{Z}$  represents the present state of the system including previous states. For example, the state variable (vector) may be the (real) temperature of a thermometer immersed into a water bath with a different temperature (see Figure 3).

State-space forms are mathematically equivalent to the description by means of ordinary differential equations (see Equation (4)); both forms can be transformed into each other. The relevant advantages of state-space forms are

- a technically easy interpretation of the state vector/variable
- having first order differential equations only
- allowing to easily derive the input and the output quantities/vectors from the state vector/variable.

Time discretisation results in a finite-state form that basically allows to treat a measuring system as a linear (and time-invariant) system at a discrete state  $\mathbf{Z}_k$ . Hence, equations (6) and (7) become

$$\mathbf{Z}_{k+1} = \mathbf{A}_k \mathbf{Z}_k + \mathbf{B}_k \cdot \mathbf{X}_{\text{IN}k} \quad (8)$$

$$\mathbf{X}_{\text{OUT}k} = \mathbf{C}_k \mathbf{Z}_k (+ \mathbf{D}_k \mathbf{X}_{\text{IN}k}) \quad (9)$$

where  $k$  indicates a discrete point in time.

With a view to evaluate the (measurement) uncertainty for a (measurement) process described in space-state form, the above vectors (variables)  $\mathbf{X}_{\text{IN}}$ ,  $\mathbf{X}_{\text{OUT}}$  and  $\mathbf{Z}$  are to be replaced with appropriate probability density functions (PDF)  $g(\mathbf{X}_{\text{IN}k})$ ,  $g(\mathbf{X}_{\text{OUT}k})$  and  $g(\mathbf{Z}_k)$  which represent the incomplete knowledge about the vectors (variables). Furthermore, based on the existing knowledge about the measuring system, both, the state equation and the output equation may be

augmented by additional noise/uncertainty components to account for the imperfection in modelling the whole process.

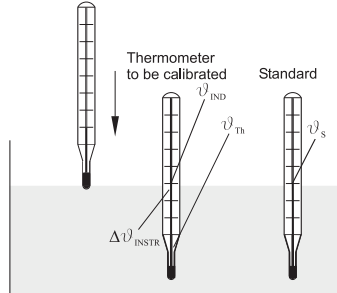


Figure 4. Example: Calibration of a thermometer with simultaneous consideration of the temperature equalisation of the instrument to be calibrated. Symbols see text.

For detailed explanation, the thermometer example given in Section 2 and Figure 3 is changed and extended to a calibration of the instantly immersed thermometer, and the bath temperature is made known by a standard thermometer (see Figure 4) [8]. The calibration aims at the theoretical error  $\Delta \vartheta_{\text{INSTR}}$ . Obviously, the (real) temperature of the thermometer to be calibrated,  $\vartheta_{\text{th}}$  might be taken as a state variable, and the bias-corrected temperature indicated by the standard,  $\vartheta_s$ , is an appropriate system input. Then, the discretised system equation formally reads to

$$\mathbf{Z}_{k+1} = \mathbf{A}_k \cdot \mathbf{Z}_k + b_k \cdot \Delta \vartheta_{\text{INSTR}} + b_k \cdot \vartheta_s . \quad (10)$$

Hence, the output equation is

$$\mathbf{X}_{\text{OUT}k} = \vartheta_{\text{IN}k} = \mathbf{Z}_k + \nu_k , \quad (11)$$

where  $\nu_k$  represents a random uncertainty component.

Figure 5 illustrates the basic structure of this model [8].

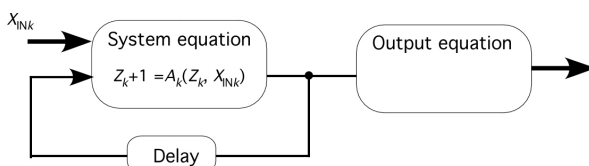


Figure 5. Basic structure of the discretised state-space model used [6, 8].

## 5. Model-Based Bayesian Estimator

Assume the following (reality-based) case: At the end of a thermometer-production process the instruments must be calibrated, and the measurand is the (steady-state) instrumental error. The calibration is carried out by immersing the thermometers automatically into a water bath of known temperature. For efficiency reasons, one can not wait until the thermal steady state is reached. Therefore, a good estimate of the unknown dynamic error is needed. This estimation can be carried out on the basis of the state-space model [8, 5, 6], Figure 6 illustrates the idea [8]: Both uncertainties for the system equation and the output equation are taken into consideration. The system input and the state vector are described by appropriate PDFs. Due to the fact that in our example the output quantity  $X_{OUTk} = V_{INDk}$  is well known, the inverse output equation might be used for obtaining a real-value based estimate of the state-vector PDF  $g_L(Z_k)$ . This estimate is used to permanently update the PDF  $g_p(Z_k)$  provided by means of the system equation. For an optimal estimation result,  $g_e(Z_k)$ , possible systematic uncertainty contribution (covariances) are to be taken into consideration. Therefore, the filter algorithm used for the Bayes step must be capable to cope with unknown correlation, such as, for example, so-called covariance bounds [8, 9, 10].

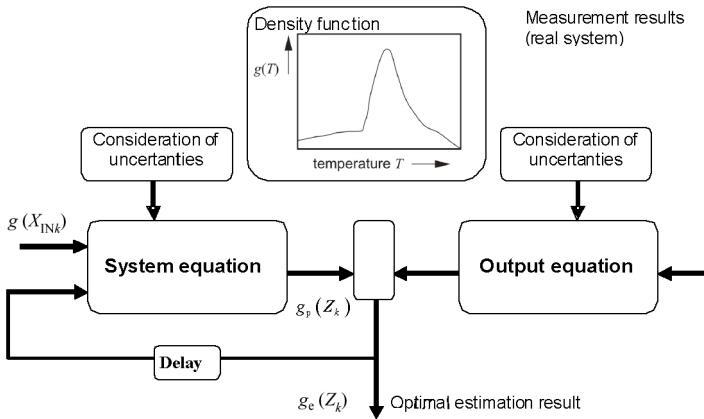


Figure 6. Model-based Bayesian estimator [8].

Figure 7 shows simulation results computed in [8] for the above described (state-space) model-based estimator along with the realistic uncertainty values for the covariance matrix. The results obtained exemplary demonstrate the

potential and performance of the suggested approach: The measurement period can be reduced to less than one third of the thermometer settling time.

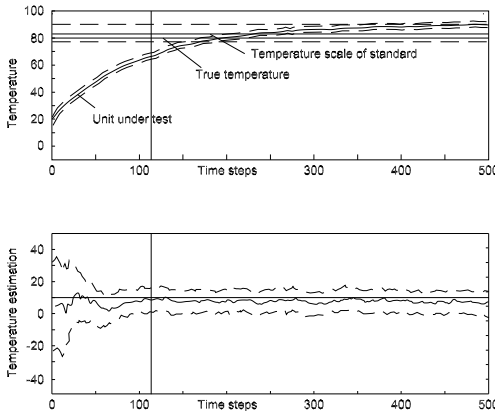


Figure 7. Exemplary simulation results computed in [8].

## 6. Conclusion

Modelling the measuring process is a necessary task for evaluating measurement results and ensuring their reliability. Since dynamic measurements gain more and more importance, modern uncertainty evaluation must develop appropriate modelling approaches. It is demonstrated that discretised state-space forms are a suitable alternative for modelling dynamic measurements for uncertainty evaluation. First results show the performance and the potential of this approach.

## References

1. ISO 1993 *Guide to the Expression of Uncertainty in Measurement* (GUM) 1<sup>st</sup> edn, corrected and reprinted 1995 (Geneva: International Organization for Standardization (ISO))
2. BIPM, IEC, IFCC, ILAC, ISO, IUPAC, IUPAP and OIML Evaluation of measurement data – Supplement 1 to the *Guide to the Expression of Uncertainty in Measurement* – Propagation of distributions using a Monte Carlo method
3. Sommer, K.-D.; Siebert, B.R.L.: Systematic Approach to the Modelling of Measurements for Uncertainty Evaluation. *Metrologia* 43 (2006) 4

4. Sommer, K.-D.: Modelling of Measurements, System Theory and Uncertainty Evaluation. In Pavese, F; Forbes, A: Data Modelling for Metrology and Testing in Measurement Science, Springer, 2008
5. Kliencke, U.; Jäkel, H.: Signale und Systeme. Oldenbourg Verlag München Wien 2005 (ISBN 3-486-57811-1)
6. Kiencke, U.; Eger, R.: 1995 *Messtechnik – Systemtheorie* für Elektrotechniker (Berlin: Springer)
7. Hemmi, P.; Profos, P.: Dynamische Messfehler. in Profos, P.; Pfeifer, T. (Hrsg.): Grundlagen der Messtechnik. R. Oldenbourg Verlag München Wien 1997 (ISBN 3-486-24148-6)
8. Sawo, F.; Hanebeck, U.D.; Sommer, K.-D.: A Bayesian Approach to Consistently Describing and Analysing Dynamic and Distributed Parameter Measurement Systems. 238<sup>th</sup> PTB Seminar on Analysis of Dynamic Measurements, Berlin, 6<sup>th</sup> November 2007
9. R.H. Deaves: Covariance bounds for augmented state Kalman filter application, Electronic Letters, Vol. 35, Iss. 23, p. 2062-2064
10. Uwe D. Hanebeck; Kai Brieche; Joachim Harm: A Tight Bound for the point covariance of two random vectors with unknown but constraint cross correlation

## OPTIMAL DECISION RULES AND LIMITS OF DETECTION

JOAO A. SOUSA\*

*LREC, Madeira, Portugal*

ALISTAIR B. FORBES

*National Physical Laboratory, Teddington, UK*

This paper describes a general approach, based on Bayesian decision analysis, to determining decision rules in the presence of uncertain knowledge taking into account the likely decision costs. It shows how the approach can be applied to limit-of-detection problems for a number of measurement models, including those associated with repeated measurements. The approach is extended to cover the case where the measurand reflects background, naturally-occurring levels of a quantity.

### 1. Introduction

In many spheres of regulation, it is required to assess whether the value of some parameter exceeds specified limits, e.g., the amount of a pollutant in air or water, or of a banned substance in a blood sample. The decision to pass or fail a sample is usually made on the basis of measurement with which there will be associated some uncertainty. As a result, there is a risk that a decision based on a measurement result may be wrong in the sense that a sample may be passed when the true value, if it were known, would result in a failure, etc. Probabilistic methods are often used to evaluate the risk of making a wrong decision<sup>2,5</sup>. The consequences of making a wrong decision will vary with context but, if costs can be associated with these consequences, decision rules can be set in such a way that the expected cost of making a wrong decision is minimised<sup>3,4,6,8</sup>. In many regulation areas, the quantities being assessed are small but necessarily nonzero. As a result, the measurement uncertainty can often be of the same order as the quantity being assessed, so that the measurement task is near the ‘limit of detection’

---

\*corresponding author: jasousa@lrec.pt

of the measuring system. Bayesian methods that can incorporate physical constraints in the model of the measurement system have been shown to be effective in such limit-of-detection cases<sup>1</sup>. A further complication may be that a small, background level of the quantity arises naturally and the assessment has to consider if an observed measurement result is consistent with expected background levels.

In section 2 we give an overview of a general approach to minimising decision costs and in section 3 we illustrate how the approach can be extended to cover a type of conformance test involving background levels of a quantity subject to non-negativity constraints. Our concluding remarks are given in section 4.

## 2. Decisions Minimising Expected Costs

Suppose the decision to be made depends on the value of one or more parameters  $\alpha \in \mathcal{A}$ ,  $\mathcal{A} \subset \mathbb{R}^n$  that describe the (true) state of a system. We assume that the cost of choosing the  $k$ th course of action,  $k = 1, \dots, n_D$ , is given by a function  $c_k(\alpha)$  of  $\alpha$  defined on  $\mathcal{A} \subset \mathbb{R}^n$ . These functions define the exact decision rule  $D^* : \mathcal{A} \mapsto \{1, \dots, n_D\}$  for exact information:  $D^*(\alpha) = j$  where  $j$  specifies a cost function  $c_j$  such that  $c_j(\alpha) \leq c_k(\alpha)$ ,  $k = 1, \dots, n_D$ . (We assume that there is a deterministic rule in the case of ties.) We also assume that the state of knowledge about  $\alpha$  is encoded in a probability distribution, usually derived from measurement data  $\mathbf{y} \in \mathcal{Y} \subset \mathbb{R}^m$ , which we denote by  $p(\alpha|\mathbf{y})$ . The expected cost  $e_k(\mathbf{y})$  of taking course of action  $k$  is given

$$e_k(\mathbf{y}) = \int_{\mathcal{A}} c_k(\alpha) p(\alpha|\mathbf{y}) d\alpha, \quad k = 1, \dots, n_D, \quad (1)$$

a function of  $\mathbf{y}$ . The optimal decision is given by

$$D(\mathbf{y}) = j, \quad e_j(\mathbf{y}) \leq e_k(\mathbf{y}), \quad k = 1, \dots, n_D, \quad (2)$$

i.e., the choice which corresponds to the minimum expected cost. The minimal expected cost corresponding to  $D$  is denoted by  $e^*(\mathbf{y}) = \min_k e_k(\mathbf{y})$ . In the illustrative example below, the cost functions  $c_k(\alpha)$  are constant in each  $I_k^*$ ,  $k = 1, \dots, n_D$ , and are therefore specified by an  $n_D \times n_D$  matrix  $C$ . Given probabilities  $p_k(\mathbf{y}) = \text{Prob}(\alpha \in I_k^* | \mathbf{y}) = \int_{I_k^*} p(\alpha|\mathbf{y}) d\alpha$ , the vector of expected costs  $\mathbf{e}(\mathbf{y}) = (e_1(\mathbf{y}), \dots, e_{n_D}(\mathbf{y}))^\top$  associated with the decisions is given by  $\mathbf{e}(\mathbf{y}) = C\mathbf{p}(\mathbf{y})$  where  $\mathbf{p}(\mathbf{y}) = (p_1(\mathbf{y}), \dots, p_{n_D}(\mathbf{y}))^\top$ . For many applications, it will be more appropriate to have varying cost functions<sup>7</sup>.

### 3. Conformance Tests Relating To Maximum Permitted Levels And Background Levels

In this section, we describe a method for making decisions about whether the value of a quantity exceeds a permitted level, with the complication that there is a natural background level of the quantity which is known imprecisely. Let  $\beta$  represent the background concentration of a substance, e.g., in a blood sample or river, and  $\alpha$  the concentration added, e.g., a banned stimulant or pollutant. Necessarily,  $\alpha$  and  $\beta$  satisfy the constraints  $0 \leq \alpha, \beta, \alpha + \beta \leq 1$ . More generally, we can apply a constraint of the form  $\alpha + \beta \leq A_{\max}, 0 < A_{\max} \leq 1$ . On the basis of a measurement of  $\alpha + \beta$ , we wish to decide whether or not the measurement result  $y$  is consistent with the expected background levels.

We use a Bayesian approach to determine  $p(\alpha|y)$ , for which a prior joint distribution  $p(\alpha, \beta)$  for  $\alpha$  and  $\beta$  is required. We first assign a prior distribution, a beta distribution<sup>4</sup>,  $\beta \sim B(p, q, 0, A_{\max})$ ,  $0 \leq A_{\max} \leq 1$ , to  $\beta$ . This distribution is nonzero on the interval  $[0, A_{\max}]$  and its shape is determined by the parameters  $p$  and  $q$ . The mean of this distribution is  $A_{\max}p/(p + q)$ . An example prior distribution for  $\beta$  is given in Figure 3. Given knowledge of  $\beta$ , the distribution for  $\alpha|\beta$  is uninformative:  $p(\alpha|\beta) = 1/(1 - \beta)$  if  $0 \leq \alpha \leq 1 - \beta$ , and  $p(\alpha|\beta) = 0$ , otherwise. In other words, given  $\beta$ , the only thing we know about  $\alpha$  is that  $0 \leq \alpha \leq A_{\max} - \beta$ . The joint prior distribution  $p(\alpha, \beta)$  is then constructed as  $p(\alpha, \beta) = p(\alpha|\beta)p(\beta)$ . Other schemes for assigning a prior joint distribution could be implemented.

We assume there are two specification limits  $L_F > L_W$ . If  $\alpha \geq L_F$  a ‘failure’ should be issued. If  $L_F > \alpha > L_W$ , a ‘warning’ should be issued. If  $\alpha \leq L_W$ , a ‘pass’ should be issued. The two limits partition the interval  $\mathcal{A} = [0, 1]$  in three regions  $I_j^*$ ,  $j = 1, 2, 3$ . We associate to the three intervals and three decisions, a  $3 \times 3$  cost matrix  $C$  where  $C_{kj}$  is the cost of taking decision  $D_k$  given that  $\alpha \in I_j^*$ .

Let  $y$  be the result of a measurement of  $\alpha + \beta$  where  $y \in N(\alpha + \beta, \sigma^2)$ , with  $\sigma$  known. This defines the sampling distribution  $p(y|\alpha, \beta)$ , the probability of observing  $y \in \mathcal{Y} = \mathbb{R}$ , given  $\alpha$  and  $\beta$ . We also consider the case where  $y$  is the mean of  $r$  repeated measurements  $y_i$ ,  $y_i \in N(\alpha + \beta, \sigma^2)$ , where  $\sigma$  is unknown. In this case  $y|\alpha, \beta$  is associated with the  $t$ -distribution  $t_{r-1}(\alpha + \beta, s)$ , where  $s$  is the observed standard deviation of  $y_i$ . Finally, we also discuss the case where an independent control measurement  $y_0 \in N(\beta, \sigma_0^2)$  of the background concentration is available.

The posterior distribution  $p(\alpha, \beta|y)$  for  $\alpha$  and  $\beta$ , given measurement re-

sult  $y$ , is such that  $p(\alpha, \beta|y) \propto p(y|\alpha, \beta)p(\alpha, \beta)$ . The marginalised posterior distributions  $p(\alpha|y)$  and  $p(\beta|y)$  are given by

$$p(\alpha|y) = \int_0^{A_{\max}} p(\alpha, \beta|y) d\beta, \quad p(\beta|y) = \int_0^{A_{\max}} p(\alpha, \beta|y) d\alpha. \quad (3)$$

Similar calculations involving  $p(y, y_0|\alpha, \beta)$  and  $p(\alpha, \beta|y, y_0)$  apply in the case of a control measurement  $y_0$ .

### 3.1. Example Calculations

The following calculations were performed for a cost matrix

$$C = \begin{bmatrix} 0 & 10 & 20 \\ 30 & 0 & 10 \\ 50 & 20 & 0 \end{bmatrix}, \quad (4)$$

$p(\beta)$  associated with the beta distribution  $B(2, 18, 0, 1)$ , i.e., with constant  $A_{\max} = 1$ , mean 0.1, and specification limits for  $\alpha$  of  $L_W = 0.2$  and  $L_F = 0.4$ . The costs are asymmetric in that issuing a fail when a pass should have been given attracts a larger cost than issuing a pass when a fail should have been given.

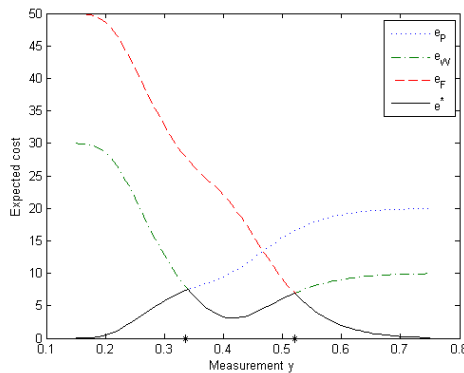


Figure 1. Expected costs as a function of measurement result  $y$ .

Figure 1 represents the expected costs  $e_F$ ,  $e_W$ ,  $e_P$  – fail, warn, pass – and their minimum  $e^*$  as a function of measurement result  $y$  for the case  $\sigma = 0.025$ . Thus,  $e_F$  gives the expected cost for issuing a fail on the basis of measurement result  $y$ . As  $y$  decreases, the expected cost increases

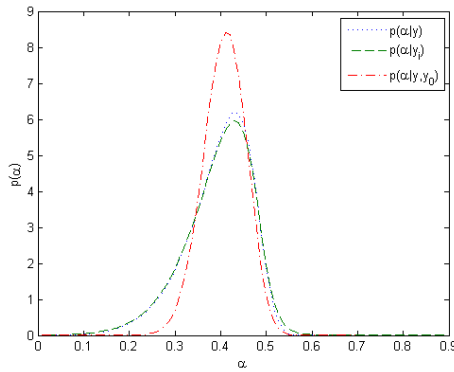


Figure 2. Posterior distributions  $p(\alpha|y)$ ,  $p(\alpha|\{y_i\})$  and  $p(\alpha|y, y_0)$  for  $\alpha$  for the three measurement experiments.

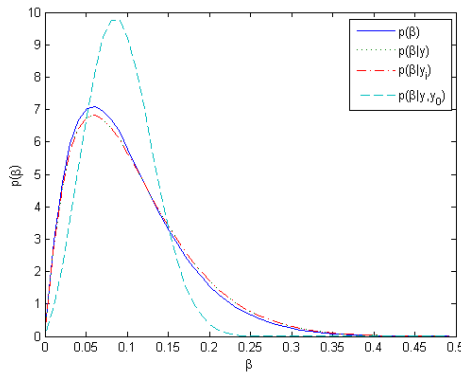


Figure 3. Prior and posterior distributions for  $\beta$  for the three measurement experiments.

to its limiting value given by  $C_{3,1} = 50$ : as  $y$  approaches zero, the probability that the true value of  $\alpha$  is greater than the specification limit 0.4 approaches zero. The asymmetric nature of the cost matrix is reflected in the individual cost functions. The decision thresholds – pass if  $y < 0.335$ , fail if  $y > 0.520$  – are given by crossover points for the cost functions. These thresholds mark the points at which the decision changes and, for a measurement system with fixed characteristics, can be calculated *a priori*. Once the measurement result is known, it can be compared with the decision thresholds and a decision made. The decision thresholds are optimal in the sense that they always lead to decisions that minimise the expected

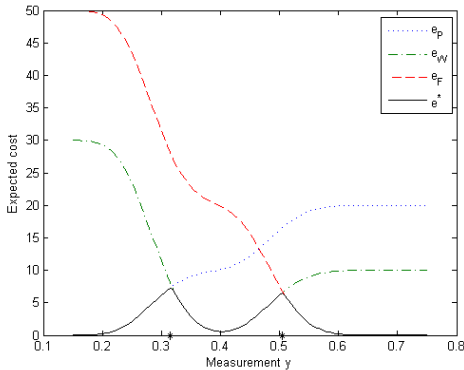


Figure 4. Expected costs as a function of measurement result  $y$ , with control measurement result  $y_0 = 0.1$ .

decision costs. Expected costs are highest for a measurement result  $y$  near the decision thresholds, i.e., where the measurement data is most ambiguous. Note that the decision thresholds relate to the measured estimate  $y$  of  $\alpha + \beta$  (and take account measurement uncertainty and the uncertain knowledge of the background concentration) while the specification limits relate to  $\alpha$  (with no reference to measurement).

Figure 2 gives the posterior distribution for  $\alpha$  for three measurement experiments i) a single measurement of  $y = 0.5$  with  $\sigma = 0.025$ , ii) 6 repeated measurements with mean  $y = 0.5$  and standard deviation  $s = 0.025$ , and iii) a measurement  $y = 0.5$  with  $\sigma = 0.025$  and a control measurement  $y_0 = 0.1$  with  $\sigma_0 = 0.05$ . Figure 3 gives the prior and posterior distributions for  $\beta$  for the same experiments. The uncertainty about the value of  $\alpha$  for the first and second experiments is largely due to the uncertainty in the background level. A measurement of the background level reduces the uncertainty about both and consequently reduces the decision costs: see Fig. 4. With the information from the control measurement  $y_0 = 0.1$ , the decision thresholds are 0.315 and 0.505.

The physical constraints associated with the parameters are incorporated into the Bayesian analysis easily through the prior distributions. The posterior distributions for  $\alpha$  and  $\beta$  will always adhere to the constraints so that, for example, a measurement result  $y$  smaller than a control measurement result  $y_0$  (which could be possible if  $\alpha$  is small) is dealt with easily. Classical approaches usually have difficulties in such circumstances.

#### 4. Summary And Concluding Remarks

In this paper, we have described a general approach to decision-making taking into account decision costs and uncertain information. The main element is using a probabilistic description of the state of knowledge to evaluate the expected costs associated with each decision choice. The approach has been illustrated on a model relating to measurements of the concentration of a substance, subject to physical constraints. The example shows how decision thresholds can be set that reflect both the costs and uncertainties and also demonstrates how the decision costs associated with different measurement strategies can be evaluated.

#### Acknowledgements

The work was funded in part by the Software Support for Metrology programme supported by UK's Department of Innovation, Universities and Skills. The authors are grateful for the helpful anonymous review comments.

#### References

1. M. G. Cox, A. B. Forbes, P. M. Harris, and J. A. Sousa. Accounting for physical knowledge in obtaining measurement results and associated uncertainties. In *IMEKO World Congress, September 18–22, 2006, Rio de Janeiro*.
2. C. D. Ferris, F. E. Grubbs, and C. L. Weaver. Operating characteristics for the common statistical tests of significance. *Ann. Math. Stat.*, 17:178–197, 1946.
3. A. B. Forbes. Measurement uncertainty and optimised conformance assessment. *Measurement*, 39:808–814, 2006.
4. A. Gelman, J. B. Carlin, H. S. Stern, and D. B. Rubin. *Bayesian Data Analysis*. Chapman & Hall/CRC, Boca Raton, Fl., second edition, 2004.
5. I. Lira. A Bayesian approach to the consumer's and producer's risk in measurement. *Metrologia*, 36:397–402, 1999.
6. H. S. Migon and D. Gamerman. *Statistical Inference: an Integrated Approach*. Arnold, London, 1999.
7. L. R. Pendrill. Operating ‘cost’ characteristics in sampling by variable and attribute. *Accred. Qual. Assur.*, 13:619–631, 2008.
8. L. R. Pendrill and H. Källgren. Decision-making with uncertainty in attribute sampling. In P. Ciarlini, E. Felipe, A. B. Forbes, F. Pavese, C. Perruchet, and B. Siebert, editors, *Advanced Mathematical and Computational Tools for Metrology VII*, pages 212–220, Singapore, 2006. World Scientific.

## VALIDITY OF EXPANDED UNCERTAINTIES EVALUATED USING THE MONTE CARLO METHOD

HIDEYUKI TANAKA, KENSEI EHARA

*National Measurement Institute of Japan, National Institute of Advanced Industrial  
Science and Technology, AIST3, 1-1-1  
Tsukuba, Ibaraki 305-8563, Japan*

The validity of expanded uncertainties evaluated using the method based on the “law of propagation of uncertainty” (LPU, GUM method) and “propagation of distribution using the Monte Carlo method” (MCM, GUM Supplement1 draft method) were investigated by using model data generated from random numbers belonging to the normal distribution. It was found that the expanded uncertainty evaluated by the MCM can be a significant overestimate, when *t*-distributions are adopted as the input distributions.

### 1. Introduction

The Monte Carlo method for propagation of distributions (MCM) [1] has been frequently used for the evaluation of uncertainties. It is often assumed that the results obtained by the MCM provide a coverage probability with accuracy greater than that obtained by the law of propagation of uncertainty (LPU) [2]. However, the validity of this assumption needs to be verified. Recently, Hall [3] investigated the validity of the MCM with regard to the magnitude of a complex-valued quantity. He showed that for a certain non-linear model of measurement, the MCM can result in an unreasonably low long-run success rate, while the LPU retains a reasonable level of success rate.

In this study, we investigated the validity of uncertainty intervals constructed by the MCM in which *t*-distributions were adopted as the distributions of input quantities. We generated a series of simulated measurement results assuming a simple linear model of measurement, and compared the success rate between the MCM and the conventional LPU method.

### 2. Verification Method

1. Suppose that the mathematical model of measurement is given by

$$Z = X + Y, \quad (1)$$

where *Z* denotes the measurand, and *X* and *Y* denote the input quantities. The two quantities *X* and *Y* are assumed to be independent. The estimates of

$Z$ ,  $X$  and  $Y$  are denoted by  $z$ ,  $x$  and  $y$ , respectively. We assume that  $x$  and  $y$  are determined from the arithmetic means of  $m$  and  $n$  repeated measurements, respectively, with  $m = 2, \dots, 10$  and  $n = 2, \dots, 10$ .

2. Generate  $m$  and  $n$  normally distributed random numbers by sampling from  $N\left(0, \left(\sqrt{m}\right)^2\right)$  and  $N\left(0, \left(\sqrt{n}\right)^2\right)$  as the measured values of  $X$  and  $Y$ .

These values are denoted by  $x_i$  and  $y_j$  ( $i = 1, \dots, m$ ;  $j = 1, \dots, n$ ). The variances of the normal distributions are so chosen that both  $x$  and  $y$  (i.e., the means of  $x_i$  and  $y_j$ ) can be regarded as samples from  $N(0, 1^2)$  and hence  $x$  and  $y$  have approximately the same size of contributions to the uncertainty of  $z$ .

- Evaluate  $z$  and its expanded uncertainty  $U$  by using the LPU and MCM. Here the coverage probability corresponding to  $U$  is chosen to be 95 %. In the LPU method, the coverage factor is determined by using the  $t$ -distribution with the effective degrees of freedom given by the Welch-Satterthwaite formula. In the MCM, the probability density functions of  $x$  and  $y$  are assumed to be scaled and shifted  $t$ -distributions with  $m - 1$  and  $n - 1$  degrees of freedom, respectively. The Monte Carlo trials are performed 10 000 times to calculate  $U$  in the MCM.
  - Check whether the interval  $z \pm U$  includes the true value of  $Z$  (in this case, the true value of  $Z$  is 0). If the true value of  $Z$  is in the interval, this trial is counted as a success.
  - Repeat steps 1–4 10 000 times, and estimate the success rate out of these 10 000 trials.

### 3. Result of Simulation

Tables 1 and 2 show the success rates attained by the MCM and LPU, respectively.

Table 1: Results of the simulation using the MCM (Unit: %)

Table 2: Results of the simulation using the LPU method (Unit: %)

$m \setminus n$	2	3	4	5	6	7	8	9	10
2	97.63	96.46	95.86	95.33	94.75	94.66	94.86	94.49	94.26
3		96.21	95.88	95.91	94.96	95.43	95.26	95.22	95.08
4			96.04	95.63	95.51	95.23	95.37	95.06	95.18
5				95.61	95.31	95.25	95.12	95.44	95.12
6					95.59	95.27	94.94	95.13	95.19
7						95.41	94.93	95.03	95.13
8							94.94	95.28	95.47
9								95.04	94.97
10									95.42

We observe that the success rate by the MCM is always larger than the assumed coverage probability of 95 %. This result demonstrates that the MCM tends to overestimate the expanded uncertainty if  $t$ -distributions are chosen to represent the input distributions. Because the present measurement model, Equation (1), is linear, the LPU is expected to perform well, resulting in the success rate by the LPU method close to 95 %. This is indeed confirmed in Table 2.

#### 4. Discussion

In determining  $U$  in the LPU method, the degree of freedom plays an essential role, while in the MCM it plays no role. However, we may introduce the apparent degrees of freedom,  $\nu_{\text{MCM}}$ , for the MCM in the following way:

1. The “effective” coverage factor  $k$  is first calculated by dividing  $U$  obtained in the MCM by the combined standard uncertainty  $u_c(z)$  which is calculated from  $x_i$  and  $y_i$ . We conduct 10 000 Monte Carlo trials of calculating  $k$ , and take their average  $\bar{k}$ .
2. We search for the degrees of freedom  $\nu$  of the  $t$ -distribution such that  $\Pr(|t| \leq \bar{k}) = 0.95$ , and regard  $\nu$  found in this way as  $\nu_{\text{MCM}}$ .

In the LPU method, the effective degrees of freedom,  $\nu_{\text{LPU}}$ , is calculated from the Welch-Satterthwaite formula. Table 3 and 4 show  $\nu_{\text{LPU}}$  and  $\nu_{\text{MCM}}$ , respectively.

Table 3: Degrees of freedom in the LPU method:  $\nu_{\text{LPU}}$ 

$m \setminus n$	2	5	10	50	100
2	1.418	3.494	6.056	19.127	31.412
5		6.876	10.531	19.147	26.576
10			16.541	33.171	39.360
50				96.166	130.479
100					196.068

Table 4: Degrees of freedom in the MCM method:  $\nu_{\text{MCM}}$ 

$m \setminus n$	2	5	10	50	100
2	0.907	1.286	1.333	1.357	1.359
5		3.979	5.500	7.066	7.300
10			9.353	15.655	16.944
50				53.068	71.052
100					107.740

It is observed that  $\nu_{\text{MCM}}$  is always significantly smaller than  $\nu_{\text{LPU}}$ . For diagonal elements (i.e.,  $m = n$ ),  $\nu_{\text{LPU}}$  is close to  $2(m - 1)$  as expected from the Welch-Satterthwaite formula, and  $\nu_{\text{MCM}}$  is approximately half this value. For off-diagonal elements when either  $m$  or  $n$  is relatively small, we observe that  $\nu_{\text{MCM}}$  is much smaller than  $\nu_{\text{LPU}}$ .

The degrees of freedom may be regarded as a measure of the credibility of the magnitude of uncertainty. The above argument suggests that the use of  $t$ -distributions as the input distributions in the MCM can lead to a significant underestimate of the credibility of the uncertainties of the input quantities.

## 5. Conclusions

We conducted numerical simulations to investigate the validity of the expanded uncertainty obtained by the MCM, assuming a simple linear model of measurement. When  $t$ -distributions are adopted as the distributions of the input quantities, the success rate attained in the MCM were found to be consistently larger than the coverage probability assumed in calculating the expanded uncertainty. This result suggests that the expanded uncertainty obtained by the MCM can be a significant overestimate, depending on the choice of input distributions.

## References

1. Joint committee for guides in metrology, “Evaluation of measurement data—Supplement 1 to the ‘guide to the expression of uncertainty in measurement’—Propagation of distributions using a Monte Carlo method” Draft, JCGM, (2007).
2. BIPM, IEC, IFCC, ISO, IUPAC, IUPAC and OIML, “Guide to the expression uncertainty in measurement 2<sup>nd</sup> edn,” ISO, ISBN 92-67-10188-9, (1995).
3. B D Hall, “Evaluating methods of calculating measurement uncertainty,” *Metrologia*, **45**, L5–L8, (2008).

## MODEL BASED UNCERTAINTY ANALYSIS IN INTER-LABORATORY STUDIES

BLAZA TOMAN, ANTONIO POSSOLO

*Statistical Engineering Division, National Institute of Standards and Technology,*

Statistical analysis of key comparison and inter-laboratory experiments is required to produce an estimate of the measurand called a reference value and further, measures of equivalence of the participating laboratories. Methods of estimation of the reference value have been proposed that rest on the idea of finding a so-called consistent subset of laboratories, that is, eliminating outlying participants. In this paper we propose an alternative statistical model, one that accommodates all of the participants' data and incorporates the dispersion among the laboratories into the total uncertainty of the various estimates. This model recognizes the fact that the dispersion of values between laboratories often is substantially larger than the measurement uncertainties provided by the participating laboratories. We illustrate the method on data from key comparison CCL-K1.

### 1. Introduction

Data from inter-laboratory experiments and key comparisons is collected to produce information about a particular measurand, or a set of measurands. In the case of key comparisons, the primary goal is to produce measures of equivalence of the participating laboratories, both unilaterally with respect to a reference value, and bilaterally with respect to each other. The understanding of the relationship between the *measurements* and the *measurand* determines how the former should be combined to produce an estimate of the latter, and how the uncertainty of this estimate should be assessed. This understanding is best expressed by means of a *statistical model* (that is, an *observation equation* [1]) that describes that relationship precisely, in particular, how the measurement values depend on the measurand. In the context of inter-laboratory studies and key comparisons, this suggests how the measurement results from the participating laboratories should be combined, and how other, pre-existing information about the measurand should be blended in.

Typically, in an inter-laboratory study, the participating laboratories provide measurements  $x_1, \dots, x_n$ , their standard uncertainties  $u_1, \dots, u_n$ , and possibly the accompanying degrees of freedom  $v_1, \dots, v_n$ . Each lab's measurement summarizes replicated measurements, each of which involves the combination of indications and measured values of participating quantities (thermal

expansion coefficient, temperature, etc.), and possibly also other pre-existing information about the measurand. The standard uncertainties are computed using methodology based on the *Guide to the Expression of Uncertainty in Measurement* (GUM) [2], combining uncertainty components from various sources, evaluated either by Type A or Type B methods. The current practice in most metrological experiments is to produce a reference value ( $x_{ref}$ ) to estimate the measurand and then, in key comparison experiments, to compute the unilateral,  $x_i - x_{ref}$ , and bilateral  $x_i - x_j$  degrees of equivalence (DoE). The reference value in a key comparison is abbreviated as KCRV. It is often the case that when a reference value and its uncertainty are computed, plots and other summaries of the data suggest that the measurements are not consistent, that is, that some of the laboratories' measurements are too far away from the reference value with respect to the accompanying uncertainties. In key comparisons, there have been proposals for formal methods to address this problem. Namely, [3,4] suggest using a hypothesis test based on a chi-square statistic to determine whether the participating laboratories belong to a consistent set. If the test determines this not to be the case then a method is proposed for finding a consistent subset of the laboratories. The key comparison reference value is then computed using only data from laboratories in the consistent subset. Even though not formally expressed in the literature, the chi-square statistic used in this method requires an assumption of a particular statistical model for the measurements. In this paper we address this issue, and propose alternative models for the analysis of key comparison and inter-laboratory data that do not require the preliminary identification of a "consistent" subset of laboratories whose measurements are combined into the KCRV, all the others being excluded. Our models are probabilistic: we use probability distributions to describe incomplete knowledge, and to describe also the dispersion of values that arise in replicated measurements. And our usage of them is statistical: we employ principles of inference to combine information (from data, and possibly from other sources) to produce estimates of the measurand, and to characterize the uncertainty of these estimates. We illustrate our methods on data from key comparison CCL-K1, calibration of gauge blocks by interferometry [5,6]. Section 2 introduces the current recommended methods, the common estimates of reference values, their uncertainties, degrees of equivalence and the consistency testing procedure. Section 3 presents proposed methodology based on the laboratory effects model, gives formulas and interpretations, and an example. A Laboratory Effects Model for experiments with multiple related measurands is shown in section 4. Conclusions follow in section 5.

## 2. Current Practice

### 2.1. Methods

Given the measurements and the standard uncertainties for a particular measurand from each of  $n$  laboratories, the two most common reference values are the arithmetic average and the weighted mean. These are frequently used statistical estimators of population means that are optimal under certain assumptions about the data. The arithmetic average  $\bar{x} = \frac{1}{n} \sum_{i=1}^n x_i$  would be optimal if the measurements were like outcomes of independent, Gaussian random variables, all with the same mean  $\mu$ , and the same variance  $\sigma^2$ . The weighted mean  $\bar{x}_w = \sum_{i=1}^n x_i / u_i^2 \Big/ \sum_{i=1}^n 1/u_i^2$  would be optimal if measurements were like outcomes of independent (assumption 1), Gaussian (assumption 2) random variables, all with the same (assumption 3) mean  $\mu$ , and different known variances given by  $u_1^2, \dots, u_n^2$  (assumption 4). We will refer to this as Model W. In most cases the standard uncertainties cannot reasonably be regarded as though they were based on infinitely many degrees of freedom. In some cases, including that of our example CCL-K1, the number of degrees of freedom associated with the standard uncertainties is available. In these circumstances it is preferable to fit yet another model (WD), which relies on the validity of assumptions 1-3, but not on 4. Under this model, the  $u_i^2$  are estimates of the true variances  $\sigma_i^2$  and behave like outcomes of chi-squared random variables: specifically,  $v_i u_i^2 / \sigma_i^2$  is like an outcome of a chi-square random variable with  $v_i$  degrees of freedom.

The weighted mean has been suggested as the preferred reference value by [3] with the condition that a consistency test is carried out using the statistic  $\chi_{Obs}^2 = \sum_{i=1}^n \frac{(x_i - \bar{x}_w)^2}{u_i^2}$  [4]. Under the assumptions of Model W, this is an observed value of a random variable with chi-square distribution with  $n-1$  degrees of freedom. The consistency test checks whether  $\chi_{Obs}^2 > \chi_{\alpha, n-1}^2$ , the  $100(1-\alpha)$  percentile of the chi-square distribution with  $n-1$  degrees of freedom. If the  $\chi_{Obs}^2$  is in fact larger than  $\chi_{\alpha, n-1}^2$ , the measurements are determined to be inconsistent. The largest subset of participants that passes this test is called the largest consistent subset (LCS) in [4] and is used to compute the reference value.

This subset is found using a sequential procedure, computing  $\chi_{Obs}^2$  for the larger subsets first.

Such consistency testing suffers from several consequential shortcomings. Most importantly, a conclusion that a set of laboratories is inconsistent appears to be interpreted as a violation of assumption 3. This is not necessarily so, in fact it could equally well reflect a violation of any of the other assumptions: particularly assumption 4, which would mean that the uncertainties are underestimated. (Also see [5]) Secondly, the proposed choice of  $\alpha$  equal to 0.05 is conventional but arbitrary. This is unfortunate because the LCS procedure may result in different subsets for different values of  $\alpha$  as is later shown for the CCL-K1 data. Matters are further complicated by the fact that the proposed procedure typically comprises a possibly large number of component tests, each of which has probability 0.05 of erroneously rejecting consistency, by chance alone 5% of the subsets will be deemed inconsistent when in fact they are not: the value of  $\alpha$  must be adjusted to compensate for this effect of multiplicity.

Another shortcoming derives from the sequential nature of the procedure. Suppose that  $\chi_{Obs}^2 > \chi_{\alpha,n-1}^2$ , and that the hypothesis of consistency was in fact incorrectly rejected. This means that purely by chance, as will occur with probability  $\alpha$ , the observed values  $x_1, \dots, x_n$  produce large values of  $\chi_{Obs}^2$ . We now proceed to the next stage of the LCS procedure, that is, to test that for a subset of laboratories (call it  $I_k$ ), of size  $n-1$ , the assumptions 1 through 4 are true (null hypothesis), versus the alternative hypothesis that this is false. We do that using the test statistic  $\chi_{Obs_k}^2 = \sum_{i \in I_k} (x_i - y_{n-1})^2 / u^2(x_i)$ . Now, simply

because by chance the data points are more spread out, this statistic will also tend to be large, larger than one would expect under the new null hypothesis if doing this test unconditionally, that is, not as a follow-up procedure to the first hypothesis test. This means that for an  $\alpha$  level test, the probability of rejecting the null hypothesis when it is true is in fact larger than  $\alpha$ . Thus  $\chi_{Obs_k}^2 > \chi_{\alpha,n-2}^2$  for the follow-up test is not as strong an evidence against the second null hypothesis as is believed, leading to incorrect conclusions.

Next we illustrate these methods using the data from key comparison CCL-K1.

## 2.2. Example CCL-K1

This key comparison was carried out to compare deviations from nominal length of several steel and several tungsten gauge blocks, and is fully described in

[6,7]. Here the results for the tungsten gauges are used to illustrate the various procedures. Table 1 has the results for the tungsten 1.1 mm gauge.

Table 1. Deviations from nominal length (in mm), standard uncertainties (in mm), and degrees of freedom for the 1.1 mm tungsten block (20'20987).

Lab	Deviation from nominal (mm)	Standard uncertainty (mm)	Degrees of Freedom
OFMET	-54	9	500
NPL	-51	14	119
LNE	-36	10	94
NRC	-51	13	9
NIST	-38	9	50
CENAM	-72	7	72
CSIRO	-32	9	207
NRLM	-66.4	10.3	5
KRISS	-62	9.4	24

Figure 1 shows a plot of the measurements with their 95% uncertainty intervals, and the weighted mean with its uncertainty, based on Model W, and on Model WD. In the plot, two laboratories appear to be clear outliers, with several others also quite far away from the weighted mean. This suggests that Model W (and Model WD) is not good choices for this particular set of data.

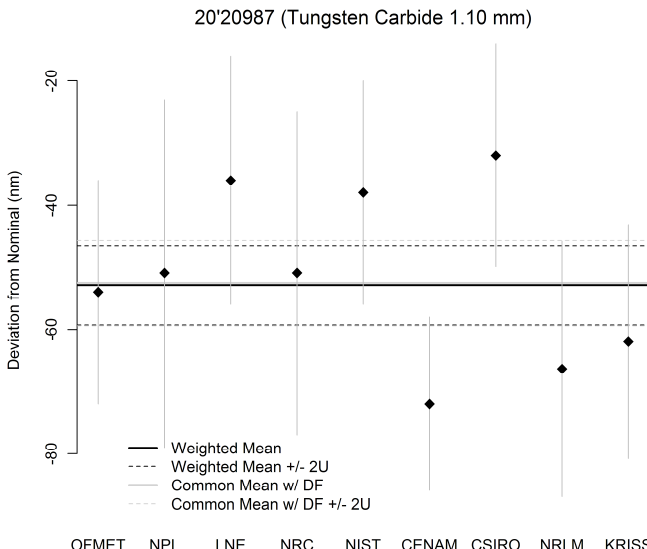


Figure 1. Laboratory measurements, 95% uncertainty intervals, weighted mean and its uncertainty for the 1.1 mm tungsten gauge.

A formal test of consistency using the chi-square statistic produces  $\chi^2_{Obs} = 21.15$ , which is larger than  $\chi^2_{0.05,8} = 15.5$ , thus confirming what the plot suggests, rejecting the full set of laboratories as consistent at this level of  $\alpha$ . The LCS procedure for  $\alpha = 0.05$  identifies CENAM as an outlier. The remaining laboratories form the LCS.

Since the level of the test is arbitrary, it is interesting to see what happens for other values of  $\alpha$ . Figure 2 contains a plot which illustrates this.

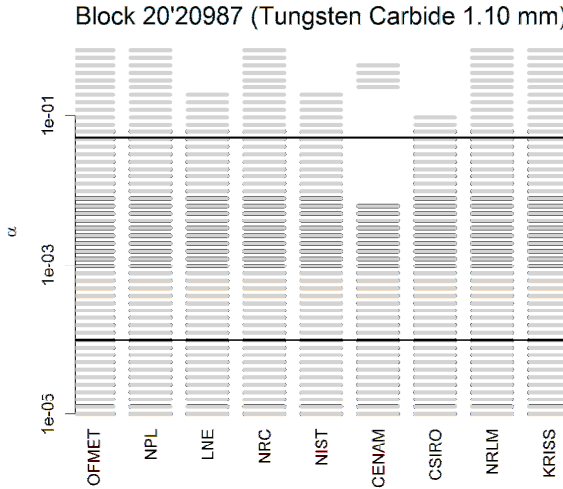


Figure 2. Consistent subsets as  $\alpha$  varies. The top horizontal line is for  $\alpha = 0.05$ . The continuous horizontal line towards the bottom is the value of  $\alpha$  that results from the so-called Bonferroni [7, Section 10.7] correction to accommodate the fact that, to find the largest consistent subset, one is either implicitly or explicitly performing  $2^n - n - 1$  separate (and statistically dependent) consistency tests.

This figure shows that the largest consistent subset (LCS) is not a monotonic function of  $\alpha$ : in other words, the LCS corresponding to a particular value of  $\alpha$  does not necessarily include the LCS corresponding to a larger value of  $\alpha$ . Since any choice of a value for  $\alpha$  is both arbitrary and influential, and the corresponding chi-squared test that is employed to judge significance (either using the chi-squared reference distribution or its counterpart determined by simulation) typically has low power to detect heterogeneity, we believe that basing the KCRV on the LCS as [9] recommends generally is imprudent. Indeed, we much prefer alternatives where the measurements provided by all the laboratories are allowed to speak, and play a role, albeit one that is modulated by their intrinsic uncertainties, and by the extrinsic dispersion of the measurements.

### 3. Laboratory Effects Model

#### 3.1. Methods

Under the Laboratory Effects Model, measurements are modeled as outcomes of independent Gaussian random variables with means  $\lambda_i$ , and variances given by  $u_1^2, \dots, u_n^2$ . (A similar relaxation of the assumption on the variances as given by Model WD can also be used here.) The means can be written as  $\lambda_i = \mu + \beta_i$ , where  $\mu$  is the measurand. There are two well-known [10,11] alternative models which differ in the definition and interpretation of the  $\beta_i$ .

The so-called Fixed Effects Model [10], assumes that the  $\beta_i$  are systematic laboratory effects (biases) which are expected to re-occur in repeated similar experiments. They are unknown constants to be estimated from the measurement data. In terms of an observation equation this model can be written as

$$\begin{aligned} X_i &= \mu + \beta_i + E_i \\ E_i &\sim N(0, u_i^2) \end{aligned} \quad (1)$$

If the measurand is known independently of the results of the interlaboratory study – for example, it pertains to a standard reference material (SRM) whose certificate puts it at  $M$ , with uncertainty  $u(M)$ , then the  $\beta_i$  can be estimated as  $x_i - M$  with uncertainty  $u_i + u(M)$ . Clearly, the unilateral DoE is  $x_i - M$ , the bilateral DoE the usual  $x_i - x_j$ . In most cases no independent information about the measurand exists and the reference value needs to be estimated from the measurements. In such a case, there is no unique solution and the  $\beta_i$  need to be constrained. Under the constraint  $\sum_{i=1}^n \beta_i = 0$ , the measurand is estimated (via least squares or maximum likelihood) as  $\bar{x}$ , and the  $\beta_i$  are estimated by  $x_i - \bar{x}$ , the unilateral DoE with respect to the arithmetic average [12]. The uncertainty of the  $\bar{x}$  is

$$u(\bar{x}) = \sqrt{\frac{1}{n} \sum_{i=1}^n u_i^2}, \quad (2)$$

the uncertainty of the unilateral DoE for the  $i$ th laboratory is

$$\sqrt{u_i^2 + \frac{1}{n^2} \sum_{j=1}^n u_j^2 - \frac{2}{n} u_i^2}. \quad (3)$$

To summarize, the Fixed Effects Model does not require a common mean but partially attributes differences among measurements from various laboratories to differences among the means of the random variables which represent the observations. The laboratory uncertainties are not increased in this model. In addition to the classical interpretation of the measurements as observations of random variables, or as sample averages, one may also interpret the measurements as expected values of belief distributions about the measurand. In this case, the  $u_i$  are interpreted as standard deviations of such belief distributions. Both interpretations lead to the same formulas and results with different interpretations of the uncertainties and uncertainty intervals. Refer to [12] for a full discussion.

The second type of Laboratory Effects Model is called the Random Effects Model [10,11]. Here the  $\beta_i$  are random biases which are *not* expected to have the *same* value on repeated similar experiments, but instead are outcomes of Gaussian random variables with mean 0 and variance  $\sigma_\beta^2$ . In terms of an observation equation this is

$$\begin{aligned} X_i &= \mu + \beta_i + E_i \\ \beta_i &\sim N(0, \sigma_\beta^2) \\ E_i &\sim N(0, u_i^2) \end{aligned} \tag{4}$$

Measurements from all laboratories have the same mean  $\mu$ , but the variances are inflated to  $u_i^2 + \sigma_\beta^2$ . Using the method of maximum likelihood [11], all of the parameters of this model can be estimated. As the laboratory effects are random variables, their estimates are really estimates of the realized values of the  $\beta_i$ . The estimated covariance matrix provides the uncertainties of the  $\hat{\mu}$  (KCRV) and of the  $\hat{\beta}_i$ . The  $\hat{\beta}_i$  can be used to compare laboratories to each other instead of the standard DoE.

To summarize, under the Random Effects Model, apparent differences among laboratory measurements are explained by an increase in the laboratory uncertainties. The measurements from all laboratories have the same mean. As the ratio of  $\hat{\sigma}_\beta^2$  to the  $u_i^2$  gets large for most or all of the laboratories, the  $\hat{\beta}_i$  approach  $x_i - \hat{\mu}$ , the usual unilateral DoE. On the other hand, as this ratio approaches zero, the  $\hat{\beta}_i$  approach 0.

As both models are designed to fit data from experiments such as key comparisons and inter-laboratory studies, it is useful to discuss when to apply one versus the other. Generally, Fixed Effects Models are meant to be used when the laboratory effects are essentially constant biases which are likely to re-

occur in similar sizes both relative to the value of the measurand and relative to each other, across similar experiments. Random effects are used for situations when there is no such expectation, or no solid documentation for such biases. That is, the laboratory biases are most likely due to some common underlying cause which acts in a *varying nature* so that the laboratories may be closer or farther from the target value in different experiments, purely by chance. There are no identifiable causes that seem responsible for these laboratory biases, hence they are treated symmetrically (relative to each other), and modeled as random variables with a common distribution, centered at 0, and whose variance captures the dispersion of the lab measurements in excess of what their respective uncertainties suggest such dispersion should be.

In each particular experiment, it may be difficult to discern the cause of the variability among laboratories and thus decide which model to use. But it will be seen in the following section that the Random Effects Model provides the most conservative solution.

### 3.2. Example

The laboratory effects models are now applied to the data from key comparison CCL-K1. Table 2 contains the estimates of  $\mu$  and of the corresponding uncertainty under the three models, Model W, the Fixed Effect Model and the Random Effects Model. All model-fitting was done in the R [13] environment for statistical computation and graphics, in particular by employing function lme [14], which fits linear Gaussian models possibly containing both random and fixed effects, as [15] describes in detail.

Table 2. Estimates of the mean deviation from nominal length (in mm), standard uncertainties (in mm) in parentheses, and estimates of the standard deviation of the laboratory effects distribution. All under the three alternative models.

Block	Model W	Fixed Effects	Random Effects	$\hat{\sigma}_\beta$
0.5	22 (3.1)	24 (3.5)	24 (4.0)	12
1.00	14 (3.1)	16 (3.5)	16 (4.0)	12
1.01	26 (3.1)	28 (3.5)	27 (3.6)	9
1.10	-53 (3.2)	-51 (3.5)	-51 (4.4)	13
6.0	-48 (3.1)	-47 (3.5)	-47 (3.4)	10
7.0	29 (3.1)	30 (3.5)	31 (3.8)	11
8.00	47 (3.1)	49 (3.5)	49 (3.3)	10
80.0	104 (4.0)	104 (4.7)	104 (4.1)	10
100.0	-76 (4.3)	-79 (5.2)	-79 (4.7)	14

The results show that estimates of the mean deviation from nominal length are quite similar under the three models. The uncertainties of the weighted mean are uniformly smaller than the uncertainties of the other two estimates. Figure 3

provides a comparison of the laboratories via their unilateral Degrees of Equivalence under Model W, and under the Fixed Effects Model. The  $\hat{\beta}_i$  are given for the Random Effects Model.

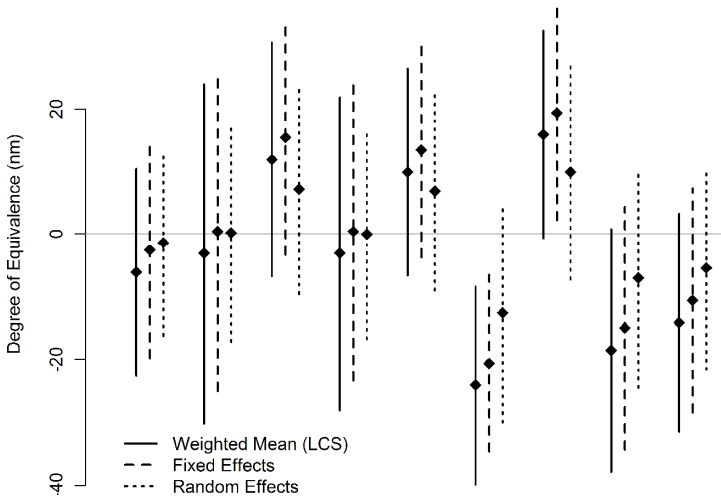


Figure 3. 95% uncertainty intervals for the DoE obtained using the LCS procedure, and using the Fixed Effects model. 95% uncertainty intervals for the estimated biases under the Random Effects model

The plot shows that there are no significant (that is, non-zero) laboratory biases under the Random Effects Model. Model W with the LCS procedure identifies CENAM as not belonging to the largest consistent subset. Thus the added variability in the form of the between-laboratory variance  $\sigma_{\beta}^2$  does explain the dispersion of the laboratory measurements under the assumption of a common mean. The Fixed Effects model on the other hand produces significant laboratory biases for CENAM and for CSIRO. The question now is whether these biases are systematic and would be repeated in additional experiments. This question is answered below.

#### 4. Laboratory Effects Model for Multiple Measurands

In CCL-K1, the participating laboratories measured nine steel gauges and nine tungsten carbide gauges, of rectangular cross-section and different lengths, using optical interferometry, applying the same method of fringe fractions, with phase corrections. (Since neither NIM nor VNIIM applied these corrections, we follow [6,7] in leaving their measurements out of this study.) Experiments such

as this, where multiple measurands are measured using essentially the same methods, afford a unique opportunity to determine whether the apparent differences between laboratories, indicated by the estimated laboratory biases, indeed remain constant across measurands. Figure 4 shows the average predicted laboratory biases from the Random Effects Model for each of the tungsten gauges with different symbols for each laboratory.

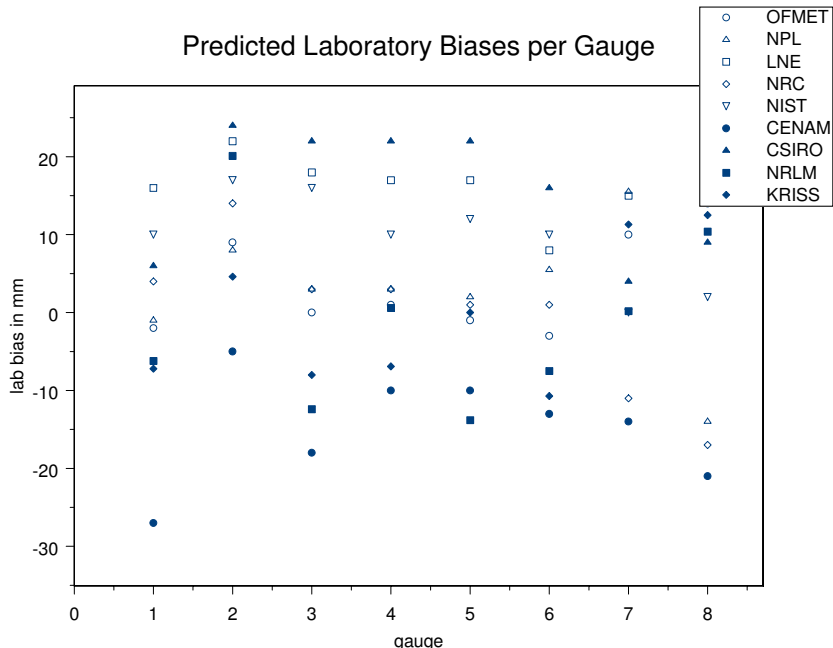


Figure 4. Average Predicted Laboratory Biases in mm.

This graph does show a pattern for the biases of several of the laboratories, particularly LNE and CSIRO tend to be high, and CENAM tends to be low, compared to the other laboratories. The following model can capture such information.

Measurements  $x_{ij}$ , where  $i$  denotes the laboratory and  $j$  denotes the gauge block, are outcomes of independent Gaussian random variables with means  $\lambda_{ij}$ , and variances given by  $u_{11}^2, \dots, u_{1p}^2, \dots, u_{n1}^2, \dots, u_{np}^2$ . The number of laboratories is  $n$  and the number of blocks is  $p$ . The means can be written as  $\lambda_{ij} = \mu_j + \beta_{ij}$ , where  $\mu_j$  are the measurands, and  $\beta_{ij}$  are the laboratory effects. For each laboratory,

the  $\beta_{ij}$  are considered to be Gaussian random variables with a mean given by  $\alpha_i$ . In terms of an observation equation this is

$$\begin{aligned} X_{ij} &= \mu_j + \beta_{ij} + E_{ij} \\ \beta_{ij} &\sim N(\alpha_i, \sigma_{\beta_i}^2) \\ E &\sim N(0, u_{ij}^2) \end{aligned} \quad (5)$$

The  $\alpha_i$  represent the average laboratory bias that applies to all blocks measured by the same laboratory. As in the simpler, Fixed Effects Model, there must be a constraint on the laboratory biases, that is,  $\sum_{i=1}^n \alpha_i = 0$ . This model can again be

fitted using maximum likelihood methods, in R or other software packages such as WinBUGS [16]. Figure 5 shows a plot of 95% uncertainty intervals for the  $\alpha_i$  for the 9 tungsten gauges in the CCL-K1 key comparison. The three laboratories LNE, CSIRO and CENAM do have non-zero average predicted biases over different sized gauges and thus appear to have systematic laboratory biases. The remaining laboratories do not appear to have such systematic biases as their uncertainty intervals for the  $\alpha_i$  include 0.

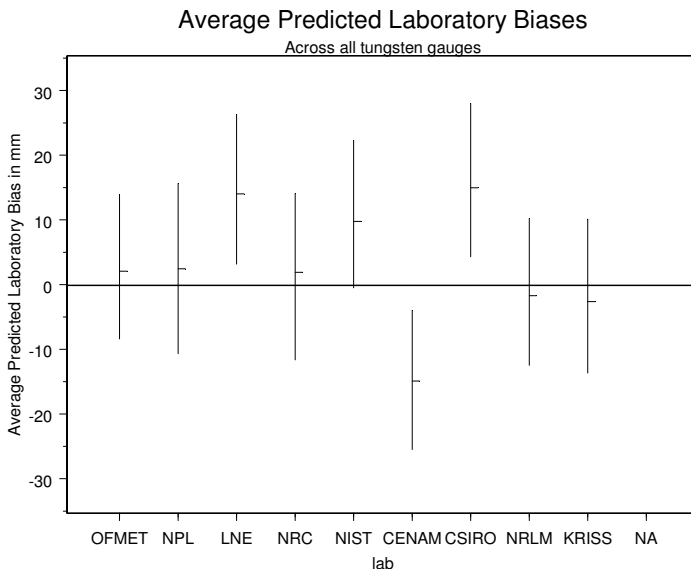


Figure 5. Average estimated laboratory biases  $\alpha_i$  (in mm) and their uncertainty intervals, estimated from the measurements of all tungsten gauge blocks

## 5. Conclusions

The laboratory effects models presented in this paper facilitate the statistical analysis of key comparison data without excluding measurements made by any of the participating laboratories. Such exclusion should be done only for cause, without which even the most discrepant measurement cannot logically be ruled out as erroneous. This inclusive policy enacts a price in uncertainty for the reference value. But this only properly reflects the common state of knowledge that results when the dispersion of the measurements exceeds what one might expect based only on the measurement uncertainties that the laboratories state. The fixed effects model allows direct computation of degrees of equivalence as required by the MRA. In the case of the random effects model, where laboratory biases are modeled as random variables with the same probability distribution, equivalence between laboratories may be measured by comparing the estimates of the realized biases. When the key comparison or inter-laboratory study includes measurements for multiple measurands measured in similar experiments, then it becomes possible to determine whether systematic biases are in fact present.

## Acknowledgments

The authors wish to thank Rudolf Thalmann, METAS, for sharing the degrees of freedom for the data from key comparison CCL-K1. The manuscript benefitted greatly by reviews from Greg Strousse, and Nien-fan Zhang, NIST, and an anonymous referee.

## References

1. Possolo A and Toman B 2007 Assessment of measurement uncertainty via observation equations *Metrologia* **44** 464-475
2. ISO Technical Advisory Group, Working Group 3, Guide to the Expression of Uncertainty in Measurement, International Organization for Standardization, Geneva (1993).
3. Cox M G 2002 The evaluation of key comparison data *Metrologia* **39** 589 – 95.
4. Cox M G 2007 The evaluation of key comparison data: determining the largest consistent subset *Metrologia* **44** 187-200.
5. Kacker R, Forbes A, Kessel R, Sommer K-D 2008 Classical and Bayesian interpretation of the Birge test of consistency and its generalized version for correlated results from interlaboratory evaluations *Metrologia* **45**, 257 - 265

6. Thalmann R 2001 CCL Key Comparison CCL-K1: Calibration of gauge blocks by interferometry — Final report. Swiss Federal Office of Metrology METAS, Wabern, Switzerland
7. Thalmann R 2002 CCL key comparison: calibration of gauge blocks by interferometry *Metrologia* **39** 165–177
8. Wasserman L 2004 All of Statistics, A Concise Course in Statistical Inference, Springer Science+Business Media, New York, NY, ISBN 0-387-40272-1
9. Decker J, Brown N, Cox M G, Steele A, and Douglas R 2006 Recent recommendations of the Consultative Committee for Length (CCL) regarding strategies for evaluating key comparison data. *Metrologia* **43**: L51-L55
10. Searle S R 1971 *Linear Models* John Wiley & Sons New York
11. Searle S R, Casella G, McCulloch C 1992 *Variance Components* John Wiley & Sons New York
12. Toman B 2007 Statistical interpretation of key comparison degrees of equivalence based on distributions of belief *Metrologia* **44** L14-L17
13. R Development Core Team (2008) R: A Language and Environment for Statistical Computing, R Foundation for Statistical Computing, Vienna, Austria, <http://www.R-project.org>
14. Pinheiro J, Bates D, DebRoy S, Sarkar D, R Core team (2008) nlme: Linear and Nonlinear Mixed Effects Models, R package version 3.1-89, <http://www.R-project.org>
15. Pinheiro J. C., Bates, D. M. (2000) Mixed-Effects Models in S and S-Plus, Springer-Verlag, New York
16. Lunn, D.J., Thomas, A., Best, N., and Spiegelhalter, D. 2000 WinBUGS -- a Bayesian modelling framework: concepts, structure, and extensibility. *Statistics and Computing*, **10**:325--337.

## GEAR METROLOGY OF STATISTICAL TOLERANCING BY NUMERICAL SIMULATION

JEAN-PAUL VINCENT, CYRILLE BAUDOUIN, JÉRÔME BRUYERE,  
JEAN-YVES DANTAN, REGIS BIGOT

*Laboratoire de Génie Industriel et de Production Mécanique.  
E.N.S.A.M. de Metz, 4 rue A. Fresnel, 57070 METZ Cedex, France.  
E-mail: [jean-yves.dantan@metz.ensam.fr](mailto:jean-yves.dantan@metz.ensam.fr)*

Tolerance verification permits to check the product conformity and to verify assumptions made by the designer. For conformity assessment, the uncertainty associated with the values of the measurands must be known. In the ISO TS 17450 part 2, the notion of the uncertainty is generalized to the specification and the verification. The uncertainty is divided into correlation uncertainty, specification uncertainty and measurement uncertainty. Correlation uncertainty characterizes the fact that the intended functionality and the controlled characteristics may not be perfectly correlated. Therefore, we propose a new specified characteristics based on the statistical tolerancing approach which is directly in relationship with the design intent: the probability distribution of maximum range of the transmission error (the transmission error is the main source of vibratory and acoustic nuisances), and the evaluation of this characteristic based on 3D acquisition by Monte Carlo simulation and Tooth Contact Analysis. Moreover, the measurement uncertainty of the evaluation of this characteristic is estimated by Monte Carlo Simulation.

### 1. Introduction

As technology increases and performance requirements continually tighten, the cost and required precision of assemblies increase as well. There is a strong need for increased attention to tolerance design to enable high-precision assemblies to be manufactured at lower costs. Tolerance verification permits to check the product conformity and to verify assumptions made by the designer. Tolerance verification defines inspection planning and metrological procedures for functional requirements, functional specifications and manufacturing specifications.

For gears, two kinds of metrology exist [1], [2]: Geometrical metrology and kinematic metrology. Geometrical metrology is performed to ensure that parts meet tolerance specified on its geometric definition. Kinematic metrology allows determining transmission error of the product. Concerning the gears standards (ANSI/AGMA 2009-B01; DIN 3962), three types of geometrical

deviation are identified: the flank deviation (profile or form deviation...), the situation deviations between flanks (cumulative and single pitch deviations...) and the situation deviations between teeth and hole (runout, ...) As geometric deviations impact the kinematic behaviour of the product, it is possible to use a computer program, able to predict the total composite deviation  $F'_1$  and the tooth-to-tooth composite deviation  $f'_1$  knowing the geometric deviation of the product. This program evaluates the virtual kinematic error based on the CMM's data points from the geometrical measurement of gears.

The notion of uncertainty is by now well entrenched in metrology. In the ISO TS17450-2, the notion of the uncertainty is generalized to the specification and the verification. In fact, the uncertainties through the product life cycle begin from the design intent to the inspection activity. The uncertainty is divided into correlation uncertainty, specification uncertainty and measurement uncertainty. Correlation uncertainty characterises the fact that the intended functionality and the controlled characteristics may not be perfectly correlated. The specification uncertainty characterizes the ambiguity in the specification expression. And the measurement uncertainty is considered by the metrologists and well described in GUM. The measurement uncertainty includes all the causes of variation from the geometric specification to the result of inspection.

To decrease the correlation uncertainty, a new specified characteristic based on a statistical tolerancing approach is proposed: the probability distribution of the transmission error of the studied gear. This characteristic is in direct relationship with the design intent: the requirement on the transmission error (this approach could be apply to others requirements – backlash, ...) In fact, it is interesting to predict the kinematic behaviour the studied gear with a gear randomly chosen from production i.e. to know the probability distribution of the transmission error of the studied gear.

## **2. Global Approach**

The objective of this paragraph is to present the global approach followed to first estimate the total composite deviation  $F'_1$  and the tooth-to-tooth composite deviation  $f'_1$  for a virtual master gear meshing with a studied gear based on its acquisition CMM's data points, and secondly to estimate the probability distribution of the transmission error of the studied gear.

The estimation of  $F'_1$  and  $f'_1$  (Approach 1) is detailed in Figure 1a):

1. To obtain an image of a manufactured gear, the acquisition equipment chosen, has been a CMM.
2. The result of the CMM acquisition is a set of points

3. A set of points of the nominal model of the master gear geometry is generated
4. Based on the result of the CMM acquisition [3], substitute tooth surfaces in the global coordinate system are reconstructed using Bezier surfaces. The geometrical modelling of parts is detailed in the third chapter.
5. Tooth Contact Analysis (TCA) [4], [6], program computes a simulated transmission error then  $F'_1$  and  $f'_1$  are calculated.

Secondly, the estimation of the probability distribution of the transmission error of a studied gear (Approach 2) is detailed in Figure 1 b):

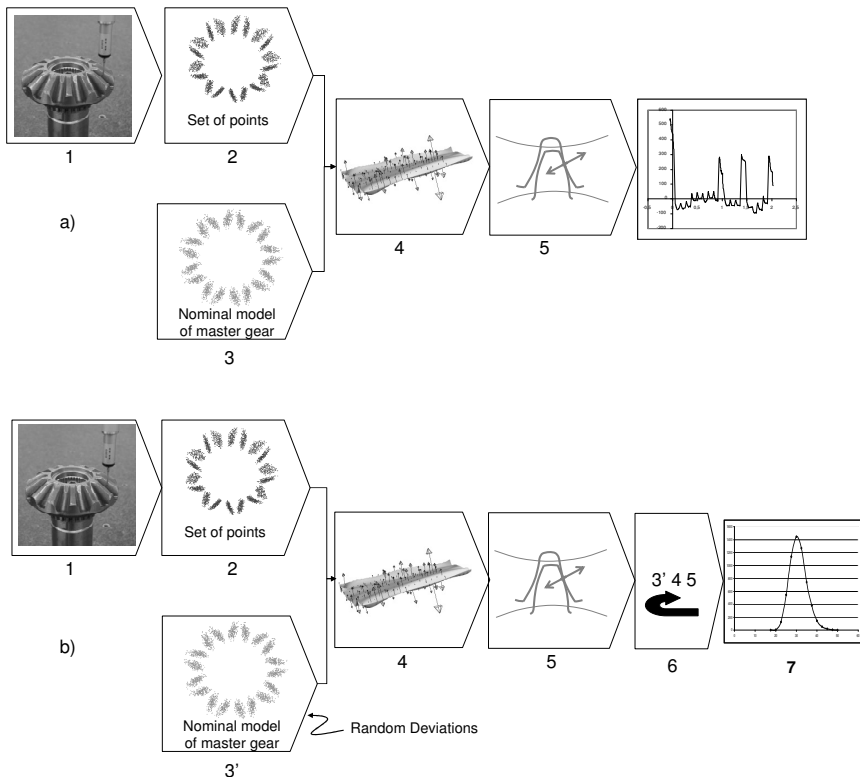


Figure 1: a) Detail of the estimation of  $F'_1$  and  $f'_1$ . b) Detail of the estimation of the probability distribution of the transmission error of a studied gear.

- 3'. The first and the second steps of this approach are the same as before. The geometrical deviations of the wheel and the assembly are modeled by random variables. These geometries provide an image of the manufactured gears.

The fourth and fifth steps of this approach are the same as before.

6. A Monte Carlo simulation computes a set of meshing simulations. Each meshing simulation is computed by a computer program based on Tooth Contact Analysis. The result of this metrology and numerical simulation.
7. The probability distribution of the maximum range of the transmission error of the measured pinion is then calculated.

To validate the program of virtual meshing simulation, a simulated kinematic error, based on the set of points of the CMM's measurement of a pair of gears, has been compared to an experimental kinematic error of this same pair of gear. Several measurements have been performed in order to assess the measurement uncertainty of the kinematic metrology. For each test, the tooth-to-tooth composite deviation has been calculated. The simulation meshing program allows evaluating the transmission error of a manufactured gears meshing with an other gear, master, or manufactured one. It provides virtual kinematic metrology estimation. In order to test the robustness of this approach, the confidence interval must be evaluated.

### **3. Confidence interval of virtual kinematic metrology**

In general, the result of a measurement is only an approximation or estimate of the value of the specific quantity subject to measurement. In this case, the measurands are the total composite deviation  $F'_1$  and the tooth-to-tooth composite deviation  $f'_1$ . The uncertainty of the result of this measurement must be evaluated by statistical methods. Furthermore, the TCA computer program is not base on an explicit model, that's why the evaluation of uncertainty by the statistical analysis is made by Monte Carlo simulation [5].

The uncertainty and confidence interval of the result given by the meshing simulation program depend on several factors like the approximation error of the fitting operation, the point's density used to reconstruct surfaces, the numerical precision of the TCA algorithm and the acquisition uncertainty due to the CMM.

In order to evaluate the effects of acquisition uncertainty of the step 1 on the result of the simulation, the following method has been followed:

- The evaluation of the acquisition uncertainty is based on CMM's manufacturer's specifications,
- The measurand  $Y$  (the total composite deviation  $F'_1$  or the tooth-to-tooth composite deviation  $f'_1$ ) is not measured directly, but is determined from  $N$  other quantities  $X_1, X_2 \dots X_N$  (the result of the acquisition: the set of points) through a functional relation:  $Y = f(X_1, X_2, \dots, X_n)$ . The input quantity  $X_i$  is

estimated from an assumed probability distribution based on the evaluation of the acquisition uncertainty.  $N$  independent observations  $X_{i,k}$  of  $X_i$  are obtained by a random generator like a Monte Carlo simulation, and the probability distribution and the combined standard uncertainty of the measurand  $Y$  is estimated (Figure 2a))

- 2'. Points of the first geometry are perturbed around there initial position. The perturbation is taken around the value of the uncertainty measurement of a CMM. For example 4  $\mu\text{m}$ . Steps 3' 4, 5, and 6 are the same as shown in section 2.

Figure 2 b) shows the set of simulations for a set of geometries (perturbed points from 4  $\mu\text{m}$  to their initial position). The confidence interval of the tooth-to-tooth composite deviations for this set of simulation is 2  $\mu\text{m}$ .

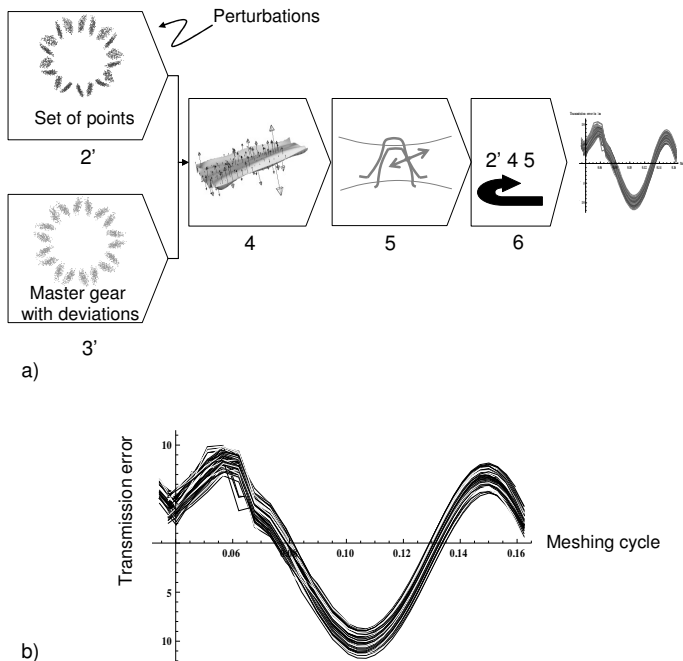


Figure 2: a) Uncertainties evaluation approach due to acquisition uncertainties, b) A set of simulations based on perturbed geometries

#### 4. Gear Metrology of Statistical Tolerancing on Transmission Error

In this part, a statistical tolerancing approach is proposed to provide a new specified characteristic: the probability distribution of the transmission error of a

studied gear. This characteristic, in direct relationship with the design intent, could decrease the correlation uncertainty (ISO TS 17450 part 2).

Statistical tolerancing is a more practical and economical way of looking at tolerances and works on setting the tolerances so as to assure a desired yield [6]. By permitting a small fraction of assemblies to not assemble or function as required, an increase in tolerances for individual dimensions may be obtained, and in turn, manufacturing costs may be reduced significantly. Statistical tolerance analysis computes the probability that the product can be assembled and will function under given individual tolerance.

Gear roll testing allows knowing the kinematic error of a gear from production meshing with a master gear, but to know how a manufactured gear behaves with others, randomly chosen from production i.e. to know the probability distribution of the kinematic error of the studied gear, a large number of meshing must be performed. To do so, geometrical deviations are introduced in the model of gears. Different models can be used to introduce these deviations i.e. vectorial tolerancing or zone tolerancing.

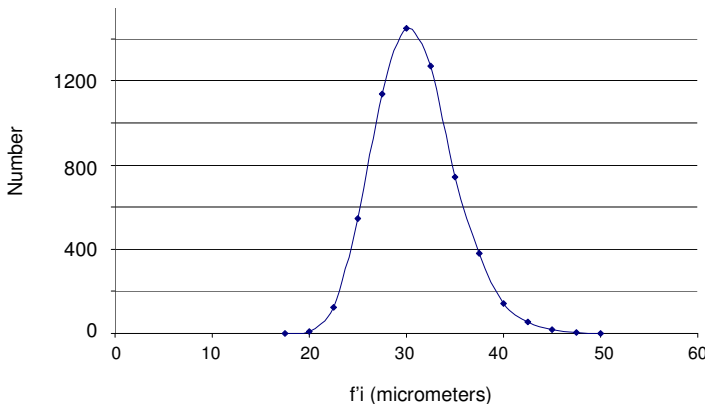


Figure 3: Probability distribution of the maximum range of the transmission error.

Usually, statistical analysis uses a relationship of the form  $Y = f(X_1, X_2, \dots, X_n)$  where  $Y$  is the response (characteristic such as gap or functional characteristics) of the assembly and  $X = \{X_1, X_2, \dots, X_n\}$  are the values of some characteristics (such as situation deviations or/and intrinsic deviations) of the individual parts.  $f$  can be an explicit function or implicit expression. As it is implicit in our case, statistical analysis methods like Linear Propagation (RSS) and Taylor series cannot be employed. Quadrature technique can be used if the

function is approximable. Monte Carlo Simulation is a powerful tool to know the probability distribution of a functional characteristic of a product for example. The following figure shows the result of a Monte Carlo simulation with 4000 samples: probability distribution of the maximum range of the transmission error: a measured pinion meshing with randomly generated geometries of wheel (equivalent to ISO Quality 6) (Figure. 3).

## 5. Conclusion

The important point of the proposed specification and metrology for a gear based on dimensional metrology and numerical simulation is to provide a solution which is in adequacy with the design intent. There is no more interpretation for the designer, the manufacturer and the metrologist. This approach could be decrease the correlation uncertainty [ISO TS 17450 – part 2]. Further more, in order to test the robustness of the proposed approach (to evaluate the impact of the measurement uncertainties on the simulated transmission error), the confidence interval of the proposed characteristic has been evaluated using Monte Carlo simulation.

## Reference

1. G. Goch, Gear metrology, keynote papers, *Annals of the CIRP*, 52(2), 1–37. (2003)
2. S. Boukebbab, H. Bouchenitfa, H. Boughouas, J. M. Linares. Applied iterative closest point algorithm to automated inspection of gear box tooth, *Computers & Industrial Engineering*, 52, 162-173. (2007)
3. C. Baudouin, R. Bigot, S. Leleu, P. Martin, Gear geometric control software: approach by entities, *The International Journal of Advanced Manufacturing Technology*.(2007)
4. F.L. Litvin, A. Funetes and K. Hayasaka. Design, manufacture, stress analysis, and experimental tests of low-noise high endurance spiral bevel gears, . *Mechanism and Machine Theory*, 41, 83-118. (2006).
5. K.D. Sommer, O. Kuehn, A. Weckenmann, Use of MCM for Uncertainty Evaluation of a Non-Linear and Multivariate Dimensional Measurement Task. *CIRP Seminar on Computer Aided Tolerancing*, Germany. (2007).
6. J. Bruyère, J.Y. Dantan, R. Bigot, P. Martin, Statistical tolerance analysis of bevel gears by Tooth Contact Analysis and Monte Carlo simulation, *Mechanism and Machine Theory*, 42( 10), 1326-135.(2007).

## TRANSFERRING MONTE CARLO DISTRIBUTIONS IN THE EVALUATION OF UNCERTAINTY

ROBIN WILLINK

*Industrial Research Ltd.,  
P.O.Box 31-310, Lower Hutt 5040, New Zealand  
E-mail: r.willink@irl.cri.nz*

The output of a Monte Carlo analysis is a large set of numbers that can be used to approximate the probability distribution of the relevant random variable. This article describes how this set can be summarized to enable the variable to function as an input to a further uncertainty calculation, in particular a further Monte Carlo calculation. The basic technique presented involves approximating the inverse distribution function of the variable, which is the *quantile function*, by a function with a simple form. This makes the subsequent generation of random samples for Monte Carlo calculations straightforward.

### 1. Introduction

The technique of studying the output of a function with random inputs by applying this function to large random samples of these inputs is called the Monte Carlo technique. This technique is advocated for the evaluation of measurement uncertainty in Ref. 1, which envisages a measurand defined by  $Y = \mathcal{F}(X_1, \dots, X_m)$  and uses probability distributions to represent belief or knowledge about the input quantities  $X_1, \dots, X_m$ . The output of the analysis is a large set of data that can be formed into a normalized histogram to approximate the corresponding probability density function (p.d.f.) of  $Y$  and ordered to approximate the cumulative distribution function (c.d.f.).

One limitation of this method of uncertainty evaluation relates to the idea that the distribution representing  $Y$  should be able to be used as an input to another calculation.<sup>2</sup> The Monte Carlo output set is too large to be suitable for written communication, and the actual distribution of  $Y$  will not exactly follow a form that is easily expressible. Accordingly, we require a summarizing representation from which we can obtain a good approximation. This paper addresses this issue for various methods of evaluation.

## 2. Transfer to an Analytical Method

Let the Monte Carlo output be the ordered set of  $M$  observations  $\{y_{(i)}\}$ , where  $y_{(1)} \leq \dots \leq y_{(M)}$ . A typical value of  $M$  is  $10^5$ . Estimates of the mean and variance of the distribution of  $Y$  are  $\hat{\mu} \equiv \sum_{i=1}^M y_{(i)}/M$  and  $\hat{\sigma}^2 \equiv \sum_{i=1}^M (y_{(i)} - \hat{\mu})^2/(M-1)$ , and estimates of the usual coefficients of skewness and excess kurtosis,  $\phi$  and  $\gamma$ , are

$$\hat{\phi} \equiv \frac{\sum_{i=1}^M (y_{(i)} - \hat{\mu})^3}{(M-1)\hat{\sigma}^3} \quad \text{and} \quad \hat{\gamma} \equiv \frac{\sum_{i=1}^M (y_{(i)} - \hat{\mu})^4}{(M-1)\hat{\sigma}^4} - 3.$$

Suppose  $Y$  is subsequently to be used as an input to an analysis carried out by the basic procedure of Ref. 2. Such an input is represented by an estimate  $y$ , the standard uncertainty  $u$  associated with this estimate, and a number of degrees of freedom  $\nu$ . If the triplet  $y, u, \nu$  is interpreted as implying that the distribution attributed to  $Y$  has mean  $y$  and standard deviation  $u$  and has the form of a  $t$ -distribution with  $\nu$  degrees of freedom, which has  $\gamma = 6/(\nu - 4)$ , then we can set  $\nu = \hat{\nu}$  where  $\hat{\nu} = 4 + 6/\max\{\hat{\gamma}, 0\}$ . So an appropriate way to summarize the Monte Carlo output in this case is to record the vector  $(y, u, \nu) = (\hat{\mu}, \hat{\sigma}, \hat{\nu})$ .

The procedure of Ref. 2 has been criticized on grounds of theoretical inconsistency.<sup>3,4</sup> By contrast, an alternative analytical procedure recently presented<sup>4,5</sup> is consistent with the view of probability implied in Ref. 1. This procedure involves treating the inputs and output as random variables, summarizing the corresponding input distributions by their moments and propagating the moments through the function  $\mathcal{F}$  analytically. If  $Y$  is to be an input to an analysis by this method then the only data required are its mean  $y$ , its standard deviation  $u$ , and its coefficients of skewness and excess  $\phi$  and  $\gamma$ . We simply set  $(y, u, \phi, \gamma) = (\hat{\mu}, \hat{\sigma}, \hat{\phi}, \hat{\gamma})$ .

## 3. Quantile Functions

The remainder of this article deals with the more difficult problem of summarizing  $\{y_{(i)}\}$  for use as an input to another Monte Carlo analysis. Consider a continuous random variable  $X$  with p.d.f.  $f(x)$ , c.d.f.  $F(x) \equiv \int_{-\infty}^x f(y) dy$  and inverse c.d.f.  $Q(p) \equiv F^{-1}(p)$ , which is also called the *quantile function*. The quantile function  $Q(p)$  contains the same information as the p.d.f. and c.d.f., and so may be regarded as defining the distribution of  $X$ . This function gives the value of  $x$  for which  $\Pr(X \leq x) = p$ , which is called the  $p$ -quantile of the distribution.

Figure 1 shows the quantile functions and p.d.f.s of the standard normal and half-normal distributions, the distribution of the sum of standardized

normal and uniform variables ( $n+u$ ), the triangular distribution on  $[-1, 1]$ , the standard Cauchy distribution and the distribution discussed in Sec. 6.

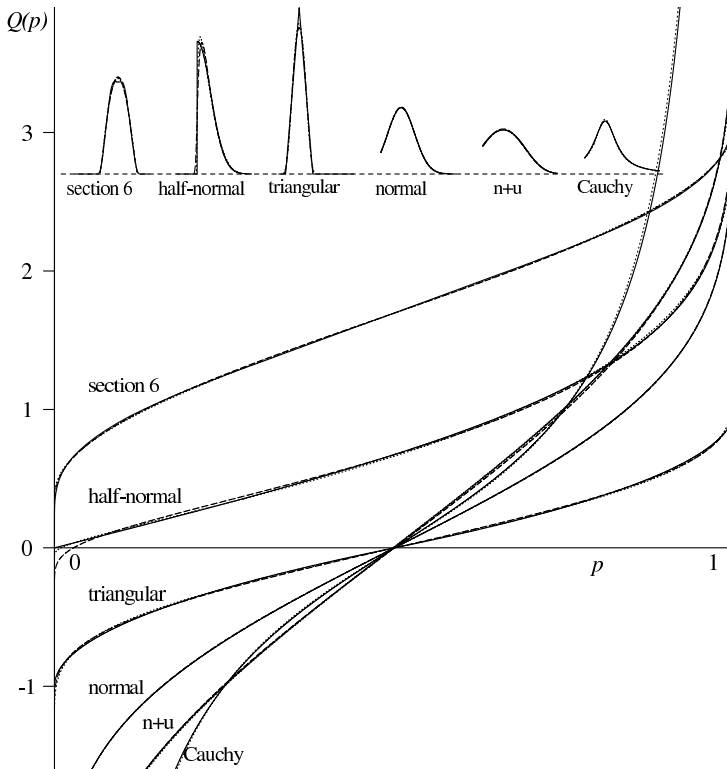


Fig. 1. Quantile functions and p.d.f.s (inset) displayed from  $Q(p) \approx -1.5$  to  $Q(p) \approx 4$ . Solid lines: exact functions. Other lines: approximations described in Secs. 5–6.

Several facts about quantile functions are relevant.

- (1) A quantile function  $Q(p)$  is defined on  $[0, 1]$  and is non-decreasing. Conversely, any non-decreasing function on  $[0, 1]$  can be a quantile function.
- (2) The p.d.f. of a random variable with quantile function  $Q(p)$  is  $f[Q(p)] = 1/Q'(p)$ , i.e.  $f(x) = 1/Q'(Q^{-1}(x))$ .
- (3) The  $r$ th moment about the point  $x$  of a variable with quantile function  $Q(p)$  is  $\int_0^1 \{Q(p) - x\}^r dp$ .
- (4) If  $p^*$  is drawn randomly from the unit uniform distribution then  $Q(p^*)$  is drawn randomly from the distribution with quantile function  $Q(p)$ .

Most familiar distributions have p.d.f.s with well-known analytical forms, but this is often associated with  $Q(p)$  having an inconvenient form. In contrast, we propose using distributions with a convenient form of quantile function. As point (4) above indicates, this makes sampling very efficient.

#### 4. Extended Lambda Distributions

A suitable family of distributions is the family with quantile function<sup>7</sup>

$$Q(p) = \begin{cases} d + (c/b)\{ap^b - (1-p)^b + 1 - a\} & b \neq 0 \\ d + c\{a \ln p - \ln(1-p)\} & b = 0. \end{cases} \quad (1)$$

The dimensionless parameters  $a$  and  $b$  determine the shape of the distribution, while  $c$  and  $d$  affect only the scale and location of the distribution. The form with  $b = 0$  is obtained from the form with  $b \neq 0$  using the relationship  $\lim_{b \rightarrow 0} [(1-x)^b - 1]/b = \ln(1-x)$  for  $0 \leq x < 1$ . The distribution with  $a = 1$  is a symmetric lambda distribution,<sup>8</sup> which has ‘ $\lambda$ ’ instead of ‘ $b$ ’.

Let us call a distribution with quantile function given by Eq. (1) an *extended lambda distribution* (ELD). Figure 2 shows that the family of ELDs covers a range of shapes. When  $b = 1$  the distribution is uniform, when  $a = 0$  and  $b = 0$  the distribution has the form of an exponential distribution, and when  $a = 1$  and  $b = 0$  the distribution has the form of a logistic distribution.

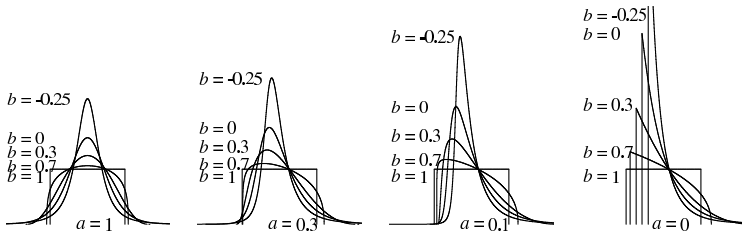


Fig. 2. Probability density functions for ELDs with  $a \leq 1$  and  $b \leq 1$ . Density functions with the same shapes but the opposite sense of skewness are obtained with  $a \geq 1$ .

We may note several facts about an ELD.

- (1) The p.d.f. is  $f[Q(p)] = c^{-1}\{ap^{b-1} + (1-p)^{b-1}\}^{-1}$ .
- (2) Necessarily  $a \geq 0$  and  $c > 0$ , else the p.d.f. takes some negative values.
- (3) If  $b > 0$  the distribution is bounded with limits  $d - ac/b$  and  $d + c/b$ .
- (4) The mean is  $\mu = d + c(1-a)/(b+1)$  and the variance is

$$\sigma^2 = \begin{cases} \left(\frac{c}{b}\right)^2 \left( \frac{a^2+1}{2b+1} - \frac{2a\Gamma(b+1)^2}{\Gamma(2b+2)} - \left(\frac{a-1}{b+1}\right)^2 \right) & b \neq 0 \\ c^2(a^2 + \pi^2 a/3 - 2a + 1) & b = 0. \end{cases}$$

- (5) If  $a < 1$  then the skewness is positive (negative) when  $b < (>)1$ .
- (6) Using  $1/a$  gives an ELD with the same shape but opposite skewness.
- (7) The  $r$ th moment of a variable  $X$  with  $Q(p) = ap^b - (1-p)^b$  is

$$E[X^r] = \sum_{j=0}^r (-1)^j \binom{r}{j} a^{r-j} \Gamma(rb - jb + 1) \Gamma(jb + 1) / \Gamma(rb + 2).$$

## 5. Fitting an Extended Lambda Distribution

The flexibility seen in Fig. 2 means that ELDs can be used to approximate many distributions that are encountered in practice, and especially those distributions only represented by Monte Carlo output.

Equation (1) involves four parameters, so in general we can find an ELD that matches four pieces of information derived from the actual distribution of interest. The dashed lines in Fig. 1 give the quantile functions and p.d.f.s of approximations obtained by matching the first four moments, and the dotted lines give approximations obtained by matching the  $p$ -quantiles for  $p = 0.025, 0.25, 0.75, 0.975$ . (Using  $p = 0$  or  $p = 1$  would preserve a limit.) The approximations for the standard normal distribution, which have parameters  $(a, b, c, d)$  equal to  $(1, 0.1349, 0.6833, 0)$  and  $(1, 0.1455, 0.6927, 0)$  respectively, are indistinguishable from the exact functions.

There are many other criteria on which the choice of an approximating ELD might be based, some of which will involve a measure of distance between the two distributions. Suppose that a variable to be approximated has p.d.f.  $f(x)$  and c.d.f.  $F(x)$ , and suppose that the approximation has p.d.f.  $g(x)$  and c.d.f.  $G(x)$ . One possible distance is the quantity  $D_1 \equiv \int_A f(x) - g(x) dx$  with  $A \equiv \{x : f(x) > g(x)\}$ , which is the maximum difference in probability that the two distributions can assign to any event; the maximum being achieved with the events  $X \in A$  and  $X \notin A$ . This *total variation distance*,  $D_1$ , might not be appropriate because it allows  $A$  to be the union of disjoint intervals. An analogous distance that only considers events of the form  $X \in [a, b]$ , with  $a$  or  $b$  possibly infinite, is  $D_2 \equiv \max_i \left\{ \int_{a_i}^{b_i} |f(x) - g(x)| dx \right\}$ , where each pair  $(a_i, b_i)$  is such that  $f(x) - g(x)$  has one sign in the interval  $[a_i, b_i]$  but has the other sign immediately outside that interval. A third measure is the Kolmogorov distance,  $D_3 \equiv \sup_x \{|F(x) - G(x)|\}$ , which is obtained by only considering events of the form  $a < X < \infty$  and  $-\infty < X \leq b$ .

One of these distances might be minimized while preserving the mean and variance, which seems important because of the role of the central limit theorem in linear problems. A different approach applicable with bounded distributions would involve minimizing  $D_4 \equiv \sup_p \{|F^{-1}(p) - G^{-1}(p)|\}$ .

## 6. Example

Suppose we seek the distribution that describes belief about the volume,  $V$ , of a cuboid when the corresponding distributions for the length, breadth and depth are independent uniform distributions with means 42.4 mm, 21.3 mm and 9.8 mm respectively, each with half-width 0.5 mm. The quantile function and p.d.f. for  $V/50 - 40\,000 \text{ mm}^3$  obtained by Monte Carlo evaluation are shown on Fig. 1. The close approximations obtained by fitting ELDs to the first four moments and to the 0.025, 0.25, 0.75 and 0.975 quantiles are also plotted. The corresponding approximations to the distribution of  $V$  have parameter vectors  $(0.9158, 0.4001, 0.5907 \times 50, 1.6656 + 40\,000)$  and  $(0.9042, 0.4277, 0.6157 \times 50, 1.6592 + 40\,000)$ . A random sample can then be obtained by applying Eq. (1) to a uniform random sample  $\{p_i\}$ .

## 7. Summary

The output distribution of a Monte Carlo evaluation of uncertainty is easily summarized for use as an input to the methods of Ref. 2 and Refs. 4–5. It can also be approximated for use in another Monte Carlo calculation by a distribution with a simple quantile function, from which resampling is straightforward. Usually a suitable approximation will exist within the family of distributions defined by Eq. (1). Further work could involve fitting these, and other, generalizations of lambda distributions to actual data.

## Acknowledgments

Much of this work was conducted while the author was a visiting scientist at the National Physical Laboratory, UK.

## References

1. Joint Committee for Guides in Metrology *Evaluation of measurement data — Supplement 1 to the “Guide to the expression of uncertainty in measurement” — Propagation of distributions using a Monte Carlo method* (2007).
2. *Guide to the Expression of Uncertainty in Measurement* (ISO, Geneva, 1995).
3. R. Kacker and A. Jones, *Metrologia* **40**, 235 (2003).
4. R. Willink, *Metrologia* **42**, 329 (2005).
5. R. Willink, *Metrologia* **43**, 522 (2006).
6. W. G. Gilchrist, *Statistical Modelling with Quantile Functions* (Chapman & Hall/CRC, Boca Raton, 2000).
7. J. S. Ramberg, A probability distribution with applications to Monte Carlo simulation studies, in *Statistical Distributions in Scientific Work vol. 2*, 51, eds. G. P. Patil, S. Kotz, J. K. Ord, (D. Reidel, Dordrecht-Holland, 1975).
8. J. Tukey, *Annals of Mathematical Statistics* **33**, 1 (1962).

## MATHEMATICAL ENTROPY AND A CRITICISM OF A USAGE OF THE PRINCIPLE OF MAXIMUM ENTROPY

ROBIN WILLINK

*Industrial Research Ltd,  
P.O.Box 31-310, Lower Hutt 5040, New Zealand  
E-mail: r.willink@irl.cri.nz*

The ‘principle of maximum entropy’ has been advocated for choosing a probability distribution to represent individual unknowns such as systematic deviations. Supporting claims like ‘the maximum-entropy distribution is minimally committal’ are indefensible in this context. The idea that entropy measures information only has meaning with sequences of categorical random variables.

### 1. The Principle of Maximum Entropy

The ‘entropy’ of the continuous random variable  $X$  with p.d.f.  $f(x)$  is

$$H(X) = - \int_{-\infty}^{\infty} f(x) \log f(x) dx. \quad (1)$$

The ‘principle of maximum entropy’ is that “when we make inferences based on incomplete information, we should draw them from that probability distribution that has the maximum entropy permitted by the information we do have”.<sup>1</sup> For example, when all we know about  $X$  is that  $a < X < b$  we obtain the uniform distribution on  $[a, b]$  and when all we know about  $X$  is its mean and variance we obtain the corresponding normal distribution.<sup>2</sup> These are the maximum-entropy distributions (MEDs) in these situations.

### 2. Unjustified Claims for Maximum-Entropy Distributions

Consider the vague claim that the MED “is maximally noncommittal with regard to missing information”.<sup>3</sup> To speak of commitment requires identifying the thing to which we are committed. The typical object of our commitment about an unknown constant  $X$ , such as a systematic deviation,<sup>2</sup> must be a hypothesis  $H: a \leq X \leq b$  in which  $a$  and  $b$  are known.

Being minimally committed to a hypothesis must mean giving it the smallest possible probability. Suppose we know only that  $0 < X < 1$ , as in

Fig. 1a. The MED is uniform on  $[0, 1]$ , and this assigns non-zero probability to  $H$ . However, there are many p.d.f.s giving  $\Pr(H) = 0$ , as with the dashed line. So the MED is not minimally committal to  $H$ . If it is legitimate to think of being committed *about* a hypothesis then being minimally committed means setting  $\Pr(H) = 0.5$ , as with the dotted line.

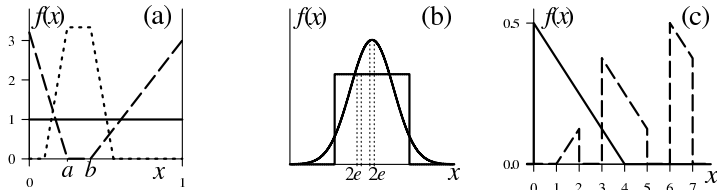


Fig. 1. (a) commitment (b) prediction (c) two distributions with equal entropy.

Perhaps ‘choosing the MED represents having minimal information’, (c.f. Ref. 4). A value  $X$  on a continuous scale cannot be represented exactly, so information about  $X$  exists only in a statement like  $a - \epsilon \leq X \leq a + \epsilon$  for known  $a$  and  $\epsilon$ . Therefore, any idea of ‘information’ about  $X$  relies on the concept of ordering of the domain, which is absent from Eq. (1); see Sec. 4.

It might be thought that ‘the MED represents maximum uncertainty’, (c.f. Ref. 3). In metrology, such a distribution must maximize the final standard uncertainty, and this distribution has maximum variance, not maximum entropy. By this argument, the p.d.f. to attribute to  $X$  when all we know is that  $a < X < b$  comprises point masses of 0.5 at  $a$  and  $b$ .

Perhaps ‘choosing the MED makes predicting the value of  $X$  as hard as possible’, (c.f. Ref. 5). Predicting a value  $X$  on a continuous scale means selecting a value  $a$  and stating ‘ $X \in [a - \epsilon, a + \epsilon]$ ’; see Fig. 1b. ‘Hard to predict’ means having a low probability of being correct, so our best choice for  $a$  is the mode. The MED when only the mean and variance are known is normal, but the corresponding uniform distribution has a smaller modal value. So choosing the MED does not make prediction as hard as possible.

### 3. The Origin of Entropy as ‘Information Rate’: An Infinite Sequence of Categorical Random Variables

Consider a random variable  $X$  with three possible categories or symbols A, M and C. A sequence of independent realizations of the random variable is a sequence of symbols, the first few of which might be MAACACMC. Any such sequence is encoded efficiently by assigning shorter binary codewords to more probable symbols. If  $\Pr(X = A) = 0.5$ ,  $\Pr(X = M) = 0.3$  and

$\Pr(X = C) = 0.2$  then a suitable assignment is  $A \rightarrow 1$ ,  $M \rightarrow 00$ ,  $C \rightarrow 01$  in which case the data segment above becomes 0011011010001. A long sequence would require  $1 \times 0.5 + 2 \times (0.3 + 0.2) = 1.5$  bits per symbol.

When  $X$  has probabilities  $\{p_s\}$ , where  $s$  indicates the category or symbol, no assignment of codewords can achieve fewer than  $\sum p_s \log p_s$  bits per symbol in the long run. This bound can be obtained in theory by assigning individual codewords to groups of symbols. e.g. AM and AAC. Therefore, as  $n \rightarrow \infty$ , the amount of information in  $n$  realizations of  $X$  is the same as in a certain binary sequence of length  $n \sum p_s \log p_s$ . This *source-coding theorem* justifies equating  $\sum p_s \log p_s$  with a ‘rate of gain of information’ from repeated observation of  $X$ . The same result can be obtained by considering the number of different messages possible in  $n$  symbols, with  $n \rightarrow \infty$ .<sup>1</sup>

The entropy of  $X$  in this foundational case is defined to be

$$H(X) = - \sum_{\text{all categories}} p_s \log p_s, \quad (2)$$

so the rate of information gained by repeated observation of  $X$  is equal to the negative of the entropy. We read: “The *average* information per single symbol interval ... of a message with  $n$  possible symbols or levels, of probability  $P_1$  to  $P_n$ , respectively, is then  $H_{av} = - \sum_{j=1}^n P_j \log P_j$  bits/interval”<sup>6</sup> and “Using bits as the unit for entropy,  $H(\mathbf{X})$  is a lower bound to the average number of binary digits (or responses to yes-no inquiries) needed to determine the value of  $\mathbf{X}$ ”.<sup>5</sup> These useful quotations can be contrasted with statements like “According to ... [information theory], the amount of information (relative to the value of a random variable) contained in a probability distribution with frequency (or density) function  $p()$  is  $I(p) = E[\log p]$ ”,<sup>4</sup> which omit the important idea that the quantification of information relates to repeated observation, i.e. to information *rate*.

#### 4. Unjustified Generalization

Our demonstration involved repeated observation of a categorical variable, which was the original context of Shannon (Parts I and II).<sup>7</sup> He obtained a similar result for a continuous numerical variable (Theorem 22) but only by assuming a certain loss function to describe information fidelity. Without clear support,<sup>3,8</sup> Jaynes<sup>1</sup> extrapolates to state “The general Principle of Maximum Entropy is applicable to any problem of inference with a well-defined hypothesis space and noiseless but incomplete data, whether or not it involves a repetitive situation ... .” But the idea that entropy relates to ‘information’ does not hold with single realizations of numerical variables.

The original definition of (mathematical) entropy is given in Eq. (2). For a discrete numerical variable  $X$  on the values  $1, \dots, n$  with  $\Pr(X = i) = p_i$ , the entropy of  $X$  has been defined as

$$H(X) = -\sum_{i=1}^n p_i \log p_i, \quad (3)$$

and for a continuous variable  $X$  the (differential) entropy is given by Eq. (1). The definition of an entropy can be generalized in this way, but it does not follow that the quantities in Eqs. (1) and (3) can be automatically identified with information rate. ‘Information’ with a numerical variable is different.

The quantities  $i$  and  $x$  in Eqs. (3) and (1) act only as labels, so reordering and rearranging the domain makes no change to the entropy; see Fig. 1c. Also, in Sec. 3, where ‘information rate’ is meaningful, there is no concept of order or distance between the symbols, i.e., the statements ‘A > M’ and ‘M ≈ C’ have no meaning. Yet the ideas of inequality and closeness contain the meaning of ‘information’ with numerical variables. For example, the statements ‘ $T < 30^\circ$ ’ and ‘ $T \approx 23^\circ$ ’ are informative. When assigning a continuous probability distribution to a constant  $X$ , information resides only in the concepts of order and distance, which are absent from the argument in Sec. 3 – on which the familiar claims about the quantity in Eq. (1) are ultimately based. Conversely, the concept of repetition, which was *essential* in Sec. 3, is ignored when assigning a MED to a single unknown constant.

## 5. Conclusion

By examining the original papers, we find that the ‘entropy’ given in Eq. (1) cannot legitimately be associated with ‘information’ and ‘uncertainty’ in the way claimed in metrology. The use of maximum-entropy distributions for modelling constants does not seem justified by theory.

## References

1. E. T. Jaynes, *Proceedings of the IEEE* **70**, 939 (1982).
2. W. Woeger, *IEEE Trans. Inst. Meas.* **IM-36**, 655 (1987).
3. E. T. Jaynes, *Physical Review* **106**, 620 (1957).
4. Y. Bard, Maximum entropy principle, Classical approach, *Encyclopedia of Statistical Sciences* vol. 5, 336 (Wiley, New York, 1985).
5. B. Harris, Entropy, *Encyclopedia of Statistical Sciences* vol. 2, 512 (eds. S. Kotz, N. L. Johnson and C. B. Read) (Wiley, New York, 1982).
6. M. Schwartz, *Information Transmission, Modulation and Noise* 3rd edn., International Student Edn., (McGraw-Hill, Auckland, 1981).
7. C. E. Shannon, *Bell Syst. Tech. J.* **27**, 379 and 623 (1948).
8. E. T. Jaynes, *IEEE Trans. Syst. Sci. Cyber.* **SSC-4**, 227 (1968).

## MULTIVARIATE AND FUNCTIONAL CLUSTERING APPLIED TO MEASUREMENTS OF LABORATORY ANALYSIS SYSTEMS

INSA WINZENBORG<sup>\*12</sup>, ANDREA GEISTANGER<sup>2</sup> and ULRICH  
STADTMÜLLER<sup>1</sup>

<sup>1</sup>*Department of Number Theory and Probability Theory, University of Ulm,  
Ulm, Germany*

<sup>2</sup>*Department of Biostatistics, Roche Diagnostics GmbH,  
Penzberg, Germany*

*\* E-mail: insa.winzenborg@roche.com*

Modern laboratory analysis systems often involve parallel components to enhance throughput. As a consequence these components need to be designed and controlled to allow for a homogeneous performance. In our case antigen-antibody-reactions take place on small measurement chips, which are processed at several units of an analysis system. Signals are measured on the two dimensional chip surface. In order to optimize the measurement process it is necessary to compare the outcome of the separate processing units and to identify the units of equal performance.

Clustering, the unsupervised partitioning of data into groups, is a task with broad application in many disciplines. We compare some cluster algorithms in the aforementioned situation. The algorithms that we analyze and compare are classical multivariate ones like K-means or hierarchical clustering, as well as a more recent one emerging from functional data analysis. The latter method is based on nonparametric functional principal component analysis. Furthermore a clustering method based on the coefficients of a parametric linear model fit is taken into consideration.

### 1. Introduction

The data we analyze are obtained by measurements carried out on a laboratory analysis system. This system can detect several analytes in a blood sample simultaneously. The measurements take place on chips with plane coated surfaces of about  $1.3 \text{ cm}^2$  in size. The coating consists of several specific binding points which are arranged in an array of up to 21 columns and 11 rows on the chip. After multiple steps of filling the chip with probe or buffer fluids, incubating, washing and drying it, the amount of specific

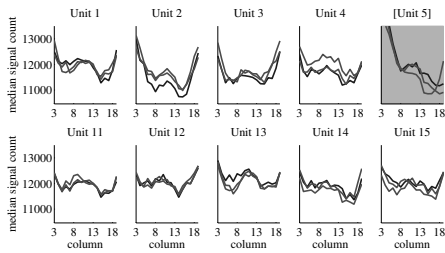


Fig. 1. Medians per column for each chip (different gray scales) and some incubator positions). Position 5 is marked because it is partly excluded in the analysis due to its obvious outlier state.

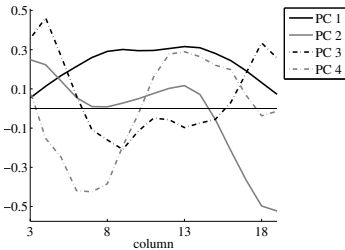


Fig. 2. Estimated functional principal components of the column medians. PC 1: 76.5% of variation, PC 2: 13.3%, PC 3: 8.0%, PC 4: 1.6%

binding reactions is determined by a camera sensitive to fluorescent light. In applications each column of spots binds specifically one analyte and the measured signal is used to estimate analyte concentrations.

In order to optimize several aspects concerning the performance of this system a special type of chip is used. These chips are coated homogeneously so that one ideally obtains a constant signal on the whole surface. Due to complex influence effects (e.g. from washing and mixing processes) the ideal situation can hardly be reached. Measurements are available at a grid of  $21 \times 11$  points per chip.

One performance aspect shall be analyzed in detail: The system consists of several parallel incubator positions to increase the throughput. An incubator position is an area where a chip stays for about 30 seconds at an ideal temperature so that binding reactions take place. Additionally, each incubator position has an air jet for probe mixing during the incubation. Due to small differences in the air jets resulting from the fabrication process, the mixing is not equal at each incubator position. This leads to visible differences in signal patterns of chips incubated at different positions. For further evaluations which should not depend on incubator positions, it is necessary to select positions which are comparable in signal height and course. This task shall be accomplished by a clustering algorithm which groups air jets and thereby incubator positions that behave similarly.

A specialty in this clustering task is the fact that the incubator positions are clustered indirectly via the signals of the chips they process. Therefore it is necessary to deal with multiple measurements per position in the clustering algorithms.

Instead of executing the cluster algorithms over the two dimensional chip

space, column medians (i.e. medians of each 11 signal values per column are calculated). This procedure for reducing the number of variables is chosen because in laboratory practice also a robust estimation of the column's mean value is evaluated. A robust estimator is necessary due to edge effects which are caused by insufficient washing and mixing power near the edges. Our data set consists of 30 incubator positions and three chips measured per position. Each of the 90 chips is described by a median signal course consisting of 21 values. Because of the mentioned edge effects only the middle 17 medians are analyzed in the following. Figure 1 shows the column medians per chip and incubator position.

In the following we present the methods used for clustering, show results of the data application, mention two simulation studies and end in a conclusion.

## 2. Methods

### 2.1. Treatment of multiple measurements

Since the task is to cluster the incubator positions and not the chips it is necessary to find a way to treat multiple measurements on one position. Two approaches are considered here. In the first approach we average the signals of the same position and use only the mean functions for clustering. The second approach is to cluster all chip signals and to assign each incubator position to the cluster where most of the chips processed by this position belong to. If the incubator position belongs to two or more clusters with equal weight it is randomly assigned (see Leisch 2007<sup>1</sup>).

### 2.2. Multivariate methods

Multivariate cluster analysis comprises essentially two methods that we also consider here: hierarchical clustering and K-means. In the following  $y_i \in \mathbb{R}^J$  denotes the  $i$ th column median vector ( $i = 1, \dots, I$ ) and  $\{S_c\}_{c=1, \dots, C}$  a cluster partition of  $\{1, \dots, I\}$ .

Hierarchical clustering creates a hierarchy of cluster partitions with decreasing fineness that is cut at a specified level. We use the agglomerative variant with complete linkage.

The aim of K-means clustering is to partition the data in a way that minimizes the within-groups sum of squares  $\sum_{c=1}^C \sum_{i \in S_c} \|y_i - \hat{\mu}^{(c)}\|_2^2$  and maximizes the between-groups variance  $\sum_{c=1}^C \|\hat{\mu}^{(c)} - \hat{\mu}\|_2^2$  in which  $\hat{\mu}^{(c)}$  with  $\hat{\mu}^{(c)}(j) = \frac{1}{|S_c|} \sum_{i \in S_c} y_i(j)$  for  $j = 1, \dots, J$  is the estimated mean of cluster  $c$  and  $\hat{\mu}$  the overall mean.

As distance measure between elements the Euclidean distance  $\|\cdot\|_2$  is applied in all algorithms. We use the functions *kmeans* and *clusterdata* of the Matlab Statistical Toolbox (Hastie et al. 2001<sup>2</sup>, Documentation Statistical Toolbox 2007<sup>3</sup>).

### 2.3. Parametric clustering

Figure 1 leads to the assumption that the column medians can be well approximated by polynomials of fourth order. Therefore a sensible way of clustering is to fit polynomials to the column median data of each incubator position and use a multivariate cluster algorithm (for example K-means) to cluster the coefficients afterwards. This method can cope with multiple measurements naturally by using the data of all multiples to fit the polynomial. We used least squared fitting. Parameters are standardized before clustering in order to have equal influence in K-means clustering.

### 2.4. Functional method: FPCA.

In this section we consider the measured signals as outcomes of a stochastic process  $Y$  over the column location interval  $\mathcal{S} \subseteq \mathbb{R}_{\geq 0}$ .  $Y$  has a mean function  $\mu(s) = E(Y(s))$  for  $s \in \mathcal{S}$  and a covariance function  $\Gamma$  with  $\Gamma(s, t) = \text{Cov}(Y(s), Y(t))$  for  $s, t \in \mathcal{S}$ . We want to examine the principal directions of  $Y$ . Analogously to the multivariate case one calculates the eigenfunctions of  $\Gamma$  (which are the principal components of  $Y$ ) by the following rule: An eigenfunction of  $\Gamma$  is a function  $\rho_l : \mathcal{S} \rightarrow \mathbb{R}$ ,  $\rho_l \neq 0$  for that a value  $\lambda_l \in \mathbb{R}$  exists s.t.  $\langle \Gamma(\cdot, t), \rho_l \rangle = \lambda_l \rho_l(t)$ <sup>a</sup> (see Ramsay and Silverman 2006<sup>4</sup>).

We assume that the eigenvalues are in non-increasing order  $\lambda_1 \geq \lambda_2 \geq \dots$ . Using its principal components one can represent the stochastic process  $Y$  via the Karhunen-Loëve representation

$$Y(s) = \mu(s) + \sum_{l=1}^{\infty} \xi_l(Y) \rho_l(s) \quad \text{for all } s \in \mathcal{S} \quad (1)$$

under certain regularity conditions (see Chiou and Li 2007<sup>5</sup> for details). The coefficients  $\xi_l$  are called principal component scores and can be calculated via projection of  $Y - \mu$  on the  $l$ th eigenfunction  $\rho_l$ :  $\xi_l(Y) = \langle Y - \mu, \rho_l \rangle$ .

In practice the mean function is estimated by local linear regression, the covariance function by two-dimensional local polynomial fitting (the

---

<sup>a</sup> $\langle \cdot, \cdot \rangle$  denotes the inner product  $\langle f, g \rangle = \int f(s)g(s)$  of two functions  $f$  and  $g$  in the Hilbert space of square integrable functions on  $\mathcal{S}$ .

definition of a bandwidth is necessary for both) and the eigenfunctions and PCA scores via discrete approximations. For details we refer to appendix A of Chiou and Li 2007<sup>5</sup>.

For clustering, the K-means method is applied to the first  $l^*$  PCA scores which describe a defined part of variation (usually 90-95 %).

Chiou and Li 2007<sup>5</sup> developed an enhancement of FPCA which calculates principal components for each cluster and re-sorts each element to that cluster where it can be best approximated via the first principal components. In our data situation, however, the calculation of principal components of each cluster does not yield useful results because the number of measurements is too small. Hence the results of the enhanced method are not shown here. We performed FPCA clustering using the method *KCFC* provided by Chiou.<sup>b</sup>

### 3. Data Analysis

K-means, hierarchical, parametric and FPCA clustering are applied to the data shown in Fig. 1. When including position 5 and splitting the data into three clusters, all algorithms separate position 5 into a singular cluster. Hence the results presented here are obtained by forming two clusters of the remaining 29 incubator positions. We do not increase the number of clusters, because the cluster sizes otherwise get to small for using only one of the clusters in later analysis. In FPCA we include the first principal components which describe 90 % of variation and use bandwidth 2 for estimating mean and covariance functions. For treatment of multiple measurements only the method of averaging before clustering is presented here because both methods lead to approximately the same results.

Agreement of different cluster partitions or of a cluster partition and the true assignment is measured by the cRate index. The index is defined as the proportion of maximal correspondences between two partitions to the total number of objects (see Chiou and Li 2007<sup>5</sup>). Results of comparing the four algorithms by the cRate index are shown in Table 1.

The multivariate methods (Fig. 3a, b) yield two clusters which clearly differ in their location. In this data set the results of K-means and hierarchical clustering differ a lot.<sup>c</sup>

---

<sup>b</sup>Download link: <http://www.blackwellpublishing.com/rss/Volumes/Bv69p4.htm> (accessed: 24 Oct 2008)

<sup>c</sup>Some data sets of other analysis systems show greater agreement between K-means and hierarchical results.

Table 1. **cRate indexes.** This table presents the cRate indexes between each pair of cluster partitions.

	K-means	hierarch.	param.	FPCA
<b>K-means</b>	1.00	0.69	0.55	1.00
<b>hierarch.</b>	0.69	1.00	0.62	0.69
<b>param.</b>	0.55	0.62	1.00	0.55
<b>FPCA</b>	1.00	0.69	0.55	1.00

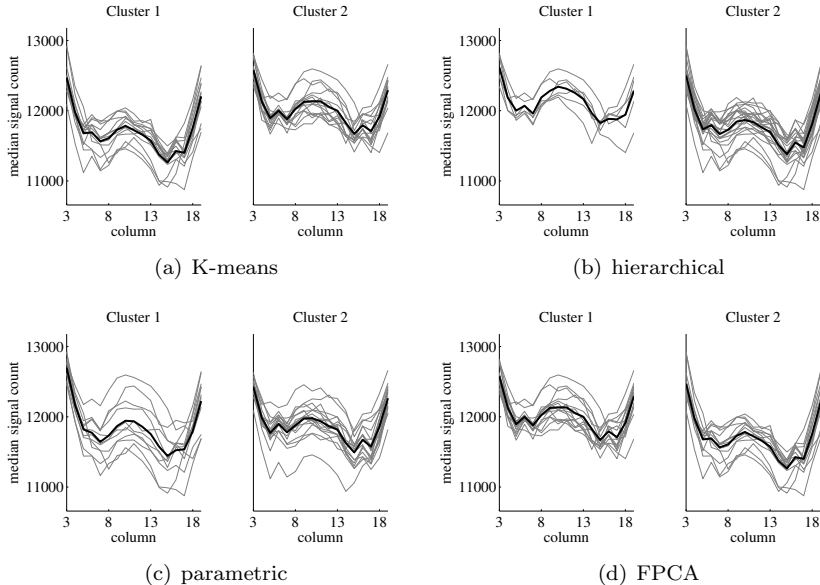


Fig. 3. **Clustering results.** These graphics show the partition of incubator positions to clusters for each algorithm. The thick lines represent cluster mean curves (*centroid*) and the finer lines mean curves per position.

Before regarding the parametric results we evaluate the fit. Residual plots demonstrate that not much information is left in the residuals (not shown here). The autocorrelation of the residuals reveals a normal extent of correlation between joining column medians. The parametric clustering results (Fig. 3c) are hard to interpret because curves belonging to one cluster show no obvious agreement in location or form.

As FPCA is based on principal components, the first four principal components of the data are shown in Fig. 2. The first principal component explains already 76.5 % of variation and describes especially variations of the locations of the inner column medians. The first three principal components describe over 90 % of variation so that the first three scores suffice

for clustering. The FPCA clustering results (figure Fig. 3d) are identical to the K-means results.<sup>d</sup>

#### 4. Simulations

We further analyze the robustness and performance of the four algorithms in simulation studies.

In the first study the original data are disturbed by multivariate normally distributed errors. Clustering the disturbed data with all methods yields that K-means, FPCA and parametric clustering are equally robust, whereas hierarchical clustering is sensitive even to little disturbance.

In the second study we simulate data of two clusters based on polynomials of fourth degree. The two clusters are best separated by K-means and FPCA clustering. The results of hierarchical clustering are a bit more imprecise, those of parametric clustering are at random level.

#### 5. Conclusion

The intention of this analysis is to examine and compare the K-means, hierarchical, parametric and FPCA clustering algorithms in their performance in a special data situation.

K-means, hierarchical and FPCA clustering yield to well interpretable results which are mainly separated by location.

The, at first glance astonishing, effect that K-means and FPCA lead to similar results, can be explained by the fact that the (most influential) first principal component score mainly describes the location of each curve and location is also the most important criterion in K-means clustering.

Due to the low performance of hierarchical clustering with the chosen settings we also tested other settings of metric and linkage, *e.g.* the ward linkage with the correlation coefficient as metric or single linkage with different metrics, but no setting leads to performance improvements. Single linkage settings even decreases the performance.

The advantage of FPCA compared to the multivariate methods is the consideration of the alignment of the columns, but at the cost of being much slower as the multivariate algorithms due to the additional calculation of functional principal components.

Regarding parametric clustering one has to consider that much of its low performance is based on the standardization of parameters before clus-

---

<sup>d</sup>Other data sets also show great agreement, but not always equal results.

tering. If not doing so, data are mainly clustered by their intercept, because this location parameter has the biggest variance. To get sensible results between the two extremes one could try to assign weights to the parameters.

In summary, regarding the interpretability of cluster results, the robustness and the performance, the algorithms K-means and FPCA are most advisable in the analyzed data situation.

## References

1. F. Leisch, *The flexclust Package (R Documentation V0.99-0)* (CRAN archive, 2008).
2. T. R. Hastie, T. and J. Friedman, *The Elements of Statistical Learning* (Springer, 2001).
3. MathWorks, *Documentation of Matlab Statistics Toolbox V6.1 R2007b*, (2007).
4. J. O. Ramsay and B. W. Silverman, *Functional Data Analysis*, 2nd edn. (Springer, 2006).
5. J.-M. Chiou and P.-L. Li, *Functional clustering and identifying substructures of longitudinal data*, *J. R. Statist. Soc. B* **69**, p. 679 (2007).

## IMPACT OF CORRELATION IN THE MEASURED FREQUENCY RESPONSE ON THE RESULTS OF A DYNAMIC CALIBRATION

GERD WÜBBELER<sup>1</sup>, ALFRED LINK<sup>1</sup>, THOMAS BRUNS<sup>2</sup>, CLEMENS ELSTER<sup>1</sup>

*Physikalisch-Technische Bundesanstalt,*

*1) Abbestr. 2-12, Berlin, 10587, Germany,*

*2) Bundesallee 100, Braunschweig, 38116, Germany*

The dynamic behaviour of accelerometers can be described in terms of a second-order model. The parameters of this model may be estimated from a measurement of the frequency response of the accelerometer as obtained in a dynamic calibration measurement. The impact of correlations of the measured frequency response on the results obtained from a subsequent analysis of this data is studied. Possible correlations are considered which arise from correlations of magnitude and phase measurements at the same frequency as well as from a common systematic influence. By using data from a dynamic calibration measurement it is shown that the considered correlations can have a large influence on the results and that they should be taken into account.

### 1. Introduction

Evaluation of measurement uncertainty according to the “propagation of uncertainties” approach of the GUM [1] or the “propagation of distributions” concept of a recent supplement to the GUM [2] both enable the treatment of correlations. Correlations are often caused by a common systematic influence and can be revealed and treated by adequate modelling. This paper illustrates such modelling and the impact correlations can have for the particular example of dynamic accelerometer calibration.

Piezoelectric accelerometers [3] are linear electromechanical transducers employed for the measurement of acceleration. The input-output behaviour of accelerometers can be modelled by a linear second-order differential equation [3]. The unknown coefficients of this differential equation can be estimated from the measurements of the frequency response of the accelerometer which is determined from dynamic calibration measurements using sinusoidal excitations. The resulting estimates of the coefficients of the differential equation and their uncertainties may then be viewed as the result of an analysis of the dynamic calibration measurements. We propose to apply essentially a weighted least-squares procedure for the estimation of the model parameters,

and determine the uncertainties associated with these estimates by means of “propagation of distributions” [2,4]. We study the impact of correlations of the measured frequency response on the resulting model parameters estimates and their uncertainties. To this end a realistic model is introduced which describes the correlation pattern of the complex-valued frequency response measurements. The resulting characteristic structures of the correlation matrix as well as its impact on the calibration results are presented using measurements of a dynamic accelerometer calibration.

## 2. Analysis Of Dynamic Calibration Of Accelerometers

In an accelerometer calibration measurement the electrical sensor output and the applied sinusoidal acceleration are measured simultaneously. From this data then the complex-valued frequency response  $G(\omega) = S(\omega)\exp(j\phi(\omega))$  is estimated in terms of amplitude estimates  $s(\omega_m)$  and phase estimates  $\phi(\omega_m)$  together with their associated uncertainties  $u(s(\omega_m)), u(\phi(\omega_m))$ . The input acceleration is generated at discrete frequencies  $\omega_m, m=1,2,\dots,L$  covering the working frequency range of the accelerometer.

The input-output behaviour of an accelerometer can be modelled by a mass-spring system with frequency response

$$G(\omega) = \Lambda / ((\Omega_0^2 - \omega^2) + 2j\Delta\Omega_0\omega), \quad (1)$$

where  $\Delta, \Omega_0, \Lambda$  denote the physical model parameters damping, resonance frequency and the transformation factor of the piezoelectric transducer.

The analysis of the calibration data can be performed as follows. By applying an appropriate nonlinear transformation of the model parameters  $\Delta, \Omega_0, \Lambda$ , their estimation is reduced to a weighted linear least squares task. Due to the involved non-linear transformation, the uncertainty matrix associated with the resulting parameter estimates can be evaluated using the GUM S1 approach [2,4]. For details cf. [3].

## 3. Modelling Systematic Influences

The above briefly described analysis was in [3] applied assuming uncorrelated data, i.e. the uncertainty matrix associated with the frequency response was assumed to be diagonal. In the following, an analysis based on an assumed correlation pattern is given. The correlation pattern follows from accounting for correlations (at the same frequency) between magnitude and phase as well as the inclusion of additional systematic influences. The resulting correlation matrix of the frequency response is derived, and its characteristic structures are discussed.

Following the concepts introduced in [5,6] for uncertainty evaluation of complex valued quantities a combined vector  $\mathbf{Y} = (Y_1, \dots, Y_{2L})$  is constructed, with  $Y_i, Y_{L+i}$  denoting the magnitudes  $Y_i = S(\omega_i)$  and the phases  $Y_{L+i} = \phi(\omega_i)$  of the frequency response at frequencies  $\omega_i, i=1,2,\dots,L$ . Systematic effects enter in the accelerometer frequency response measurements since a correction is applied to account for the influence of the employed amplifier, and because the employed devices may be affected by constant offsets. It is here assumed that the systematic influences are described by the following model

$$\begin{aligned} Y_i &= X_i - \Delta_1 \\ Y_{L+i} &= X_{L+i} - \Delta_2, \end{aligned} \quad (2)$$

where  $X_i, X_{L+i}$  denotes the frequency response as indicated by the calibration measurement and  $\Delta_1, \Delta_2$  denote unknown, frequency independent offset corrections to the indicated magnitude and indicated phase. For the offset corrections, the estimates  $\delta_1 = \delta_2 = 0$  are used with associated uncertainties  $u(\delta_1)$  and  $u(\delta_2)$ , respectively. The estimates of  $X_i, X_{L+i}$  are given by  $x_i$  and  $x_{L+i}$  with uncertainties  $u(x_i)$  and  $u(x_{L+i})$ , respectively.

In order to cover correlations between magnitude and phase of the frequency response two types of correlation are considered. First, the magnitude and phase offset corrections may be related by a correlation  $\rho_1$

$$\rho_1 = u(\delta_1, \delta_2) / (u(\delta_1)u(\delta_2)). \quad (3)$$

Second, a correlation  $\rho_2$  of magnitude and phase of the indications  $X_i, X_{L+i}$  is considered

$$\rho_2 = u(x_i, x_{L+i}) / (u(x_i)u(x_{L+i})). \quad (4)$$

All remaining correlations of the input quantities in (2) are assumed to be zero. The resulting correlation matrix of the complex valued frequency response  $\mathbf{Y}$  is composed by the four ( $L \times L$ ) sub-matrices

$$\mathbf{R} = \begin{pmatrix} \mathbf{R}_{11} & \mathbf{R}_{12} \\ \mathbf{R}_{12}^T & \mathbf{R}_{22} \end{pmatrix}. \quad (5)$$

The sub-matrix covering the magnitude-magnitude correlations is given by

$$[\mathbf{R}_{11}]_{ik} = \frac{\delta_{ik}u^2(x_i) + u^2(\delta_1)}{\sqrt{u^2(x_i) + u^2(\delta_1)}\sqrt{u^2(x_k) + u^2(\delta_1)}}, \quad (6)$$

for  $i, k = 1, \dots, L$  where  $\delta_{ik} = 1$  for  $i = k$  and zero otherwise.

The phase-phase correlation sub-matrix reads

$$[\mathbf{R}_{22}]_{ik} = \frac{\delta_{ik} u^2(x_{L+i}) + u^2(\delta_2)}{\sqrt{u^2(x_{L+i}) + u^2(\delta_2)} \sqrt{u^2(x_{L+k}) + u^2(\delta_2)}}, \quad (7)$$

and the sub-matrix for the magnitude-phase correlations

$$[\mathbf{R}_{12}]_{ik} = \frac{\delta_{ik} \rho_2 u(x_i) u(x_{L+k}) + \rho_1 u(\delta_1) u(\delta_2)}{\sqrt{u^2(x_i) + u^2(\delta_1)} \sqrt{u^2(x_{L+k}) + u^2(\delta_2)}}. \quad (8)$$

In order to illustrate the characteristic structures of the resulting correlation matrix  $\mathbf{R}$  a synthetic complex-valued frequency response with frequency dependent uncertainties associated with magnitude and phase estimates has been assumed using  $L=11$  frequency values. In Figure 1 the resulting correlation matrices are illustrated. As can be seen in Figure 1b and 1c the uncertainties associated with the offset corrections of magnitude respectively phase cause here a frequency dependent correlation. Due to (7) and (8) the according correlation coefficients are always greater than zero. In Figure 1d a correlation of magnitude and phase at the very same frequency can be noted resulting from a non-zero correlation coefficient  $\rho_2$  in (4). By combining the influences of both offset corrections with the correlation coefficient  $\rho_1$  in (3), the characteristic pattern in Figure 1e is obtained. In Figure 1f the correlation effects are summarized by considering all correlation influences simultaneously.

#### 4. Results

Using measurements from a dynamic calibration experiment, the impact of correlation has been studied by repeatedly analyzing these data for various settings of the correlation parameters  $u(x_i), u(x_{L+i}), u(\delta_1), u(\delta_2), \rho_1$  and  $\rho_2$ . The uncertainties associated with the estimates of the input quantities  $X_i, X_{L+i}$  and  $\Delta_1, \Delta_2$  were chosen in such a way, that the diagonal elements of the uncertainty matrix associated with the estimate of  $\mathbf{Y}$  are retained to their values given by the calibration data. This enabled a reasonable interpretation of the obtained results, when studying the impact of correlations. The correlation matrix was evaluated according to (5)-(8) and the corresponding altered uncertainty matrix of the frequency response was calculated as  $(\mathbf{U}_Y)_{i,k} = u(y_i)u(y_k)[\mathbf{R}]_{ik}$  with  $i, k = 1, 2, \dots, L$ . By feeding this altered uncertainty matrix into the analysis of the calibration data (cf. section 2), the impact of the correlations on the resulting estimates of the model parameters as well as on their associated uncertainty matrix has been studied.

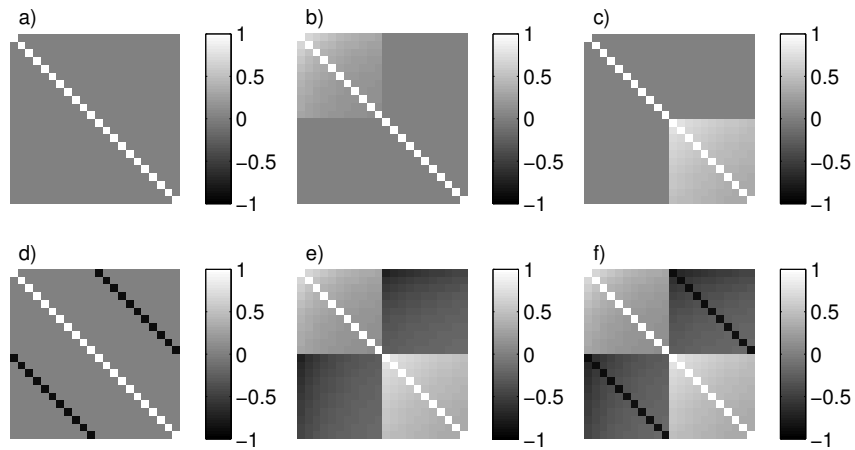


Figure 1. Characteristic patterns of the correlation matrix  $\mathbf{R}$  as obtained by the proposed model: a)  $u(\delta_1)=u(\delta_2)=\rho_2=0$ , b)  $u(\delta_1)>0$ , c)  $u(\delta_2)>0$ , d)  $\rho_2<0$ , e)  $u(\delta_1)>0, u(\delta_2)>0, \rho_1<0$  and f)  $u(\delta_1)>0, u(\delta_2)>0, \rho_1<0, \rho_2<0$ . The right-hand bars indicate the correlation values.

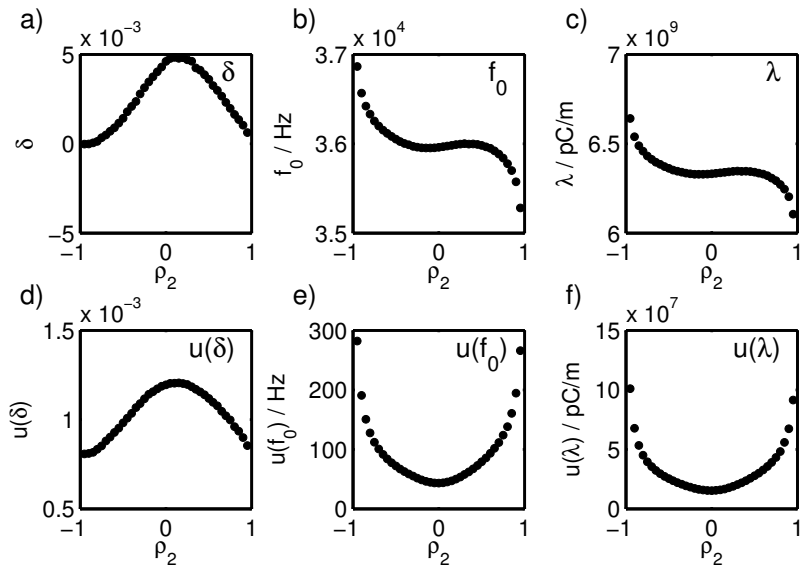


Figure 2. Impact of the correlation  $\rho_2$  defined in (9) on the analysis of calibration data of an accelerometer: a), b), c) show the  $\rho_2$  dependence of the estimates  $\delta, f_0 = \omega_0/(2\pi), \lambda$  and d), e), f) the  $\rho_2$  dependence of their associated uncertainties.

In Figure 2 the impact of the correlation coefficient  $\rho_2$  in (4) is shown exemplarily. Since the uncertainty matrix  $U_Y$  enters into the weighting scheme of the least-squares analysis, the parameter estimates (Figure 2a-2c) display systematic variations with varying correlation. Moreover, the uncertainties associated with these estimates exhibit substantial variations with respect to the degree of correlation. For individual model parameters variations of uncertainty of more than 50 % are observed (Figure 2d-2f).

## 5. Conclusion

A model covering correlations and common systematic influences possibly arising in the measurement of a complex-valued frequency response has been considered. Based on this model the resulting correlation matrix has been derived and the characteristic matrix structures generated by the different influences were discussed. The model has been used to study the impact of such correlations on the analysis of a dynamic accelerometer calibration measurement. As a result, the estimated model parameters display a significant variation with respect to the degree of correlation. An even more pronounced dependence has been observed for the uncertainties associated with the parameter estimates. The results imply that correlations should be accounted for when analyzing data from dynamic calibration measurements.

## References

1. BIPM, IEC, IFCC, ISO, IUPAC, IUPAP and OIML. Guide to the Expression of Uncertainty in Measurement. Geneva, Switzerland: International Organization for Standardization ISBN 92-67-10188-9 (1995).
2. BIPM, IEC, IFCC, ILAC, ISO, IUPAC, IUPAP, and OIML. Evaluation of measurement data — Supplement 1 to the “Guide to the expression of uncertainty in measurement” — Propagation of distributions using a Monte Carlo method. Joint Committee for Guides in Metrology, Bureau International des Poids et Mesures, JCGM 101, to appear
3. A. Link, A. Täubner, W. Wabinski, T. Bruns, C. Elster. Modelling accelerometers for transient signals using calibration measurements upon sinusoidal excitation. *Measurement* **40**, 928 (2007).
4. M. G. Cox and B.R.L. Siebert. The use of a Monte Carlo method for evaluating uncertainty and expanded uncertainty. *Metrologia* **43** 178 (2006).
5. N. M. Ridler and M. J. Salter. An approach to the treatment of uncertainty in complex S-parameter measurements. *Metrologia* **39** 295 (2002).
6. B. D. Hall. On the propagation of uncertainty in complex-valued quantities. *Metrologia* **41** 173 (2004).

## UNCERTAINTY OF STANDARD CONCENTRATIONS, CALIBRATION LINE AND PREDICTIONS

CATHERINE YARDIN, SACKO KABA

*Laboratoire National d'Essais et de Métrologie, Paris 75724, France,  
[catherine.yardin@lne.fr](mailto:catherine.yardin@lne.fr)*

This article discusses the GLS method which estimates the calibration line taking into account unequal variances and covariances associated with responses and standard concentrations. As these two variables are not pair correlated, we use a simplified GLS estimator.

### 1. Introduction

The ordinary least squares method (OLS) does not allow proper estimation of the straight line calibration curve,  $y_t = a + bx_t$ , where  $y_t$  is the response of the measuring system and  $x_t$  is the standard. It does not take into account all the information relating to the uncertainty of the variables.

The OLS estimators are biased, not consistent, and the uncertainty associated with the calibration curve is underestimated.

In the general linear model, where only the response  $y_t$  have uncertainty, the generalized least squares method (GLS), addresses the case of heteroscedastic or autocorrelated  $y_t$ . The well known weighted least squares method (WLS) is a particular case of the GLS.

The errors-in-variables model considers the case where the two variables  $x_t$  and  $y_t$  have uncertainty. Among the various estimation methods proposed for this model, the recently Bivariate Least Squares method (BLS) applies to the case where each variable is heteroscedastic and not autocorrelated. The two variables are pair correlated for the same observation only.

Following this example, we modified the GLS estimator, used in the general linear model, and adapted it to the errors-in-variables case, to take into account the covariances of the standards  $x_t$ .

Methods were defined for the case where the  $x_t$  and  $y_t$  variables have a general variance-covariance matrix: Generalised Gauss Markov Regression [1] or minimum distance estimator [2]. In this article, we used a simplified estimator as we have no correlation between  $x_t$  and  $y_t$ .

## 2. The GLS and the General Linear Model

In the case of a straight line, the general model written in matrix notation is  $\mathbf{Y} = \mathbf{XB} + \mathbf{e}$  where  $\mathbf{Y}$  is the vector of the observations of the response variable,  $\mathbf{X} = (1 \ x)$  is a matrix composed with a column of units and the independent variable  $x$ ,  $\mathbf{B} = (a \ b)$  is the vector of the parameters and  $\mathbf{e}$  is the vector of the errors.

The most important assumptions on this model are: the  $x_t$  variable is certain, the errors  $e_t$  are random variables with zero mean, constant variances and zero covariances. So  $\mathbf{V}(e) = \sigma^2 \mathbf{I}$ , where  $\mathbf{I}$  is the identity matrix. From  $x_t$  is a certain variable, we have:  $\mathbf{V}(\mathbf{Y}) = \mathbf{V}(e)$ .

The OLS method minimises the residuals sum of squares  $S_{OLS} = \mathbf{e}'\mathbf{e}$  and the estimators are given by  $\mathbf{B}_{OLS} = (\mathbf{X}'\mathbf{X})^{-1}\mathbf{X}'\mathbf{Y}$  and  $\sigma^2_{OLS} = S_{OLS}/(n - 2)$ . The variance-covariance matrix of  $\mathbf{B}_{OLS}$  is  $\mathbf{V}(\mathbf{B}_{OLS}) = \sigma^2_{OLS}(\mathbf{X}'\mathbf{X})^{-1}$ .

When the errors are heteroscedastic and (auto)correlated,  $\mathbf{V}(e) = \mathbf{W}$  with variances on the principal diagonal and covariances out of the diagonal. The GLS (also called « Aitken's estimator ») method minimises the sum of the weighted square residuals  $S_{GLS} = \mathbf{e}'\mathbf{W}^{-1}\mathbf{e}$  with respect to  $a$  and  $b$  parameters. The estimator is given by :

$$\mathbf{B}_{GLS} = (\mathbf{X}'\mathbf{W}^{-1}\mathbf{X})^{-1}\mathbf{X}'\mathbf{W}^{-1}\mathbf{Y} \quad (1)$$

and its variance-covariance matrix is:

$$\mathbf{V}(\mathbf{B}_{GLS}) = (\mathbf{X}'\mathbf{W}^{-1}\mathbf{X})^{-1} \quad (2)$$

This GLS estimator is described in [3]. As  $\mathbf{W} = \mathbf{P}'\mathbf{P}$ , it is equivalent to using the OLS method on the transformed model  $\mathbf{P}'\mathbf{Y} = \mathbf{P}'\mathbf{XB} + \mathbf{P}'\mathbf{e}$ .

When  $\mathbf{W} = \sigma^2 \mathbf{V}$ , is known up to a scalar,  $\mathbf{B}_{GLS} = (\mathbf{X}'\mathbf{V}^{-1}\mathbf{X})^{-1}\mathbf{X}'\mathbf{V}^{-1}\mathbf{Y}$  and  $\mathbf{V}(\mathbf{B}_{GLS}) = \sigma^2_{V-GLS} (\mathbf{X}'\mathbf{V}^{-1}\mathbf{X})^{-1}$  where  $\sigma^2_{V-GLS} = (\mathbf{e}'\mathbf{V}^{-1}\mathbf{e})/(n - 2)$  is the estimator of  $\sigma^2$ . The estimate  $\sigma^2_{W-GLS} = (\mathbf{e}'\mathbf{W}^{-1}\mathbf{e})/(n - 2)$  will approximate 1, when  $\mathbf{W}$  is fully known. This result is used to check the adequacy of the model, the uncertainty information and the results of the regression.

The matrix  $\mathbf{W}$  is invertible if the variables are not perfectly correlated.

The general linear model is called « model with an error on the equation » to distinguish it from the « error in variables model » discussed now.

## 3. The Errors-in-Variables Model

In this model, the true variables  $x_t$  and  $y_t$  are related by the straight line,

$$y_t = a + b x_t \quad (3)$$

but they are not observed. They are measured with a zero mean random error:  $Y_t = y_t + v_t$  and  $X_t = x_t + u_t$ . The model written in terms of observed variables is:

$$Y_t = a + b X_t + e_t \quad (4)$$

where the term error  $e_t = v_t - b u_t$  is correlated with the independent variable  $X_t$ . The number of unknowns to be determined and the estimation method used depend on the assumptions about the errors, the true variables and the relation (3). In the following, we give the assumptions which best represent the metrological context.

The true variables  $x_t$  may be certain or random if they are derived from a random drawing in the population of the concentrations. The case where  $x_t$  is certain is more convenient for the calibration context where the analyst chooses the level of the calibration points. The model is called functional model, the true variables  $x_t$ , associated with the  $n$  observations, are  $n$  supplementary unknowns to estimate.

The errors or the observed variables may be homoscedastic or heteroscedastic, correlated or not. In the metrological context, the uncertainties vary with the level of the variables so the errors are heteroscedastic. The responses may be not correlated. The values of the standards, usually derived from the same primary standard or the same preparation process, are correlated.

The responses and the standards are not pair correlated:  $\text{Cov}(X_t, Y_t) = 0$ . The equation (3), derived from the measuring system, has no error.

#### 4. The Bivariate Least Squares

This method is detailed in [4], [5]. The BLS deals with a model  $Y_t = a + bX_t + e_t$  in which  $X_t$  and  $Y_t$  are random variables, heteroscedastic and not (auto) correlated. The two variables are correlated only for the same observation:  $\text{Cov}(X_i, Y_i) \neq 0$  and  $\text{Cov}(X_i, Y_j) = 0$  for  $i \neq j$ .

As GLS, the BLS method minimises the sum of the weighted square residuals  $S = \mathbf{e}' \mathbf{W}^{-1} \mathbf{e}$  with respect to  $a$  and  $b$ . As in the particular case of WLS, the weights are the inverse of the variances of the errors; but these variances now depend on the uncertainties of  $X_t$  and  $Y_t$ :  $s^2 e_t = s^2 Y_t + b^2 s^2 X_t - 2 b \text{Cov}(X_t, Y_t)$ . In the metrological context, the variables are often not correlated,  $\text{Cov}(X_t, Y_t) = 0$  so these variances are:

$$s^2 e_t = s^2 Y_t + b^2 s^2 X_t \quad (5)$$

The estimator is determined by a system of two non linear equations in the unknown parameters. This system is simplified as:

$$\begin{vmatrix} \sum \frac{1}{s^2 e_t} & \sum \frac{X_t}{s^2 e_t} \\ \sum \frac{X_t}{s^2 e_t} & \sum \frac{X_t^2}{s^2 e_t} \end{vmatrix} \times \begin{vmatrix} a \\ b \end{vmatrix} = \begin{vmatrix} \sum \left( \frac{Y_t}{s^2 e_t} \right) \\ \sum \left( \frac{X_t \cdot Y_t}{s^2 e_t} + \left( \frac{e_t}{s^2 e_t} \right)^2 \cdot b \cdot s^2 X_t \right) \end{vmatrix} \quad (6)$$

Written in matrix notation, (6) is  $\mathbf{R}\mathbf{B}_{\text{BLS}} = g$ . This system is solved using an iterative process with the OLS estimates as initial values of the parameters. The variance-covariance matrix of the estimator is  $\mathbf{V}(\mathbf{B}_{\text{BLS}}) = \mathbf{R}^{-1a}$ .

This estimator is a particular case of GLS estimator. First, it is approximately GLS in the general linear model (1) where the  $\mathbf{W}$  matrix is diagonal, with variances (5) as elements, and fully known (when  $b$  is determined):  $\mathbf{B}_{\text{BLS}} = (\mathbf{X}' \mathbf{W}^{-1} \mathbf{X})^{-1} \mathbf{X} \mathbf{W}^{-1} \mathbf{Y}$ . Second, BLS is the GLS estimator proposed by Sprent for the errors-in-variables model, when the model is functional, the errors heteroscedastic and correlated only for the same observation [5].

## 5. The GLS and the Errors-in-Variables Model

In this paragraph, we adapt the BLS principle to the case of (auto)correlated errors. We assume that we have only covariances on the standard concentrations.

The covariance of the errors is:  $\text{Cov}(\mathbf{e}_t, \mathbf{e}_l) = b^2 \text{Cov}(X_t, X_l)$  where  $\text{Cov}(X_t, X_l)$  is the covariance of the two standards  $X_t$  and  $X_l$ . The variance of the errors is still given by (5).

The  $\mathbf{W}$  matrix is now, for example  $n = 3$ :

$$\text{Cov}(\mathbf{e}) = \begin{pmatrix} s^2 Y_1 + b^2 s^2 X_1 & b^2 \text{cov}(X_1, X_2) & b^2 \text{cov}(X_1, X_3) \\ b^2 \text{cov}(X_1, X_2) & s^2 Y_2 + b^2 s^2 X_2 & b^2 \text{cov}(X_2, X_3) \\ b^2 \text{cov}(X_1, X_3) & b^2 \text{cov}(X_2, X_3) & s^2 Y_3 + b^2 s^2 X_3 \end{pmatrix} \quad (7)$$

This matrix depends on the unknown parameter  $b$ .

The simplified GLS estimator (s-GLS) is the estimator (1) described in the paragraph 2, where  $\mathbf{W}$  is given by (7). This matrix  $\text{Cov}(\mathbf{e})$  must be invertible. The estimates of the parameters are obtained by an iterative process with  $b_{\text{OLS}}$  as initial value of  $b$ . The variance-covariance matrix of  $\mathbf{B}$  is estimated by (2).

---

<sup>a</sup> In [5],  $\mathbf{V}(\mathbf{B}_{\text{BLS}}) = s^2 \mathbf{R}^{-1}$  where  $s^2 = (\mathbf{e}' \mathbf{W}^{-1} \mathbf{e}) / (n - 2)$  is the estimation of the experimental error.

The full GLS estimator considers the distances between the observed and the true variables:  $(X_t - x_t)$ ,  $(Y_t - (a - bx_t))$ . The BLS and the simplified GLS deal with these distances:  $(Y_t - (a - bX_t))$  in taking into account the uncertainties on the  $X_t$ . In some particular cases, these estimators give same values for the parameters of the calibration line.

## 6. Examples

The methods were tested on two examples of measurement where the standards are highly correlated ( $r(X_i, X_j) > 0.8$ ). The calibration line is used to predict a mean response  $Y_0$  (first example) and the unknown concentration  $X_0$  corresponding to a measured response (second example).

Three methods were used : OLS, BLS and s-GLS. We checked the validity of the results with Monte Carlo method (500 000 simulations). Two sets of assumptions were tested : correlated standards (called MC – with) as GLS and uncorrelated standards (called MC – without) as BLS.

Table 1. Example 1

	OLS	BLS	MC – without	s-GLS	MC - with
$a$	1.84	1.79	1.91	1.81	1.84
$u(a)$	0.18	0.71	0.70	0.19	0.19
$b$	2.58	2.59	2.55	2.59	2.57
$u(b)$	0.07	0.29	0.29	0.09	0.09
$\sigma$	0.029	0.262	not computed	0.965	not computed
$Y_0$	8.276	8.277	8.28	8.277	8.28
$U(Y_0)$	0.024	0.060	0.06	0.113	0.11

Table 2. Example 2

	OLS	BLS	MC – without	s-GLS	MC - with
$A$	16582	19557	20347	19707	16564
$u(a)$	22223	28759	29260	24104	23989
$B$	1784	1778	1777	1777	1784
$u(b)$	43	59	60	53	52
$\sigma$	0.182	0.756	not computed	1.173	not computed
$X_0$	504.35	504.35	504.35	504.5	504.4
$u(X_0)$	2.4	5.8	5.8	8.1	8.1

Methods give the same predictive value for the response or the concentration. But the uncertainties are very different: OLS and BLS give low values. In the case of s-GLS, we check the adequacy between the input uncertainty information and the estimation results ( $\sigma$  is about 1). In the second example, the standard concentrations have a standard uncertainty from 5.4 ng to 7.6 ng.

## References

1. M G Cox, A B Forbes, P M Harris, The classification and solution of regression problems for calibration, NPL Report CMSC 24/03, (2004)
2. Malinvaud, Méthodes statistiques de l'économétrie, Dunod, (1978)
3. Johnston, Econometric methods, International student edition, (1972)
4. J. Riu and F.X. Rius, Univariate regression models with errors in both axes, Journal of chemometrics, VOL. 9, 343-362 (1995)
5. F. Javier del Rio, Jordi Riu and F. Xavier Rius, Prediction intervals in linear regression, taking into account errors on both axes, Journal of chemometrics, 15, 773 – 788 (2001)
6. C. Cheng, J. Riu, On estimating linear relationships when both variables are subject to heteroscedastic measurement errors, Technometrics, VOL. 48, NO. 4 (2006)

## THE CONCEPT OF “VIRTUAL MICROSCOPE” FOR NANOMETROLOGY

A.V. ZABLOTSKIY, A.S. BATURIN, V.S. BORMASHOV

*Moscow Institute of Physics and Technology (State University),  
Institutskiy per. 9, Dolgoprudny, Moscow region, 141700, Russia*

To prove the reliability of nanoscale measurements a new approach is proposed, which assumes joined analysis of experimental image and its analog produced by simulation in “virtual microscope”. Uncertainties of “measured” parameters are evaluated using cross-correlation dependences between the parameters describing specimen shape and parameters of simulated image.

### 1. The Concept of Nanoscale Measurements

Development of nanotechnologies requires a forward development of metrology at nanometer scale [1]. Nanotechnology deals with nanoscale objects so the most important issue is the development of procedures and tools for measurements of linear dimensions in nanoscale. Finite probe size of scanning electron microscope (SEM) or atomic force microscope (AFM) leads to discrepancy between image and true shape of studied nanoobjects. This is a principal limitation for usage SEM or AFM as tool for nanometrology. To solve this problem we propose to supplement real experimental data with simulation results obtained by “virtual microscope” [2] (see Figure 1).

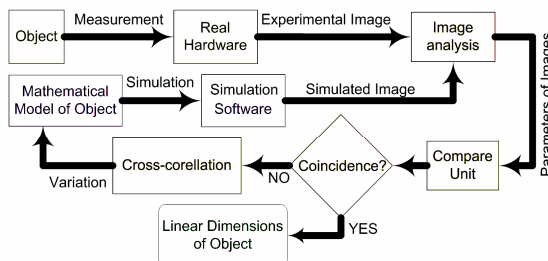


Figure 1. Concept of “virtual microscope” measurements

We propose to append the results of measurement simulations by “virtual microscope” modeling AFM or SEM to experimental results. “Virtual

“Virtual microscope” represents a numerical model of SEM or AFM operation and is used to simulate measurements of real object which is described as some mathematical shape with a set of properties. Object dimensions could be found by means of variation of shape parameters to obtain the best coincidence between simulated and experimental images. Using proposed algorithm multiple direct problem to predict a measurements result from different specimen shapes instead of inverse task should be solved.

## **2. Measurement algorithm**

“Virtual microscope” is a measurement complex that consists of:

- Measurement hardware instrument – SEM or AFM
- Test-object generation software
- SEM or AFM simulation software
- Image processing software

To provide measurements of liner dimensions and to obtain value of uncertainties one should fulfill following procedures (see Figure 2).

1. One should obtain image of studied specimen using calibrated measurement hardware (SEM or AFM).
2. Taking in account obtained image and initial hypothesis about specimen structure one should define parameters of studied object model. Test-object generation software can get these parameters and provide mathematical model of specimen which describes a specimen shape with a finite set of parameters.
3. One should put this mathematical model of specimen to SEM or AFM simulation software input and adjust simulation parameters in correspondence of real hardware parameters used at step 1.
4. One should start measurement simulation. Model image of specimen model is obtained as simulation software output.
5. One should use image processing software to handle real image (step 1) and model one (step 4) to acquire images parameters.
6. Parameters of real image and model one are compared with each other.
7. Steps 2-6 are repeated varying parameters of mathematical model of specimen until the best coincidence between parameters of real image and model one.
8. Cross correlation dependences between parameters of specimen mathematical model and model image parameters are composed.
9. One should take into account real experimental measurement hardware uncertainties (noise level, pixel precision) and slope of cross-correlation curves to obtain linear dimensions of specimen and measurements errors.

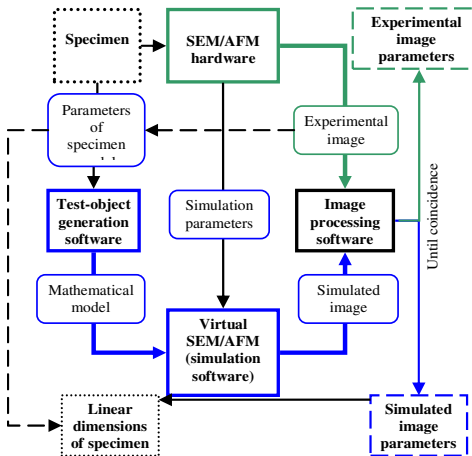


Figure 2. Logical scheme of “virtual microscope” operation.

### 3. Calibration

To provide measurements in nanoscale one should provide translation of length unit from primary standard of length to nanoscale range with appropriate accuracy to be able to calibrate measurements hardware instrument.

There is a reference object for SEM and AFM calibration introduced by Russian national standards (GOST R 8.628-2007, GOST R 8.629-2007). These requirements are realized in calibration grating (measure) GWPS-2.0Si [4]. We proposed to use it for the calibration of “virtual microscope”. Naturally it is possible to calibrate “virtual microscope” using another appropriate reference object.

### 4. Conclusions

To solve a problem of measurements in nanoscale which is originated from physical foundation of SEM or AFM operation and comparability of its probe size to dimension of investigated specimen we propose concept of “virtual microscope”. On the first step one obtains an image of investigated nanoobject utilizing SEM or AFM. At the second step one makes an initial hypothesis about nanoobject relief. Then one generates mathematical model of investigated relief using a library of mathematical test-objects. At the next step one simulates an image with help of virtual microscope. The simulated image is parameterized and cross-correlation between parameters of test-object and simulated image are estimating. The parameters of the test-object are varying until the best

coincidence of simulated image and measured one. The accuracy of found value of test-object parameters is estimated from the experimental uncertainties and cross-correlation curves.

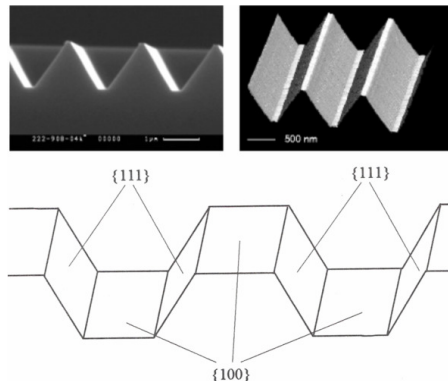


Figure 3. Reference objects GWPS-2.0Si for calibration. The trapezoid trenches produced by anisotropic etching of silicon along crystallographic axis {111} that provides extremely stability of the side wall projection length. Russian standards (GOST R 8.628-2007, GOST R 8.629-2007).

## Acknowledgements

Authors acknowledge the Russian Ministry of Education and Science (Federal Agency of Science and Innovation, contract 02.513.11.3224 and Grant of Federal Agency of Education RNP.2.1.2.9353) for financing of this research.

## References

1. Yu. A. Novikov, A. V. Rakov, P. A. Todua, *Proceedings of the Prokhorov General Physics Institute*, 62, pp.3-13, (2006).
2. A. V. Zablotskiy, A. S. Baturin, V. S. Bormashov, R. M. Kadushnikov, N. A. Shturkin, *Book of abstracts International Conference “Mirco- and nanoelectronics – 2007”*, P2-42, (2007).
3. A. V. Zablotskiy, A. S. Baturin, V. S. Bormashov, R. M. Kadushnikov, N. A. Shturkin, *Nanotechnology in Russia*, N 11-12, V.2, pp. 40-48, (2007).
4. Yu. A. Novikov, Yu. V. Ozerin, Yu. I. Plotnikov, A. V. Rakov, P. A. Todua, *Proceedings of the Prokhorov General Physics Institute*, 62, pp. 36-76, (2006).

## ORTHOGONAL DISTANCE FITTING OF PRECISION FREE-FORM SURFACES BASED ON $L_1$ NORM

XIANGCHAO ZHANG, XIANGQIAN JIANG

*Centre for Precision Technologies, University of Huddersfield, Queensgate,  
Huddersfield, HD1 3DH, UK*

PAUL J. SCOTT

*Taylor Hobson Ltd, PO Box 36, 2 New Star Road, Leicester LE4 9JQ, UK*

Precision free-form surfaces are widely used in advanced optical and mechanical devices. In order to evaluate the form quality of a free-form surface, it is required to fit the measurement data with the design template and compare the relative deviation between them. A common approach is to minimize the sum of squared differences in the  $z$  direction. Its solution is not robust enough and may be biased due to outliers. This paper presents a fitting algorithm which employs the sum of orthogonal distances to evaluate the goodness of fit. The orthogonal projection points are updated simultaneously with the shape and motion parameters. Additionally, the  $L_1$  norm is adopted to improve the robustness of the solution. The Monte-Carlo simulation demonstrated that the bias in the fitted intrinsic characteristics of this method is much smaller than the traditional algebraic fitting, whereas the fitted motion parameters have no distinct difference.

### 1. Introduction

Compared with traditional industrial elements which have simple geometrical shapes, free-form components occupy superior optical and aerodynamic properties, and are crucial to the development of optical and mechanical devices [1]. Surface form plays an essential role in the characteristics of these components. To assess the form quality of a free-form surface, a nominal template is required. The form error is obtained from the relative deviation between the measurement data and the template. However, usually the two surfaces do not exactly lie in the same coordinate system, thus the best *fitting* (or *matching*) needs to be established between them under some error criterion, e.g. least squares,

$$E = \sum_{i=1}^N [z_i - f(x_i, y_i)]^2 \quad (1)$$

where  $[x_i, y_i, z_i]^T = p_i$ ,  $i = 1, 2, \dots, N$  are the data points after transformation and  $z = f(x, y)$  is the nominal template function. Sometimes the template is only supplied as an analytical function, and some intrinsic characteristics (shape parameters) need to be specified as well.

In the above equation, only the deviation in the  $z$  direction is considered, which is called *algebraic fitting* [2]. This approach is commonly adopted

because of its ease of implementation. However, its definition of error distances does not coincide with measurement guidelines and the estimated fitting parameters will be biased, especially when there exist errors in the explanatory variables [2-4]. Consequently researchers have developed the *orthogonal distance fitting* (ODF, also termed *geometric fitting*) method. This technique intends to minimize the sum of squared orthogonal distances from the measurement points to the nominal surface. It can effectively overcome the bias problem of the algebraic fitting. But for free-form surfaces, the orthogonal distances are not straightforward to obtain and the computational cost may increase dramatically. This paper tries to solve this problem.

## 2. The Orthogonal Distance Fitting Algorithm

Suppose the explicit function of a template is given as  $z = f(x, y; \mathbf{a})$ . We aim to determine the intrinsic characteristics  $\mathbf{a}$ , an optimal rotation matrix  $\mathbf{R}$  and a translation vector  $\mathbf{t}$  to minimize the sum of squared orthogonal distances from all the measurement points to the template,

$$\min_{\mathbf{a}, \mathbf{R}, \mathbf{t}} \sum_{i=1}^N \| \mathbf{R}\mathbf{p}_i + \mathbf{t} - \mathbf{q}_i \|^2 = \min_{\mathbf{a}, \mathbf{R}, \mathbf{t}} \sum_{i=1}^N \| \mathbf{p}'_i - \mathbf{q}_i \|^2 \quad (2)$$

Here  $\mathbf{p}'_i = \mathbf{R}\mathbf{p}_i + \mathbf{t} = [x'_i, y'_i, z'_i]^T$  is an arbitrary measurement point after motion and  $\mathbf{q}_i$  is the closest point on the template corresponding to  $\mathbf{p}'_i$ .

The coordinates of  $\mathbf{q}_i$  are represented as,

$$\mathbf{q}_i = [x'_i + \xi_i, y'_i + \zeta_i, f(x'_i + \xi_i, y'_i + \zeta_i; \mathbf{a})]^T$$

and the weighting technique is incorporated. Then the error metric in Equation (2) can be rewritten as,

$$E = \sum_{i=1}^N w_i^2 [z'_i - f(x'_i + \xi_i, y'_i + \zeta_i; \mathbf{a})]^2 + \sum_{i=1}^N u_i^2 \xi_i^2 + \sum_{i=1}^N v_i^2 \zeta_i^2 = \mathbf{G}^T \mathbf{G} + \mathbf{H}^T \mathbf{H} \quad (3)$$

with  $\mathbf{G} \in \Re^{N \times l} : G_i = w_i [z'_i - f(x'_i + \xi_i, y'_i + \zeta_i; \mathbf{a})]$ ,  $i = 1, \dots, N$

$$\text{and } \mathbf{H} \in \Re^{2N \times l} : H_j = \begin{cases} -u_{(j+1)/2} \xi_{(j+1)/2}, & j = 1, 3, \dots, 2N-1 \\ -v_{j/2} \zeta_{j/2}, & j = 2, 4, \dots, 2N \end{cases}$$

If regarding  $\{\xi_i\}$  and  $\{\zeta_i\}$  as unknown variables, we can solve them simultaneously with the intrinsic characteristics  $\mathbf{a} \in \Re^{p \times l}$  and the six motion parameter  $\theta_x, \theta_y, \theta_z, t_x, t_y$ , and  $t_z$ .

Boggs *et al* [5] proposed a method to solve this nonlinear least squares problem based on the Levenberg-Marquardt algorithm.

Denoting the shape and motion parameters with a vector  $\mathbf{m} \in \Re^{(p+6) \times l}$  and denoting  $\{\xi_i\}$  and  $\{\zeta_i\}$  with a vector  $\beta \in \Re^{2N \times l}$ , then Equation (3) can be solved iteratively by,

$$\begin{bmatrix} \mathbf{J} & \mathbf{V} \\ 0 & \mathbf{D} \\ \lambda^{1/2}\mathbf{S} & 0 \\ 0 & \lambda^{1/2}\mathbf{T} \end{bmatrix} \begin{bmatrix} \delta\mathbf{m} \\ \delta\beta \end{bmatrix} = - \begin{bmatrix} \mathbf{G} \\ \mathbf{H} \\ 0 \\ 0 \end{bmatrix} \quad (4)$$

with  $\mathbf{J} \in \Re^{N \times (p+6)} : J_{ij} = \partial g_i / \partial m_j, i=1, \dots, N, j=1, \dots, p+6,$

$\mathbf{V} \in \Re^{N \times 2N} : V_{ij} = \partial g_i / \partial \beta_j = -w_i \partial f_i / \partial \beta_j, i=1, \dots, N, j=1, \dots, 2N$

and  $\mathbf{D} \in \Re^{2N \times 2N} : \mathbf{D} = -\text{diag}\{u_1, v_1, u_2, v_2, \dots, u_N, v_N\}$

Here  $\lambda > 0$  is a damping factor and  $\mathbf{S} \in \Re^{(p+6) \times (p+6)}$  and  $\mathbf{T} \in \Re^{2N \times 2N}$  are two scaling matrices. Employing damping terms can greatly improve the numerical stability of the system and guarantee the convergence of its solution. The damping factor  $\lambda$  need to be selected properly according to the specific problem. If the value of  $\lambda$  is too large, the step length of the updates  $\delta\alpha$  and  $\delta\beta$  will be very small, consequently leading to a rather slow convergence speed; On the other hand, a  $\lambda$  too small cannot significantly affect the system's numerical property. The normal function of Equation (4) is,

$$\begin{bmatrix} \mathbf{J}^T \mathbf{J} + \lambda \mathbf{S}^2 & \mathbf{J}^T \mathbf{V} \\ \mathbf{V}^T \mathbf{J} & \mathbf{V}^T \mathbf{V} + \mathbf{D}^2 + \lambda \mathbf{T}^2 \end{bmatrix} \begin{bmatrix} \delta\mathbf{m} \\ \delta\beta \end{bmatrix} = - \begin{bmatrix} \mathbf{J}^T \mathbf{G} \\ \mathbf{V}^T \mathbf{G} + \mathbf{D}\mathbf{H} \end{bmatrix} \quad (5)$$

So that  $\delta\mathbf{m} = -(\mathbf{J}^T \mathbf{M} \mathbf{J} + \lambda \mathbf{S}^2)^{-1} \mathbf{J}^T \mathbf{M} (\mathbf{G} - \mathbf{V} \mathbf{E}^{-1} \mathbf{D}\mathbf{H})$  (6)

and  $\delta\beta = -\mathbf{E}^{-1} [\mathbf{V}^T \mathbf{M} (\mathbf{G} + \mathbf{J} \delta\mathbf{m} - \mathbf{V} \mathbf{E}^{-1} \mathbf{D}\mathbf{H}) + \mathbf{D}\mathbf{H}]$  (7)

In the equation  $\mathbf{M} = \mathbf{I} - \mathbf{V} (\mathbf{V}^T \mathbf{V} + \mathbf{E}^2)^{-1} \mathbf{V}^T$ . In fact, it is a diagonal matrix

$$\mathbf{M} = \text{diag} \left\{ 1 / \left[ 1 + \left( w_i \frac{\partial f_i}{\partial \xi_i} \right)^2 / E_{2i-1} + \left( w_i \frac{\partial f_i}{\partial \zeta_i} \right)^2 / E_{2i} \right] \right\}, \quad i = 1, \dots, N,$$

and  $\mathbf{E} = \mathbf{D}^2 + \lambda \mathbf{T}^2$  is diagonal as well.

### 3. Improving the Robustness of the Solution Based on the $l_1$ Norm

The least squares approach is commonly adopted as in Equation (2) for its ease of calculation. It is unbiased when the error is normally distributed [6]. However, measurement outliers and manufacturing defects can make the result distorted, or even break down.

To improve the robustness of the fitting results, various improvements have been proposed [7]. Among these methods, the  $l_1$  norm pays less attention to the wild points and concentrates on the vast majority of the data points. But it has discontinuous derivatives and consequently difficult to solve. Hunter and Lange [8] proposed an algorithm based on the Majorize-Minimize theory. A continuous surrogate function is adopted to approximate the initial  $l_1$  norm objective function.

For the  $l_1$  norm fitting problem,

$$E = \sum_{i=1}^N \|Rp_i + t - q_i\| = \sum_{i=1}^N r_i \quad (8)$$

A small perturbation  $\varepsilon > 0$  is introduced,

$$E^\varepsilon = \sum_{i=1}^N \rho^\varepsilon(r_i) = \sum_{i=1}^N [r_i - 2\varepsilon \ln(\varepsilon + |r_i|)] \quad (9)$$

It turns out that for a given residual  $r^{(k)}$  at the  $k$ -th iteration,  $\rho^\varepsilon(r)$  is majorized by  $\psi^\varepsilon(r|r^{(k)}) = \frac{r^2}{\varepsilon + |r^{(k)}|} + c$ , i.e.  $\begin{cases} \psi^\varepsilon(r^{(k)}|r^{(k)}) = \rho^\varepsilon(r^{(k)}) \\ \psi^\varepsilon(r|r^{(k)}) \geq \rho^\varepsilon(r) \text{ for all } r \end{cases}$ , thus the new objective function will be

$$E^\varepsilon = \sum_{i=1}^N \psi^\varepsilon(r_i) = \sum_{i=1}^N \left[ \frac{r_i^2}{\varepsilon + |r_i^{(k)}|} + c_i \right] \quad (10)$$

It can be proved that  $|E^\varepsilon - E| \leq -2\varepsilon N \ln \varepsilon$ , hence the constant  $\varepsilon$  can be determined according to the overall error threshold  $\tau = -2\varepsilon N \ln \varepsilon$ .

Obviously the constants  $\{c_i\}$  do not affect the solution. Therefore, the  $l_1$  norm optimization becomes a reweighted least squares problem with  $w_i = 1/(\varepsilon + |r_i^{(k)}|)$ . Now recall the weights of the ODF algorithm. We set them as  $\begin{cases} u_i = aw_i, i = 1, 2, \dots, N \\ v_i = bw_i \end{cases}$ . Here  $a, b \geq 0$  are utilized to measure the relative influence of the lateral and vertical deviations onto the error metric. In practice if there is noise in all the  $x$ ,  $y$ , and  $z$  coordinates, we set  $a, b > 0$ . On the contrary, if only  $z$  coordinates contain errors, we set  $a = b = 0$ , i.e. algebraic fitting will be adopted.

#### 4. Numerical Example and Discussion

A biconic surface is adopted for numerical simulation [9],

$$z = \frac{c_x x^2 + c_y y^2}{1 + \sqrt{1 - (1 + k_x)c_x^2 x^2 - (1 + k_y)c_y^2 y^2}} \quad (11)$$

In the equation, the intrinsic characteristics are set to be  $c_x = 2/9 \text{ mm}^{-1}$ ,  $c_y = 2/7 \text{ mm}^{-1}$ ,  $k_x = -0.3$ , and  $k_y = 0.3$ .  $100 \times 100$  points are sampled within the area  $-2.5 \text{ mm} \leq x, y \leq 2.5 \text{ mm}$  as measurement data and transformed with  $\theta_x = -2^\circ$ ,  $\theta_y = 4^\circ$ ,  $\theta_z = 3^\circ$  and  $t = [-1.0 \text{ mm}, -2.0 \text{ mm}, 1.5 \text{ mm}]^T$ . Gaussian noise of  $N(0, (0.5 \mu\text{m})^2)$  is introduced onto the  $x$  and  $y$  directions and  $N(0, (0.1 \mu\text{m})^2)$  onto the  $z$  direction. 200 points are randomly sampled and Gaussian error of  $N(0, (50 \mu\text{m})^2)$  is added on them as outliers. Defects are also involved as shown in Figure 2.

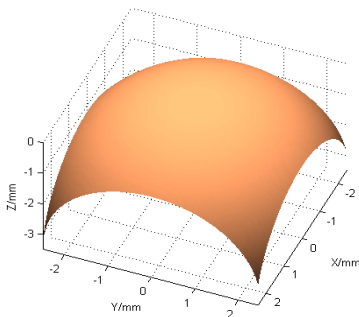


Figure 1. Biconic surface

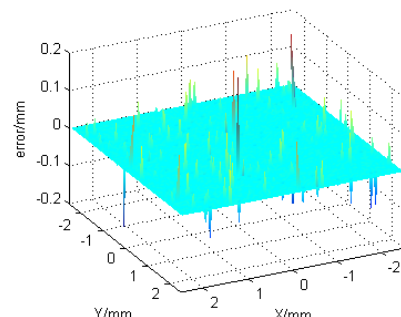


Figure 2. Defects and noise

Here we compare the  $l_1$  norm geometric fitting,  $l_2$  norm geometric fitting, and  $l_1$  norm algebraic fitting. These programs are coded in MATLAB R2007a and run on a Pentium 4 PC with 3.0GHz, 2.00GB RAM. In order to make the fitting results more reliable, the Monte-Carlo simulation is employed and the fitting procedure is run 500 times. The average values of the 500 fitting errors are adopted to measure the bias of each method; and the standard deviations ( $\sigma$ ) to assess the uncertainty. The uncertainty of the three algorithms turns out to be not significantly different, with  $l_2$  norm ODF a little poorer. The reason is that the uncertainty of the fitted parameters is mainly determined by the amplitude of the introduced random noise. The biases of the six intrinsic characteristics and six motion parameters are listed in Table 1.

Table 1. Biases of three fitting methods

Method	$l_1$ Norm ODF	$l_2$ Norm ODF	$l_1$ Algebraic fitting
$c_x$	$-2.85 \times 10^{-6} \text{ mm}^{-1}$	$-6.04 \times 10^{-5} \text{ mm}^{-1}$	$-1.17 \times 10^{-4} \text{ mm}^{-1}$
$c_y$	$1.75 \times 10^{-5} \text{ mm}^{-1}$	$1.36 \times 10^{-4} \text{ mm}^{-1}$	$-1.13 \times 10^{-4} \text{ mm}^{-1}$
$k_x$	$4.20 \times 10^{-4}$	$3.62 \times 10^{-3}$	$1.73 \times 10^{-3}$
$k_y$	$-3.28 \times 10^{-4}$	$-4.13 \times 10^{-3}$	$1.50 \times 10^{-3}$
$\theta_x$	$-0.0736^\circ$	$0.116^\circ$	$-0.231^\circ$
$\theta_y$	$-0.166^\circ$	$-0.711^\circ$	$-0.0755^\circ$
$\theta_z$	$1.22 \times 10^{-3}^\circ$	$2.09 \times 10^{-2}^\circ$	$7.69 \times 10^{-4}^\circ$
$t_x$	$11.6 \mu\text{m}$	$49.1 \mu\text{m}$	$5.33 \mu\text{m}$
$t_y$	$-3.66 \mu\text{m}$	$5.34 \mu\text{m}$	$-11.5 \mu\text{m}$
$t_z$	$-0.0210 \mu\text{m}$	$-0.157 \mu\text{m}$	$0.108 \mu\text{m}$
Running time	1.570 sec	1.539 sec	0.253 sec

It can be seen that the biases of the intrinsic characteristics of the  $l_1$  norm geometric fitting are at least one order smaller than the other two methods. It demonstrates that ODF technique can effectively overcome the bias problem and the  $l_1$  norm error metric can greatly improve the system stability and robustness against outliers and defects.

The geometric fitting shows no significant superiority over algebraic fitting on motion parameters. In fact, it holds true for most smooth surfaces. Therefore, when the shape of the surface is completely fixed, the motion parameters can be calculated using the conventional algebraic fitting algorithm, which is relatively simpler and quicker to implement.

## 5. Conclusions

Orthogonal distance fitting shows obvious superiority on accuracy and unbiasness over algebraic fitting methods, especially when the surface is highly curved and both its lateral and vertical coordinates contain errors. The error metric of ODF is consistent with the standard error definition. Numerical simulation shows the fitting accuracy of the intrinsic characteristics can be greatly improved. Moreover, real measurement data may be polluted by outliers, missing data or defects, consequently causing serious error in the least-squared fitted parameters. In this case, the  $l_1$  norm regression can be adopted to improve the robustness of the system. On the other hand, if the specific distribution of the noise has been known beforehand, we will try to transform the corresponding objective function into an appropriate reweighted least squares problem, so that the Boggs algorithm can still be employed.

## References

- [1] X Jiang, P J Scott, D J Whitehouse et al. Paradigm shifts in surface metrology II. The current shift. Proc Royal Soc. A. 2007; 463: 2071-2099
- [2] S J Ahn, W Rauh et al. Least-squares orthogonal distances fitting of circle sphere, ellipse, hyperbola and parabola. Patt. Recog. 2001; 34: 2283-2303
- [3] DIN 32880-1, Coordinate Metrology; Geometrical Fundamental Principles, Terms and Definitions, German Standard, Beuth Verlag, Berlin, 1986
- [4] W Sun. Precision Measurement and Characterisation of Spherical and Aspheric Surfaces. Ph.D Thesis, Univ. of Southampton, UK. May 2007
- [5] P T Boggs, R H Byrd and R B Schabel. A stable and efficient algorithm for nonlinear orthogonal distance regression. SIAM J Stat Comput. 1987; 8(6): 1052-1078
- [6] R M Barker, M G Cox, A B Forbes and P M Harris. Discrete modelling and experimental data analysis. Version 2. NPL Report. 2004
- [7] W J J Rey. Introduction to Robust and Quasi-Robust Statistical Methods. Springer-Verlag. 1983
- [8] D R Hunter and K Lange. Quantile regression via an MM Algorithm. Journal of Computational and Graphical Statistics. 2000; 9(1): 60-77
- [9] ZEMAX Optical Design Program, User's Guide, April 2006

## ALLAN VARIANCE AND THE UNCERTAINTY OF AUTOCORRELATED MEASUREMENTS

NIEN FAN ZHANG

*Statistical Engineering Division, National Institute of Standards and Technology,  
Gaithersburg, MD 20899, USA  
Email: zhang@nist.gov*

In metrology, the uncertainty of the mean of repeated measurements is often calculated by the sample standard deviation of the measurements divided by the square root of the sample size. When the measurements are autocorrelated, in particular when they are from a stationary process, a recent paper in *Metrologia* (Zhang 2006) provided an approach to calculate the corresponding uncertainty. However, when the measurements are from a nonstationary process, how to assess their uncertainty remains unresolved. Allan variance or two-sample variance has been used for more than three decades as a substitute for the classical variance to characterize the stability of clocks or frequency standards when the underlying process is a  $1/f$  noise process. Recently, from the point of view of the time domain, a paper in *Metrologia* (Zhang, 2008) studied the Allan variance and its properties for stationary processes, random walk, and long-memory processes such as the fractional difference processes. This paper discusses the use of Allan variance as an alternative measure of uncertainty for measurements from time series models. The results show that the Allan variance is a better measure of the process variation than the classical variance of the random walk and the nonstationary fractional difference processes including the  $1/f$  noise.

### 1. Introduction

It is a common practice in metrology that the dispersion or standard deviation of the average of repeated measurements is calculated by the sample standard deviation of the measurements divided by the square root of the sample size. When the measurements are autocorrelated, this calculation is not appropriate as pointed out by the Guide to the Expression of Uncertainty in Measurement (GUM) [3], 4.2.7. Thus, appropriate approaches are needed to calculate the corresponding uncertainty. Recently, a practical approach was proposed in [1] to calculate the uncertainty of the mean of autocorrelated measurements when the data are from a stationary process. To explain that approach, some basic concepts of time series models, in particular the stationary processes are needed.

Consider a discrete weakly stationary process  $\{X(t), t = 1, 2, \dots\}$ . Namely,  $E[X(t)] = \mu$  (constant) and the covariance between  $X(t)$  and  $X(t + \tau)$

( $\tau = 0, \pm 1, \dots$ ) is finite and depends only on  $\tau$ , i.e.,

$$r(\tau) = Cov[X(t), X(t+\tau)] = r(-\tau). \quad (1)$$

In particular, the process variance is  $\sigma_x^2 = r(0)$ .  $r(\tau)$  is the autocovariance function at lag  $\tau$ . The autocorrelation function of  $\{X(t)\}$  is  $\rho(\tau) = r(\tau)/r(0)$ . Obviously,  $\rho(0) = 1$ . The simplest stationary process is white noise, which has a mean of zero and  $\rho(\tau) = 0$  for all  $\tau \neq 0$ . We define the process  $\{Y_n(T), T = 1, 2, \dots\}$ ,  $n \geq 2$ , of arithmetic means of  $n$  consecutive  $X(t)$ 's ( $n > 1$ ) or moving averages as

$$Y_n(T) = \frac{X((T-1)n+1) + \dots + X(Tn)}{n} \quad (2)$$

for  $T = 1, 2, \dots$ . It is obvious that

$$E[Y_n(T)] = \mu. \quad (3)$$

As shown in [1], the variance can be expressed as

$$Var[Y_n(T)] = \frac{\sigma_x^2}{n} \left[ 1 + \frac{2 \sum_{i=1}^{n-1} (n-i) \rho(i)}{n} \right] = Var[\bar{X}], \quad (4)$$

where  $n \geq 2$ . In particular, when  $\{X(t)\}$  is an independently identically distributed (i.i.d.) sequence,  $Var[Y_n(T)] = \sigma_x^2/n$ . This fact has been used in metrology to reduce the standard deviation or uncertainty of the  $Y_n(T)$  or  $\bar{X}$ , using a large sample size  $n$ . When  $\{X(t)\}$  is autocorrelated, the variance of  $Y_n(T)$  or  $\bar{X}$  can be calculated from (4) and is used to calculate the uncertainty of the mean of autocorrelated measurements when they are from a stationary process. In practice, the uncertainty of  $Y_n(T)$  can be calculated by substituting  $\sigma_x^2$  by the sample variance  $S_x^2$  and substituting  $\rho(i)$  by the corresponding sample autocorrelation  $\hat{\rho}(i)$  and thus given by

$$u_{Y_n(T)}^2 = \frac{S_x^2}{n} \left[ 1 + \frac{2 \sum_{i=1}^{n-1} (n-i) \hat{\rho}(i)}{n} \right], \quad (5)$$

where  $n_c$  is a cut-off lag estimated from the data. The details are referred to [1]. A simple example of a stationary process is an first order autoregressive (AR(1)) process, i.e.,

$$X(t) - \mu - \phi[X(t-1) - \mu] = a(t) \quad (6)$$

with  $|\phi| < 1$ . The process  $\{a(t)\}$  is white noise with a variance of  $\sigma_a^2$ . The above expression can be rewritten as

$$(1 - \phi B)[X(t) - \mu] = a(t), \quad (7)$$

where  $B$  is the back shift operator, i.e.,  $B[X(t)] = X(t-1)$ . Without loss of generality, we assume that the means for AR(1) and other stationary processes in this paper are zero. When  $\{X(t)\}$  is an AR(1) process, it is given in [1] that

$$\text{Var}[Y_n(T)] = \frac{n - 2\phi - n\phi^2 + 2\phi^{n+1}}{n^2(1 - \phi)^2} \sigma_x^2. \quad (8)$$

In this case, the variance of  $Y_n(T)$  or  $\bar{X}$  still decreases with a rate of  $1/n$  when the sample size  $n$  increases.

However, as stated in [1], if measurements are from a nonstationary process, using the average value and the corresponding variance to characterize the measurement standard may be misleading. [2] studied properties of Allan variance and its use as an alternative measure of uncertainty.

For some processes, which are not stationary, it is shown later that the variance of  $Y_n(T)$  or  $\bar{X}$  may not decrease with rate of  $1/n$  or even may not always decrease when  $n$  increases. For these processes, continued averaging of repeated measurements does not reduce the uncertainty and improve the quality of measurements as when the measurements are statistically independent or from a stationary process. This concern was the main reason to use Allan variance in [4]. In Section 2, Allan variance is introduced for a weakly stationary process in general and its properties are studied for the first order autoregressive (AR(1)) processes. Sections 3 and 4 discuss the Allan variance for random walk and the fractional difference autoregressive-moving average (ARFIMA)(0,  $d$ , 0) processes, including the case where  $d = 0.5$ , respectively. In Section 5, two examples are presented followed by the conclusions.

## 2. Allan variance for a weakly stationary process

In time and frequency metrology, Allan variance or two-sample variance has been used for a long time as a substitute for the classical variance to characterize the stability of clocks or frequency standards. GUM [3], 4.2.7 states that specialized methods such as the Allan variance should be used to treat autocorrelated measurements of frequency standards. As discussed in [5], [6], [7], and [8], it has been found empirically that random fluctuations in standards can be modeled or at least usefully classified by a power law of the power spectral density given by

$$f(\omega) = \sum_{\alpha=-2}^2 h_\alpha \omega^\alpha, \quad (9)$$

where  $f(\omega)$  is the spectral density at the Fourier frequency  $\omega$  and the  $h_\alpha$ 's are intensity coefficients. When a process has the property that  $f(\omega) \sim 1/\omega$  when  $\omega \rightarrow 0$ , it is called  $1/f$  noise. For such processes, it was concluded that the process variance is infinite while its Allan variance is finite. Recently, [7] and [8] found that the measurements of Zener-diode voltage standards retain some “memory” of its previous values and can be modeled as  $1/f$  noise. In [7] and [8] Allan variance was used to characterize the noise of Zener-diode voltage standards, though it has been used mostly for its properties related to the power spectrum density for a variety of stochastic process, in particular, the  $1/f$  noise. Allan variance has been applied to the the processes, which are characterized by power law of frequencies as in (9). In [2], the properties of the Allan variance for a wide range of time series in the time domain were studied.

In [7], the two-sample variance or Allan variance of a stationary  $\{X(t)\}$  for the average size of  $n \geq 2$  is defined as

$$AVar_n[X(t)] = \frac{E[(Y_n(T) - Y_n(T-1))^2]}{2}. \quad (10)$$

When  $\{X(t)\}$  is stationary, the Allan variance can be expressed as

$$AVar_n[X(t)] = \frac{Var[Y_n(T) - Y_n(T-1)]}{2}. \quad (11)$$

It is shown in [2],

$$AVar_n[X(t)] = \frac{n[1 - \rho(n)] + \sum_{i=1}^{n-1} i[2\rho(n-i) - \rho(i) - \rho(2n-i)]}{n^2} \sigma_x^2. \quad (12)$$

From (4) and (12), the variance of moving averages and the Allan variance of a stationary process are closely related and both of them are functions of the autocorrelation function, the size of the average, and the variance of the process. From (11), for a given time series data set of  $\{X(1), \dots, X(N)\}$ , the Allan variance for the average size of  $n$  is estimated by

$$\overline{AVar}_n[X(t)] = \frac{\sum_{i=2}^m [Y_n(i) - Y_n(i-1)]^2}{2(m-1)} \quad (13)$$

for  $m = [N/n]$ , which is unbiased. In [2] the properties of Allan variance for several stationary time series models were investigated. We describe the main properties in the following subsections.

## 2.1. Independently identically distributed sequence

When  $\{X(t)\}$  is an i.i.d. sequence or a stationary sequence and uncorrelated process,  $\rho(i) = 0$  when  $i \neq 0$  and  $\rho(0) = 1$ . From (11),

$$AVar_n[X(t)] = Var[Y_n(T)] = \frac{\sigma_x^2}{n}. \quad (14)$$

That is, in the case of an i.i.d. sequence, the Allan variance equals the variance of the sample average.

## 2.2. AR(1) processes

Assume that  $\{X(t)\}$  is an AR(1) process as given in (6). When  $|\phi| < 1$ ,  $\{X(t)\}$  is stationary. In this case,  $\rho(i) = \phi^i$  for  $i = 1, 2, \dots$ . From [2],

$$\begin{aligned} AVar_n[X(t)] &= \frac{n - 3\phi - n\phi^2 + 4\phi^{n+1} - \phi^{2n+1}}{n^2(1-\phi)^2} \sigma_x^2 \\ &= \frac{n - 3\phi - n\phi^2 + 4\phi^{n+1} - \phi^{2n+1}}{n^2(1-\phi)^2(1-\phi^2)} \sigma_a^2 \end{aligned} \quad (15)$$

since  $\sigma_x^2 = \sigma_a^2 / (1 - \phi^2)$ . Note that when  $\phi = 0$ ,  $X(t) = a(t)$ , which is a white noise process, then (15) becomes (14). We now consider the case that the values of the Allan variance when  $n$  increases. From (15), when  $n \rightarrow \infty$ ,

$$AVar_n[X(t)] \sim \frac{\sigma_a^2}{n(1-\phi)^2} \quad (16)$$

Namely, for a fixed  $|\phi| \neq 1$ , the Allan variance approaches zeros with a rate of  $1/n$  when  $n \rightarrow \infty$ . In [2], the results were extended to the general autoregressive-moving average (ARMA) processes when such a process is stationary.

### 3. Allan variance for Random walk

A random walk process  $\{X(t), t = 0, 1, \dots\}$  is defined as follows (see [11], p. 10):  $X(0) = 0$  and

$$X(t) = X(t-1) + a(t) \quad (17)$$

for  $t > 1$ , where  $a(t)$  is white noise with variance of  $\sigma_a^2$ . From [1],

$$Var[X(t)] = t \cdot \sigma_a^2 \quad (18)$$

Since

$$Y_n(T) = \frac{X((T-1)n+1) + \dots + X(Tn)}{n},$$

from (17)

$$Var[Y_n(T)] = \frac{\sigma_a^2}{n} \frac{2n^2(3T-2) + 3n + 1}{6}. \quad (19)$$

Thus, the variance of  $Y_n(T)$  depends on  $T$  and approaches infinity with rate of  $n$  when  $n$  increases. Although a random walk is not stationary, we can treat it as a limiting case of an AR(1) process (with  $X(0) = 0$ ) when  $\phi \rightarrow 1$ . From [2], the Allan variance of random walk  $\{X(t)\}$  is given by

$$AVar_n[X(t)] = \frac{2n^2 + 1}{6n} \sigma_a^2. \quad (20)$$

Note that the Allan variance of a random walk is independent of  $T$ , the time index and depends on  $n$  only. In that sense, it is a better measure than the variance of the moving averages.

#### 4. Allan variance for Fractional difference ARFIMA(0, $d$ , 0) process

The fractional difference model was proposed by [12] and [13]. In particular, the ARFIMA(0,  $d$ , 0) is defined as

$$(1-B)^d X(t) = a(t), \quad (21)$$

where  $B$  is the back shift operator,  $\{a(t)\}$  is white noise, and  $d$  can be any real number. By a binomial series the fractional difference  $(1-B)^d$  is defined as

$$(1-B)^d = 1 - dB - \frac{d(1-d)}{2} B^2 - \frac{d(1-d)(2-d)}{6} B^3 - \dots$$

When  $d = 1$  and  $X(0)=0$ , it is random walk. When  $d$  is not an integer,  $\{X(t)\}$  is called a fractional difference process. When  $d < 0.5$ , the process is stationary and when  $d > -0.5$  it is invertible [13]. When  $d < 0.5$ , [11] shows that the spectrum density of a stationary  $\{X(t)\}$  has the property:

$$f(\omega) = \frac{\sigma_a^2}{2\pi(2\sin\frac{\omega}{2})^{2d}} \quad (22)$$

for  $-\pi \leq \omega \leq \pi$ . When  $\omega \rightarrow 0$

$$f(\omega) \sim \omega^{-2d}$$

Thus, it is a long-memory process. [13] shows that the autocovariance function at lag  $k$  of  $\{X(t)\}$  is expressed by gamma functions as

$$r(k) = \frac{(-1)^k \Gamma(1-2d)}{\Gamma(k-d+1) \cdot \Gamma(1-k-d)} \sigma_a^2 \quad (23)$$

for  $k = \pm 1, \pm 2, \dots$ . In particular, the variance of  $\{X(t)\}$  is

$$Var[X(t)] = \frac{\Gamma(1-2d)}{[\Gamma(1-d)]^2} \sigma_a^2. \quad (24)$$

Obviously, when  $d \rightarrow 0.5$ ,  $\text{Var}[X(t)] = \sigma_x^2 \rightarrow \infty$ . The autocorrelation function of  $\{X(t)\}$  is

$$\rho(k) = \frac{d \cdot (1+d) \cdot \dots \cdot (k-1+d)}{(1-d) \cdot (2-d) \cdot \dots \cdot (k-d)} = \frac{\Gamma(1-d)\Gamma(k+d)}{\Gamma(d)\Gamma(k+1-d)} \quad (25)$$

for  $k = 1, 2, \dots$ . From (4),

$$\text{Var}[Y_n(T)] = \left[ 1 + \frac{2 \sum_{i=1}^{n-1} (n-i)\rho(i)}{n} \right] \frac{\Gamma(1-2d)}{[\Gamma(1-d)]^2} \frac{\sigma_a^2}{n}. \quad (26)$$

Similarly, from (12) when  $n \geq 2$ , the Allan variance can be expressed as

$$\text{AVar}_n[X(t)] = \frac{n[1-\rho(n)] + \sum_{i=1}^{n-1} i[2\rho(n-i) - \rho(i) - \rho(2n-i)]}{n^2} \frac{\Gamma(1-2d)}{[\Gamma(1-d)]^2} \sigma_a^2 \quad (27)$$

Thus, by (25) and (27) for given  $d$  and  $n$ , the Allan variance for a stationary fractional difference process can be calculated.

As shown in [13], when  $d > -0.5$ , an ARFIMA  $(0,d,0)$  is invertible. In particular, when  $d = -0.5$ , this is called flicker phase noise (see Table 1 in [14]). The process is stationary but not invertible as described in [13]. From (22),

$$f(\omega) = \frac{\sin \frac{\omega}{2}}{\pi} \sigma_a^2 \quad (28)$$

for  $-\pi \leq \omega \leq \pi$ . Obviously, when  $\omega \rightarrow 0$ ,  $f(\omega) \sim \omega$ . It is shown in [2] that

$$\text{Var}[Y_n(T)] \sim \frac{\ln n}{n^2} \quad (29)$$

which is faster than the rate of  $1/n$  as expected. From [2], it was shown that the Allan variance will go to zero when  $n$  increases. Similar to the argument for the rate of convergence for the variance of  $Y_n(T)$ , the rate of the Allan variance when  $n$  approaches infinity is  $\ln n / n^2$ , which is faster than the rate of  $n^{2d-1}$  for  $-0.5 < d < 0.5$ .

We now consider the fractional difference process when  $d = 0.5$ . First we know that in this case, the process has long-memory and is not stationary. From (22), the spectral density (as a limit) of the process,

$$f(\omega) = \frac{\sigma_a^2}{4\pi \sin \frac{\omega}{2}} \sim \omega^{-1} \quad (30)$$

as  $\omega \rightarrow 0$ . Because of the limiting behavior of the spectrum density this process is a flicker frequency process (see Table 1 in [14]) or a discrete  $1/f$  noise as indicated in [11]. As shown in [12] when  $d = 0.5$ ,  $\sigma_x^2$  is infinite, which is true when  $d \rightarrow 0.5$  in (24). It is shown in [2] that when  $d \rightarrow 0.5$ ,  $\text{Var}[Y_n(T)]/\text{Var}[X(t)] \rightarrow 1$  for any fixed  $n$ . That is, when  $d \rightarrow 0.5$ ,  $\text{Var}[Y_n(T)]$  and  $\text{Var}[X(t)]$  goes to infinite with a same rate. Hence,  $\text{Var}[Y_n(T)]$  is not a good measure of uncertainty of ARFIMA(0,0.5,0). For a fixed  $n$ , e.g.,  $n=2$ , analytically, it seems intractable to find the limit of Allan variance in (27) when  $d \rightarrow 0.5$ . Numerically, for a fixed  $n$  the Allan variance of ARFIMA(0, $d$ ,0) can be calculated from (27) for  $d$ 's very close to 0.5. For example, when  $n = 2$ , the limit seems equal to  $0.5093 \cdot \sigma_a^2$  when  $d \rightarrow 0.5$ . In general, we found that for a fixed  $n$ , the Allan variance increases when  $d \rightarrow 0.5$ . On the other hand, for a fixed  $d$ , the Allan variance decreases when  $n \rightarrow \infty$ , which is reasonable. The computation results show that when  $d \geq 0.49999$  and  $n \geq 100$ , Allan variance stabilized at the value of  $0.4413 \cdot \sigma_a^2$ , which is close to  $(2 \ln 2/\pi) \sigma_a^2$ . Namely, when  $n \geq 100$  and  $d \rightarrow 0.5$ ,  $AVar_n[X(T)]$  closes to  $(2 \ln 2/\pi) \sigma_a^2$ , which to a great extent is consistent with the Allan variance of a  $1/f$  in the frequent domain and listed in Table 1 in [8] and the observations by [10], where the property of a stabilized Allan variance was exploited to test whether the measurements of the Zener-diode standards is  $1/f$  noise. As pointed earlier that the variance of a moving average of ARFIMA(0, $d$ ,0) will approach infinity when  $d$  approaches to 0.5, it is clear that using Allan variance has an advantage over using the variance of the moving average. Figure 1 shows the behaviors of Allan variance for AR(1) with  $\phi = 0.75$  and 0.9, ARFIMA(0,0.499,0), ARFIMA(0,0.25,0), and ARFIMA(0,-0.5,0) when  $n$  increases. For these processes, we let the white noise variance  $\sigma_a^2 = 1$ . The Allan variances are calculated by (15) and (27), respectively. The figure shows that the Allan variances of stationary AR(1) processes increase first when  $n$  increases then decrease and approach zero. It also shows that the Allan variance of ARFIMA(0,0.499,0) with  $\sigma_a^2 = 1$ , which is close to  $1/f$  noise

is almost flat at the level of 0.44 when  $n > 20$ . As noted in [7], for  $1/f$  noise the increase of  $n$  will not reduce the uncertainty. It is clear that the convergent rates of Allan variance for stationary fractional difference processes are slower than that of stationary AR processes when  $0 \leq d < 0.5$  and vice versa when  $-0.5 \leq d < 0$ .

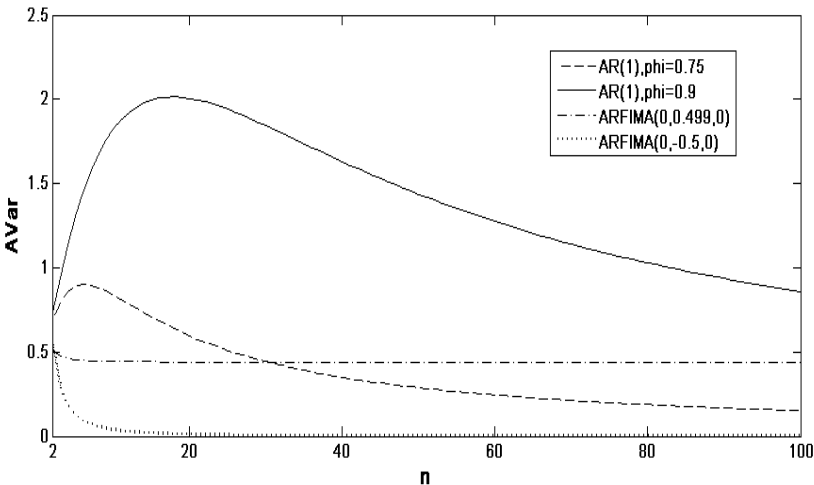


Figure 1. Allan variance as a function of the average size for various processes

In [2], the results for ARFIMA(0,  $d$ , 0) were extended to the general ARFIMA( $p$ ,  $d$ ,  $q$ ) process, especially when  $d \rightarrow 0.5$ .

## 5. Examples

We use two examples to illustrate the Allan variance for autocorrelated data. The first example is a series of 217 high precision weight measurements of 1 kg check standard weight described in [1]. The differences (in micrograms) from 1 kg were plotted in Figure 3 in [1]. An autocorrelation function plot presented in [1] shows that the data are autocorrelated. A time series analysis shows that the data can be treated as from a stationary process. From [1], the uncertainty of the sample average is 0.0067 given by (5). Namely,  $\text{Var}[Y_{217}(1)] = 0.0067^2$ . From (12), the Allan variance for  $n = 2, \dots, 40$  were calculated and plotted in Figure 2. Obviously, the Allan variance decreases when  $n$  increases.

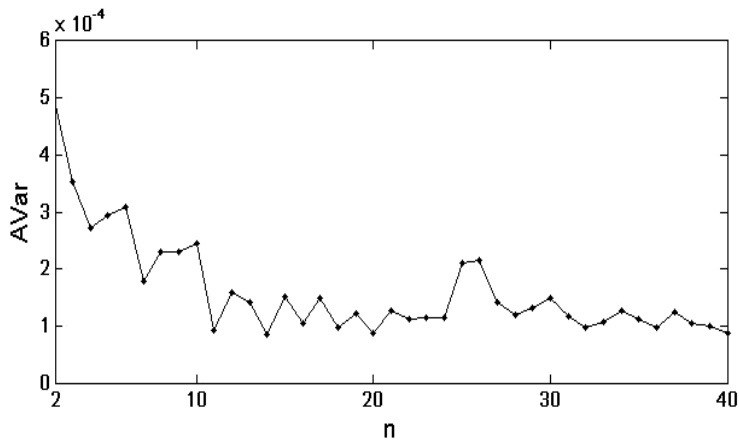


Figure 2. Allan variance for the time series of the differences of the measurements of weight from 1 kg.

The second example is a series of a Zener voltage standard measured against a Josephson voltage standard. Figure 3 shows the time series of the differences of the 8192 voltage measurements in the units of microvolt. The time interval between successive measurements is 0.06 second.

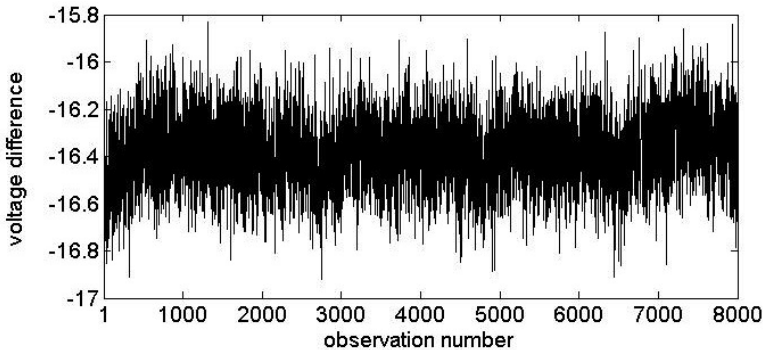


Figure 3. The differences between the measurements from a Zener voltage standard and Josephson voltage standard in the unit of microvolt ( $\mu\text{V}^2$ )

An autocorrelation function plot was presented in [2] and shows that the autocorrelations are significant even for lags larger than 250. [2] shows that a ARFIMA (5,0.497,0) model is a good fit for the data. Thus, it can be treated as a

$1/f$  noise process. The Allan variance in Figure 4 decreases slowly when the size of the average increases and becomes stabilized at the level of 0.006 (a  $1/f$  noise floor) when  $n > 100$ .

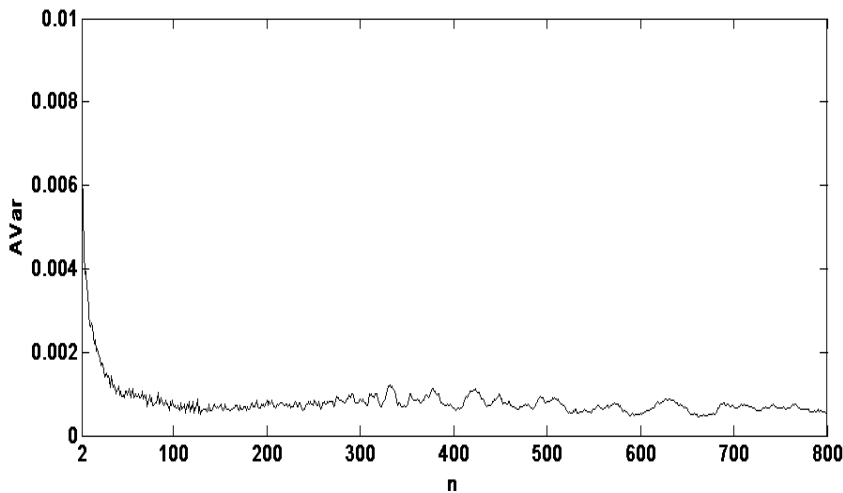


Figure 4. Allan variance for the time series of voltage differences

## 6. Conclusions

In this paper, Allan variance as an alternative measure of uncertainty is investigated for time series models. The variance of moving averages and the Allan variance of a stationary AR(1) process are closely related. They decrease with a same rate when the size of the average increases. For a random walk process, which is a nonstationary process, the variance of the moving averages of it will go to infinity when the size of the averages increases. While Allan variance of random walk also approaches infinity with the same rate for the variance of the moving averages when the size of the averages increases, it is independent of the time. For a nonstationary fractional difference process when  $d = 0.5$ , which is a  $1/f$  noise process, we have demonstrated that its Allan variance is stabilized at a certain level when the size of the averages is large enough while the variance of the moving averages will approach infinity.

In summary, the variance of moving averages and Allan variance are two similar measures of uncertainty for measurements from stationary processes. Each of them is a function of the size of average. For measurements from a stationary process, the traditional standard deviation of the sample average (i.e., the size of average equals the sample size) by [1] is used as the measure of the uncertainty. However, for the measurements from a nonstationary ARFIMA (0,0.5,0) or a  $1/f$  noise process, Allan variance is stabilized when the size of the averages increases and thus a better uncertainty measure than the variance of the moving averages to characterize the process.

## References

1. Zhang N F 2006 Calculation of the uncertainty of the mean of autocorrelated measurements *Metrologia* 43 S276 – S281
2. Zhang N F 2008 Allan variance for time series models for measurement data, *Metrologia*, 45, 549-561
3. ISO/IEC 1995 Guide to the Expression of Uncertainty in Measurement (Geneva: International Organization for Standardization)
4. Allan D 1987 Should the classical variance be used as a basic measure in standards metrology? *IEEE Transactions on Instrumentation and Measurement* 36(2) 646-654
5. Rutman J 1978 Characterization of phase and frequency instabilities in precision frequency sources: fifteen years of progress, *Proc. IEEE* 66(9) 1048-1075
6. Barnes J, Chi A R, Cutler L S, Healey D J, Leeson D B McGunigal T E, Mullen Jr J A, Smith W L Sydnor R L Vessot R F C, and Winker G M R 1971 Charaterization of requence stability *IEEE Trans. Instrum. Meas.* 20(2) 105-120
7. Rutman J and Walls F L 1991 Characterization of frequency stability in precision frequency sources *Proc. IEEE* 79(6) 952-960
8. Witt T 2000 Testing for correlations in measurements, *Advanced Mathematical and Computational Tools in Metrology IV* edited by P Ciarlini, A B Forbes, F Pavese & D Richter 273-288 Singapore: World Scientific
9. Witt T and Reymann D 2000 Using power spectra and Allan variances to characterize the noise of Zener-diode voltage standards *IEE Proc.-Sci. Meas. Technol.* 147(8) 177-182
10. Witt T and Tang Y 2005 Investigations of noise in measurements of electronic voltage standards *IEEE Trans Instrum. Meas.* 54 567 -570
11. Brockwell P J and Davis A D 1987 *Time Series: Theory and Methods* New York: Springer-Verlag

12. Granger C W J and Joyeux R 1980 An introduction to long-range time series models and fractional differencing *Journal of Time Series Analysis* 1 15-30
13. Hosking J R M 1981 Fractional differencing *Biometrika* 68 165-176
14. Schmidt L 2003 Atomic clock models using fractionally integrated noise processes, *Metrologi*, 40 S305-S311

## **Author Index**

- A Allard, 1  
N Almeida, 28  
N Anwer, 73  
S Aranda, 7  
  
M Bär, 142  
T Barashkova, 14  
I M Barbosa, 20  
E Batista, 28  
A S Baturin, 32, 381  
C Baudouin, 344  
R Bigot, 344  
V S Bormashov, 32, 381  
S Botta, 118  
H Bouchenitfa, 37  
S Boukebbab, 37  
P Bourdet, 73  
T Bruns, 204, 369  
J Bruyere, 344  
  
N Chevassus, 73  
P Clarkson, 44  
A Clément, 298  
M L Collucci da Costa Reis, 20  
C O Costa, 273  
M G Cox, 213, 273  
  
J-Y Dantan, 344  
L Del Dossi, 54  
E del Moral Hernandez, 20  
G E D'Errico, 50  
M Do Céu Ferreira, 90  
R J Douglas, 61  
M Douilly, 73  
  
K Ehara, 326  
C Elster, 80, 213, 369  
T J Eward, 44  
  
O A De Faria Mello, 20  
E Filipe, 28, 90, 96  
N Fischer, 1  
A B Forbes, 104, 319  
E Franke, 204  
P Fritz, 291  
A Furtado, 90  
  
C Galvan, 243  
B Gapinski, 113  
A Geistanger, 361  
V Giovanetti, 118  
S Giunta, 118  
R V Goldshtein, 32  
V A Granovsky, 123  
N Greif, 130  
D Grientschnig, 136  
H Gross, 142  
  
C Hajiyev, 148, 154  
B D Hall, 158  
U Hanebeck, 309  
P M Harris, 44, 273  
J P Hessling, 164  
  
X Q Jiang, 385  
  
R Kaarls, 171  
S Kaba, 375  
R Kacker, 195

- D A Kenett, 183  
R S Kenett, 183  
R Kessel, 195  
M Kobusch, 204  
M Krystek, 309  
  
P Le Vacon, 73  
J-M Linares, 7, 37, 219  
K J Lines, 44  
A Link, 80, 369  
I Lira, 213  
  
J Mailhe, 219  
P Marcarino, 118  
G P Mauris, 225  
A Merlone, 118  
L D Milici, 231  
M R Milici, 231  
M Moinet, 298  
M Müller, 237  
J A Muñoz-Gómez, 243  
  
F O Onakunle, 44  
  
G Parkin, 130  
F Pavese, 249  
M Pawłowski, 113  
L R Pendrill, 256  
A Possolo, 330  
M Priel, 262  
  
A Rathsfeld, 142  
A S Ribeiro, 273  
G B Rossi, 279  
M Rösslein, 237  
R Rotar, 231  
M Rucki, 113  
  
F Sawo, 309  
R Schmitt, 291  
P J Scott, 385  
P Serré, 298  
T N Siraya, 123  
I M Smith, 44  
  
K-D Sommer, 309  
J A Sousa, 273 319  
J-M Sprauel, 7, 219  
U Stadtmüller, 361  
A G Steele, 61  
  
H Tanaka, 326  
B Toman, 330  
  
K B Ustinov, 32  
  
J-P Vincent, 344  
  
R Willink, 351, 357  
I Winzenborg, 361  
W Wöger, 213  
M Wolf, 237  
G Wübbeler, 369  
  
C Yardin, 375  
  
A V Zablotskiy, 32, 381  
D Zappa, 54  
X C Zhang, 385  
N-F Zhang, 391